R&D PROJECT

IDENTIFICATION OF VULNERABLE AREAS IN HIMALAYAN WATERSHEDS

Sponsor: Indian National Committee for Hydrology (INCOH), National Institute of Hydrology, Roorkee, (Ministry of Water Resources, Government of India)

Submitted By

Surendra Kumar Mishra, Associate Professor and Principal Investigator
Manoj Kumar Jain, Assistant Professor and Investigator

Dept. of Water Resources Development and Management
INDIAN INSTITUTE OF TECHNOLOGY ROORKEE
Roorkee 247 667, Uttarakhand, India
March 2012

PREFACE

Identification of vulnerable areas in a drainage basin helps improve the planning of soil conservation systems. It basically involves the knowledge of the quantity of sediment yield production by a watershed. The vulnerability increases with the increase in sediment yield, and vice versa. To simulate the process of sediment yield generation, a number of distributed sediment delivery models are available in literature which can be derived from basic principles and linked with a personal computer-based, low cost, geographic information system (GIS) to facilitate preparation, examination, and analysis of spatially distributed input parameters as well as to link the sediment delivery from a micro-scale to the drainage basin-scale. Normally, for field applications, the heterogeneous and complex land surface within the drainage basin is divided into a number of sub-areas and spatially distributed data on vegetative cover can be derived from the digital analysis of satellite images.

Limited studies reported in literature for steep Himalayan catchments indicate that the rate of soil erosion from these catchments is increasing at an alarming rate due to heavy deforestation, urbanization and other developmental activities, and the lack of proper conservation measures. Therefore, a systematic study for quantification of soil erosion, sediment yield and areas vulnerable to soil erosion from the Upper Ramganga catchment was carried out in the form of an R&D project on Identification of Vulnerable Areas in Himalayan Watersheds. The study area lies in the foothills of Himalayas in the Uttaranchal State of India. In this study, the processes of sediment erosion and its transport in Chaukhatia, Gagas, and Naula watersheds of the upper Ramganga catchment were simulated using historical data and these were tested for their efficacy to prediction of sediment yield for identification of vulnerable zones. The project was financially supported by the Indian National Committee on Hydrology, Ministry of Water Resources (MoWR), Govt. of India.

Dr. S K Mishra (PI)

Dr. M K Jain

ACKNOWLEDGEMENT

The investigators of the project owe to the sponsoring agency the Indian National Committee on Hydrology, Ministry of Water Resources (MoWR), Govt. of India, for their financial support. The project could be successfully completed with the timely availability of funds and the support of the INCOH personnel/staff at its Head Quarter New Delhi and at its Secretariat National Institute of Hydrology (NIH), Roorkee. Thanks are especially due to the present NIH Director Sh. R.D. Singh and the Ex-Director Dr. K.D. Sharma and the Member Secretary Dr. Rakesh Kumar for their full moral support. The project handling was fully facilitated by the DEAN (SRIC) and his office staff at the institute level and by Dr. Nayan Sharma, Professor & Head, Dept. of Water resources Development and Management (WRDM), faculty colleagues, and staff of WRDM. The cooperation extended by the field engineers during field visits, especially Sh. Piyush Chandra Gaur, S.E., Ramganga Dam Circle; Sh. Suresh Chandra Sharma, Executive Engineer, Sh. Satya Prakash Naroria, Asstt. Engineer (Second), and Sh. Rajnish Kumar, Asstt. Engineer (First), Sh. Ramganga Dam Division, Kalagarh, is fully acknowledged. In addition, the project could be successfully completed only because of the whole-hearted support and dedication of the project staff Dr. P.K. Singh, Mr. S.S. Rawat, Mr. P. Rang Rao Patil, Ms. Vibha Agarwal, and other Research/M.Tech scholars. The appreciation of the referees/ reviewers of the project report was remarkable and it is greatfully acknowledged.

Dr. S K Mishra (PI)

Dr. M K Jain

CONTENTS

LIST OF FIGURES

LIST OF TABLES

LIST OF SYMBOLS

a	Area drained by unit length of contour
A	Area of the basin
a	Recession constant
A_c	Watershed area
A_i	Mean stream area
a_i	Upslope catchment area per unit contour length draining to a point in catchment
A_i	Fractional area associated with topographic index class 'i'
AVP	Average annual rainfall
AVQ	Average annual runoff
b_c	Depletion coefficient
b_f	A factor describing base flow
BFI_{max}	Maximum value of the baseflow index that can be measured
C	A parameter that allows the shape of the separation to be altered
C	Cover and management factor
CC	Correlation coefficient
CE	Coefficient of efficiency
ChVel	Effective surface routing velocity for scaling the distance/area
CN	Curve number
CN_d	Curve number for the drainage flow
COUR	Courant number
C_r	Runoff coefficient
D	Deposition in cell
D	Number of days between the storm crest and the end of quickflow
d	Euclidean distance
D_d	Drainage density
DO	Sum of the routed rainfall excess
DP	Average daily depletion
D_R	Sediment delivery ratio
$\Delta\Sigma_\mu$	Soil moisture storage
E	Kinetic energy of rainfall
E	Annual Gross Soil Erosion
E	Lake evaporation
E	Computed soil loss per unit area
EFF	Nash and Sutcliffe efficiency
E_t	Average monthly lake evaporation for day t
ET	Evapotranspiration

EV	Volumetric error
EV_{t-1}	Previous day's evapotranspiration
F	Cumulative infiltration
F	Infiltration depth
f	Any kind of model structure (linear or nonlinear)
f	Infiltration rate at time t
f(d)	Nonlinear function
f_c	Final infiltration rate
f_o	Initial infiltration rate at time t= 0
F_r	Actual retention after flow begins
F_s	Stream frequency
g_0, g_1, g_2	Base flow routing coefficients
H	Total relief (Relative relief) of the basin
λ_l	Topographic index
I_{30}	Maximum intensity of rainfall during a continuous period of 30 minutes
I_a	Initial abstraction
I_i	Average intensity of rainfall intensity in the ith increment
IV	Initial variance
k	Scale parameter (T)
k	Filter parameter given by the recession constant
K	Storage coefficient
K	Monthly crop coefficient determined from experimental data
K	Soil erodibility facto
K_b	Base flow storage coefficient
K_{TC}	Transport capacity coefficient
L	Length of main channel or highest order stream
λ	Catchment average topographic index value
L	Effective contour length orthogonal to the direction of flow
L	Slope length factor
L_b	Basin length
L_g	Length of overland flow
L_i	Mean stream length
L_u	Total stream length of the order 'u'
Lu	Stream length
L_{u-1}	Total stream length of its next lower order
M	Soil moisture
M	Number of training instances in that cluster

m_2'	Second dimensionless moment about the centre of area of the IUH
M_t	Soil moisture index at any time t
n	Number of downward stream direction
n	Number of rainstorms per year
n	Shape parameter equal to m_2^{-1}
N	Total number of UH ordinates
n	Total number of observations
N_i	Total No. of stream
NLAG	Lag parameter
n_s	Shape parameter
N_u	Total no. of stream segments of order 'u'
N_{u+1}	Number of segments of the next higher order
n_x and n_y	Positive integer numbers reflecting the memory length of the watershed
O	Outflow
O_b	Baseflow
O_t	Total runoff hydrograph
P	Basin perimeter
P	Total rainfall
P	Rainfall of the respective day
P	Support practice factor
PANC	Pan coefficient
PBIAS	Deviation of streamflow discharge expressed as a percent
PET	Potential evapotranspiration
P_i	Depth of rainfall in the ith increment
Q	Direct surface runoff
$q_{(i)}$	Original stream flow for the i^{th} sampling instant
$q_{(i-1)}$	Original stream flow for the previous sampling instant to i
q(t)	Discharge ordinates
$q_{b(i)}$	Filtered base flow response for the i^{th} sampling instant
$q_{b(i-1)}$	Filtered base flow response for the previous sampling instant to i
Q_{comp}	Simulated runoff
Q_d	Drainage flow depth
$q_{f(i)}$	Filtered quick flow for the i^{th} sampling instant
$q_{f(i-1)}$	Filtered quick flow for the previous sampling instant to i
q_i	Stream flow at time step i
Q_i	Observed runoff for i^{th} day

q_j '	Down slope flow beneath the water table per unit contour length
Q_i	Output of function layer
Q_{kobs}	Observed streamflow
Q_{ksim}	Simulated streamflow
Q_{mean}	Mean observed streamflow during the evaluation period
Q_{obs}	Observed runoff
q_p	Peak Flow Rate
$Q_{ps(c)}$	Computed peak sediment flow rate
$Q_{ps(o)}$	Observed sediment flow rate
Q_s (t)	Output from the watershed system
$Q_{s(c)}$	Computed total sediment outflow
$Q_{s(o)}$	Observed total sediment outflow
q_{vi}	Vertical flux through the unsaturated zone
$q_{vi}A_i$	Recharge rate to the saturated zone at any time step from the unsaturated zone
R	Inflow
R	Rainfall erosivity factor
R	Rainfall Erosivity Factor
R_a	Stream area ratio
R_A	Aarea ratio
R_B	Bifurcation ratio
R_c	Circularity ratio
R_e	Elongation ratio
RE	Relative Error
$RE_{(Qps)}$	Relative errors in peak sediment flow rates
$RE_{(Qs)}$	Relative errors in total sediment outflow
R_f	Form factor
R_h	Relief ratio
r_i	Recharge rate
R_L	Stream length ratio
RMSE	Root mean square error
RO_i	Rainfall excess
R_t	Drainage texture
RV	Remaining variance
S	Potential maximum retention
S	Storage

Y_s	Mobilized sediment per storm
$\hat{y}$	Estimated runoff
y_i	Observed runoff
Y_T	Total amount of mobilized sediment per storm
$\hat{Q}_i$	Computed runoff for i^{th} day
$\overline{Q_i}$	Overall mean daily runoff
$I_{sl}(t)$	Sediment inflow rate to the first reservoir
$Q_{sl}(t)$	Sediment outflow rate
K_S	Sediment storage coefficient
E_i	Kinetic energy of the rain in the i^{th} increment
ΔS	Change in storage
F	Monthly consumptive use factor
F_{t-1}	Previous day's infiltration
k	Decay constant
m	Transmissivity decay parameter
T	Number of days between the storms
Δt	Storm duration
μ	Mean
α	Learning rate
α, α_q	Filter parameters
β	Shape factor
γ, C1, C3	Physically based parameters
Δt	Data sampling interval
Δwij	Change in weight
λ	Initial abstraction coefficient
σ	Spread
σ^2	Variance
$\Gamma(\,)$	Gamma function
$\overline{y}$	Mean observed Runoff
$S_{SS}(t)$	Sediment storage within the reservoir

EXECUTIVE SUMMARY

EXECUTIVE SUMMARY

The concept of a Research and Development (R&D) project on Identification of Vulnerable Areas in Himalayan Watersheds was envisioned in 2006 and proposal was submitted to Indian National Committee on Hydrology (under Ministry of Water Resources (MoWR), Govt. of India), with its secretariat at National Institute of Hydrology, Jal Vigyan Bhawan, Roorkee-247 667 (UK), for possible financial support. The project proposal was considered for its review and it was finally approved by the Ministry of Water Resources (MoWR) under its R&D program for grant of Rs. 21.55 lacs (Rs. Twenty one lacs and fifty five thousand only) vide letter no. 23/58/2006-R&D/2502-14 dated 30.10.2006. Since the first grant was released vide letter no. 23/58/2006- R&D/3001-14 dated 05.12.2006, the project could formally start from January 2007. It was initially approved for three years, but later, it was extended for one more year for completing the project work without any additional financial outlay. Thus, the project is planned to be completed by 31.01.2011. This executive summary presents a brief of the works carried out in accordance with the original project proposal.

Technical Background

Identification of vulnerable pockets within a drainage basin facilitates improvements in planning of soil conservation systems. It basically involves the knowledge of the quantity of sediment yield production by a watershed. The vulnerability increases with the increase in sediment yield, and vice versa. To simulate the process of sediment yield generation, a number of distributed sediment delivery models are available in literature which can be derived from basic principles and linked with a personal computer-based, low cost, geographic information system (GIS) to facilitate preparation, examination, and analysis of spatially distributed input parameters as well as to link the sediment delivery from a micro-scale to the drainage basin-scale. Normally, for field applications, the heterogeneous and complex land surface within the drainage basin is divided into a number of sub-areas and spatially distributed data on vegetative cover can be derived from the digital analysis of satellite images.

, Limited studies reported in literature for steep Himalayan catchments indicate that the rate of soil erosion from these catchments is increasing at an alarming rate due to heavy deforestation, urbanization and other developmental activities, and the lack of proper conservation measures. Therefore, a systematic study for quantification of soil erosion, sediment yield and areas vulnerable to soil erosion from such catchments is a pressing need of the time. In this study, the sub-watersheds of Upper Ramganga catchment, Viz., Chaukhutia and Naula was taken up to develop and test the modeling tools useful for identification of vulnerable zones for taking up soil conservation measures.

Study Area

The Upper Ramganga catchment lies in the foothills of Himalayas in the Uttaranchal State of India. River Ramganga is a major tributary of River Ganga and emerges out of the hills at Kalagarh (District Almora) where a major multi-purpose Ramganga dam is situated. Up to Ramganga dam, the river is joined by several main tributaries: Ganges, Binoo, Khatraun, Nair, Badangad, Mandal, Helgad, and Sona Nadi. Its catchment (area = 3134 sq. km) lies between elevation 262 and 2926 m above the mean sea level and it is considerably below the perpetual snow line of the Himalayas. About 50% of the drainage basin is covered with forest, 30% is under cultivation on terraced fields, and the remaining 20% is urban/barren land. The Ramganga valley experiences approximately an annual rainfall of 1550 mm. The raingauge network consists of Ranikhet, Chaukhatia, Naula, Marchulla, Lansdowne and Kalagarh. The life of the Ramganga dam is estimated to be of the order of 100 years based on the sediment rate of 4.25 ha-m/100 sq. km per year based on Khosla theory of sedimentation in reservoirs. However, a systematic study does not appear to have been taken for reliable assessment of sedimentation in the reservoir and, in turn, taking up ameliorative measures to control it. In this study, using the historical data, it is planned to model sediment erosion and its transport in Chaukhatia, Gagas, and Naula, watersheds of the upper Ramganga catchment and develop/test suitable models for prediction of sediment yield for identification of vulnerable zones.

Tasks Proposed under Different Heads of the Original Project Proposal

a) Finding answers to as yet answered questions.

Fundamental to the identification of vulnerable areas in a watershed is the problem related with the computation of the sediment yield which, in turn, associates with the problem of soil erosion and its transport by rainfall-generated runoff and it is too complex to replicate exactly. Specific to Himalayan catchments, there exists a little understanding on the processes of rainfall-runoff-sediment yield. Therefore, the aim of the present study is to identify vulnerable zones in a degraded Himalayan watershed.

b) Development of a new computational procedure

Since the present work primarily deals with the estimation of rainfall-generated runoff and sediment yield, the following research and development studies were carried out in the process of understanding the involved hydrological processes:

Investigation of unit hydrograph (UH) approach: It is of common experience that the popular UH approach is severely restricted for its application to hilly watersheds for reasons of the underlying assumptions in UH derivation, which are of linearity, uniformity, and superposition. In this study, the applicability of UH concept is tested in terms of its derivation from the catchment characteristics derived with the help of GIS coupled with probability density function (pdf). Out of the three pdf-based distributions, the two-parameter inverse Gamma function (2PIGD) is found to perform the best based on three goodnesss-of-fit criteria. Using the same GIUH concept, the best performing 2PIGD model is also applied to the data of Ramgamga catchment for SUHs derivation for different dynamic velocities useful for direct field applications.

Investigation of SCS-CN method: The Soil Conservation Service-Curve Number (SCS-CN) methodology is a concept of paramount importance in the field of surface water hydrology. It is used to estimate the direct surface runoff from the total amount of

rainfall. It has significantly widened its scope since its inception in 1957. In the present study, its applicability is has been investigated in terms of its utility in long-term hydrologic simulation, and consequently, a four-parameter long-term rainfall-runoff model is proposed and tested on the data of Ramganga catchment. The model generally performed well in both calibration and validation on the data of Ramganga catchment. The resulting efficiencies for all the years varied in the range of 81.82 to 73.62%, showing a satisfactory fit and, in turn, satisfactory model performance. To check its versatility, it was applied to six other watersheds located in different hydro-meteorological settings. It performed satisfactorily on the high runoff producing watersheds, which is appreciable in terms of only a few (only four) parameters and its simplicity.

Application of TOPMODEL: The TOPMODEL is a distributed, topographically based hydrological model and it was applied to simulate daily runoff from Chaukhutia watershed. It is based on the concept of variable contributing area and topography controls the soil water storage and runoff generation. The total flow is computed as the sum of surface runoff and flow in the saturated zone. The model performed less than satisfactorily to less than satisfactorily largely due to watershed's moderate to steep sloping topography whereas TOPMODEL is suitable for moderate topography only and deep forest contributes less to saturation-excess runoff, an important TOPMODEL assumption for runoff generation.

Application of SWAT model: The Soil and Water Assessment Tool (SWAT) has gained much popularity in the recent past for it is a distributed watershed model and predicts several hydrological variables satisfactorily in complex watersheds. It however requires a significant amount of data for runoff simulation. This study investigates its applicability to runoff simulation in Chaukhutia watershed, for it is said to be applicable to moderately sloping watersheds only. The model was calibrated and validated with different datasets, and finally a sensitivity analysis of model parameters was carried out. The Nash and Sutcliffe efficiency ranging from 0.70 to 0.85 indicated a satisfactory model fit, implying that the SWAT model is applicable to even forested sub-Himalayan watersheds.

Application of ANN technique: The Artificial Neural Network (ANN) models have been widely and successfully used in almost all branches of engineering. In this study, a radial basis function ANN (RBFANN) was developed to simulate rainfall-generated runoff for Ramganga basin and its two sub-watersheds namely Chaukhutia and Naula. The Radial Basis Function is found to be a solution for rainfall-runoff modeling. The proposed model performed very well in calibration, cross-validation, and verification for both Chaukhutia and Naula watersheds. However, in case of Ramganga watershed the model performed very well in calibration and cross-validation whereas it performed satisfactorily during verification.

Determination of sediment graph: Sediment graphs are useful for quick estimation of peak rates of sediment yield in a rain storm. In this study, concepts of Nash-based Instantaneous Unit Sediment Graph (IUSG), SCS-CN method, and power law were amalgamated to develop a simple sediment yield model for computation of sediment graphs. The resulting higher model efficiency (varying from 90.52% to 95.41%) and lower values of relative errors in total sediment outflow (from 2.49% to 10.04%) and peak sediment flow rate (9.69% to 16.42%) suggest the model's suitability for computation of sediment graph and total sediment outflow.

Identification of vulnerable areas: In order to meet the primary objective of the project, i.e. the identification of vulnerable areas in Himalayan watersheds, a sediment accumulation limited approach was suggested and employed to the data of Chaukhutia and Naula watersheds of Ramganga catchment. The procedure involved preparation of various thematic layers representing different factors of USLE to compute spatially distributed gross soil erosion maps using recorded rainfall for 18 years, transport capacity (TC) maps, transport capacity limited (TCL) sediment outflow maps. Such maps give amount of sediment flowing from a particular grid in spatial domain. The sediment yield was computed with errors ranging from -40% (over-estimation) to +41% (under-estimation). Finally, maps for deposition/erosion of sediment were obtained for identifying areas vulnerable to silt deposition in the catchment, which are useful in planning conservation measures.

c) Development of a new software/application

For testing the approaches suggested for the above R&D studies, several computer programs were developed for facilitating the computations. In addition, guidelines are provided in Chapter 9 for developing software for the approach suggested for identification of vulnerable zones.

d) Development of a new field technique

The models available in literature are generally applicable to plain areas. In this study, new techniques for derivation of unit hydrograph, *SCS-CN-based* rainfall-runoff modeling, and sediment graph were proposed. For identification of vulnerable areas in sub-watersheds of Ramganga, a sediment accumulation limited approach has been suggested.

e) Investigation of the behaviour of a natural process

During the course of investigating the behaviour of a complex natural process of sediment erosion and its transport in the catchment by runoff, the research was carried out on the fundamental aspects of the applicability of unit hydrograph, SCS-CN, TOPMODEL, SWAT, ANN, and USLE approaches. All these approaches were found to be reasonable applicable to the studied hilly watersheds, except TOPMODEL which exhibited a less than satisfactory model performance. The concept of sediment accumulation limited transport for computation of sediment yield worked satisfactorily and it was taken as the basis for identification of vulnerable areas.

f) Contribution to Water Resources Development

The importance of the study of rainfall-runoff-sediment yield process is an extremely complex phenomenon at catchment scale. It is of common knowledge that the Himalayan catchments contribute significantly to the water resources of Northern India. Literature survey reveals that only a few studies have focused on the process of rainfall-

runoff-sediment yield in hilly catchments which are quite prone to soil erosion. In other words, only a little understanding is available on the runoff and sediment generation mechanisms from these catchments. The present study provides a greater insight to the complex phenomenon of runoff and sediment yield generation. The major contributions are as follows:

a) Development of a GIUH- and pdf-based approach for derivation of synthetic unit hydrograph for ungauged hilly watersheds.
b) Development of an SCS-CN-based long-term simulation model for a hilly watershed.
c) Less satisfactory TOPMODEL performance on forest hilly Chaukhutia watershed, applicability of SWAT and ANN models to Chaukhutia watershed.
d) Development of a new sediment graph model based on Nash IUSG, SCS-CN, and power law concepts.
e) Development of a sediment transport limited based procedure for identification of vulnerable areas in Chaukhutia and Naula watersheds.

g) Dissemination of the Research for Use in Field

A training program was organized for the field engineers of State Irrigation Departments and Dept. of Forest at the Engineers' Academy, Kalagarh during November 22-23, 2010. A brief of the training program is provided in Appendix-I. The engineers of Uttar Pradesh Irrigation Department helped in providing the necessary data required for this project work. In addition, for putting the research to use, a pamphlet (Appendix-II) was prepared for easy dissemination, transmission, and understanding of the research output. The research material is planned to be presented on the World Wide Web.

In brief, all major objectives of the proposed research project were fulfilled. For the development of computer software for identification of vulnerable areas, guidelines have been provided in Chapter 9 of this project report. It would however require not only a skilled computer personnel but also ample time and resources for preparation.

CHAPTER 1

INTRODUCTION

CHAPTER 1

INTRODUCTION

Over the last decade, the major emphasis in the field of land resource management has been on the development of strategies to ensure sustainable use of land. The primary aim of any policy dealing with sustainable use of soils is to maintain soil quality, properties, processes and diversity. At the same time soil erosion continues to degrade the global land resource base with approximately 30 per cent of the present cultivated area having been significantly affected. According to National Commission on Agriculture, 175 million hectares are degraded all over the world. The current rate of annual top soil loss in the world due to water and wind erosion ranging from 20 to 100 tons per ha. This is 16 to 100 times greater than the natural accumulation range, which is estimated at about one centimeter of topsoil formation in 200 years under normal Agricultural practices. Soil erosion rates have increased to such an extent that the material delivery from rivers to the oceans has increased from just 8 billion tons to over 23 billion tons a year, the largest discharge of over 10 billion tons per year coming from Asian rivers alone. If the present trend in the erosion of fertile topsoil of over 23 billion tons per year continues, it will result in the loss of 30 per cent of global soil inventory by 2050.

Identification of vulnerable areas within a drainage basin helps improve the planning of soil conservation systems. It basically requires determination of the quantity of sediment yield produced by a watershed. The vulnerability increases with the increase in sediment yield, and vice versa. The process of soil erosion involves the processes of detachment, transportation & accumulation of soil from land surface due to either impact of raindrop, splash due to rain impact, shearing force of flowing water, wind, sea waves or moving ice. Erosion due to water is an area of interest to hydrologists and sedimentologists. Various forms of soil erosion due to water are inter-rill, rill, gully & stream channel erosion. Apart from rainfall and runoff, the rate of soil erosion from the area also strongly relies on its soil, vegetation & topographic characteristics. During the process of erosion and transportation to downstream side, some part of the eroded material may gets opportunity to deposit. The deposition of sediment transported by a river into a reservoir reduces the reservoir capacity, thereby adversely affecting the water availability for power generation, irrigation, domestic & industrial use.

Notably, the soil erosion is a serious problem in Himalayan watersheds and foothill ecosystem. Sustainable use of mountains depends on conservation and sustainable use of land and water resources systems. High population growth has placed a demand on limited natural resources present in the hills. High rainfall coupled with fragile rocks, and high relief conditions in Himalayas are conducive to soil erosion. Rapid increase in the developmental activities, mining and deforestation etc. are major factors contributing to soil erosion and increased erosion susceptibility; and thus leading to land degradation. Therefore, a systematic study for quantification of soil erosion, sediment yield and identification of vulnerable areas in Himalayan watersheds was carried out in this project using different newly developed methodologies/ procedures, GIS-coupled process-based models.

1.1 OBJECTIVE OF THE STUDY

The objectives of the present project report, as envisaged at the stage of proposal formulation, are as follows:

- To investigate the processes of rainfall-runoff-sediment yield in Himalayan watersheds, viz., Ramganga catchment its sub-catchments.
- To investigate the available process-based models and suggest a suitable model for Himalayan watersheds, viz., Ramganga catchment its sub-catchments.
- To develop a simple physically based mathematical model for rainfall-runoff-sediment yield simulation.
- To identify vulnerable zones in a degraded Himalayan watershed.
- To develop a computer software for identification of vulnerable areas.

1.2 ORGANIZATION OF THE PROJECT REPORT

The report has been organized in the following chapters:

Chapter 1 introduces the project work, sets the objectives, and presents the organization of the project report.

Chapter 2 describes the study area on the data of which the proposed methodology was employed for identification of vulnerable areas and the research was carried out for

CHAPTER 2

STUDY AREA

CHAPTER 2

STUDY AREA

Since this study deals with the identification of vulnerable areas in a Himalayan watershed, i.e. Ramganga catchment, the prime emphasis has been on this catchment or its three sub-catchments, viz., Chaukhutia, Naula, and Gagas. The other catchments were primarily used for testing the versatility of the proposed/employed technique. Thus, this chapter deals with a general description of all the catchments used in this study. However, study specific catchment characteristics and hydro-meteorological data have been detailed in the respective chapters only.

2.1. RAMGANGA CATCHMENT

The Ramganga River is a major tributary of the Holy River Ganga and drains a catchment area of 3,134 km^2. Its catchment lies in the Sivalik ranges of Himalayas and the valley is known as Patlei Dun. River Ramganga originates at Diwali Khel in the district of Chamoli. It emerges out of the hills at Kalagarh (District Pauri Garwhal) where a major multipurpose Ramganga dam is situated. Its catchments lie between elevation 338 and 3088 m above mean sea level, and it is considerably below the perpetual snow line of the Himalayas. The map of Ramganga catchment is shown in Figure 2.1.

The river traverses approximately 172 km before it meets the reservoir and then continues its journey in the downstream plains for 370 km before joining River Ganga at Farrukhabad district of Uttar Pradesh. During its travel up to Ramganga dam, the river is joined by main tributaries: Gagas, Bino, Khatraun, Nair, Badangad, Mandal, Helgad, and Sona Nadi. Figure 2.1 shows Ramganga catchment along with the major sub-catchments as discussed above. About 50% of the drainage basin is covered with forest, 30% is under cultivation on terraced fields, and the remaining 20% is urban/barren land. The catchment receives approximately rainfall of 1550 mm annually. The records of river stages, instantaneous as well as monthly, are available at Kalagarh since 1958. At the outlet of the Upper Ramganga catchment, i.e. Kalagarh, there exists a multi-purpose Ramganga dam. The specific characteristics of the dam are given here as below:

- Sanctioned in 1973-74
- Dam: 127.5 m high earth and rock-fill dam

- Storage capacity = 2448 MCM at FRL
- Purposes:
    - Irrigation = 0.575 million ha in 11 districts of UP,
    - Drinking water = 5.5 cumec to Delhi
    - Hydro-power = 198 Mega Watt (MW)
    - Flood protection
    - Tourism.
- Estimated life = 100 years
    - based on the estimated sediment rate = 4.25 ha-m/100 sq. km per year

Figure 2.1: Ramganga catchment

2.2. CHAUKHUTIA WATERSHED

2.2.1. Geographic Location

The Chaukhutia watershed is the uppermost Himalayan catchment of Ramganga River comprising of an area of 572 sq. km. The Chaukhutia watershed is located in Almora and Chamoli districts of the State of Uttrakhand. Geographically the entire boundary of Chaukhutia watershed is situated between latitudes of 29^0 46' 35" to 30^0 06' 11" North and longitudes of 79^0 11' 23" to 79^0 31' 21" East vide Survey of India, Toposheet nos. 53N/4,53N/8, 53O/1,53O/5 and 53O/9, all available in the scale of 1:50,000. The district boundary of Chaukhutia watershed is Chamoli in the north, Almora in the south, Pauri Garhwal & Almora in the west and Almora & Chamoli in the east. Small townships of Chaukhutia and Dwarahat are situated in Chaukhutia watershed and these townships come under Almora district. Other small towns situated in Chaukhutia watershed are Gairsen and Mehalchauri which comes under Chamoli district. Entire Chaukhutia watershed falls under Kumaon region of Western Himalayas. The outlet of Chaukhutia watershed is located in Chaukhutia block headquarter under Ranikhet sub division of Almora district. The Index map of Chaukhutia watershed is shown in Fig. 2.2.

2.2.2. Geology

Chaukhutia watershed consists of crystalline and sedimentary rocks of calcareous zone. Crystalline occurs as vast sequence of low to medium grade metamorphic associated with coarse to medium grained granites. A thin zone of porphyritic rocks exposed along the Almora fault is known as Chaukhutia Quartz Porphyry. These rocks are highly crushed and fine grained with porphyro-blasts of quartz and feldspar, and also show development of schistose structure. Sedimentary rocks of Calc zone is found north of Dwarahat around Dhunagiri hill and Ramganga valley near Mehalchauri. South of Mehalchauri north-east trending open faults of large wavelength are superimposed by the tight isoclinical folds trending north-west. A series of gently plunging open folds of 27.432 m to 36.576 m wavelength are exposed in the Ramganga valley south-east of Mehalchauri. Tightness of folds increases in upper level and assumes a recumbent to overturned posture towards Chaukhutia. Regional trend of folds is from north to north-west which are reoriented and refolded near the contact with Almora crystalline.

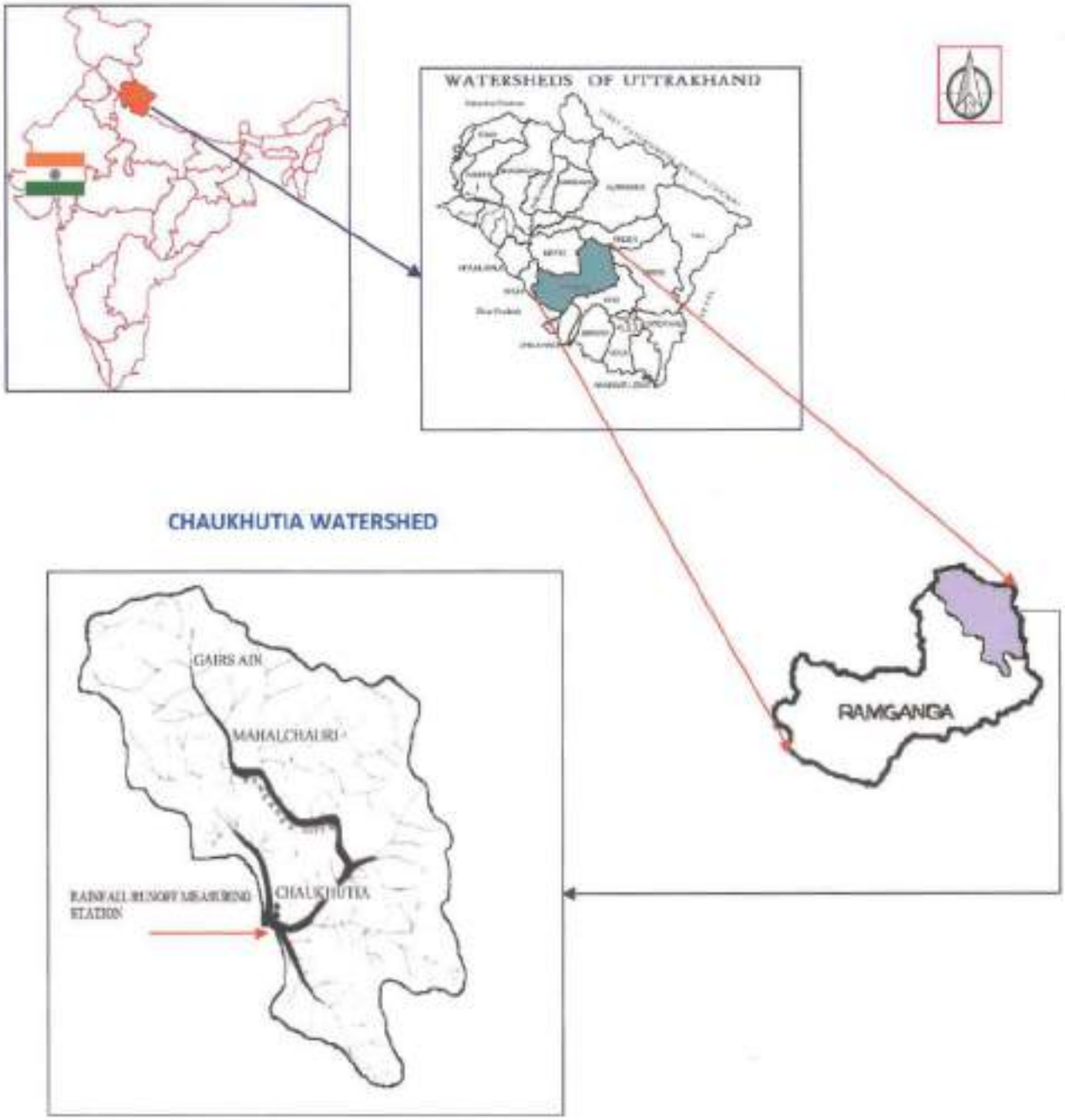

Figure 2.2: Location Map of Chaukhutia Watershed

2.2.3. Climate

The Chaukhutia watershed lies in sub-Himalayan zone of Western Himalaya. The variation in altitude influences the climate of the watershed. The climate varies from sub-tropical in the lower region to sub-temperate and temperate in upper region with a mean annual temperature of 24.5 ^{0}C and a mean minimum temperature of 17.3 ^{0}C. Winter rainfall occurs during December to February. The mean maximum and minimum temperatures, relative humidity, evapotranspiration, sunshine hours and average monthly and annual temperatures of Chaukhutia watershed are presented in Table 2.1.

2.2.4. Topography

The Chaukhutia watershed is a hilly catchment of the river Ramganga. The maximum and minimum elevations within this watershed are 3098.95 m and 939.05m above mean sea level, respectively. The outlet is situated at an elevation of 939.053 m in south-western boundary of the watershed as shown in location/index maps. This watershed consists mostly of rolling and undulating topography having very steep irregular slopes.

2.2.5. Land Resources

In terms of land resources, the Chaukhutia watershed is covered with forest, pasture, agriculture, settlement, fallow/rocky/waste lands, river and road.

2.2.5.1. Forest Land

Forest land of Chaukhutia watershed is dominated by dense mixed jungle mainly having Pine and Banj. Chir, pine (Pinus Roxburghii) and broad-leaved Banj (Quercus Leuchotrichophora) are the major forest species. Most of the forest areas are under Reserve Forest. The forest cover of Chaukhutia watershed is about 49% of the total area of this watershed. Forest area of this watershed is under the jurisdiction of Divisional Forest Office (Soil Conservation), Ranikhet, Almora, Uttrakhand.

Table 2.1: Mean, maximum and minimum temperatures, relative humidity, evapotranspiration and sunshine hours of Chaukhutia Watershed

Sl. No.	Month	Mean Maximum Temperature (^{0}C)	Mean Minimum Temperature (^{0}C)	Relative Humidity (%)	Evapo-transpiration (mm)	Sunshine Hours (hrs)	Average Temperature (^{0}C)
1	2	3	4	5	6	7	8
1	Jan	19.8	5.8	58.6	111.7	7.30	12.8
2	Feb	24.7	9.9	50.8	126.4	7.03	17.3
3	Mar	30.8	14.4	45.5	178.2	8.38	22.6
4	Apr.	36.8	19.2	39.1	209.3	8.72	28.0
5	May	37.8	22.6	41.5	239.9	9.53	30.2
6	Jun	38.6	24.4	48.4	244.1	9.49	31.5
7	Jul	35.8	24.5	51.2	243.4	9.67	30.2
8	Aug	36.5	24.4	51.1	232.1	9.22	30.4
9	Sep	33.7	22.8	51.5	200.5	8.33	28.2
10	Oct	31.9	19.0	44.5	183.6	7.99	25.4
11	Nov	29.1	11.9	45.2	145.5	7.19	20.5
12	Dec	23.3	9.1	52.5	125.0	7.15	16.2
	Average	31.6	17.3	48.3	186.6	8.33	24.5

2.2.5.2. Pasture Land

The Chaukhutia watershed consists of pasture land having an area of about 16% of the total area of this watershed.

2.2.5.3. Agriculture Land

Agriculture land in this watershed consists of hill-slope cultivation, level terrace cultivation and valley cultivation. The percentage of agriculture land area is about 12.41% of the total area of this watershed.

2.2.5.4. Settlement

The area covered by urban and rural settlements in this watershed is about 8.19% of the total area of this watershed. Mostly settlement is along Ranikhet – Badrinath State Highway which crosses the Chaukhutia watershed from its southern boundary to northern boundary. In addition, the area of different types of road is about 2.98% of the total area of this watershed.

2.2.5.5. Other Land Types

Within the other land the area of water bodies is about 4.83% and the area of fallow/rocky/waste land is about 6.57% of the total area of this watershed.

2.2.6. Soil Type

The soils in Chaukhutia watershed vary in texture, depth and slope. Broadly, soils of this watershed may be classified as loamy soils. Depth of soil varies from shallow to deep and slope varies from steep to very steep. Hydrologic Soil Groups of the soil of this watershed vary from B to C. Soil map of the watershed was taken from soil survey of this watershed carried out by NBSS&LUP (2004). Detailed information for different mapping units is given in Table 2.2. In this table Hydrologic Soil Group has been decided as per User Manual of SWAT 2005 (Neitsch et al., 2005).

2.2.7. Rainfall

The significant portion of total precipitation in the form of rainfall in the watershed occurs mainly during the four months of the monsoon, i.e. from June to September, with a mean annual total precipitation of 1388.7 mm. In fact, the monsoon contributes about 74.2% of the total annual rainfall. Total annual rainfall varies from 967.9 mm (1981) to 1985.1 mm (1998). Mean monthly rainfall varies from 6.9 mm in the month of November to 344.3 mm in the month of July. The entire hydro-meteorological characteristics of the watershed are characterized by the high precipitation generating peak monsoon flows and low precipitation during the dry season

resulting in low flows. These figures are based on the rainfall data at Chaukhutia which were collected from Ramganga Dam Division, Kalagarh (Pauri Garhwal) under the Department of Irrigation, Government of Uttar Pradesh.

Table 2.2: Soil legend of Chaukhutia watershed

Sl. No.	Map Unit	Texture	Depth	Erosion	Slope	Surface	Drainage	Stoniness	HYDGRP
1	2	3	4	5	6	7	8	9	10
1	14	Thermic fine loamy to loamy skeletal soils	Moderately shallow	Moderate	Moderate	Loamy	Excessively drained	Slight	C
2	23	Thermic to course loamy soils	Shallow to moderately shallow	Severe to moderate	Steep	Loamy to sandy	Excessively drained	Strong to moderate	B
3	28	Thermic skeletnl to course loamy soils	Moderately deep to moderate shallow	Moderate	Moderate steep to steep	Loamy	Excessively drained		B
4	36	Thermic course to fine loamy soils	Moderately deep	Moderate to slight	Moderate steep	Loamy	Excessively drained	Strong to moderate	C
5	38	Thermic loamy skeletal to fine loamy soils	Moderately shallow deep to moderate deep	Moderate to slight	Steep to moderate steep	Loamy	Excessively drained	Strong to moderate	C
6	45	Thermic course to fine loamy soils	Moderately deep to deep	Moderate to slight	Moderate	Loamy	Well drained		C
7	48	Thermic sandy skeletal soil	Very shallow	Very severe	Very steep	Sandy	Excessively drained	Strong	B

2.3 NAULA WATERSHED

The Rāmgangā river system drains an area of 1074 km^2 at Naula, referred hereafter as Naula Watershed. Spatial extent of Naula watershed is between 29°44' N and 30°6'20"N latitude and 79°6'15" E and 79°31'15" longitude in the Ranikhet forest sub-division. The entire watershed is spread over three districts namely Chamoli in North, Almora in South, Pauri Gharwal & Almora in West and Almora & Chamoli in East. Small townships of Chaukhutia and

Dwarahat are situated in Chaukhutia Block and come under Almora District. Other small towns situated in Chaukhutia watershed are Gairsen, Mehalchauri, which comes under Chamoli district and Bhikiyasain comes under Ranikhet sub-division of district Almora. Location map of the watershed is shown in Fig 2.3.

2.3.1 Climate

The watershed lies in sub-Himalayan zone of Western Himalaya. Its climate varies from sub-tropical in the lower region to sub-temperate and temperate in upper region with mean annual temperature of 24.5 ^{0}C and mean minimum temperature of 17.3 ^{0}C. Variation in altitude influences the climate of the watershed. Mean monthly values for maximum and minimum temperatures, relative humidity, evapotranspiration, sunshine hours and average monthly and annual temperatures of watershed were collected from Ramganga Dam Division and State forest departments and are given in Table 2.3.

2.3.2 Topography

The watershed under study is a hilly watershed of the river Ramganga. The maximum and minimum elevations within this watershed are 3097 m and 778 m above mean sea level, respectively. The gauging outlets at Chaukhutia, draining an area of approximately 573 sq. km, and Naula draining the entire watershed area (approximately 1074 sq. Km) are situated at an elevation of 937.0 m and 778.0 m, respectively. The topography of the watershed is undulating and irregular with slope varying from moderate to steep.

2.3.3 Soil type

Soils of the watershed are acidic in nature having pH between 4.5 and 6.5. Broadly, particle size of soils of this watershed may be classified as fine loamy to coarse-loamy. Depth of soil varies from shallow to deep and slope varies from moderate to very steep. Soil of this watershed can be categorized as hydrologic soil group B and C. Soil map and other soil characteristics of the watershed were taken from soil survey report of watershed carried out by

National Bureau of Soil Survey and Land Use Planning (NBSSLUP, 2004). The NBSSLUP had assigned Soil Mapping Units (SMU) to different soils based on soil characteristics and the same is taken in this study for assigning values of different soil related parameters. Detailed information for different soil mapping units is given in Table 2.4.

2.3.4 Geology

Naula Watershed falls under lesser Himalayas, a massive mountainous tract and tangled mass of series of ridges being divided from each other by deep valleys. The watershed consists of crystalline and sedimentary rocks of Calc zone. Crystalline occurs as vast sequence of low to medium grade metamorphics associated with coarse to medium grained granites. A thin zone of porphyritic rocks exposed along the Almora fault is known as Chaukhutia Quartz Prophyry. These rocks are highly crushed and fine grained with prophyro-blasts of quartz and feldspar, and also show development of schistose structure. Sedimentary rocks of Calc zone is found north of Dwarahat around Dhunagiri hill and Ramganga valley near Mehalchauri. South of Mehalchauri north-east trending open faults of large wavelength are superimposed by the tight isoclinical folds trending north-west. A series of gently plunging open folds of 27.432 to 36.576 m wavelength are exposed in the Ramganga valley south-east of Mehalchauri. Tightness of folds increases in upper level and assumes a recumbent to over tuned posture towards Chaukhutia. Regional trend of folds is from north to north-west which are reoriented and refolded near the contact with Almora crystallines (Sharma and Sinha, 1972).

2.3.5 Land use

The land cover in study watershed consists of forest, pasture, agriculture, settlement, fallow/rocky/waste lands, river and road etc. Satellite image of Indian Remote Sensing-Linear Imaging and Self Scanning Sensors (IRS-LISS III) with a spatial resolution of 23.5 m was available and used for classifying area under different land uses.

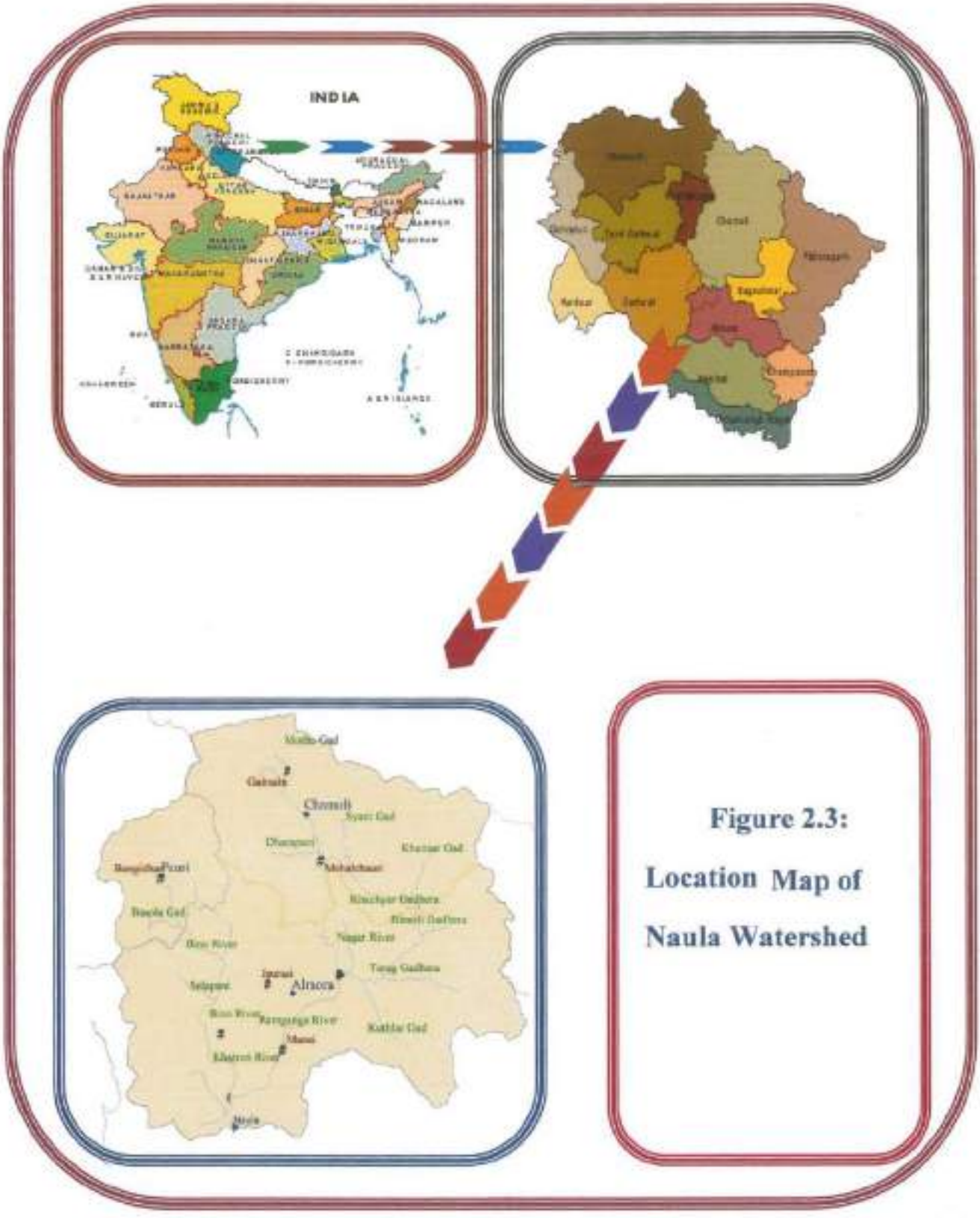

Figure 2.3:

Location Map of

Naula Watershed

Table 2.3: Monthly Values for Various Climatic Parameters

Month	Mean Maximum Temperature (°C)	Mean Minimum Temperature (°C)	Relative Humidity (%)	Evapotra-nspiration (mm)	Sunshine Hours (hrs)	Average Temperature (°C)
Jan	19.8	5.8	58.6	111.7	7.30	12.8
Feb	24.7	9.9	50.8	126.4	7.03	17.3
Mar	30.8	14.4	45.5	178.2	8.38	22.6
Apr.	36.8	19.2	39.1	209.3	8.72	28.0
May	37.8	22.6	41.5	239.9	9.53	30.2
Jun	38.6	24.4	48.4	244.1	9.49	31.5
Jul	35.8	24.5	51.2	243.4	9.67	30.2
Aug	36.5	24.4	51.1	232.1	9.22	30.4
Sep	33.7	22.8	51.5	200.5	8.33	28.2
Oct	31.9	19.0	44.5	183.6	7.99	25.4
Nov	29.1	11.9	45.2	145.5	7.19	20.5
Dec	23.3	9.1	52.5	125.0	7.15	16.2
Average	**31.6**	**17.3**	**48.3**	**186.6**	**8.33**	**24.5**

2.3.6 Forest land

Naula watershed is rich in forest resources and dominated by major species of dense mixed Chir Pine (Pinus Roxburghii) and Banj trees (Quercus Leuchotrichophora). The forest cover accounts for more than 54% of the total area of the watershed. The economy and livelihood pattern of the people of the watershed is primarily built around the forests. Further, about four million livestock population in the state (according to the Livestock Census, 2003) is dependent on forests for fodder. Most of the forests in watershed comes under reserve forest category and falls under jurisdiction of Divisional Forest Office (Soil Conservation), Ranikhet, Almora.

2.3.7 Agriculture Land

Agriculture land consists about 15% of the total watershed area. The agriculture is practiced under hill slope cultivation, level terrace cultivation and valley cultivation. Major crops grown in the area are madua-wheat and sewa-wheat. About 70% inhabitants of watershed primarily depend on agriculture for livelihood.

2.3.8 Settlements

The area being utilized for urban and rural settlements constitutes approximately 12% of the total watershed area. Mostly, settlement is found along water sources and Ranikhet–Badrinath State Highway which crosses the Chaukhutia from its southern boundary to northern boundary.

2.3.9 Other Land Type

Approximately 13% of the watershed area comes under pasture and facing severe degradation of land because of over exploitation of natural resources by the inhabitants for subsistence living far beyond its capacity to regenerate. The rest of the area of the watershed is under various land uses viz. roads and open water bodies.

Table 2.4: Soil Properties Table

Soil Mapping Unit	Zone	Surface Form	Soil Depth (c.m.)	Particle Size	Soil Temp. Regime	Soil Reaction (pH)	Drainage	Surface Texture	Slope	Erosion	Surface Stoniness	Soil Taxonomy	Hydrologic Soil Group
SMU14	Lesser Himalayas Soil on Summits and Ridge Tops	Ridges (R)	Moderately Shallow (50-75) (3)	Fine Loamy (M)	Thermic (15-22°C) (T)	Slightly Acidic (5.5-6.5) (3)	Somewhat Excessively Drained (6)	Loamy (L)	Moderately Sloping (8-15%) (d)	Moderate (2)	Slight (<15%) (1)	Dystric Eutrochrepts & Typic Hapludolls	C
SMU23	Lesser Himalayas Soil on Side Slopes	Steep (S)	Shallow (25-50) (2)	Loamy (L)	Thermic (15-22°C) (T)	Moderately Acidic (4.5-5.5) (2)	Excessively Drained (7)	Loamy (L)	Very Steeply Sloping (>50%) (g)	Severe (3)	Strong (>40%) (3)	Lithic Udorthents	B
SMU28	Lesser Himalayas Soil on Side Slopes	Steep (S)	Moderately Deep (75-100) (4)	Loamy Skeletal (K)	Thermic (15-22°C) (T)	Slightly Acidic (5.5-6.5) (3)	Excessively Drained (7)	Loamy (L)	Moderately Steep Sloping (15-30%) (e)	Moderate (2)	Moderate (15-40%) (2)	Typic Udorthents	B
SMU34	Lesser Himalayas Soil on Side Slopes	Steep (S)	Moderately Deep (75-100) (4)	Coarse Loamy (R)	Thermic (15-22°C) (T)	Slightly Acidic (5.5-6.5) (3)	Excessively Drained (7)	Loamy (L)	Moderately Steep Sloping (15-30%) (e)	Moderate (2)	Strong (>40%) (3)	Typic Udorthents	C
SMU38	Lesser Himalayas Soil on Side Slopes	Steep (S)	Moderately Shallow (50-75) (3)	Loamy Skeletal (K)	Thermic (15-22°C) (T)	Slightly Acidic (5.5-6.5) (3)	Excessively Drained (7)	Loamy (L)	Steeply Sloping (30-50%) (f)	Moderate (2)	Strong (>40%) (3)	Typic Udorthents & Dystric Eutrochrepts	C
SMU45	Lesser Himalayas Soil on Fluvial Valleys	Valleys (V)	Moderately Deep (75-100) (4)	Coarse Loamy (R)	Thermic (15-22°C) (T)	Neutral (6.5-7.5) (4)	Well Drained (5)	Loamy (L)	Moderately Sloping (8-15%) (d)	Moderate (2)	Strong (>40%) (3)	Typic Udorthents	C
SMU48	Lesser Himalayas Soil on Cliffs	Steep (S)	Very Shallow (10-25) (1)	Sandy Skeletal (Z)	Thermic (15-22°C) (T)	Slightly Acidic (5.5-6.5) (3)	Excessively Drained (7)	Sandy (S)	Very Steeply Sloping (>50%) (g)	Very Severe (4)	Strong (>40%) (3)	Lithic Udorthents	B

2.4 GAGAS CATCHMENT

The Gagas catchment is one of the sub-catchments of the Ramganga river catchment located in the Himalayan region of India having an area of 506 km^2 and lies between latitudes 29^0 35' 20" N and 29^0 51'N, and longitudes 79^0 15'E and 79^0 35' 30"E as shown in Fig. 2.4. The catchment is approximately rectangular in shape with a minimum elevation of 772 m at the outlet e.g., Bhikiasen and a maximum of 2744 m above mean sea level at the upstream end of the catchment. The catchment area in general has a hilly terrain with undulating and irregular slopes ranging from relatively flat in narrow river valley to steep towards ridge.

The mean annual rainfall varies from 903 to 1281 mm with a mean value of 1067 mm (Kumar and Kumar, 2008). The soils of the catchment are highly coarse textured, varying from coarse sand to gritty sandy loam, and slightly acidic to neutral in nature. The hydrologic data regarding runoff hydrograph, effective rainfall for six isolated storms were obtained from the Divisional Forest Office, Ranikhet, Uttarakhand.

Figure 2.4: Gagas catchment

2.5 HEMAVATI CATCHMENT

River Hemavati is a tributary of River Cauvery, originating in Ballaiarayanadurga in the Western Ghats in Mundgiri Taluk of Chikmanglur district in Karnataka State (Mishra and Singh, 2003b). It passes through a region of heavy rainfall in its early reaches, in the vicinity of Kotigehara and Mudigere. It has Yagachi and Algur tributaries and drains an area of 600 km^2 up to Sakleshpur as shown in Figure 2.5.

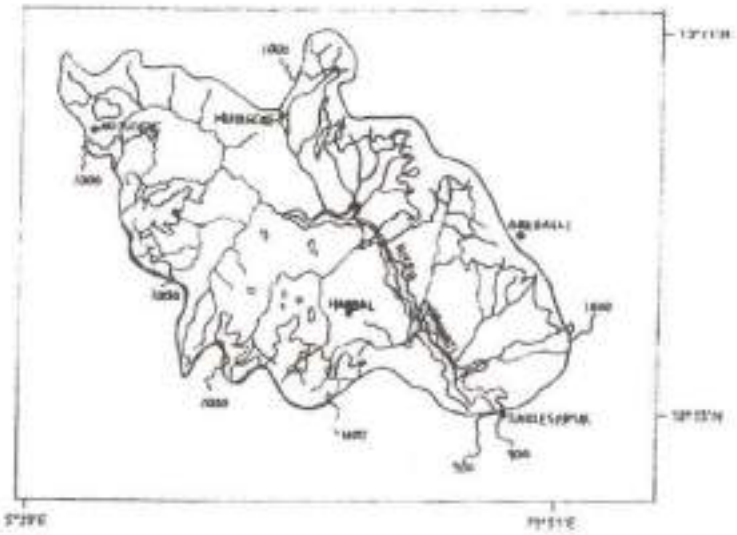

Figure 2.5: Hemavati catchment

The catchment of Hemavati lies between 12° 55′ and 13° 11′ north latitude and 75° 20′ and 75° 51′ east longitude (Fig. 2.5). It is a hilly catchment with steep to moderate slopes (Mishra and Singh, 2003b). The upper part of the catchment is hilly with an average elevation of 1,240m above the mean sea level and the lower part forms a plain terrain with an average elevation of 890m. Agriculture and plantation are major industries of the basin. Its land use can be characterized by forests (12%), coffee plantations (29%), and agricultural lands (59%). The principal soil types are red loamy soil (67%) and red sandy soil (33%). Soils in the forest area and coffee plantations are greyish due to high humus content.

2.6 NARMADA CATCHMENT

The River Narmada (Fig. 2.6) is one of the major rivers with 41 tributaries flowing through central parts of India. It rises from the Amarkantak plateau of the Maikala range in Shahdol district in Madhya Pradesh at an elevation of about 1059 m above mean sea level. The river travels a distance of 1312 km before it joins the Gulf of Cambay in the Arabian Sea near Bharuch in Gujarat. The stream flow data used in the study belong to the River Narmada at Manot, Banjar at Hridaynagar and Burhner at Mohegaon and described briefly below.

(a) **Narmada up to Manot**: The Narmada catchment up to Manot lies between north latitudes 22° 26' to 23° 18' and east longitudes 80° 24' to 81° 47'. The length of the River Narmada from its origin up to Manot is about 269 km, with a drainage area of 5032 km^2. The catchment is covered by forest and its topography is hilly. Its elevation ranges from 450 m near Manot site to 1110 m in the upper part of the catchment. It has a continental type of climate classified as sub-tropical and sub-humid, with average annual rainfall of 1596 mm. It is very hot in summer and cold in winter. In the major part of the catchment, soils are red, yellow and medium black with shallow to very shallow depth. In some small pockets of plain land, soils are moderately deep dark greyish clay. Approximately, 52% of the catchment area is under cultivation, about 35% under forest and 13% under wasteland.

(b) **Banjar up to Hridaynagar**: The Banjar River, a tributary of Narmada in its upper reaches, rises from the Satpura range in the Durg district of Madhya Pradesh near Rampur village at an elevation of 600 m at north latitude 21° 42' and east longitude 80° 50'. Its catchment area up to Hridaynagar is about 3370 km^2 and the elevation drops from 600 m to 372 m at Hridaynagar gauging site. The climate of the basin can be classified as sub-tropical and sub-humid, with average annual rainfall of 1178 mm. About 90% of the annual rainfall is received during the monsoon season (June–October). The estimates of evapotranspiration

(c) **Burhner up to Mohegaon:** The Burhner River rises in the Maikala range, south-east of Gwara village in the Mandla district of Madhya Pradesh at an elevation of about 900 m at north latitude 22° 32' and east longitude 81° 22'. It flows in a westerly direction for a total length of 177 km to join the Narmada near Manot. The Burhner drains a total area of

about 4661 km^2 and its catchment area up to Mohegaon is about 4103 km^2. The elevation at Mohegaon gauging site drops to 509 m. The climate of the basin can be classified as sub-tropical and sub-humid, with average annual rainfall of 1547 mm. The evapotranspiration varies from 4 mm/day in winter to 10 mm/day in summer. The catchment area comprises both flat and undulating lands covered with forest and cultivated lands. Soils are mainly red and yellow silty loam and silty clay loam. Forest and agricultural lands share nearly 58% and 42% of the catchment area, respectively.

Figure 2.6: Narmada Basin

2.7 KALU CATCHMENT

The River Kalu (Fig. 2.7) is a tributary of the Ulhas River in the Thane district of Konkan region in Maharashtra. It originates near Harichandragad in Murbad Taluka of Thane district at an elevation of 1200 m above mean sea level and extends between east longitude 73° 36′ to 73° 49′ and north latitude 19° 17′ to 19° 26′. The steep terrain watershed (area = 224 km^2) experiences an average annual rainfall of 2450 mm, which varies from 2794 to 5080 mm in different parts of the watershed. Most of the rains are received during June to

October. The existing crop pattern of the cultivation covers 46% paddy, 16% nanchani vari, 3% pulses and 35% grass. The catchment is covered with 50% thickly wooded forest, and 50% is cultivated area. A dam is proposed across the Kalu River near the village of Khapri about 31 km downstream of the origin to serve for irrigation as well as water supply.

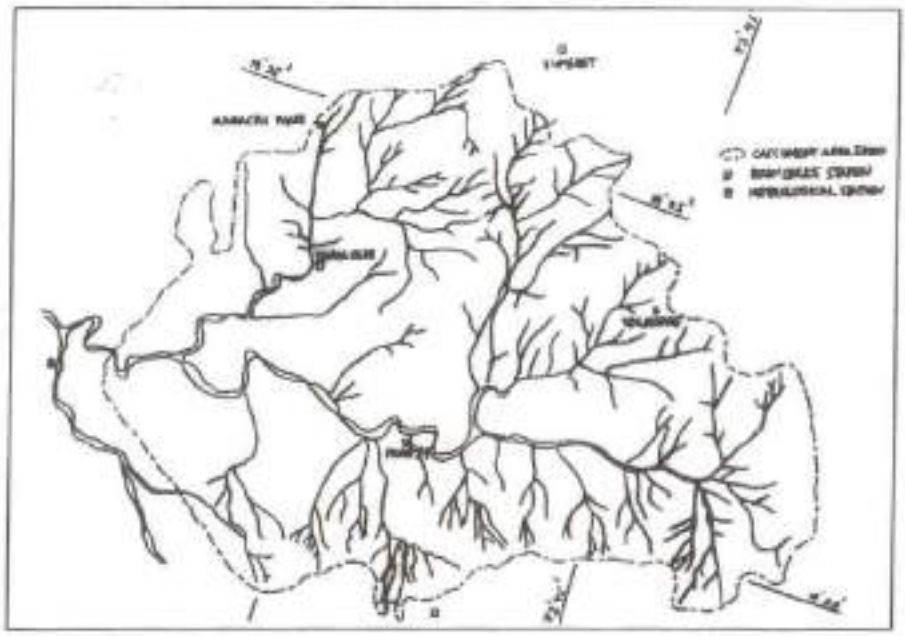

Figure 2.7: Kalu watershed

2.8 GHODAHADO CATCHMENT

Rushikulya is a major river in the State of Orissa (Fig. 2.8). It originates from Rushamala hills of the eastern ghats in Phullabani district. It is 165 km long with 8900 sq. km of catchment area. Ghodahado is a tributary of Rushikulya in Ganjam district near Degapahandi block. It extends between east longitude 84° 27' to 84° 40' and north latitude 19° 17' to 19° 28'. The watershed having area of 138 km^2 experiences an average annual rainfall of 1476 mm, having mean maximum summer temperature of 37°C and 10.3°C in winter. Most of the rainfall occurs during June to October. The watershed is situated in the East and South Eastern coastal Plain with hot and moist sub- humid climatic condition. The broad soil group of this area is Red soils, has blocky structures of either granular or sub granular geometry, and it is dominated by Kaolinites and illites. The land use pattern of the watershed

is 40% of forest area, permanent pastue is 3%, culturable waste is about 2%, non-agril land use is 5% and 50% of area is under net sown area.

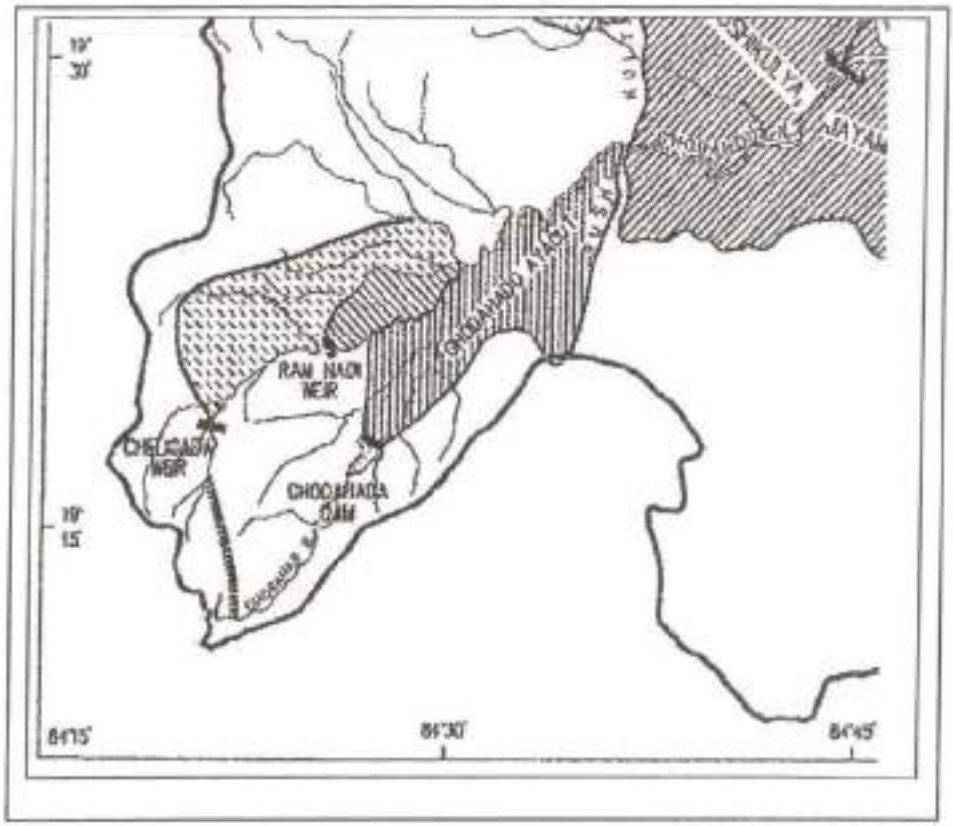

Figure 2.8: Rushikulya basin showing Ghodahado catchment

CHAPTER 3

A REVISIT TO UNIT HYDROGRAPH CONCEPT

CHAPTER 3

A REVISIT TO UNIT HYDROGRAPH CONCEPT

The unit hydrograph (UH) method introduced by Sherman (1932) for runoff estimation has immense significance due to its basic simplicity of the definition, i.e., the direct runoff resulting from unit depth of excess rainfall produced by storm of uniform intensity and specified duration. In order to explore the simplicity and less data requirement of UH approach, McCarthy (1938) and Snyder (1938) developed synthetic unit hydrograph (SUH) for ungauged catchments using some empirical equations to derive the salient points of the hydrograph. Similar expressions were later given by Edson (1951), Gray (1961), and Haan et al. (1984). All these methods begin by obtaining the salient points of the UH, and a smooth curve is fitted through these points to obtain a SUH; thus a large degree of subjectivity is involved in manual fittings, as simultaneous adjustments are also required for the area under the UH to represent unit runoff volume. Since UH approach relies on rain duration, a number of UHs of different durations can exist for a catchment.

Clark (1945) was probably the first to propose the Instantaneous Unit Hydrograph (IUH) theory. The main advantage of IUH is that it is independent of the duration of effective rainfall and thus has one parameter less than unit hydrograph. Nash (1957), for the first time, derived the IUH as two parameter gamma distribution (2PGD) by simulating the whole catchment by "n" identical conceptual cascaded linear reservoirs. Due to similarity in typical shape and unit area of a probability distribution function (PDF) curve, various suitable distributions have been explored by Gray (1961), Croley (1980), Aron and White (1982), Koutsoyiannis and Xanthopoulos (1989), Haktanir and Sezen (1990), Singh (2000), and Bhunya et al. (2004, 2007, and 2009) for SUH derivation. Nandrajah (2007) suggested eleven different flexible PDFs ranging from one parameter to three parameters for UH derivation. One of the major advantages of the application of PDFs is the subjectivity that existed in manual fitting of the UH in earlier methods was eliminated. With the coupling of Horton's geomorphic parameters and hydrological parameters by Rodriguez-Iturbe & Valdes (1979) and further refinement by

Gupta et al. (1980), the IUH theory (called GIUH) became more promising for ungauged or scantily gauged catchments. Since the theory represented hydrological parameters in terms of geomorphological characteristics of river basin, and thus, requirement of landuse and climatic parameters (like in Clarks, 1945 and Nash, 1957) are obviously omitted. A number of studies (Bhaskar et al., 1997; Lee, 1998; Karvonen et al. 1999; Hall et al., 2001; Jain et al., 2003; Kumar et al., 2007; Bharda et al., 2008) have been conducted to investigate hydrological response of the catchment by using the basin geomorphologic parameters according to GIUH concept.

Estimation of the geomorphologic parameters using manual methods is a tedious and time consuming process. With the recent advancements in the field of geo-spatial technologies like Geographical Information System (GIS) and Remote Sensing (RS), Digital Elevation Model (DEM) or Digital Terrain Model (DTM) has gained much impetus in hydrology from last two decades (Tarboton et al., 1991; Moore et al., 1992; Maathuis and Sijmons, 2005; and Hengl et al., 2006). In general, DEM/DTM is prepared from the digitalization of the contours from concerned toposheet or mosaic of toposheets of study area, which is very painstaking and time consuming process, especially when the area of interest is very large. Furthermore, readily available and probably cost free Shuttle Radar Topography Mission (SRTM) data plays a vital role to extract the catchment's geomorphological parameters.

3.1 OBJECTIVES

Based on the foregoing deliberations, the present study was specifically carried out with the following objectives: (i) to explore the potential of Two-parameter Inverse Gamma distribution (2PIGD), Two-parameter Weibull (2PWD) distribution, and Two-parameter Nash geomorphological model (2PNGM) for fitting UH, where an analytical approach is followed to estimate the distribution parameters; worth mentioning that 2PIGD has not been attempted in past; (ii) the UH parameters, viz., peak discharge, time to peak, etc. are accomplished using Horton order ratios given by Rodriguez-Iturbe and Valdes (1979); (ii) to extract the geomorphological parameters of the catchments from easily available and perhaps most updated SRTM data in a GIS environment; (iii) the

workability of this approach for UH derivation is demonstrated using data of Gagas watershed (a sub-watershed of Ramganga catchment); and finally (iv) based on the potentiality of the proposed models, i.e., 2PIGD, 2PWD and 2PNGM, the best performing model is to be further applied on the data of Ramganga catchment for SUHs derivation for different dynamic velocities using GIUH (Rodriguez-Iturbe and Valdes, 1979) concept and simple regression models for q_p and t_p are developed for direct field applications.

3.2 MATERIALS AND METHODS

As discussed in the previous section, the parametric expressions of the three proposed models, i.e., Two-parameter inverse gamma distribution (2PIGD), Two-parameter Weibull distribution (2PWD), and Two-parameter Nash Gamma model (2PNGM) are diagnosed and simple analytical procedures are proposed for parameter estimation using GIUH concept, as discussed in the following sub-sections.

3.2.1 Two-Parameter Inverse Gamma Distribution (2PIGD)

The parametric expression of the probability density function (pdf) of the 2PIGD model (Fig. 3.1) is given as:

$$f(x)=\frac{a^b}{\Gamma b}x^{-b-1}\exp\left(-\frac{a}{x}\right); \qquad \text{for } x>0,\ a>0, \text{ and } b>0 \qquad (3.1)$$

where a and b represent the shape and scale parameters of 2PIGD.
Similarly, the expression for cumulative distribution function (cdf) can be given as:

$$F(x)=\frac{\Gamma(b,a/x)}{\Gamma b} \qquad (3.2)$$

The mean (μ) and variance (σ^2) of the distribution, respectively, are given as:

$$\mu_x = \frac{a}{b-1}; \quad \text{for } b>1; \ \sigma_x^2 = \frac{a^2}{(b-1)^2(b-2)}; \quad \text{for } b>2 \tag{3.3}$$

Now, taking the parametric expression of 2PIGD as the discharge ordinates q(t) of UH and x as time t, Eq. (3.1) is redesigned as:

$$q(t) = \frac{a^b}{\Gamma b} t^{-b-1} \exp\left(-\frac{a}{t}\right); \quad \text{for } t > 0 \tag{3.4}$$

3.2.1.1 Derivation of Expressions for Peak Flow Rate (q_p) and Time to Peak (t_p)

At time to peak (t_p), the slope of the UH, i.e., dq(t)/dt shall be equal to zero. Therefore, the first derivative of Eq. (3.4) can be expressed as:

$$\frac{dq(t)}{dt} = \frac{d}{dt}\left[\frac{a^b}{\Gamma b} t^{-b-1} \exp\left(-\frac{a}{t}\right)\right] = 0 \tag{3.5}$$

Derivation of Eq. (3.5) results into

$$\frac{a^b}{\Gamma b} t^{-b-1} \exp\left(-\frac{a}{t}\right)\left(\frac{a}{t^2}\right) + \frac{a^b}{\Gamma b} t^{-b-2}(-b-1)\exp\left(-\frac{a}{t}\right) = 0 \tag{3.6}$$

Further simplification of Eq. (3.6) yields:

$$\frac{a^b}{\Gamma b} t^{-b-2} \exp\left(-\frac{a}{t}\right)\left[\frac{a}{t} + (-b-1)\right] = 0 \tag{3.7}$$

Two different conditions can be observed from Eq. (3.7), i.e., either [(a/t) + (-b-1)] = 0, which results into:

$$t_p = \frac{a}{(b+1)} \tag{3.8}$$

or

$$\frac{a^b}{\Gamma b} t^{-b-1} \exp\left(-\frac{a}{t}\right) = 0 \tag{3.9}$$

On expansion of exponential series and truncating the third term, Eq. (3.9) takes the form as (1-a/t) = 0, which yields; $t_p = a$.

Substitution of Eq. (3.8) in Eq. (3.4), gives the expression for peak ordinates, expressed as:

$$q_p = \frac{1}{a\Gamma b}(b+1)^{-b-1} \exp(-b-1); \qquad \text{for } a \neq 0, b \neq 0 \tag{3.10}$$

3.2.1.2 Estimation of 2PIGD Parameters

Defining shape factor β as the product of q_p (Eq. 3.10) and t_p (Eq. 3.8) (Bhunya et al., 2003; 2009) results into

$$\beta = q_p t_p = \frac{(b+1)^b}{\Gamma b} \exp[-(b+1)] \tag{3.11}$$

An assumption of (b+1) = m in Eq. (3.11) results into

$$\beta = \frac{m^{m-1}}{\Gamma(m-1)} \exp(-m) \tag{3.12}$$

Now using the property of Gamma function, i.e., Γ(m) = (m-1)Γ(m-1), Eq. (3.12) can be re-written as:

$$\beta = \frac{(m-1)m^{m-1}}{\Gamma(m)}\exp(-m) \tag{3.13}$$

Using Stirling's formula (Abramowitz & Stegun, 1964), the Gamma function can be expanded as:

$$\Gamma m = \sqrt{2\pi m}\left[m^{m-1}\exp(-m)\right]\left\{1 + \frac{1}{12m} + \frac{1}{288m^2} - \frac{139}{51840m^3} - \frac{571}{2488320m^4}\ldots\right\} \tag{3.14}$$

Considering the first two terms of Eq. (3.14) in the parenthesis, Eq. (3.13) can be simplified as:

$$\beta = \frac{m-1}{\sqrt{2\pi m}\left(1 + \frac{1}{12m}\right)} \tag{3.15}$$

The term $[1 + 1/(12m)]$ in Eq. (3.15) can be approximated by $[1 + 1/(6m)]^{1/2}$, then Eq. (3.15) simplifies to:

$$\beta^2 = \frac{(m-1)^2}{\left(2\pi m + \frac{\pi}{3}\right)} \tag{3.16}$$

Substitution of (b+1) = m in Eq. (3.16) reduces to

$$\beta^2 = \frac{b^2}{\left(2\pi(b+1) + \frac{\pi}{3}\right)} \tag{3.17}$$

Finally, Eq. (3.17) can be expressed as:

$$3b^2 - 6\pi\beta^2 b - 7\pi\beta^2 = 0 \tag{3.18}$$

The roots of the above quadratic equation (Eq. 3.18) can be written as:

$$b = \pi\beta^2 \pm \beta\sqrt{\pi^2\beta^2 + 7\pi/3} \tag{3.19}$$

Hence, for the known values of the shape factor β the scale parameter b from Eq. (3.19). Once b is obtained, the shape parameter a can be estimated from Eq. (3.8) and the complete shape of UH using Eq. (3.4).

3.2.2 Two-Parameter Weibull Distribution (2PWD)

The parametric expression of the probability density function (pdf) of two-parameter Weibull distribution (2PWD) model (Fig. 3.1) can be expressed as:

$$f(x) = \frac{b}{a}\left(\frac{x}{a}\right)^{b-1} \exp\left[-\left(\frac{x}{a}\right)^{b}\right]; \text{ for } a>0,\ b>1,\ t>0 \tag{3.20}$$

where a is the scale parameter and b is the shape parameter. For b = 1, Eq. (3.20) reduces to exponential distribution function. Thus, the exponential distribution is a special case of the Weibull distribution (Singh, 1987).

The cumulative density function (cdf) can be expressed as:

$$F(x) = 1 - \exp\left[-\left(\frac{t}{a}\right)^{b}\right] \tag{3.21}$$

The mean (μ) and variance (σ^2) of the pdf are given as:

$$\mu = a\Gamma\left(1+\frac{1}{b}\right) \quad \sigma^2 = a^2\Gamma\left(1+\frac{2}{k}\right) - a^2\left[\Gamma\left(1+\frac{1}{b}\right)\right]^2 \tag{3.22}$$

Considering the UH similar to the Weibull distribution with discharge ordinate q(t) on the y axis and x axis as time (t), Eq. (3.20) can be used to describe the UH as:

$$q(t) = \frac{b}{a}\left(\frac{t}{a}\right)^{b-1} \exp\left[-\left(\frac{t}{a}\right)^{b}\right] \tag{3.23}$$

3.2.2.1 Derivation of Expressions for Peak Flow Rate (q_p) and Time to Peak (t_p)

For the condition of time to peak (i.e., $t = t_p$), the slope of tangent to UH, i.e. dq(t)/dt should be zero. Hence, Eq. (3.23) reduces to:

$$\frac{b}{a^2}\left(\frac{t}{a}\right)^{b-1} \exp\left\{-\left(\frac{t}{a}\right)^{b}\right\}\left[(-b)\left(\frac{t}{a}\right)^{b-1} + (b-1)\left(\frac{t}{a}\right)^{-1}\right] = 0 \tag{3.24}$$

Now, two conditions can be observed from Eq. (3.24) as either: (i) $\left[(-b)\left(\frac{t}{a}\right)^{b-1} + (b-1)\left(\frac{t}{a}\right)^{-1}\right] = 0$ or (ii) $\frac{b}{a^2}\left(\frac{t}{a}\right)^{b-1} \exp\left\{-\left(\frac{t}{a}\right)^{b}\right\} = 0$; which yields;

$$t_p = a\left(1 - \frac{1}{b}\right)^{\frac{1}{b}}; \; t_p = a \tag{3.25a\&b}$$

Substitution of $t_p = a\left(1 - \frac{1}{b}\right)^{\frac{1}{b}}$ in Eq. (3.23) gives the expression for peak flow rate (q_p) as:

$$q_p = \frac{b}{a}\left(1 - \frac{1}{b}\right)^{1-\frac{1}{b}} \exp\left[1 - \left(1 - \frac{1}{b}\right)\right] \tag{3.26}$$

3.2.2.2 Estimation of 2PWD Parameters

The expression for shape factor or the dimensionless term (β) in this case can be obtained by multiplying the terms q_p (Eq. 3.26) and t_p (Eq. 3.25a) as:

$$\beta = q_p t_p = (b-1)\exp\left[-\left(1-\frac{1}{b}\right)\right] \tag{3.27}$$

A further simplification and expansion of the exponential term up to third term yields

$$b^3 - (e\beta)b^2 - (1/2)b - (1/2) = 0 \tag{3.28}$$

The solution of the above equation can be expressed as (Abramowitz and Stegun, 1964):

$$b = (S_1 + S_2) - a_2/3 \tag{3.29}$$

where $S_1 = \left[B + (A^3 + B^2)^{1/2}\right]^{1/3}$ and $S_2 = \left[B - (A^3 + B^2)^{1/2}\right]^{1/3}$; $a_2 = (-e\beta)$; $A = a_1/3 - a_2^2/9$; $B = (a_2a_1 - 3a_0)/6$; $a_1 = (-1/2)$; and $a_0 = (-1/2)$.

Thus, for known values of the shape factor β, the shape parameter '*b*' can be estimated from Eq. (3.29) and the scale parameter 'a' from Eq. (3.25a), and finally, the complete shape of UH using Eq. (3.23).

3.2.3 The Geomorphological Instantaneous Unit Hydrograph (GIUH) Model

Linking quantitative geomorphology with basin hydrologic characteristics can provide a simple way to understand the hydrologic behavior of different basins, particularly the ungauged ones. Rodriguez-Iturbe and Valdes (1979) expressed the initial state probability of one droplet of rainfall in terms of geomorphological parameters as well as the transition state probability matrix. The final probability density function of droplets leaving the highest order stream into the trapping state is nothing but the GIUH. An exponential holding time mechanism, equivalent to that of a linear reservoir, was assumed. The expression derived by Rodriguez-Iturbe and Valdes (1979) yields full analytical, but complicated expressions for the instantaneous unit hydrograph (IUH). They suggested that it is adequate to assume a triangular instantaneous unit hydrograph and only specify the expressions for the time to peak

and peak value of the IUH. These expressions are obtained by regression of the peak as well as time to peak of IUH derived from the analytic solutions for a wide range of parameters with that of the geomorphologic characteristics and flow velocities. The model was parameterized in terms of Horton's order laws (Horton 1945) of drainage network composition and Strahler's (1957) stream ordering scheme. The expressions for peak flow (q_p) and time to peak (t_p) of the IUH are given as:

$$q_p = \left(\frac{1.31}{L}\right) R_L^{0.43} v \tag{3.30}$$

and

$$t_p = 0.44\left(\frac{L}{v}\right) R_B^{0.55} R_A^{-0.55} R_L^{-0.38} \tag{3.31}$$

where L is the length of main channel or length of highest order stream in kilometres, v is the average peak flow velocity or characteristic velocity in m/s, q_p and t_p are in units of h^{-1} and h, respectively. R_B, R_A, and R_L represent the bifurcation ratio, area ratio, and length ratio.

Rodriguez-Iturbe and Valdes defined the dimensionless shape factor β as:

$$\beta = 0.584\left(\frac{R_B}{R_A}\right)^{0.55} R_L^{0.05} \tag{3.32}$$

It is observed from Eq. (3.32) that β is independent of velocity v and length of highest order stream or scale variable L, thereby, on the storm characteristics and hence is a function of only the catchment characteristics. Alternatively, Eqs. (3.30) and (3.31) can also be expressed as (Rosso, 1984):

$$q_p = 0.364 R_L^{0.43} v L^{-1} \tag{3.32a}$$

and

$$t_p = 1.584 (R_B/R_A)^{0.55} R_L^{-0.38} v^{-1} L \tag{3.33}$$

where q_p, t_p, L and v must be in coherent units.

3.2.4 Geomorphological UH Based Two Parameters Nash Model (2PNGM)

The possibility of preserving the form of the SUH through a two-parameter gamma pdf was analyzed by Rosso (1984), where Nash model parameters were related to Horton ratios as discussed here. The parametric expression for 2PNGM (Fig. 3.1) is given as:

$$q(t) = \frac{1}{k\Gamma(n)}\left(\frac{t}{k}\right)^{n-1} e^{-\frac{t}{k}} \tag{3.34}$$

where k is the scale parameter (T), n is the shape parameter equal to m_2^{-1}; where m_2 is the second dimensionless moment about the centre of area of the IUH, and $\Gamma(\ )$ is the gamma function. The mean (μ) and variance (σ^2) are described as:

$$\mu = n\,k;\ \sigma^2 = n\,k^2 \tag{3.35a\&b}$$

For the condition: at time to peak ($t = t_p$), $dq(t)/dt = 0$, Eq. (3.34) yields the following expression relating n and k as:

$$k = t_p/(n-1) \tag{3.36}$$

Following the similar procedures as to 2PIGD and 2PWD, the expression for dimensionless shape factor (β) can be obtained in the simpler form as:

$$\beta = q_p t_p = \frac{(n-1)^{n-1} e^{-(n-1)}}{\Gamma(n-1)} \tag{3.37}$$

Rosso (1984) equated both the expressions of β, i.e., Eqs. (3.32) & (3.37) and used an iterative computing scheme to develop the expressions for the parameters n and k as:

$$n = 3.29(R_B / R_A)^{0.78} R_L^{0.07} \quad (3.38)$$

$$k_* = 0.70[R_A / (R_B R_L)]^{0.48} \quad (3.39)$$

where $k_* = kvL^{-1}$ is a dimensionless scale parameter. Thus, for a known value of v, the parameters of the 2PNGM and hence the UH shape can be computed from the geomorphological parameters of the catchment. Thus, for an observed v, the parameters of the 2PNGM and the UH shape can be computed from the geomorphological parameters of the catchment.

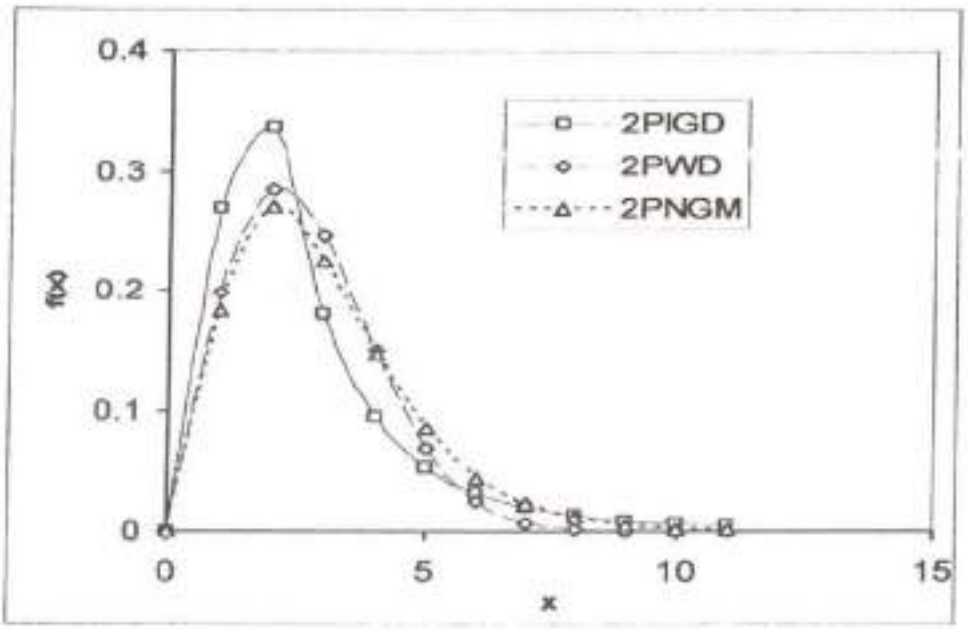

Figure 3.1: The pdf shapes of 2PIGD (a = 6, b = 3), 2PWD (a =3, b = 2) and 2PNGM (n = 3, k = 2).

3.2.5 Extraction of Geomorphological Parameters Using SRTM and GIS

Certain characteristics of the drainage basins reflect hydrologic behavior and are therefore, useful when quantified in evaluating the hydrologic response of the basins. These characteristics relate to the physical characteristics of the drainage basin as well as of the drainage network. In this study, the geomorphological parameters of the

catchments are extracted from Shuttle Radar Topography Mission (SRTM) DEM using ILWIS 3.31 GIS environment as described below. The SRTM data of 3-arc second (≈ 90 m) resolution used in this study was downloaded from website Global Land Cover Facility (GLCF) and imported into ILWIS through "import via Geo-gateway" command.

To delineate the catchment boundaries of Gagas and Ramganga catchments and consistent drainage networks, the SRTM mosaics were passed through subsequent processes like fill sinks, flow direction, flow accumulation, drainage network extraction, drainage network ordering, catchment extraction and finally catchment merge according to the location of outlet of the catchment. These all modules are well embedded in the ILWIS and given under "DEM Hydro-Processing" operation, however at some steps user interference are required to schematize and parameterize more realistic drainage network. Once catchment and drainage network delineated, the geomorphologic parameters such as drainage area, perimeter of the basin, length of the basin, maximum and minimum elevation, watershed relief, relief ratio, elongation ratio, mean slope, drainage density, stream frequency, circulatory ratio, farm factor, Horton's bifurcation ratio length ratio stream-area ratio, can be easily estimated using the formulae summarized in Table 3.1.

In this section, the proposed distribution function based models, i.e., 2PIGD, 2PWD, and 2PNGM are applied to the data of Gagas watershed (a sub-watershed of Ramganga catchment) for UH derivation as is being discussed here. Basic description about Gagas watershed has already been given in Chapter 2. For geomorphologic analysis, a detailed DEM of the catchment was prepared using SRTM data having fineness of 3-arc second spatial resolution, which was downloaded from the website Global Land Cover Facility (www.landcover.org/data/srtm/). The UH characteristics for the Gagas watershed are given in Table 3.2.

Figure 3.2 represents the resulting drainage network map of the Gagas catchment having fourth order. The Horton's plot drawn with X-axis as Strahler order and number of stream channels, average stream length (km), average stream area (km^2) calculated by least square method were plotted on a log transformed Y-axis as shown in Fig. 3.3a.

Table 3.1: Formulae Used to Estimate Different Geomorphological Parameters

Sl. No.	Geomorphological Parameters	Formula	Reference
1	Stream order	Hierarchical rank	Strahler (1964)
2	Stream length (Lu)	Length of the stream	Horton (1945)
3	Stream length ratio (R_L)	$R_L = L_u / L_{u-1}$ L_u = The total stream length of the order 'u' L_{u-1} = The total stream length of its next lower order	Horton (1945)
5	Bifurcation ratio (R_b)	$R_b = N_u / N_{u+1}$ N_u = Total no. of stream segments of order 'u' N_{u+1} = Number of segments of the next higher order	Schumn (1956)
6	Relief ratio (R_h)	$R_h = H / L_b$ H = Total relief (Relative relief) of the basin (m); L_b = Basin length	Schumn (1956)
7	Drainage density (D_d)	$D = L_u / A$ L_u = Total stream length of all orders; A = Area of the basin (km^2)	Horton (1932)
8	Stream frequency (F_s)	$F_s = N_u / A$ N_u = Total no. of streams of all orders	Horton (1932)
9	Drainage texture (R_t)	$R_t = N_u / P$ N_u = Total no. of streams of all orders; P = Perimeter (km)	Horton (1945)
10	Compactness factor	$0.2821*P/A^{0.5}$	
11	Form factor (R_f)	$R_f = A / L_b^2$	Horton (1932)
12	Circularity ratio (R_c)	$R_c = 4 * \pi * A / P^2$ P = Basin perimeter (km)	Miller (1953)
13	Elongation ratio (R_e)	$R_e = 2(A/\pi)^{0.5} / L_b$	Schumn (1956)
14	Length of overland flow (L_g)	$L_g = 1 / (2*D)$ where, L_g = Length of overland flow; D = Drainage density	Horton (1945)

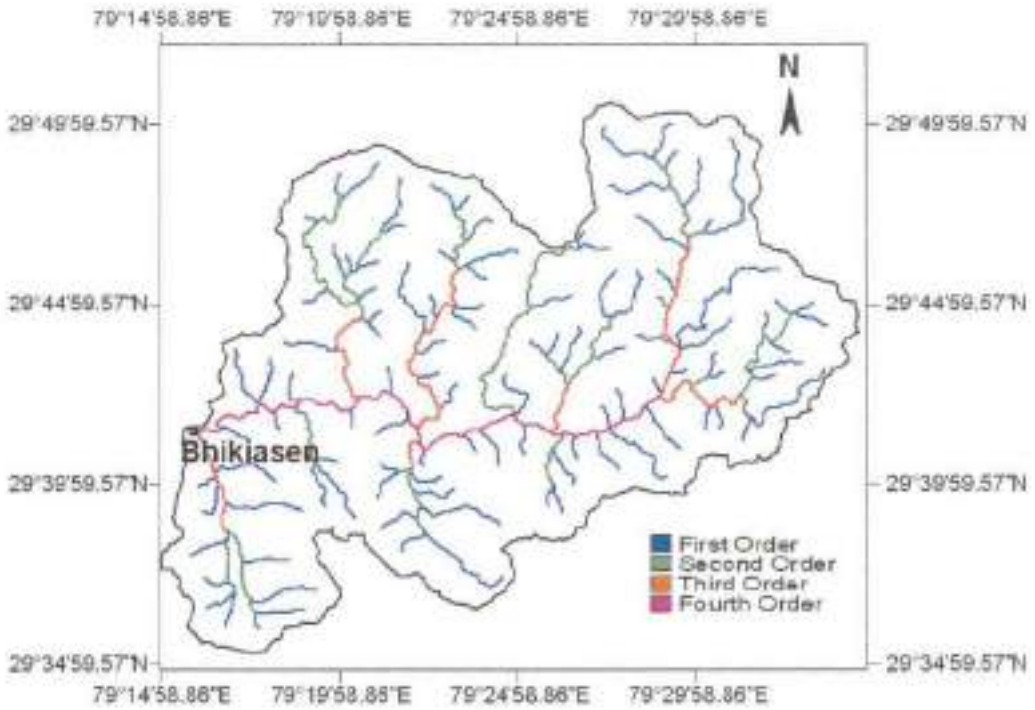

Figure 3.2: Drainage Network Map of Gagas catchment.

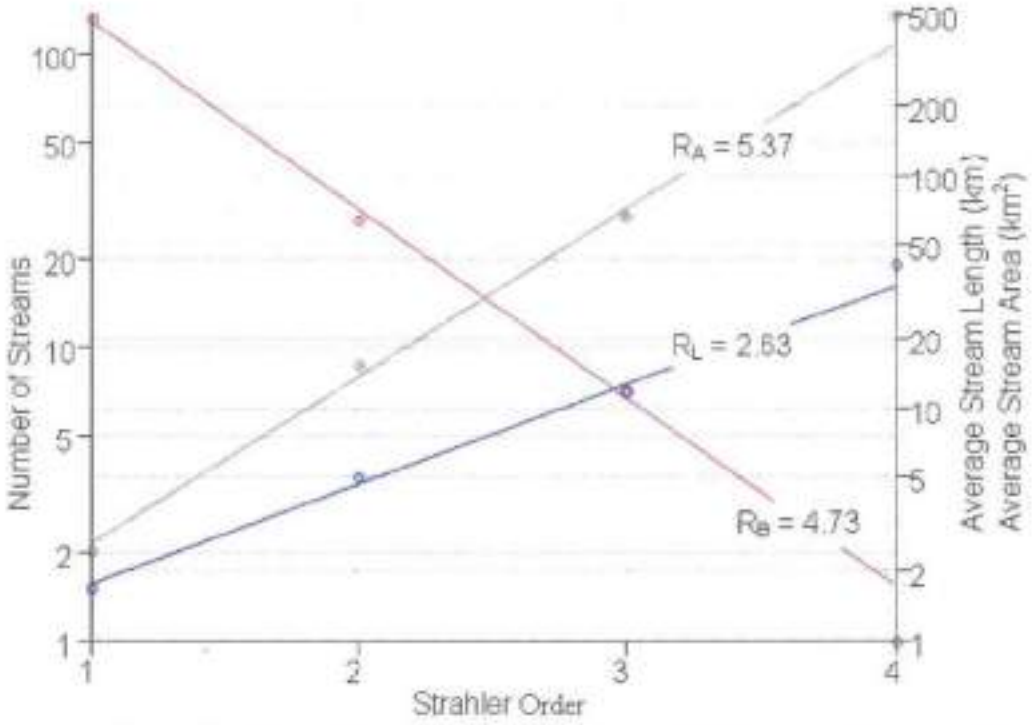

Figure 3.3a: Horton's plot showing Strahler order in relation to number of streams, average stream length, and average catchment area for Gagas catchment.

From the Horton's plot the Horton's ratios, i.e., the bifurcation ratio (R_B), length ratio (R_L), and area ratio (R_A) are found to be 4.73, 2.63, and 5.37, respectively as shown in Table 3.2. These values are very close to the corresponding values, i.e., $R_B = 4.82$, $R_L = 2.39$ and $R_A = 5.37$ for the Gagas watershed derived from cartographic data and as reported by Kumar and Kumar (2008). Further, these values are also within the range as suggested by Rodriguez-Iturbe and Valdes, i.e., $2.5 \le R_B \le 5.0$, $3.0 \le R_A \le 6.0$ and $1.5 \le R_L \le 4.0$. In addition to this, the close fitting of extracted number of stream, average stream length, average catchment area for different Strahler orders in a straight line, as shown in Fig. 3.3, indicates that they are good representative of the catchment.

Table 3.2: Geomorphological Parameters Extracted from SRTM DEM Using ILWIS 3.3 for Gagas watershed

Stream Order	Total No. of Stream (N_i)	Mean Stream Length (L_i)	Mean Stream Area (A_i)	Stream Area ratio (R_a)	Bifurcation Ratio (R_b)	Stream Length Ratio (R_L)
1	118	2.16	2.88	5.37 (5.37)*	4.73 (4.82)*	2.63 (2.39)*
2	24	5.39	17.37			
3	7	12.07	66.81			
4	1	41.49	506.00			

*Represent the values obtain from cartographic data by Kumar & Kumar (2008)

3.3 APPLICATION OF THE PROPOSED MODELS ON GAGAS WATERSHED

The potentiality of 2PIGD, 2PWD, and 2PNGM models was examined considering the catchment as ungauged and having partial data availability only, i.e., few observations from the observed UH, i.e., q_p and t_p are to be used. As discussed above, six storm events have been used as given in Table 3.3. For the storm event of June 25, 1978: when q_p is considered to be known and t_p is calculated as follows: using Eq. (3.32), $q_p = 0.364(2.63)^{0.43}$ vL^{-1}; $vL^{-1} = 0.34/\ [0.364(2.63)^{0.43}] = 0.617\ h^{-1}$; using Eq. (3.33), $t_p = 1.584(4.73/5.37)^{0.55}2.63^{-0.38}\ v^{-1}L = 1.656$ h and $\beta = 0.340 \times 1.656 = 0.564$. Taking these values, the estimated parameters of 2PIGD and 2PWD are given in Table 3.2. However,

for 2PGNM (Rosso, 1984), the parameters are calculated using $n = 3.29 \times (4.73/5.37)^{0.78} \times 2.63^{0.07} = 3.183$ and $k = 0.70[2.63/(4.73 \times 5.37)]^{0.48} \times 1.62 = 0.759$, as given in Table 3.3. A similar procedure was followed for parameter estimation of the proposed models for the rest of the storm events and the computed values are given in Table 3.2. Using above parameters, the SUHs were derived using 2PIGD, 2PWD, and 2PNGM methods as shown in Figures 3.3 to 3.8. For visual comparison, it can be observed from these figures that the computed UHs are in good matching with the observed UHs with respect to peak flow rate, time to peak, time to base, and overall shape of for all the storm events. However, the UHs computed by 2PIGD are in much better resemblance than the rest of the two models, i.e., 2PWD and 2PNGM as for as the rising segment, crest segment and recession segment is concerned.

Table 3.3: Storm characteristics and parameters of the three models for partial data availability condition for Gagas watershed

Date of Storm	UH Characteristics		Parameters of:					
			2PIGD		2PWD		2PNGM	
	Q_p (m^3/s)	t_p (h)	a	b	a	b	n	k
June 25, 1978	47.93	2.0	6.326	2.820	2.421	1.926	3.183	0.759
June 20, 1981	48.35	2.0	6.279	2.820	2.404	1.926	3.183	0.753
July 31, 1982	50.40	2.0	5.982	2.820	2.290	1.926	3.183	0.718
August 30, 1984	46.03	2.0	6.583	2.820	2.520	1.926	3.183	0.790
August 10, 1985	49.09	2.0	6.160	2.820	2.358	1.926	3.183	0.739
August 15, 1985	50.90	2.0	5.948	2.820	2.277	1.926	3.183	0.713

To further evaluate the performance of these models, the goodness-of-fit was evaluated using the following statistical indices: (i) Standard Error (STDER); (ii) Nash-Sutcliffe Efficiency (NSE); and (iii) Root Mean Square Error (RMSE), as discussed here.

Standard Error (STDER): it represents the absolute sum of the mismatching areas to the total hydrograph area, mathematically expressed as (HEC-1, 1990):

$$\text{STDER} = \left[\left(\sum_{i=1}^{N}(U_{oi} - U_{ci})^2 W_i\right)/N\right]^{1/2} ; W_i = (U_{oi} - U_{av})/2U_{av} \qquad (3.40)$$

where U_{oi} is the i^{th} ordinate of observed UH, U_{ci} the i^{th} ordinate of the computed UH, W_i the weighted value of i^{th} UH ordinate, U_{av} the average of the observed UH ordinates, and N the total number of UH ordinates.

NS-Coefficient of Efficiency (NSE): It was given by Nash and Sutcliffe (1970) on a scale of 0-100, expressed as:

$$\text{NSE}(\%) = 1 - \left[\sum_{i=1}^{N}(U_{oi} - U_{ci})^2 \Big/ \sum_{i=1}^{N}(U_{oi} - U_{av})^2\right] \text{x}100 \qquad (3.41)$$

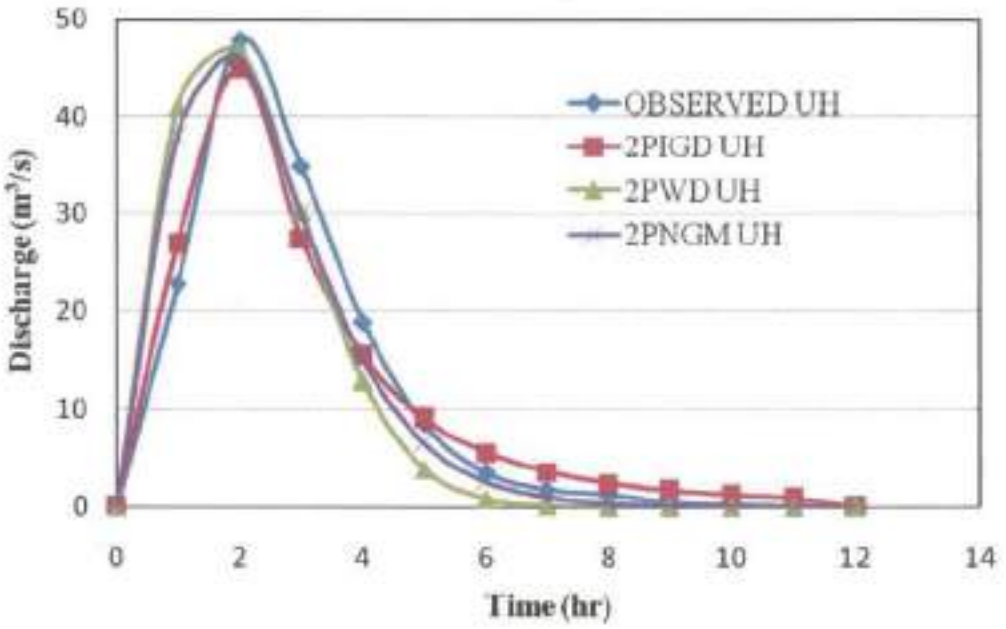

Figure 3.3b: Comparison between observed and computed UHs for Gagas catchment for the storm of June 25, 1978.

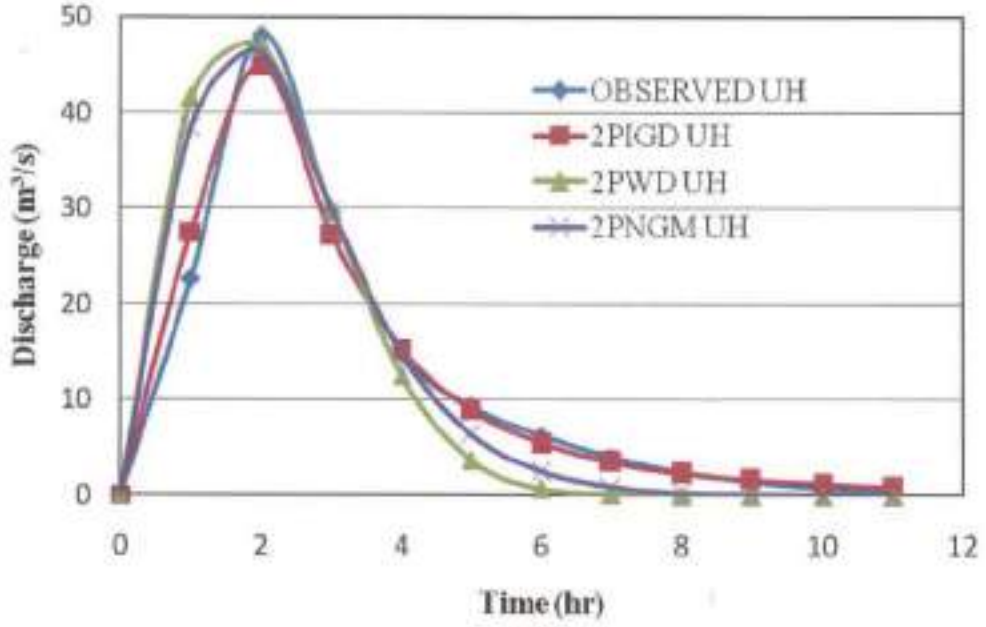

Figure 3.4: Comparison between observed and computed UHs for Gagas catchment for the storm of June 20, 1981.

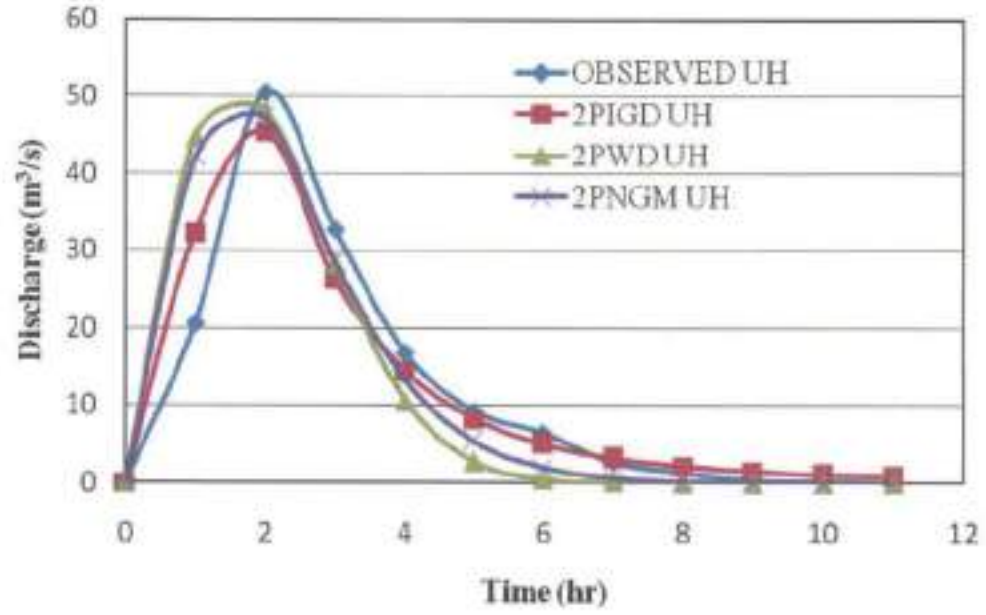

Figure 3.5: Comparison between observed and computed UHs for Gagas catchment for the storm of June 31, 1982.

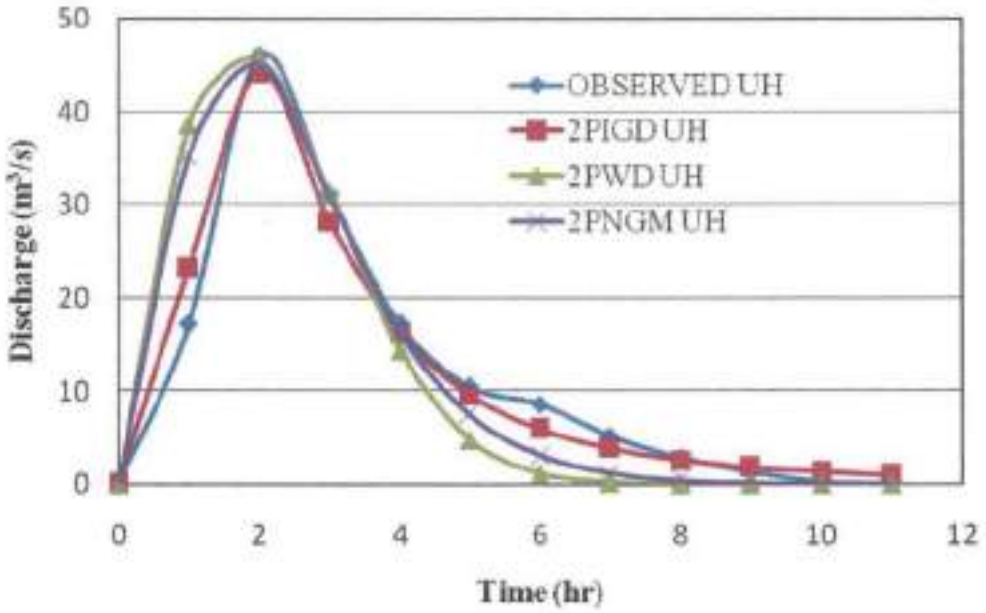

Figure 3.6: Comparison between observed and computed UHs for Gagas catchment for the storm of August 30, 1984.

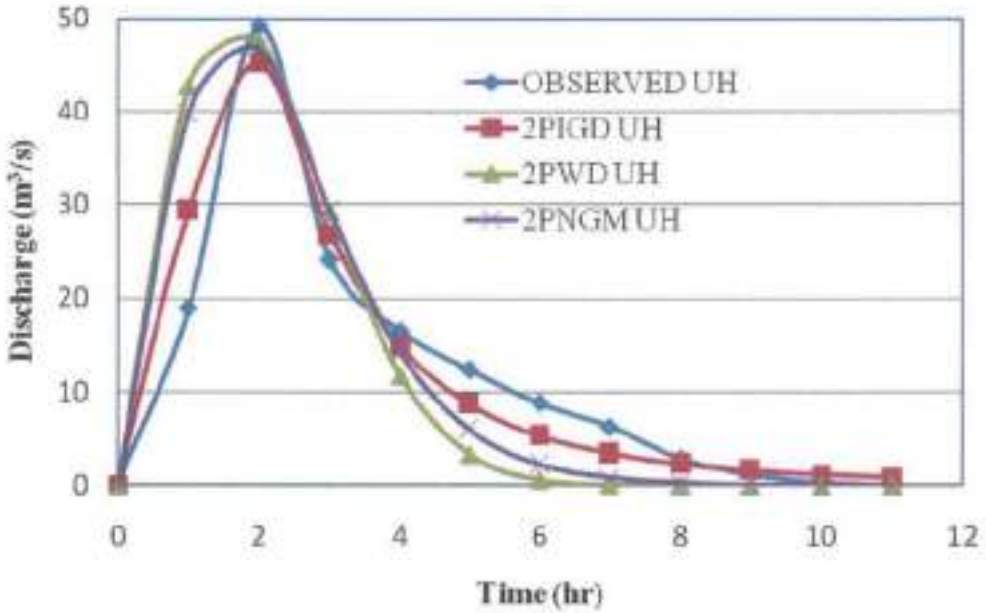

Figure 3.7: Comparison between observed and computed UHs for Gagas catchment for the storm of August 10, 1985.

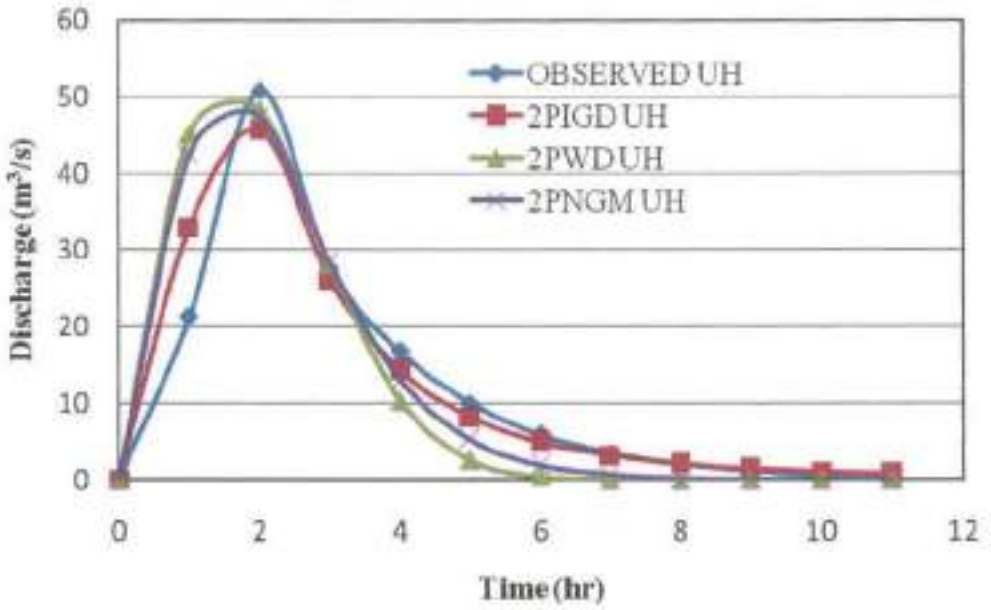

Figure 3.8: Comparison between observed and computed UHs for Gagas catchment for the storm of August 15, 1985.

Root Mean Square Error (RMSE): It represents an index of variation between computed and observed runoff values (Madsen et al. 2002; Itenfisu et al. 2003; and Moradkhani et al. 2004), expressed as:

$$RMSE = \left[\sum_{i=1}^{N} \{U_{ai} - Uci\}^2 / N \right]^{0.5} \qquad (3.42)$$

The results of the above indices for goodness-of-fit criteria are given in Table 3.4. It can be observed from the Table 3.3 that 2PIGD model has lower values of STDER and RMSE and higher values of NSE as compared to 2PWD and 2PIGD for all the storm events.

Table 3.4: Storm-wise statistical indices of goodness-of-fit for 2PIGD, 2PWD, and 2PNGM models Gagas watershed

Date of Storm	Statistical Indices for Goodness-of-Fit:								
	STDER			NSE (%)			RMSE		
	2PIGD	2PWD	2PNGM	2PIGD	2PWD	2PNGM	2PIGD	2PWD	2PNGM
June 25, 1978	3.89	7.19	5.95	93.6	78.2	85.1	2.85	5.76	4.65
June 20, 1981	4.22	12.08	9.94	97.0	75.4	83.4	1.86	6.13	4.96
July 31, 1982	11.71	19.59	17.08	87.6	65.3	73.6	4.26	7.84	6.72
August 30, 1984	3.76	11.01	9.03	96.5	70.0	79.8	2.24	6.99	5.69
August 10, 1985	6.39	13.37	11.53	89.9	55.8	67.1	3.77	8.27	7.07
August 15, 1985	7.31	13.50	11.73	89.2	63.2	72.2	3.85	7.77	6.64
Average	**6.21**	**12.79**	**10.88**	**92.3**	**68.0**	**76.9**	**3.14**	**7.13**	**5.96**

These results indicate the suitability of 2PIGD over 2PWD and 2PNGM models for SUH derivation from ungauged catchments based on geomorphological model of a catchment response. It can be observed from Table 3.4 that the STDER values are found to vary from 3.76 % to 11.71% with an average value of 6.21 for 2PIGD model; 7.19 to 19.59 with an average value of 12.79 for 2PWD model; and 5.94 to 17.8 with an average value of 10.88 for 2PNGM model. The RMSE values are found to vary from 1.86 to 4.26 with an average value of 3.14 for 2PIGD model; 5.76 to 8.27 with an average value of 7.13 for 2PWD model; and 4.65 to 7.07 with an average value of 5.96 for 2PNGM model. Similarly, the NSE values are found to vary from 89.2 to 97.0% with an average value of 92.3% for 2PIGD model; 55.8 to 78.2% with an average value of 68% for 2PWD model; and 67.1 to 85.1% with an average value of 76.9% for 2PNGM model. From the overall results (visual comparison as well as goodness-of-fit in terms of statistical indices), it can be concluded that 2PIGD performs much better than 2PWD and 2PNGM model for SUH derivation from ungauged catchments.

3.4 APPLICATION TO RAMGANGA CATCHMENT

As discussed in section 3.1 part (iv), the best performing model is to be further applied on the data of Ramganga catchment for UHs derivation for different dynamic velocities using GIUH (Rodriguez-Iturbe and Valdes, 1979) concept and simple

regression models for q_p and t_p are to be developed for direct filed applications. Hence based on the results obtained from application of the proposed models, the Two-parameter inverse gamma distribution (2PIGD) is further applied to the data of Ramganga catchment as follows.

A general description about Ramganga catchment is given in Chapter 2.0. To extract the geomorphologic features of the basin, the SRTM data of 3 arc-second resolution was used. The DEM of Ramganga river basin was prepared from SRTM data set using ILWIS 3.31 GIS environment as depicted in Figure 3.9. The drainage network was also extracted from the DEM of Ramganga catchment following the standard procedure discussed above. Figure 3.10 shows the extracted drainage lines of different Strahler order of Ramganga basin and has the highest order of basin as 5, i.e., a fifth order basin. The maximum length of the river is found to be 172 km. The number of streams of different orders, length, corresponding area and the extracted geomorphologic parameters such as drainage area, perimeter of the basin, length of the basin, maximum and minimum elevation, watershed relief, relief ratio, elongation ratio, mean slope, drainage density, stream frequency, circulatory ratio, farm factor, Horton's bifurcation ratio, length ratio, stream-area ratio, etc. are also summarized in Table 3.5.

Using the computed Horton's ratios and the length of highest order stream (L), the parameters of 2PIGD are estimated for different assumed dynamic flow velocities. Noteworthy, the dynamic velocity flow component of GIUH can also be computed using the approach suggested by Kumar et al. (2002), provided the necessary data such as characteristics of the cross-sections, roughness coefficients, velocities at different locations, etc. is available. However in this study the dynamic flow velocity component could not be computed due to lack of observed velocities at different locations.

The computed values of the distribution parameters a & b at various assumed flow velocities are given in Table 3.5. Finally, using the computed values of a & b at different flow velocities v, the UHs for different velocities are computed using Eq. (3.4) as shown in Fig. 3.11.

Table 3.5: Extracted Geomorphological Parameters for Ramganga Catchment

Parameters		Value	
Area (Km^2)		3134	
Perimeter (Km)		379.65	
Length of Basin (Km)		173	
Maximum Elevation (m)		3088	
Minimum Elevation (m)		356	
Stream Characteristics (Number, Length and Area)			
Order of Stream	**Number**	**Mean length (Km)**	**Mean area (Km^2)**
1	681	2.17	2.89
2	135	3.45	18.67
3	33	7.28	85.29
4	6	24.13	500.57
5	1	101.15	3134.66
Ratios & Other Geomorphological Parameters			
Bifurcation ratio (R_b)		5.04	
Area ratio (R_a)		5.45	
Length ratio (R_l)		2.65	
Drainage density		0.774	
Stream Frequency (Km^{-2})		0.273	
Elongation Ratio		0.365	
Circulatory Ratio		0.273	
Farm Factor		0.105	
Shape Factor		9.550	
Compactness Factor		1.913	
Relief ratio (m/km)		15.792	
Drainage texture		2.255	
Length overland flow		0.646	

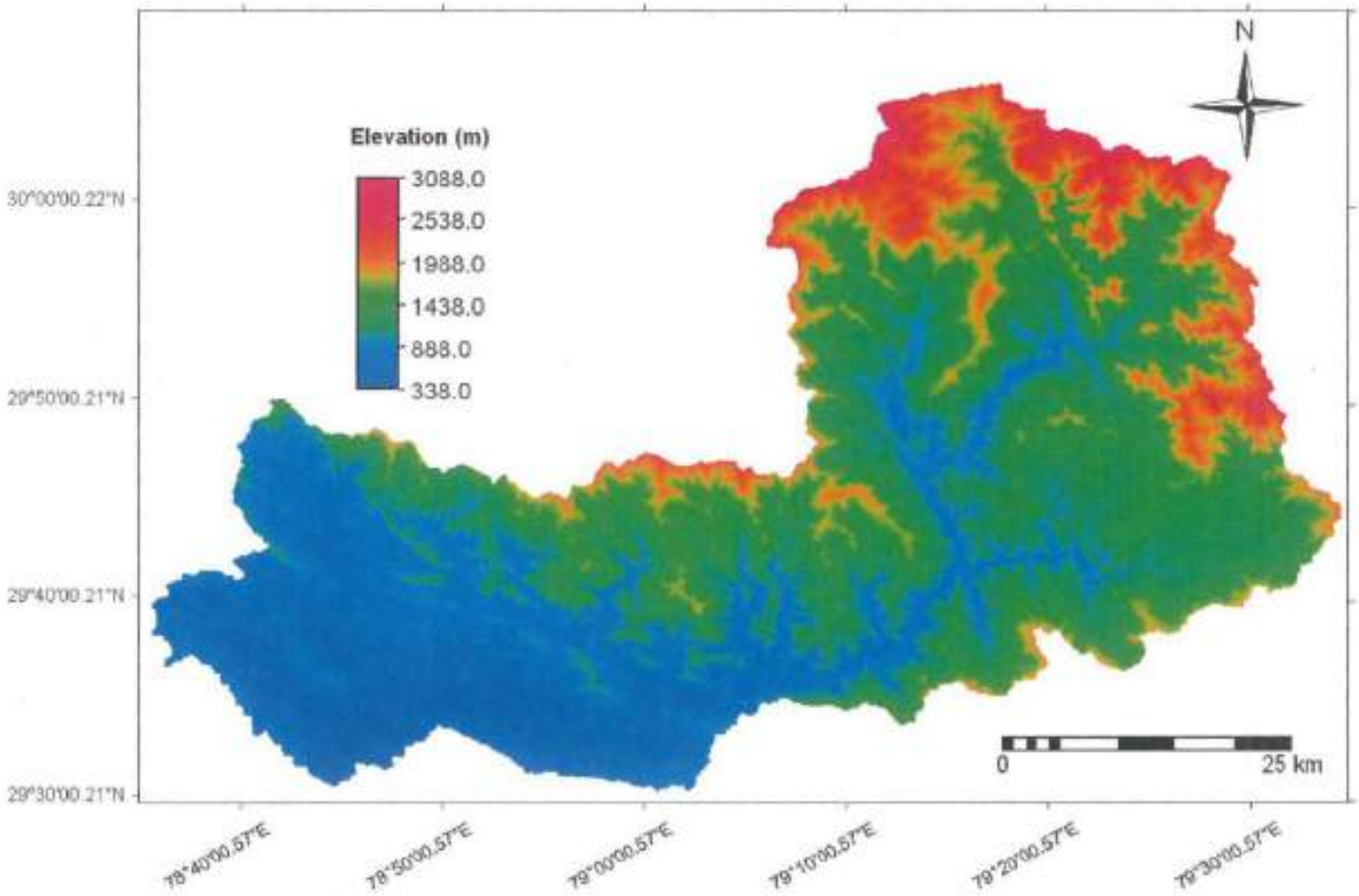

Figure 3.9: Digital Elevation Model (DEM) of Ramganga catchment extracted from SRTM and ILWIS 3.31.

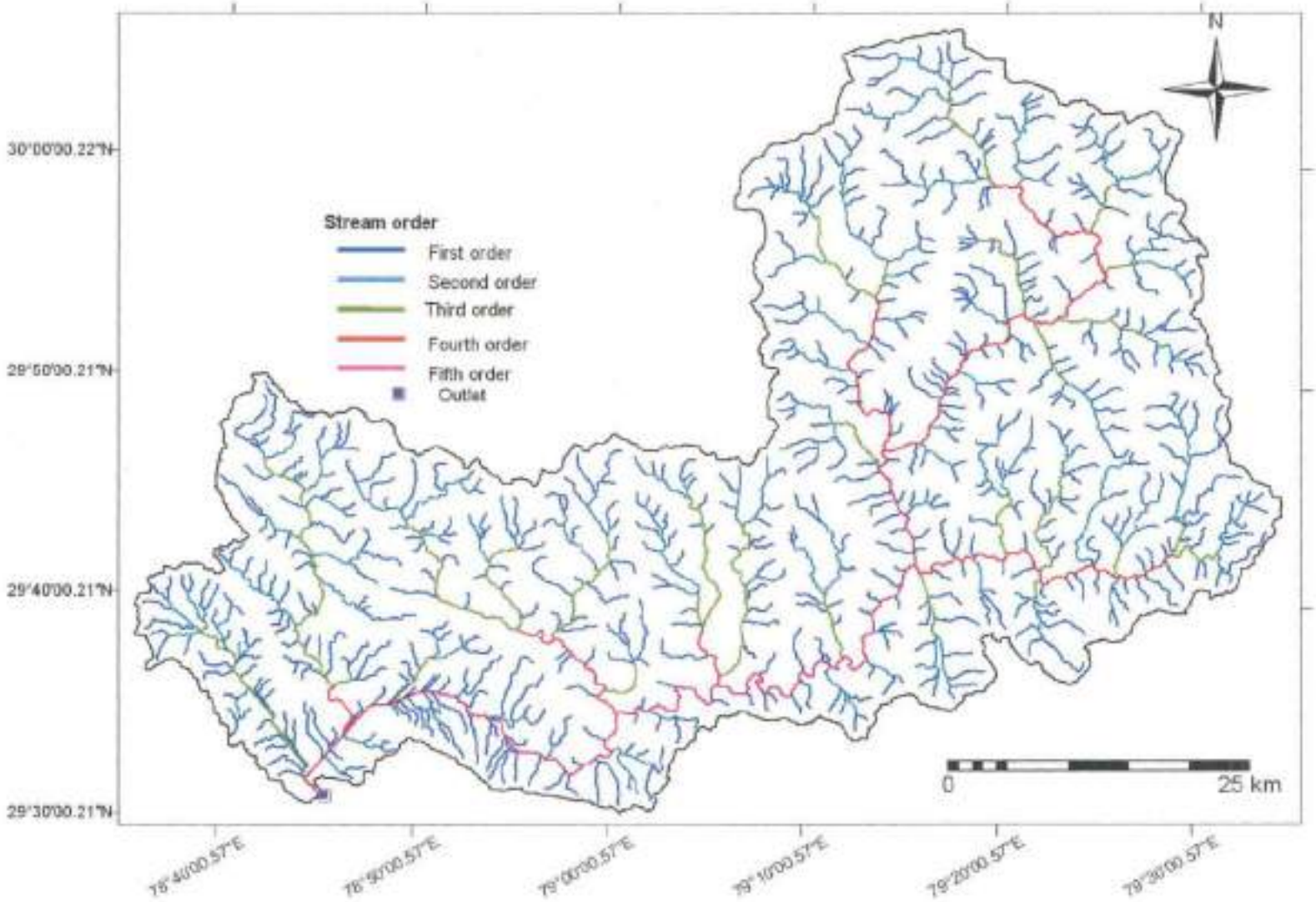

Figure 3.10: Map showing the drainage line of different Strahler order of Ramganga catchment extracted from SRTM DEM and ILWIS 3.31.

Table 3.6: Estimated values of Inverse Gamma distribution parameters at different velocity for Ramganga catchment

v (m/s)	a (hr)	b	v (m/s)	a (hr)	b
2	59.0499	2.9987	4.5	2.9987	26.2444
2.5	47.2399	2.9987	5	2.9987	23.6200
3	39.3666	2.9987	5.5	2.9987	21.4727
3.5	33.7428	2.9987	6	2.9987	19.6833
4	29.5250	2.9987	6.5	2.9987	18.1692

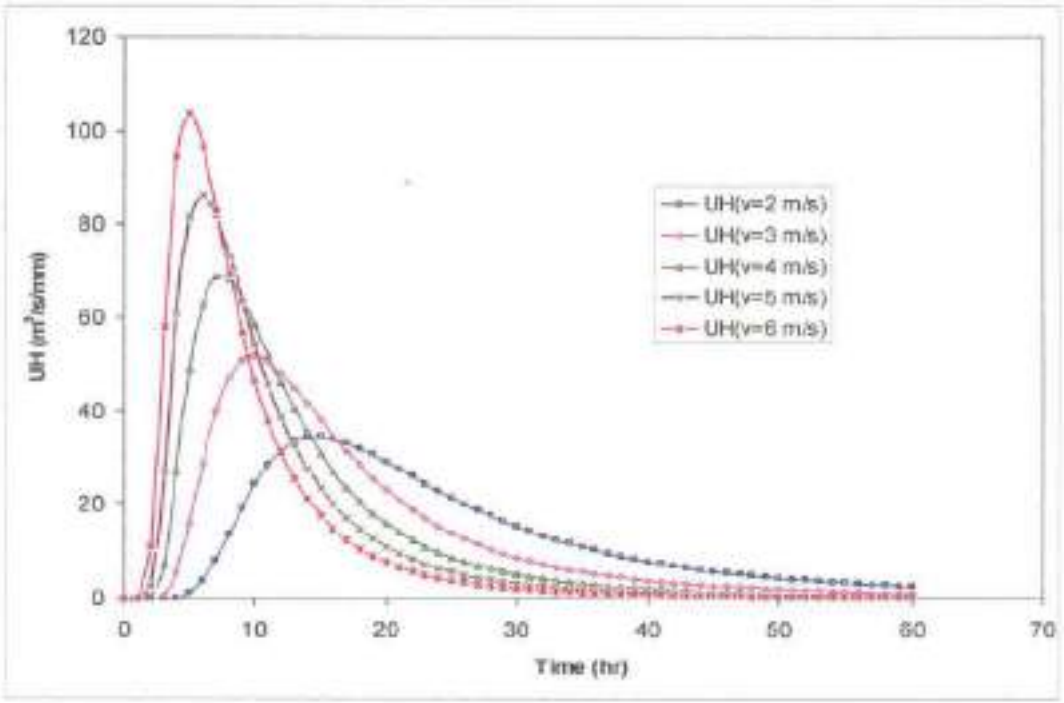

Figure 3.11: UHs derived for Ramganga catchment at different flow velocities using inverse gamma distribution and geomorphological parameters

As discussed in section 3.1 part (iv), simple regression models for q_p and t_p are to be developed using the GIUH governing equations given by Rodriguez-Iturbe and Valdes (1979) for direct field applications, where only flow velocities are available. Corresponding to different assumed flow velocities, q_p and t_p were calculated using the GIUH governing equations as shown in Figure 3.12. Finally, a linear regression model was fit to get the simple models relating q_p and t_p with dynamic flow velocity, expressed as:

$$q_p = 17.149 * V + 0.1361 \qquad (R^2 = 0.999) \qquad (3.43)$$

$$t_p = 29.535 * V^{-1} \qquad (R^2 = 1) \qquad (3.44)$$

where, q_p is the peak flow rate ($m^3/s/mm$), v is the dynamic velocity of flows (m/s), and t_p is the time to peak (hours).

The practical utility of the above models can be understood as one can directly compute the magnitudes of q_p and t_p (hence the complete shape of UH) utilizing only the dynamic flow velocities at a given basin channel section outlet without extracting the geomorphological parameters. Hence, these linear models can be of immense importance for the field engineers as well as hydraulic engineers for design of hydraulic structures and development of flood prediction and warning systems, particularly for Ramganga catchment.

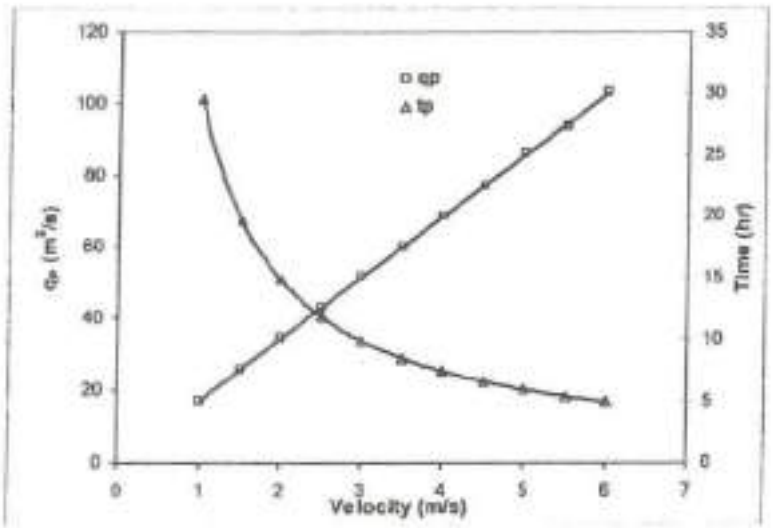

Figure 3.12: Relationship between q_p and t_p with dynamic flow velocity v for Ramganga catchment

3.5 CONCLUSIONS

This study explored the potential of the density functions of Two-parameter Inverse Gamma distribution (2PIGD), Two-parameter Weibull (2PWD) distribution, and Two-parameter Nash geomorphological model (2PNGM) for deriving SUH based on GIUH approach (Rodriguez-Iturbe and Valdes, 1979) for limited data availability condition for Gagas watershed of Ramganga catchment. The geomorphological parameters of the catchments were extracted from easily available and most updated SRTM data in ILWIS 3.3 GIS environment. Based on the goodnesss-of-fit (GOF) criteria, 2PIGD is found to perform significantly better than 2PWD and 2PNGM models. Finally, the 2PIGD model (the best performing model) was further applied to the data of Ramgamga catchment for SUHs derivation for different dynamic velocities using GIUH concept which resulted into simple regression models for q_p and t_p for direct field applications. These linear models can be of immense importance to the field engineers as well as hydraulic engineers for design of hydraulic structures and development of flood forecasting and warning systems, particularly for Ramganga catchment.

CHAPTER 4

A REVISIT TO SCS–CN MODEL

CHAPTER 4

A REVISIT TO SCS–CN MODEL

Rainfall-runoff modeling is now-a-days a dynamically developing field of hydrology and water management. This development is primarily caused by the rapid progress of computers and information technology. This evolution provides the mankind with new possibilities to use water as its basic need and at the same time to evolve an affective protection against it. Rainfall-runoff modeling is meant to model the hydrological processes of the land phase of the hydrological cycle which inputs the rainfall and other hydrologic, climatic, and basin parameters and produces the desired output such as runoff, peak discharge etc. In other words, a rainfall - runoff model is a hydrological model which determines the runoff from the rainfall. Obviously hydrological processes are complex phenomena and certain degree of simplification is always involved in modeling. For estimation of runoff, a number of models varying from the simplest empirical relations to the most complex physically based models are available in literature. Since the rainfall data are generally available for a much longer period than the stream flow data, long – term hydrologic simulation helps to extend the gauged data required for the applications in water resources planning and watershed management. Much of the current research in catchment hydrology as well as practical management of water resources is based on computer models for estimating runoff from rainfall and evaporation data. Most of the modern rainfall–runoff models that now number in thousands will give reliable results where some stream flow data are available for calibration of model parameters. However, very little progress has been made in use of these models on ungauged catchments where calibration data are not available.

The response of the catchment for a particular rainfall event is runoff. Stream flow representing the runoff phase of the hydrologic cycle is the most important data for hydrologic studies. The first and foremost requisite for the planning of water resources development is accurate data of stream flow, or in other words, the surface runoff for a considerable period of time to determine the extent and pattern of the available supply of water. The usual practical objective of a hydrologic analysis is to determine the characteristics of the hydrograph that may be expected from a stream

draining any particular watershed. Surface runoff is that part of the precipitation which, during and immediately following a storm event, ultimately appears as flowing water in the drainage network of a watershed. Such flow may result from direct movement of water over the ground surface, precipitation in excess of abstraction demands, or it may result from emergence of soil water into drainage ways.

The long-term daily hydrologic simulation is useful in augmentation of hydrologic data, water resources planning and watershed management (Mishra and Singh, 2003, 2004) and is efficacious in describing the performance of a water resource system under climatic variations of rainfall and other aspects (Kottegoda et al., 2000). The computer-based lumped, conceptual rainfall–runoff models have been widely applied in hydrological modelling since they were first introduced in the late 1960s and early 1970s. Among a multitude of models, a few well known and some recent storage concept-based models worth citing are: Stanford Watershed Model IV (SWM IV) (Franchini and Pacciani, 1991; Singh, 1989), Boughton model (Johnston and Pilgrim, 1976; Mein and Brown, 1978), Kentucky Watershed model (Moore et al., 1983; James, 1972), Institute of Hydrology model (Nash and Sutcliffe, 1970), HYDROLOG (Poter and McMahon 1976), MODHYDROLOG model (Chiew et al., 1993), and Hydrology and River Hydraulics at University of Tokushima (HRUT) model (Yao et al., 1996). Using the storage concept, the Soil Conservation Service Curve Number (SCS-CN) model has also been widely employed in the past for long-term hydrologic simulation (Mishra et al., 1998; Mishra and Singh, 2003, 2004).

Estimation of runoff from a particular rainfall event is of vital significance in planning for irrigation, hydropower, flood control, water supply and navigation. In general rainfall- runoff modeling is basic to design of a wide variety of hydraulic structures, environmental impact assessment, evaluation of the impact of climatic change, irrigation scheduling, flood forecasting, planning of tactical military operation, augmentation of runoff records, pollution abatement, watershed management & so on.

4.1 OBJECTIVES

As runoff data are missing or only available during short periods, they can be generated using rainfall – runoff relationship or long- term hydrologic simulation models. This analysis however considers the model application to the catchment as a

whole. This chapter aims at to conceptualize and develop a lumped model based on the popular SCS – CN technique for long daily rainfall- runoff simulation model and test its workability using the data of Ramganga catchment, a sub-himalayan catchment, and further verify its applicability to other catchments located in different geo-hydro-meteorological settings. Finally, the study also compares the model performance with another lumped conceptual model (Geetha et al., 2007) on different watersheds.

4.1.1 General Study Layout

The chapter is divided into following sections:

- Envisages the hydrologic modelling and objectives of the study.
- Summarizes various rainfall – runoff simulation methods, historical background, and other specific details relevant to the study.
- Deals with development of the proposed long daily runoff simulation model based on SCS- CN method.
- Provides a brief description of the watersheds and the data available for model application.
- Provides a discussion of the results of model calibration and validation and its comparison with the existing model.

4.2 RAINFALL – RUNOFF MODELLING

The simulation of rainfall-generated runoff is very important in various activities of water resources development and management such as flood control and its management, irrigation scheduling, design of irrigation and drainage works, design of hydraulic structures, and hydro-power generation etc. Ironically, determining a robust relationship between rainfall and runoff for a watershed has been one of the most important problems for hydrologists, engineers, and agriculturists since its first documentation by P. Perrault (In: Mishra and Singh 2003) about 330 years ago.

4.3 RAINFALL-RUNOFF APPROACHES AND CONCEPTUALIZATION

The process of transformation of rainfall to runoff is highly complex, dynamic, non-linear, and exhibits temporal and spatial variability, further affected by many and often interrelated physical factors. However an understanding of various hydrologic variations (spatial and temporal) over long periods is necessary for identification of these complex and heterogeneous watershed characteristics. The hydrological cycle is a continuous process in which water circulates from the oceans through the atmosphere and rivers, and finally backs to the oceans. Among the various components of hydrological cycle, the term precipitation denotes all forms of water that reach the earth from the atmosphere. Rain (precipitation) is the major object of hydrologic cycle and the primary cause of runoff. The rainfall is subjected to the physical processes which depend on climatological factors like temperature, humidity, wind velocity, cloud cover, evaporation and evapotranspiration, topographical features like depressions, slope of the catchments, vegetation and land use pattern, the soil characteristics like permeability, antecedent moisture content and irrigability characteristics; and the hydrological condition like rock formation, elevation of water table and sub-surface channels too affect this process considerably.

Runoff is defined as the portion of the precipitation that makes its way towards river or ocean etc. as surface and subsurface flow. Runoff, representing the response of a catchment to precipitation, reflects the integrated effect of a catchment, climate & precipitation characteristics. Under these influencing parameters, it is utmost difficult task to estimate the likely runoff from a particular storm. The precipitation responsible for the runoff is known as effective precipitation. For a given precipitation the evapotranspiration, initial loss, infiltration and detention storage requirements will have to be first satisfied before the commencement of runoff. When these are satisfied the excess precipitation moves over the land surface to reach smaller channels. The portion of the runoff is called as overland flow and involves building up of storage over the surface and draining the same. Flows from several small channels join bigger channels and flows from there and, in turn, combine to form a large stream and so on till the flow reaches the catchment's outlet. The flow in this mode where it travels all the time over the surface as overland flow and through the channels as open channel flow and reaches the catchment's outlet is called surface runoff. A part of precipitation that infiltrates moves laterally through upper crust of

the soil and returns to the surface at some location away from the point of entry into the soil. This component of the runoff is known as interflow. Precipitation (rain) falling on the land surface has several pathways as shown in Figure 4.1.

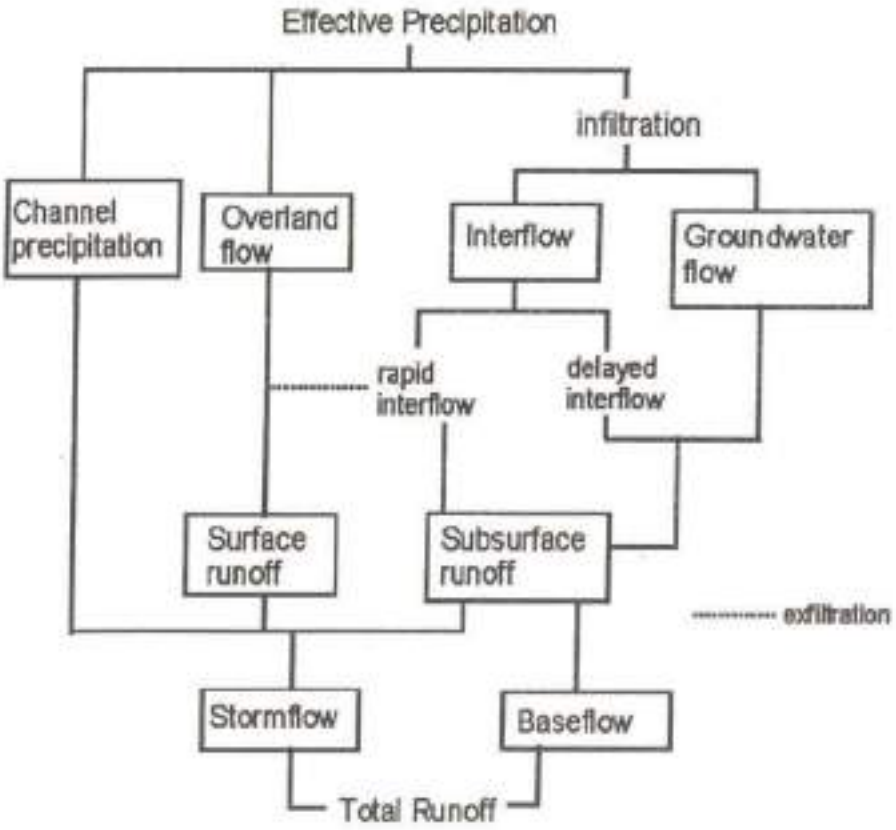

Figure 4.1: Generation of runoff from effective rainfall in a catchment (source: - www.cartage.org.lb/.....sourcesofrunoff.htm)

The amount of interflow depends on the geological condition of the soil. Depending upon the time delay between the infiltration and outflow, the interflow is sometimes classified into prompt interflow or rapid interflow i.e. the interflow with the least time lag and delayed interflow. Another route for the infiltrated water is to undergo deep percolation and reach the ground water storage in the soil. The time lag i.e. difference in time between the entry into the soil and outflow from it is very large, being of the order of months and years. This part of runoff is called groundwater runoff or groundwater flow.

Based on the time delay between the precipitation and the runoff, runoff is classified into two categories as direct runoff or storm runoff and base flow. Direct runoff is the part of runoff which enters the stream immediately after the precipitation. It includes surface runoff, prompt interflows and precipitation on channel surface. The delayed flow that reaches stream essentially as groundwater flow is called as base flow. Rainfall-runoff models may be grouped into two general classifications that are illustrated in Figures 4.2 and 4.3. The first approach uses the concept of effective rainfall in which a loss model is assumed which divides the rainfall intensity into losses and an effective rainfall hyetograph. The effective rainfall is then used as input to a catchment model to produce the runoff hydrograph. It follows from this approach that the infiltration process ceases at the end of the storm duration.

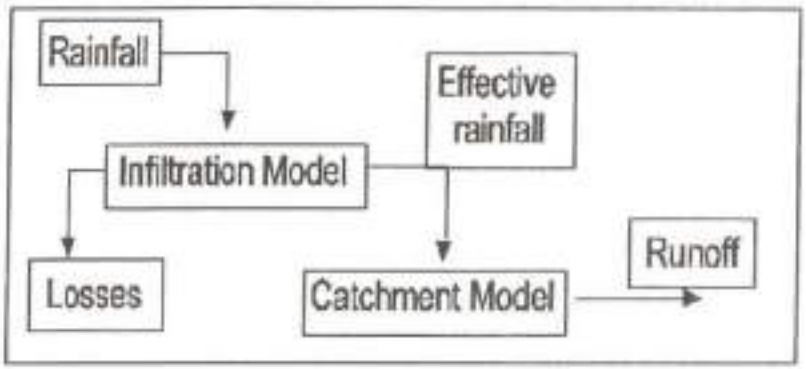

Figure 4.2: A rainfall-runoff model using effective rainfall
(Source: - www.alanasmith.com/theory-calculating../runoff models.htm)

An alternative approach that might be termed as surface water budget model incorporates the loss mechanism into the catchment model. In this way, the incident rainfall hyetograph is used as input and the estimation of infiltration and other losses is made as an integral part of the calculation of runoff. This approach implies that infiltration will continue to occur as long as the average depth of excess water on the surface is finite. Clearly, this may continue after the cessation of rainfall. The origin of rainfall- runoff modelling, widely used for flow simulation, can be found in the second half of the 19th century when engineers faced the problems of urban drainage and river training networks. During the last part of 19th century and early part of 20th century, the empirical formulae were in wide use (Dooge, 1957, 1973).

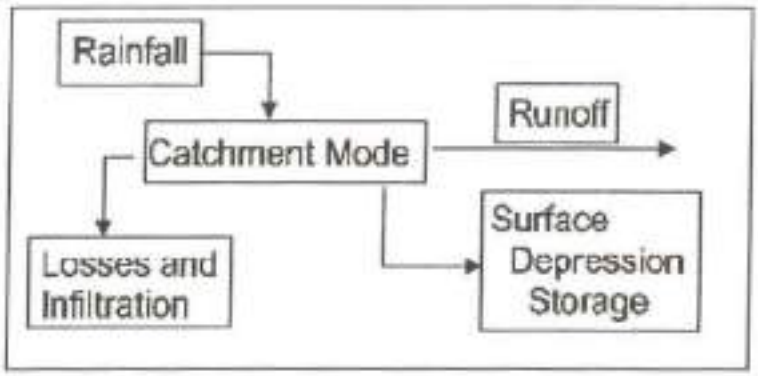

Figure 4.3: A rainfall-runoff model using a surface water budget
(Source: - www.alanasmith.com/theory-calculating../runoff models.htm)

The approaches were mainly confined to small and mountainous watersheds. Later attempts were mainly confined to their application to larger catchments. In 1930's the popular unit hydrograph techniques were developed. With the advent of computers in 1950's, sophistication to models through mathematical jugglery was introduced with the objective of providing the generality of available approaches. The subsequent era saw the development of a number of models and evoked the problem of classification. The relation between precipitation (rainfall) and runoff is influenced by various storm and basin characteristics. Because of the complexities and frequent paucity of adequate runoff data, many approximate formulae have been developed to relate runoff with rainfall. The earliest of these were usually crude empirical statements, whereas the trend now is to develop descriptive equations based on physical processes.

4.4 CLASSIFICATION OF HYDROLOGICAL MODELS

The simulation of rainfall-runoff (R-R) relationships has been an unavoidable issue of hydrological research for several decades and has resulted in plenty of models proposed in literature. In recent decades the science of computer simulation of groundwater and surface water resources systems has passed from scattered academic interest to a practical engineering procedure. A few of the most descriptive

classifications are presented. The available hydrological models can be broadly classified into Deterministic vs. Stochastic / Probabilistic, Conceptual vs. Physically Based Models, Lumped Models vs. Spatial Distributed Models, a brief description of which is provided as follows:

4.4.1 Deterministic vs. Stochastic / Probabilistic models

Water balance models can be referred to as "deterministic" if the statistical properties of input and output parameters are not considered. On the other hand, probabilistic models include random variations in input parameters, whereby known probability distributions are used to determine statistical probabilities of output parameters; i.e. deterministic models permit only one outcome from a simulation with one set of input and parameter values. Stochastic models allow for some randomness or uncertainty in the possible outcomes due to uncertainty in input variables.

4.4.2 Conceptual vs. Physically Based Models

Conceptual models rely primarily on empirical relationships between input and output parameters. These are based on overall observations of system behaviour (sometimes called "black box" models). The modeling systems may or may not have clearly defined physical, chemical or hydraulic relationships. Physically based models seek to describe water movement based on physical laws and principles. This may result in more reliable descriptions of water balance relationships. This type of model demands appropriate data for input and requires documentation of processes and assumptions.

4.4.3 Lumped Models vs. Spatially Distributed Models

Lumped models treat a sub-watershed as a single system and use the basin-wide averaged data as input parameters. This method assumes that the hydrologic characteristics of sub-watersheds are homogeneous. A spatially distributed model accounts for variations in water budget characteristics. Various methods are available, such as division of the watershed into grid cells or use of Hydrological Similar Units (HSU). For example, a grid cell model uses data for each grid cell inside the basin to compute flow from cell to cell. By this method, the spatial variation in hydrologic

characteristics can be handled individually (i.e. assuming homogeneity for each cell), and therefore, may be a more appropriate treatment. Spatially distributed models are suitable for GIS applications.

In this study a simple, lumped, conceptual, and empirical Soil Conservation Service Curve Number (SCS–CN) method has been used in long-term hydrological simulation. Here, it is notable that since its inception in 1956, the SCS-CN method/concept has been employed in several fields other than the original intended one, i.e. event-based rainfall-runoff modelling. An updated review this method is provided in Appendix-III. The forthcoming section presents SCS-CN method in brief and its application to long-term hydrologic modelling.

4.5 SCS-CN METHODOLOGY

The curve number is used to determine the amount of rainfall-excess that results from a rainfall event over the basin. This methodology is a standard hydrologic analysis technique that has been applied in a variety of settings and the development and application of the curve number is well documented in Section 4 of the National Engineering Handbook (NEH) in 1956. The Natural Resource Conservation Service - Curve Number (NRCS-CN) model, formerly known as Soil Conservation Service - Curve Number (SCS-CN) model (SCS 1956, 1964, 1969, 1971, 1972, 1985, 1993), is one of the popular models for computing the volume of surface runoff from small to medium-sized agricultural watersheds for a given rainfall event. The SCS-CN technique (USDA, 1972) is an empirical method based on the characteristics of soil type, land use, and the hydrological condition in the watershed. It is a well known and practical tool that is used to estimate direct runoff from rainfall. This technique was originally derived from the examination of annual flood event data. Its application is therefore most suited to designs involving high runoff events (Young et al., 2006). Even though the curve number technique is appropriately used for rainfall – runoff event simulation, it has also been widely used in a number of continuous simulation models since the 1980's.

The SCS-CN model converts rainfall to surface runoff (or rainfall-excess) using a single parameter, called curve number (CN) which is derived from watershed characteristics and 5-day antecedent rainfall. Some of the reasons for its popularity are that (1) it is simple (Bales and Betson, 1981); (2) it is a familiar procedure that has

been used for many years around the world; (3) it is computationally efficient; (4) the required inputs are generally available; and (5) it relates runoff to soil type, land use, and management practices. The use of readily available daily rainfall is particularly an important input to the SCS-CN model. This model however has its own limitations and assumptions, which lead to many questionable arguments on its applications. Since its inception, the SCS-CN model has been improved, extended and modified in various ways

The method which is derived to compute the surface runoff from rainfall in small agricultural watersheds is based on water balance equation and the two hypotheses (SCS, 1956; Mishra and Singh 1999, 2003). The curve numbers are a function of the land use type, soil texture type, hydrologic condition and antecedent moisture condition (AMC). Estimation of it requires mapping of the soil and land use with the drainage basin boundaries and specification of unique soil texture type.

The SCS curve number method is a simple, widely used and efficient method for determining the direct runoff from a rainfall event in a particular area. Although the method is designed for a single storm event, it can be scaled to find average annual runoff values. The requirements for this method are very low, rainfall amount and curve number. The curve number is based on the area's hydrologic soil group, land use, treatment and hydrologic condition; the former two being of the greatest importance. In the SCS-CN-based long-term hydrologic simulation, daily computation of direct surface runoff largely depends on AMC dependent CN. The computed direct surface runoff (or rainfall excess) is routed to the outlet of the catchment. Since the SCS-CN method is an infiltration loss model (Ponce and Hawkins, 1996), a portion of the infiltrated water is taken as base flow routed to the catchment outlet. The total runoff is the sum of the routed direct surface runoff and base flow.

The existing SCS–CN method (SCS, 1956) consists of the following three equations (Mishra and Singh, 2003):

Water Balance Equation:

$$P = I_a + F + Q \qquad (4.1)$$

Proportionality Hypothesis:

$$\frac{Q}{P-I_a}=\frac{F}{S} \tag{4.2}$$

I_a–S Hypothesis:

$$I_a=\lambda S \tag{4.3}$$

where P = total rainfall, I_a = initial abstraction, F = cumulative infiltration, Q = direct surface runoff, S = potential maximum retention, and λ = initial abstraction coefficient. All quantities in above equations are in depth or volumetric unit. Combination of these equations leads to the following popular form of the SCS – CN method, expressed as:

$$Q=\frac{(P-I_a)^2}{P-I_a+S} \tag{4.4}$$

Here, $P > I_a$ and Q = 0 otherwise. By using the volumetric concept of soil water air, Mishra (1998) defined S as the maximum amount of space available in the soil profile under given antecedent moisture. The relation between S and CN is usually expressed in SI units as:

$$S=\frac{25400}{CN}-254 \tag{4.5}$$

where S is in mm and CN = curve number. CN is taken as CN_0 valid for AMC II (normal condition), for the first five days beginning from the first day of simulation (June 1 to June 5). As the time (day) advances, CN varies with AMC levels (Hawkins 1978; Mishra et al. 1998) dependent on the amount of antecedent rainfall (ANTRF):

$$ANTRF_t=P_{(t-1)}+P_{(t-2)}+P_{(t-3)}+P_{(t-4)}+P_{(t-5)} \tag{4.6}$$

where, t = current day, and P = rainfall of the respective day. AMC II (average or normal condition) is taken as the basis from which adjustments to daily curve numbers are made so that they correspond to AMC I or AMC III (Hjelmfelt, 1991).

Different AMC class limits (Table 4.1) are provided for the dormant and growing seasons based on five-day antecedent precipitation, i.e., ANTRF and presented in (Mishra et al., 1998; Ponce, 1989; Hawkins et al., 1985).

Variation in curve numbers based on the total rainfall in the five days preceding the storm under consideration (Woodward and Croshney, 1992), CN_t of t^{th} day which corresponds to CN_{II} is converted to CN_I or CN_{III} as follows (Hawkins et al., 1985):

$$CN_I = \frac{CN_{II}}{2.3 - 0.013CN_{II}} \tag{4.7}$$

$$CN_{III} = \frac{CN_{II}}{0.43 - 0.0057CN_{II}} \tag{4.8}$$

Table 4.1: Antecedent Moisture Conditions

AMC	Total 5-day antecedent rainfall (cm)	
	Dormant season	**Growing season**
I	Less than 1.3	Less than 3.6
II	1.3 to 2.8	3.6 to 5.3
III	More than 2.8	More than 5.3

which are valid for AMC I or AMC III.

4.6 AVAILABLE LONG-TERM SIMULATION MODELS

Long-term hydrological simulation is required for augmentation of hydrological data. It is useful for water resources planning and watershed management. Long-term daily flow data are specifically needed for analysis of water availability, computation of fortnightly or monthly flows for reservoir operation and drought analysis. As the rainfall data are generally available for much longer periods than the stream-flow data, long-term hydrological simulation helps extend the gauged stream-flow data required for the applications.

There exist a multitude of models for hydrological simulation. In 1991, the U. S. Bureau of Reclamation prepared an inventory of 64 watershed models into four categories and the inventory is currently being updated. Burton (1993) compiled Proceedings of the Federal Interagency Workshop on Hydrologic Modeling Demands

for the 1990's, which contains several important watershed hydrology models. Singh (1995) edited a book that summarized 26 popular models from around the globe. The subcommittee on hydrology of the Interagency Advisory Committee on Water Data (1998) published Proceedings of the First Federal Interagency Hydrologic Modeling Conference, which contains many popular watershed hydrology models developed by federal agencies in the USA. Wurbs (1998) listed a number of generalized water resources simulation models in seven categories and discussed their dissemination.

The hydrological models vary in description of the components of the hydrological cycle, degree of complexity of inputs, number of parameters to be determined, time interval used in simulation, error and risk analyses, and output generated. Most of the models, such as the Hydrologic Simulation Package Fortran (HSPF), USDAHL (Holtan and Lopez, 1971) and its variants, System Hydrologic Europeen (SHE) (Abbott et al., 1986a, b), Hydrologic Engineering Centre Hydrologic Modeling System (HEC-HMS) (HEC, 2000), etc., have a number of parameters, usually use a short time interval, produce hydrographs as well as water yield and provide continuous simulation. The HSPF and SHE models are not applicable to ungauged watersheds for the reason that their application requires a priory calibration with measured runoff data for each watershed. The USDAHL model can, however, be used for ungauged watersheds, but the prediction accuracy is not commensurate with the input detail. These models are better suited for detailed scientific, hydrologic studies. Holtan and Lopez (1971) found the USDAHL model to explain about 90% of the variation in the monthly runoff for four watersheds up to 40 sq. km. The Hann (1975) model has four parameters, uses a 1- d time interval (except for a 1- d interval is used during rains), has simple inputs, and only outputs the runoff volume. In testing, this model was reported to explain about 80% of the variation in the monthly runoff from 46 watersheds of generally less than 100 sq. km. However, no provision exists for estimating the parameters of this model for its employment to ungauged watersheds. Woodward and Gburek, (1992) compared some of the available models and found them widely varying in their degree of success.

Despite their comprehensive structure, many of these models have not yet become standard tools in hydrological practice in developing countries, such as India, Pakistan, Nepal, and other countries of Asia as well as African countries. The reason is twofold. First, most basins in these countries are ungauged and there is little hydrological data available. Second, these models contain too many parameters,

which are difficult to estimate in practice and vary from basin to basin. Although some of these models have been applied to ungauged basins, the fact is that they are not easy for practical applications. Furthermore, when these models are compared on the same basin, they are found widely varying in their performance (Woodward and Gburek, 1992). Thus, what is needed in developing countries is simple models which can provide reasonable simulations and need few data. The Soil Conservation Service Curve Number (SCS-CN) based simulation models do satisfy these criteria.

The SCS-CN method is an infiltration loss model and, therefore, its applicability is supposedly restricted to modelling storms (Ponce and Hawkins, 1996). Notably, the SCS – CN method is theoretically applicable to any watershed of any size as long as the measured runoff corresponds to the observed rainfall amount (Mishra and Singh, 2003). However, some restrictions regarding its application to watershed of less than 250 sq. km, for practical reasons, have been reported in literature (for example Ponce and Hawkins, 1996). Using theoretical arguments, it is possible to apply the SCS-CN method for long-term hydrological simulation to any basin. It is for this reason that the SCS – CN method computes the rainfall – excess that equals the direct surface runoff. In large watersheds, routing plays an important role in converting the rainfall-excess to the surface runoff hydrograph produced at the basin outlet. On the other hand, small watersheds require minimal routing in long-term hydrological simulation utilizing a time interval of 1 day or larger. Consequently, the SCS-CN method has been used on small basins for long-term hydrological simulation and several models have been developed in the past two decades. The models of Williams and LaSeur (1976), Huber et al. (1976), Hawkins (1978), Knisel (1980), Soni and Mishra (1985) and Mishra et al. (1998) are notable.

4.6.1 Williams–LaSeur (1976) model

Williams and LaSeur (1976) proposed a model based on the existing SCS – CN method which is based on water balance equation and two fundamental hypotheses (methodology). The SCS – CN parameter potential maximum retention S is linked with the soil moisture (M) as:

$$M = S_{abs} - S \qquad (4.9)$$

where, S_{abs} is the absolute potential maximum retention equal to 20 inches. M is depleted continuously between storms by evapotranspiration and deep storage. Depletion is high when soil moisture and lake evaporation is high, the most rapid immediately after a storm (high M). M is assumed to vary with the lake evaporation as:

$$\frac{d(M)}{dt} = -b_c M^2 E \tag{4.10}$$

where, t is the time, b_c is the depletion coefficient, and E is the lake evaporation. Eq. (4.2) represents a second- order process. The lake evaporation is used as a climatic index. According to Williams and LaSeur, Eq. (4.10) works well for the average monthly values for runoff predictions. They found their model to perform poorly when daily pan evaporation and temperature were used as climatic indices. From Eq. (4.10) M is solved as:

$$M_t = \frac{M}{1.0 + b_c M \sum_{t=1}^{T} E_t} \tag{4.11}$$

where, M is the soil moisture index at the beginning of the first storm, M_t is the soil moisture index at any time t, E_t is the average monthly lake evaporation for day t, and T is the number of days between the storms.

For model operation, the amount of water infiltrated during a rainstorm (= rainfall P – direct surface runoff Q) is added to the soil moisture. The rainfall of the first day of the T – day period is added to M before Eq. (4.11) is solved. However, runoff is not abstracted from rainfall until the end of the T – day period, for the reason that runoff lags rainfall and may be subjected to depletion for several days on large watersheds. Thus Eq. (4.11) is modified for rainfall P as:

$$M_t = \frac{M + P}{1.0 + b_c M \sum_{t=1}^{T} E_t} - Q \tag{4.12}$$

where, P and Q are, respectively, the rainfall and runoff for the first storm. The retention parameter S is computed from equation $S = S_{abs} - M$ for $S_{abs} = 20$ inches for computing runoff for the second storm using the popular form of the existing SCS – CN method, expressible as:

$$Q = \frac{(P - 0.2S)^2}{P + 0.8S} \tag{4.13}$$

The procedure is repeated for each storm in the rainfall series. Thus, the Williams and LaSeur model can also be applied to the pre- identified rainstorms other than 1 day. The model is calibrated with data from a gauged watershed by adjusting the depletion coefficient, b_c, until the predicted average annual runoff matches closely with the measured average annual runoff. The initial estimation of b_c is derived from the average annual rainfall and runoff values as:

$$DP = \frac{AVP - AVQ}{365} \tag{4.14}$$

where, DP is the average daily depletion, AVP is the average annual rainfall, and AVQ is the average annual runoff. The value of b_c can be computed from Eq. (4.12) assuming that (a) T = 1; (b) M is the average soil moisture index, M_A; (c) E is the average lake evaporation; and (d) P= Q=0 for the day. For this situation, Eq. (4.12) can be recast as:

$$M_t = \frac{M_A}{1.0 + b_c M_A E_t} \tag{4.15}$$

In which, M_A is computed from equation $S = \frac{1000}{CN} - 10$ and $S = S_{abs} - M$ for CN corresponding to AMC II. The average daily depletion computed from Eq. (4.14) is set equal to the change in soil moisture for 1 day as:

$$DP = M_A - M_t \tag{4.16}$$

Combining Eqs. (4.15) & (4.16), one obtains

$$DP = M_A - \frac{M_A}{1.0 + b_c M_A E_t} \tag{4.17}$$

From which b_c can be derived as:

$$b_c = \frac{-DP}{E_t M_A (DP - M_A)} \tag{4.18}$$

The simulation begins 1 year before the actual calibration period because of a priori determination of the initial soil moisture index. At the end of one year, the soil moisture is taken to represent the actual soil moisture conditions. Here the initial estimate of M is M_A.

In brief, the Williams–LaSeur model has one parameter, uses a 1-day or any other pre-determined time interval, has simple inputs and only outputs the runoff volume. It eliminates, to certain extent, sudden jumps in the CN values when changing from one AMC to the other. Its operation requires (i) an estimate of the AMC-II curve number, (ii) measured monthly runoff, (iii) daily rainfall and (iv) average monthly lake evaporation. The model-computed b_c forces an agreement between the measured and the predicted average annual runoff. The model can be applied advantageously to nearby ungauged watersheds by adjusting the curve number for the ungauged watershed in proportion to the ratio of the AMC-II curve number to the average predicted curve number for the calibrated watershed.

The model, however, has its limitations. It utilizes an arbitrarily assigned value of 20 inches for S_{abs} and simulates runoff on monthly and annual bases although runoff is computed daily, treating rainfall of a day as a storm. Several adjustments for b_c loss the physical soundness of the model apart from the undesirable loss of 1-year rainfall–runoff information (Singh et al., 2001). Owing to physically unrealizable decay of soil moisture with lake evaporation, the model contradicts the SCS-CN approach, as shown below.

Taking $S_{abs} = S_0 = S$, which represents S at the beginning of a storm under fully dry conditions, equation $M = S_{abs} - S$ can be written for time t as: $M_t = S_0 - S_t$, if $S_t = 0$ at time $t = 0$, $M_t = S_0$. Its substitution into Eq. (4.11) leads to

$$(S_0 - S_t)/S_0 = \frac{1}{(1 + b_c S_0 \overline{E}t)} \tag{4.19}$$

where, E is the average rate of evapotranspiration. Here, $(S_0 - S_t) / S_0 = F/ S_0$, consistent with the description of Mishra (1998) and Mishra and Singh (2002a, b). With the assumption that $P/ S_0 = b_c S_0 E_t$ and $I_a = 0$ (here, P/t = uniform rainfall intensity $i_o = b_c S_0^2 E$), a substitution of these relationships into equation $P = I_a + F + Q$ yields $Q = PS_0/(S_0+P)$, which actually holds for F in the existing SCS-CN approach, rather than Q, and therefore, Eq. (4.11) is physically unrealizable.

4.6.2 Hawkins Model

Hawkins (1978) derived a daily simulation model by expressing Eq. (4.13) as:

$$Q = P - S\left(1.2 - \frac{S}{(P + 0.8S)}\right) \tag{4.20}$$

which is valid for $P \geq 0.2S$. It is evident from this equation that as $P \rightarrow \infty$ the maximum possible water is equal to S_t and it is computed as:

$$S_t = 1.2\, S \tag{4.21}$$

which can be derived from equation $S_T = (1 + \lambda)S$, assuming $\lambda = 0.2$. Substitution of equation $S = \frac{1000}{CN} - 10$ for S into Eq. (4.21) yields a storage relation for any time t as:

$$S_{T(t)} = 1.2S_t = 1.2\left(\frac{1000}{CN_t} - 10\right) \tag{4.22}$$

where, subscript 't' represents the time level. Taking into account the evapotranspiration (ET), the maximum water loss at a higher time level (t + Δt), where Δt is the storm duration, can be derived from the moisture balance as:

$$S_{T(t+\Delta t)} = S_{T(t)} + \left[ET - (P-Q)_{(t+\Delta t)}\right] \tag{4.23}$$

where, the last term in the bracket corresponds to the Δt duration between time t and (t+Δt), denoted by subscript (t, t+Δt). Following the above argument, Eq. (4.23) can be alternatively written as:

$$S_{T(t+\Delta t)} = 1.2\, S_{(t+\Delta t)} \tag{4.24}$$

Here it is noted that ET also intuitively accounts for the interim drainage, if any. Coupling of Eq. (4.23) with Eq. (4.24) and substitution of equation $S = \frac{1000}{CN} - 10$ into the resulting expression leads to

$$1.2\left(\frac{1000}{CN_t} - 10\right) + \left[ET - (P-Q)\right]_{(t+\Delta t)} = 1.2\left(\frac{1000}{CN_{t+\Delta t}} - 10\right) \tag{4.25}$$

which can be solved for $CN_{t+\Delta t}$ as:

$$CN_{t+\Delta t} = \frac{1200}{\frac{1200}{CN_t} + \left[ET - (P-Q)\right]_{(t+\Delta t)}} \tag{4.26}$$

Since ET, P, Q in Eq. (4.26) correspond to the time duration Δt and these are known quantities, Q can be computed from Eq. (4.13) for a given CN_t. Input of these values along with the known value of ET yields CN at time level (t+Δt).

It is apparent from the above that the Hawkins model accounts for the site moisture on a continuous basis using the volumetric concept. It is worth emphasizing here that the Hawkins model is analogous to a bottomless reservoir, implying that the reservoir never depletes fully or the reservoir is of infinite storage capacity. Such a description is, however, physically realizable in terms of $\psi - \theta$ relationship, according

to which S is directly proportional to the average ψ which approaches infinity as $\theta \rightarrow 0$. Under the situation that the soil is fully saturated or $\theta \rightarrow \eta$ (soil porosity), $\psi \rightarrow 0$. Thus, similar to S, S_t will also vary from 0 to ∞. Following this argument, $S_{abs} = 20$ inches in the Williams–LaSeur model appears to be a forced assumption. While applying the Hawkins model, Soni and Mishra (1985) also employed a similar assumption by fixing the depth of the soil profile to the root zone depth of 1.2 m for computing S.

The advantage of the Hawkins model is that it also eliminates sudden quantum jumps in the CN values when changing from one AMC level to the other, similar to the Williams–LaSeur model. However, the Hawkins model also has the following limitations.

1. It does not distinguish the dynamic infiltration from the static one. The water drained down to meet the water table may not be available for evapotranspiration.
2. The interim drainage is coupled with the evapotranspiration intuitively.
3. According to the model formulation (Eq. (4.20)), the term $(I_a + S)$ takes part in the dynamic infiltration process, rather than the S alone, where I_a = initial abstraction. As the initially adsorbed water ($= I_a$) as a result of very high capillary suction is not available for transpiration, I_a does not play a part in the dynamic infiltration process.
4. The follow up of the above 3 leads to the assumption of the SCS-CN method to be based on the $(I_a - S)$ scheme, whereas I_a is separate from S. It is noted that the Hawkins model considers the maximum F amount equal to $(I_a + S)$.
5. Substitution of $P = 0$ in Eq. (4.20) yields $Q = 0.05S$, which is impossible. Although equation $P = I_a + F + Q$, where P = Total rainfall, F = Actual infiltration, Q = Direct surface runoff is stated to be valid for $P \geq 0.2S$, Eq. (4.20) carries its impacts by allowing an additional storage space of 20% of S available for water retention at every time level and, in turn, leads to unrealistic negative infiltration at $P \rightarrow 0$. Thus, S at time t ($= S_t$) corresponds to CN at time t ($= CN_t$). Eq. (4.20) therefore needs modification by substitution of 1000 for 1200.

4.6.3 Pandit and Gopalakrishnan (1996) Model

Pandit and Gopalakrishnan (1996) suggested a continuous simulation model for computing the annual runoff for determination of annual pollutant loads. This model is specifically useful for urban areas characterized primarily by the percentage imperviousness, and involves the following steps.

1. Determine the pervious curve number for AMC II.
2. Determine the directly connected impervious area of the urban watershed according to SCS (1956).
3. Estimate the daily runoff depth for both pervious and impervious areas separately using Eq. (4.13).
4. Determine the actual AMC based on the previous 5-day rainfall and modify CN as:

$$CN_{I} = \frac{CN_{II}}{2.281 - 0.01281CN_{II}}; r^2 = 0.996 \text{ and SE} = 1.0 \text{ CN} \qquad (4.27a)$$

$$CN_{III} = \frac{CN_{II}}{0.427 - 0.00573CN_{II}}; r^2 = 0.994 \text{ and SE} = 0.7 \text{ CN} \qquad (4.27b)$$

   CNs are modified such that these do not exceed 98. NEH – 4 identified three antecedent moisture conditions (AMC): AMC I, AMC II, AMC III for dry, normal and wet conditions of the watershed, respectively. As shown in Figure (4.4), AMC I corresponds to the lower enveloping CN, and AMC III the upper enveloping CN. NEH- 4 provides conversion table from CN for AMC II to corresponding CNs for AMC I and AMC III.
5. Calculate the yearly storm runoff depth by summing the runoff for each .day.

In summary, the method is very simple, allows sudden jumps in the CN values and ignores evapotranspiration, drainage contribution and watershed routing. Since routing is ignored, it is useful for small watersheds, where routing is minimal in daily runoff computation. This model is a specific form of the Mishra et al. (1998) model described subsequently.

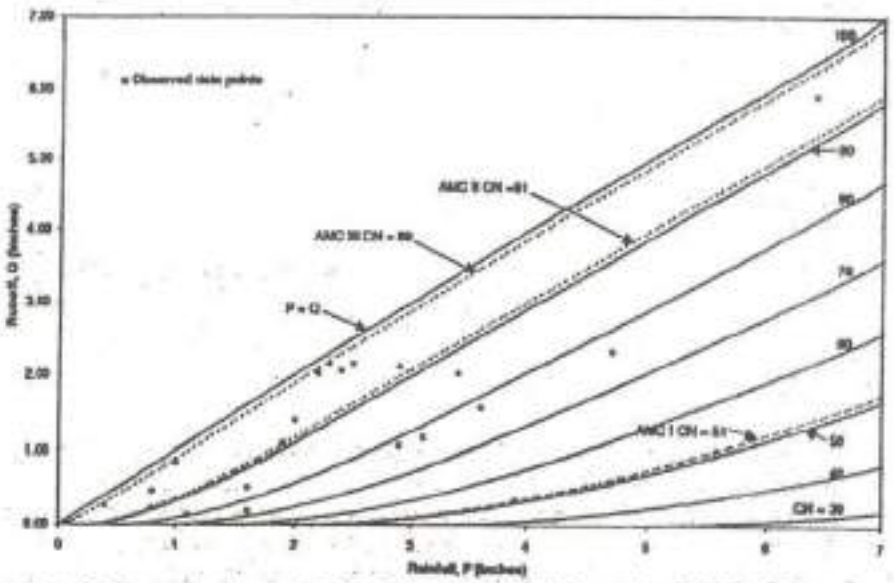

Figure 4.4: Determination of CN for AMC I through AMC III using existing SCS-CN method

4.6.4 Mishra et al. Model

The Mishra et al. (1998) model assumes CN variation with time t dependent on AMC (Ponce and Hawkins, 1996) only. The computed rainfall-excess Q (Eq. 4.13) is transformed to direct runoff amount DO_t using a linear regression approach, analogous to the unit hydrograph scheme. Taking base flow (O_b) as a fraction of F along with the time lag, the total daily flow, Q_t, is computed as the sum of DO_t and O_b. The model parameters are optimized utilizing the objective function of minimizing the errors between the computed and observed data.

The initial value of CN = CN_0 at the start of simulation, an optimized value, corresponds to AMC II. Thus,

$$S_t = S_0 \quad \text{for} \quad S_t \geq S_0 \tag{4.28}$$

where S_0 corresponds to CN_0, derivable from Eq. (4.5).

The potential water retention is defined as the maximum possible pore space available for retention of moisture in the soil store after the loss, which is in the form of evapotranspiration and the outflow in the form of base flow. Potential maximum retention S is the maximum depth of storm rainfall that could potentially be abstracted

by a given site (Ponce and Hawkins, 1996). The potential retention on the current day is calculated by considering the space availability after evapotranspiration and infiltration inputs, as below:

$$S_t = S_{(t-1)} - (1 - b_f)F_{(t-1)} + EV_{(t-1)} \tag{4.29}$$

where S_t = space available for water retention for the current day; S_{t-1} = previous day's potential maximum retention (mm); EV_{t-1} = previous day's evapotranspiration (mm), computed using Penman coefficients taken as 0.8 for June – September, 0.6 for October–January, and 0.7 for February–May; and F_{t-1} = previous day's infiltration (mm), computed using the water balance equation

$$F_{(t-1)} = P_{(t-1)} - I_{a(t-1)} - RO_{(t-1)} \tag{4.30}$$

Here, if $P_{e(t)} \geq 0$, $F_t \geq 0$. The quantity $(1-b_f)\ F_{(t-1)}$ is assumed to be a part of the infiltration available in the soil store on the previous day for balancing the soil storage for moisture retention, and b_f is taken as a factor describing base flow.

Base flow is assumed to be a fraction, b_f, of infiltration F and it is routed to the watershed outlet using the lag and route method as follows:

$$q_{b(t+NLAG)} = b_f F_t \tag{4.31}$$

where NLAG = lag parameter.

The advantage of the above Mishra et al. (1998) model is that it allows the transformation of rainfall-excess to direct runoff and takes into account the base flow, enabling its application to even large basins. The model, however, has the following limitations.

1. It does not distinguish between dynamic and static infiltration, similar to the Williams–LaSeur and Hawkins models.
2. It allows sudden jumps in CN values when changing from one AMC to another AMC level.

3. The use of a linear regression equation invokes the problem of mass balance, for the sum of the regression coefficients is seldom equal to 1.0 in long-term hydrological simulation.
4. The base flow is taken as a fraction of F, which is not rational. The water retained in the soil pores may not be available for base flow, rather the water that percolates down to meet the water table may appear at the outlet as base flow.

Thus, there exists a need for an improved model that eliminates for the most part of these limitations, leading to the formulation of a model based on the modified SCS-CN method (Mishra and Singh, 2002a; Mishra et al., 2003). In the present work, since the SCS–CN concept is utilized for computation of base flow, which is an integral part of total runoff from the watershed, a brief review of baseflow computation is in order.

4.7 BASE FLOW COMPUTATION

Base flow analysis, with a wide availability of methodologies, is a valuable strategy to understand the dynamics of groundwater discharge to streams. Stream flow data is commonly collected and made publicly available, so is amenable to desktop analysis prior to any detailed field investigations. However, it is important to remember that the assumption that base flow equates to groundwater discharge is not always valid. Water can be released into streams over different timeframes from different storages such as connected lakes or wetlands, snow or stream banks. As the hydrographical record represents a net water balance, base flow is also influenced by any water losses from the stream such as direct evaporation, transpiration from riparian vegetation, or seepage into aquifers along specific reaches. Water use or management activities such as stream regulation, direct water extraction, or nearby groundwater pumping can significantly alter the base flow component. Hence, careful consideration of the overall water budget and management regime for the stream is required.

Subsurface runoff analysis considers the movement of water throughout the entire hydrologic cycle. The prediction of subsurface runoff is performed with models of varying complexity depending on the application requirements and constraints. The

models used may be categorized as event-oriented or continuous simulation. Event-oriented models utilize relatively simple techniques for estimating subsurface contributions to a flood hydrograph. Continuous simulation models continuously account for the movement of water throughout the hydrologic cycle. Continuous accounting of water movement involves the consideration of precipitation, snow melt, surface loss, infiltration, and surface transport processes that have been discussed previously. Other processes that need to be considered are evapotranspiration, soil moisture redistribution, and groundwater transport.

A stream hydrograph is the time-series record of stream conditions (such as water level or flow) at a gauging site. The hydrograph represents the aggregate of the different water sources that contribute to stream flow. These components can be subdivided into quick flow and base flow.

(i) Quick flow – the direct response to a rainfall event including overland flow (runoff), lateral movement in the soil profile (interflow) and direct rainfall onto the stream surface (direct precipitation), and;

(ii) Base flow – the longer-term discharge derived from natural storages.

The relative contributions of quick flow and base flow components change through the stream hydrographic record. The flood or storm hydrograph is the classic response to a rainfall event and consists of three main stages (Figure 4.5).

(i) Prior low-flow conditions in the stream consisting entirely of base flow at the end of a dry period;

(ii) With rainfall, an increase in stream flow with input of quick flow dominated by runoff and interflow. This initiates the rising limb towards the crest of the flood hydrograph. The rapid rise of the stream level relative to surrounding groundwater levels reduces or can even reverse the hydraulic gradient towards the stream. This is expressed as a reduction in the base flow component at this stage;

(iii) The quick flow component passes, expressed by the falling limb of the flood hydrograph. With declining stream levels timed with the delayed response of a rising water table from infiltrating rainfall, the hydraulic gradient towards the stream increases. At this time, the base flow component starts increasing. At

some point along the falling limb, quick flow ceases and streamflow is again entirely base flow. Over time, base flow declines as natural storages are gradually drained till the dry period is up and until the next significant rainfall event.

Another complication is that base flow is also influenced by any water losses from the stream. The hydrographic record essentially represents the net balance between gains to and losses from the stream. These losses include direct evaporation from the stream channel or from any connected surface water features such as lakes and wetlands, transpiration from riparian vegetation, evapotranspiration from source groundwater seepages, leakage to the underlying aquifer, or rewetting of stream bank and alluvial deposits (Smakhtin, 2001). These processes are often aggregated into a transmission loss for the reach of the stream. Specific activities that can influence base flow include:

(i) Stream regulation where flow is controlled by infrastructure such as dams or weirs. Releases from surface water storages for downstream users can make up the bulk of stream flow during dry periods. Base flow analysis should be undertaken in unregulated reaches, or at least the regulated catchment area should be no more than 10% of the catchment area of the stream flow gauge (Neal et al. 2004);

(ii) Stream regulation where flow is controlled by infrastructure such as dams or weirs. Releases from surface water storages for downstream users can make up the bulk of stream flow during dry periods. Base flow analysis should be undertaken in unregulated reaches, or at least the regulated catchment area should be no more than 10% of the catchment area of the stream flow gauge (Neal et al. 2004);

(iii) Direct pumping of water from the stream for consumptive uses such as irrigation, urban supply or industry;

(iv) Artificial diversion of water into or out of the stream as part of inter-basin transfer schemes;

(v) Direct discharges into the stream, such as from sewage treatment plants, industrial outfalls or mine dewatering activities;

(vi) Seasonal return flows from drainage of irrigation areas;

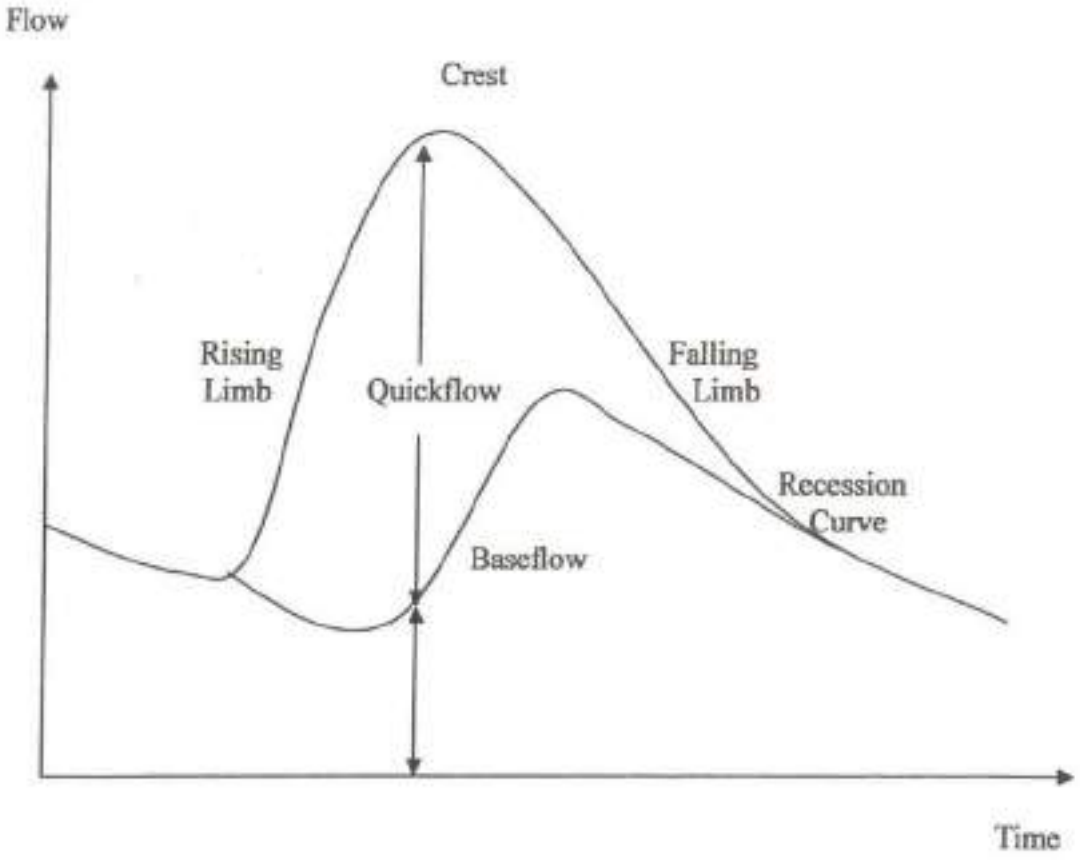

Figure 4.5: Components of a typical flood hydrograph

(vii) Artificial drainage of the floodplain, typically for agricultural or urban development, which can enhance rapid runoff and reduce delayed drainage;

(viii) Changes in land use, such as clearing, re-afforestation or changes in crop type, which can significantly alter evapotranspiration rates;

(ix) Groundwater extraction, sufficient to lower the water table and decrease or reverse the hydraulic gradient towards the stream. Careful consideration of the overall water budget and management regime for the stream is required before the assumption that base flow equates to groundwater discharge can be made.

Several methods for base flow separation are used when actual amount of base flow is unknown. During large storms, the maximum rate of discharge is only slightly affected by base flow, and inaccuracies in separation are fortunately not important.

4.7.1 Base Flow Separation

From the hydrological process view point, baseflow is considered to be that component of the total flow hydrograph that is derived from runoff processes that operate relatively slowly. Thus many of the traditional hydrograph separation approaches have focused on trying to distinguish between rapidly occurring surface runoff, slower moving interflow and even slower discharge from groundwater. However, the conceptual basis for such distinctions can only really apply in small catchments where differential travel times, due to distance from the catchment outlet, play a minor role. In larger catchments the situation is far more complex and hydrograph shapes can be affected by a multitude of processes, some dominated by topography, others by subsurface (soils and geology) characteristics and others by spatial variations in rainfall inputs.

Baseflow separation techniques use the time-series record of stream flow to derive the baseflow signature. The common separation methods are either graphical which tend to focus on defining the points where baseflow intersects the rising and falling limbs of the quickflow response, or involve filtering where data processing of the entire stream hydrograph derives a base flow hydrograph (www.connectedwater.gov.au/framework/baseflow_separation).

4.7.1.1.Graphical Separation Methods

Graphical methods are commonly used to plot the baseflow component of a flood hydrograph event, including the point where the baseflow intersects the falling limb (Figure 4.6). Stream flow subsequent to this point is assumed to be entirely baseflow, until the start of the hydrographic response to the next significant rainfall event. These graphical approaches of partitioning baseflow vary in complexity and include

(i) An empirical relationship for estimating the point along the falling limb where quickflow has ceased and all of the stream flow is baseflow;

$$D = 0.827A^{0.2} \qquad (4.32)$$

where, D is the number of days between the storm crest and the end of quickflow, and A is the area of the catchment in square kilometres. The value of the exponential constant (0.2) can vary depending on catchment characteristics such as slope, vegetation and geology.

(ii) The constant discharge method assumes that baseflow is constant during the storm hydrograph. The minimum stream flow immediately prior to the rising limb is used as the constant value.

(iii) The constant slope method connects the start of the rising limb with the inflection point on the receeding limb. This assumes an instant response in baseflow to the rainfall event.

(iv) The concave method attempts to represent the assumed initial decrease in baseflow during the climbing limb by projecting the declining hydrographic trend evident prior to the rainfall event to directly under the crest of the flood hydrograph (Linsley et al. 1958). This minima is then connected to the inflection point on the receding limb of storm hydrograph to model the delayed increase in baseflow.

(v) Using the trends of the falling limbs before and after the storm hydrograph to set the bounding limits for the baseflow component.

(vi) Using the Boussinesq equation as the basis for defining the point along the falling limb where all of the stream flow is base flow.

4.7.1.2 Filtering Separation Methods

The base flow component of the streamflow time series can also be separated using data processing or filtering procedures. These methods tend not to have any hydrological basis but aim to generate an objective, repeatable and easily automated index that can be related to the base flow response of a catchment. The base flow index (BFI) *or* reliability index, which is the long-term ratio of base flow to total streamflow, is commonly generated from this analysis. Other indices include the mean annual base flow volume and the long-term average daily base flow.

Examples of continuous hydrographic separation techniques based on processing or filtering the data record include;

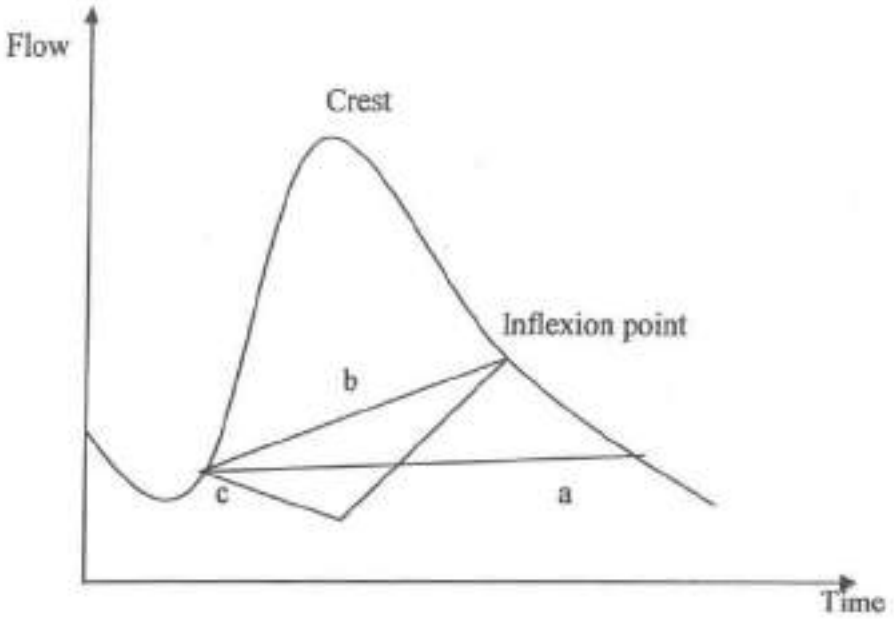

Figure 4.6: Graphical base flow separation techniques including (a) constant discharge method, (b) constant slope method, (c) concave method

1. Increasing the base flow at each time step, either at a constant rate or varied by a fraction of the runoff;
2. The smoothed minima technique which uses the minima of 5-day non-overlapping periods derived from the hydrograph. The baseflow hydrograph is generated by connecting a subset of points selected from this minima series. The HYSEP hydrograph separation program uses a variant of this called the local-minimum method;
3. The fixed interval method discretises the hydrographic record into increments of fixed time. The magnitude of the time interval used is calculated by doubling (and rounding up) the duration of quickflow. The baseflow component of each time increment is assigned the minimum stream flow recorded within the increment;
4. The sliding-interval method assigns a baseflow to each daily record in the hydrograph based on the lowest discharge found within a fixed time period before and after that particular day;
5. Recursive digital filters, which are routine tools in signal analysis and processing, are used to remove the high-frequency quickflow signal to derive the low-

frequency baseflow signal. Table 4.2 outlines some of the digital filters that have been applied to smooth hydrographic data. Eckhardt (2005) has developed a general formulation that can devolve into several of the commonly used one-parameter filters:

$$q_{b(i)} = \frac{(1 - BFI_{max})aq_{b(i-1)} + (1 - a)BFI_{max}q_i}{1 - aBFI_{max}} \quad (4.33)$$

where, $q_{b(i)}$ is the baseflow at time step i, $q_{b(i-1)}$ is the baseflow at the previous time step i-1, q_i is the stream flow at time step i, a is the recession constant and BFI_{max} is the maximum value of the baseflow index that can be measured; and

6. The streamflow partitioning method uses both the daily record of streamflow and rainfall. Baseflow equates to streamflow on a given day, if rainfall on that day and a set number of days previous is less than a defined rainfall threshold value. Linear interpolation is used to separate the quickflow component during high rainfall events.

where:

- $q_{(i)}$ is the original stream flow for the i^{th} sampling instant
- $q_{b(i)}$ is the filtered base flow response for the i^{th} sampling instant
- $q_{f(i)}$is the filtered quick flow for the i^{th} sampling instant
- $q_{(i-1)}$ is the original stream flow for the previous sampling instant to i
- $q_{b(i-1)}$is the filtered base flow response for the previous sampling instant to i
- $q_{f(i-1)}$is the filtered quick flow for the previous sampling instant to i
- k is the filter parameter given by the recession constant
- α, α_q are filter parameters
- C is a parameter that allows the shape of the separation to be altered
- γ, c_1, c_3 are physically based parameters

Along with the above methods for base flow separation, there are also other methods to calculate base flow as, for example, given below:

Table 4.2: Recursive digital filters used in base flow analysis (Grayson *et al*, 1996; Chapman, 1999; Furey and Gupta, 2001)

Filter Name	Filter Equation	Source	Comments
One-parameter algorithm	$q_{b(i)} = \frac{k}{2-k} q_{b(i-1)} + \frac{1-k}{2-k} q_{(i)}$	Chapman and Maxwell (1996)	$q_{b(i)} \leq q_{(i)}$ Applied as a single pass through the data.
Boughton two-parameter algorithm	$q_{b(i)} = \frac{k}{1+C} q_{b(i-1)} + \frac{C}{1+C} q_{(i)}$	Boughton (1993) Chapman and Maxwell (1996)	$q_{b(i)} £ q_{(i)}$ Applied as a single pass through the data Allows calibration against other base flow information such as tracers, by adjusting parameter C
IHACRES three-parameter algorithm	$q_{b(i)} = \frac{k}{1+C} q_{b(i-1)} + \frac{C}{1+C}\left(q_{(i)} + \alpha_s q_{(i-1)}\right)$	Jakeman and Homberger (1993)	Extension of Boughton two-parameter algorithm
Lyne and Hollick algorithm	$q_{f(i)} = \alpha q_{f(i-1)} + \left(q_{(i)} - q_{(i-1)}\right)^* \frac{1+\alpha}{2}$	Lyne and Hollick (1979) Nathan and McMahon, (1990)	$q_f(i) \leq 0$ α a value of 0.925 recommended for daily stream data .filter recommended to be applied in three passes Base flow is $q_b = q - q_f$
Chapman algorithm	$q_{f(i)} = \frac{3\alpha - 1}{3-\alpha} q_{f(i-1)} + \frac{2}{3+\alpha}\left(q_{(i)} - \alpha q_{(i-1)}\right)$	Chapman (1991) Mau and Winter (1997)	Baseflow is $q_b = q - q_f$
Furey and Gupta filter	$q_{b(i)} = (1-\gamma) q_{b(i-1)} + \gamma \frac{c_2}{c_1} * \left(q_{(i-d-1)} - q_{b(i-d-1)}\right)$	Furey and Gupta (2001)	Physically-based filter using mass balance equation for baseflow through a hillside

1. It is known that infiltration depends on rainfall. Therefore, if P – I_a is less than the gravitational infiltration F_c on a given day, then F_c = P - I_a and direct surface runoff ROt = 0 or dynamic infiltration Fd_t= 0. It implies that F_c exists even prior to the satisfaction of the capillary demand, which is in contrast with reality. This is because of the assumed equivalence between F_c and the minimum infiltration rate

at a time approaching infinity. Considering that the water infiltrating after saturation through F_c percolates down to the water table, it finally appears at the outlet of the basin with assumptions that the basin boundary coincides with the aquifer boundary and no lateral flow contributes to the water table from across the defined watershed boundary. Thus, applying continuity and storage equations, the baseflow (O_b) can be computed as:

$$O_{b(t+\Delta t)} = g_0 F_{a(t)} + g_1 F_{a(t)} + g_2 O_{b(t)} \quad (4.34)$$

where,

$$g_0 = \frac{\Delta t / K_b}{2 + \Delta t / K_b}; \quad (4.35a)$$

$$g_1 = g_0; \quad (4.35b)$$

$$g_2 = \frac{2 - \Delta t / K_b}{2 + \Delta t / K_b}; \quad (4.35c)$$

K_b is the base flow storage coefficient [T]; and g_0, g_1, g_2 are the base flow routing coefficients.

2. The concept behind the SCS – CN method can also be applied to determination of surface drainage flow from rainfall (Yuan et. al., 2001). The work of Andrews (1954) and Mockus (1964) was the basis for the generalized SCS rainfall-runoff relationship, which can be expressed as follows: when accumulated natural runoff is plotted against accumulated natural rainfall, runoff starts after some rainfall has accumulated, and the line of the relation curve becomes asymptotic to a line of 45° slope, as illustrated in Figure 4.7.

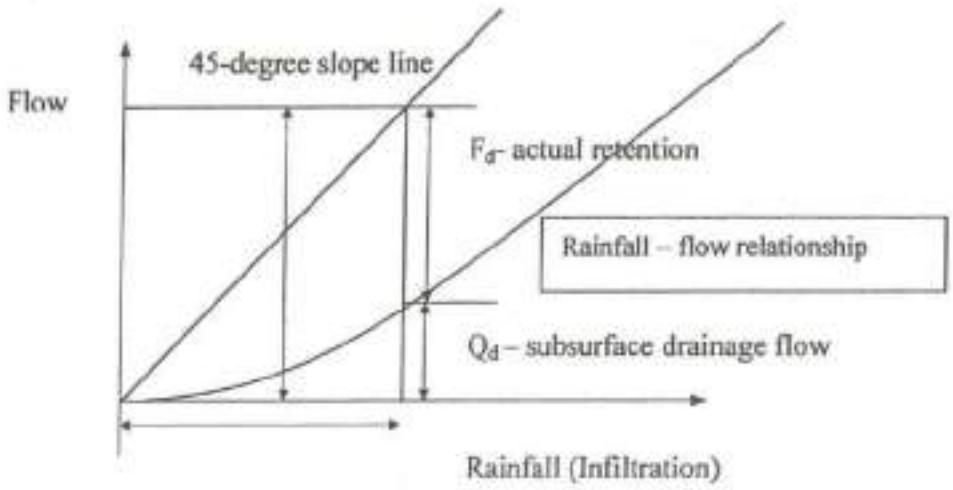

Figure 4.7: Typical rainfall and flow relationship (Source: Yuan et al., 2001)

By analogy, for subsurface drainage flow, equation becomes:

$$\frac{F_r}{S_d} = \frac{Q_d}{F} \tag{4.36}$$

where F_r = actual retention after flow begins, S_d = potential maximum retention of watershed, Q_d = drainage flow depth ($F > Q_d$), and F= infiltration depth.

If there are no initial abstractions, or if one begins the water accounting after initial abstractions, then Eq. (4.36) can be rewritten as:

$$\frac{F - Q_d}{S_d} = \frac{Q_d}{F} \tag{4.37}$$

However, initial abstractions, in the form of soil moisture changes, must be considered, and the amount of infiltration available for drainage flow is $F - \Delta S_m$. By substituting $F - \Delta S_m$ for F in Eq. (4.37), the following equation results:

$$\frac{F - \Delta S_m - Q_d}{S_d} = \frac{Q_d}{F - \Delta S_m} \tag{4.38}$$

where F = infiltration depth, ΔS_m = soil moisture storage, Q_d = drainage flow depth ($F > Q_d$), S_d = potential maximum retention of watershed. If no surface runoff occurs, then:

$$F = P - I_a \tag{4.39}$$

where P = rainfall depth ($P > I$), I_a = interception. If surface runoff occurs, then

$$F = P - I_a - Q_s \tag{4.40}$$

where P = rainfall depth ($P > I$) , I_a = interception, Q_s = surface runoff.

If, for simplicity, we assume that there is no surface runoff and substitute Eq. (4.39) into Eq. (4.38), we obtain:

$$\frac{P - I_a - \Delta S_m - Q_d}{S_d} = \frac{Q_d}{P - I_a - \Delta S_m} \tag{4.41}$$

If we assume,

$$I_d = I_a + \Delta S_m \tag{4.42}$$

where I_d is the initial abstraction for subsurface drainage flow. A substitution of Eq. (4.42) into Eq. (4.41) yields

$$\frac{P - I_d - Q_d}{S_d} = \frac{Q_d}{P - I_d} \tag{4.43}$$

Solving for Q_d results in

$$Q_d = \frac{(P - I_d)^2}{P - I_d + S_d} \qquad (P > I_d) \tag{4.44}$$

$$Q_d = 0 \qquad (P < I_d) \tag{4.45}$$

Eq. (4.44) and (4.45) can be used to estimate subsurface flow (Q_d) from storm rainfall. If surface runoff occurs then Eq. (4.41) can be written as:

$$\frac{P - I_a - Q_s - \Delta S_m - Q_d}{S_d} = \frac{Q_d}{P - I_a - Q_s - \Delta S_m} \tag{4.46}$$

Solving Eq. (4.46) for Q_d results in,

$$Q_d = \frac{(P - I_d - Q_s)^2}{P - I_d - Q_s + S_d} \qquad (P > I_d) \tag{4.47a}$$

$$Q_d = 0 \qquad (P < I_d) \tag{4.47b}$$

Eq. (4.47) can be used for computation of base flow. The methodology proposed here for base flow computation is largely based on this concept and its development is discussed in the forthcoming section.

4.8 PROPOSED LONG-TERM SIMULATION MODEL

Based on the existing SCS–CN method, a new method is proposed for long-term hydrologic simulation. Here the direct surface runoff is computed based on the SCS – CN based hydrological simulation and it is routed to the outlet of the catchment. Since the SCS – CN method is an infiltration loss model, a portion of the infiltration is taken as base flow, as described above. The total runoff is the sum of the surface runoff and base flow.

4.8.1 Computation of Direct Surface Runoff

Replacing Q by RO (surface runoff) in Eq. (4.4) can be rewritten (for clarity in text) for daily runoff with time t as subscript) yields,

$$RO_{(t,t+\Delta t)} = \frac{(P_{(t,t+\Delta t)} - I_{a(t)})^2}{P_{(t,t+\Delta t)} - I_{a(t)} + S_t} \tag{4.48}$$

where,

$$I_{a(t)} = \lambda S_t \tag{4.49}$$

$$S_t = \frac{25400}{CN_t} - 254 \tag{4.50}$$

Equation (4.48) is valid for $P_{(t,t+\Delta t)} \geq I_{a(t)}$, $RO_{(t,t+\Delta t)} = 0$ otherwise. Here P = total rainfall, I_a = initial abstraction, S = potential maximum retention, and λ = initial abstraction coefficient.

4.8.2 Soil Moisture Budgeting

The total infiltration (F) consists of static infiltration component (Q_d) and dynamic infiltration component (F_t) (Mishra.et.al, 2004) as shown in Fig. 4.8. The

dynamic infiltration component of infiltration that occurred during the time period can be computed from water balance equation as:

$$F_{r(t,t+\Delta t)} = F_{(t,t+\Delta t)} - Q_{d(t,t+\Delta t)} \quad (4.51)$$

where,

$$F_{(t,t+\Delta t)} = P_{(t,t+\Delta t)} - I_{a(t)} - RO_{(t,t+\Delta t)} \quad (4.52)$$

which is valid for $RO_{(t,t+\Delta t)} \geq 0$, $F_{r(t,t+\Delta t)} = 0$ otherwise. The term $F_{r(t,t+\Delta t)}$ also represents an increase in the amount of soil moisture in the soil profile during the time period, which when added to its antecedent moisture leads to the antecedent moisture amount for the next day as:

$$M_{(t,t+\Delta t)} = M_{(t)} + F_{r(t,t+\Delta t)} - ET_{(t,t+\Delta t)} \quad (4.53)$$

where $M_{(t,t+\Delta t)}$ varies from 0 to S_{abs}, S_t can be modified for the next day by balancing the soil moisture as:

$$S_{(t+\Delta t)} = S_{(t)} - M_{(t+\Delta t)} \quad (4.54)$$

4.8.3 Computation of Evapotranspiration

The daily evapotranspiration (ET) can be computed using the pan evaporation as:

$$PET_{(t,t+\Delta t)} = PANC \times E_{(t,t+\Delta t)} \quad (4.55)$$

where E is the pan evaporation based on field data and PANC is the pan coefficient, assumed as 0.8 for June – September, 0.6 for October – January and 0.7 for February – May in this study.

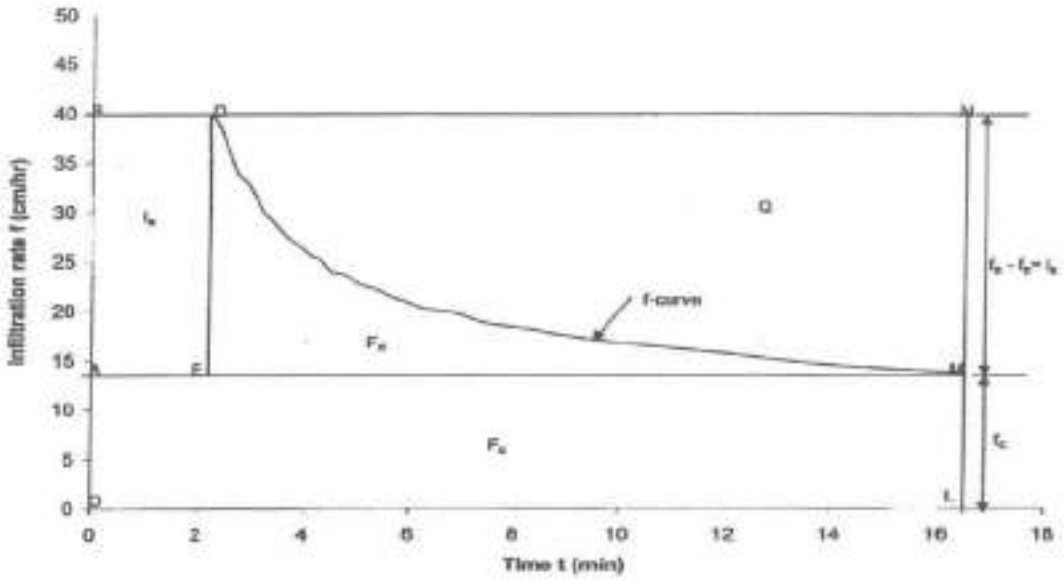

Figure 4.8: A descriptive infiltration curve of Columbia sandy loam (Mishra and Singh, 2003)

4.8.4 Base Flow

Based on the general hypothesis of SCS – CN method, base flow is computed as:

$$Q_{d(t,t+\Delta t)} = \frac{(P_{(t,t+\Delta t)} - I_{a(t)} - RO_{(t,t+\Delta t)} - I_{d(t)})^2}{P_{(t,t+\Delta t)} - I_{a(t)} - RO_{(t,t+\Delta t)} - I_{d(t)} + S_d} \quad (4.56)$$

where

$$I_{d(t)} = \lambda S_{d(t)} \quad (4.57)$$

$$S_{d(t)} = \frac{25400}{CN_{dt}} - 254 \quad (4.58)$$

Eq. (4.56) is valid for $(P_{(t,t+\Delta t)} - I_{a(t)} - RO_{(t,t+\Delta t)}) \geq I_{d(t)}$, $Q_{d(t,t+\Delta t)} = 0$ otherwise. Here RO = direct surface runoff, I_d = initial abstraction, S_d = potential maximum retention, and λ = initial abstraction coefficient for subsurface drainage.

The initial abstraction for drainage flow depends on the soil moisture storage, S_d or (CN_d) for next day is varied by balancing the soil moisture storage follows:

$$S_{d(t+\Delta t)} = S_{d(t)} - \left(M_{(t+\Delta t)} - M_{(t)}\right) \tag{4.59}$$

4.8.5 Flow Routing

Based on the principle of continuity and storage equations, the daily rainfall excess is routed to the outlet of the catchment using single linear reservoir (Mishra and Singh, 2004) as:

$$R - O = \frac{\Delta S}{\Delta t} \tag{4.60}$$

$$S = KO \tag{4.61}$$

where K = storage coefficient (day); R = inflow (mm/day); O = outflow (mm/day); S = storage (mm). Here, the time step is considered as one-day interval. Δt /K is defined as the Courant number (Ponce, 1989). The rainfall excess RO_t corresponding to P_e can be computed only if rainfall P exceeds initial abstraction (I_a), it is otherwise zero. Then RO_t is routed to the outlet of the basin using the single linear reservoir as below:

$$DO_{(t+\Delta t)} = C0RO_t + C1RO_{t-1} + C2DO_{t-1} \tag{4.62}$$

where

$$C0 = \frac{COUR}{2 + COUR} \tag{4.63a}$$

$$C1 = C0 \tag{4.63b}$$

$$C2 = \frac{2 - COUR}{2 + COUR} \tag{4.63c}$$

$$COUR = \frac{1}{K} \tag{4.64}$$

In Eqs. (4.63a-c), COUR = courant number.

It is known that infiltration depends on rainfall. Therefore, if P- I_a is less than F on a given day, then F = P- I_a. It emphasized that under such situation, $RO_t = 0$. Applying Eq. (4.62), base flow can be computed as:

$$Q_{b(t+\Delta t)} = C0Q_{dt} + C1Q_{d(t-1)} + C2Q_{b(t-1)} \quad (4.65)$$

where

$$C0 = \frac{COUR}{2 + COUR} \quad (4.66a)$$

$$C1 = C0 \quad (4.66b)$$

$$C2 = \frac{2 - COUR}{2 + COUR} \quad (4.66c)$$

$$COUR = \frac{1}{K_b} \quad (4.67)$$

In Eqs. (4.66a-c), K_b is the base flow storage coefficient.

Thus, the total runoff hydrograph, "O" appearing at the outlet of the catchments is computed as the sum of the routed rainfall excess, DO, and the base flow, O_b. Expressed mathematically as:

$$O_t = DO_{(t)} + O_{bt} \quad (4.68)$$

which actually represents the computed total runoff hydrograph.

4.9 MODEL PARAMETERS

The proposed model has parameters CN, CN_d, K [T] and K_b [T]. The parameter CN represents the curve number on the simulation, assuming that the maximum pore space is available in the soil for water storage or retention on that day of simulation. The curve number can vary from 0 to 100. CN_d is the curve number for the drainage flow and it depends on the soil moisture storage. It also varies from 0 to 100. Parameter K represents the storage coefficient of the surface runoff hydrograph and is analogous to the time lag of the watershed. Parameter K_b, represents the storage coefficient of the base flow appearing at the outlet of the watershed.

4.10 APPLICATION

4.10.1 Study Area and Data Availability

The SCS-CN model is applied to daily rainfall-runoff data of Ramganga catchment. Apart from this catchment, the proposed model is also applied to different

catchments falling under different climatic and geographic settings of India. The daily monsoon (June–November) data of the catchments, Hemavati, a tributary of River Cauvery in Karnataka state; Hridaynagar, Manot, and Mohegaon catchments, tributaries of River Narmada in Madhya Pradesh; Kalu catchment, a tributary of River Ulhas, in Maharashtra; and Ghodahado catchment, a tributary of River Rushikulya, in Orissa, State of India, observed at respective gauging stations are used in the analysis. A detailed description about these catchments has been provided in Chapter 2. However, the hydro-meteorological and other essential data pertaining to the present study has also been described here as follows. Data availability for all the study catchments as described as follows.

4.10.1.1 Ramganga Catchment

The climatic condition of the river basin is largely influenced by the orographic effect. The area receives the majority of precipitation in the form of rainfall. The daily rainfall and evaporation data were available from 1985 to 1990 (five years). The runoff data is available for the same period. These data have been processed for the application of the model.

(a) **Rainfall:** The Ramganga valley experiences approximately an annual precipitation of 1,550 mm. The raingauge network consists of Ranikhet, Chaukhutia, Naula, Marchulla, Lansdowne and Kalagarh besides the other existing stations.

(b) **Evaporation:** The daily pan evaporation data are available for the catchment, but for a limited period only.

(c) **Runoff:** Stream flow records of the Ramganga River, including river stages, instantaneous as well as monthly, are available at Kalagarh.

4.10.1.2 Other Indian Catchments

The data used in the present study include daily rainfall, evaporation, and runoff for a total length ranging from 5 to 10 years. For Hemavati catchment, data of five years (June 1974–May 1979) were collected and for Kalu catchment, daily rainfall, evaporation, and stream gauge records of four years (1990–1993) were used,

but only during monsoon period (June to November). Daily rainfall, evaporation, and runoff data for nine years (June 1981 –May 1990) were available for Manot catchments. For Mohegan catchments, the data were available for eight years (June 1981 – May 1989), and for Hridayanagar catchments, these were for eight years (June 1981 – May 1989). These are used in the study. For Ghodahado, the data available for June 1993–May 1996 and June 1987–May 1989 are used in the analysis. A time step of one day is used in simulation. Table 4.3 presents the area and the data length used in model calibration and validation for each catchment.

Table 4.3: Catchments area and data used in model calibration and validation

Catchment	Area (sq. km)	Data length	
		Calibration	Validation
Hemavati	600	1974 - 1977 (3 years)	1977 - 1979 (2 years)
Manot	5032	1981 - 1986 (5 years)	1986 - 1990 (4 years)
Hridaynagar	3370	1981 - 1986 (5 years)	1986 - 1990 (4 years)
Mohegaon	4661	1981 - 1985 (5 years)	1986 - 1989 (3 years)
Kalu	224	1990 - 1992 (3 years) Monsoon period	1993 (1 year) Monsoon period
Ghodahado	138	1993 - 1996 (3 years)	1987 - 1989 (2 year)

4.10.2 Parameter Estimation

The application of the proposed SCS – CN based long term hydrological simulation model requires daily data of rainfall, runoff and evaporation of the above described watersheds. The proposed model has four parameters CN, CN_d, K [T] and K_b[T]. The optimal estimates of model parameters were obtained by using the non-linear Marquardt algorithm (Mishra and Singh, 2003) coupled with trial and error.

Although these parameters can be determined by trial and error for obtaining the maximum efficiency, it is also possible to derive these parameters physically or from rainfall– runoff data. As also discussed earlier in section 4, the parameter CN represents the curve number in runoff simulation, assuming that the maximum pore space is available in the soil for water storage or retention on that day of simulation. The curve number can vary from 0 to 100. CN_d is the curve number for the drainage flow and it depends on the soil moisture storage. It also varies from 0 to 100.

Parameter K represents the storage coefficient of the surface runoff hydrograph and is analogous to the time lag of the watershed. It can also be derived from the rainfall–runoff data by plotting them on a semi-logarithmic paper. The slope of the fit represents K. The rainfall–runoff data set selected for the derivation should correspond to high rainfall–runoff events excluding base flow. Similarly, parameter K_b, which represents the storage coefficient of the base flow appearing at the outlet of the watershed, can be derived for low rainfall–runoff events or using other methods suggested in standard text books, for example, in the text books by Ponce (1989), Singh (1992) and Singh and Singh (2001), among others.

For describing the range of variation of these parameters, the lower bound is taken as zero, because all the parameters are physically non-negative. The upper bound values are, however, decided from the trial runs whether the estimated parameter values are well within the supplied range. If the estimated parameter value corresponds to the upper bound of the described range, the upper bound is increased to the extent that the estimate falls in the prescribed range. The ranges/values of parameters selected for trials and optimization are given in Table 4.4.

Table 4.4: Ranges and Initial Estimates of Model Parameter

Parameters		CN	CN_d	K	K_b
Range		0.001-99.999	0.001-99.999	0.001 - 5.0	1 - 360
Initial value	Ramganga	99	80	0.01	20
	Hemavati	98.9	95	0.1	30.5
	Manot	85	76.9	0.91	15
	Hridaynagar	65	60	0.9	21
	Mohegaon	80	70	0.80	20
	Kalu	85	70	0.05	10.5
	Ghodahado	90	80	0.1	10

4.10.3 Model Efficiency

The efficiency (Nash and Sutcliffe, 1970) of both models is computed using the expression as:

$$\text{Efficiency} = \left[1-\left(\frac{RV}{IV}\right)\right]\times 100 \tag{4.69}$$

where,

$$RV = \sum_{i=1}^{n}\left(Q_i - \hat{Q}_i\right)^2 \tag{4.70a}$$

$$IV = \sum_{i=1}^{n}\left(Q_i - \bar{Q}_i\right)^2 \tag{4.70b}$$

where RV = remaining variance; IV = initial variance; Q_i = observed runoff for i^{th} day; $\hat{Q}_i$ = computed runoff for i^{th} day; n =total number of observations; and $\overline{Q}_i$ = overall mean daily runoff. Efficiency is used for evaluating the model performance. Efficiency varies at the scale of 0 to 100. It can also assume a negative value if RV > IV, implying that the variance in the observed and computed values is greater than the model variance. The efficiency of 100 implies that the computed values are the same as the observed ones, which is the perfect fit.

The Relative Error (RE) is also computed to see the deviation between the observed and simulated runoff, with respect to the observed runoff and it is determined as:

$$RE\ (\%) = \left(\frac{Q_{obs} - Q_{comp}}{Q_{obs}}\right)\times 100 \tag{4.71}$$

Here, Q_{obs} = observed runoff and Q_{comp} = simulated runoff. The higher RE is indicative of greater deviation from the observed, and vice versa.

4.10.4 Model Calibration and Validation for Ramganga Catchment

For model calibration and validation, the available five years data set of Ramganga catchment was split into two parts. For calibration, three years (1985 – 1988) of data have been considered. The estimated values of the four parameters (CN, CN_d, K and K_b) along with their initial values and model efficiencies in calibration are given in the Table 4.5. It is apparent from the table that the values of the parameters

CN, CN_d, and K decrease as the number of years data increase from 1- 3 years, and vice versa holds for K_b. From the results due to 3-year dataset, it is also seen that the CN value of the watershed is of the order of 80, indicating a good runoff producing watershed; CN_d of the order of 74, which is lower than CN indicating less baseflow production potential than the runoff generation from rainfall; K of the order of 2 days, a reasonable value of the lag in runoff hydrograph for Ramganga catchment (catchment area = 3134 sq. km); and K_b of the order of 30 days, which is also reasonable for mid-size watershed.

The resulting efficiencies are seen to vary from 81.82 to 73.62%, as the number of years of data varies from 1- 3 years. Though the efficiencies show a decreasing trend with the increase in the data length, these are indicative of adequate and satisfactory performance of the proposed model in calibration. Then taking the initial and final parameter values corresponding to three years of data in model calibration (Table 4.5), the model was tested on the remaining two years (1988- 90) data. The resulting efficiency of two year data was found to 75.46% which indicates a satisfactory model performance. The daily variation of observed and computed runoff along with the rainfall is depicted in Figs. 9-11 for calibration and in Figs. 12-13 for validation.

As seen from Figures. 4.9-4.11, the computed runoff fairly simulated the observed runoff, except for a few peaks in years 1985 (Figure 4.9) and 1986 (Figure 4.10). From these three figures, it is interesting to note that the computed non-monsoon flows closely follow the trend exhibited by the observed runoff, indicating the satisfactory performance of the proposed SCS-CN-based base flow model (Section 4.8).

Similar to the above trends can be observed from the Figures. 4.12 and 4.13 that show the validation results of the proposed model. Except for two largest runoff peaks in both the years 1988 (Figure 4.12) and 1989 (Figure 4.13), the computed runoff closely matches the observed runoff values, indicating again that the model performs satisfactorily on the data of Ramganga catchment, and there, is suitable for this catchment.

To further test the proposed model applicability to Ramganga catchment, the percent relative errors (Eq. 4.71) were computed and these are shown in Table 4.6. In this table, the resulting positive and negative values of the relative errors, respectively, show the underestimation and over-estimation of the yearly runoff by the

proposed model. Apparently, except for 1987-88, the model has under-estimated the yearly runoff in all the years. The relative error values are seen to vary from 8.92 to ±29.66%, which indicate a reasonably satisfactory performance of the proposed model in yearly runoff computation.

Table 4.5: Parameters from Simulation of Different Time Periods

No of years of data used in simulation	Parameters (Calibration)				
	CN	CN_d	K	K_b	Efficiency (%)
	Initial Estimate				
	99	80	0.01	20	
	Final Estimate				
1	83.88	76.82	2.29	24.32	81.82
2	81.73	76.62	2.5	30.55	76.95
3*	80.38	74.4	2.25	30.99	73.62

*used as calibration dataset

Table 4.6: Observed and Simulated Runoff and Computed Relative Error

Year	Observed runoff (mm)	Simulated runoff (mm)	Relative Error (%)
1985 – 86	675.63	585.75	13.30
1986 – 87	539.36	491.26	8.92
1987 – 88	270.54	350.78	-29.66
1988 – 89	641.42	524.66	18.20
1989 – 90	443.40	397.71	10.30
Average	514.07	470.03	8.57

4.10.5 Sensitivity Analysis

The purpose of such an analysis lies in distinguishing the parameters that are more sensitive, for their cautious and judicious derivation and employment in the field. Therefore, to assess the sensitivity of the above described four parameters of the model, a sensitivity analysis is carried out. To this end, the parameters calibrated for the year 1985 – 88 were varied for evaluating the impact of their variation on the model performance described above in terms of efficiency resulting from the model application to calibration dataset. For sensitivity, all the parameters were varied from

±5% to ±30%, and the corresponding efficiency computed. The changes in efficiency due to variation in the four parameters are shown in Figures. 4.14 to 4.17 and these are discussed below.

An increase in the value of parameter CN by ±30% of the calibrated value (Table 4.5) results into efficiencies varying in the range of 73.678% to 66.717% (Figure 4.14). Notably, there is not much change in the efficiency as the parameter (CN) value increased up to 20%, but further increasing in the value shows a sudden drop in the efficiency (73.66 to 66.72%). On the other hand, the second parameter CN_d appears to be less sensitive than CN (Figure 4.15), for the efficiency varies a little with the change in the parameter value by the same extent. It can be seen that the variation of CN_d from ±5 to ±30% leads to change in efficiencies in the range 73.68 – 73.66%, which exhibits a much lesser range than that due to CN. From Figure 4.15, it is apparent that the efficiency does not change significantly, only from 73.68% to 73.56% with an increase or decreased in the K values by the same (as above) extent. Thus the parameter is less sensitive than CN. A reduction or increase in K implies that the computed rainfall- excess is allowed to reach the outlet earlier or later than required and it results in the decrease in the model efficiency. Figure 4.17 shows a variation in efficiency (from 73.678% to 73.66%) with an increase in the value of parameter K_b by ±30. Here also the graph shows the less sensitivity of the parameter K_b than CN and K. From all the figures (4.9- 4.17) it is clear that the four parameters are sensitive in the following order: $CN > K > CN_d > K_b$.

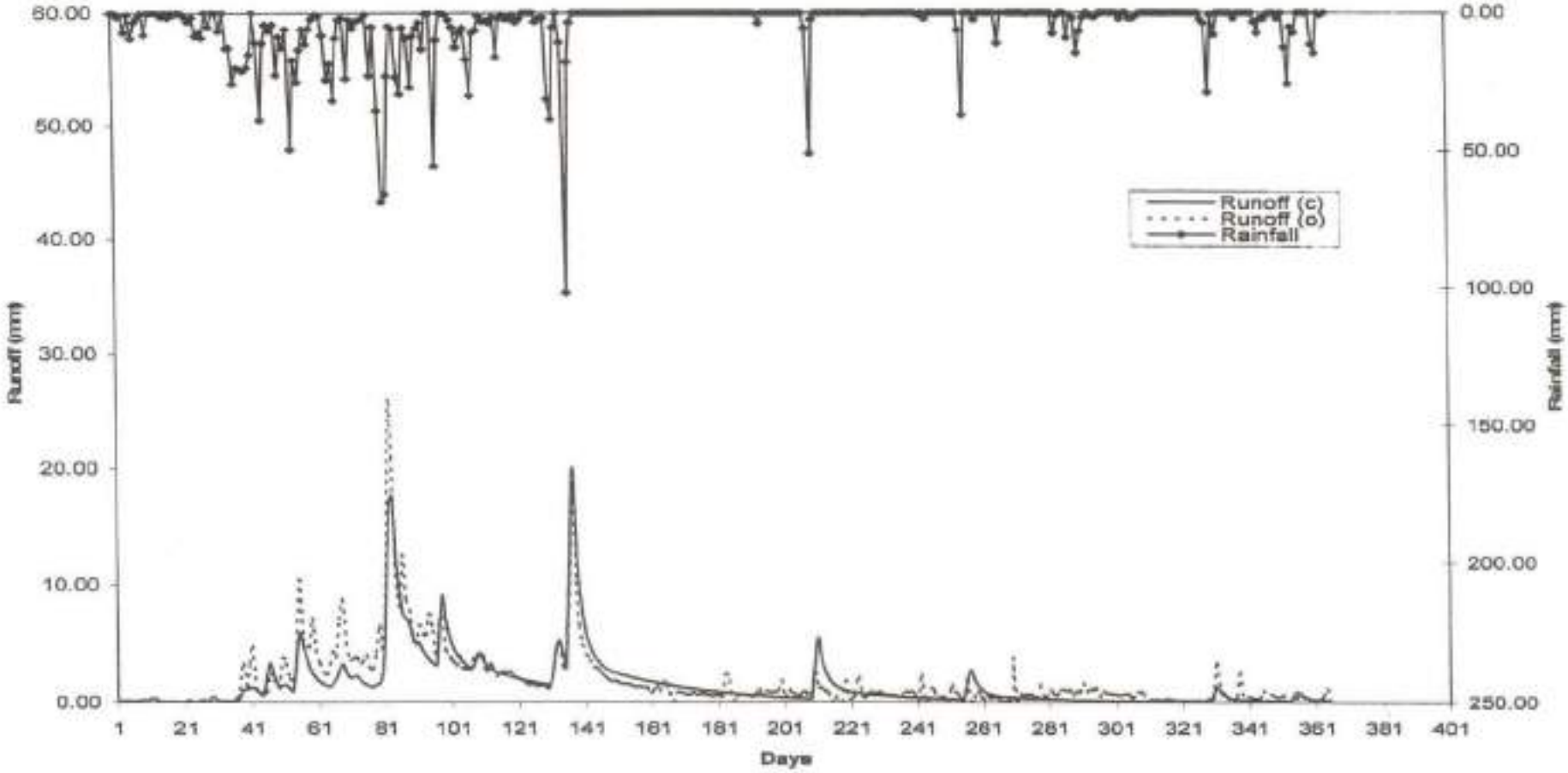

Figure 4.9: Model calibration for Ramganga catchment (June 1985- May 1986) Day 1 represents June 1, 1985

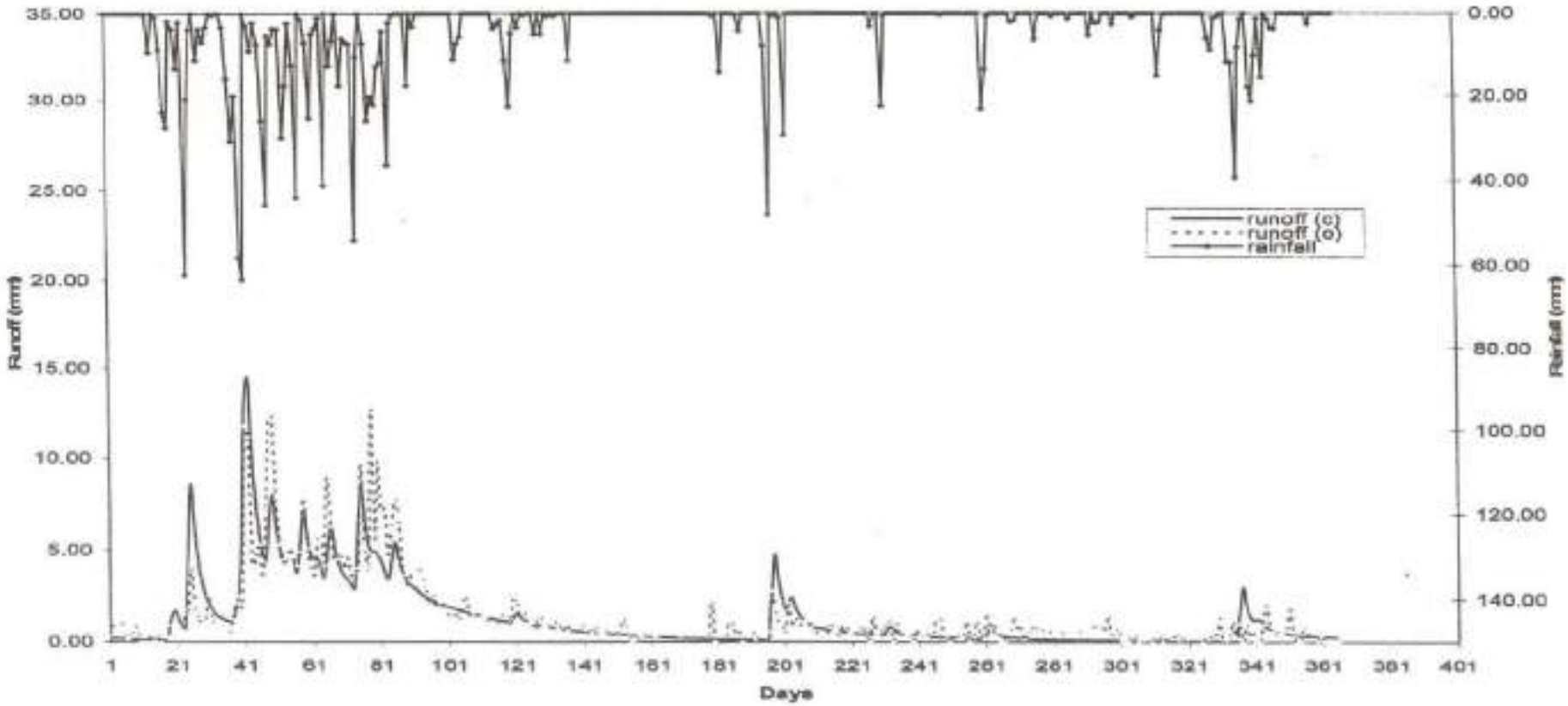

Figure 4.10: Model calibration for Ramganga catchment (June 1986- May 1987) Day 1 represents June 1, 1986

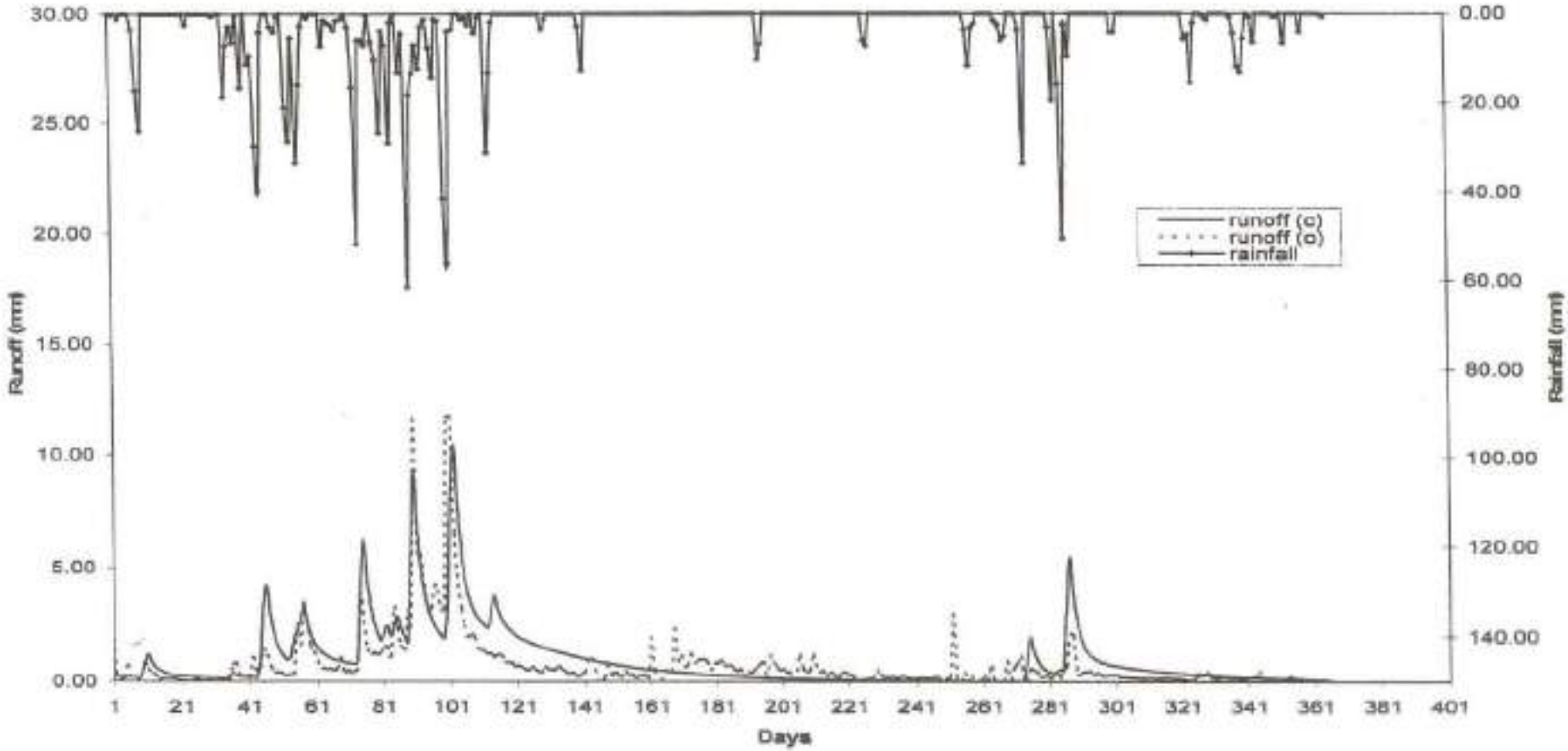

Figure 4.11: Model calibration for Ramganga catchment (June 1987- May 1988) Day 1 represents June 1, 1987

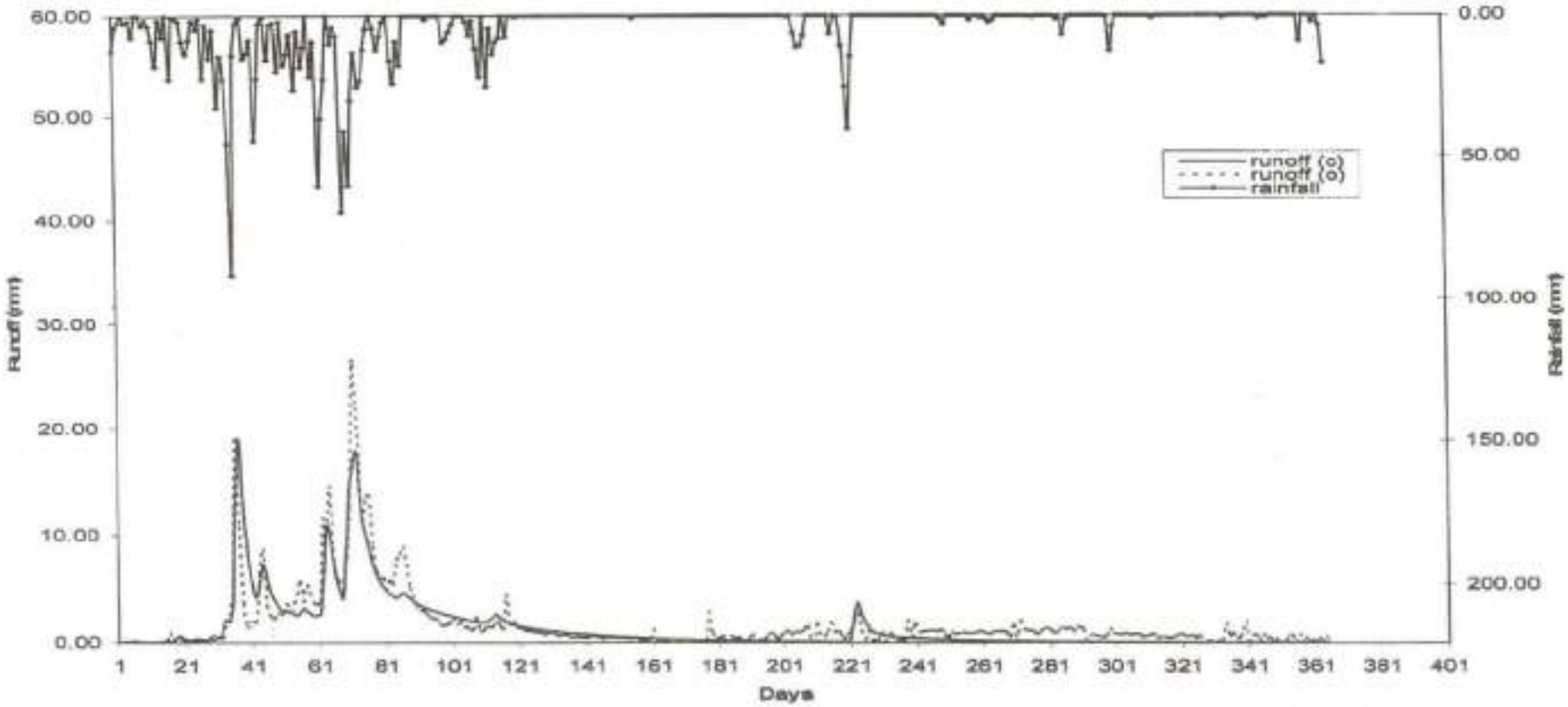

Figure 4.12: Model validation for Ramganga catchment (June 1988- May 1989) Day 1 represents June 1, 1988

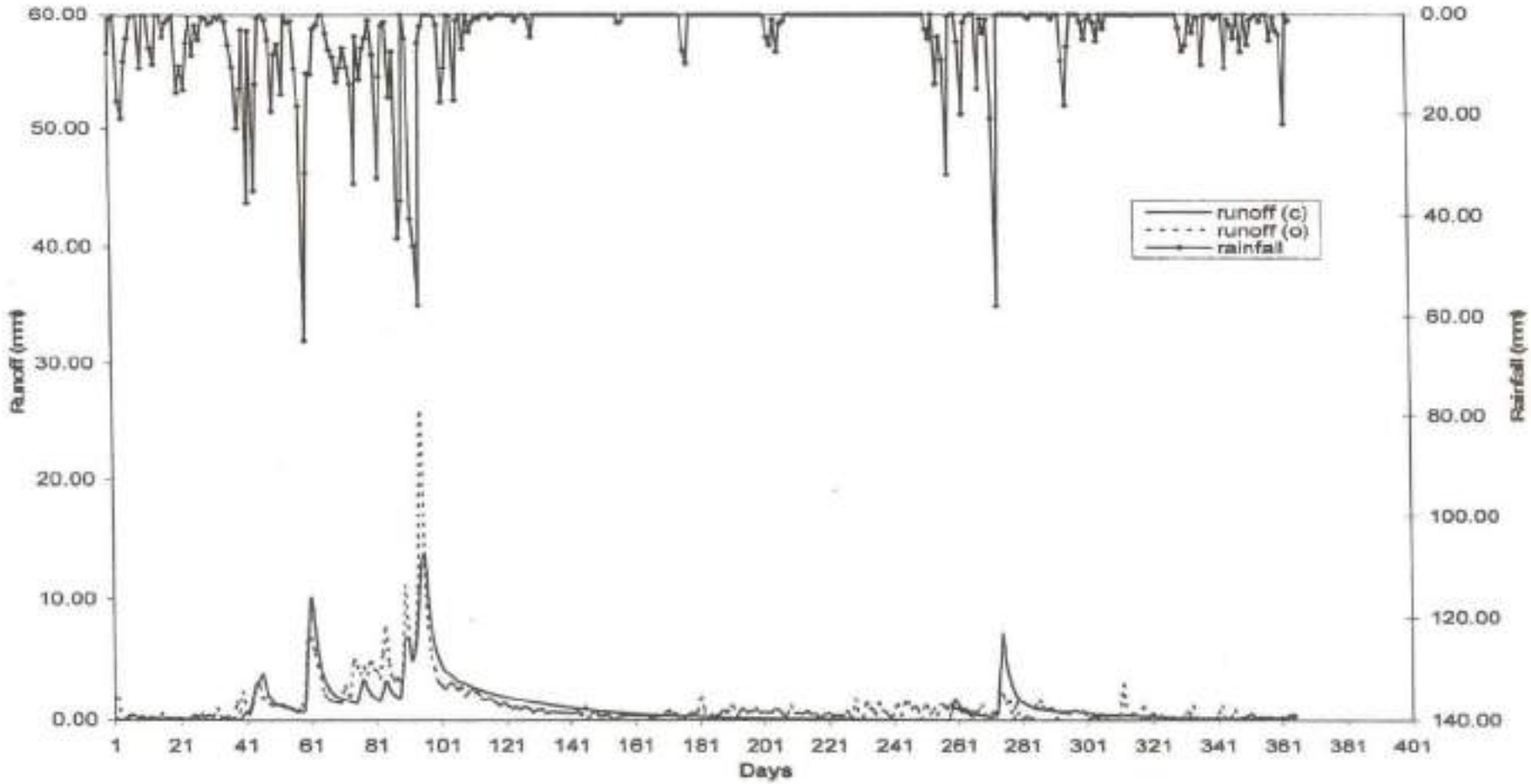

Figure 4.13: Model validation for Ramganga catchment (June 1989- May 1990) Day 1 represents June 1, 1989

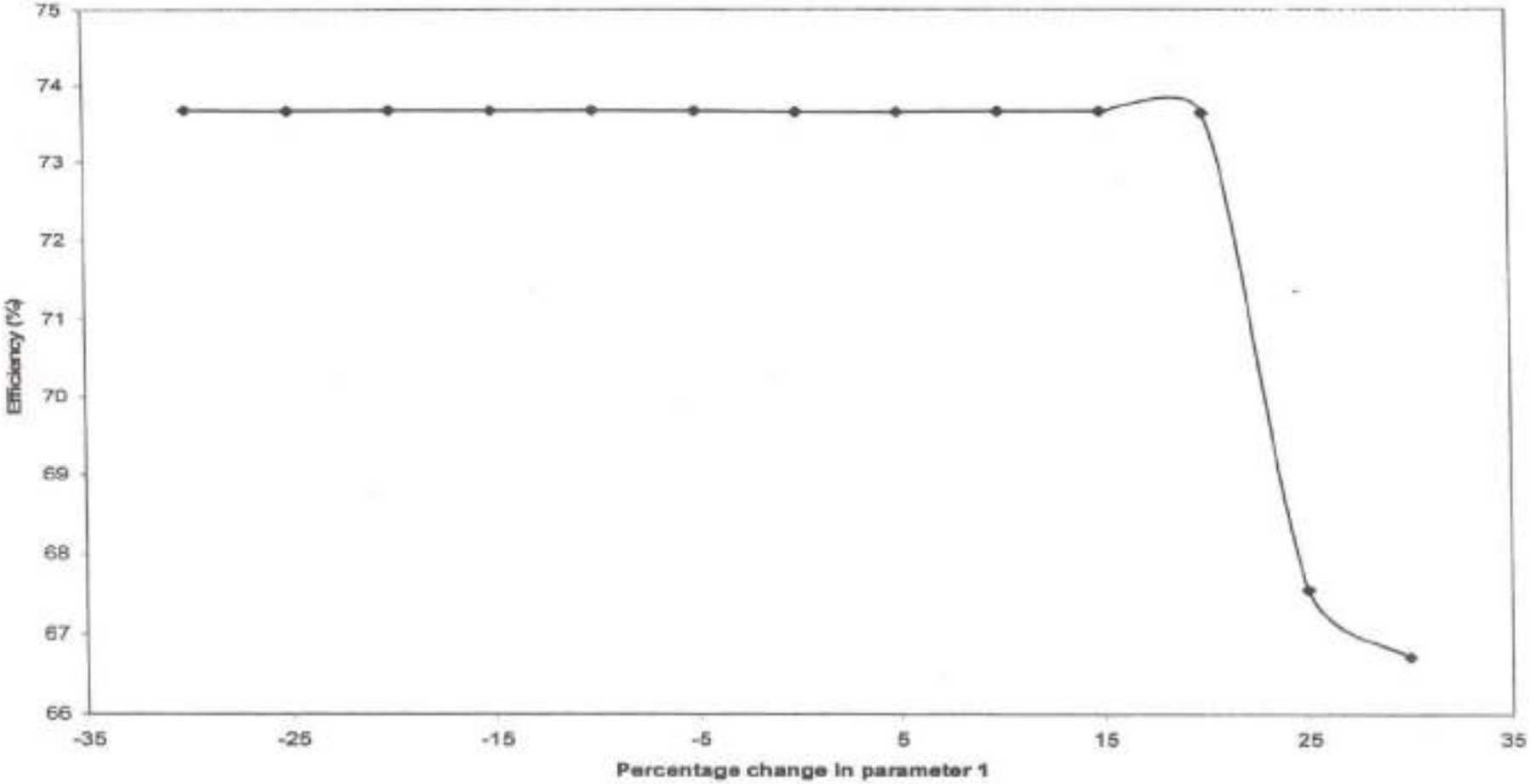

Figure 4.14: Sensitivity of model parameter CN (Ramganga catchment)

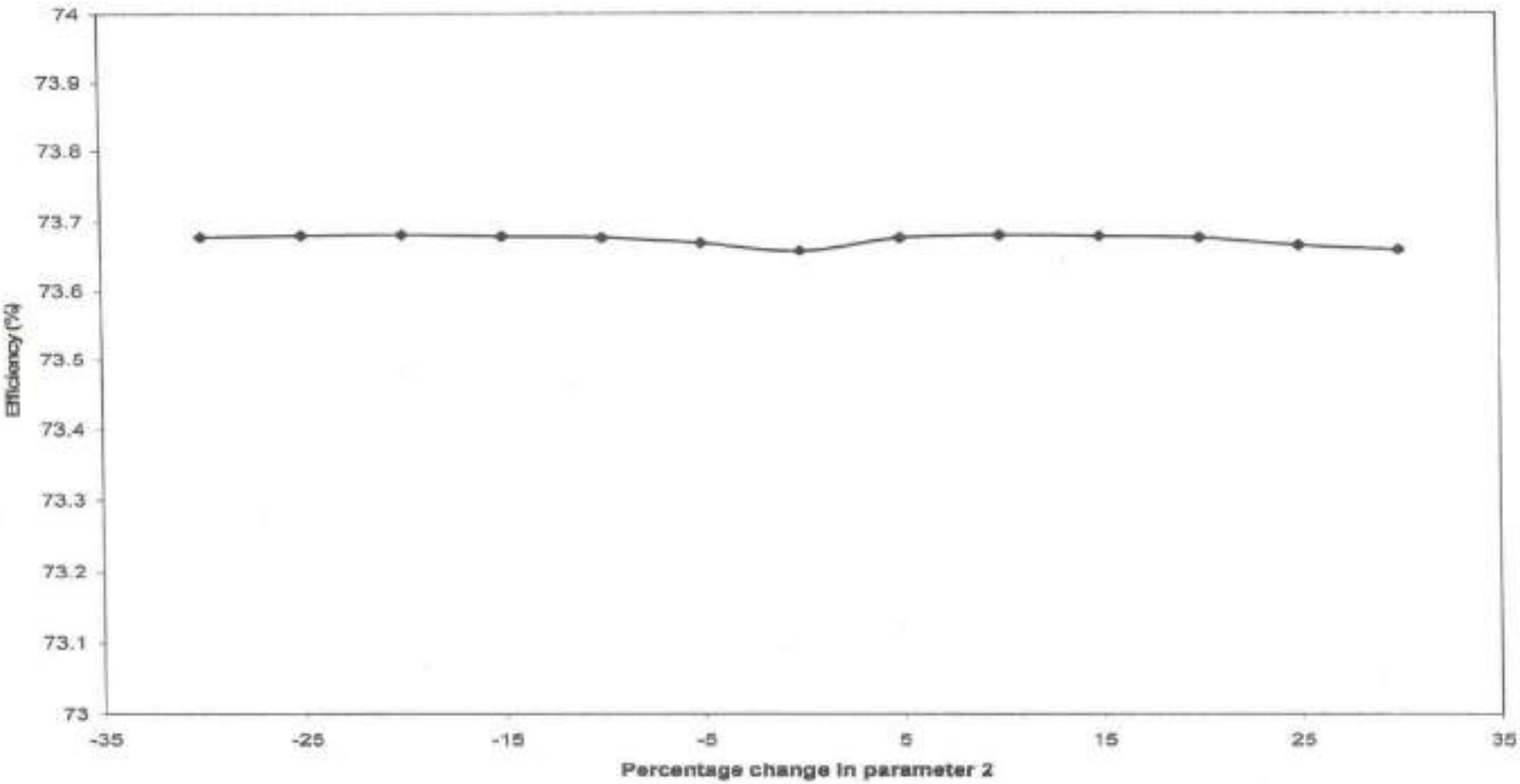

Figure 4.15: Sensitivity of model parameter CN_d (Ramganga catchment)

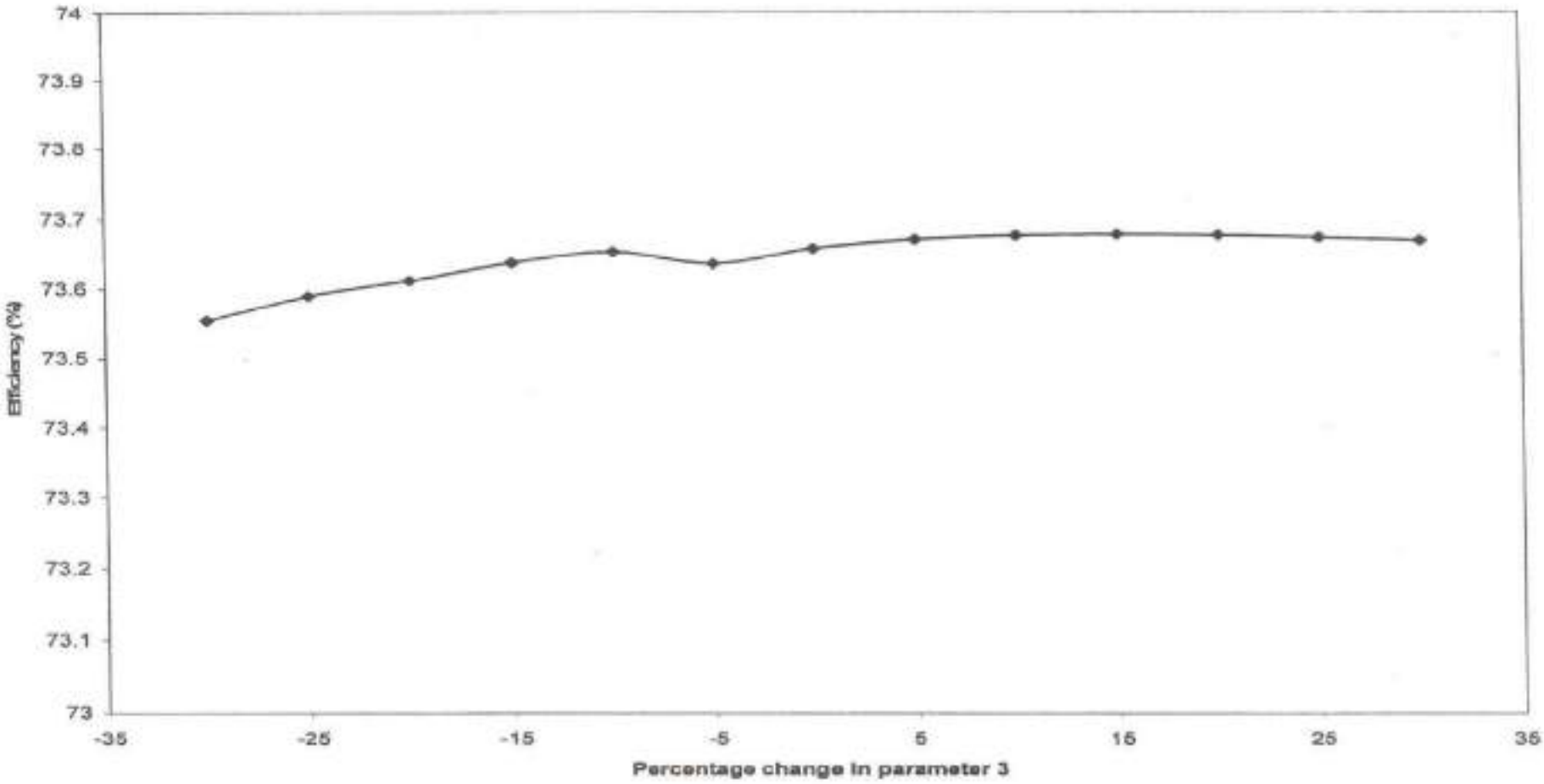

Figure 4.16: Sensitivity of model parameter K (Ramganga catchment)6

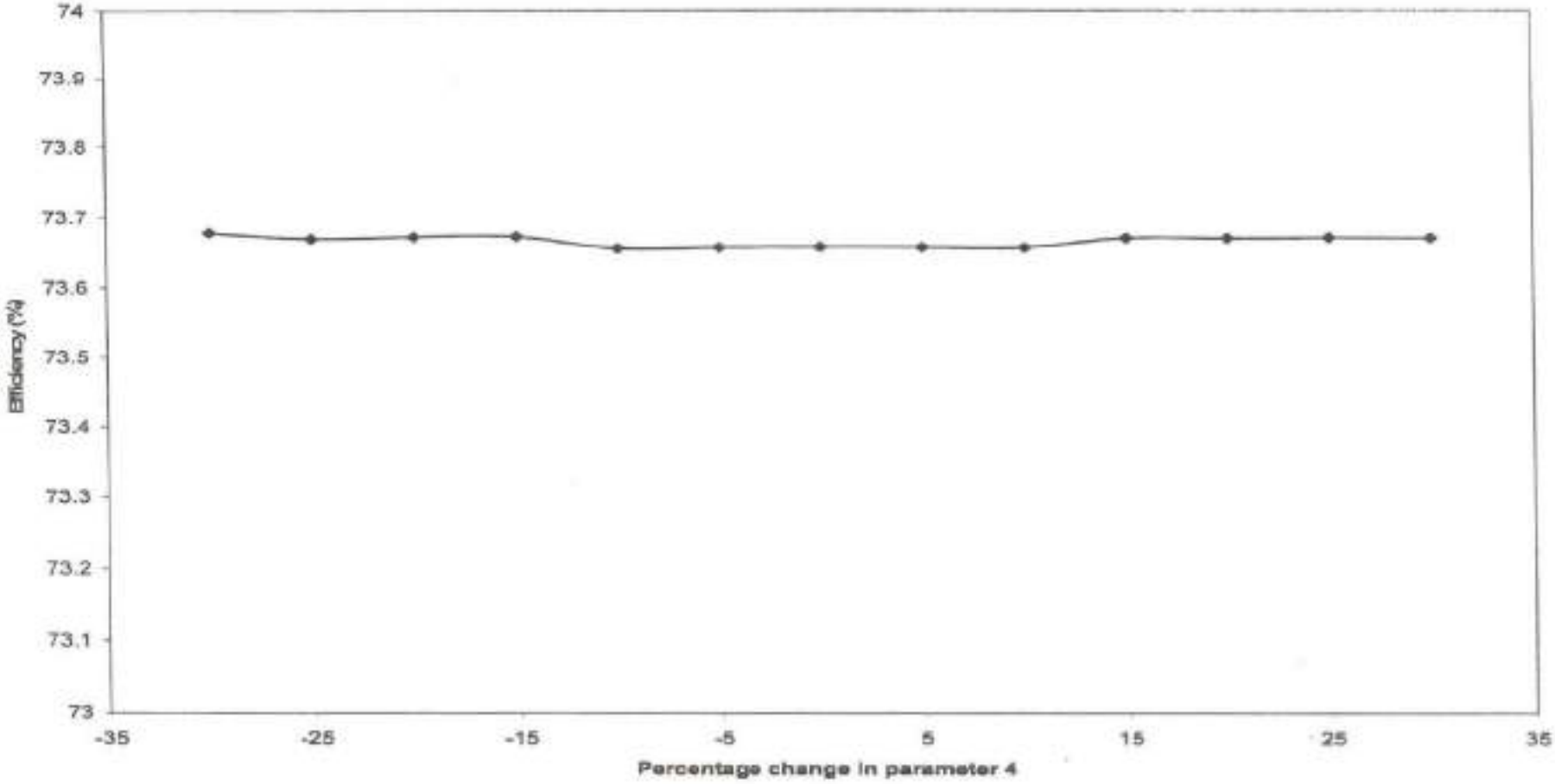

Figure 4.17: Sensitivity of model parameter K_b (Ramganga catchment)

4.10.6 Model Testing On Other Watersheds

4.10.6.1 Model Calibration

The proposed model is calibrated using rainfall, evaporation, and runoff data of the other watersheds located in different hydro-meteorological conditions (Section 4.11). Three years of data were used for Hemavati (1974-1977), Kalu (1990-1992) and Ghodahado (1993- 1996) catchments. For Narmada basin nine years of data were available, out of which five years of data of Manot, Hridaynagar and Mohegaon sites were used in calibration. The values of parameters computed in calibration for all the watersheds are given in Table 4.7, and discussed below.

Table 4.7: Estimates of Model Parameters

Parameters	CN	CN_d	K	K_b
Hemavati	91.65	85.57	2.24	50.35
Manot	88.26	74.03	0.57	21.23
Hridaynagar	72.31	37.59	2.06	29.31
Mohegaon	76.6	44.71	0.1	21.73
Kalu	85.49	72.85	0.66	28.89
Ghodahado	82.71	78.07	3.20	37.16

The optimal estimates of model parameter were obtained by using non-linear Marquardt algorithm (Mishra and Singh, 2003) coupled with trial and error. The estimated values of the four parameters (CN, CN_d, K and K_b) along with their initial values (Table 4.4) and the estimated values of model parameters in calibration for other watersheds are given in Table 4.7. It is apparent from the table that the values of the parameter CN varies in the range of 72 to 91 for all the six catchments. This demarcates a maximum value of 91.65 for Hemavati which interprets it to be a good runoff producing watershed, whereas the minimum value occurs at Hridaynagar with a value of 72.31 representing it to be a less runoff producing watershed. Similarly, the CN_d value of the watershed varies in the range from 35 to 85 for all the considered catchments. The maximum value of 85.57 for Hemavati indicates good base flow production potential, and on the other hand, the catchment which produces the lowest CN_d value of 37.59 is Hridaynagar shows less baseflow production potential. K-values are seen to vary from 3 hrs to 3day, whereas the time of travel for base flow,

K_b varies in the order of 20 days to 50 days, which is also reasonable for mid-size watersheds.

Table 4.8 shows the resulting efficiencies along with runoff coefficients for each catchment. It is seen that Hridayanagar and Mohegaon catchments show the least runoff coefficient of 0.25 and 0.29, indicating them to be dry catchments (Gan et. al., 1997) whereas Hemavati and Kalu can be classified as high runoff producing catchments with their coefficient values of 0.8 and 0.91, respectively. The runoff coefficients for Manot and Ghodahado are 0.45 and 0.47 respectively, describing them to lie in the intermediate category of dry and wet. The model yields maximum efficiency of 83.27% in Hemavati catchment whereas Hridayanagar catchment produces the least efficiency of 42.08%. The other catchments like Manot, Mohegaon, Kalu and Ghodahado exhibit 60.75, 62.72, 62.85 and 59.35% efficiencies.

Table 4.8: Model Efficiencies in Calibration and Runoff Co-efficient

Catchment	Data length	Efficiency (%)	Runoff coefficient
Hemavati	1974 - 1977 (3 years)	83.27	0.80
Manot	1981 - 1986 (5 years)	60.75	0.45
Hridaynagar	1981 - 1986 (5 years)	42.08	0.25
Mohegaon	1981 - 1986 (5 years)	62.72	0.29
Kalu	1990 - 1992 (3 years) Monsoon period	62.85	0.91
Ghodahado	1993 - 1996 (3 years)	59.35	0.47

Figure 4.18 shows the daily variation of observed and computed runoff along with the rainfall for the Hemavati catchment from 1974-77. From this figure it can be interpreted that the observed runoff and the computed runoff follow a close trend except for the deviation at peaks of the hydrographs. Similar inferences can be drawn from the graphs for other catchments. From the figures, it is noted that the model underestimates the peaks, like for Hemavati in the year 1974, for Kalu in the year 1991, for Manot in year 1985 and for Mohegaon in year 1985. Since the proposed model accounts for baseflow, it appears that the model is not suitable for prediction of high flows.

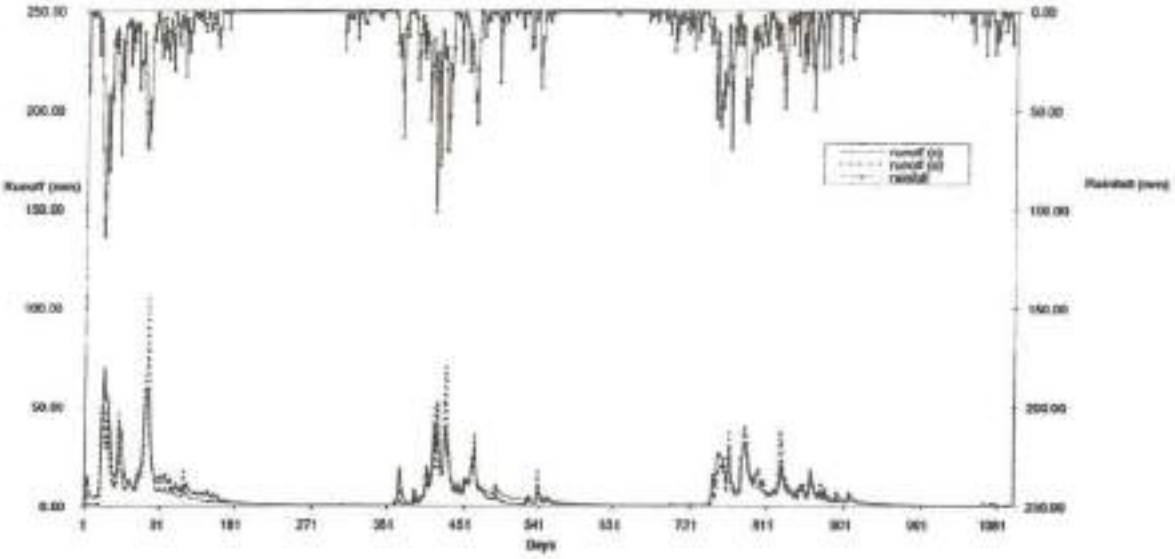

Fig: 4.18 Daily variation of Rainfall, observed runoff and simulated runoff in Hemavati catchment (calibration)

4.10.6.2 Model Validation

Taking the parameter values corresponding to the data available for different catchments (Table 4.7) in model calibration, the model was tested on the remaining years data for the corresponding catchments. Two years of data were used for Hemavati and Ghodahado catchments for validation. From the available nine-year dataset for Narmada River at Manot, Hridaynagar and Mohegaon the remaining four years of data were used for validation. For Kalu catchments, four years data for monsoon period only were available for the analysis, out of which three years ware used for calibration and one year for validation. The efficiencies resulting from model application to the remaining data of different catchments are given in Table 4.9, which indicates a satisfactory model performance only on those watersheds for which runoff coefficient value is high, such as Hemawati and Kalu watersheds. On other watersheds, the model performs poorly.

Like in calibration, the catchments having higher runoff coefficient produces higher efficiencies in validation also. Hemavati catchment shows a better efficiency (= 84.82%) than others. Kalu stands next to Hemavati in efficiency which is 80.77%, indicating satisfactory model performance. But in case of Manot, Mohegaon, Hridaynagar and Ghodahado catchments, the efficiencies are low, viz., 54.06, 42.17, 34.88 and 32.31%, respectively, as shown in Table 4.9. The model efficiencies being

too low on these catchments indicate its non-suitability to these watersheds. Alternatively, the proposed model is not applicable to watersheds of low runoff production potential.

Table 4.9: Model Efficiencies in Validation and Runoff Co-efficient

Catchment	Data Length	Efficiency (%)	Runoff Co-efficient
Hemavati	1977 - 1979 (2 years)	84.82	0.83
Manot	1986 - 1990 (4 years)	54.06	0.39
Hridaynagar	1986 - 1990 (4 years)	34.88	0.20
Mohegaon	1986 - 1989 (3 years)	42.17	0.23
Kalu	1993 (1 year) Monsoon period	80.77	0.99
Ghodahado	1987 - 1989 (2 year)	32.31	0.52

To further test the proposed model applicability, the percent relative errors (Eq. 4.71) for six watersheds were computed and these are shown in Table 4.10. The table shows yearly rainfall along with the observed and calculated runoff for the described watersheds. The average annual value of relative error ranges from 17.71% to ± 24.61%, with an average value of ± 3.57% for Hemavati catchment over the study period of five years. This watershed experienced an average annual rainfall of 2854 mm which varies from 2651 mm to 3064 mm in different years. The average annual runoff calculated is 2312 mm whereas the observed runoff is 2233 mm. Apparently, except for 1977-78, the model has over-estimated the yearly runoff in all the years. For Kalu watershed the average annual rainfall is 2944 mm which varies from 1903 mm to 3355 mm in these three years and the average annual runoff calculated is 2858 mm and observed runoff is 2930 mm annually. The relative error values are seen to vary from 8.08 to ±7.09% with an average value of 2.45%, which indicate a reasonably satisfactory performance of the proposed model in yearly runoff computation. Similarly for Manot, the relative error varies in the range of 34.88% to ± 44.54% with average value of 4.59. Average annual rainfall for the catchment is 1264 mm, whereas the calculated and observed runoff is 559 mm and 533 mm,

respectively. The proposed model underestimated the yearly runoff in years 1981-82, 1983-84, 1984-85 and 1989-90, but in other years it overestimated.

Similarly for other catchments, such as Mohegaon and Hridayanagar deviation in annual runoff, in both calibration and validation is in the range of 46.93% to ± 13.08 (average value of 25.03%) and 51.46% to ± 40.53% (average value of 8.10%), respectively for both the catchment (Table 4.10). The average annual rainfall, runoff calculated and observed for Mohegaon are 1231 mm, 431mm and 323 mm and for Hirdayanagar are 1443 mm, 357mm and 328mm respectively. It is also observed that in some cases, the relative errors are negative, implying that the model overestimates the runoff. But in case of Ghodahado catchment, it shows maximum deviation in the observed and simulated one as the relative error is more, varying in the range of 8.46% to ±93.25%. This shows a poor model fit to the data of this catchment. But for other catchments with high runoff coefficient, the proposed model shows satisfactory results.

4.10.7 Comparison with an Existing Model

This section compares the application of two models, viz., the proposed SCS – CN based model accounting on base flow computation and an available lumped conceptual model (Geetha, 2007) on different watersheds. Tables 4.11 and 4.12 compare the model efficiencies and average relative error values due to the above models. Both the models show a satisfactory performance on higher runoff producing catchments, like Hemavati and Kalu catchments. The catchment like Manot shows a low efficiency, as the runoff coefficient is low. The Ramganga catchment is however an exception.

The comparison of model efficiencies reveals that, the proposed model yields a maximum efficiency of 83.27% in calibration and 84.82% in validation in Hemavati catchment, whereas the existing model yields 83.5% and 87.72%, respectively in calibration and validation for the same catchment. For Ramganga catchment the proposed model yields efficiencies of 73.62% and 75.46% in calibration and validation, respectively and the existing model shows efficiencies of 65.48 and 41.64%, respectively in calibration and validation. Similarly for other catchments like Manot and Kalu catchments the proposed model shows respective efficiencies of

60.75 and 63.895% in calibration, and in validation these are 54.06 and 82.014%, whereas the existing method shows higher efficiencies in case of Kalu catchment.

Table 4.10: Observed and Simulated Runoff and Relative Error

Sl. No	Year	Rainfall	observed runoff	Simulated runoff	Relative Error
		(mm)	(mm)	(mm)	%
HEMAVATI					
1	1974 -75	2938	2553	2551	0.06
2	1975 - 76	2651	1718	2066	-20.26
3	1976 - 77	2676	1894	1959	-3.43
4	1977 - 78	2942	2937	2417	17.71
5	1978 - 79	3064	2062	2569	-24.61
Average		2854	2233	2312	-3.57
KALU					
1	1990	3347	3529	3245	8.06
2	1991	3169	3060	3277	-7.09
3	1992	1903	1602	1663	-3.81
4	1993	3355	3529	3249	7.95
Average		2944	2930	2858	2.45
MANOT					
1	1981 - 82	1136	383	553	-44.54
2	1982 - 83	1024	371	327	11.89
3	1983 - 84	1391	567	671	-18.36
4	1984 - 85	1303	616	703	-14.15
5	1985 - 86	1264	713	483	32.24
6	1986 - 87	1379	708	564	20.37
7	1987 - 88	1347	767	500	34.88
8	1988 - 89	1309	631	623	1.23
9	1989 - 90	1220	277	377	-36.39
Average		1264	559	533	4.59
MOHEGAON					
1	1981 - 82	1240	334	357	-6.93
2	1982 - 83	1113	339	183	46.06
3	1983 - 84	1533	486	301	37.99
4	1984 - 85	1295	518	586	-13.08

5	1985 - 86	1329	579	453	21.79
6	1986 - 87	1356	471	387	17.75
7	1987 - 88	1125	377	200	46.93
8	1988 - 89	1166	550	332	39.75
9	1989 - 90	926	227	111	51.21
Average		1231	431	323	25.03
HRIDAYANAGAR					
1	1981 - 82	1587	319	448	-40.53
2	1982 - 83	1462	314	333	-6.07
3	1983 - 84	1937	380	430	-13.07
4	1984 - 85	1300	299	368	-23.27
5	1985 - 86	1457	258	326	-26.03
6	1986 - 87	1815	601	292	51.46
7	1987 - 88	881	182	229	-26.06
8	1988 - 89	1377	568	284	50.06
9	1989 - 90	1171	289	241	16.73
Average		1443	357	328	8.10
GHODAHADO					
1	1993 - 94	947	145	263	-81.24
2	1994 - 95	1983	486	939	-93.25
3	1995 - 96	1483	1080	879	18.57
4	1987 - 88	1493	826	756	8.46
5	1988 - 89	1475	434	786	-81.21
Average		1476	594	725	-21.97

It is apparent from Table 4.12 that the proposed model performs with the average relative error ranging from -7.15 to 8.57%, whereas the existing model ranges from 7.42 to 43.13%. Thus, the comparison based on average relative error indicates the proposed model to perform much better than the existing one in majority of the watersheds considered in this study.

4.11 SUMMARY AND CONCLUSIONS

Information regarding flow rates at any point of interest along a stream is necessary in the analysis and design of many types of water resources projects.

Although many streams have been gauged to provide continuous records of stream flow, planners and engineers are sometimes faced with little or no available stream flow information and must rely on synthesis and simulation as tools to generate artificial flow sequences for use in rationalizing decisions regarding structure size, the effect of land use, flood control measures, water supplies, and the effect of natural or induced watershed or climatic change.

Table 4.11: Data Length and Model Efficiency (%) With Runoff Coefficient

Catchment	Area Km^2	Efficiency (%)				Runoff coefficient
		Proposed model		Existing model		
		Calibration	Validation	Calibration	Validation	
Ramganga	3134	73.62	75.46	54.26	-18.79	0.33
Hemavati	600	83.27	84.82	83.50	87.72	0.80
Manot	5032	60.75	54.06	60.65	43.91	0.45
Kalu	224	63.89	82.01	63.33	76.15	0.91

Table 4.12: Annual Average Rainfall, Observed Runoff and Relative Error (%)

Catchment	Average rainfall (mm)	Average observed runoff (mm)	**Proposed model**		**Existing model**	
			Average simulated runoff (mm)	Average Relative Error (%)	Average simulated runoff (mm)	Average Relative Error (%)
Ramganga	1492.78	514.07	470.03	8.57	633.13	35.89
Hemavati	2854.19	2233	2312.47	-3.57	1986.87	9.78
Manot	1263.59	559	533.50	4.59	304.38	43.13
Kalu	2887.12	3338	3577.00	-7.15	2546.73	7.42

The long-term hydrologic simulation plays an important role in water resources planning and watershed management, specifically for analysis of water availability; computation of daily, fortnightly, and monthly flows for reservoir operation and drought analysis. In this chapter, popular Soil Conservation Service Curve Number (SCS – CN) based long term rainfall runoff model was proposed, and

tested on the data of Ramganga catchment (area = 3134 km^2) using split sampling. The proposed model has four parameters, CN, CN_d, K and K_b. The first two parameters are the curve number for surface flow and drainage flow respectively, K is the catchment storage coefficient (day), and K_b is the ground water storage coefficient (day).

To check the versatility of the proposed model, the model was further applied to different watersheds located in different hydro-meteorological conditions. These are the catchments of Hemavati, Manot, Hridaynagar, Mohegaon, Kalu and Ghodahado. The following conclusions were derived from this study:

1. The model generally performed well in both calibration and validation on the data of Ramganga catchment. The resulting efficiencies for all the years varied in the range of 81.82 to 73.62%, showing a satisfactory fit and, in turn satisfactory model performance.
2. The comparison of model efficiencies resulting from model application to other catchments reveals that Hemavati yields maximum efficiency of 83.27% in calibration and 84.82% in validation. The other catchments like Manot, Kalu and Ghodahado exhibit 60.75, 63.895 and 59.35% efficiencies, respectively in calibration and 54.06, 82.014 and 32.31% in validation. The efficiencies of all catchments, except Hemavati and Ramganga, are higher in calibration than in validation, but reverse holds for the others.
3. It is seen that the catchment of Hemavati and Kalu can be classified as high runoff producing catchments with runoff coefficient values of 0.83 and 0.91 respectively. Hridaynagar, Mohegaon catchments with low runoff coefficients of 0.25 and 0.27 respectively behave as dry catchments.
4. The model simulated the yearly runoff values with relative error in the range (-29.66 to 18.20%) for Ramganga catchment. For other catchments it falls within the range of (-21.97 to 8.10%). These significantly low values indicate a satisfactory model performance. The negative (-) values of relative error indicate that the model overestimates the runoff values.
5. The satisfactory model performance on the high runoff producing watersheds is further appreciable in view of the limited number of model parameters (only four) and its simplicity.

CHAPTER 5

APPLICATION OF TOPMODEL

CHAPTER 5

APPLICATION OF TOPMODEL

The flow of water on the surface of the earth has long perplexed the human mind. The desire to understand the movement of water has mainly arisen from the need to evaluate the amount of water available at a particular location to meet local demand as well as risk of flooding due to excess water. Hydrological processes within a catchment are complex involving macropores, heterogeneity and local pockets of saturation. Catchment direct runoff response to rainfall involves generation of rainfall-excess (runoff response) and the transfer of this rainfall-excess to the catchment outlet via land surface and through linked channels (channel response). The representation of runoff formation process has been accomplished, over the decades, with methods which vary according to the purpose and application of the model. These range from simple calculation of design discharge to the two-dimensional representation of various processes, based on suitably conditioned mass balance, energy and momentum equations and to the three-dimensional representation of all exchanges.

Runoff in wet region is mainly produced by saturation-excess runoff. This means that the spatial distribution of soil moisture storage will result in varied surface runoff production. For a large area, the saturation-excess runoff will occur in a certain portion of the area with no soil moisture deficit, say, ground water goes up to ground surface. Both models and data have shown that within a catchment substantial soil moisture heterogeneity exists at almost any scale and that a major control on the distribution of soil moisture is topography. Even though there are many surface runoff models based on saturation-excess runoff mechanism, only a few models take the topography influence on the spatial distribution pattern of soil moisture into consideration and, in turn, on runoff production. The TOPMODEL (Beven, 1986a) is a variable contribution area conceptual model in which the predominant factors determining the formation of runoff are represented by the topography of the basin and a negative exponential law linking the transmissivity of soil with the vertical distance from ground level.

5.1 OBJECTIVES

The TOPMODEL is one of the few conceptual models, in which physical reality is represented in a simplified manner, that incorporate explicitly the saturation-excess overland flow mechanism and integrates the variable contributing area concept, both of which are essential to model the catchment accurately. It is a topography based watershed hydrology model that has been used to study a range of topics, including spatial scale effects on hydrological process, topographic effects on stream flow, and the identification of hydrological flow path etc. This chapter evaluates the applicability of TOPMODEL to simulate runoff from Chaukhutia watershed, a forested Himalayan watershed of Ramganga River catchment system, in GIS environment.

5.1.1 General Layout

The applicability of TOPMODEL is tested systematically as follows:

1. Generate digital elevation model (DEM) for Chaukhutia watershed.
2. Calculate the Topographic index from DEM for use in TOPMODEL.
3. Calibrate and validate TOPMODEL from observed data of Chaukhutia watershed.
4. Perform sensitivity analysis of model parameters using Monte Carlo simulations and analyze the results obtained.

5.2 RAINFALL RUNOFF MODELLING APPROACHES

The fundamental characteristic of catchment hydrology is in the form of mass balance equation for a specified time interval and is represented by

$$R = P - ET - \Delta S \qquad (5.1)$$

where R is runoff, P is precipitation, ET is evapotranspiration, and ΔS represents change in storage which includes surface water, soil moisture, groundwater, and snow pack. Over short periods, ground water storage and spatial distribution of soil

moisture content will change in response to the prevailing inputs and climate. Consequently, investigation of hydrologic processes on these time scales require detailed knowledge of water including fluxes, changes in storage, and transfers throughout the catchment.

The literature contains many works which summarize the current level of understanding of physics of the complex process of rainfall-runoff transformation, and still more work is continuing to bring in possible improvements in schematizing the whole process so as to develop hydrologically sound mathematical models (Todini 1988). In fact the representation of runoff transformation processes has been accomplished, over the decades, with models which vary according to the purpose and application.

Theoretical models presumably are the consequences of most important laws governing the phenomena. A theoretical or physical model has a logical structure similar to the real world system and may be helpful under changed circumstances. The parameters of a physically based model can be measured directly or in-situ. Watershed runoff models based on St. Venant's equation are the example of physical models, such as System Hydrologique European (SHE) model (Abbott et al., 1986) and others. On the other hand, an empirical model is not based on physical laws governing the phenomena. It merely presents the facts, that is, it is a representation of data. If the conditions change, it has no predictive capability. Rational method, unit hydrograph models, etc. fall under the category of empirical models. For a conceptual model, the physical reality is represented in simplified manner. Conceptual models consider physical laws but in highly simplified form. Thus, the conceptual models lie intermediate between theoretical and empirical models. Examples of conceptual models may include rainfall-runoff models based on the spatially lumped form of continuity equation and the storage discharge relationship. Models of Nash (1957) and Dooge (1959) are conceptual models. Theoretical models aid in understanding a process and generally yield information in greater detail in both time and space. Empirical models do not aid in physical understanding. Conceptual models provide useful results efficiently and economically for some problems. They contain parameters, some of which may have direct physical significance and can, therefore, be estimated by using concurrent observations of input and output.

TOPMODEL, which is the abbreviation of Topography based hydrologic MODEL, is a conceptual model developed by Kirkby and Weyman (1974) and refined by Beven and Kirkby (1979) to simulate runoff from a catchment based on the concept of saturation-excess overland flow and subsurface flow and places emphasis on the role of catchment topography in the runoff generation process. An implicit assumption is that the local groundwater table has the same slope as the watershed surface. This allows for the modeling of sub-surface flow using the surface topographic slope.

5.3 TOPMODEL APPLICATIONS IN RAINFALL-RUNOFF MODELLING

TOPMODEL represents a set of modeling tools that combines the computational and parametric efficiency of a lumped modeling approach with a link to physical theory. TOPMODEL has been successfully used in humid temperate regions (Beven and Wood, 1983; Hornberger et al., 1985; Beven, 1993; Robson et al., 1993, Lamb et al, 1998; Guntner et al., 1999), drier Mediterranean regimes (Durand et al., 1992; Pinol et al., 1997), small humid tropical catchments such as Booro catchment in Irovy coast (Quinn et al., 1991) and in a forested head water catchment of a river Sinnamary in French Guiana (Molicova et al., 1997). TOPMODEL was applied to simulate continuously the runoff hydrograph of medium sized humid tropical catchment (Campling et al., 2002). The model simulated well the fast subsurface and overland flow events superimposed on seasonal rise and fall of the base flow. A study of rainfall-runoff response for a catchment in the upper reaches of Yangtze river was done by Shufen and Huiping (2004) using TOPMODEL coupled with the simple water cycle model. Nageshwar et al. (2005) studied the rainfall-runoff response of Tygarts Creek catchment in eastern Kentucky using TOPMODEL. The calibration results were in good agreement with the results documented from previous studies using TOPMODEL.

Molicova et al. (1997) used the TOPMODEL for modeling the hydrological patterns within a humid, tropical catchment. They tested its validity in modeling the stream flow dynamics (hydrograph) in a 1 ha tropical rain forest catchment in French Guiana. The field validation of the temporal and spatial hydrodynamics across a rainfall-runoff event revealed that TOPMODEL might be suited for applications to this particular rain forest environment. In fact, this was the first successful application

of such a model within the humid tropics. The main reason for success of the model was low hydraulic conductivity of subsoil coupled with the absence of an additional deep ground water body, and the contributions which has caused difficulties in application of topographic based runoff models elsewhere in humid tropics.

Pinol et al. (1997) applied the distributed TOPMODEL concepts in an application to the strongly seasonal contributing area responses in two adjacent small Mediterranean catchments in the Parades region of Catalonia, Spain. A perceptual model of hydrological response in these catchments was used to suggest possible modifications in the model, in a hypothesis testing framework, including an attempt to modify the topographic index approach to reflect the expansion of effective area of subsurface flow during the wetting-up sequence. It was found that slight improvements in modeling efficiency were possible but that different model parameter distributions were appropriate for different parts of the record. The model was much more successful for the catchment producing the higher runoff volumes.

Campling et al. (2002) applied the TOPMODEL to simulate the runoff hydrograph for a medium sized humid tropical catchment (379 km^2). The objectives were to relate hydrological responses to runoff generation mechanisms operating in the catchment and to estimate the uncertainty associated with runoff prediction. Field observations indicated that water tables were not parallel to the surface topography, particularly at the start of wet season. A reference topographic index λ_{REF} was therefore introduced into the TOPMODEL structure to increase the weighting of local storage deficits in upland areas. The model adaptation had the effect of depending water tables with distance from river channel. The generalized likelihood uncertainty estimation (GLUE) framework was used to asses the performance of the model with randomly selected parameter sets, and to set simulation confidence limits. The model simulated well the fast subsurface and overland flow events superimposed on the seasonal rise and fall of the base flow. The top ranked parameter sets achieved modeling efficiencies of the order of 0.943 and 0.849. The GLUE analysis showed that exponential decay parameter m, controlling the base flow and local storage deficit, was the most sensitive parameter. Uncertainty increased in simulation of storm events during the early and late phases of the season due to combination of errors in detecting the rainfall depths for conventional rainfall events, the treatment of

rainfall as a catchment areal value, and the strong seasonality in runoff response in humid tropics.

Shufen & Huiping (2004) used TOPMODEL to study the rainfall-runoff response of a catchment (around 2500 km^2) in the upper reaches of Yangteze river. They developed a simple water cycle model, for estimating other components of the surface water cycle, which was implemented into the TOPMODEL to integrate the water cycle of the catchment. Using the output of a DEM from 100m x 100m resolution data and a single flow direction algorithm, the index distribution function was calculated for the catchment under different channel initiation thresholds. Finally, the daily and monthly rainfall-runoff response from year 1960 to 1987 for Soumon River Catchment (a tributary of the Yangtze River) was simulated with TOPMODEL. To evaluate the general quality of model, percentage of efficiency E for each year with Channel Initiation Threshold (CIT) equal to 0.01 km^2, 0.1 km^2 and 5.0 km^2 was calculated and it was found that values of E didn't show a large variation (for channel initiation threshold (CIT) = 0.5, 1 and 5 km^2, the values for E were almost the same) from each other with different CIT values except for a very small CIT. They found that E values are large for most years which means TOPMODEL works well in simulating the runoff of Soumon River catchment. Hence, it was concluded that TOPMODEL works well in catchments with a hill slope region, with moist soil, and with a shallower ground water table.

Bhaskar et al. (2005) studied the rainfall-runoff response of a mountainous catchment, Tygarts Creek, using TOPMODEL. Unlike the traditional application of this model to continuous rainfall-runoff data, its applicability to single storm event-runoff modeling, specifically floods, was explored. The topographic index values within the catchment were determined using the digital terrain analysis procedures in conjunction with digital elevation model (DEM) data. Select parameters such as surface transmissivity T_o, transmissivity decay parameter m, and initial moisture deficit in root zone, S_m were calibrated using an iterative procedure to obtain the best fit runoff hydrograph. These parameters were calibrated using three additional storm events. They found the calibration results to be in general agreement with the results documented from previous studies. However, the model did not perform well in verification, and consequently, a universal set of TOPMODEL parameters could not be recommended for simulating runoff from Tygarts Creek catchment.

Nachabe (2005) proposed an equivalence between TOPMODEL and NRCS Curve Number (NRCS-CN) method for predicting variable runoff source areas. They found that NRCS-CN model can be used successfully to describe the probability distribution function of moisture deficit in a catchment calculated by TOPMODEL. His approach was to constrain 'S' parameter in NRCS-CN model by the physical soil and topography characteristics of the catchment and depth to water table. By giving a clear physical meaning for 'S' he provided better estimation of this parameter in humid vegetated landscape, where runoff production is controlled by rising water table. The study showed that a distributed model might be equivalent to a lumped parameter model, especially when the objective is to predict a spatially integrated response, like runoff at catchment outlet.

Wang et al. (2006) used the TOPMODEL's rainfall – runoff hydrologic concept, based on soil saturation process, in representing hydrograph recession curve by power function decay of hydraulic conductivity with soil depth. They developed a power function formulation of Green and Ampt infiltration equation to represent field measurements in Ward Pound Ridge watershed in New York City drinking water supply area. They used power function decay to compute Topographic Index distributions of soil saturation of TOPMODEL and found that soil hydraulic conductivity values had power function decay with soil depth.

Venkatesh and Jain (2000) applied TOPMODEL to Malaprabha catchment (520 km^2) in Karnataka state to simulate the daily flows. The topographic index for Malaprabha catchment was derived by developing a digital elevation model (DEM) by interpolating the contours in the basin at 300 m grid size. The results indicated that the model could be used to simulate the flows in the catchment quite accurately. The efficiency of model was found to be 0.89 and 0.79, respectively, in calibration and validation. Also the model was able to simulate the timing and magnitude of the peak flow satisfactorily.

Jain (1996) tested the applicability of TOPMODEL for simulating rainfall-runoff response of Hemavathy catchment in Western Ghats. NS efficiency (Nash-Sutcliffe, 1970) was more than 0.84 both for model calibration and validation on independent data series. This show TOPMODEL works well in simulating rainfall-runoff response for a catchment.

A look at the applications of TOPMODEL shows its suitability to widely differing catchments in respect of size, climate and land cover conditions. However,

the model has certain limitations as: (i) The model only simulates watershed hydrology; (ii) it can be applied most accurately to watersheds that do not suffer from excessively long dry periods and have shallow homogeneous soil and moderate topography; and (iii) the model results are sensitive to grid size, and grid size ≤ 50 m is recommended.

Very few studies have been carried out for Indian catchments, and yet the model has not been explored for their applicability to hilly watersheds, particularly for Himalayan watersheds. In this chapter, the applicability of TOPMODEL is tested for simulating rainfall-runoff response of Chaukhutia watershed, a hilly catchment of Ramganga river catchment using daily rainfall-runoff data as discussed below.

5.4 TOPMODEL DESCRIPTION

TOPMODEL is a set of conceptual tools that can be used to reproduce the hydrological behaviour of the catchments in a distributed or semi-distributed way, in particular the dynamics of surface or subsurface contributing areas. The model simulates hydrologic fluxes of water (infiltration excess, overland flow, infiltration, subsurface flow, evapotranspiration and channel routing) through a watershed. The model simulates explicit groundwater / surface water interactions by predicting the movement of water table which determines where saturated land surface areas develop and have the potential to produce saturation overland flow.

5.4.1 Model Assumptions

(i) The hydraulic gradient of subsurface flow is equal to the land surface slope.

(ii) The actual lateral discharge is proportional to specific watershed area (drainage area per unit length of contour line).

(iii) The redistribution of water within the subsurface can be approximated by a series of consecutive steady states.

(iv) The soil profile at each point has a finite capacity to transport water laterally down slope.

(v) The saturated hydraulic conductivity decreases exponentially as depth below land surface increases.

5.4.2 Model Theory

In TOPMODEL, the topography dominated rainfall-excess generation process is described by using a topographic index $\lambda_i = \ln (a/\tan \beta_i)$, where a_i is upslope catchment area per unit contour length draining to a point 'i' in the catchment and tan β_i is the local surface topographic slope (assumed equal to hydraulic gradient of saturated zone) at the same location. This index is used to calculate the average moisture deficit over the entire catchment and the local moisture deficit at any location 'i' within the catchment. Hence it can be used to characterize how the moisture deficit at any particular location within the catchment deviates from the average moisture deficit of entire catchment. Thus, the main goal of TOPMODEL is to compute storage deficit in water table depth at any location for every time step. The theory relates mean watershed storage deficit to local storage deficits using the local value of a function of the topographic index.

The TOPMODEL parameters in runoff simulation examined in the past studies are surface transmissivity 'T_o' and transmissivity decay parameter 'm'. According to Beven (1997), the concept of transmissivity, as used in TOPMODEL, does not have the traditional meaning of groundwater mechanics, where transmissivity refers to the rate at which water is transmitted through a unit width of aquifer under unit hydraulic gradient. The transmissivity values obtained using TOPMODEL are for down slope subsurface flow, where the unit hydraulic gradient is equal to surface topographic slope. The other TOPMODEL parameter 'm' reflects the decay rate of assumed transmissivity profile (relationship between the subsurface transmissivity, T, at any depth to the surface transmissivity, T_o). The slope of stream flow recession curves during period of no recharge to the groundwater table can be analyzed to get an initial estimate of parameter 'm'. In original version of TOPMODEL, the soil hydraulic conductivity on the soil transmissivity is assumed to decay following a negative exponential law. In this case, the expression that estimates the value of local storage deficit or water table depth is given in terms of topographic index ln (a / tan β). Other forms of soil hydraulic conductivity decay function lead to

different index functions. When distributed values of soil transmissivity, T_o, are known, a soil topographic index may be considered, ln ($a/T_o \tan\beta$).

5.5 RUNOFF PRODUCTION IN TOPMODEL

Runoff generation at a point depends on:

(i) Rainfall intensity or amount

(ii) Antecedent soil moisture conditions

(iii) Soils and vegetation

(iv) Depth to water table i.e. topography

(v) Time scale of interest.

These vary spatially which suggest a spatial geographic approach to runoff estimation. The soil profile is defined by a set of stores. The upper one is the root zone storage, where rainfall infiltrates until the field capacity is reached. In this store, evapotranspiration is assumed to take place at the potential rate to decrease at a linear rate when the root zone becomes depleted. Once the field capacity is exceeded, a second store starts filling until the water content reaches saturation. The gravity drainage store links the unsaturated and saturated zones, according to a linear function that includes a time delay parameter for vertical routing through the unsaturated zone. When the deficit in the gravity drainage store or water table depth equals zero, the saturation condition is reached and the rainfall produces direct surface runoff.

TOPMODEL primarily estimates runoff at the catchment outlet from the saturation excess at the surface and from the subsurface flow. The rainfall runoff equations used are derived from:

(i) Darcy's law

(ii) The continuity equation

(iii) The assumption that the saturated hydraulic conductivity decreases exponentially as depth below the land surface increases.

Darcy's Law:

Darcy's law in TOPMODEL takes the form

$$q_i = T_o (\tan \beta_I) \exp (-S_i / m) \qquad (5.2)$$

where index 'i', refers to a specific location in the catchment, q_i = down slope flow beneath the water table per unit contour length (m^2/h); tan β_i = average inflow slope angle; T_o = surface transmissivity (m^2/h) at location I; m = transmissivity decay parameter; S_i = moisture deficit at location i in (m).

Continuity Equation:

The continuity equation is represented by quasi-steady state recharge rate to the water table, expressed as:

$$q_i = r_i\, a_i \tag{5.3}$$

where r_i is the recharge rate (m/h) to the water table a_i is the upslope contributing area per unit contour length (m^2/m) at any location i in the catchment. Combining Equations (5.2) and (5.3) and rearranging gives an expression for moisture deficit S_i at any particular location 'i' within the catchment, expressed as:

$$S_i = -\, m \ln (r_i\, a_i / T_o \tan \beta_i) \tag{5.4}$$

The variable S_i in the above equation can be expressed in terms of average moisture deficit, $\overline{S}$, for the entire catchment or sub catchment as:

$$S_i = \overline{S} - m[(\lambda_i - \lambda) - (\ln T_o - \ln T_e)] \tag{5.5}$$

where $\lambda_i = \ln (a_i / \tan \beta_i)$ is the local topographic index and T_e is the average transmissivity value for the entire catchment or sub-catchment and is equal to

$$T_e = \left(\frac{1}{A}\right)\sum \ln T_o \tag{5.6}$$

where A is entire area of catchment; λ = the catchment average topographic index value and is given by

$$\lambda = \left(\frac{1}{A}\right)\sum_i \ln(a_i / \tan\beta_i) \tag{5.7}$$

Equation (5.7) is the fundamental equation for describing runoff production within TOPMODEL because it defines the degree of saturation for each topographic index value λ_i at any location within the catchment.

By assuming T_e equal to T_o, S_i depends on $\overline{S}$ and the deviation of the local topographic index, λ_i from λ. Since small values of S_i are associated with larger values of the topographic index λ_i, the higher the topographic index value at any location in the catchment, the smaller amount of moisture that will be needed to saturate the soil profile for that location.

In TOPMODEL, it is assumed that the hydraulic conductivity, K, decreases exponentially with depth. The hydraulic conductivity and transmissivity have the relation T = bK, where b is assumed average depth of soil moisture deficit zone. Hence the transmissivity below the catchment surface can be expressed as:

$$T = T_o \exp^{(-S_i/m)} \tag{5.8}$$

where T (m^2/h) is the transmissivity value for a local moisture deficit, S_i. This relationship is used in the development of Equation (5.5).

There are three main soil profile zones, namely root zone, unsaturated zone and saturation zone. When the root zone exceeds the field capacity of the soil, excess moisture contributes to moisture storage is the unsaturated zone. Beven et al. (1995) describes the equation describing the flow through the unsaturated and saturated zones in TOPMODEL, which are:

1. The vertical flux through the unsaturated zone is represented by

$$q_{vi} = S_{uz} / S_i t_d \tag{5.9}$$

where q_{vi} has units of (m/h), S_{uz} is the moisture storage in unsaturated zone at each time step at location i (m), S_i is moisture deficit in the unsaturated zone at location 'i' at each time step in (m), t_d is the time delay per unit depth of deficit (h/m). The term $S_i t_d$ represents a time constant that increases with the soil moisture deficit.

2. The recharge rate to the saturated zone at any time step from the unsaturated zone is $q_{vi}A_i$ where A_i is the fractional area associated with topographic index class 'i'. This recharge is summed over the total number of topographic index classes, n, to get the total recharge to the saturated zone Q_v.

At current time step, $$Q_v\,(m/h) = \sum_i q_{vi} A_i \qquad (5.10)$$

Once Q_v enters the saturated zone, the flow in the saturate zone on subsurface flow, Q_b (m/h), is

$$Q_b = Q_o \exp^{(-\bar{S}/m)} \qquad (5.11)$$

The flow Q_b can also appear at the surface when the soil profile is fully saturated, such as at the bottom of a hill slope, Q_o (m/h) in Equation (5.11) is the subsurface flow when the soil is fully saturated (i.e. when S = 0)

$$A_o = Ae^{-Y} \qquad (5.12)$$

where Y is the average soil-topographic index and A is the total catchment area. The average soil topographic index Y is given by

$$Y = \frac{1}{A}\sum \ln(a_i / T_o \tan\beta_i) \qquad (5.13)$$

For constant transmissivity T_o, within the catchment

$$Y = \frac{1}{T_o} \qquad (5.14)$$

The recharge rate to the saturated zone, Q_v and subsurface flow from the saturated zone, Q_b, are used to update the value of average moisture deficit, in the catchment at each time step at (h). This is represented by

$$\overline{S}_t = \overline{S}_{t-1} + (Q_{0,t-1} - Q_{v,t-1}).\Delta t \qquad (5.15)$$

where the subscript t represents the current time interval. The initial value of $\overline{S}$ (i.e. when t = 0) is calculated from Equation (5.11) using the initial value of the observed hydrograph as Q_b. The total contribution to the catchment outlet at any time step, Q_i (simulated flow), is the sum of subsurface flow, Q_b, and the saturation-excess overland flow, Q_{ovr}. The overland flow Q_{ovr} is calculated as the product of the depth of saturation-excess and the fractional area of topographic index values that are generating the saturation-excess.

Routing is necessary to recognize the effects of travel time within the catchment. The routing method used in TOPMODEL resembles Clark's (1945) method, which is a time-area routing method. In the time-area method of catchment routing, the travel time in the catchment is divided into equal intervals. At each time interval, it is assumed that the area within the catchment boundaries and the specific distance increment will contribute to the flow at the catchment outlet. The partial flow at the catchment outlet from each sub-area is equal to the product of the rainfall excess produced times the area of the contributing portion of the catchment. Summing the partial flows of all contributing areas at each time step gives the total flow at the catchment outlet for each time step in the hydrograph (Ponce 1989).

5.5.1 Procedure for Computation of ln(a/tanβ) Index for a Grid

In order to calculate ln (a/tanβ) index in each grid square, the contributing area for that grid square must be calculated and then divided by the tangent of the slope relevant to that grid. Only the downward direction is considered below. If it is assumed that all the directions have the same water transportation probability, then the area drained by unit length of contour can be calculated as:

$$a = A / nL \qquad (5.16)$$

where n = number of downward stream direction, L = effective contour length orthogonal to the direction of flow, and A = total area drained by current grid square (total upslope area).

The value of tan β can be computed as:

$$\tan\beta = \frac{1}{n}\sum_{i=1}^{n}\tan\beta_i \tag{5.17}$$

where tan β_i is the slope of the line connecting the current grid square with the further most grid square in the i^{th} downstream direction. Therefore,

$$\frac{a}{\tan\beta} = \frac{A}{L\sum_{i=1}^{n}\tan\beta} \tag{5.18}$$

and

$$\ln\left(\frac{a}{\tan\beta}\right) = \ln\left[\frac{A}{L\sum_{i=1}^{n}\tan\beta i}\right] \tag{5.19}$$

The amount of area A that contributes in each i^{th} downstream direction is thus calculated as:

$$\Delta A_i = \left[\frac{A_i \tan\beta_i}{\sum_{i=1}^{n}\tan\beta_i}\right] \tag{5.20}$$

The procedure is repeated on all cells of the DEM proceeding downstream.

5.5.2 Approaches for Computation of Topographic Index

Various procedures have been implemented to determine the spatial distribution of the topographic index ln (a/tanβ). The development of these procedures can be attributed to the manifold potential of the geographic information systems (GIS) which by means of its integration with hydrological modules greatly facilitates the estimation of the index in catchment areas.

Topographic index using single flow direction algorithm proposed by Jenson and Dominique (1988) is the most commonly used method of computing topographic index due to its simplicity and wide availability in most GIS systems. In this method,

starting from a DTM, the cumulative upslope area drained through a generic cell of the DTM is computed by allowing flow of water to occur in one of the possible eight neighbouring cells by means of a moving window of 3 x 3 points centered on the analysis point (I, J) (commonly known as D8 algorithm) which, along the direction of maximum slope, moves sequentially from higher to lower DTM levels. At the end of this elaboration, it is possible to associate the cumulative upslope area that has drained through the element considered, the theoretical path taken by flow and the topographic gradient in the direction of maximum slope to each DTM element (I, J).

Greater detail can be obtained by introducing a stochastic component inside the D8 algorithm, along the N-E, S-E, S-W and N-W directions (Fairfield and Leymarie, 1991). This improvement, known as Rho8 procedure, is more often found more suitable in those moderately sloping areas along which the automatically extracted channel network would tend to runoff in parallel along the preferential directions, according to the D8 approach. The D8 and Rho8 procedures produce similar distribution function of topographic index, however, the same procedures do not represent completely the flow path of surface runoff, especially in those areas typified by divergent surfaces.

Freeman et al. (1991) introduced a multiple direction approach, defined as FD8, for theoretical evaluation of the concentration of surface runoff by considering the accumulated upslope area for any one cell is distributed amongst all those of downstream direction according to weighted percentages relative to the slope. They however demonstrated that FD8 algorithm cannot simulate well in certain topographic conditions, such as those found in alluvial plains. In these circumstances a pronounced expansion of surface runoff along the alluvial plains is noticeable instead of well-delineated stream channels. The FD8 algorithm, therefore, has to be modified according to the river network and local soil depth variations.

A mixed scheme namely, FRho8 (Medicino and Sole, 1997) allows the evaluation of theoretical path of flow related to the permanent drainage system. Runoff coming from slopes (scheme FD8), after having reached one of the channels of the river network, must remain in it (scheme Rho8) until it reaches the basin outlet.

Quinn et al. (1995) suggested a specific procedure for hydrological applications using TOPMODEL. This is based on the analysis of distribution functions of the topographic index obtained for different value of channel initiation threshold, CIT which is minimum drainage area required to initiate a channel.

Variations in the CIT produce different resolution levels of the channel network because of different cataloging of a certain number of DTM cells ("Channel" cell, on "slope" cells).

Therefore, different procedures imply variation in the shape of the topographic index distribution function, channels of the network are characterized by a greater concentration of surface runoff with respect to the slopes, and therefore, by higher values of topographic index. If a high starting value of CIT is selected (low network resolution level), and ever decreasing values are considered (level increase), the 'channel' cells propagate upwards involving the 'slope' cells that contain a channel, and which are thus characterized by lower index values. This leads to a small increase in the peak of the topographic index distribution function. These variations are contained up to a threshold value of CIT for which there is a rapid rise and a noticeable shift of the distribution peak towards lower index values. This threshold values according to Quinn et al. (1995) should be more suitable for identification of the permanent channel network in the case of hydrological applications conducted exclusively with TOPMODEL relative to basic resolution of current DTM.

In the above procedures there are two important restrictions. The first involves the formation of runoff within DTM, which, as well as having a pixel, origin is routed downwards by means of a line (one dimensional). The second refers to runoff directions, which are limited to the eight possibilities of neighbouring points of cell under consideration. These problems can be overcome by a DTM cell is routed downwards by means of a surface, analogous to that produced by the procedure proposed by Costa-Carbal and Burger (1994), called DEMON. In this procedure, according to contour based stream tube approach used originally by Beven and Kirkby (1979), runoff is generated by area and not by a pixel origin. Runoff produced by DTM cell is routed downwards by means of a surface, analogous to that produced by the projection of a stream tube on to a plane. Different stream tubes, or flow paths, are identified locally as line intersection points, traced in aspect direction, with the edges of the DTM cell. The width will vary according to morphology in the DTM, increasing for divergent surfaces and decreases in relation to convergent surfaces.

Currently a digital terrain model (DTM) or digital elevation model (DEM) is extensively used to calculate the spatial distribution of the topographic index in a catchment (Saulnir et al. 1997). However, there are two factors which affect the pattern of the topography index distribution; the resolution of the topography used in

the DTM and the way to define a grid as containing the river channel or not in a catchment. If a grid, which originally is one containing a river channel by one threshold setting, which is used to decide whether the grid contains the river channel or not, is considered as one of the water collection area without the river channel by another threshold setting, the number of grids with high topography index will increase and the distribution of topography index in a catchment will move to the end of high value and, in turn, the average topography index of the catchment will enlarge. In order to reduce the effect of the way to consider a grid as containing the river channel on not, a channel initiation threshold (CIT), is set up. If a grid with area 'a' draining water through it greater than CIT, the grid is considered as one containing water channel; otherwise the grid is considered as one without the water channel inside and as an area collecting water flow from upstream.

5.6 STUDY AREA AND DATA AVAILABILITY

A brief description of the Chaukhutia watershed is given in Chapter 2. However, as per the requirements of TOPMODEL, a diagnosis of landuse and soil classification and hydrological data has been discussed herein as follows.

5.6.1 Soil Type

A description of soil types of Chaukhutia watershed has been given in Chapter 2. However, this description meets the requirements of the present study, which is preparation of soil map for Chaukhutia watershed. Broadly soils of this watershed may be classified as loamy soils. Depth of soil varies from shallow to deep and slope varies from steep to very steep. Hydrologically, soils present in the watershed can be grouped into A through C as per SCS (1956). Figure 5.1 depicts the soil map (NBSSLUP, 2004) of the watershed.

5.6.2 Land Use

A description of landuse types has been provided in Chapter 2. However, this description meets the requirements of the present study, which is preparation of land

use map for Chaukhutia watershed. In terms of land resources, the Chaukhutia watershed is covered with forest, pasture, agriculture, settlement, and fallow/rocky/ waste lands. The forest cover of Chaukhutia watershed is about 50% of the total area of this watershed. The percentage of agricultural land area is about 12.0% of the total area of the Chaukhutia watershed. About 15% area of the watershed is covered by pasture. The area covered by urban and rural settlements in this watershed is about 8.0% of the total area. In addition, the area under different roads is about 2.0% of the total area. Besides, other land types such as water bodies (about 5.0%) and area under fallow/rocky/waste lands is about 8.0% of the total area of this watershed. Land cover map of the watershed obtained after classification of LISSIII satellite image of IRS system is shown in Figure 5.2.

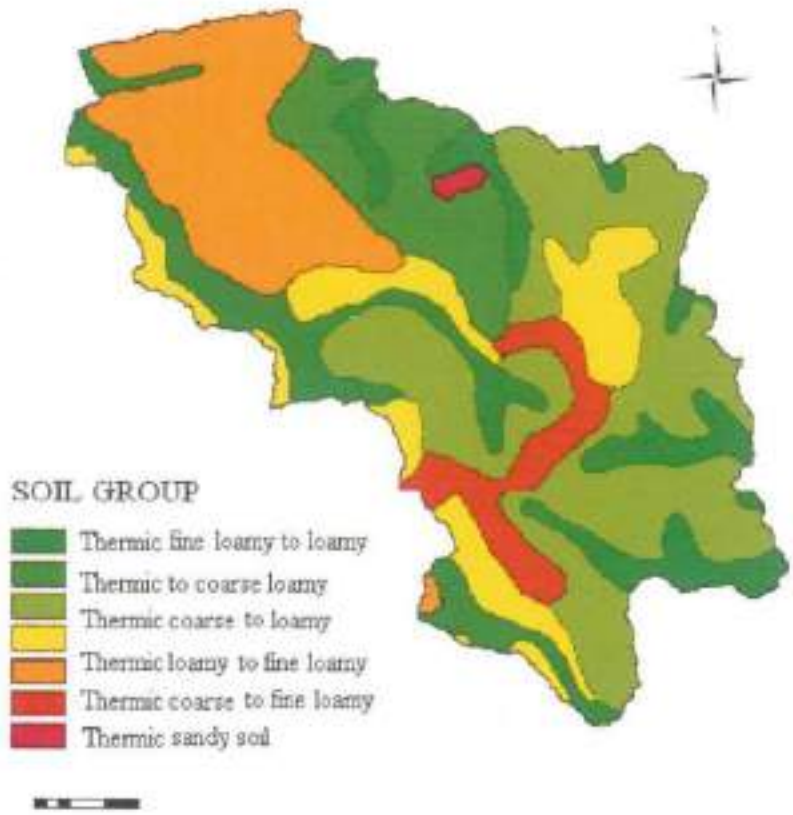

Figure 5.1: Soil Map of Chaukhutia Watershed

5.6.3 Stream Network

The watershed is drained by a dense river network having high slopes. There are two major streams that meet the river Ramganga at Chaukhutia namely Kurhlar Gad which is 16 km long meeting the main river from south-east direction and Khachyar Gadhera which is about 14 km long and meets the main streams north direction of Chaukhutia. Drainage map of Chaukhutia watershed is shown in Figure 5.3.

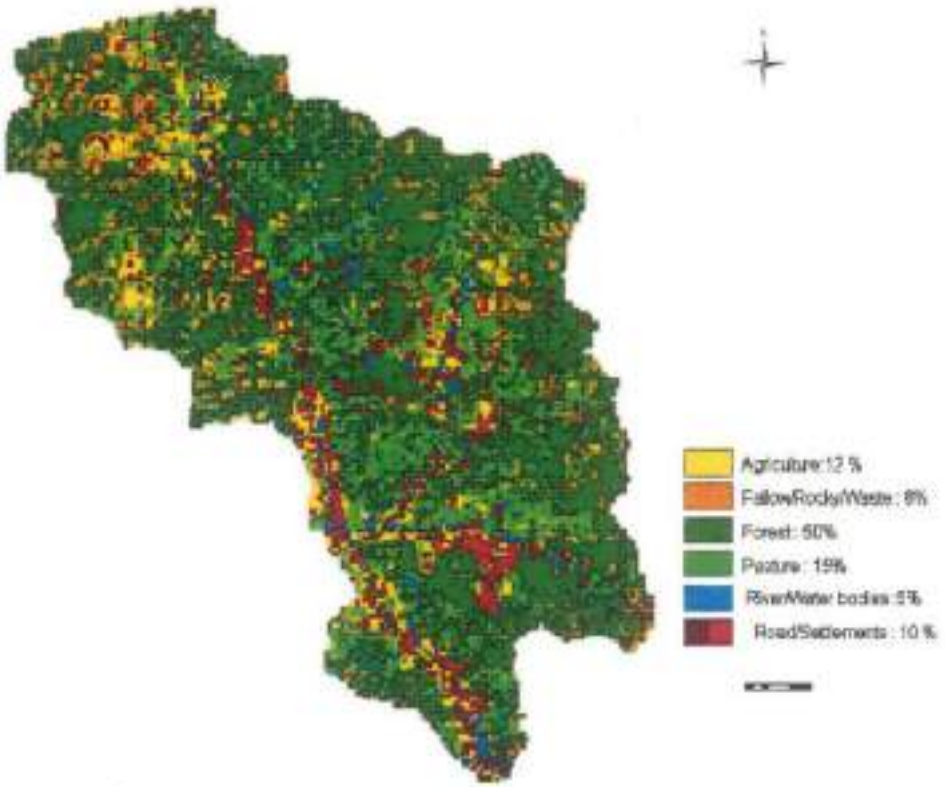

Figure 5.2: Land use Map of Chaukhutia watershed

5.6.4 Data Availability

Basic topographic details were available from the Survey of India toposheets (Nos. 53N4, 53N8, 53O1, 53O5 and 53O9) at the scale of 1:50000. Daily rainfall and runoff data for the years 1975-78 and June 1979 – May 1981 were available.

Temperature data for the corresponding period was also available and these were used for computation of daily evapotranspiration of the watershed due to nonavailability of its observations.

Figure 5.3: Drainage Map of Chaukhutia Watershed

5.7 TOPMODEL APPLICATION

This section deals with the application of TOPMODEL to Chaukhutia watershed in a step-to-step procedure as follows.

5.7.1 Data Processing

Application of TOPMODEL involves **(i)** generation of digital elevation model (DEM); **(ii)** determining the topographic index distribution of watershed from generated DEM, after making it sink free; **(iii)** preparing the necessary input and catchment data files from hydrological and topographic index distribution data.

5.7.1.1 DTM Generation and Analysis

In the present study scanned topographic maps in scale of 1:50000 were used to derive spatial information such as contours, drainage, spot height etc. Georeferencing of scanned topographic maps was done using ERDAS IMAGINE image processing system (ERDAS, 2001). The objective of Georeferencing is to provide a rigid spatial framework by which positions of the real world features are measured, computed and analysed in terms of length of a line, size of an area and shape of a feature. The primary aim of a reference system is to locate a feature on earth surface.

All these maps were first registered in Geographic coordinate system (latitude, longitude) and then re-projected in polyconic projection system with reference spheroid as Everest 1956 (Indo-Nepal) by invoking geometric correction function of data preparation menu of ERDAS IMAGINE. Then all the point features, line features, such as contours and streams, and area features, such as lakes, ponds etc, were digitized as vector layer in ERDAS. All these files were exported to ArcGIS (ESRI, 2000) to assign associated attribute information elevation of contours etc. and further processing.

The digitized contour map was interpolated using interpolation tools available in ArcGIS to produce DEM of Chaukhutia watershed. By using Topo to raster option of Raster Interpolation menu, hydrologically correct DEM at a finer resolution of 20m was made. Generated DEM was further aggregated to 100 m pixel size to fit into rows and column limits imposed in TOPMODEL program. Aggregated DEM of 100 m resolution was analysed further by TauDEM terrain analysis extension to ArcGIS (Tarboton, 1997). Using terrain analysis functions available in TauDEM extensions, a sink free DEM was generated. Location of the outlet of watershed was marked on sink free DEM. For this, a shape file with point feature class was created in ArcMap and outlet was located on the stream path by selecting Editor/Start and Stop Editing and save edits options of ArcMap. Selecting this output file in Network Delineation menu watershed was delineated. After masking operation Raster Digital Elevation was masked and all pixels lying outside of watershed were assigned a value greater than 9999.0m. The masked DEM of watershed is shown in Fig. 5.4.

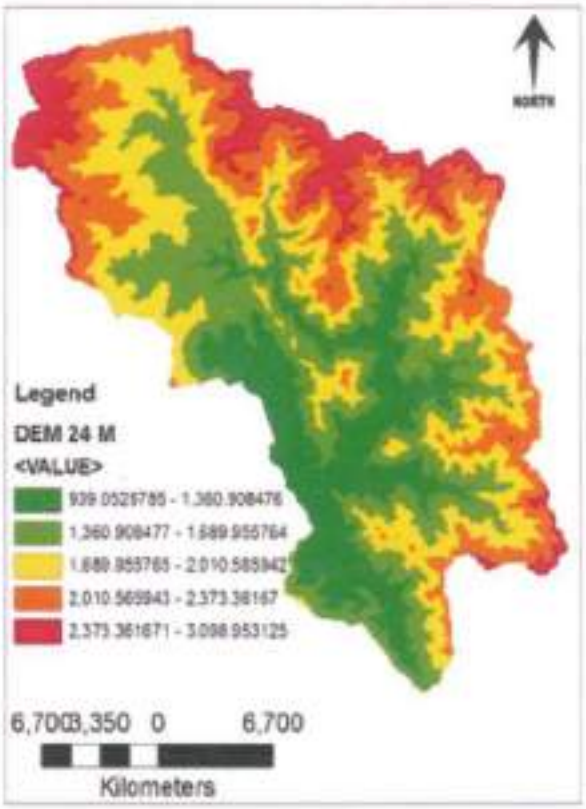

Figure 5.4: DEM of Chaukhutia watershed

5.7.1.2 Determination of Topographic Index

The generated DEM was exported to ASCII format for inputting into DTM analysis program of TOPMODEL. The input elevation file is a file of elevation in meters, listed in order from bottom left hand (South West) corner, row by row, working northwards. Only the elevation of points within the catchment is used, all other values in the matrix is set to a value greater than 9999.0 (m), for Topographic Index calculation. Values of topographic index $\ln(a/\tan\beta)$ were calculated using single and multiple direction flow algorithm (Quinn et al., 1995).

By choosing Topographic Index distribution option of the program, output files, with information of topographic index $\ln(a/\tan\beta)$, % contributing area $\Delta A_c/A$, cumulative contributing area and number of sinks and lake pixels, was obtained. The single flow direction does not require a contour length term as every pixel has the same contour length. However, multiple flow direction algorithms have variable outflow directions that are dependent on a cell's neighbors, hence contour length is also considered for this flow direction. For this weighting factor of 0.5 was considered

for cardinal directions and 0.35 for a diagonal direction for partitioning of flow (Quinn et al. 1991). These topographic index distribution values were reclassified into 27 classes to fit in dimensional limitation of less than or equal to 30 classes of the TOPMODEL program available. Figs. 5.5a&b shows the spatial distribution of Topographic Index in the catchment computed using single and multiple flow direction algorithms. Fig. 5.6 shows cumulative frequency distribution of Topographic Index $\ln(a/\tan\beta)$ for single and multiple flow direction algorithm. As can be seen from Fig. 5b, the curves showing cumulative frequency distributions for single and multiple flow direction have same shape but index values computed by single flow direction algorithm have higher values near channel cells due to concentration of flow which can be seen clearly from this figure. Overall the distribution of topographic index well spread across the catchment and nearly all high index areas are located near the streams. In general, the index map corresponds well with the catchment wetness.

5.7.1.3 Preparation of Input Files

For setting up of a model for a watershed, input data files are required to be prepared. The input files for application of the TOPMODEL consist of project file of the watershed having information of text description of application, Catchment Data file name, Hydrologic Input Data file name and Topographic Index Map file name. The Catchment data file was prepared with all necessary data regarding log(a/tanβ) distribution class values, stream channel distance increment with contributing area for channel routing and five model parameters, namely, parameter of exponential transmissivity function (m), the natural logarithm of effective transmissivity of the soil when just saturated ($\ln(T_o)$), the profile storage available for transpiration (SR_{max}), initial storage deficit in root zone (SR_{int}), and effective surface routing velocity for scaling the distance/area (ChVel), with initial, minimum and maximum values of the parameters.

Hydrological input Data file was prepared with the available daily rainfall, runoff and temperature data of the watershed. As reported previously, daily potential evapotranspiration data were not available, monthly Potential evapo-transpiration was calculated by an empirical formula given by Blaney and Criddle (1962). In this

method potential evapotranspiration is estimated by correlating it with sunshine hour and temperature. Sunshine at a place is dependent on latitude of the place and varies with month of the year. PET for a crop during its growing season is given as:

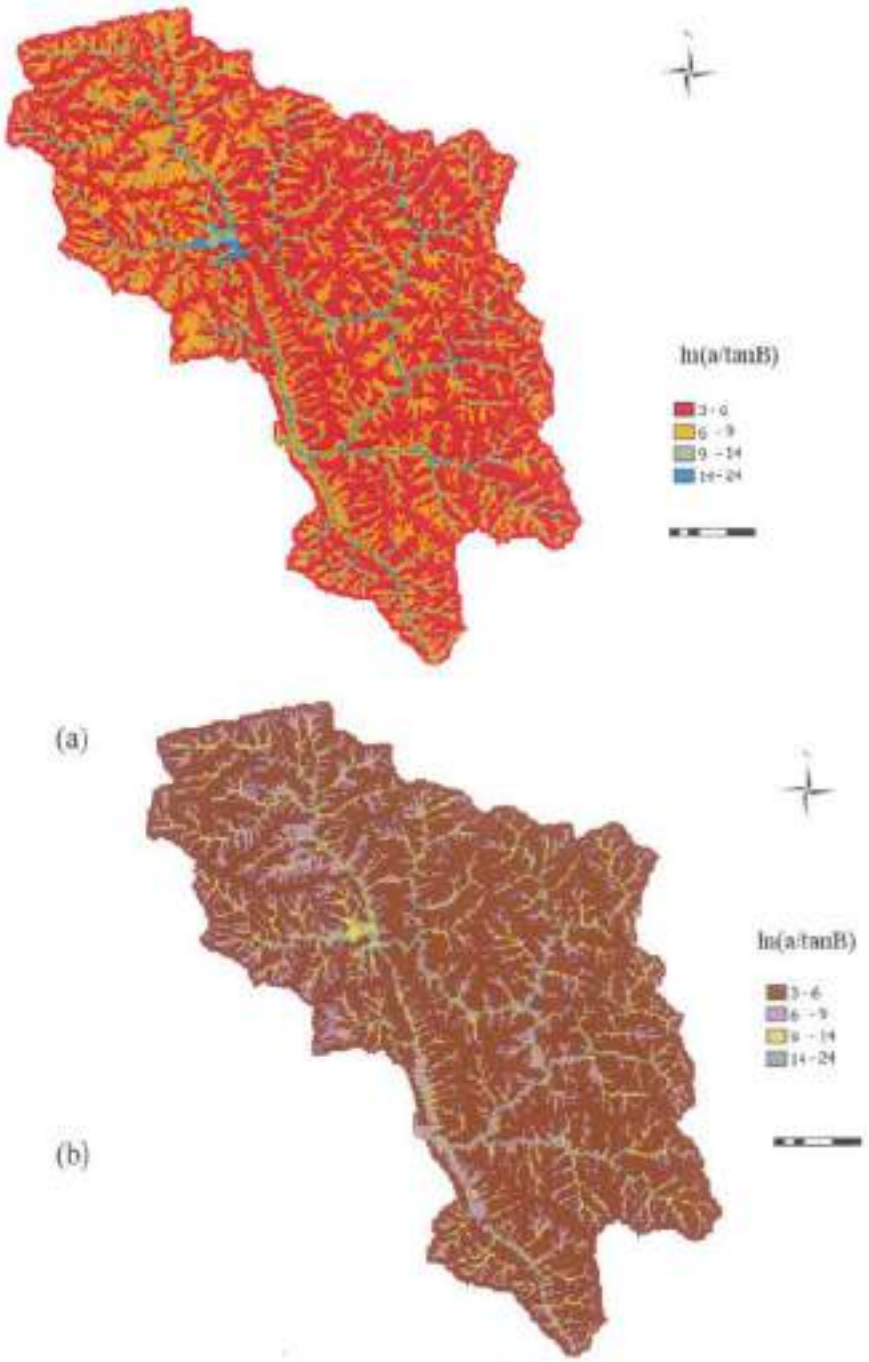

Figure 5.5: Topographic Index Map of Chaukhutia watershed (a) Multiple direction of flow, (b) Single direction of flow

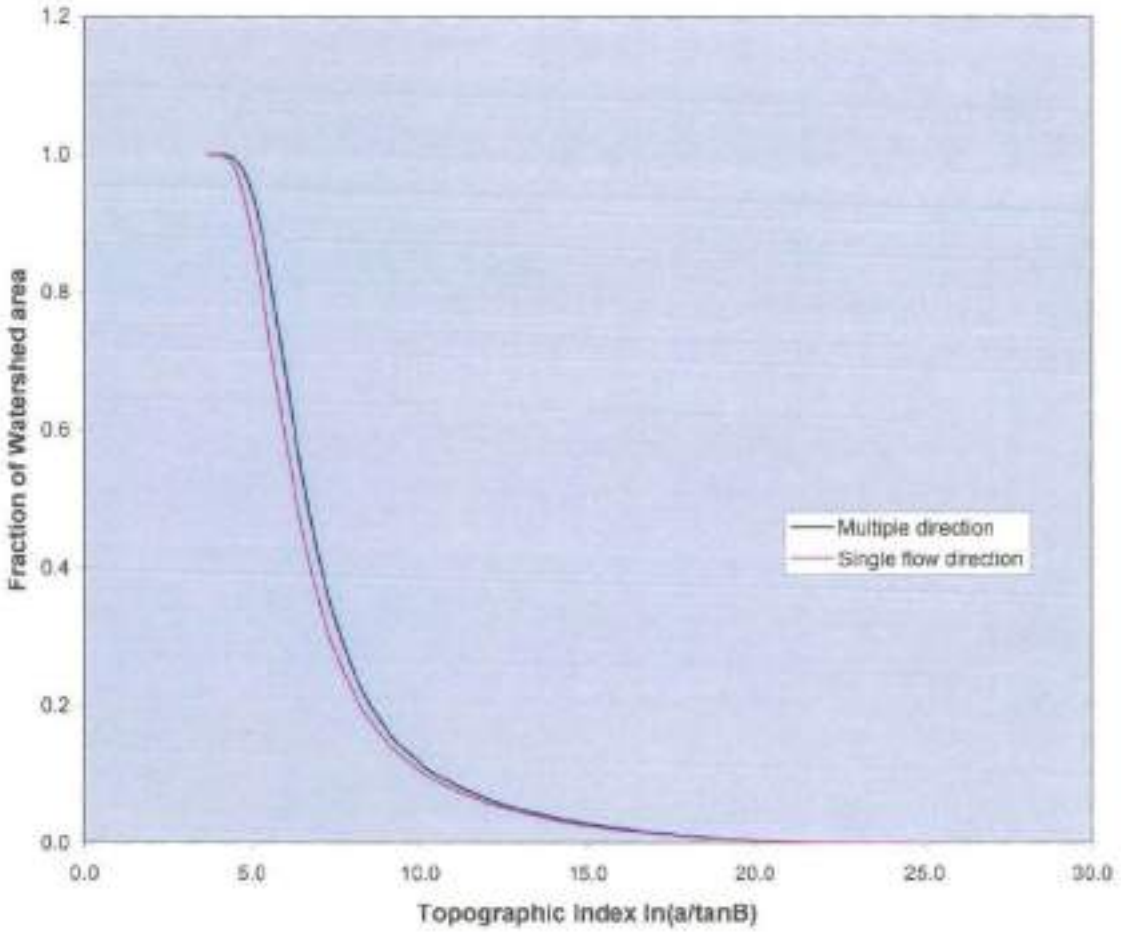

Figure 5.6: Cumulative frequency distribution of Topographic Index for Single and Multiple direction of flow

$$PET = \sum K*F \tag{5.21}$$

where, K is monthly crop coefficient determined from experimental data and F is monthly consumptive use factor, given as:

$$F = (0.0457T_m + 0.8128)\ P \tag{5.22}$$

where PET is the potential evapotranspiration in cm; T_m is the mean monthly temperature in ^{o}C and P, the monthly percentage of bright sunshine hour in the year.

5.8 ANALYSIS AND DISCUSSION OF RESULTS

In this section, the model is calibrated and validated for its applicability to the data of Chaukhutia watershed for runoff simulation, and the sensitivity analysis of various model parameters is also carried out as discussed in next sections.

5.8.1 Model Calibration and Validation

For calibration and validation of the model parameters, the available observed data was split into two groups. The first group of data for years 1975 to 1978 was used for calibration of the model and the remaining data for years 1979 to 1981 was used to validate the model results.

5.8.1.1 Model Calibration

Each formulation of the TOPMODEL may present an individual parameter set to be calibrated. However, in the version of the TOPMODEL used in the present study, there are five critical parameters that directly control model response. These are

1. 'm' : the parameter of exponential transmissivity function or recession curve (units of depth, m).
2. $\ln(T_0)$: The natural logarithm of effective transmissivity of the soil when just saturated. A homogeneous soil throughout the catchment is assumed.
3. SR_{max} : The soil profile storage available for transpiration i.e. available water capacity (units of depth, m).
4. SR_{init} : The initial storage deficit in the root zone (units of depth, m).
5. ChVel : Effective surface routing velocity for scaling the distance/area or network width function. Linear routing is assumed (units of m/hr).

The model was applied on a continuous basis over a period of 4 years (Jan. 1975 to Dec. 1978) for calibration of model parameters for the watershed. A time step of 1 day was selected for computations to calibrate the model. As detailed earlier, all five parameters were assigned with initial values. The calibration of parameters was systematically performed starting with parameter 'm'. The value of parameter m was varied, holding values of remaining four parameters at initial value and value of

parameter m was determined which yields the highest Nash and Sutcliffe efficiency value, 'EFF'. Subsequently, the parameter m was assigned the just determined value and next parameter $\ln(T_0)$ was varied with an effort to further maximize efficiency. This was repeated for remaining parameters in succession to arrive at a set of parameters which gave highest value of efficiency EFF. These parameters were further refined by giving computed parameters as initial guess in second round of execution runs with narrow band of upper and lower limits and in this way a set of parameters was chosen which gave highest value of EFF. After each run of the model, four indices of goodness of fit were considered for evaluation. These are:

- The Nash and Sutcliffe efficiency, $EFF = (1 - \sigma_i^2/\sigma^2_{obs})$ where σ_i^2 is residual variance and σ^2_{obs} is the observed variance. (5.24)
- Sum of squared errors, $SSE = \sum_{1}^{n} (Q_{obs} - Q_{simu})^2$ (5.25)
- Sum of squared log error, $SLE = \sum_{1}^{n} \{\log(Q_{obs}) - \log(Q_{simu})\}^2$ (5.26)
- Sum of absolute errors, $SAE = \sum_{1}^{n} |Q_{obs} - Q_{simu}|$ (5.27)

The calibration of model parameters was done by considering values of topographic index computed by single as well as multiple flow direction algorithms. For computation of topographic index using single flow direction, weighting factor 'H' was taken equal to 5.0 and for multiple flow direction 'H' was taken as 1 for 100 m pixel size used in the present analysis (Quinn et al.,1995). The values of model parameters obtained through calibration and values and error statistics for entire calibration period obtained using topographic index values for single and multiple direction algorithms are shown in Table 5.1. Yearly values of Nash-Sutcliffe efficiency using multiple direction flow algorithm based topographic index are shown in Table 5.2. As can be seen from Table 5.2 the efficiency of model varies from year to year with a high value of 0.86 for year 1976 and lowest value for year 0.33 for year 1978.

The result shows that there is little variation in efficiency as well as value of the parameters in both single and multiple direction flows suggesting insignificant effect on computed results due to choice of computation method used for deriving

topographic index. Figs. 5.7 through 5.10 show the simulated and observed hydrographs for calibration period for years 1975 through 1978, respectively. As can be seen from Fig. 5.7 the match of observed and simulated runoff is very good. However, the observed and simulated runoff shown in Fig. 5.10 does not match well.

Table 5.1: Values of calibrated parameters and error statistics for calibration run

Flow direction	m	$Ln(T_0)$	SR_{max}	SR_{init}	Chvel	EFF	SSE	SLE	SAE
Multiple (H =1.0)	0.005	2.0	0.0015	0.001	3600	0.584	9.27E-6	3.73E+2	0.058
Single (H = 5)	0.0048	2.0	0.0015	0.001	3600	0.583	9.29E-6	3.58E+2	0.057

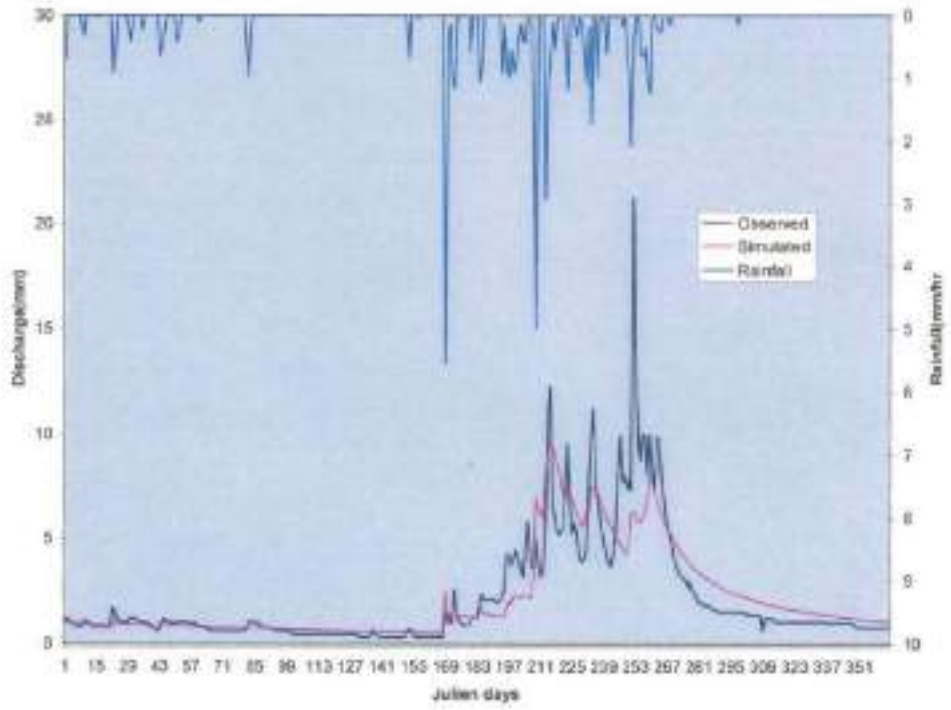

Figure 5.7: Observed and simulated hydrograph of Chaukhutia watershed (calibration year 1975)

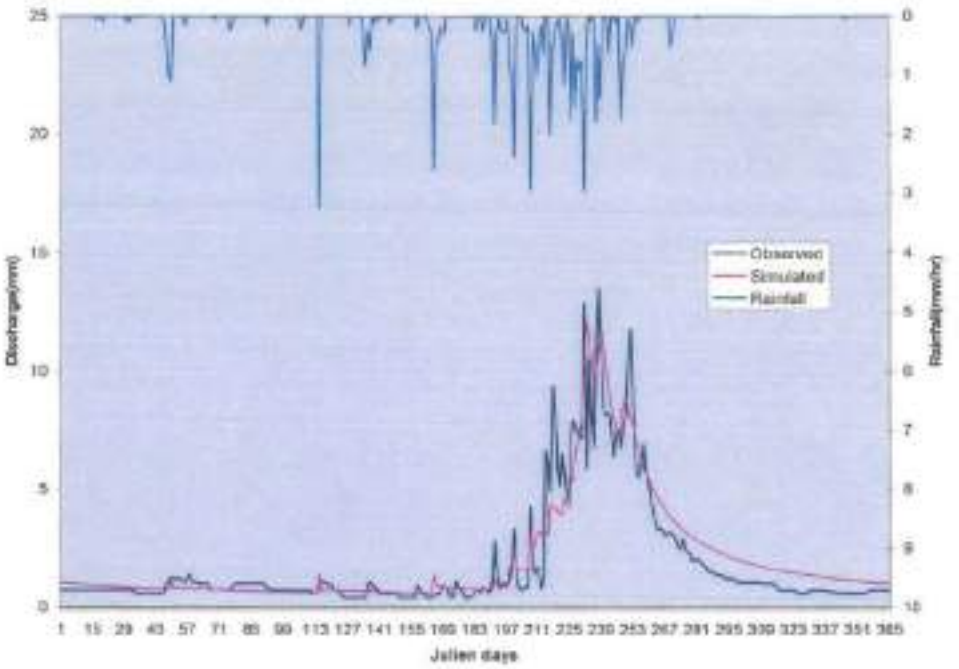

Figure 5.8: Observed and simulated hydrograph of Chaukhutia watershed (calibration year1976)

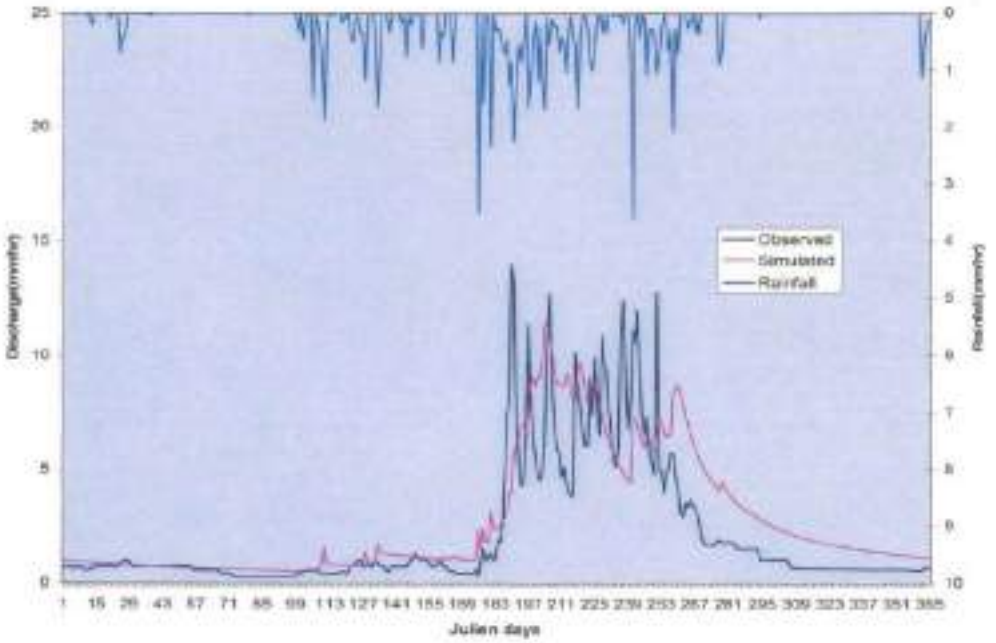

Figure 5.9: Observed and simulated hydrograph of Chaukhutia watershed (calibration year1977)

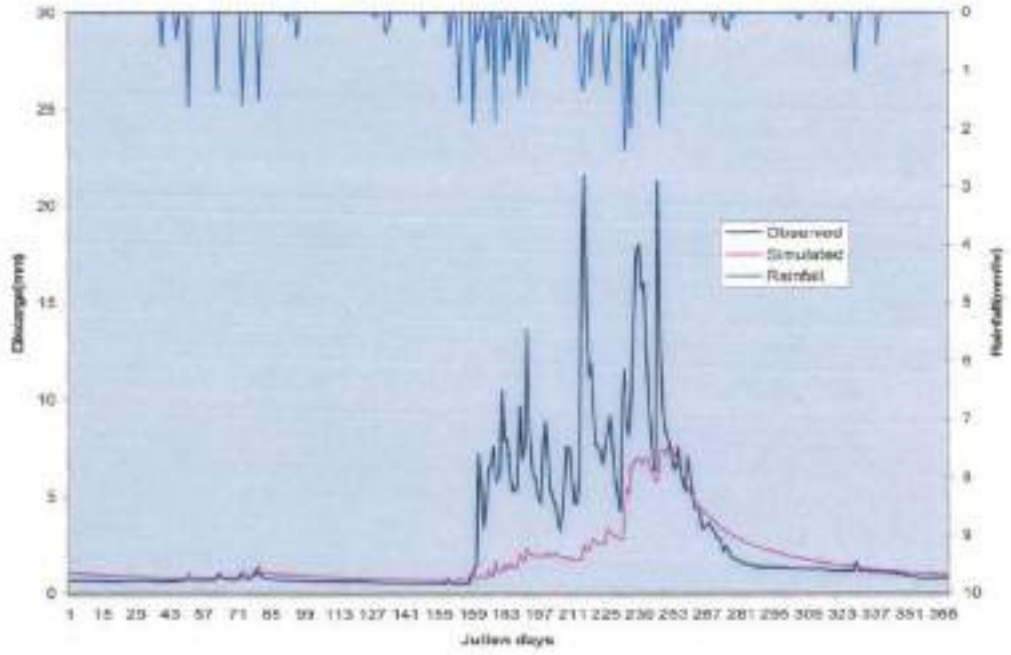

Figure 5.10: Observed and simulated hydrograph of Chaukhutia watershed (calibration year 1978)

Table 5.2: Yearly values of Nash-Sutcliffe efficiency for calibration run

Calibration year	NS Efficiency
1975	0.73
1976	0.862
1977	0.605
1978	0.336

5.8.1.2 Model Validation

The model was run further with above parameter values for validation data series and the resulting efficiency was compared with the calibration efficiency. Validation was carried out for the period different from the one used for calibration. Same set of optimized parameters as found during calibration were used to run the model. The average values efficiency and other goodness of fit indices for validation period are given in Table 5.3. Yearly values of Nash-Sutcliffe efficiency using multiple direction flow algorithm based topographic index are shown in Table 5.4 for

validation period. As can be seen from Table 5.4 the efficiency of model varies from year to year with highest value of 0.695 for year 1980-81 and lowest value of 0.419 for year 1979-80. Figs. 5.11 & 5.12 show the simulated and observed hydrographs for validation period for years 1979-80 and 1980-81, respectively. As can be seen from Fig. 5.12 the match of observed and simulated runoff is very good however the observed and simulated runoff shown in Fig. 5.11 does not match well.

Table 5.3: Values of error statistics for validation run

Flow direction	EFF	SSE	SLE	SAE
Multiple (H=1.0)	0.649	4.27E-6	2.64E+2	0.028
Single (H=5)	0.665	4.07E-6	2.52E+2	0.027

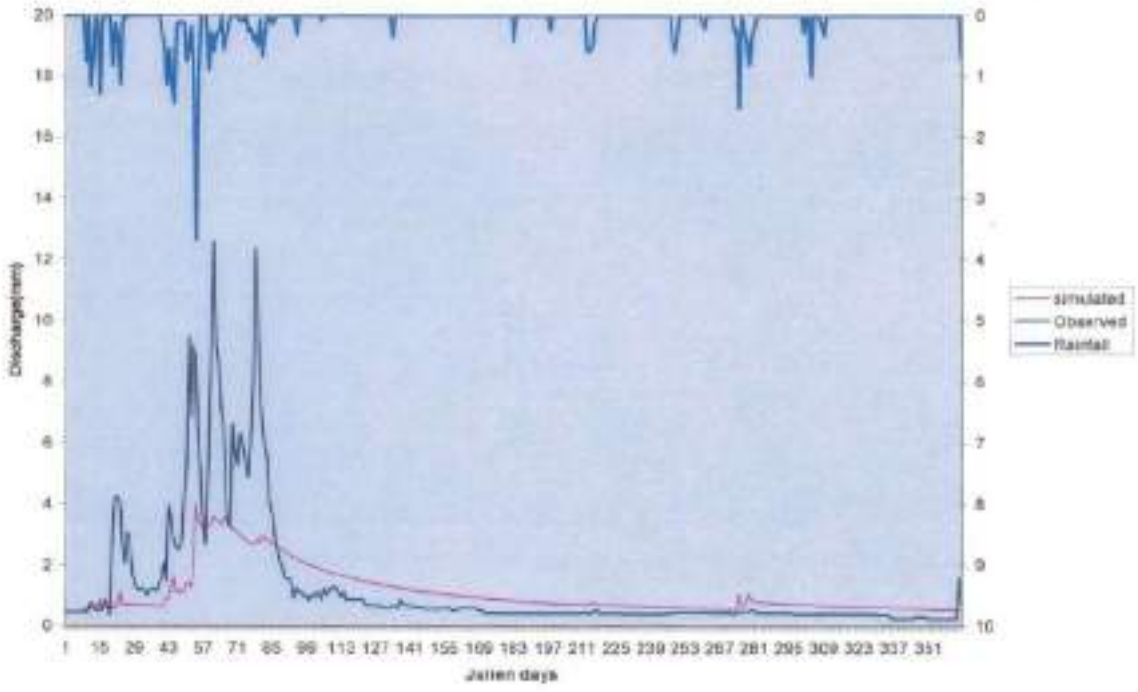

Figure 5.11: Observed and simulated hydrograph of Chaukhutia watershed (Validation year 1979-80).

Table 5.4: Yearly values of Nash-Sutcliffe efficiency for validation run

Validation year	Efficiency
1979-80	0.419
1980-81	0.695

5.8.2 Discussion of Results

It is evident from the results of model performance based on efficiency and other goodness of fit indices that there is a minor difference in efficiency for single and multiple direction flows. This may be due to marginal difference in values of topographic index distribution in single as well as multidirectional flows.

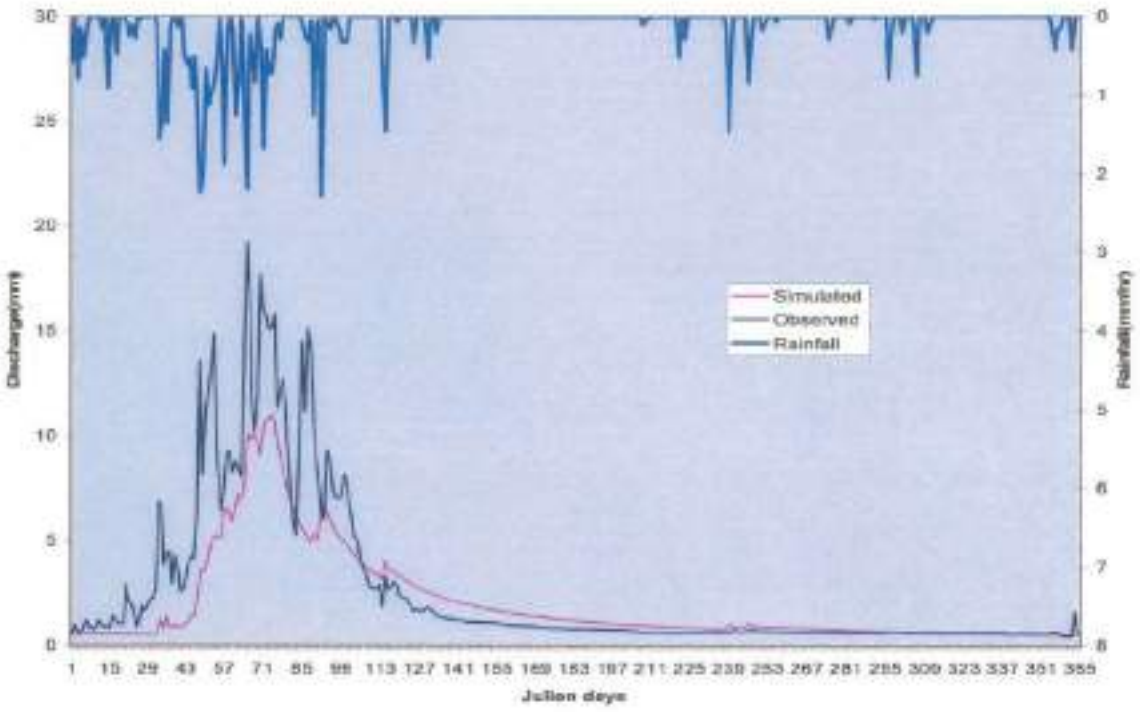

Figure 5.12: Observed and simulated hydrograph of Chaukhutia watershed (Validation year 1980-81)

Topographic index indicates the propensity of landscape areas to become wet. The maximum Topographic Index class was 25.0 and minimum Topographic

Index class was 3.5. High index values are associated with river channel and low with upland areas which do not contribute directly to runoff. From the Topographic index distribution Map of Chaukhutia watershed it can be seen that most of the watershed areas are in lower index class values. This is due to coverage of watershed with deep forest (about 50%) which contributes a little towards infiltration-excess runoff. This may be a reason behind the low average Nash and Sutcliffe efficiency value of 0.58, for calibration and 0.649 for validation periods.

The model simulated the rise and fall of seasonal base flow through the season with superimposed overland and fast subsurface flow events. Simulations improved as the rainfall events became more frequent and contributing areas were more established through wetting up. The calibration period plot of observed and simulated hydrographs showed that the model reproduced the rise and fall of seasonal base flow but under-estimated some of the high runoff producing storm events. This phenomenon was also visible in validation period plot of observed and simulated hydrographs. This resulted in overall low efficiency of model. It is also observed during calibration run that influence of parameter like SR_{init} and ChVel on runoff estimation is negligible. It may be due to coverage of watershed by deep forest with the large moisture holding capacity. Deep forest also causes more evaporation. This causes less initial root zone deficit to occur at the start of next rainy season.

5.8.3 Sensitivity Analysis

The sensitivity analysis was carried out to evaluate the sensitivity of the objective function due to change in the values of model parameters in predefined range. An initial run of the model was made with the current value of parameters and efficiency as objective function. Then value of each of the parameters was altered in specified lower and upper limits of the parameters and results for different combinations of parameters set were obtained. A result for plots of efficiency with change in values of individual parameters is shown graphically in Fig. 5.13. As can be seen from Fig. 5.13, only three parameters namely 'm', $\ln(T_o)$ and SR_{max} are affecting model efficiency and change in values for parameters SR_{ini} does not affect model efficiency.

5.8.4 Monte Carlo Analysis

To evaluate model performance further, Monte Carlo simulation runs were taken using uniform random samples of the parameters chosen for inclusion in the analysis. Values of the other parameters were kept constant at their current values. The result was analyzed by Generalized Likelihood Uncertainty Estimation (GLUE) program.

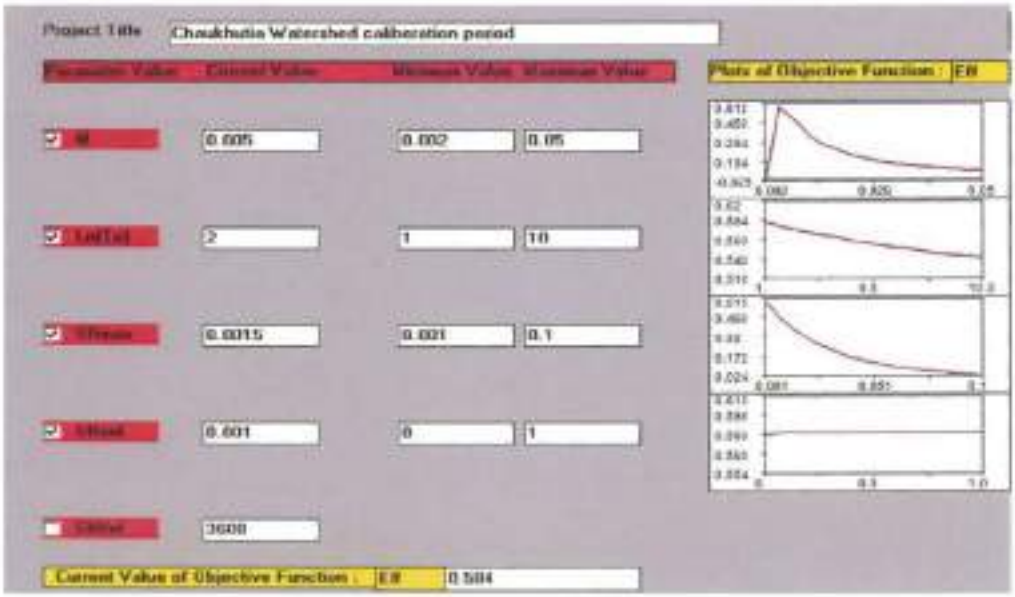

Figure 5.13: Sensitivity analysis of parameters of Chaukhutia watershed

Generalized Likelihood Uncertainty Estimation (GLUE)

The purpose of model calibration was to determine uncertainty associated with model prediction estimates derived from simulation for the entire season. The GLUE procedure requires a number of choices to be made (Beven and Binley, 1992):

1. Sampling a range for each parameter;
2. Methodology for sampling the parameter space;
3. A likelihood measure of model performance;
4. A criterion for acceptance or rejection of models; and
5. A methodology for updating likelihood measures.

Random values of parameters m, $\ln(T_0)$, SR_{max}, SR_{init}, and Ch Vel were drawn from uniform distributions over specified ranges. 1000 sets of five randomly generated parameters were supplied to TOPMODEL. The likelihood measure to evaluate model performance was the modeling efficiency of Nash and Sutcliffe (1970):

$$L(\Theta_i \mid \underline{Y}) = [1 - \sigma_i^2/\sigma^2_{obs}] \qquad (5.28)$$

where $L(\Theta_i \mid \underline{Y})$ is the likelihood measure for the 'i^{th}' model conditioned on the observations, σ^2_{obs} is the observed variance for the period under consideration, and σ_i^2 is the associated error variance for the 'i^{th}' model. The 1000 parameter sets were selected for calibration period. The criterion for behavioral parameter sets was selected as $E > 0.5$, and all others rejected.

From the result of Monte Carlo Analysis run, scatter plots of maximum likelihood versus different parameters were obtained. Dotty plots of 'E' versus parameters (Fig. 5.14) were used to assess the sensitivity of parameters to model performance. All the parameters have showed good or bad simulations over wide ranges of parameter space. It can be concluded from plots that 'm' and 'SR_{max}' parameters are sensitive to simulation due to clustering of dots in a certain range of parameter space. Based on Monte Carlo analysis list of top 20 ranked parameter sets are shown in Table 5.5. Among these twenty sets, only four parameter sets have efficiency $E > 0.5$. This indicates that model simulated the daily flows of Chaukhutia watershed less than satisfactorily.

5.9 SUMMARY & CONCLUSIONS

This chapter evaluated the applicability of TOPMODEL to daily flow simulation of Chaukhutia watershed of Ramganga catchment, a forest and sub-Himalayan watershed. As discussed in section 5.3, such an evaluation does not appear to have been reported in recent past. TOPMODEL, a distributed, topographically based hydrological model was applied to simulate continuously the runoff hydrograph of Chaukhutia watershed. It is a variable contributing area conceptual model in which topography controls the soil water storage and runoff generation. In this model, the total flow is calculated as the sum of two terms: surface runoff and flow in the

saturated zone. The TOPMODEL is attractive because of its structural simplicity and consideration of only a few parameters.

Table 5.5: List of top ranked parameter sets as per Monte Carlo simulation

Rank	M	$Ln(T_0)$	SR_{max}	SR_{init}	Efficiency
1	0.005	3.626	0.001	0.179	0.578
2	0.004	5.823	0.003	0.102	0.533
3	0.005	4.409	0.004	0.701	0.509
4	0.006	3.12	0.004	0.269	0.504
5	0.004	4.652	0.007	0.312	0.493
6	0.004	7.382	0.006	0.386	0.491
7	0.005	9.329	0.005	0.974	0.473
8	0.006	3.034	0.006	0.236	0.449
9	0.005	0.562	0.007	0.151	0.447
10	0.003	8.481	0.012	0.664	0.426
11	0.006	8.649	0.005	0.399	0.419
12	0.005	2.415	0.011	0.051	0.398
13	0.006	6.436	0.008	0.966	0.391
14	0.007	4.281	0.006	0.963	0.379
15	0.005	2.915	0.014	0.604	0.378
16	0.002	2.448	0.013	0.394	0.377
17	0.003	1.714	0.001	0.342	0.373
18	0.008	2.564	0.006	0.715	0.368
19	0.005	4.712	0.013	0.146	0.368
20	0.009	2.496	0.003	0.177	0.36

Raster DEM input for the model is generated through Arc GIS after digitization contour map from Survey of India toposheets. For model calibration and validation, the available data was split into two groups: the first set (1975 – 78) was used for calibration of the model, and the other set (1979 – 81) for validation. The model efficiency was 0.58 in calibration and 0.649 in validation period. The simulations provided an insight into the response of the catchment at different periods of the season. TOPMODEL performed only reasonably well as a continuous

hydrograph simulator in the Chaukhutia watershed. The model simulates well the base flow events but most of the peaks were under-simulated. Although top-ranked parameter sets achieved modeling efficiency of E = 0.57, and thus, simulation results are less than encouraging. This may be due to topography of watershed area which has a moderate to steep sloping surface covered with deep forest whereas TOPMODEL is suitable for moderate topography only. Furthermore, deep forest contributes less to saturation excess runoff.

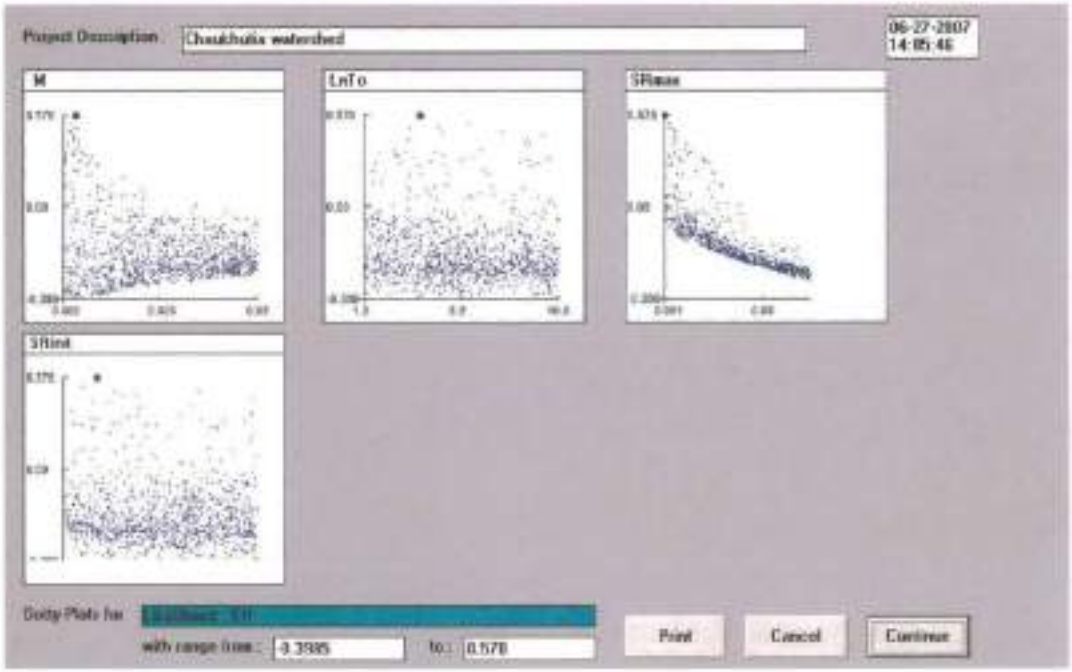

Figure 5.14: Dotty plots of parameters of Chaukhutia watershed for Efficiency

CHAPTER 6

APPLICATION OF SWAT MODEL

CHAPTER 6

APPLICATION OF SWAT MODEL

Water is the most precious and prime natural resource and a major constituent of all known forms of living matter on the planet earth. It is the single most important requirement for life. It is probably the only natural resource to touch all aspects of human civilizations- from agriculture and industrial development to the cultural and religious values embedded in society. As water brings life, water can also take life away. Large volumes of flowing water carry tremendous energy resulting in flooding and related phenomenon such as mudslides. For these reasons, throughout history, human beings have attempted to understand the behavior of water in order to reap the benefits it provides, while minimizing its potential for destruction. Over the year's rapid growth in population, urbanization and industrialization and changes in economic and social activities have resulted in increased and diversified demand of water. As the quantity of available water has remained constant, water has progressively emerged as the most important national and international issue. So there is need to simulate the runoff with reasonable accuracy by considering various factors affecting runoff. Numerous models are available to simulate hydrological regime from catchments.

The Soil and Water Assessment Tool (SWAT) is a distributed watershed model developed by Agricultural Research Service (ARS) of United States Department of Agriculture (USDA) to predict the impact of land management practices on water, sediment and agricultural chemical yields in complex watersheds. It is a comprehensive model which requires a significant amount of data and parameters for simulation of runoff and loadings mainly from rural catchments. To set up the SWAT model, a watershed is subdivided into a number of sub watersheds. These watersheds are further subdivided into Hydrologic Response Units (HRU) which are units of unique intersection of land use and soil. Watershed map inputs i.e. topographic, land use and soil maps, are provided to this model in the form of well treated digital raster maps in addition to several model compatible databases prepared by using latest Remote Sensing and Geographical Information System techniques. Most of the equations are solved at HRU

level in SWAT. Thus, this evaluates the applicability of SWAT model to simulation runoff from sub-Himalayan Chaukhutia watershed.

The Chaukhutia watershed is the uppermost Himalayan catchment of Ramganga river in the State of Uttrakhand. This watershed is situated in hilly terrain consisting of rolling and undulating topography having very steep irregular slopes. Soils of this watershed vary in texture, depth and slope. Hydrologic soil group also varies from B to C at different segments of this watershed. In terms of land resources, this watershed is dominantly covered by forests along with pasture, agriculture, fallow/rocky/waste land, settlements, road and stream networks. Thus, the Chaukhutia watershed consists of a complex terrain and there exists heterogeneity in land use and soil structures in this watershed. So simulation of runoff using any lumped model for this watershed may not produce good results. Hydrologic simulation models using distributed information of the watershed may be more suitable in modeling such complex watersheds.

6.1 OBJECTIVES

Broadly, this chapter aims at to discuss the suitability of SWAT model to simulate runoff in a predominantly forested mountainous catchment of Ramganga at Chaukhutia. The general layout of the study is as follows:

- Creation of Digital Elevation Model (DEM) of the study area.
- Creation of land use map of the study area using satellite data.
- Creation of digital soil map of the study area.
- Creation of data base compatible with SWAT model.
- Simulation of runoff using the latest AVSWATX extension of SWAT-2005 model
- Calibration and validation of the model with different data sets.
- Sensitivity analysis of the model.

6.2 SWAT MODEL

SWAT is a river basin, or watershed, scale model originally developed by Jeff Arnold for the United States Department of Agriculture (USDA) - Agricultural Research Service (ARS) (Liew et al., 2007 & Neitsch et al., 2005). SWAT was developed to predict the impact of land management practices with reasonable accuracy, on water, sediment, and agricultural chemical yields in large complex watersheds with varying soils, land use, and management conditions over long periods of time. This model was obtained by merging the models: Simulators for Water Resources in Rural Basins (SWRRB) (William et al., 1985; Arnold et al., 1990) and Routing Outputs to the Outlet (ROTO) (Arnold et al., 1995). The goal of developing SWRRB model was mainly the prediction of effect of management decisions on water and sediment yields with reasonable accuracy for ungauged rural basins throughout United States (Arnold and William, 1987). The other specific models that contributed significantly to the development of SWAT were: Chemicals, Runoff and Erosion From Agricultural Management Systems) (CREAMS) (Knisel, 1980), Ground Water Loading Effect on Agricultural Management Systems (GLEAMS) (Leonard et al., 1987), and Erosion-Productivity Impact Calculator (EPIC) (Williams et al., 1984).

SWRRB was initially developed from modifications to the daily rainfall hydrologic model from CREAMS. The major changes were model expansion to allow simultaneous computations and addition of storage components, weather generator, EPIC crop growth model, improved peak runoff predictions, flood routing component, transmission loss and sediment transport calculations.

Models were developed primarily to assess water quality issues in the 1980's, and SWRRB was a good model for simulating just that. In the late 1980's, the need to analyze larger, more complex watersheds arose. At this time, SWRRB was limited to ten sub basins in which water and sediment transport was routed from each subbasin directly to the outlet of the watershed. The development of a model called ROTO allowed the outputs from SWRRB to be routed through channels and reservoirs. SWRRB and ROTO were merged together to form SWAT.

SWAT (written in **FORTRAN 90**) was created in the early 90s, and since then it has undergone continued review, expansion of capabilities and extensive validation. The most significant improvements of the model between releases include:

SWAT94.2: Multiple hydrologic response units (HRUs) incorporated.

SWAT96.2: :Auto-fertilization and auto-irrigation added as management options;
:Canopy storage of water incorporated;
:Carbon Dioxide component added to crop growth model for climatic change studies;
:Penman-Monteith PET equation added;
:Lateral flow of water in the soil based on kinematic storage model incorporated;
:In-stream pesticide routing and nutrient water quality equations from QUAL2E added;

SWAT98.1: :Snow melt routines and in-stream water quality improved;
:Nutrient cycling routines expanded;
:Grazing, manure applications, and tile flow drainage added as management options;
:Model modified for use in Southern Hemisphere.

SWAT99.2: :Nutrient cycling and rice/wetland routines improved, Rservoir/pond/ wetland nutrient removal by settling added;
:Bank storage of water in reach and routing of metals through reach added;
:All year references in model changed from last 2 digits of year to 4- digit year;
:Urban build up/wash off equations from SWMM added along with regression equations from USGS;

SWAT2000: : Bacteria transport routines, Green & Ampt infiltration added;
: Weather generator improved;
: Daily solar radiation, relative humidity, and wind speed allowed to be read in or generated;
: All PET methods reviewed and allowed its values for watershed to be read in or calculated;
: Elevation band processes improved;
: Simulation of unlimited number of reservoirs enabled;
: Muskingum routing method added;
: Dormancy calculations for proper simulation in tropical areas was modified

SWAT2005: AVSWAT-X, [Beta version of SWAT2005]
: Weather forecast scenarios added;
: Bacteria transport routines improved;
: Sub daily precipitation generator added;
: Retention parameter used in the daily CN calculation may be a function of soil water content or plant evapotranspiration;
: Interfaces for the model have been developed in Windows (Visual Basic) **GRASS**, and **ArcView, ArcGIS.** SWAT has undergone extensive validation.

The world wide application of SWAT reveals that it is a versatile model that can be used to integrate multiple environmental processes, which support more effective watershed management and development for better policy decisions. The SWAT is a very flexible and robust tool that can be used to simulate variety of watershed problems. The SWAT model has proven to be an effective tool for assessing water resources and diffuse pollution problems for a wide range of scales and environmental conditions across the globe. In USA, SWAT is increasingly being used to support Total Maximum Daily Load (TDML) analysis (Mausbach and Dedrick, 2004), the effectiveness of conservation

practices in Conservation Effect Assessment Project (CEAP), macro scale studies covering Upper Mississippi River Basin and even entire US (Benaman et al., 2005), and a wide variety of other water use and water quality applications. Similar SWAT application trends have also emerged in Europe and other countries (Arnold & Fohrer, 2005).

6.3 SWAT APPLICATIONS- CASE STUDIES

6.3.1 International Applications

Upper Mississippi River Basin (US): A simulation study using SWAT has been initiated to access current and alternative nutrient, cropping and management practices in Upper Mississippi River Basin. Preliminary results indicate that the result is viable for predicting UMRB flows. The study is being carried out by Gassman et al., (2003).

Mekong River Basin (MRB): Mekong river is the 12th largest river in the world with a total length of 4800 km and a basin area of 795,000 km^2 for which it is ranked 21st. It is also ranked 8th in the world for its average annual rainfall of 475,000 Million m^3 (575.5 mm). The basin is composed of portions of several countries, including **China** (21%), **Myanmar** (3%), **Laos** (25%), **Thailand** (23%), **Cambodia** (20%), and **Vietnam** (8%). The SWAT model has been embedded into the Decision Support Framework as the first official hydrological model of the Mekong River Commission (MRC) and is used to generate runoff at the sub basin level. Presently, SWAT has been used to generate runoff from each sub basin under historical climate conditions and land cover change. In the future, the MRC will improve the Mekong SWAT model in various aspects such as better calibration results and land cover change. The SWAT capability in water quality and sedimentation will also be tested and applied. The study is being carried out by Jirayoot and Trung (2005).

Exe Catchment (UK): The Exe Catchment has a total area of 1530 km^2 is a large rural and agricultural catchment located in southern England. SWAT model was applied and

calibrated, verified and validated for hydrology and this has been taken as a sufficient base for modeling contaminants. The study is being carried out by White et al., (2005).

Elbe River Basin: The Elbe river basin covers large parts of **Eastern Germany** (2/3 portion) and **Czech Republic** (1/3 portion). The river is 1092 km. long and drainage area is 148268 km^2. Soil and Water integrated model based on SWAT was able to illustrate with a reasonable accuracy the basic hydrologic processes, the cycling of nutrients in the soil and their transport with water, the growth and yield of major crops and the dynamic features of soil and erosion and sediment transport under different environment conditions in catchment of temperate climate zones. The study was carried out by Krysanova et al. (2005).

Cannata Basin: Cannata is an ephemeral mountainous tributary of the Flascio river in Eastern Silicy (Europe). The basin covers 1.3 km^2 between 903 m and 1270 m above sea level with an average slope of 21%. The overall result of SWAT performance evaluation carried out for the Cannata basin was found to be very promising. The model was found to be efficacious in simulating surface runoff.

Terou Catchment: Terou catchment is a sub catchment of the Oueme River in sub humid African catchment. SWAT 2003 verison was found to be appropriate to adequately simulate changes in land use and precipitation. Further, reasonable values for future changes in runoff and erosion rates were obtained. The study was carried out by Busche et al., 2005.

Naivasha Lake Basin: Naivasha Lake is located within the eastern branch of Great Rift Valley of Kenya occupying a basin area of about 3200 km^2. SWAT model was applied to estimate spatial distribution of the flow in the basin to lake Naivasha and also to estimate lake water level fluctuation. Due to the altitudinal differences diverse climatic conditions were found in the basin. SWAT model was found to simulate the stream flow from year 1935 to 1965 with an acceptable accuracy. The study was carried out by Muthuwatta, (2004).

Upper Uma Oya Catchment: Upper Uma Oya catchment is a main tributary of Mahaweli River and flows into Ratnambe Reservoir in Sri Lanka. It covers approximately 89 km^2 with a high spatial variation of topography, rainfall and vegetation. SWAT model was found to simulate the hydrological condition of the catchment with an acceptable accuracy. The results shows that the changes in the land use greatly affect the hydrological characteristics of the catchment, especially increase the soil erosion in steep sloping areas with tea compared to natural forests.

Amameh Catchment: Amameh catchment in Iran is a mountainous and snow bound region having area of 37.20 km^2. The SWAT model was applied for water and sediment yield simulations and it was found that the structure of the SWAT model proved to be very stable, but the snow component of the model needed improvement and was therefore modified accordingly. The results were promising for water and sediment yield simulations. The study was carried out by Gholami & Gosain, (2005).

Yellow, Heihe River Basin: Runoff changes were studied for the Yellow river (China) headwaters under different climate and land coverage scenarios. Non point source pollution problems mainly caused by livestock over the Heihe river basin (7241.0 km^2) were studied and evaluated by using SWAT model. Based on the sensitivity analysis for different livestock scenarios, an effective strategy was proposed for having sustainable development for the study area. SWAT model was applied to Luxi watershed to simulate runoff time series. The study was done by Hao et al., (2005).

Woady Yaloak River Basin: Woady Yaloak river basin is located in Corangamite region in South Victoria, Australia and has an area of about 1463 sq. km. SWAT model was applied to predict the impacts of future land use changes within the basin. The results were very conducive and it was found that the model has very good potential for being adopted as a management tool to predict the impacts of future land use changes across the Corangamite region of Australia. The study was carried out by Watson et al., (2003).

Yongdam & Bocheong Watersheds: SWAT model was applied to estimate daily stream flow of Yongdam and Bocheong watersheds in Korea having catchments areas of 930 sq. km and 348 sq. km, respectively. It was found that the model performed successfully for these watersheds. The calibration and validation results showed a good agreement with the simulated and observed daily stream flow. The study was performed by (Kim et al., 2003).

Big Creek Watershed: The Big Creek Watershed situated in U.S.A., having an area of 133 sq. km., not only contributes significant amounts of flow to the Lower Cache River, but also carries a higher sediment load than other tributaries located in the area. Detailed sensitivity and feasibility analysis were performed for the SWAT model. Its feasibility analysis results demonstrate the suitability of SWAT for use in future decision support models that support comprehensive watershed management. The feasibility analysis demonstrates that SWAT is capable of identifying environmentally friendly land use and management practices and is a suitable watershed simulation model for use as a component of integrative watershed management tools. The study was conducted by Muleta et al. (2007).

Colworth Catchment: Kannan et al. (2007) applied SWAT-2000 model on a small catchment of 141.5 ha in the Unilever Colworth estate, in Sharnbrook, Bedfordshire, United Kingdom. The performance of SWAT model in different combinations of runoff generation and evapotranspiration methodologies available for hydrological modeling was explored and the following conclusions were drawn from the study:

a. Identification of the correct combination of ET and runoff generation methods is crucial for getting reasonably good results in hydrological modelling.
b. Calibrating the SWAT model using data from a wet period produces better results than calibrating it using data from a dry period.
c. The temperature-based Hargreaves method appears to be at least as good as the more complex energy-based Penman-Montieth method in predicting daily evapotranspiration.

d. The curve number method performed better than the Green and Ampt method in modelling runoff.

Five USDA-ARS Experimental Watersheds: Liew et al. (2007) evaluated the performance of SWAT model under a range of climatic, topographic, soils, and land use conditions in compliance with U.S. Senate Document. Hydrologic responses were simulated on five USDA Agricultural Research Service watersheds that included Mahantango Creek Experimental Watershed (7 sq. km.) in Pennsylvania, Reynolds Creek Experimental Watershed (239 sq. km.) in Idaho in the northern part of the United States, Little River Experimental Watershed (334 sq. km.) in Georgia, Little Washita River Experimental Watershed (610 sq. km.) in Oklahoma and Walnut Gulch Experimental Watershed (149 sq. km.) in Arizona in the south. A long record of multigauge climatic and streamflow data on each of the watersheds was used for model calibration and validation. The newly developed auto calibration tool in **AVSWAT-X [Beta version of SWAT2005]** was used to calibrate stream flow response in the model. Test results demonstrate the uniqueness of each calibrated parameter set and corresponding hydrologic response. SWAT exhibits an element of robustness in simulating stream flow responses for a range in topographic, soils, and land use conditions. Differences in model performance, however, are noticeable on a climatic basis in that, except when explicitly calibrated, SWAT performs better on watersheds in more humid climates than in desert or semi-desert climates.

6.3.2 National Applications

Nagwan Watershed: The Nagwan watershed having an area of 90.23 km^2 is located in the upper Damodar-Baraker Valley in the state of Jharkhand in eastern India. Tripathi et al. (2005) conducted a study to test the applicability of SWAT model for runoff, sediment yield, and nutrient loss simulations for Nagwan watershed in a GIS environment. GIS was used to delineate the watershed and was further sub-divided into 12 sub-watersheds on the basis of topography. SWAT model was found to be successful to simulate

accurately daily and monthly runoff, sediment yield and nutrient losses, particularly from small agriculture watersheds.

Banha Watershed: Banha watershed having an area of 1695 hectare is situated in Damodar Valley Corporation (DVC) command in Hazaribag district of Jharkhand state in India. The watershed has three on stream check dams. Using SWAT model, Mishra et al. (2003) studied various aspects of the hydrology of Banha watershed. The SWAT model was found in accounting for different processes in small watersheds. The model made accurate estimation of the deposited sediment in check dams, and also how the removal of sediments and sands over time can improve watershed management.

Palleru Sub Basin: The Palleru sub-basin lies entirely in the state of Andhra Pradesh, India. The length of the Palleru River from its source to its outfall is 152 km. Gosain et al. (2005) tested the suitability of SWAT model using daily rainfall-runoff data from year 1972 to 1994. The results obtained were very promising and indicating model's suitability for ungauged catchments.

Salasi Khad Watershed: Salasi Khad watershed is situated in Hamirpur district of Himachal Pradesh having an area of 3171.805 ha. SWAT model was run using eight years of daily weather data (1998 to 2005) with changing proposal of land use pattern and it was found that SWAT model has the capability of providing very crucial information at the watershed scale. Further, the authors found that it is also possible to generate scenario with respect to the interventions that are proposed to be implemented and simulate their possible impacts before these are actually implemented. The study was conducted by Gosain et al., (2006).

Dudhi and Bewas Watersheds: Two adjacent micro-watersheds Dudhi (catctment area = 5.989 km^2) and Bewas (catchment area = 7.554 km^2) are situated in the district of Raisen of Madhya Pradesh. Dudhi watershed has been extensively developed as part of a Watershed Management Programmme, whereas Bewas is a virgin watershed. Gosain et al. (2006) tested the applicability of SWAT model using nine years daily weather data

(1994 to 2002) for both watersheds for different proposed changes in land use pattern. The authors also found that using SWAT model it is also possible to generate scenario with respect to the interventions that are proposed to be implemented and simulate their possible impacts before these are actually implemented.

Major Indian River Basins: Gosain et al. (2005 & 2006) conducted a comprehensive hydrological study using SWAT model to determine the spatio-temporal water availability in the various river systems of India. Simulation over twelve river basins of the country namely Brahmani, Cauvery, Ganga, Godavari, Krishna, Luni, Mahanadi, Mahi, Narmada, Pennar, Sabarmati and Tapi, were carried out using 40 years (20 years belonging to control or present and 20 years for GHG (Green House Gas) or future climate scenario) of simulated weather data. The initial analysis has revealed that under the GHG scenario, severity of droughts and intensity of floods in various parts of the country may get deteriorated. Moreover, they found a general reduction in the quantity of the available runoff under the current GHG scenario.

6.4 STUDY AREA AND DATA AVAILABILITY

This section deals with the specifically required characteristics/data of the watershed and availability of hydro-meteorological data to test the applicability of SWAT model to the data of Chaukhutia watershed. A general description of Chaukhutia watershed has been given in Chapter 2.

6.4.1 Hydro-Meteorological Data

This sub-section deals with availability of various types of hydrological-meteorological data as discussed here.

6.4.1.1 Rainfall

A significant portion of total precipitation in the form of rainfall in the watershed occurs mainly during the four months of the monsoon, i.e. from June to September with a

mean annual total precipitation of 1357.8 mm. In fact, the monsoon contributes about 74.2% of the total annual rainfall. Total annual rainfall varies from 967.9 mm (1981) to 1985.1 mm (1998). Mean monthly rainfall varies from 6.9 mm in the month of November to 344.3 mm in the month of July. Daily rainfall data recorded at Chaukhutia for the period from January 1962 to October 2006 were obtained and analyzed to arrive at data required for making weather generation tables for the SWAT model.

6.4.1.2 Runoff

There is a stream gauge station for measuring runoff of the river Ramganga at Chaukhutia. Geographic location of this stream gauge station is having latitude of 29^0 53' 10" and longitude of 79^0 20' 40" and this is situated at an altitude of 939.05 m above mean sea level (MSL). Daily runoff data from January 1975 to December 1978, Jun 1979 to December 1980 were available and used in the present study.

6.4.1.3 Climate

The Chaukhutia watershed lies in Sub Himalayan zone of Western Himalaya. The variation in altitude influences the climate of the watershed. The climate of this watershed varies from sub-tropical in the lower region to sub-temperate and temperate in upper region with a mean annual temperature of 24.5^0C and a mean minimum temperature of 17.3^0C. The mean maximum and minimum temperatures, relative humidity, evapotranspiration, sunshine hours and average monthly and annual temperatures of Chaukhutia watershed are presented in Table 2.1.

6.5 DATA PROCESSING

The latest AVSWATX [Beta Version of SWAT2005] works on ArcView Interface (3.1 or later) as an extension. To create AVSWATX database, the interface needs two types of information about watershed, viz. map themes and database files.

(A). **Map Themes:** It requires:

a. ArcInfo-ArcView Grid-Digital Elevation Model (DEM).
b. ArcInfo-ArcView Grid or Shape Land use/Land cover map.
c. ArcInfo-ArcView Grid or Shape soil map.
d. ArcInfo-ArcView Grid or Shape-DEM mask.

(B). **Database Files:** It requires:

- Precipitation data table.
- Runoff data table.
- Temperature data table.
- Weather generation table.
- Location tables of outlet of watershed, Rain gauge, Temperature gauge, Weather generation gauge.
- Solar radiation, Wind speed, Relative humidity tables.
- Land use look up tables.
- Soil look up table.

The methodology adopted in preparation of above map themes and databases is discussed in the following sections.

6.6 SOFTWARES USED

To prepare the Map themes and Database files, following softwares were used as shown in Table 6.1.

6.7 MAP THEMES

This section deals with the methodology adopted in preparation of map themes as discussed in the following sub-sections.

Table 6.1: Softwares Used For Preparation of Map Themes and Database Files

Sl. No.	Layer	Layer Format	Source	File Type	Software Used
1	Contour	Polyline	Topomaps	Shape File	ArcGIS9.0 & ERDAS8.5
2	Point Elevation	Point	Topomaps	Shape File	ArcGIS9.0 & ERDAS8.5
3	Drainage/ Stream	Polyline	Toposheet	Shape File	ArcGIS9.0 & ERDAS8.5
4	Land use map	Raster	Satellite Imagery	Imagery File	ERDAS8.5
5	Soil map	Polygon	Imagery	Shape File	ArcGIS9.0 & ERDAS8.5
6	DEM	Raster	Shape File	.img	ArcGIS9.0
7	Database	Tabular	Data Record	.dbf	Microsoft Excel

6.7.1 Digital Elevation Model (DEM)

Digital Elevation Model is sampled array of elevations (Z) that are regularly spaced intervals in the X & Y directions. DEM of the study area was prepared from digitized contour information from topomaps. Scanned topographic maps were geo-referenced in ERDAS system in polyconic projection system using Spheroid Everest 1956 and datum Indian (India/Nepal). Contour map was digitized using "On-Screen" (heads-up) method of digitization in ERDAS8.5 / ArcGIS9.0 software. On screen digitizing involves bringing a scanned map into the GIS software and tracing the features using a mouse. Digitization is vector based application of GIS. Vector based GIS stores map features as points, lines and polygons with high accuracy. Generated DEM of Chaukhutia watershed is presented in Fig. 6.1.

6.7.2 Landuse Map

Land use map was prepared using IRS-LISS-III imagery having spatial resolution of 23.5 m. Un-supervised classification was done in ERDAS8.5 software initially assigning 125 numbers of classes. These classes were merged in to seven classes based on the information available from toposheets/reports etc. Some relevant features such as roads,

urban areas were also digitized from toposheets. On combining these two image features final land use map was prepared.

Seven different classes of land use were generated as given in Table 6.2 and land use map of Chaukhutia watershed has been shown in Fig. 6.2. This land use map has been converted into grid form which is compatible with SWAT model using ArcGIS9.0 software.

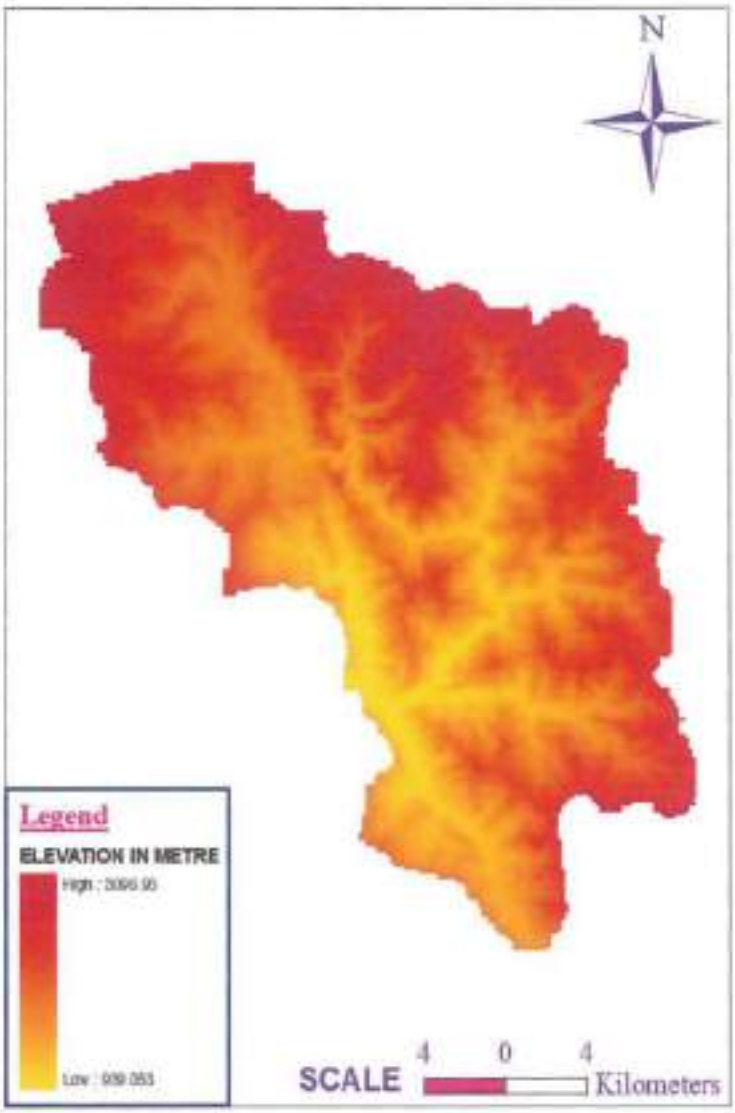

Figure 6.1: Digital Elevation Model of Chaukhutia watershed

Table 6.2: Land Use Class for Chaukhutia Watershed

Sl. No.	Land use class	Area (Ha)
1	Agriculture	7125.235
2	Fallow / Rocky / Waste	3759.725
3	Forest	28106.669
4	Pasture	9191.232
5	River	2777.184
6	Road	1704.154
7	Settlement	4692.960
	Total	57357.158

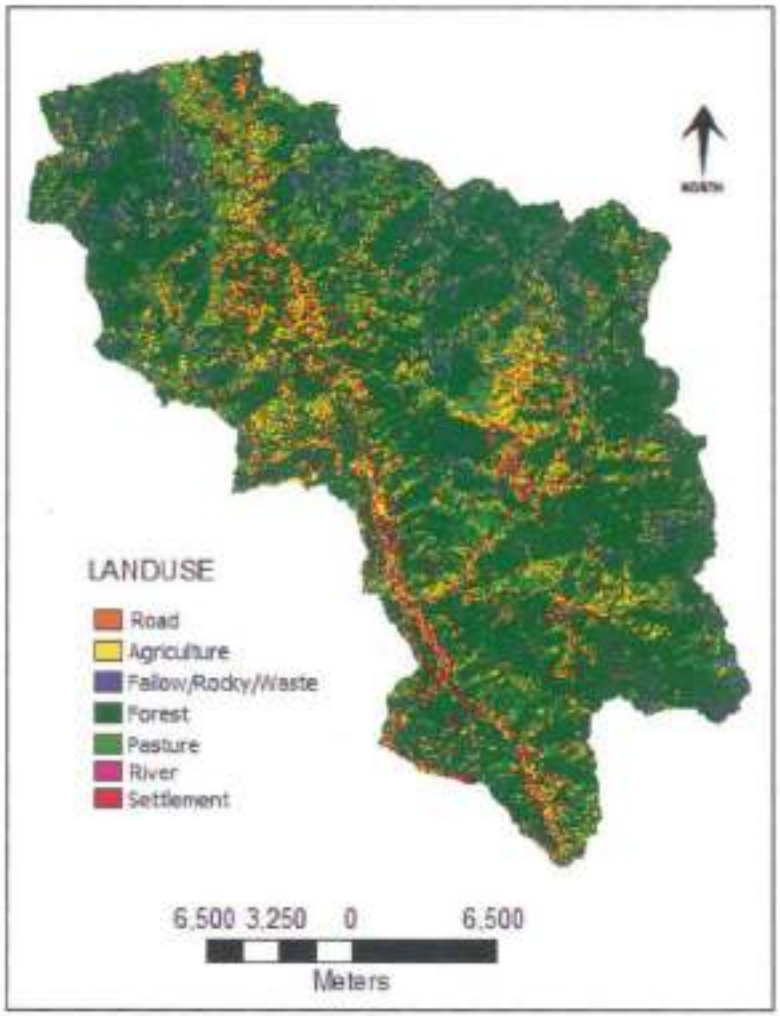

Figure 6.2: Land use map of Chaukhutia watershed

6.7.3 Soil Map

Soil map of the Chaukhutia watershed was extracted from available soil map (NBSS&LUP) of the State of Uttrakhand. Hardcopy map was scanned and the scanned image was used to digitize boundaries of various soil units using ArcGIS9.0 software. Soil map of Uttrakhand has been divided into 97 soil mapping units out of which seven numbers of soil mapping units viz Soil Mapping Units 14,23,28,36,38,45 and 48 falls under Chaukhutia watershed as given in Table 2.2. On adding above digitized shape file of soil map of Chaukhutia and AOI of Chaukhutia watershed as input, desired soil map of Chaukhutia watershed was obtained. Respective soil mapping units of the soil map as given in soil legend of Uttrakhand were also added in the attribute table of soil map of Chaukhutia as shown in Fig. 6.3.

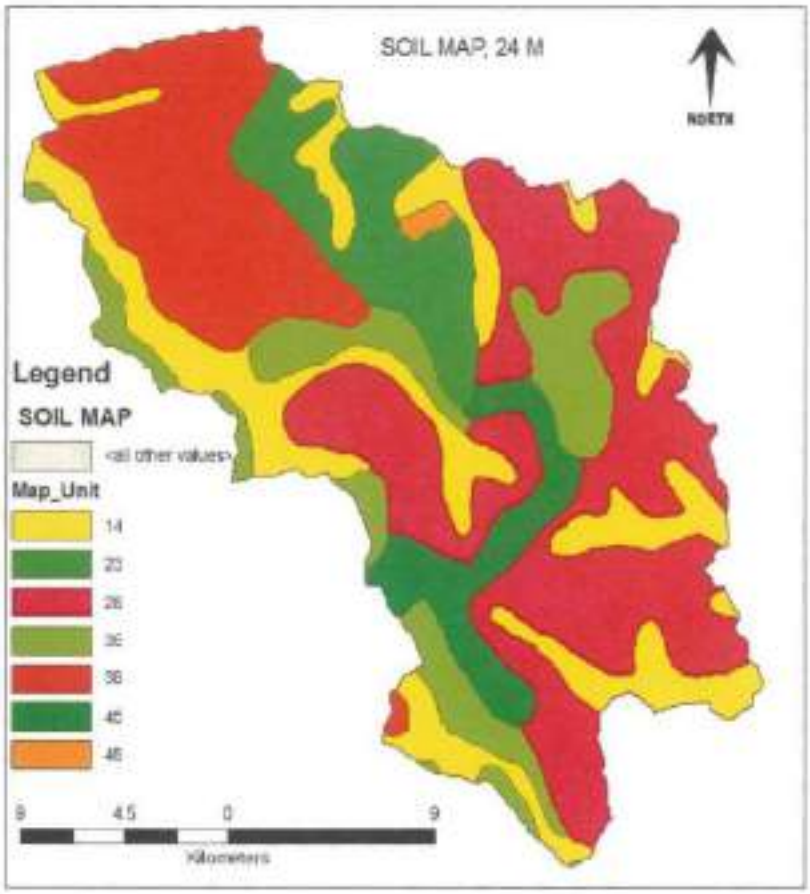

Figure 6.3: Soil map of Chaukhutia watershed

6.8 DATABASE FILES

Following databases were processed and prepared as per Soil and Water Assessment Tool, Theoretical Documentation, Version 2000 (SWAT 2000) (Neitsch et al., 2002), Soil and Water Assessment Tool, Users Manual, Version 2000 (SWAT 2000) (Neitsch. et al., 2002) and ArcView Interface for SWAT 2000, User's Guide (Luzio et al., 2002), as discussed below.

6.8.1 Precipitation Data Table

SCS-CN method was chosen in the SWAT model for simulating runoff for which precipitation data is required in dBase (.dbf) format as specified in the above SWAT manual. Daily precipitation (mm) data for the simulation period from January 1975 to December 1980 were used to run the model. Daily precipitation data for the period from January 1975 to December 1978 was used for calibration and from June 1979 to December 1980 was used for validation.

6.8.2 Runoff Data Table

To simulate runoff from SWAT model, observed runoff is not required as input to the model. However, if option for automatic calibration, sensitivity and uncertainty analysis of the SWAT model is used then observed runoff is supplied as text file. Runoff data table for the periods from January 1975 to December 1978 was prepared in text (.txt) format as specified in the above SWAT manual.

6.8.3 Temperature Data Table

Temperature data table is used to store daily maximum and minimum air temperatures. These temperatures can either be used to read by the model or may be generated by the model for simulation. Temperature data (^{0}C) table was prepared in

dBase (.dbf) format as specified in the SWAT model manual for the above simulation period.

6.8.4 Weather Generation Table

Weather generator database contains the statistical data required to generate representative daily climate data for the sub basins. SWAT model requires daily precipitation, maximum and minimum air temperature, solar radiation, wind speed and relative humidity. Values of all these parameters may be directly read from records of observed data or they may be generated. In the present study observed records of precipitation and maximum and minimum air temperatures were available and have been directly used. Data for remaining parameters such as solar radiation, wind speed and relative humidity were not available and therefore generated by SWAT software based on weather generator data base table described below. This database consists of the following variables arranged in dBase (.dbf) format as specified in the above SWAT manual:

(i) **Title**: Simply title of the file and it is not processed by the model.

(ii) **WLATITUDE**: Latitude of the weather station used to create statistical parameters. This value of latitude was given as 29.886 degrees.

(iii) **WLONGITUDE**: Longitude of the weather station. This value of longitude was given as 79.344 degrees.

(iv) **WELEV**: Elevation of weather station in meter. This value of elevation was given as 939.050 m.

(v) **XPR**: X projected coordinate of the weather station location. This value of coordinate was given as 57437.

(vi) **YPR**: Y projected coordinate of the weather station location. This value of coordinate was given as 70607.

(vii) **RAIN_YRS**: Number of years of maximum monthly 0.5 h rainfall data used. It was taken as 45 years. Daily rainfall recorded at Chaukhutia watershed outlet for the period from January 1962 to November 2006 (Total 45 years, given in

Appendix A) has been used to generate different variables of this weather generation database.

(viii) **TMPMX**: Average daily maximum air temperature for the month in ^{0}C. These values were computed by summing the maximum air temperature for every day in the month for all years of record and dividing by the number of days summed. These values are shown in Table 6.3.

Table 6.3: Average daily maximum air temperature in ^{0}C

Month	Jan	Feb	Mar	Apr	May	Jun	Jul	Aug	Sep	Oct	Nov	Dec
TMPMX	19.95	24.61	30.69	36.77	37.81	38.60	35.84	36.54	33.69	31.87	29.10	23.25

(ix) **TMPMN**: Average daily minimum air temperature for the month in ^{0}C. These values were computed by summing the minimum air temperature for every day in the month for all years of record and dividing by the number of days summed. These values are shown in Table 6.4.

Table 6.4: Average daily minimum air temperature in ^{0}C

Month	Jan	Feb	Mar	Apr	May	Jun	Jul	Aug	Sep	Oct	Nov	Dec
TMPMN	5.84	9.93	14.27	19.35	22.62	24.38	24.55	24.37	22.79	18.98	11.89	9.13

(x) **TMPSTDMX**: Standard deviation for daily maximum air temperature in the month. This parameter quantifies the variability in maximum temperature for each month. These values are shown in Table 6.5.

Table 6.5: Standard deviation for daily maximum air temperature

Month	Jan	Feb	Mar	Apr	May	Jun	Jul	Aug	Sep	Oct	Nov	Dec
TMPSTDMX	3.49	4.13	3.74	2.76	3.09	2.99	3.00	3.03	3.00	3.23	2.47	3.48

(xi) **TMPSTDMN**: Standard deviation for daily minimum air temperature in the month. This parameter quantifies the variability in minimum temperature for each month. These values are shown in Table 6.6.

Table 6.6: Standard deviation for daily minimum air temperature

Month	Jan	Feb	Mar	Apr	May	Jun	Jul	Aug	Sep	Oct	Nov	Dec
TMPSTDMN	2.83	3.76	4.00	4.25	3.96	3.31	3.19	3.38	2.13	3.96	3.77	3.76

(xii) **PCPMM**: Average total monthly precipitation in mm of water. These values were computed on the basis of daily precipitation for the period from January 1962 to November 2006 as shown in Table 6.7.

Table 6.7: Average total monthly precipitation in mm of water

Month	Jan	Feb	Mar	Apr	May	Jun	Jul	Aug	Sep	Oct	Nov	Dec
PCPMM	45.72	55.57	49.93	40.48	75.49	183.38	348.28	326.26	178.46	28.62	5.36	20.26

(xiii) **PCPSTD**: Standard deviation for daily precipitation in the month. This parameter quantifies the variability in precipitation for each month. These values are shown in Table 6.8.

Table 6.8: Standard deviation for daily precipitation

Month	Jan	Feb	Mar	Apr	May	Jun	Jul	Aug	Sep	Oct	Nov	Dec
PCPSTD	11.12	11.71	9.59	10.01	12.60	16.86	19.64	17.22	17.34	14.88	8.66	15.06

(xiv) **PCPSKW**: Skew coefficient for daily precipitation in the month. This parameter quantifies the symmetry of the precipitation distribution about the monthly mean. These values are shown in Table 6.9.

Table 6.9: Skew coefficient for daily precipitation

Month	Jan	Feb	Mar	Apr	May	Jun	Jul	Aug	Sep	Oct	Nov	Dec
PCPSKW	1.77	1.80	1.91	2.48	2.67	2.53	2.45	2.07	2.59	3.99	1.47	2.28

(xv) **PR_W(1, mon)**: Probability of a wet day following a dry day in the month. These values were computed on dividing the number of times a wet day followed a dry day in the month for the entire period of record by the number of dry days in the month during the entire period of record. These probability values are shown in Table 6.10.

Table 6.10: Probability of a wet day following a dry day

Month	Jan	Feb	Mar	Apr	May	Jun	Jul	Aug	Sep	Oct	Nov	Dec
PR_W(1)	0.09	0.12	0.11	0.10	0.16	0.31	0.48	0.46	0.26	0.06	0.02	0.04

(xvi) **PR_W(2, mon)**: Probability of a wet day following a wet day in the month. These values were computed on dividing the number of times a wet day followed a wet day in the month for the entire period of record by the number of wet days in the month during the entire period of record. These probability values are shown in Table 6.11.

Table 6.11: Probability of a wet day following a wet day

Month	Jan	Feb	Mar	Apr	May	Jun	Jul	Aug	Sep	Oct	Nov	Dec
PR_W(2)	0.38	0.36	0.37	0.40	0.42	0.53	0.72	0.75	0.61	0.33	0.21	0.34

(xvii) **PCPD**: Average number of days of precipitation in the month. These values were computed on dividing the number of wet days in the month during the entire period of record by number of years of record. These values are shown in Table 6.12.

Table 6.12: Average number of days of precipitation

Month	Jan	Feb	Mar	Apr	May	Jun	Jul	Aug	Sep	Oct	Nov	Dec
PCPD	4.07	5.16	5.07	4.56	7.05	12.64	19.69	20.38	12.24	2.62	0.66	1.73

(xviii) **RAINHHMX**: Maximum 0.5 h rainfall in entire period of record for month. This value represents the most extreme 30-minute rainfall intensity recorded in the entire period of record. These values are shown in Table 6.13.

Table 6.13: Maximum 0.5h rainfall in mm

Month	Jan	Feb	Mar	Apr	May	Jun	Jul	Aug	Sep	Oct	Nov	Dec
RAINHHMX	9.33	10.00	10.00	10.53	13.37	22.17	26.60	20.40	29.67	19.00	5.50	12.63

(xix) **SOLARAV**: Daily average solar radiation for month in MJ/m^2/day. This value is calculated by summing the total solar radiation for every day in the month for all years of record and dividing by the number of days summed. In the present study this value has been taken from text book of Hydrology and Water Resources Engineering (Patra, 2008) with some modification as per sample data attached with SWAT model. These values are shown in Table 6.14.

Table 6.14: Daily average solar radiation (MJ/m^2/day)

Month	Jan	Feb	Mar	Apr	May	Jun	Jul	Aug	Sep	Oct	Nov	Dec
SOLARAV	10.33	13.09	17.10	19.76	22.99	24.92	24.45	23.35	17.99	16.41	12.38	9.96

(xx) **DEWPT**: Average daily dew point temperature in the month in ^0C. In the present study this value has been taken to be the same as per sample data attached with SWAT model, which has been shown in Table 6.15.

Table 6.15: Average daily dew point temperature in ^{0}C

Month	Jan	Feb	Mar	Apr	May	Jun	Jul	Aug	Sep	Oct	Nov	Dec
DEWPT	0.76	2.42	4.85	10.55	16.45	19.86	20.56	20.07	17.15	11.38	5.80	1.66

(xxi) **WNDAV**: Daily average wind speed in the month in m/s. This value is calculated by summing the average wind speed values for every day in the month for all years of record and dividing by the number of days summed. In the present study this value has been taken from nearby observed data with some modification, which are shown in Table 6.16.

Table 6.16: Daily average wind speed in m/s

Month	Jan	Feb	Mar	Apr	May	Jun	Jul	Aug	Sep	Oct	Nov	Dec
WNDAV	2.40	2.67	3.06	3.40	3.65	3.40	3.23	3.09	2.74	2.19	1.94	2.08

6.9 LOCATION TABLES

Location tables for outlet of watershed, rain gauge, temperature gauge and weather generation gauge were made in dBase (.dbf) format as per above User's Guide for SWAT2000. Coordinates have been provided in terms of X and Y projected coordinates of all the above stations and watershed outlet.

6.9.1 Solar Radiation, Wind Speed & Relative Humidity Tables

In the present study options were selected at the time of simulation to generate solar radiation, wind speed and relative humidity as per above weather generation table.

6.9.2 Land Use Look Up Table

This table is used to specify the SWAT land cover plant/urban land code to be modeled for each category in the land use map grid. It was formatted in dBase (.dbf) table

as per above User's Guide for SWAT2000. Data contained in this table has been shown in Table 6.17. Codes contained in this table are for Agriculture, Fallow / Rocky / Waste land, Forest, Pasture, River, Road and Settlement respectively.

Table 6.17: Land use look up table

Value	1	2	3	4	5	6	7
Land use	AGRL	SPAS	FRSE	PAST	WETN	UTRN	URLD

6.9.3 Soil Look Up Table

This table is used to specify the type of soil to be modeled for each category in the soil map grid. The soil input file defines the physical properties of the soil layers. This table consists of the following variables:

(i) **Title:** Simply title of the file and it is not processed by the model.

(ii) **SNAM:** Soil name. As soil has been classified into seven categories as per "Soil Legend of Uttranchal" provided by National Bureau of Soil Survey and Land Use Planning (NBSSLUP), Govt. of India, New Delhi, following soil name has been given to above seven categories: SMU14, SMU23, SMU28, SMU36, SMU38, SMU45 and SMU48. Here SMU stands for Soil Mapping Unit.

(iii) **HYDROLOGIC SOIL GROUP:** Based on the definitions for the different classes of hydrologic soil group, as given in different text books and above soil user manual, broadly two types of hydrologic soil group has been decided which are B & C.

(iv) **SOL_ZMX:** Maximum rooting depth of soil profile (mm). This value was taken from above SWAT User's Manual.

(v) **ANION_EXCL:** Fraction of porosity. It was taken from text book on Applied Hydrology **(Chow et al., 1988).**

(vi) **SOL_CRK:** Maximum crack volume of soil profile expressed as a fraction of the total soil volume. Default values from the software (AVSWATX) were adopted.

(vii) **TEXTURE:** Texture of soil layer. This data is not processed by the model. Textural characteristics were taken from above "Soil Legend of Uttranchal".

(viii) **SOL_Z:** Depth of soil surface from bottom of layer in mm. Values were taken from above SWAT User's Manual.

(ix) **SOL_BD:** Moist bulk density in g/cm^3. It's values were taken from text book on Design Hydrology and Sedimentology for Small Catchments (Haan et al. 1994).

(x) **SOL_AWC:** Available water capacity of the soil layer in mm of water. Values were taken from book on Watershed Management (Tideman, 1999).

(xi) **SOL_K:** Saturated hydraulic conductivity in mm/hr. Values were taken from text book on Applied Hydrology (Chow, 1988).

(xii) **SOL_CBN:** Organic carbon content (% soil weight). Values were taken from AVSWATX database.

(xiii) **CLAY:** Clay content (% soil weight). Values were taken from text books.

(xiv) **SILT:** Silt content (% soil weight). Values were taken from text books.

(xv) **SAND:** Sand content (% soil weight). Values were taken from text books.

(xvi) **ROCK:** Rock content (% soil weight). Values were taken from text books.

(xvii) **SOL_ALB:** Moist soil albedo. Value was taken from AVSWATX database.

(xviii) **USLE_K:** USLE equation's soil erodibility factor (units: 0.013 (metric ton m^2 hr)/(m^3-metric ton cm)). Values were taken from text book on Design Hydrology and Sedimentology for Small Catchments (Haan et al. 1994).

All the above variables of soil look up table are shown in Table 6.18.

6.10 APPLICATION, RESULTS AND DISCUSSION

To run the SWAT model, extension of the model available for ArcView GIS (AVSWATX (Beta version of SWAT2005)) was installed. Using the detailed instructions available for setting up of SWAT model from its user's manual (SWAT, 2005), the model was setup for Database of the Chaukhutia watershed generated in the previous sections. This section deals with setting-up of model, calibration, validation and sensitivity analysis as discussed below.

6.10.1 SWAT Model Setup

All the required map themes (DEM, Mask and Land use in grid format and Soil map in shape file) and database sets prepared as discussed earlier sections were placed in a newly created sub-directory namely 'Chaukhutia' under "avswatdb" directory of AVSWATX Extension of SWAT2005. Weather generation and soil database tables already prepared in dBase (.dbf) format were directly placed in the above 'avswatdb' directory in the form of user weather generation table and user soil database.

Table 6.18: Soil database

Sl. No.	Variable	SMU14	SMU23	SMU28	SMU36	SMU38	SMU45	SMU48
1	2	3	4	5	6	7	8	9
1	HYDGRP	C	B	B	C	C	C	B
2	SOL_ZMX	2000.00	2000.00	2000.00	2000.00	2000.00	2000.00	2000.00
3	ANION_EXCL	0.464	0.501	0.501	0.464	0.464	0.464	0.501
4	SOL_CRK	0.500	0.500	0.500	0.500	0.500	0.500	0.500
5	TEXTURE	TFL-LSS	T-CLS	TS-CLS	TC-FLS	TLS-FLS	TC-FLS	TSSS
6	SOL_Z	500.00	500.00	500.00	500.00	500.00	500.00	500.00
7	SOL_BD	1.45	1.45	1.45	1.45	1.45	1.45	1.45
8	SOL_AWC	0.17	0.18	0.18	0.17	0.17	0.17	0.18
9	SOL_K	1.00	5.00	5.00	1.00	1.00	1.00	5.00
10	SOL_CBN	0.988	1.125	1.125	0.988	0.988	0.988	1.125
11	CLAY	30.00	20.00	20.00	30.00	30.00	30.00	20.00
12	SILT	50.00	50.00	50.00	50.00	50.00	50.00	50.00
13	SAND	20.00	30.00	30.00	20.00	20.00	20.00	30.00
14	ROCK	0.00	0.00	0.00	0.00	0.00	0.00	0.00
15	SOL_ALB	0.03	0.03	0.03	0.03	0.03	0.03	0.03
16	USLE_K	0.32	0.24	0.24	0.32	0.32	0.32	0.24

6.10.2 Stream and Watershed Delineation

First of all preprocessing of the DEM grid as already prepared for Chaukhutia and its surrounding area was done. The preprocessing module generates a stream network from the DEM based on user defined channel initiation threshold (CIT) value. The value of CIT depends on topography of the area and is generally decided based on level of channel generation desired. For the present study, CIT value of 2500 hectare was chosen as this value resulted in generation of all major channel networks in the watershed. Based on the generated channel network, the preprocessor delineated sub-watersheds for each of

the junction of the streams. The location of the watershed outlet was manually supplied to the preprocessor in the form of a dbase table. Generated sub-watersheds with location of the watershed outlet are shown in Fig. 6.4. Sub-basin parameters have also been calculated by the model and watershed and sub-basin wise elevation report was obtained. The elevation statistics and area for each sub-basin and entire watershed is shown in Table 6.19.

6.10.3 Land Use and Soil Delineation and Distribution

Land use grid map has been clipped to the watershed area and then reclassified as per SWAT codes. Soil map was also clipped using the watershed boundary and tagged to user soil database based on soil mapping units (SMU, Table 2.2) already added to the model in the form of user soil database. Fig. 6.5 shows reclassified soil map. By overlaying of land use and soil maps, report for distribution of land use & soil in each of the sub-basins and entire watershed was obtained. Hydrologic response units (HRU) were demarcated according to multiple hydrologic response unit option on setting a threshold value of 10% for each of land use and soil class which resulted in creation of 133 numbers of HRUs in the watershed. Report of HRU's for different sub basin was obtained, however the same is not produced here to save space. The report for landuse and soil distribution (after application of threshold) for entire watershed is shown in Tables 6.20 and 6.21 respectively.

6.10.4 Generation of Hydrological Database

Daily precipitation, daily maximum and minimum temperatures and generated weather databases were loaded as input for simulation. Solar radiation, wind speed and relative humidity were opted to be simulated by the model itself due to lack of records. The model was run on yearly, monthly and daily basis for the period from January 1975 to December 1978 and for calibrating model parameters. The validation of the calibrated model was done using data for period June 1979 to December 1980.

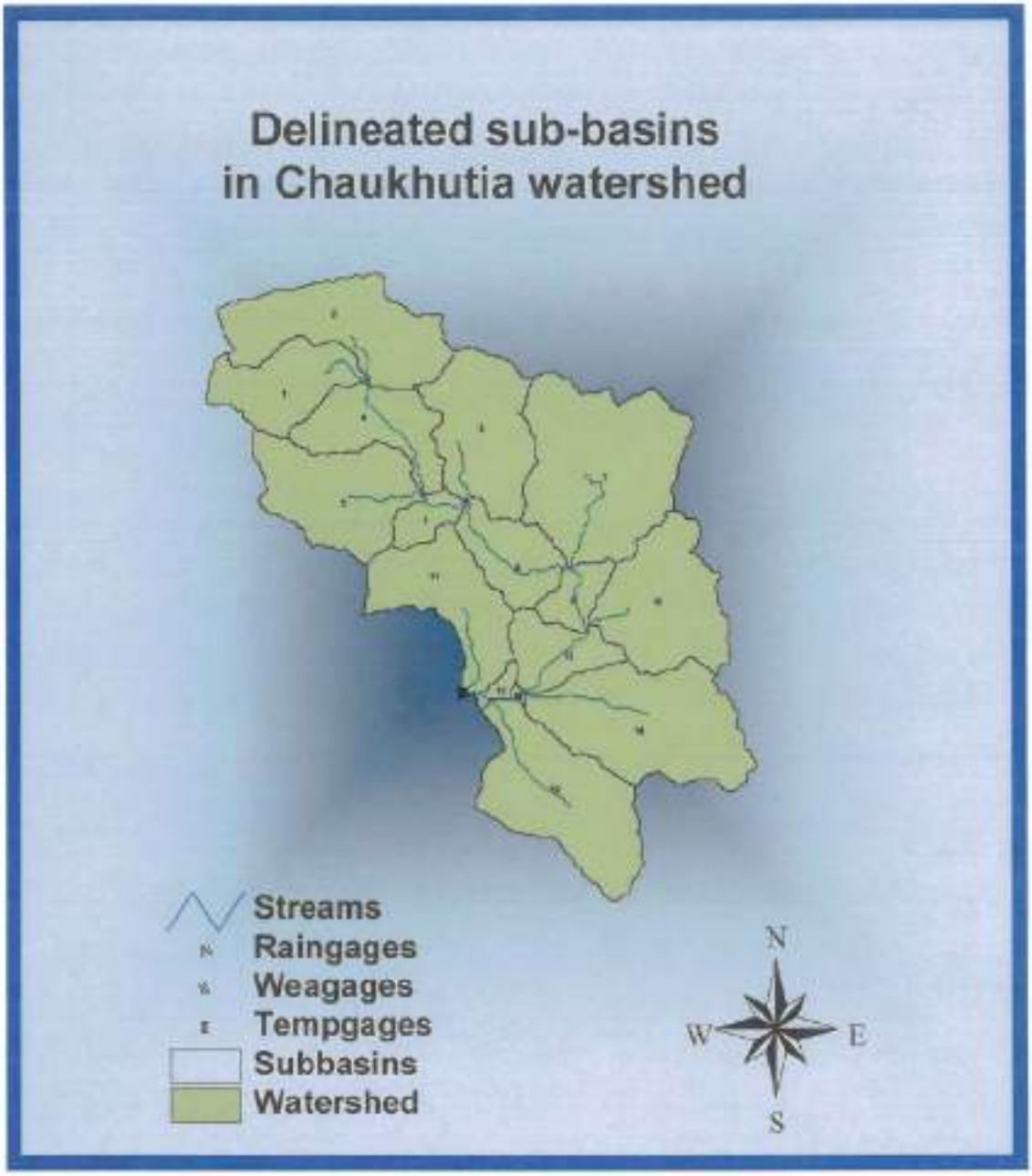

Figure 6.4: Sub-basins of Chaukhutia watershed

Table 6.19: Elevation statistics for Chaukhutia watershed

Sl. No.	Basin	Minimum Elevation (m)	Maximum Elevation (m)	Mean Elevation (m)	Standard Deviation	Area (Ha)	% Area
1	Entire watershed	934.845	3099.29	1782.74	424.33	57229	100.00
2	Subbasin 1	1544.1	3099.29	2117.36	347.684	3059	5.34
3	Subbasin 2	1533.26	3055.35	2182.83	341.186	5303	9.27
4	Subbasin 3	1287.28	2486.02	1784.86	269.743	4680	8.18
5	Subbasin 4	1286.06	2543.76	1799.27	259.042	3062	5.36
6	Subbasin 5	1250.21	3067.22	2126.74	341.019	4620	8.07
7	Subbasin 6	1251.24	1972.76	1511.91	136.765	886	1.55
8	Subbasin 7	1058.31	3063.88	1959.69	403.165	7961	13.91
9	Subbasin 8	1062.16	2405.6	1579.84	281.909	2389	4.17
10	Subbasin 9	1019.84	2150.74	1382.16	245.776	1105	1.93
11	Subbasin 10	1021.05	2456.06	1800.71	322.057	4999	8.74
12	Subbasin 11	934.845	2088.12	1335.15	259.504	4106	7.17
13	Subbasin 12	940.23	2119.68	1382.34	268.773	1969	3.44
14	Subbasin 13	941.564	1695.59	1191.53	212.609	300	0.52
15	Subbasin 14	949.517	2752	1756.55	362.944	6713	11.73
16	Subbasin 15	943.8	1479.97	1100.47	144.224	76	0.13
17	Subbasin 16	943.409	2300.42	1433.66	284.447	5999	10.48

Table 6.20: Land use report of Chaukhutia watershed after threshold application

Sl. No.	Land use	SWAT code	SWAT Description	Area in Ha.	% Area
1	Agriculture	AGRL	Agricultural Land-Generic	6255	10.93
2	Fallow / Rocky / Waste	SPAS	Summer Pasture	2708	4.73
3	Forest	FRSE	Forest-Evergreen	33871	59.18
4	Pasture	PAST	Pasture	10763	18.81
5	River	WETN	Wetlands-Non-Forested	216	0.38
6	Settlement	URLD	Residential-Low Density	3415	5.97
			Total	572289	100

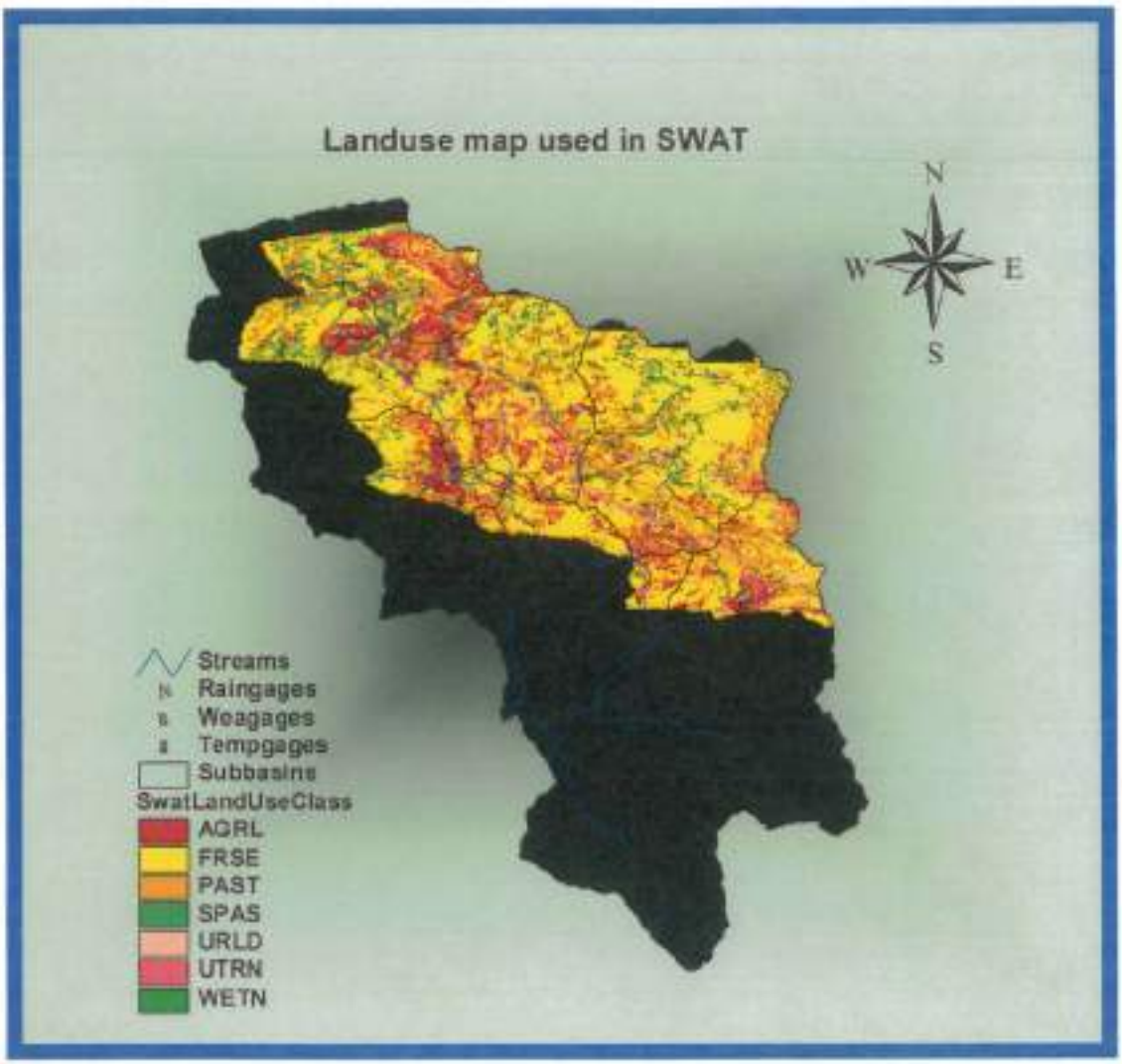

Figure 6.5: Reclassified land use map

6.11 Model Calibration and Validation

For this investigation, ten calibration parameters of SWAT which govern the rainfall-runoff process were selected for calibration using the data of the Chaukhutia watershed. Model parameters were grouped into three categories (Table 6.23), which were considered to predominantly govern surface, subsurface, and basin response. Table 6.22 lists parameters, descriptions, and units that were calibrated with the auto calibration

tool for the Chaukhutia watersheds. A brief description of each parameter is given as below:

Table 6.21: Soil report of Chaukhutia watershed after threshold application

Sl. No.	Soil Code	Description of soil	Area in Ha.	% Area
1	SMU14	Soil Mapping Unit 14	12503	21.85
2	SMU23	Soil Mapping Unit 23	5771	10.08
3	SMU28	Soil Mapping Unit 28	19785	34.57
4	SMU36	Soil Mapping Unit 36	6490	11.34
5	SMU38	Soil Mapping Unit 38	10123	17.69
6	SMU45	Soil Mapping Unit 45	2557	4.47
		Total	57229	100

6.11.1 Parameters Governing Surface Response

Calibration parameters governing the surface-water response in SWAT include the runoff curve number, the soil evaporation compensation factor, and the available soil water capacity. The runoff curve number for AMC II (CN_2) is used to compute runoff depth from total rainfall depth. It is a function of watershed properties that include soil type, land use and treatment, ground surface condition, and antecedent moisture condition. The soil evaporation compensation factor adjusts the depth distribution for evaporation from the soil to account for the effect of capillary action, crusting, and cracks. The available soil water capacity (SOL_AWC) is the volume of water that is available to plants if the soil was at field capacity. It is estimated by determining the amount of water released between in situ field capacity and the permanent wilting point.

Table 6.22: Parameters calibrated in SWAT

Sl.No.	Parameter	Description	Units
Parameters governing surface water response			
1	CN2	SCS runoff curve number	none
2	ESCO	Soil evaporation compensation factor	none
3	SOL_AWC	Available soil water capacity	mm/mm
Parameters governing subsurface water response			
4	GW_REVAP	Groundwater "revap" coefficient	none
5	REVAPMN	Minimum threshold depth of water in the shallow aquifer for "revap" to occur	mm
6	GWQMN	Minimum threshold depth of water in the shallow aquifer required for return flow to occur	mm
7	GW_DELAY	Groundwater delay	days
8	ALPHA_BF	Baseflow alpha factor or recession constant	days
Parameters governing basin response			
9	SURLAG	Surface runoff lag time	days
10	CH_K2	Channel hydraulic conductivity	mm/h

6.11.2 Parameters Governing Subsurface Response

Six calibration parameters govern the subsurface water response in SWAT. One of these parameters is referred to as the groundwater "revap" coefficient (GW_REVAP), which controls the amount of water that will move from the shallow aquifer to the root zone as a result of soil moisture depletion and the amount of direct groundwater uptake from deep-rooted trees and shrubs. Another parameter that governs the subsurface response is the threshold depth of water in the shallow aquifer for revap to occur (REVAPMN). Movement of water from the shallow aquifer to the root zone or to plants is allowed only if the depth of water in the shallow aquifer is equal to or greater than the minimum revap. A third parameter is the threshold depth of water in the shallow aquifer

required for return flow to occur to the stream (GWQMN). Two other parameters that govern watershed response include the base flow alpha factor and groundwater delay. The base flow alpha factor (ALPHA_BF), or recession constant, characterizes the groundwater recession curve. This factor approaches one for flat recessions and approaches zero for steep recessions. The groundwater delay (GW_DELAY) is the time required for water leaving the bottom of the root zone to reach the shallow aquifer. A sixth factor is the deep aquifer percolation fraction that governs the fraction of percolation from the root zone to the deep aquifer (RCHRG_DP).

6.11.3 Parameters Governing Basin Response

Two parameters that govern basin response in SWAT were calibrated in this study. These included channel hydraulic conductivity (CH_K2) that governs the movement of water from the stream bed to the subsurface for ephemeral or transient streams, and the surface runoff lag time SURLAG that provides a storage factor in the model to allow runoff to take longer than one day to reach a sub basin outlet. Five other basin parameters that govern snowfall and snowmelt in SWAT were not used as the Chaukhutia watershed does not have contribution from snow melt.

The runoff data (processed in text format) observed at Chaukhutia watershed outlet for the period from January 1975 to December 1978 was used for model calibration. Initial values of all the parameters discussed above were assigned to different parameter files and response of the model was observed by running model on calibration dataset. Based on performance statistics it was felt that the parameters need to be calibrated for improving simulated results from the model. Accordingly, a range of minimum and maximum values for each of the model parameters was workout from guide values given in SWAT user's manual and were used to calibrate model using auto-calibration tool. After successful execution of the model, a set of parameter values were obtained which gave minimum value of the objective function. Parameter values calibrated in the model using auto calibration tool are given in Table 6.23. Results of simulation from the model with calibrated values of the model parameters were then obtained both for calibration and validation period (June 1979 to December 1980).

Table 6.23: Calibrated Parameter Values

Sl. No.	Parameter	Initial value	Calibrated value
1	CN2	Varies with land use and soil	10% increase everywhere
2	SOL_AWC	0.54	0.39
3	ESCO	0.95	0.91
4	GW_REVAP	0.07	0.02
5	REVAPMN	1.00	430.00
6	GWQMN	1380	0.00
7	ALPHA_BF	0.0480	0.02
8	CH_K2	0.00	150.00
9	SURLAG	4	5
10	GW_DELAY	31	31

6.12 Discussion of Results

Year wise daily observed and simulated runoff along with daily precipitation values for the years 1975 through 1979 (from Jun. to Dec.) and 1980 are graphically presented in Figs. 6.6 to 6.11 respectively. Monthly observed and simulated runoffs for the above years in the shapes of bar charts are shown in Figs. 6.12 to 6.17 respectively. Annual observed and simulated runoff is presented in Fig. 6.18. Out of the above daily graphs, first four graphs (Figs. 6.6 to 6.9) were obtained after calibrating the model with known values of daily runoff. Rest two graphs (Figs. 6.10 and 6.11) are of the validation period.

6.13 Performance Evaluation

Five evaluation criteria were used to assess monthly and daily stream flows simulated by SWAT. The first two criteria were quantitative statistics that measured the agreement between simulated and observed values, and the rest three criteria were a visual comparison of plots of simulated and observed values as discussed below.

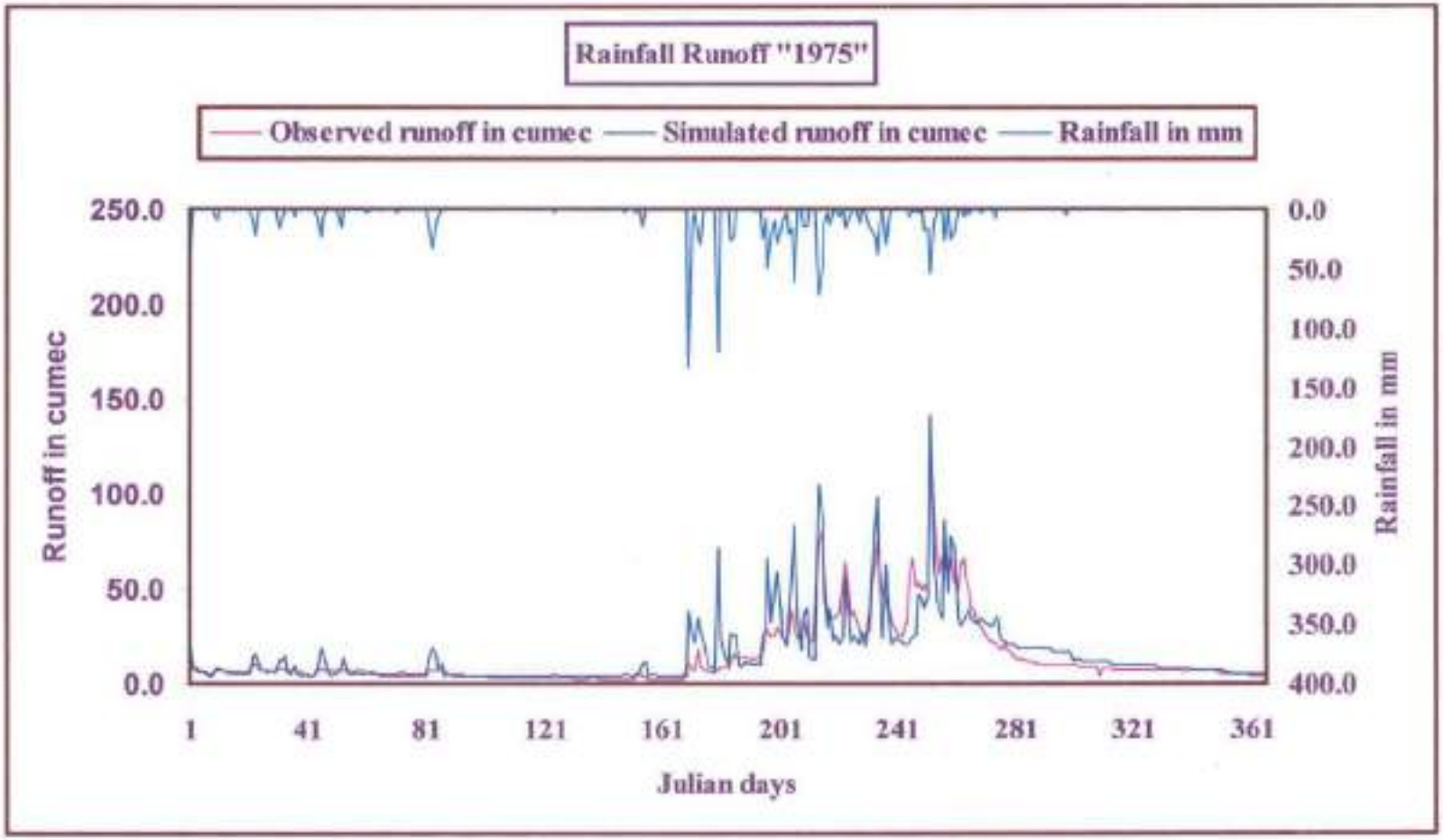

Figure 6.6: Daily observed and simulated runoff for the year 1975

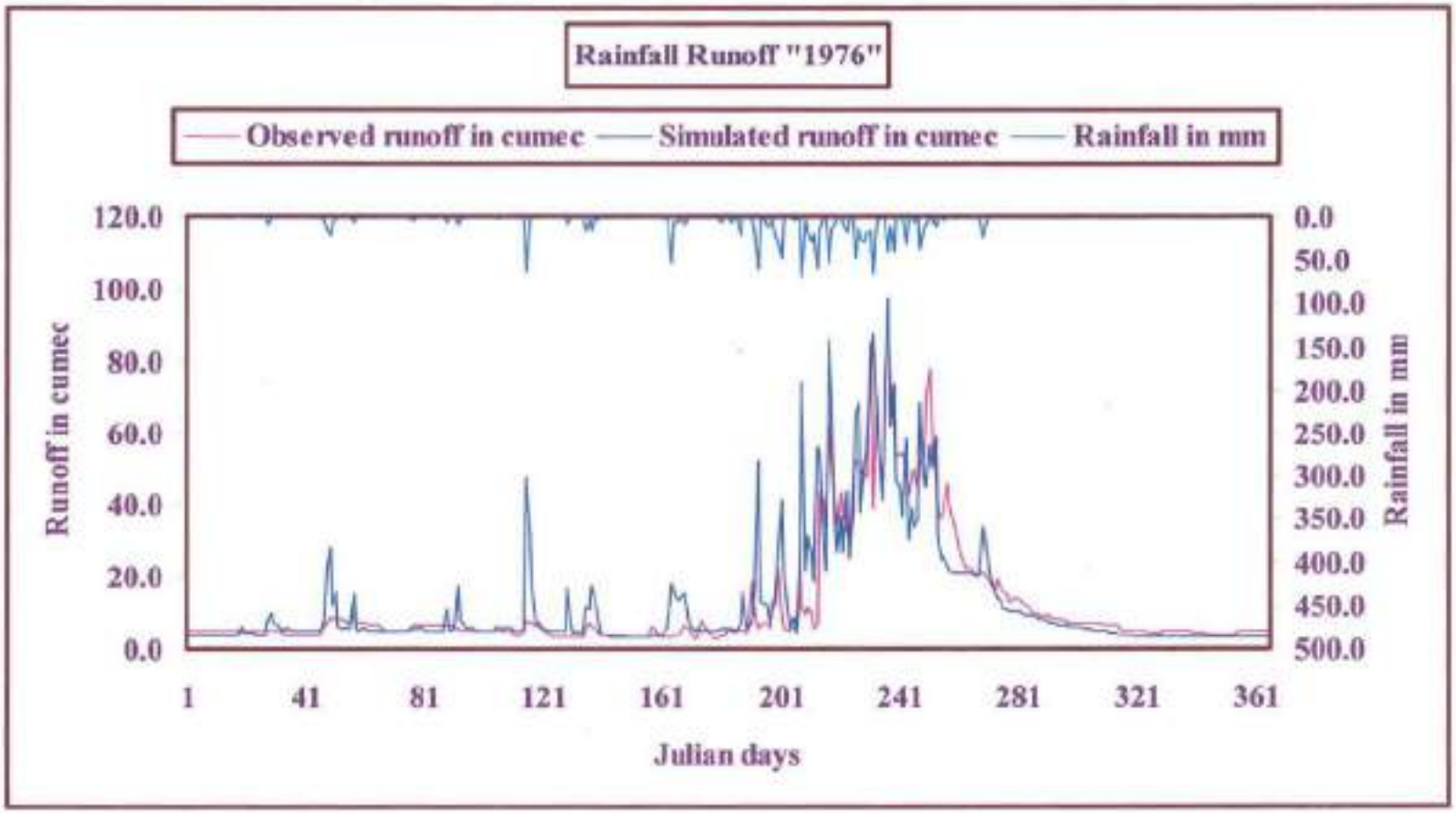

Figure 6.7: Daily observed and simulated runoff for the year 1976

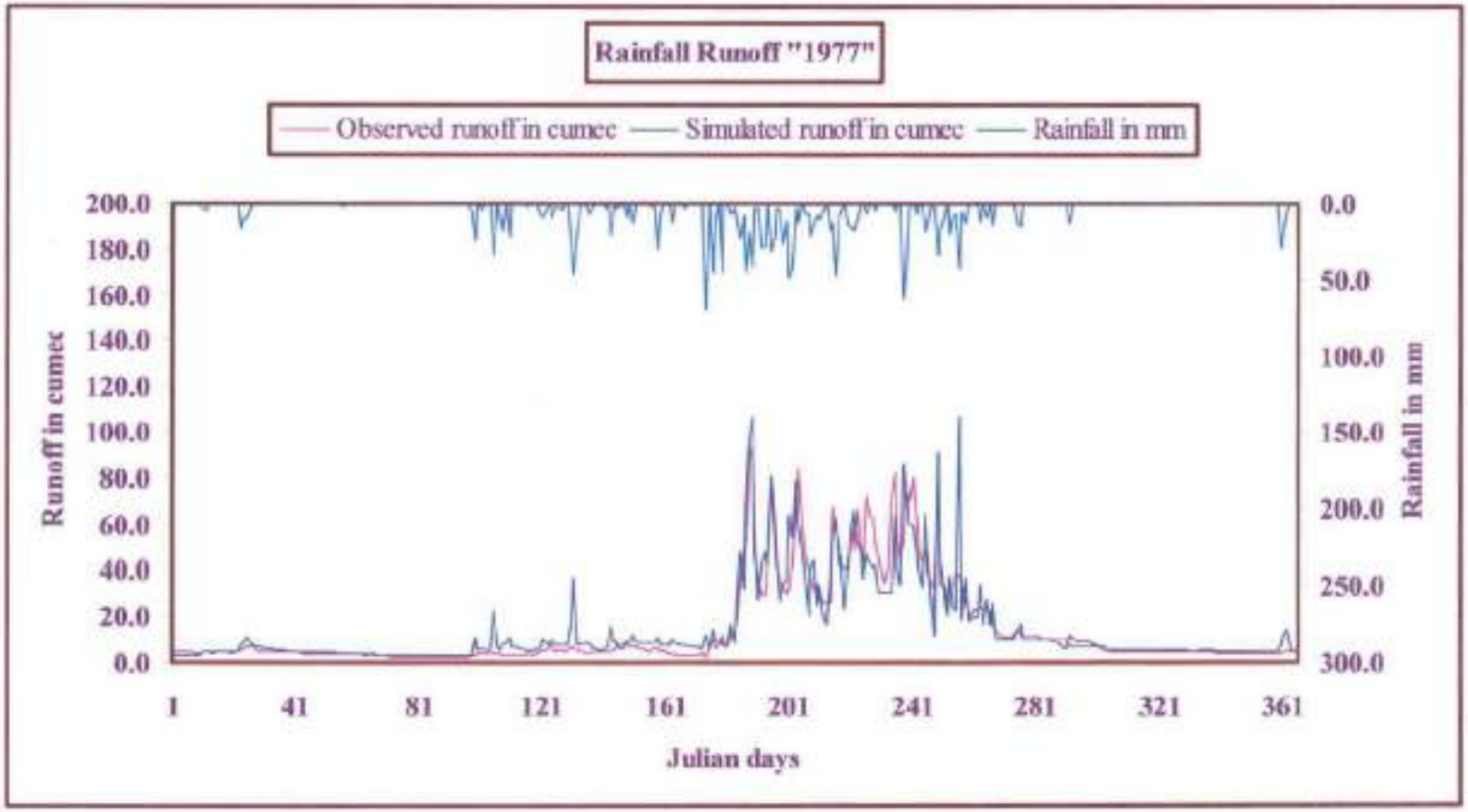

Figure 6.8: Daily observed and simulated runoff for the year 1977

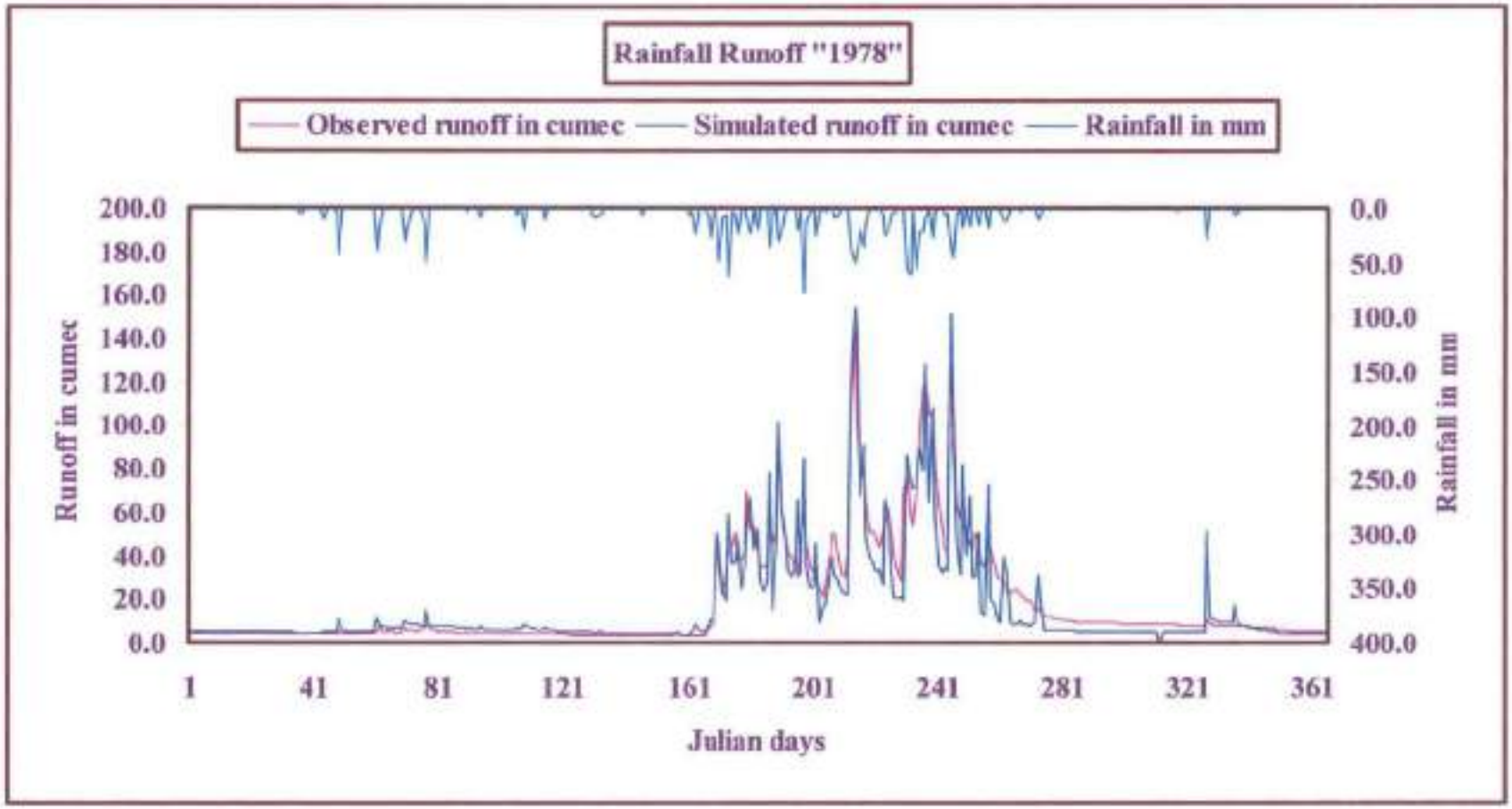

Figure 6.9: Daily observed and simulated runoff for the year 1978

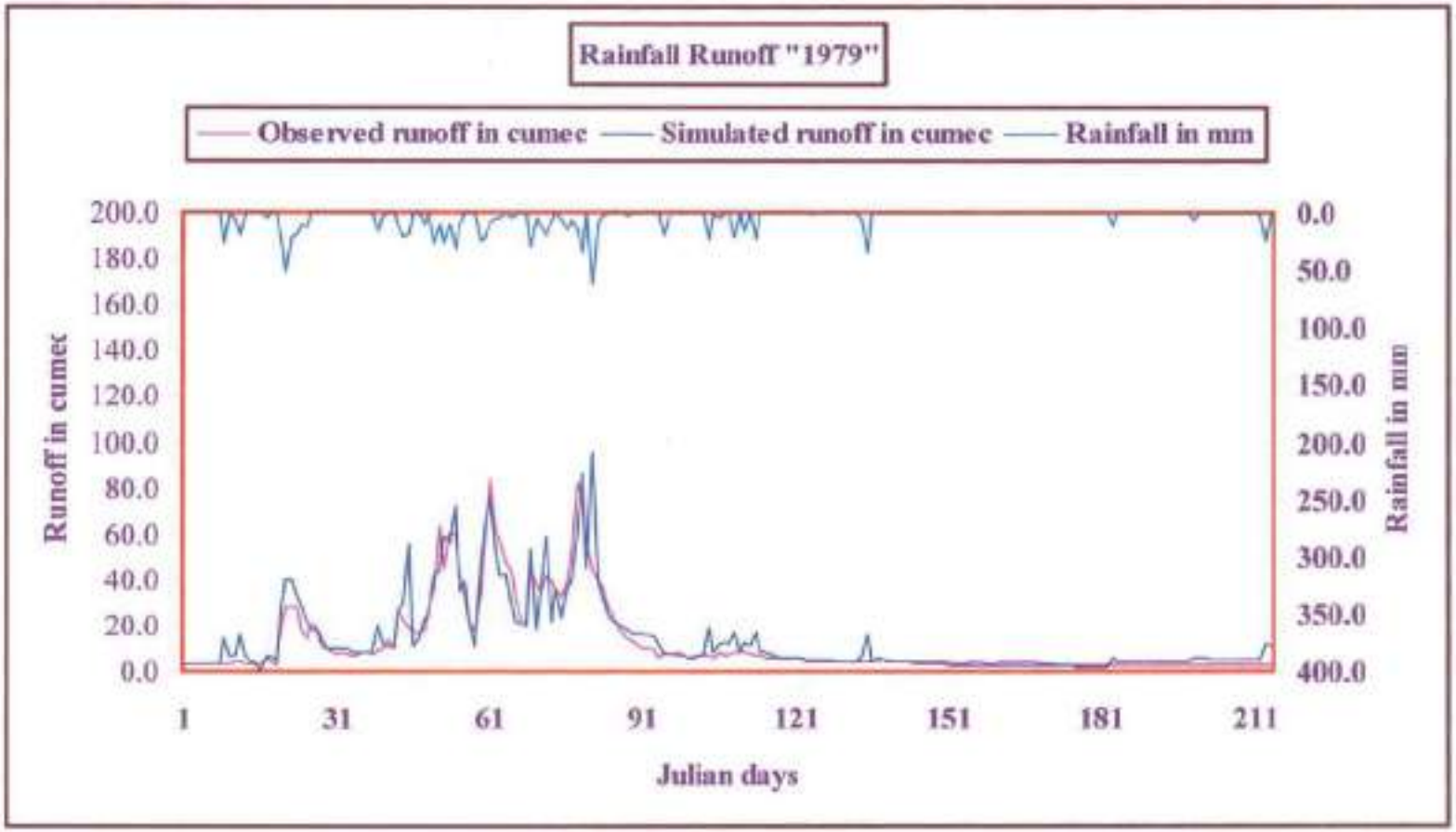

Figure 6.10: Daily observed and simulated runoff for the year 1979(July to December)

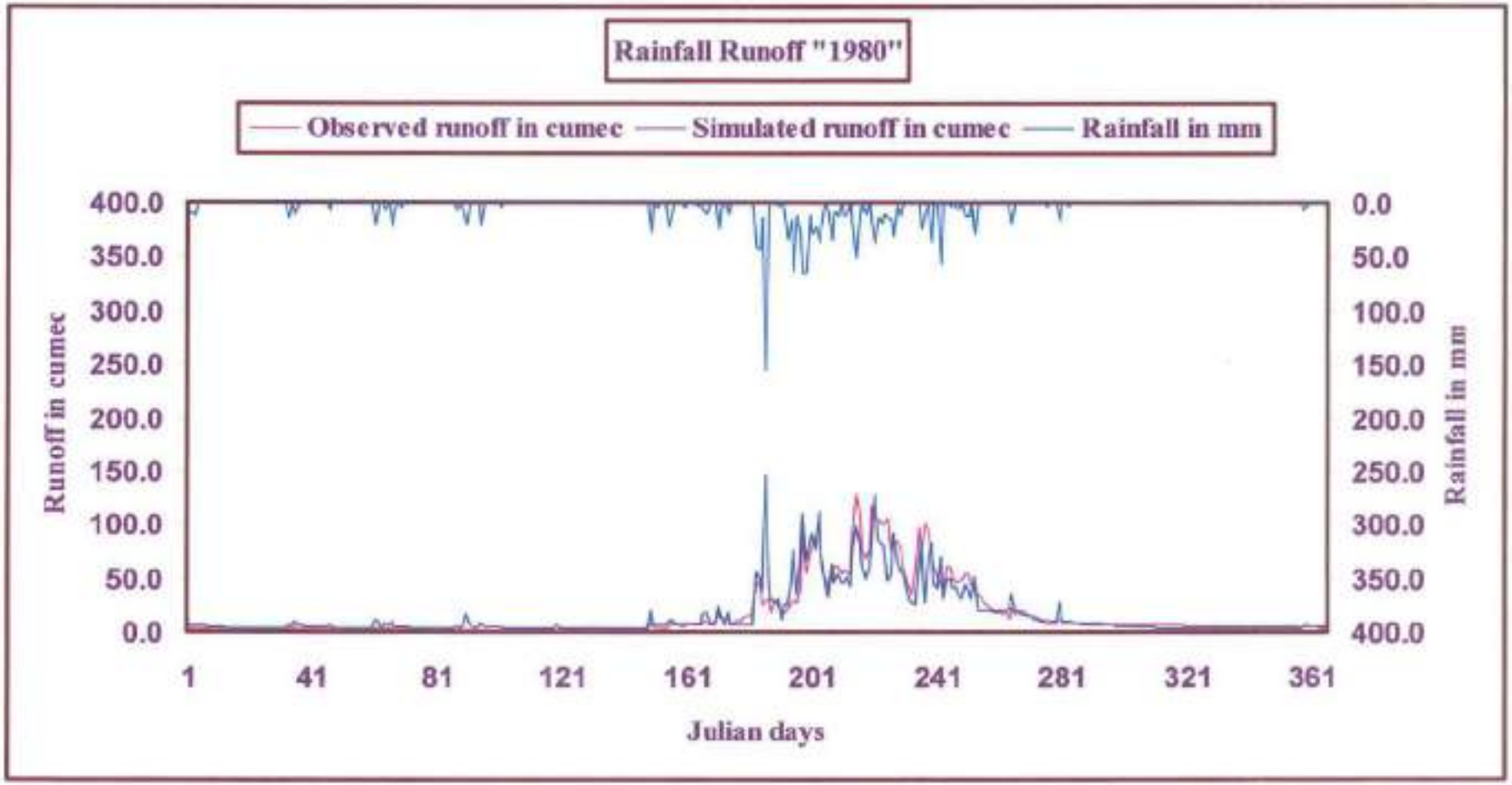

Figure 6.11: Daily observed and simulated runoff for the year 1980

Figure 6.12: Monthly observed and simulated runoff for the year 1975

Figure 6.13: Monthly observed and simulated runoff for the year 1976

Figure 6.14: Monthly observed and simulated runoff for the year 1977

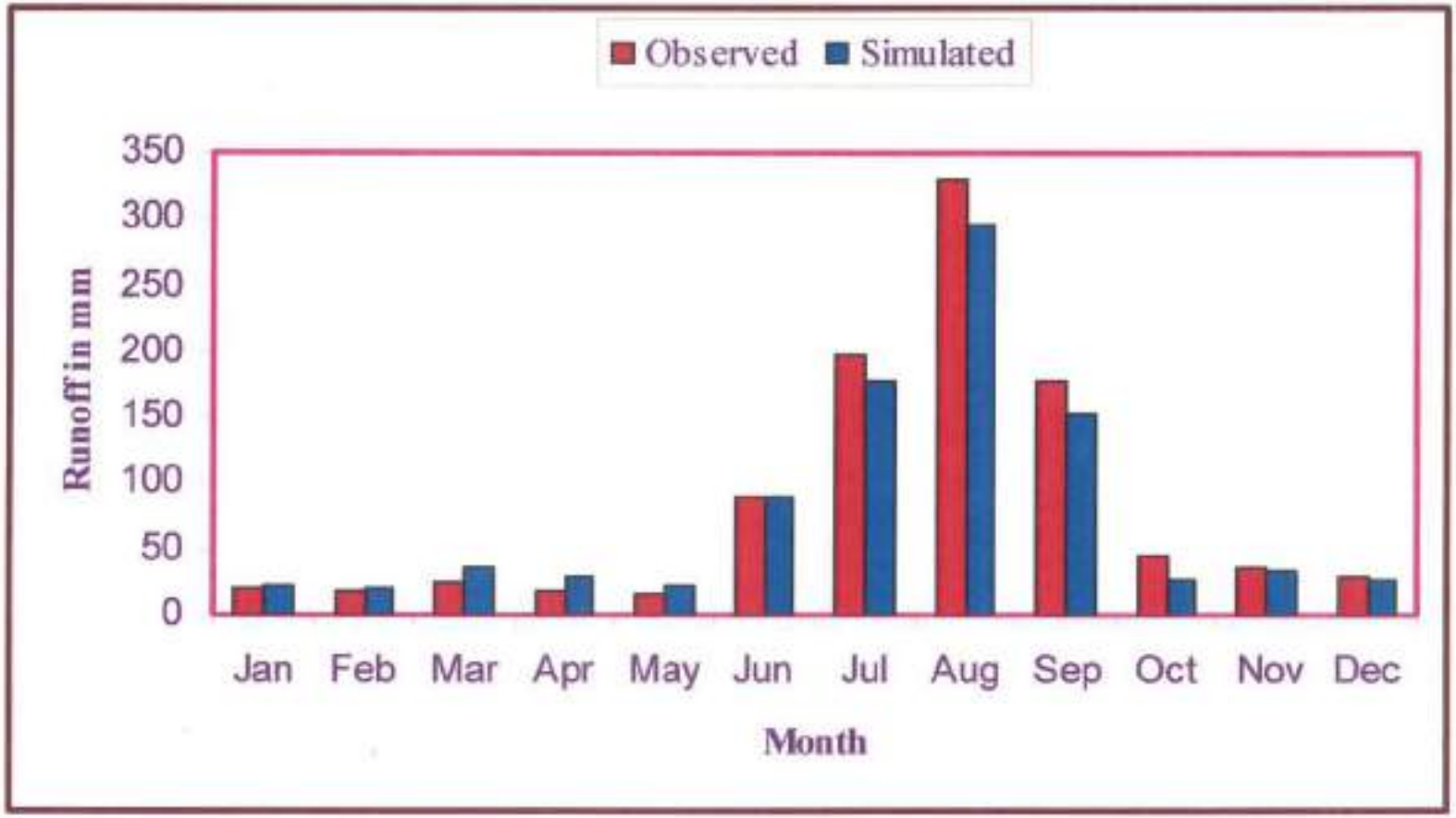

Figure 6.15: Monthly observed and simulated runoff for the year 1978.

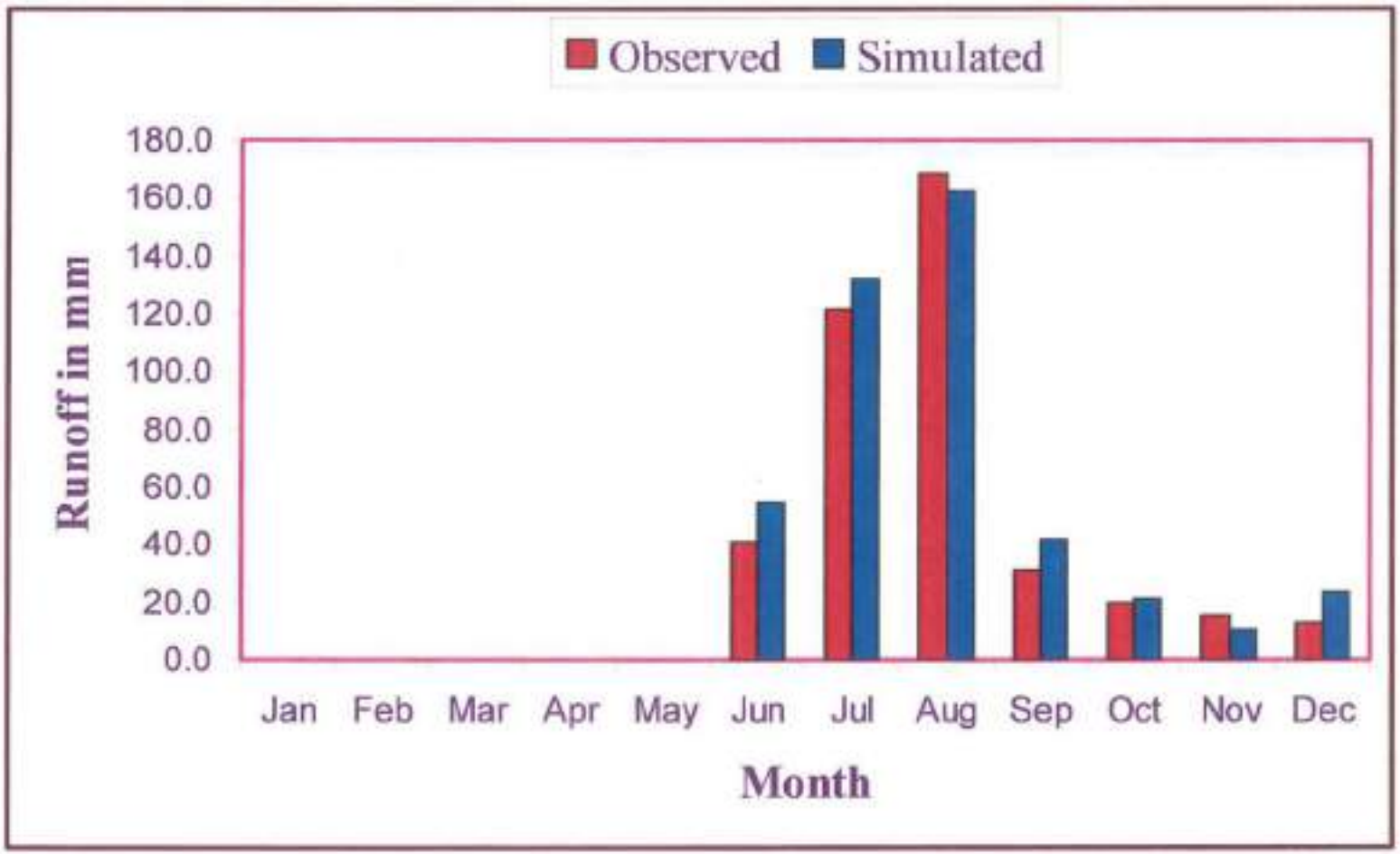

Figure 6.16: Monthly observed and simulated runoff for the year 1979.

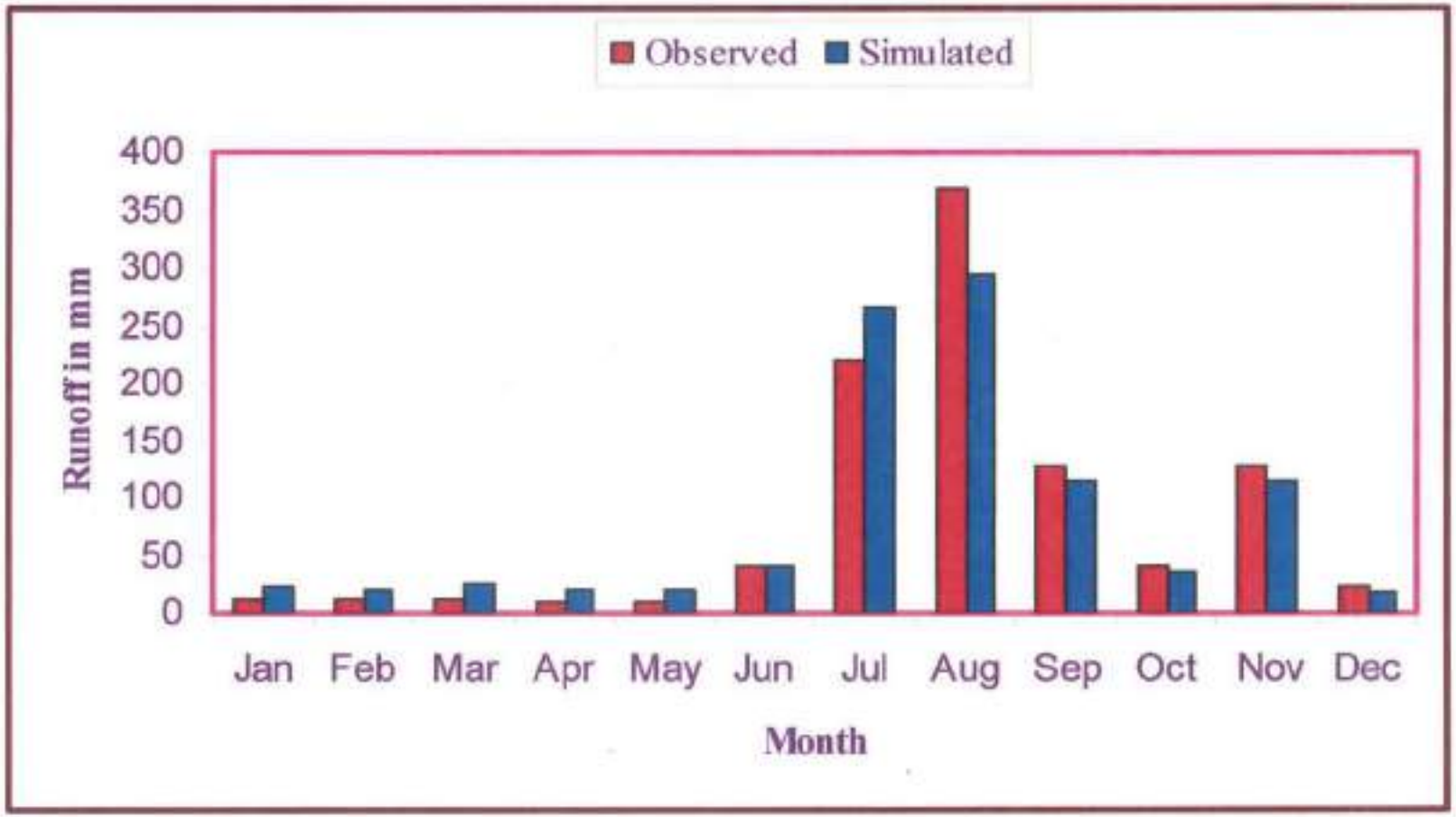

Figure 6.17: Monthly observed and simulated runoff for the year 1980.

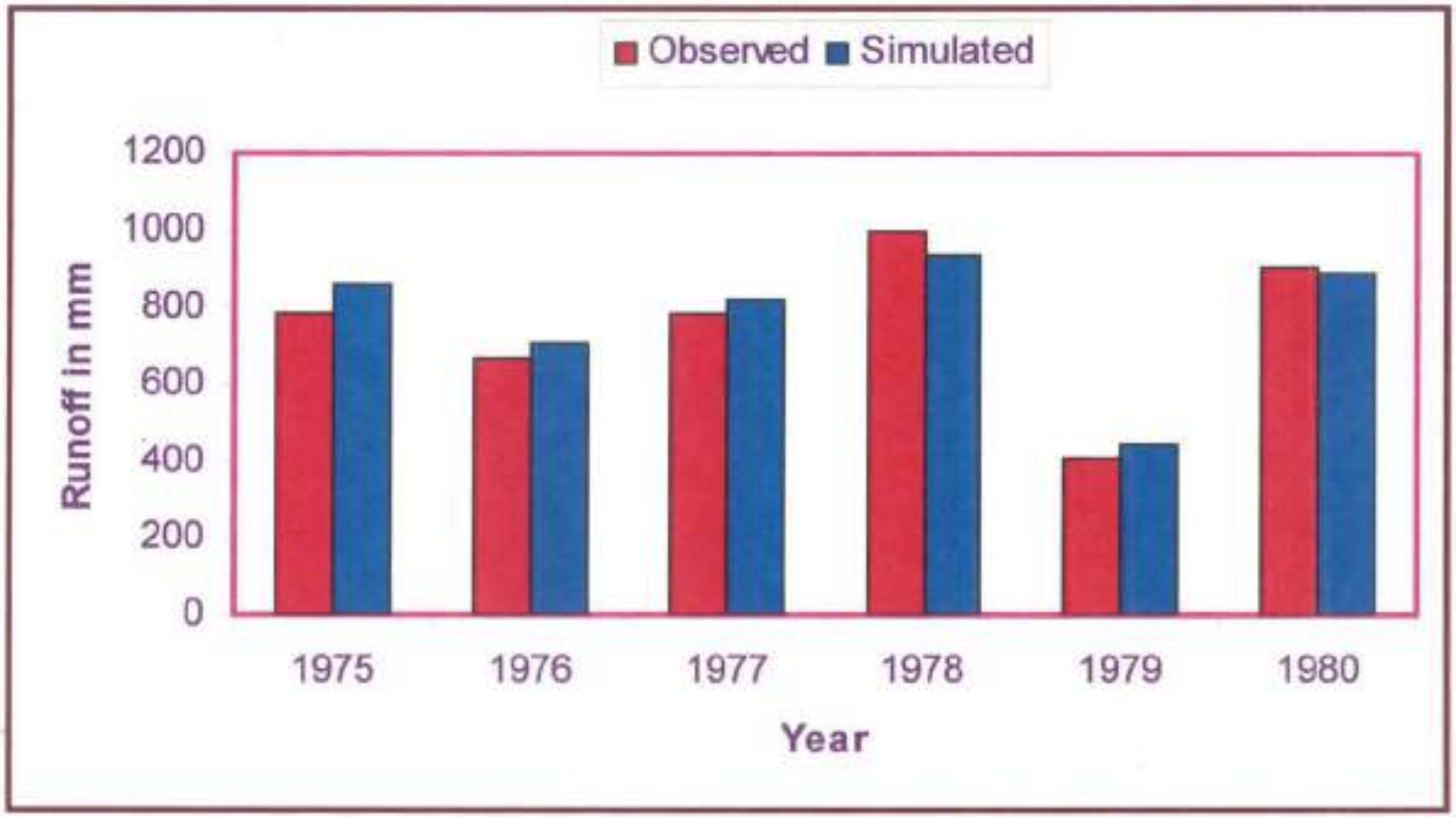

Figure 6.18: Annual observed and simulated runoff

6.13.1 Quantitative Evaluation

The first evaluation criterion used was the percent bias (PBIAS), which is a measure of the average tendency of the simulated flows to be larger or smaller than their observed values. The optimal PBIAS value is 0.0; a positive value indicates a model bias toward underestimation, whereas a negative value indicates a bias toward overestimation (Gupta et al., 1999). PBIAS may be expressed as:

$$PBIAS = \frac{\sum_{k=1,n}^{n}(Q_{kobs} - Q_{ksim})}{\sum_{k=1,n}^{n}(Q_{kobs})}(100) \qquad (6.1)$$

where PBIAS = deviation of streamflow discharge expressed as a percent; Q_{kobs} = Observed streamflow (m^3/s or (cm/s)); and Q_{ksim} = Simulated streamflow (m^3/s or (cm/s)).

Donigian et al. (1983) considered HSPF model performance "very good" if the absolute percent error is <10%, "good" if the error is between 10 and <15%, and "fair" if the error is between 15 and <25% for calibration and validation. Measurement errors associated with streamflow as recommended by Harmel et al. (2006) follow the same standard. This standard was therefore adopted for PBIAS evaluation criterion used in this study, with PBIAS values ≥ 25% considered as unsatisfactory.

The second evaluation criterion was the model coefficient of efficiency (Nash Sutcliffe coefficient of efficiency (NSE) (Nash and Sutcliffe 1970), which Sevat and Dezetter (1991) found to be the best objective function for reflecting the overall fit of a hydrograph. NSE expresses the fraction of the measured stream flow variance that is reproduced by the model.

$$NSE = 1 - \left[\frac{\sum_{k=1,n}^{n}(Q_{kobs} - Q_{ksim})^2}{\sum_{k=1,n}^{n}(Q_{kobs} - Q_{mean})}\right] \qquad (6.2)$$

where, NSE = Nash Sutcliffe coefficient of efficiency and Q_{mean} = Mean observed streamflow during the evaluation period (cm/s).

As per NSE criteria simulation results are considered to be very good for values of NSE > 0.75, whereas for values of NSE between 0.75 and 0.36, the simulation results are considered to be satisfactory (Motovilov et al., 1999).

As described above, Nash Sutcliffe coefficient of efficiency (NSE) (Nash and Sutcliffe, 1970) and Percent Bias (PBIAS) (Gupta et al., 1999) were used to assess daily runoff simulated by SWAT model. The values of NSE and PBIAS on the daily basis are tabulated in Table 6.24.

Table 6.24: NSE and PBIAS on daily basis.

Sl. No.	Year	PBIAS (%)	NSE
1	1975	-9.99	0.70
2	1976	-5.68	0.72
3	1977	-5.02	0.83
4	1978	6.66	0.85
5	1979	-9.26	0.82
6	1980	1.74	0.81
Overall		**-2.43**	**0.80**

Here, negative value of PBIAS indicates a bias towards overestimation whereas its positive value indicates a model biased towards underestimation. The optimal PBIAS value is zero. Our model overall biased towards overestimation with a little value of about 2.4% and hence as per PBIAS criteria model performance may be termed as "very good".

NSE expresses the fraction of the observed stream flow variance that is produced by the model. On the basis of these NSE criteria our model results for the years 1975 and 1976 are satisfactory and for rest years the model is considered as reasonably satisfactory.

6.13.2 Visual Evaluation

Average monthly measured and simulated streamflow for the calibration and validation periods were analyzed. Fig. 6.19 shows a graphical representation of the observed and simulated monthly mean of runoff which has been derived from daily observed and simulated records of runoff at Chaukhutia watershed outlet. From this graph it is observed that the simulated value of runoff is in close agreement with the observed runoff. The simulated runoff values are somewhat higher than the observed mean runoff. It is also evident from PBIAS quantitative method that this model setup is giving a little bit over estimated values.

Monthly and daily hydrographs are shown in Figs. 6.20 to 6.25 and Figs. 6.6 to 6.11 respectively. Monthly runoff drawn in bar chart is shown in Figs. 6.12 to 6.17. Apparently, the simulated base flow is in close agreement with the observed during the lean period. However, during monsoon, a little deviation is apparent between the observed and simulated values. In addition, the simulated runoff appears to have a lag just before the start of monsoon. Daily flow duration curves (Figs. 6.6 to 6.11) also indicate some deviation between the actual and simulated flows, which may be attributed largely to error in measurements. Apparently, the rainfall of 353 mm exhibits a runoff value of only 22 mm in monsoon, which is unreliable.

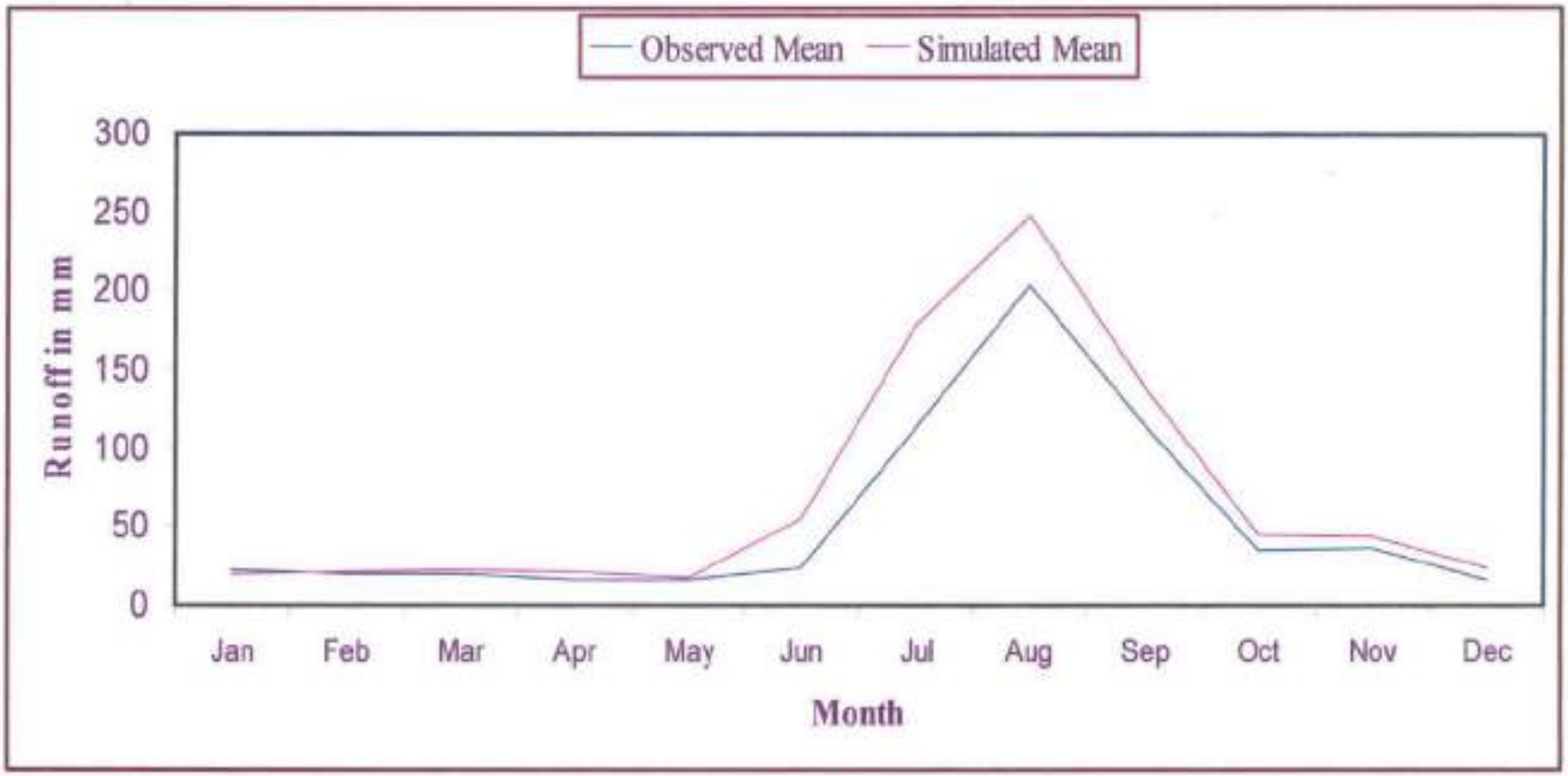

Figure 6.19: Mean monthly observed and simulated runoff

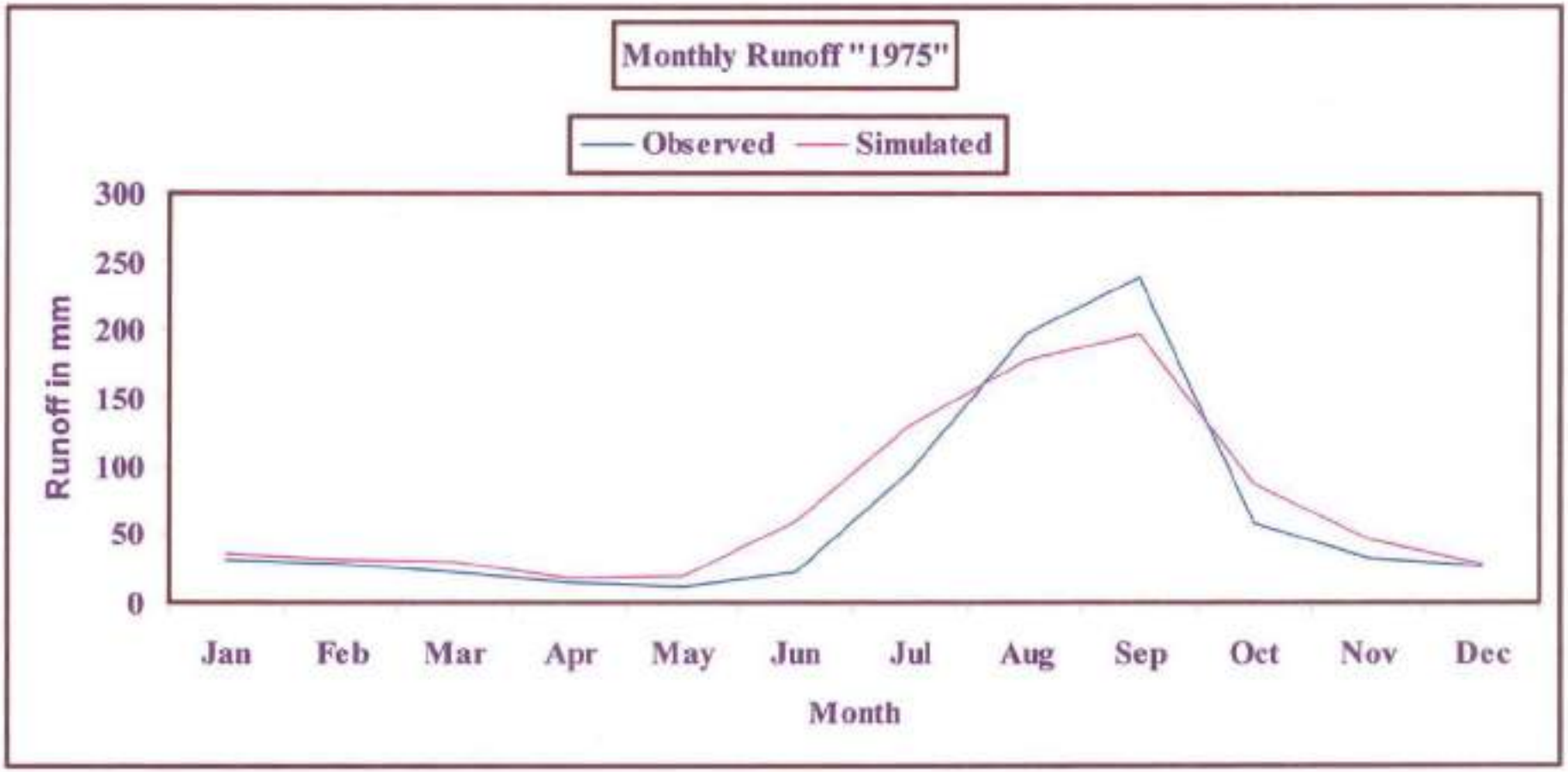

Figure 6.20: Monthly runoff for the year 1975

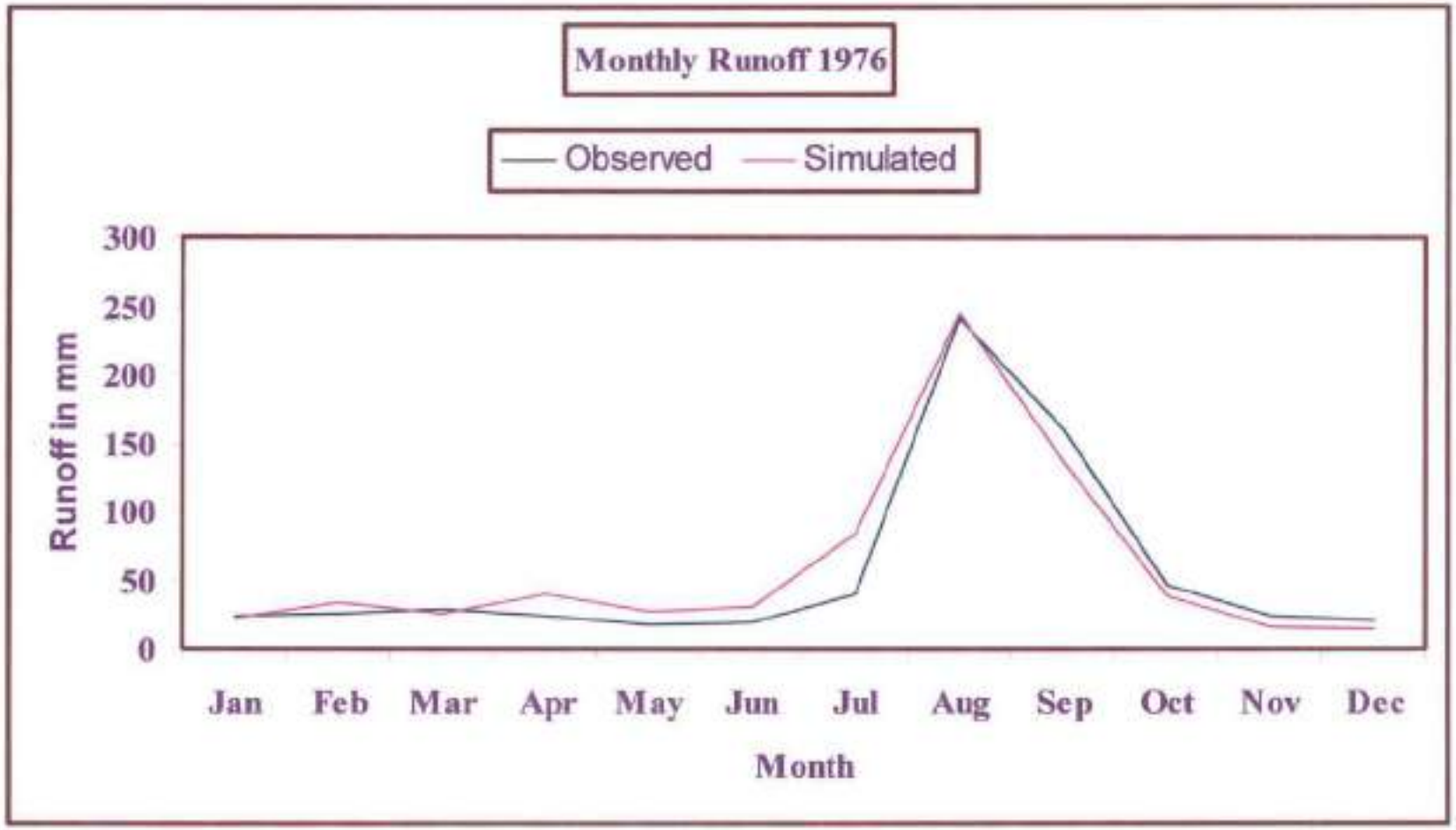

Figure 6.21: Monthly Runoff 1976

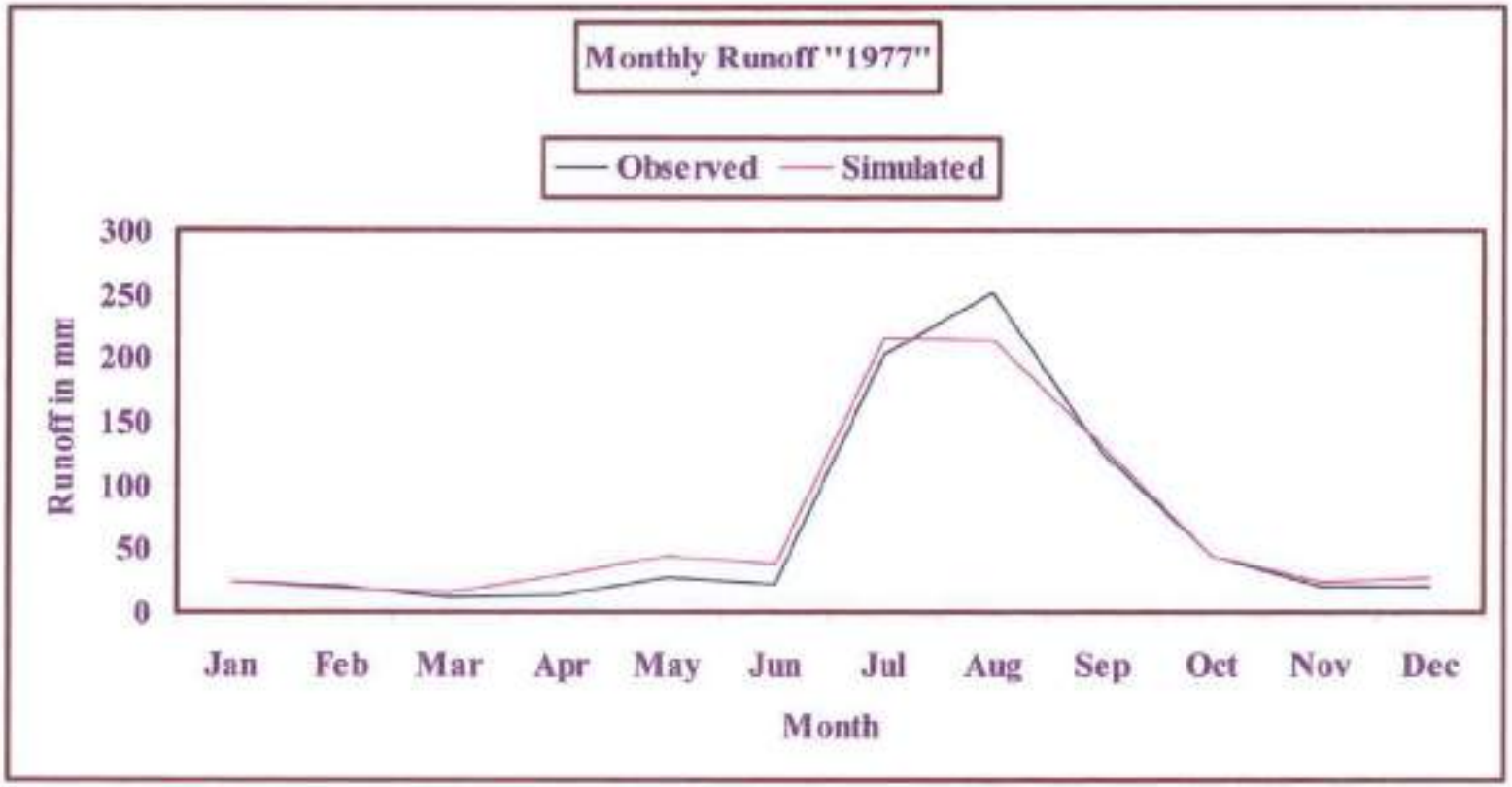

Figure 6.22: Monthly Runoff 1977

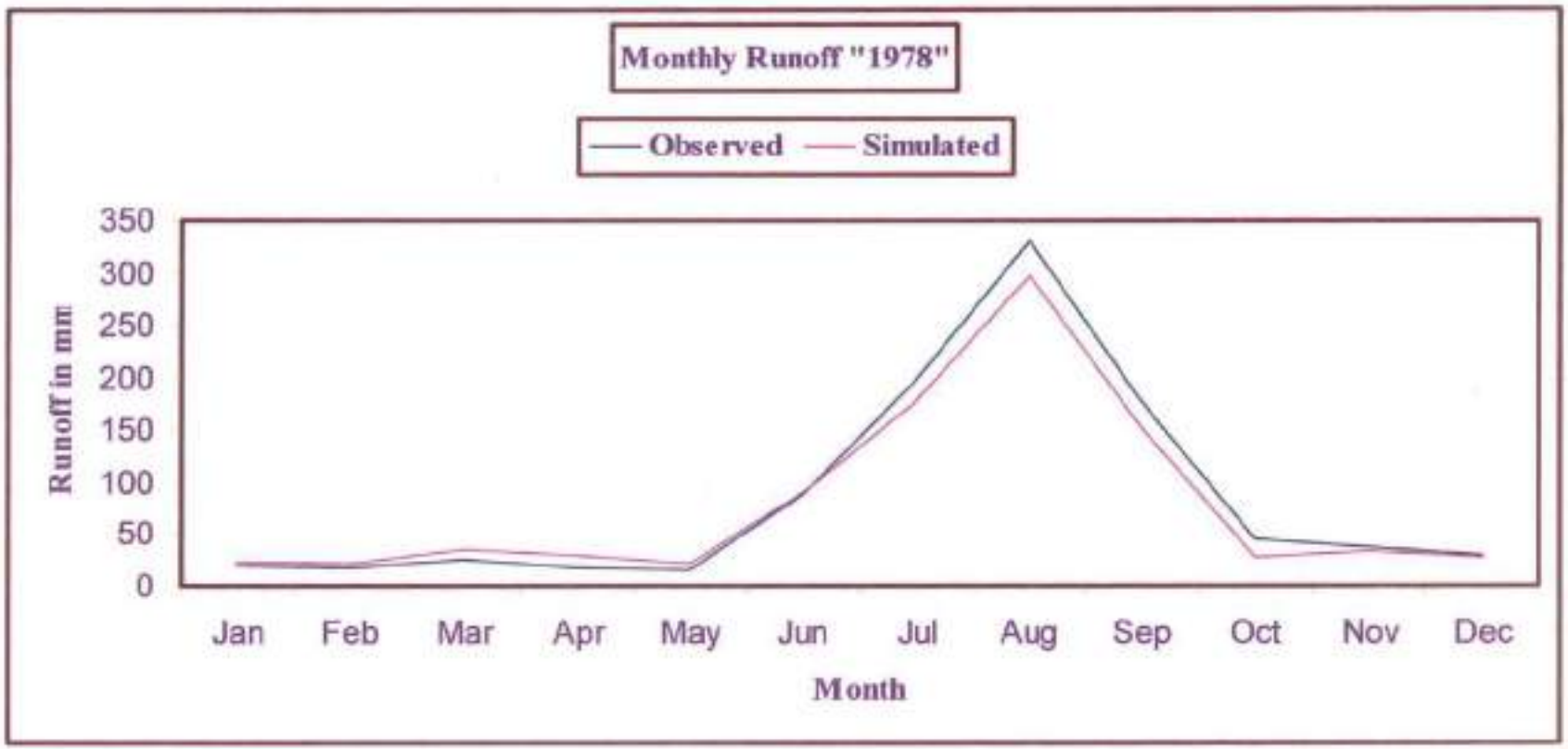

Figure 6.23: Monthly Runoff 1978

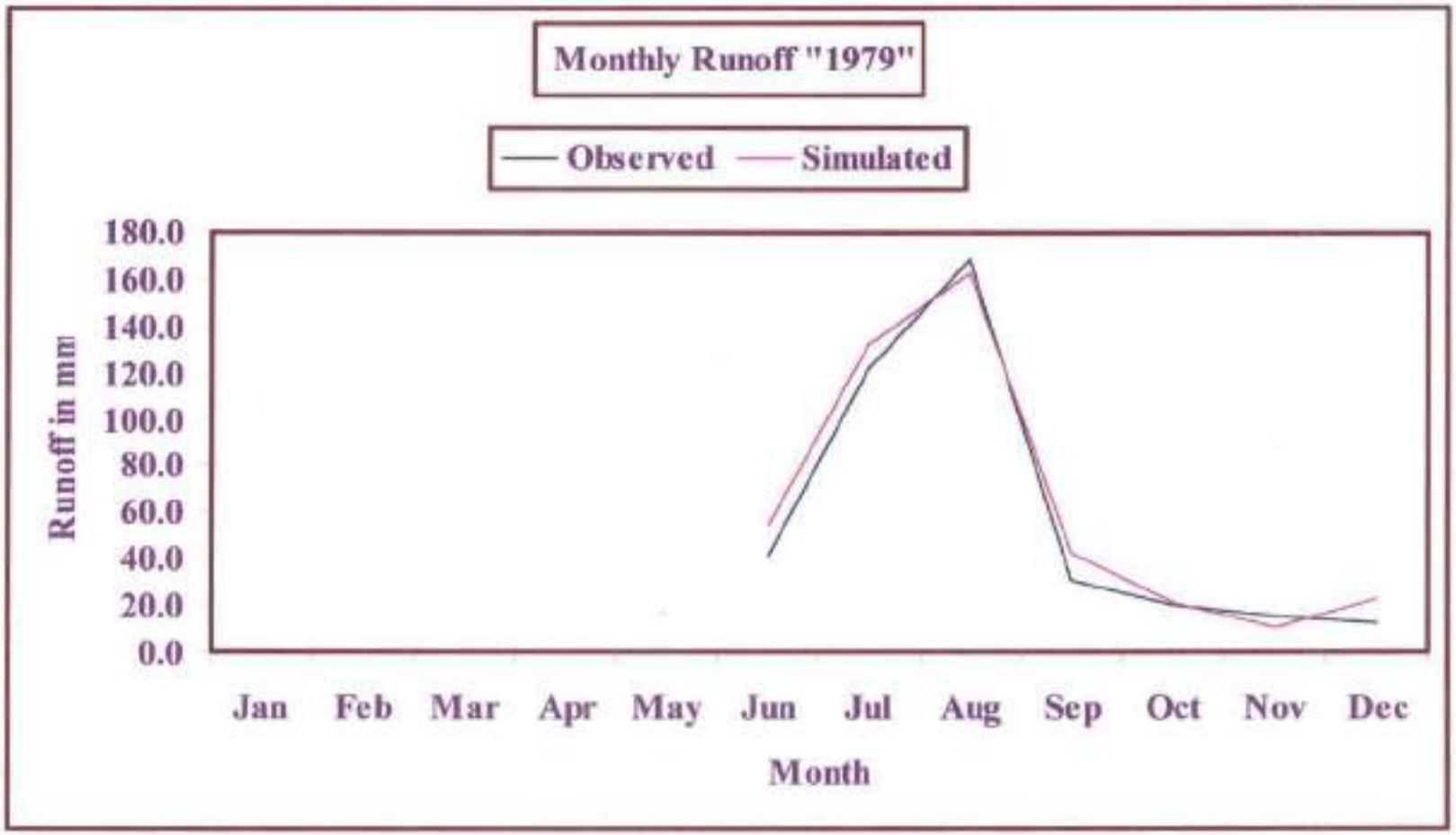

Figure 6.24: Monthly Runoff 1979

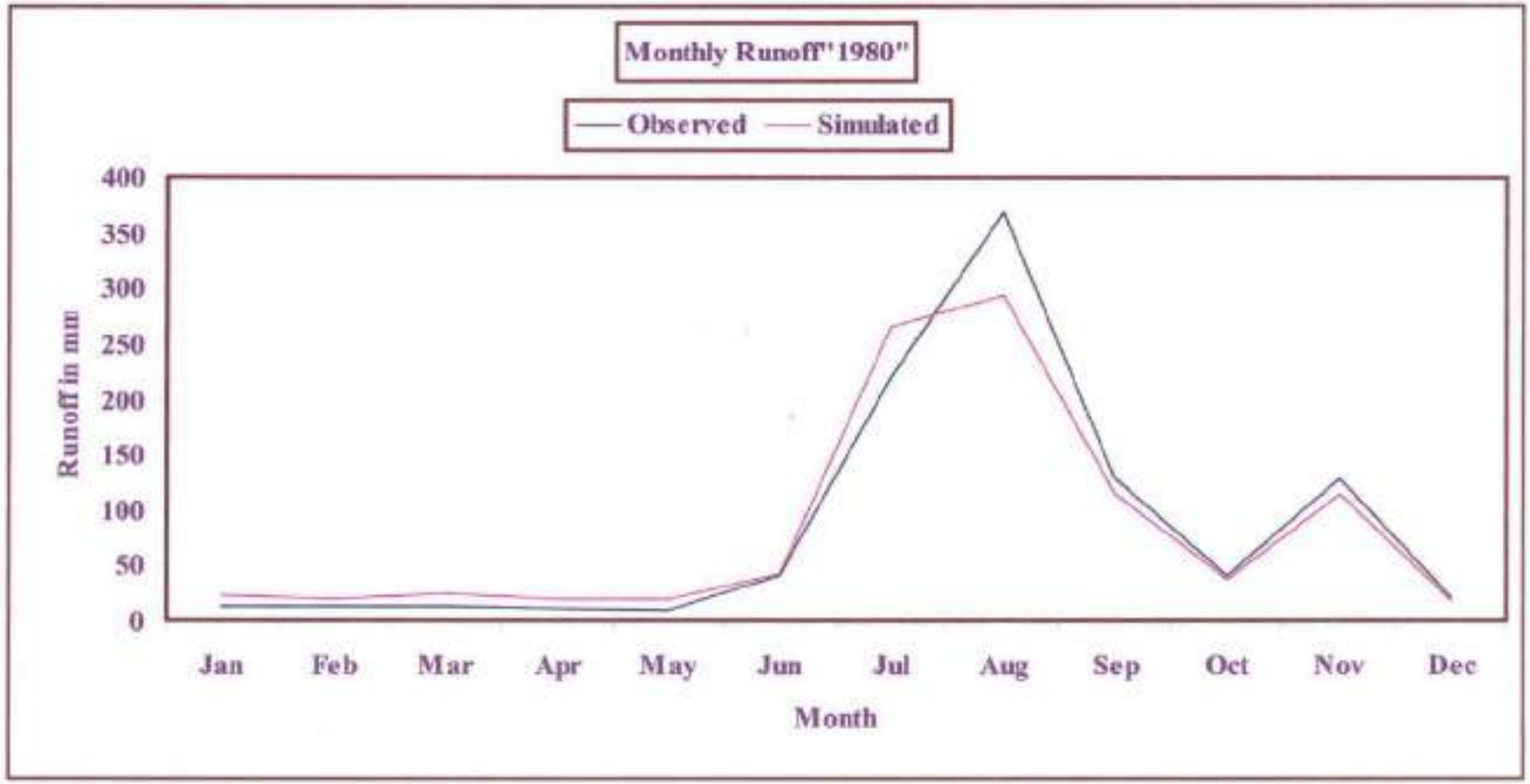

Figure 6.25: Monthly Runoff 1980.

6.14 SENSITIVITY ANALYSIS

SWAT model is a comprehensive conceptual model that requires a lot of data to run. For useful model results, every parameter is required to have a sensible value. To this end, calibration is usually undertaken to reduce the uncertainties associated with the estimation of model parameters. To ensure efficient calibration, a sensitivity analysis is conducted to identify the most sensitive parameters.

The SWAT model uses many different parameters whose values vary widely in space and time. To reduce the uncertainties posed by the variation of model parameters, a calibration process becomes necessary. In addition, access difficulties for measurement of parameters and budget constraints for the project increase the difficulty of working with models. A successful and efficient trial and error calibration is practically impossible. Although, automated calibration procedures have been successfully used for hydrological modelling with SWAT (Eckhardt and Arnold, 2001). However, due to the number of simulations required, time taken and computational requirements, the use of such automated calibration procedures is not widespread. Addressing this problem, a trade-off between simplicity and automation of calibration is attempted. A sensitivity analysis is usually the first step towards model calibration because it answers several questions such as (Cho and Lee, 2001): (a) where data collection efforts should focus; (b) what degree of care should be taken for parameter estimation; and (c) the relative importance of various parameters. A sensitivity analysis also identifies the most sensitive parameters, which ultimately dictates the set of parameters to be used in the subsequent calibration process.

A sensitivity analysis was conducted to identify the sensitive parameters affecting stream flow for subsequent application in stream flow calibration. Available interface provides the analysis using predefined sets of input variables as given on page 66 of the AVSWAT-X short tutorial (Luzio et al., 2005) out of which only ten parameters were chosen for sensitivity analysis. These were CN2, ESCO, SOL_AWC, GW_REVAP, REVAPMN, GWQMN, GW_DELAY, ALPHA_BF, SURLAG and CH_K2. Details of these codes are already given in Table 6.22 and Parameter values calibrated using auto calibration tool are given in table 6.23. The following sensitive parameters were identified:

Available water capacity of soil (SOL_AWC): Available water capacity has an inverse relationship with various water balance components. An increase in AWC value will decrease the base flow, tile drainage, surface runoff and hence water yield. All water balance components are sensitive to AWC.

Sensitivity of the curve number (CN): The result shows that the water balance components are not sensitive to the CN value adopted. This could be for two main reasons. The first is that the range assumed for assessing the sensitivity of CN is low (original CN value for a particular soil group-land use hydrologic condition combination ±2) when compared to other studies (Lenhart et al., 2002; Eckhardt and Arnold, 2001). The second potential cause of low sensitivity is that there exists an explicit provision in the SWAT model to update the CN value for each day of simulation (i.e. a daily CN value in SWAT) based on available water content in the soil profile. Therefore, a change in the initial CN value will not greatly affect the water balance components.

6.15 SUMMARY AND CONCLUSIONS

Among the myriad rainfall-runoff models available in literature, the Soil and Water Assessment Tool (SWAT) has gained popularity in the recent past, because it is a distributed watershed model developed by Agricultural Research Service of United States Department of Agriculture to predict the impact of land management practices on water, sediment and agricultural chemical yields in complex watersheds. It is a comprehensive model which requires a significant amount of data and parameters for simulation of runoff and loadings mainly from rural catchments. This study aimed at to test the applicability of SWAT model to simulate runoff response from sub-Himalayan Chaukhutia watershed.

For model run Digital Elevation Model (DEM), land use map of the study area using satellite data, digital soil map were prepared for the study area, and finally data base compatible with SWAT model was prepared. Then, runoff was simulated using the latest SWAT-2005 model, it is calibrated and validated with different data sets, and finally a sensitivity analysis of model parameters was carried out. The following conclusions can be briefly derived from this study:

1. The entire Chaukhatia watershed lies between the elevation 934.845 m and 3099.29 m indicating a mountainous watershed. Its total geographical area is of the order of 57229 ha. The SWAT model has been suggested to be applicable to only moderately sloping watersheds.
2. The Chaukhatia watershed can be broadly categorized as a forest (evergreen) watershed with 33871 ha (of the order of 59%). It is based on the channel initiation threshold (CIT) value of 2500 hectare. Notably the SWAT model has not been tested for its applicability to such watersheds in the past.
3. In general, 133 hydrologic response units (HRU) and 17 sub-basins were considered to be reasonably sufficient to describe the hydrologic response of the watershed.
4. In daily flow simulation for the years 1975 to 1980, the values of PBIAS ranged from -9.99 to 6.66 indicated that in some years the runoff was over-estimated (negative PBIAS values) and in others it was under-estimated (positive PBIAS values), but not significantly as the Nash and Sutcliffe efficiency (NSE) ranged from 0.70 to 0.85 indicating a reasonable to very good model fit. It follows that the SWAT model is applicable to even forested sub-Himalayan watersheds.
5. The SWAT model parameter "Available water capacity of soil (SOL_AWC)" was found to be the most sensitive parameter for accurate runoff simulation. It implies that this is the most crucial parameter to be assessed from field measurements.

CHAPTER 7

APPLICATION OF ANN MODEL

CHAPTER 7

APPLICATION OF ANN MODEL

Accurate estimation of runoff from catchment rainfall is crucial for judicious planning and management of water resources. The rainfall-runoff process is based on so many factors that will not always contribute to the same effect to produce runoff. Thus, the modeling of rainfall-runoff should be carried out with utmost care by considering non-linearity of the model. Rainfall-runoff modeling is one of the most complex and non-linear process of the nature. Understanding its dynamics constitutes one of the most important problems in hydrology.

The runoff from a catchment mainly depends on its physical characteristics like land use, vegetation, soil type, drainage area, basin shape, elevation, slope, topography, direction/ orientation, drainage network pattern and also on the climatological factors like sunshine, temperature, humidity, and wind velocity. Thus, modeling of rainfall-runoff process needs determination of a number of physical as well as hydrological parameters. Their spatial and temporal variability further complicates the problem of their determination and makes the task costly. In general, the model is based on two main aspects. First, the model should accurately map the input variables to output variables as is observed from the field. Secondly, the model should be a best fit with representation of a system's internal physical nature. The ultimate aim of the models must be to deliver an improved estimate to aid in decision making of hydrological problems such as irrigation, flood protection, water resources planning, reservoir operation, hydropower generation, and inland navigation. Finally, the developed model should also be useful to other similar catchments. Owing to all these reasons, a significant amount of research has focused on the development of rainfall-runoff models that comply with the demands of high accuracy, low uncertainty, and consistency with reality (Wagener, 2003).

7.1 RAINFALL-RUNOFF MODELS

Numerous models have been developed for different climatic zones and basin parameters. The modeling objective has always been to improve the accuracy and reduce the cost of modeling. Broadly, the rainfall-runoff model can be categorized in three major groups viz., Physically based models, Stochastic models, and Black box models. The physical models consist of mathematical equations of mass and energy transfer. In general, it consist the systems of ordinary or partial differential equations. These models try to represent the underlying physical relationship between the variables involved. The benefit of physical models is that they are based on a deep and thorough understanding of the system. However, the limitations of these models include the difficulty of setting up and solving complex differential equations analytically, as well as determining equation coefficients and initial and boundary conditions (Coppola et al. 2005). Moreover, these models utilize many parameters in their operation in a direct relation to topology, soil, vegetation and geological characteristics of catchments which are not always directly measured everywhere. However, stochastic models for rainfall-runoff modeling belong to the class of Autoregressive Integrated Moving Average (ARIMA) models (Makridakis et al. 1983; Cryer, 1986). The popularity of these models in many areas resulted from having quite flexible of the model, due to the inclusion of both autoregressive and moving average terms (Kadri and Ahmet, 2005). These models may not pick up some of the more subtle features of time series and not suitable for long time prediction (Graham Elliott et al., 2006).Furthermore, the back box models do not use any explicit or well-defined representation of the physical process and governing equations of the phenomena. These models are fully based on observational data and on the calibrated input-output relationship without description of individual processes.

The Artificial Neural Network (ANN) is one such black box model that has been applied to myriad diverse hydrological problems and the results in each case have been very encouraging. ANNs are capable to handle nonlinearity of the complex systems to be modeled with flexible mathematical structure along with the activation function. The important characteristics of ANNs include their adaptive nature and learning by examples (Deco and Obradovic, 1996; Haykin, 1999). ANN can find useful relationships between

different inputs and outputs without even attempting to understand the nature of the phenomena.

7.2 ARTIFICIAL NEURAL NETWORK (ANN) MODEL

ANN models are developed using the measured time series instead of utilizing mathematical expressions describing the physical processes of the catchment. ANN is one such technique in series that provides reliable estimation without considering the physical nature of the process. Besides their application in hydrology, ANNs have been successfully applied in handling extraordinary range of problem domains, in areas as diverse as medicine (Venkatesan and Anitha, 2006), aero dynamic optimization (Wei et al. 2008); construction cost forecasting (Zhigang and Yajing, 2009), pattern recognition (Miyoung and Cheehang, 2000) etc. The nonlinear nature of the relationship, universal function approximation, robustness, ability to learn, and the complexity of physically based models are some of the factors that have suggested the use of ANN in rainfall-runoff modeling (ASCE, 2000).

Numerous researchers have attempted to study the basic nature of ANN, and consequently, derived learning algorithms for its efficient usage in various applications. Jalili et al. (2004) proposed a uniform weight learning algorithm to improve fault tolerance of neural network. Peralta et al. (2007) coupled ANN with genetic algorithm for direct encoding system, in which the information is placed in chromosomes. Slawomir Golak (2005) designed induced weights of ANN to reduce the time-consuming task of pre-processing patterns. Vieira (2005) proposed iterative neural network approach for high dimensional data and described it as robust, relatively simple to implement, and able to handle many features, even if they are irrelevant for solution. Lin and Chen (2004) approached the systematic input to neural network so that it reduces unnecessary trials.

7.3 HYDROLOGICAL APPLICATIONS OF ANN

In hydrological applications, ANN has been extensively used in almost all problems. Bhattacharya and Solomatine (2000) found in their study the superiority of

ANN over the conventional linear approaches (regression and ARIMA) in the development of stage-discharge relationship. For simulating the sediment yield of Vamsadhara river basin Agarwal et al. (2004) applied linear transfer (LTF) function model and back propagation-based ANN basin. Based on selected performance evaluation criteria, they found the pattern-learned BPANN models to perform better than batch-learned models irrespective of their high convergence. On the other hand, the pattern-learned BPANN models generalized with cross-validation performed better than those generalized with a high level of iteration and LTF models. To avoid the waterlogging in coastal areas due to intrusion of sea water, Nayak et al. (2006) applied ANN to forecast the ground water level up to 4 months in advance reasonably well. Bustami et al. (2007) used back propagation neural network successfully for determination of the missing precipitation data and prediction of water level in Bedup River. Mean and maximum River water can be determined by incorporating several input parameters using ANN (Chenard and Caissie (2008). ANN requires less data incomparison to standard and conventional penman-Monteith method for determining most complicated phenomenon like evapotranspiration (Jain et al., 2008).

In addition, ANNs have been applied in hydrological study for rainfall estimation (Zhang et al. 1997; Kuligowski and Barros, 1998), flood forecasting (Fernando and Jayawardena, 1998), ground water modeling (Yang et al. 1997; Krishna et al. 2008), reservoir inflow forecasting (Coulibaly et al. 1998; Jain et al. 1999), suspended sediment estimation (Agarwal et al., 2005) and evapo-transpiration modeling (Jain et al. 2008). The texts of ASCE Task Committee (2000), Maier and Dandy (2000), and Dawson and Wilby (2001) provided a good overview of ANN applications in hydrology.

7.3.1 ANN-Based Rainfall-Runoff Modeling

In rainfall-runoff modeling, potential of ANN has been explored by many researchers such as by French et al. (1992), Hsu et al. (1995), Raman and Sunilkumar (1995), Minns and Hall (1996), Shamseldin (1997), Fernando and Jayawardena (1998), Marina et al. (1999), Tokar and Johnson (1999), Abrahart and See (2000), Komda and Makarand (2000), Tokar and Markus (2000), Gaume and Gosset (2003), Anetil et al.

(2004), Chiang et al. (2004), Jain and Srinivasulu (2004), Rajurkar et al. (2004), Lin and Chen (2004), de Vos and Rientjes (2005) and many others. Mason et al. (1996) found RBFANN networks to be more effective in modeling runoff for a large rainfall data base with radial centers fixed by a suitable data clustering technique than the traditional neural network learning procedures, such as back propagation because of slow convergence and expensive. Fernando and Jayawardena (1998) used RBFANN networks with orthogonal least square algorithm for forecasting runoff from Kamihonsha catchment in Uratsukuba. They found the OLS algorithm to be capable of synthesizing the suitable network architecture, reducing the time consuming trial and error approach.

Lin and Chen (2004) simulated the rainfall-runoff process in the Fei-Tsui reservoir watershed in northern Taiwan using RBFANN with supervised learning and hybrid-learning, for setting up the number of hidden layer neurons. The fully supervised learning algorithm was found to provide better training and accuracy than the network trained using the hybrid-learning algorithm. Zakermoshfegh et al. (2004) applied RBFANN and BPANN to forecast mean daily discharge of the Sulaghan River at Kan hydrometric station located few kilometers in the west of Tehran, Iran. The performance of RBFANN network greatly relied on the number of the input variables in both training and verification periods. Removing the non-effective inputs can improve the RBFANN network performance. Comparatively, the RBFANN network required more hidden neurons but trained faster than the BPANN network. Napiorkowski et al. (2005) used Volterra net, BPANN networks, and RBFANN networks for rainfall-runoff simulation and river flow forecasting in Nysaklodzka catchment. In comparison, neural networks performed better than Volterra net. In neural networks, BPANN networks performed better than RBFANN networks, but the latter allows a lesser number of input values due to curse of dimensionality. Kumar et al. (2005) fixed the structure of RBFANN networks using an appropriate training algorithm while simulating the rainfall-generated runoff, whereas BPANN networks requires a long trial-and-error procedure to fix the optimal number of hidden nodes. Piotrowski et al. (2006a) applied RBFANN, Fuzzy, and BPANN, Nearest Neighbour approach, linear regression, and classical empirical formulae for determination of longitudinal dispersion coefficient for a river reach. The results from neural networks were better than those due to empirical formulae, regression method, and

Nearest Neighbour approach. The results of BPANN networks were more precise than RBFANN and fuzzy models. Sudheer et al. (2008) used ANN-based hybrid model (ANNHM) and the linear parametric-based hybrid model (LPHM) for modeling annual stream flows of rivers. The ANNHM reproduced the skewness present in stream flows better than the LPHM, owing to the effective capturing of the non-linearity. Being a completely data-driven model, ANNHM reproduced the features of the marginal distribution more closely than the LPHM, but with less smoothing and little extrapolation value. Despite a better preservation of the linear dependence structure, LPHM did not predict the variation of critical drought duration effectively with respect to truncation level. In contrast, ANNHM simulated the variation of critical drought duration better even though the preservation of linear dependence structure is inferior to the LPHM. In brief, ANN models have its unique application in water resources and they have been applied in different ways in hydrologic literature. In relation to RBFANN networks, BPANN networks are sometimes poorer to converge, better in generalization, and poorer in performance.

7.4 OBJECTIVES

In this study, a computer program was developed using k-means clustering algorithm for the RBF neural network to carry out rainfall-runoff modeling of the Upper Ramganga river basin located in Himalayan region of Uttrakhand State of India. The program code was written in FORTRAN environment. The best input combination was decided by cross-correlation matrix method and it consists of rainfall and discharge values. In present study, dynamic types of approach have been applied for calculation of spread value in radial basis function neural network. The performance of the model is improved by proper selection of suitable learning rates and optimized number of iterations to train the network. The results of method are compared with the observed output.

7.5 STUDY WATERSHEDS AND DATA AVAILABILITY

In this study the Ramganga watershed and its two sub-watersheds namely Chaukhutia and Naula are taken for rainfall-runoff modeling by ANN. A detailed description of these watersheds has been given in Chapter 2. The Ramganga reservoir catchment mainly consists of 12 sub-watersheds namely Chaukhutia, Gagas, Bino, Naula, Mandal, Nair, Middle Ramganga, Haldgad, Sona Nadi, Badangad, Lower Ramganga (L), and Lower Ramganga (R). Out of these twelve sub-watersheds, the Chaukhutia and Naula (Upper Ramganga) are the two most runoff and sediment producing sub-watersheds of Ramganga river basin and consist of one third part of the total catchment area.

7.5.1 Hydro-Meteorological Data

The hydro-meteorological data of Chaukhutia and Naula watershed were collected from the Divisional Forest Office (Soil Conservation) Ranikhet, Govt. of Uttarakhand. However, the data were collected from Ramganga dam authority at Kalagarh. The rainfall is measured in mm/day, and runoff in hectare-meter (ha-m)/day. Fourteen years daily rainfall-runoff data for monsoon season (1st June – 31st September) vary from 1974 to 1987, 1974 to 1988 (except 1984), and 1979 to 1992 were collected for Chaukhutia, Naula, and Ramganga watersheds, respectively. Year 1984 could not be included in case of Naula watershed due to non-availability during June-July. The rainfall data is recorded with the help of non-recording gauges at different locations of watershed and the runoff is estimated by stage-discharge curve at three different sites along the Ramganga river namely Chaukhutia, Naula, and Kalagarh.

The above daily rainfall (mm/day) and runoff (m^3/s) data of monsoon period for years 1974-1987, 1974-1988, and 1979-1992 for three watersheds were processed. Weighted rainfall for the study area was estimated using Thiessen weights. Six rain gauge stations located at Gairsen, Mehalchauri, Vungidhar, Chaukhutia, Bhirapani, and Binta installed in/outside of Chaukhutia watershed were used to calculate the weighted rainfall of Chaukhutia watershed. For Naula watershed, ten station data (Naula, Kedar,

Tamadhanu, Jourasi, and six station of Chaukhutia watershed) were used for estimation of weighted rainfall. However, in addition to Naula watershed rain gauge stations, four more station installed at Ranikhet, Bhikiasen, Marchulla, and Kalagrah station rainfall were used for estimation of weighted rainfall of Ramganga watershed.

With the help of weighted average rainfall and runoff, runoff coefficients were calculated for each year of monsoon period and these are reported in Tables 7.1-7.3 for Ramganga, Naula, and Chaukhutia watersheds, respectively. It can be seen from these tables that Chaukhutia, Naula are the high runoff producing watersheds and Ramganga is however the low runoff producing watershed. It is notable here that Chaukhutai and Naula are typical hilly watersheds and hence very sensitive to runoff and sediment production. The runoff coefficient varies from and 0.19 to 0.40 for Ramganga watershed (Table 7.1), from 0.49 to 0.75 for Naula (Table 7.2), and from 0.52 to 0.79 for Chaukhutia (Table 7.3).

Table 7.1: Summary of Hydrological Data of Ramganga Watershed

Year	Annual Weighted Rainfall (mm)	Annual Average Runoff (m^3/s)	Runoff Coefficient
1979	781.3	9229.5	0.33
1980	1072.0	13749.1	0.35
1981	862.0	10523.7	0.34
1982	937.9	10211.1	0.30
1983	1111.4	13661.7	0.34
1984	1022.7	13145.9	0.35
1985	1182.7	13546.0	0.32
1986	1084.4	13214.8	0.34
1987	846.8	5947.0	0.19
1988	1385.8	15690.8	0.31
1989	1067.1	10023.0	0.26
1990	1425.6	20514.2	0.40
1991	942.5	9386.1	0.27
1992	1080.5	10426.5	0.27

Table 7.2: Summary of Hydrological Data of Naula Watershed

Year	Annual Weighted Rainfall (mm)	Annual Average Runoff (m3/s)	Runoff Coefficient
1974	834.4	4858.7	0.50
1975	1105.4	7335.2	0.57
1976	1006.6	7328.8	0.62
1977	1145.6	10048.5	0.75
1978	1440.3	12561.8	0.75
1979	716.6	5048.0	0.60
1980	1098.0	7424.5	0.58
1981	603.3	4029.4	0.57
1982	959.2	5931.2	0.53
1983	1102.4	7988.6	0.62
1985	799.2	5754.7	0.62
1986	931.5	8007.7	0.74
1987	581.8	3345.7	0.49
1988	1052.3	6844.7	0.56

Table 7.3: Summary of Hydrological Data of Chaukhutia Watershed

Year	Annual Weighted Rainfall (mm)	Annual Average Runoff (m^3/s)	Runoff Coefficient
1974	843.3	2735.5	0.62
1975	1068.5	3682.1	0.66
1976	1073.4	3583.8	0.64
1977	1295.0	4044.0	0.60
1978	1444.2	5269.2	0.70
1979	826.0	2396.0	0.55
1980	1329.5	4921.8	0.71
1981	680.5	1835.7	0.52
1982	1156.8	3935.3	0.65
1983	1302.4	5038.2	0.74
1984	1175.1	4169.7	0.68
1985	1009.7	3147.5	0.60
1986	1138.6	4687.8	0.79
1987	719.9	2003.8	0.53

7.5.2 Preparation of Input Data

The model was calibrated with data from 1979 to 1984; however data from 1985 to 1988 and 1989 to 1992 were used for cross-validation and verification, respectively for Ramganga watershed. In case of Naula watershed, the model was calibrated using data from 1974-1979, and data from 1980-1983 and 1985-1988 were used for cross-validation and verification, respectively. The data from 1974 to 1979 were used for model calibration whereas the data from 1980-1983 and 1984-1987 were respectively used for cross-validation and verification for Chaukhutia watershed. The daily data of the active period of monsoon (June 1st to September 31st) of water years were used to model the rainfall-runoff process. Based on cross-correlation matrix best combination of rainfall and runoff was selected for the input of the model for all three watersheds.

7.5.3 Data Normalization

Data were normalized (between 0-1) before the start of model training using following equation given as:

$$x_n = \frac{x_0}{x_{max}} \tag{7.1}$$

where x_n and x_o represent the normalized and original data, respectively; and x_{max} is the maximum value of the selected variable. After training the network, the de-normalization is performed at the output nodes.

7.6 ANN METHODOLOGY

This section describes the methodology adopted for development of ANN based rainfall-runoff model for Ramganga watershed and its sub-watershed namely Naula and Chaukhutia.

7.6.1 Radial Basis Function ANN (RBFANN)

The Radial Basis Function ANN (RBFANN) network has gained popularity and momentum in hydrological science in recent years (Fernando and Jayawardena, 1998; Dawson et al., 2002; Moradkhani et al., 2004). These networks were introduced into the ANN literature by Broomhead and Lowe (1988). The RBF network model is motivated by the locally tuned response. The same response can be found in nervous system, for example, cells in the visual cortex sensitive to bars oriented within a small region of the visual field (Poggio and Girosi, 1990). These locally tuned neurons show response characteristics bounded to a small range of the input space. RBFs are embedded in a two-layer neural network, where each hidden unit implements a radial activation function in hidden layer. The basic idea is to force each neuron of the hidden layer to represent a given region of the input space. In other words, each hidden unit must contain a prototype of a cluster in the input space. When a new pattern is presented to the network, the hidden unit with the most similar prototype will activate a decisional path inside the network that will lead to the final result.

Thus, the activation function of the new hidden units must include the concept of prototype of a region and the concept of similarity of an input pattern with this prototype. This can be translated into a measure of distance. Several distance measures have been proposed, and several training algorithms designed, to define the input cluster and its prototype associated with each hidden unit of the network. RBFANN holds the universality property and is usually accompanied by much faster learning algorithm than Back Propagation ANN (BPANN).

The output units implement a weighted sum of hidden unit outputs. The input into an RBFANN network is nonlinear while the output is linear. Due to their nonlinear approximation properties, RBFANN networks are able to model nonlinear dynamic processes, at the same time BPANN networks can only model by means of multiple intermediary layers. In RBFANN networks, instead of hidden layer as in BPANN, the term function layer is being used. In BPANN network, the weighted summation of the inputs is processed from the neurons of the input layer to neurons of the hidden layer. IN RBFANN network, the input layer does not transform the pattern, but forward an image

of variables to each node in the function layer. Learning of a RBFANN network is generally divided into two phases. The first phase is unsupervised learning in which the function unit parameters depends on the input distribution adjustment. The second phase is a supervised learning in which the weights between function and linear output layer are adjusted using gradient descent techniques.

7.6.2 Advantages of RBFANN over BPANN

- During training of BPANN network, updates take place in all units independently from their contribution to the final outputs. The interferences among hidden units produce a highly nonlinear updating process with problems of local minima. This can lead to a very slow convergence of the training algorithm. On the other hand, in a RBFANN neural structure, for any given input pattern forms its own clusters in which the input vector nearer to center will respond with significantly large activation values. This limits the number of hidden units that need to be evaluated for each training and leads to more efficient training algorithms than BPANN.
- BPANN network separates the input pattern distribution by building hyperplanes in the input space (Figure 7.1a). Usually several hyper-planes have to be combined to form closed separation surfaces. But an RBFANN networks divide the input space into a number of sub-spaces and each subspace is represented by only a few functional RBF units. The function layer activates the RBF units representing the input cluster. From the function to output layer, the activated RBF units produce the appropriate output value. This builds closed separation surfaces among groups of data in the input space (Figure 7.1b). Because of the locality property that leads to closed separation surfaces within the cluster.
- The dimensionality of the data is reduced by projecting a large input space on to a smaller number of hidden units and forcing the data through a bottle neck, but RBF works opposite to this condition.
- The number of hidden units in back propagation is more. On the other hand, in RBFANN, the minimum number of hidden node is sufficient to implement a given task.

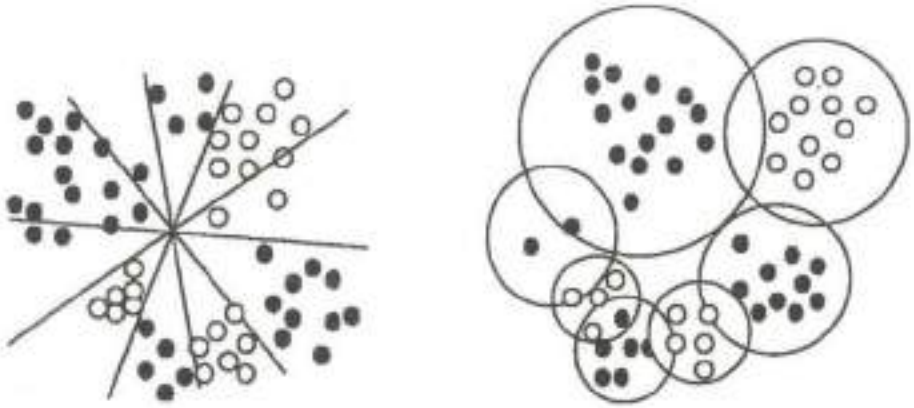

[a] [b]

Figure 7.1: Surface separation created by: [a] Back Propagation Artificial Neural Network and [b] RBF Artificial Neural network

7.6.3 Network Topology

A RBFANNs having input, function, and output layers of nodes with j, i, and k are respectively, shown in Figure 7.2. The structure of RBFANN shows jj-dimensional input pattern (x) being mapped to kk-dimensional output (O). The values j and k are problem dependent, the value i is to be determined by the network designer. In RBFANN operation, input of n^{th} pattern with each pattern made up of jj variables represents a point in the jj -dimensional input space. It enters the network at the input layer such that one variable is fed into one node. The input layer does not transform the pattern, but it transfers a copy of variables to each node in the function layer. The nodes in each function layer are specified by a transfer function f (d), which radially transforms the incoming information.

For n input patterns x having jj dimensionality (x^n_{jj}), the response of O_i of function layer, through radial transformation, can be expressed in mathematical terms as:

$$Q_i = f(d) \qquad (7.2)$$

where Q_i is the output of function layer and f(d) is a nonlinear function.

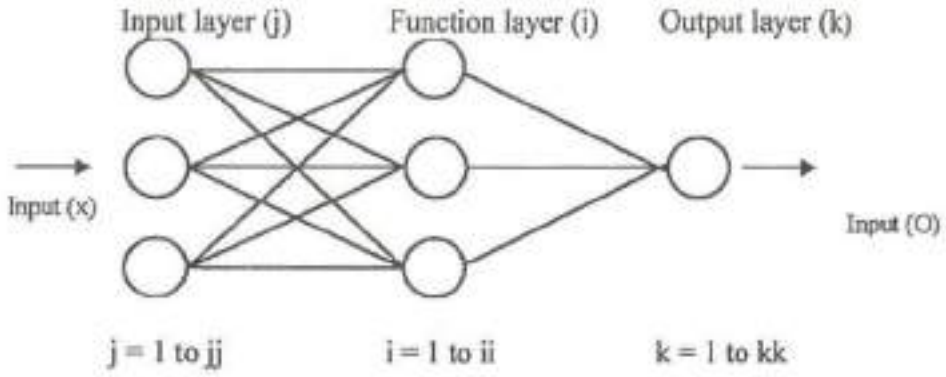

Figure 7.2: Structure of RBFANN

7.7 CONCEPTS OF MODEL DEVELOPMENT

For a discrete lumped hydrological system, the rainfall-runoff relationship can be generally expressed as (Hsu et al., 1995):

$$Q_t = f\left[R(t), R(t-\Delta t).....R(t-n_x\Delta t), Q(t-\Delta t).....Q(t-n_y\Delta t)\right] \quad (7.3)$$

where R represents rainfall, Q represents runoff at the outlet of the watershed, f is any kind of model structure (linear or nonlinear), Δt is the data sampling interval, n_x and n_y are positive integer numbers reflecting the memory length of the watershed. An ANN architecture clearly shows the network topology with the input determination and the activation function used (Fig. 7.3).

7.7.1 Activation Function Used

Normally BPANN uses sigmoidal function as an activation function in its hidden layer. But it belongs to the set of monotonic basis and unit step functions have a slowly decaying behavior in a large area of its arguments. Because of this consequence of using

sigmoidal function, one needs locally restricted basis functions, such as a Gaussian function, bell-shaped function, wavelets or the B-spline functions.

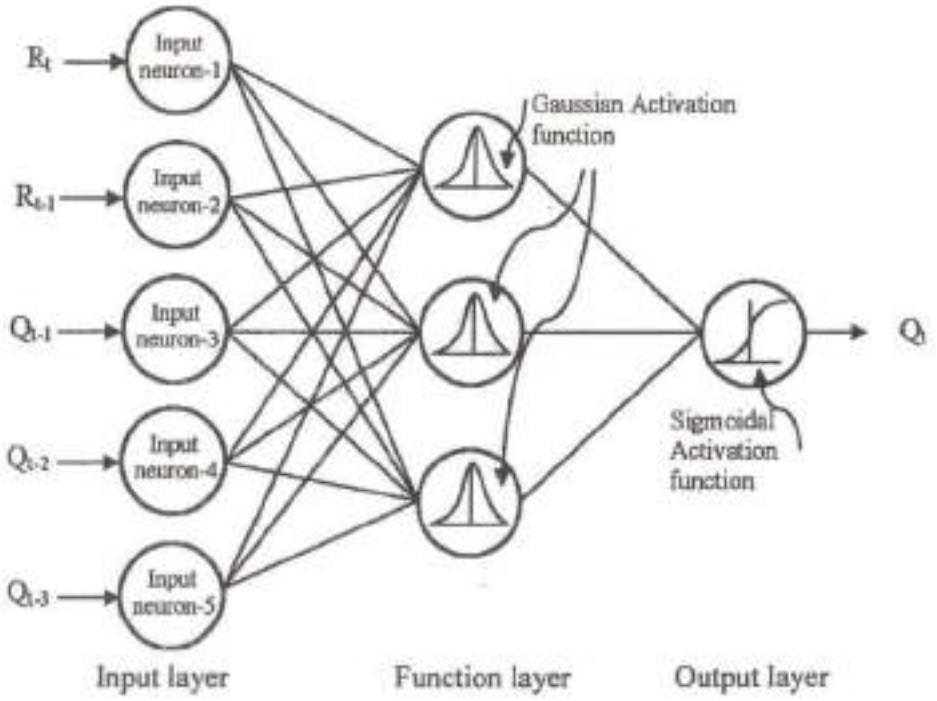

Figure 7.3: Configuration of an RBFANN with model input

In this study, the Gaussian activation function is selected as activation function (Fig. 7.4). The mathematical structure of this function is given as:

$$f(d) = e^{-(d^2/\sigma^2)} \tag{7.4}$$

when $d = 0$, then $f(d) = 1$,

$d = \infty$ then $f(d) = 0$

where d = euclidean distance and σ = spread. In general, the RBF nodes are locally tuned, i.e. to be active only for a delimited region of the input space. The selected

Gaussian function is radially-symmetric with a single maximum at the origin, dropping off rapidly to zero for large distances. Locally tuned receptive fields are widely found in biology, even though they are not single cell properties, but usually emerge from groups of cells.

7.7.2 Euclidean Distance

The euclidean distance'd' is calculated between the set of inputs and respective center of variable is given as:

$$d_{ij} = \| x_j - c_i \| \tag{7.5}$$

The main objective of the transfer function is to minimize the Euclidean distance to produce the maximum function output.

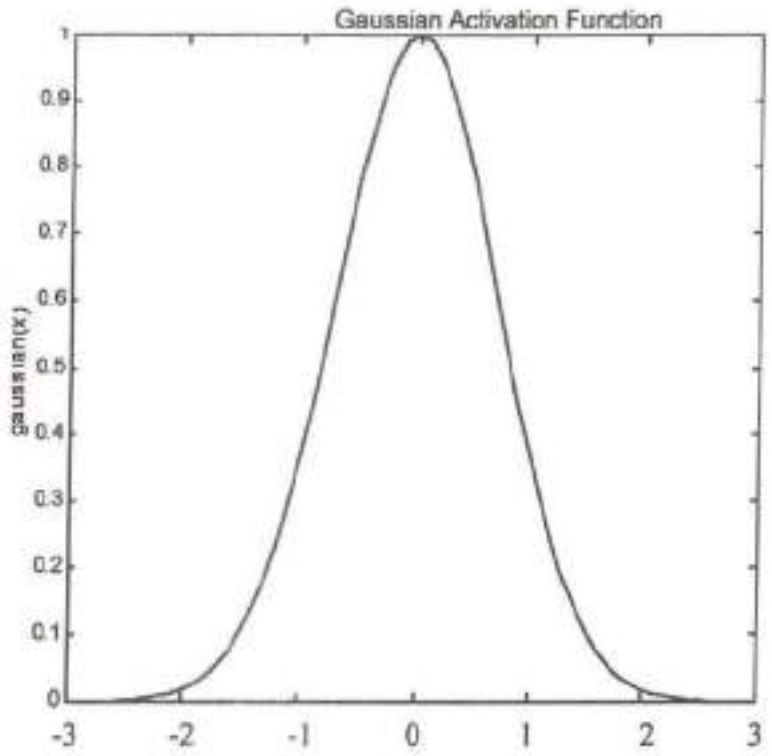

Figure 7.4: Gaussian activation functions

7.7.3 Determination of RBF Center

Performance of the radial basis function network critically depends on the chosen center. The selection of center could be through an arbitrary selection from the data points of the subset or the mean of data points of the subset or ordinary least square of subset or orthogonal least square of subset. If less data is available, there exists no option to position the centers of radial basis functions at the data points. However, such problems may be ill-posed and lead to poor generalization. If more training data presented, several solutions are possible:

- Randomly select the centers of basis functions from the available training data.
- Following the k-means rule, allocate each point to a particular radial basis function such that the greatest component of the hidden layer's activation comes from a particular neuron.

7.7.4 Estimation of Spread

The function spread around the center determines the ratio of the function decay with its distance from the centre. Based on the spread value used in Eq. (7.4), the model has been separated into two types i.e. static and dynamic. In this study, we will deal with only dynamic model. In dynamic model, the spread value is calculated from the input pattern. The value changes from pattern to pattern and in successive iterations as well. This model has good flexibility to adapt complex nature of the environment. Based on the data distribution and cluster formation, the model has a choice to activate the cluster which is nearest to the particular instance. In general, hydrological processes are complex and the output from these processes is complex. The distribution of data is very large and it does not have a definite boundary. The measure of spread (σ) is commonly described as the average distance between the cluster and training instances (number of input variables) in that cluster as:

$$\sigma_i^2 = \frac{1}{M} \sum_{j=1}^{ij} x_j w_{ij} - c_i \qquad (7.6)$$

where M is the number of training instances in that cluster.

Finally, the transformation of information is the response of each function unit and is scaled by its connecting weights to the output units and then summed to produce the overall network output. The overall response of network is calculated as:

$$O_k = \sum w_{jk} f(d) \qquad (7.7)$$

where w_{jk} is the weight coefficient between (j) the hidden unit and $(k)^{th}$ output unit.

7.7.5 Training Algorithm

Finding the RBF weights is called network training. Using the known input and output dataset (called training set), the optimization of the network parameters fits the network outputs to the given inputs. The fit is evaluated by statistical means such as root mean square error, correlation coefficient, and coefficient of efficiency. In general, two types of learning methods are being adopted (supervised learning and unsupervised learning).

In supervised learning, a standard gradient descent procedure can be used. This involves the minimization of an objective function with respect to the actual output. However, such procedures are liable to be trapped in local minimum of the parameter space. In unsupervised learning, k- means clustering algorithm is used. The algorithm k-means (MacQueen, 1967) is one of the simplest unsupervised learning algorithms that solve the well known clustering problem. The procedure follows a simple and easy way to classify a given dataset through a certain number of clusters. The main idea is to define k-centroids, one for each cluster. These centroids should be placed in such a way that different locations yield different results. Therefore, a better choice is to place them as

much far away from each other as possible. The next step is to take each point belonging to a given dataset and associate it to the nearest centroid. After grouping all points with nearest centroids, the recalculation of k-new centroid from the previous centroids value is calculated by initializing suitable weights. All connecting weights adjacent to the winner node are adjusted by making a weight movement proportional to a Mexican hat function (Ralph et al., 2008). The construction of the Mexican hat function is a second derivative of the Gaussian function ($\exp-(d^2/2)$) as:

$$f''(d) = (d_{ij}^{2} - 1) * \exp(d_{ij}^{2}/2) \tag{7.8}$$

The proportional movement related to the Mexican hat function may be explained with the third derivative of the Gaussian function as:

$$f'''(d) = \Delta w_{ij} = (3d_{ij}^{2} - d_{ij}^{3}) * \exp(d_{ij}^{2}/2) \tag{7.9}$$

The Mexican hat function has the effect in moving near neighbors close or no movement while neurons slightly away moved closer and the neurons still further away will have their weights moved away from the input space. Based on the change in weight from the Mexican hat function, the move is calculated as follows:

$$move_{ij} = (x_j - w_{ij}) * \Delta w_{ij} * \alpha \tag{7.10}$$

where Δw_{ij} = change in weight and α= learning rate. The new updated weight for the next iteration is given as:

$$w_{ij}(t) = w_{ij}(t-1) = move_{ij} \tag{7.11}$$

As a result of this, the k centroids change their location step by step until no more changes are done. In other words centroids do not move any more. The influence of

activation function decreases according to the euclidean distance from the center. This means that data samples located at a large euclidean distance from the RBF center will fail to activate that basis function. The maximum activation is achieved when the data sample coincides with the mean vector. Finally, this algorithm aims to attain the minimum euclidean distance between the set of inputs and respective center of variable. Training of weights between the function and the output layer nodes are weighted according to their strengths. The response of the function layer neurons are summed up according to these output layer weights by the nodes in the output layer.

Learning in radial basis network can be divided into two stages. For any iteration, first the learning is carried out in function layer that is followed by learning in output layer. The learning in function layer is performed using unsupervised method, such as the k-means clustering algorithm. While learning in the output layer used supervised methods, such as the initial solution is obtained by this approach, a supervised learning algorithm (back propagation) could be applied in both the layers to fine-tune the weights of the network as an optional strategy.

7.7.6 Outline of Algorithm of Dynamic Model

The algorithm of dynamic model can be outlined as follows:

1. Initialize the weights to small random values and take the average of weights for the calculation of center.
2. Select an input pattern (x) from the training set and present it to the network.
3. Calculate the spread value based on the input, weight vector, and cluster center.
4. Find the best matching or "winning" node whose weight vector wij is closest to the current input vector x using the vector distance (i.e. euclidean distance).
5. Find the network response for the winning node by Gaussian activation function.
6. Update the weight values using Mexican hat function.
7. Repeat Steps 1-6 with a number increase in iterations until weights are stabilized.

7.8 MODEL EVALUATION

The model is evaluated both statistically and hydrologically as discussed here.

7.8.1 Statistical Evaluation Criteria

The statistical evaluation for performance is usually practiced in cross-validation, primarily to improve generalization and to stop the convergence or training of network. The network is trained on the training dataset and its performance is evaluated both in training and in cross-validation for all iterations. The training stops when there is no more improvement both in training and in cross-validation. The statistical performance evaluation criteria include root mean square error (RMSE), correlation coefficient (CC), coefficient of efficiency (CE), and volumetric error (EV).

7.8.1.1 Root Mean Square Error (RMSE)

An alternate criterion of residual error is the mean square error (Yu et al., 1994) expressed as a measure of mean of the residual variance summed over the period, that is $\hat{y}$ as:

$$\text{RMSE} = \sqrt{\frac{1}{n}\sum_{i=1}^{n}(\hat{y}_i - y_i)} \qquad (7.12)$$

7.8.1.2 Correlation Coefficient (CC)

Correlation between the observed and estimated values is accounted by the correlation statistic, called the correlation coefficient. The correlation coefficient is estimated as:

$$CC = \frac{\sum_{i=1}^{n} \left[(y_i - \hat{y}_i).(\tilde{y}_i - \hat{y}_i)\right]}{\sqrt{(y_i - \bar{y}_i)^2 . \sum_{i=1}^{n} (\tilde{y}_i - \hat{y}_i)^2}} \qquad (7.13)$$

7.8.1.3 Coefficient of Efficiency (CE)

Nash and Sutcliffe (1970) proposed the criterion on the basis of standardization of the residual variance with initial variance and named it as the coefficient of efficiency. Since this criterion is based on standardized variance, it can be used to compare the relative performance between different catchments. The dimensionless criterion of coefficient of efficiency is estimated as follows:

$$CE = \left\{1 - \frac{\text{residual variance}}{\text{intial variance}}\right\} x100 \qquad (7.14a)$$

$$CE = 1 - \frac{\sum_{i=1}^{n} (y_i - \hat{y}_i)^2}{\sum_{j=1}^{n} (y_i - \bar{y}_i)^2} \qquad (7.14b)$$

Thus, a perfect agreement between observed and estimated values yields the coefficient of efficiency as 100 percent. For a zero agreement, all the estimated values must be equal to the observed mean. A negative efficiency represents that the estimated values are less than the observed mean. As the efficiency depends strongly on the initial variance of the observed records, it is still not entirely valid to use this criterion to compare the model performance between two catchments (Nash and Sutcliffe, 1970).

7.8.2 Hydrological Evaluation Criterion: Volumetric Error (EV)

This is also called as absolute prediction error (Kachroo and Natale, 1992) and is estimated as:

$$EV = \left\{ \frac{\sum_{i=1}^{n} (\bar{y}_i - y_i)^2}{\sum_{j=1}^{n} y_i} \right\} x100 \qquad (7.15)$$

where y_i is the observed runoff in m^3/s , $\bar{y}$ is the mean observed Runoff in m^3/s, $\hat{y}$ is the estimated runoff in m^3/s, and y is the mean of estimated runoff in m^3/s. This is mainly used to represent error in peak observation, error in low observation, and error in time to peak. The applicability of the evaluation criteria should be assessed carefully and must be properly understood.

7.9 RESULTS AND DISCUSSION

In this section, the results obtained from ANN are discussed. The model developed was applied to the data of three watersheds of above-described Ramganga river basin. The daily fourteen years rainfall-runoff data of monsoon period (June 1st to September 31st) for the years 1979-1992, 1974-1988 (except 1984), and 1974-1987, were used for rainfall-runoff modeling of Ramganga, Naula, and Chaukhutia watersheds, respectively. The data from 1979 to 1984 were used for model calibration whereas the data from 1985 to 1988 and 1989 to 1992 were used for cross-validation and verification of the model, respectively, for the Ramganga watershed. In case of Naula watershed, the data from 1974 to 1979 were used for calibration whereas the data from 1980 to 1983 and 1985 to 1988 were used for cross-validation and verification of the model, respectively. The data from 1974 to 1979 were used for calibration and the data from 1980 to 1983 and 1984 to 1987 were used for the cross-validation and verification of the model, respectively, for Chaukhutia watershed. The model performance has been evaluated

through the normally adopted statistical and hydrological performance evaluation criteria, viz., Root Mean Square Error (RMSE), Correlation Coefficient (CC) and Coefficient of Efficiency (CE), and Volumetric Error (EV).

7.9.1 RBFANN Model

The RBFANN model is trained by both k-means clustering algorithm and gradient descent algorithm employing the best trained input to the network which consists of daily rainfall and discharge values. Considering different inputs, the following model is finalized using correlation matrix method, maintaining the parsimony of the model for all three study watersheds:

$$Q_t = f\left(R_t, R_{t-1}, Q_{t-1}, Q_{t-2}\right) \tag{7.16}$$

where Q_t represents the runoff at time (t) and R_t represents rainfall at time (t). In this study, the dynamic RBFANN model is developed based on the criteria to estimate spread. The spread value is described as the average distance between the cluster center and training instances (number of input variables) in that cluster. The detailed explanation about the spread estimation is given in sub-section 7.74. In dynamic model, the value of spread is estimated using Eq. (7.5). Learning rate for models is selected in such a way that it should increase the convergence ability of the network. The learning rate cannot be negative because this would cause the change of weight vector to move away from ideal weight vector position. If the learning rate is zero, no learning takes place and hence the learning must be positive. In this work, the learning rate in the function layer (ALR) and learning rate in output layer (ALRG) has been selected by choosing proper values through the network behavior. The detailed selection of ALR and ALRG has been mentioned in dynamic model from the lower to higher network.

The program code was developed in FORTRAN environment for the dynamic RBFANN model. The program code was developed with the objective that a user can alter the program for different conditions and can see the network behavior. This is the

major advantage of this model. However, in already developed MATLAB RBF Neural Network models, such a change is difficult.

7.9.2 Dynamic Spread RBF Neural Network Model

In dynamic model, the spread value changes in successive iteration, and therefore, not required to be fixed; and two different values of learning rate have been used as ALR in unsupervised part and ALRG in supervised part. For estimation of ALR value in function node, the value of ALRG is again fixed constant as 0.5, consistent with the work of Agarwal (2002). Based on experience, the number of initial iterations was finalized and fixed at 1000. To ensure the proper selection of ALR from lower network to higher network, three network structures (5-4-1, 5-16-1 and 5-32-1) are selected. In this study, a particular value of ALR, ALRG, and number of iteration has been selected through the network behavior for three selected watershed one by one, and described as follows.

7.9.2.1 Ramganga Watershed

The model performance for different ALR values and three different networks for fixed ALRG (0.5) and iterations (1000) was evaluated and the results are presented in Table 7.4. As seen from Table 7.4, in network 4-4-1, RMSE increases and CC and CE decrease when ALR increases beyond ALR = 20 in cross-validation and verification. Theses values are however constant in calibration. Low values of Volumetric Error (EV) in calibration, cross-validation, and verification support that the model performed best at ALR = 20. The model performance is very poor for ALR value of 0.5. Overall, the performance evaluation criteria, viz., RMSE, CC, CE, and EV together (Table 7.4) suggest that the model performed well for ALR value of 20 and nearly well for a value of 15. In case of Network 4-16-1, RMSE, CC, and CE significantly increase up to ALR = 20. However, beyond 20, no significant improvement is seen in RMSE, CC, and CE. It is further seen from Table 7.4 that volumetric errors increase in cross-validation and verification beyond ALR = 15. However, EV values are comparable for ALR values of 15 and 20. Notably, RMSE, CC, and EV values indicate a better model performance at

ALR= 20 than that at ALR = 15 especially in verification. For network 4-32-1 (Table 7.4), no significant improvement in model efficiency is seen in calibration for ALR = 20 and larger, and it decreases in cross-validation. EV increases when ALR varies higher and lower side of 20.

From the above, it can be concluded that the model performed best at ALR = 20 in all three networks. Furthermore, model efficiency increases from network 4-4-1 to 4-32-1. The maximum coefficient of efficiency (CE) was obtained 76%, 77.68%, and 68.25% in calibration, cross-validation, and verification, respectively, for the network 4-32-1. After fixing the ALR value as 20, the emphasis has been focused towards the selection of learning rate in output layer (ALRG). To identify proper value of ALRG, different values varying from 0.5 to 10 have been tried and the results presented in Table 5.2 for network 5-4-1, 5-16-1, and 5-32-1. No variation is seen in RMSE, CC, CE, and EV in all testing periods for ALRG ranging from 0.5 to 10 in network 4-4-1. Therefore, any value of ALRG can be taken to optimize the model performance; a lower value is however preferable. On the other hand, a little improvement is seen (Table 7.5) in RMSE, CC, and CE when ALRG varies from 0.5 to 10 in the network 4-16-1. However, considerable increase in volumetric error (EV) with increasing ALRG from 0.5 to 10 in all three periods does not support the suitability of higher value of ALRG. Therefore, ALRG = 0.5 can be as the best for optimizing the model performance with network (4-16-1). The performance of 5-32-1 model is found similar to 5-16-1 model, and similar inference can be drawn for 5-32-1 model (Table 7.5). ALRG = 0.5 is also supported by the literature (Agarwal, 2002) to run the model in the range of all networks selected for the study.

After fixing the values of ALR as 20 and ALRG as 0.5, the initial selection of number of iteration is rechecked. To fix the optimum number of iteration, the system is run from lower to higher number of iterations and for three different networks, 5-4-1, 5-16-1, and 5-32-1. The number of iterations is varied from 100 to 10000 and the results presented in Table 7.6 for all three networks, viz., 5-4-1, 5-16-1, and 5-32-1. For the network (4-4-1), no significant improvement in RMSE, CC, and CE values is seen with increase in the number of iterations from 100 to 1000 in calibration, cross-validation, and verification. The volumetric error has however improved considerably up to 1000

iterations in calibration and cross-validation, and verification. Considering the volumetric error, the model performance can be treated as the best with about 1000 iteration. In case of network (4-16-1), CE increases rapidly up to 500 iterations, and thereafter, it gradually increases up to 1000 iterations in calibration, cross-validation, and verification. However, EV improved as the number of iterations increased up to 500. A further increase in iteration from 500 to 10000 resulted into increase in volumetric error. Overall, the model performed well with around 500 iterations. The performance of 5-32-1 model is similar to 5-16-1. Similar inferences can be drawn for 5-32-1 model (Table 7.6).

Moreover, it can be extended that the number of iterations required for best optimization of networks (4-4-1), (4-16-1), and (4-32-1) is around 1000, 500, and 500, respectively. Finally, it can be inferred that for a lower network, the higher number of iterations is required and with increase in network to 4-4-1 to 4-32-1, the number of iterations required for best optimization decreases.

In dynamic model development for Ramganga watershed, the value of ALR is fixed as 20 for all RBFANN structures. The lower network structure is independent of the variation in ALRG values and model performed equally well for its any value ranging from 0.5 to 10. However, with increase the level of network structure, the lower value of ALRG (0.5) is adequate for optimal results. The higher values of ALRG with higher network yield high volumetric error, and therefore, not suitable for optimal solution. Therefore, ALRG was taken as 0.5. The number of iterations required for lower networks is higher (generally 1000), however it reduces (up to 500) for higher network structure.

The observed and estimated values of runoff in calibration, cross-validation and verification for the networks (4-4-1), (4-16-1), and (4-32-1) with ALR = 20 and ALRG = 0.5 are shown in Figures 7.5 to 7.13. It can be seen from all theses figures that the daily runoff pattern is well simulated by the proposed dynamic based RBFANN model in calibration, cross-validation, and verification. However, it is also seen from Figures 7.5 to 7.13 that the sudden high flows are underestimated by all networks.

Table 7.4: Performance of (4-4-1), (4-16-1), and (4-32-1) dynamic RBFANN models. ALRG = 0.5, No. of Iterations = 1000, and ALR = 0.5 to 25 for Ramganga watershed

Period	RMSE			CC			CE			EV		
	4*	16*	32*	4*	16*	32*	4*	16*	32*	4*	16*	32*
						ALR = 0.5						
Calibration	217.7	213.7	211.8	53.74	54.81	55.3	-350.1	-333.8	-326.2	160.52	152.86	149.49
Cross-validation	223.6	219.3	217.4	50.11	51.11	51.52	-244.1	-231.1	-225.2	159.3	151.59	148.06
Verification	235.7	230.6	228.4	45.73	47.04	47.64	-262.4	-247.2	-239.9	168.6	161.13	157.2
						ALR = 5						
Calibration	76.63	75.06	71.31	78.83	79.37	79.03	44.24	46.51	51.72	-7.65	-7.61	-3.23
Cross-validation	80.5	79.07	78.7	79.78	80.31	78.47	55.4	56.98	57.38	-1	-0.71	0.25
Verification	90.13	88.31	91.15	74.29	74.76	71.27	47	48.53	45.79	-3.29	-2.98	-0.25
						ALR = 10						
Calibration	59.14	55.35	54.39	83.37	84.21	84.91	66.79	70.91	71.92	-2.02	-0.15	4.27
Cross-validation	65.07	63.87	62.98	84.37	84.91	85.59	70.86	71.93	72.71	1.18	1.2	5.78
Verification	79.11	77.55	77.05	77.3	77.96	78.45	59.16	60.76	61.26	-0.09	0.14	3.78
						ALR = 15						
Calibration	55.34	53.22	51.5	84.39	85.51	86.54	70.93	73.11	74.81	-0.91	0.01	2.79
Cross-validation	62.82	62.2	59.9	85.44	85.81	87.1	72.84	73.38	75.31	1.15	2.04	5.19
Verification	77.08	75.71	72.4	78.26	79.22	81.42	61.23	62.6	65.8	-0.1	-0.06	2.61
						ALR = 20						
Calibration	54.77	52.44	50.27	84.57	85.96	87.19	71.52	73.89	76	-0.61	0.25	1.31
Cross-validation	62.85	61.51	56.95	85.71	86.18	88.34	72.82	73.97	77.68	1.13	2.81	4.35
Verification	77.06	74.14	69.75	78.42	80.87	82.84	61.25	65.13	68.25	-0.11	0.17	1.27
						ALR = 25						
Calibration	54.76	52.16	50.19	84.5	86.12	87.23	71.52	74.17	76.08	-0.39	0.35	1.15
Cross-validation	63.22	60.94	57.29	85.7	86.43	88.16	72.5	74.44	77.42	1.16	3.29	4.43
Verification	77.47	73.79	69.32	78.34	81.09	83.1	60.84	65.43	68.65	-0.25	0.45	1.25

Note: * indicates the number of neurons in functional layer of a network.

Table 7.5: Performance of (4-4-1), (4-16-1), and (4-32-1) dynamic model. ALR = 20, no. of iterations = 1000, and ALRG = 0.5 to 10 for Ramganga watershed

Period	RMSE			CC			CE			EV		
	4*	16*	32*	4*	16*	32*	4*	16*	32*	4*	16*	32*
						ALRG = 0.5						
Calibration	54.77	52.44	50.27	84.57	85.96	87.19	71.52	73.89	76.1	-0.61	0.25	1.31
Cross-validation	62.85	61.51	56.95	85.71	86.18	88.34	72.82	73.97	77.68	1.13	2.81	4.35
Verification	77.06	74.14	69.75	78.42	80.27	82.84	61.25	64.13	68.25	-0.21	0.17	1.27
						ALRG = 1						
Calibration	54.41	51.31	48.49	84.8	86.62	88.19	71.89	75	77.67	-0.4	0.81	1.98
Cross-validation	62.74	60.16	54.79	85.89	86.85	89.33	72.92	75.1	79.34	0.97	3.74	5.31
Verification	76.95	72.32	67.16	78.58	81.43	84.37	61.37	65.87	70.56	-0.35	0.51	1.44
						ALRG = 2						
Calibration	54.25	50.28	47.36	84.93	87.26	88.42	72.06	76	78.7	-0.24	1.32	2.37
Cross-validation	62.71	58.74	53.72	86.07	87.59	89.77	72.94	76.26	80.15	0.89	4.46	5.86
Verification	76.92	70.82	65.99	78.71	82.43	85.02	61.39	67.27	71.58	-0.45	0.69	1.31
						ALRG = 5						
Calibration	54.22	49.23	46.22	84.99	87.89	89.41	72.09	76.99	79.72	0.01	2.09	3.34
Cross-validation	62.7	56.75	52.82	86.19	88.57	90.13	72.95	77.84	80.8	1.04	5.34	6.63
Verification	76.96	69.19	66.1	78.76	83.42	84.92	61.36	68.77	71.5	-0.35	1.23	1.82
						ALRG = 10						
Calibration	54.23	48.56	45.46	84.99	88.27	89.8	72.08	77.61	80.38	0.39	3.37	4.18
Cross-validation	62.7	55.55	52.28	86.19	89.14	90.35	72.95	78.77	81.19	1.4	6.52	7.32
Verification	76.98	68.66	65.89	78.74	83.6	84.97	61.33	69.23	71.67	0	2.49	2.89

Note: * indicates the number of neurons in functional layer.

Table 7.6: Performance of (4-4-1), (4-16-1), and (4-32-1) dynamic RBFANN model. ALR = 20, ALRG = 0.5, and No. of iterations = 100 to 10000 for Ramganga watershed

Period	RMSE			CC			CE			EV		
	4*	16*	32*	4*	16*	32*	4*	16*	32*	4*	16*	32*
ITERATION = 100												
Calibration	56.2	56	55.63	83.77	83.8	84.04	70.1	70.23	70.62	-1.76	-1.08	-1.06
Cross-validation	63.77	65.24	65.23	85.07	84.57	84.42	72.1	70.72	70.72	1.78	2.83	1.89
Verification	77.64	70.34	79.52	77.95	76.96	76.76	60.67	58.92	58.74	0.33	0.28	0.24
ITERATION = 500												
Calibration	55.28	53.49	52.16	84.28	85.35	86.14	70.98	72.84	74.17	-0.9	0.02	0.65
Cross-validation	63.1	62.71	59.65	85.5	85.64	87.07	72.6	72.94	75.51	1.21	2.2	2.39
Verification	77.24	75.96	73.07	78.25	79.13	80.86	61.1	62.35	65.16	-0.18	0.06	0.15
ITERATION = 1000												
Calibration	54.77	52.44	50.27	84.57	85.96	87.19	71.52	73.89	76.01	-0.61	0.25	1.31
Cross-validation	62.85	61.51	56.95	85.71	86.18	88.34	72.82	73.97	77.68	1.13	2.81	4.35
Verification	77.1	74.15	69.75	78.42	80.27	82.85	61.25	64.13	68.25	-0.21	0.17	1.27
ITERATION = 2000												
Calibration	54.42	51.33	48.5	84.79	86.26	88.18	71.89	74.99	77.66	-0.44	0.67	1.67
Cross-validation	62.74	60.16	54.77	85.89	86.85	89.33	72.91	78.1	79.36	0.93	3.61	5.01
Verification	76.95	72.35	67.19	78.58	81.42	84.36	61.36	65.85	70.54	-0.38	0.38	1.15
ITERATION = 5000												
Calibration	54.25	50.03	47.07	84.95	87.42	88.96	72.1	76.24	78.97	-0.34	0.9	1.41
Cross-validation	62.72	58.23	53.38	86.11	87.84	89.86	72.93	76.67	80.39	0.76	4.12	4.95
Verification	76.94	70.43	65.97	78.72	82.7	85.03	61.37	67.63	78.6	-0.59	0.22	0.29
ITERATION = 7500												
Calibration	54.24	49.59	46.54	84.98	87.69	89.23	72.1	76.65	79.44	-0.33	0.83	1.28
Cross-validation	62.72	57.31	52.93	86.17	88.28	90.02	72.93	77.4	80.72	0.73	4.13	4.77
Verification	76.96	69.69	66.07	78.75	83.16	84.96	61.35	68.31	71.51	-0.64	0.08	-0.01
ITERATION = 10000												
Calibration	54.24	49.31	46.17	84.98	87.84	89.4	72.1	76.91	79.96	-0.33	0.77	1.19
Cross-validation	62.71	56.69	82.63	86.19	88.57	90.13	72.94	77.88	80.94	0.72	4.11	4.61
Verification	76.97	69.24	66.16	78.75	83.4	84.89	61.34	68.71	71.14	-0.66	0.01	-0.19

Note: * indicates the number of neurons in functional layer

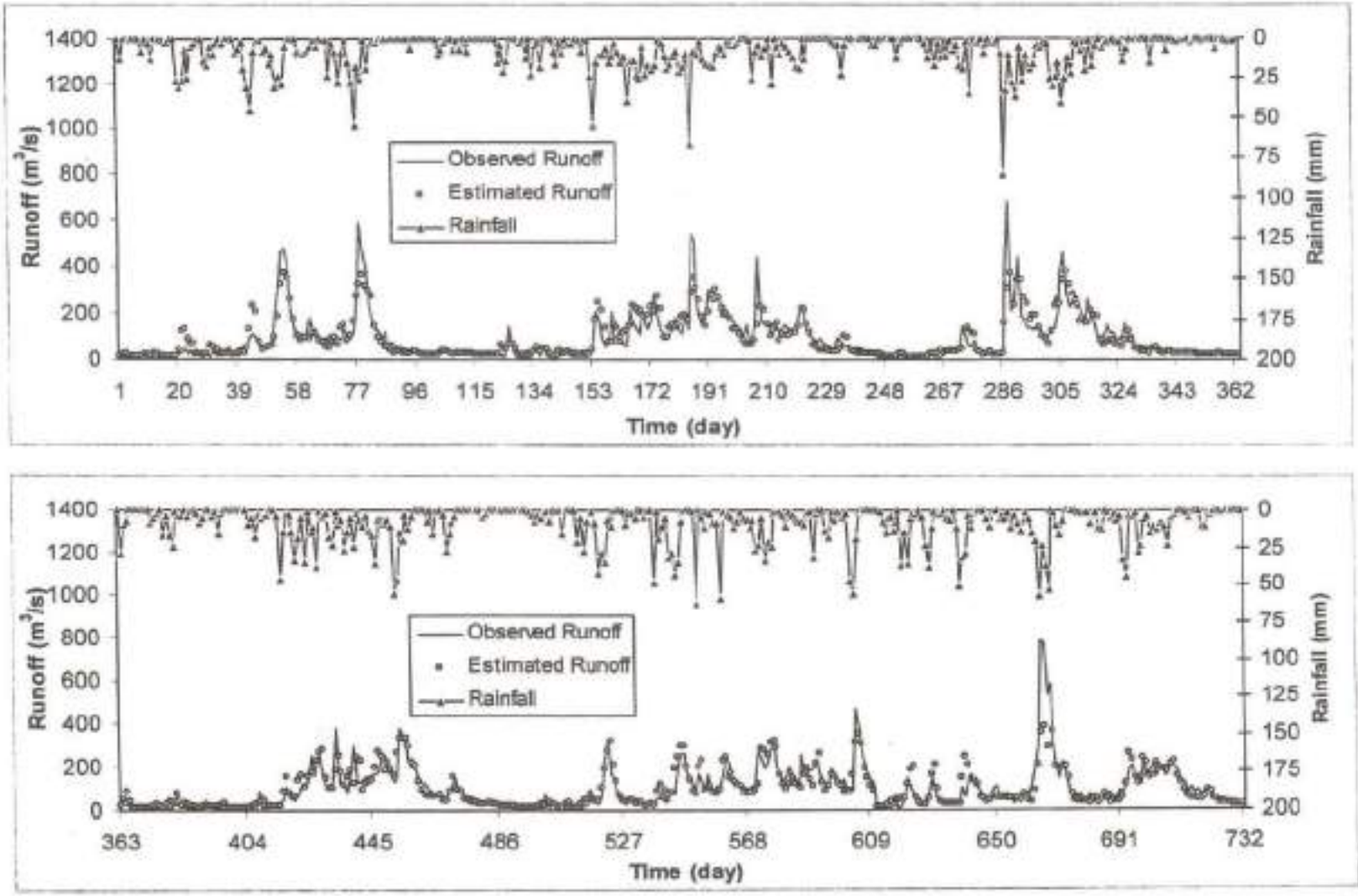

Figure 7.5: Observed and estimated runoff by dynamic RBFANN model during the period of calibration (1979-1984) for (4-4-1) network with ALR as 20 and ALRG as 0.5 for Ramganga watershed

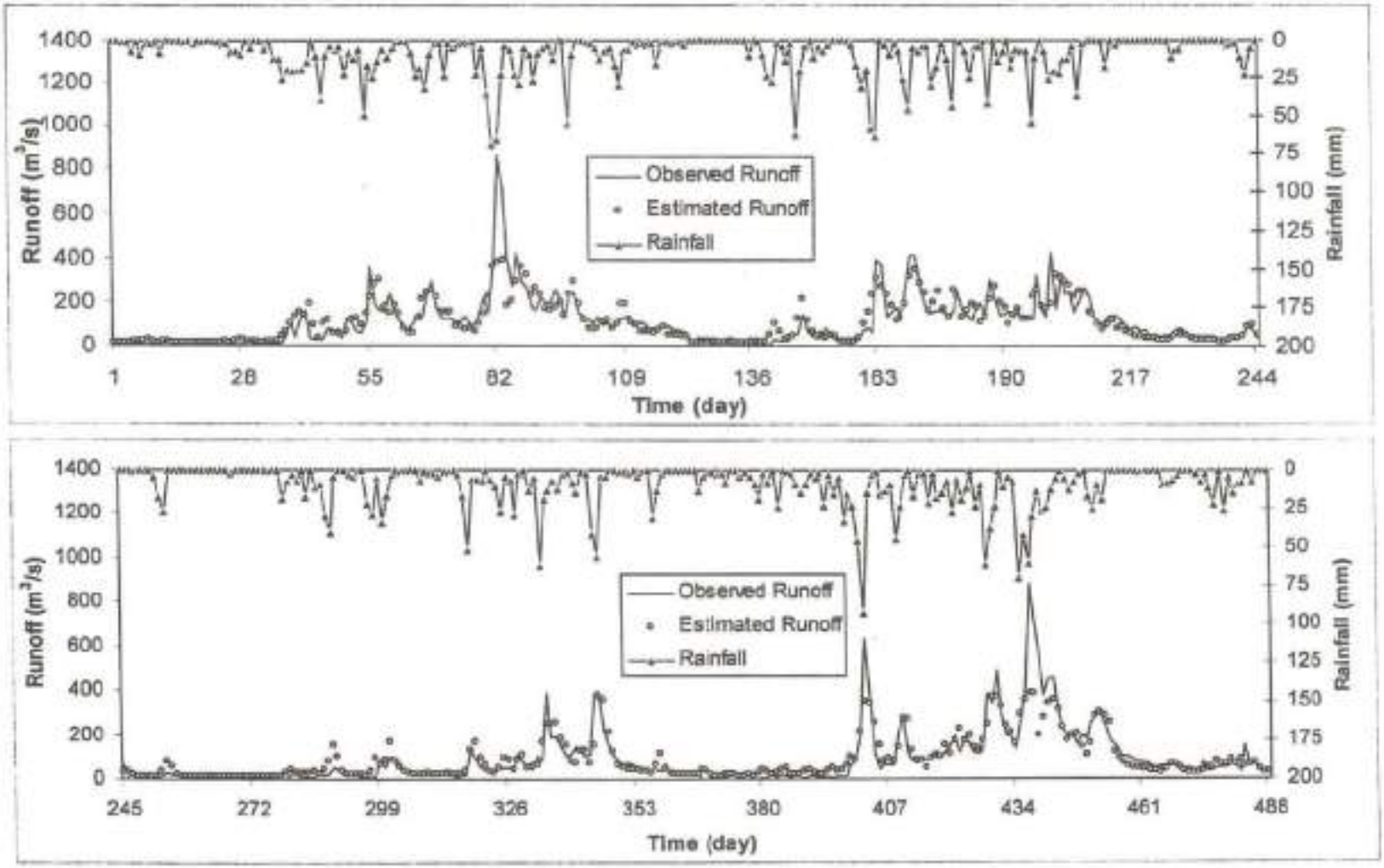

Figure 7.6: Observed and estimated runoff by dynamic RBFANN model during the period of cross-validation (1985-1988) for (4-4-1) network with ALR as 20 and ALRG as 0.5 for Ramganga watershed

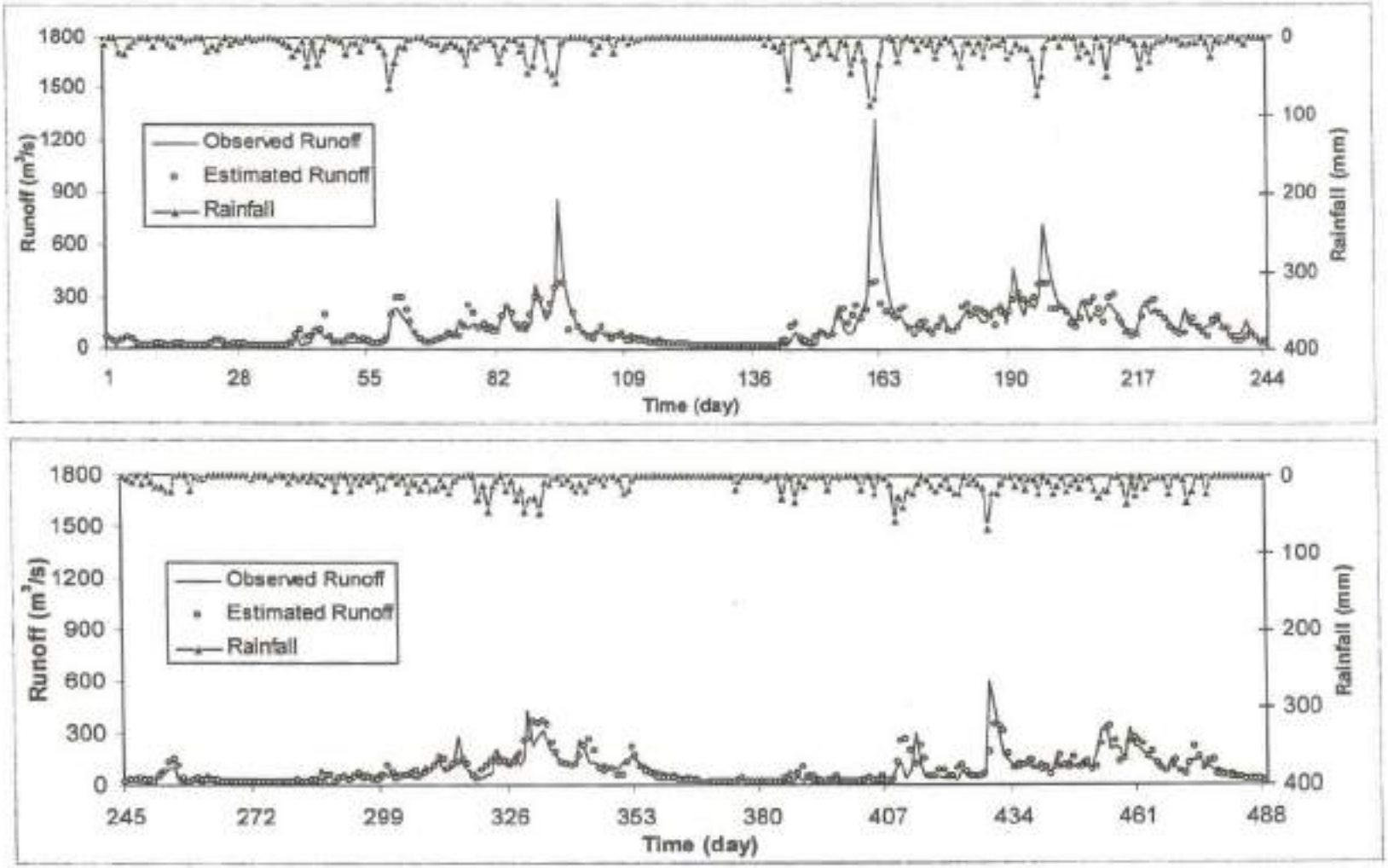

Figure 7.7: Observed and estimated runoff by dynamic RBFANN model during the period of verification (1989-1992) for (4-4-1) network with ALR as 20 and ALRG as 0.5 for Ramganga watershed

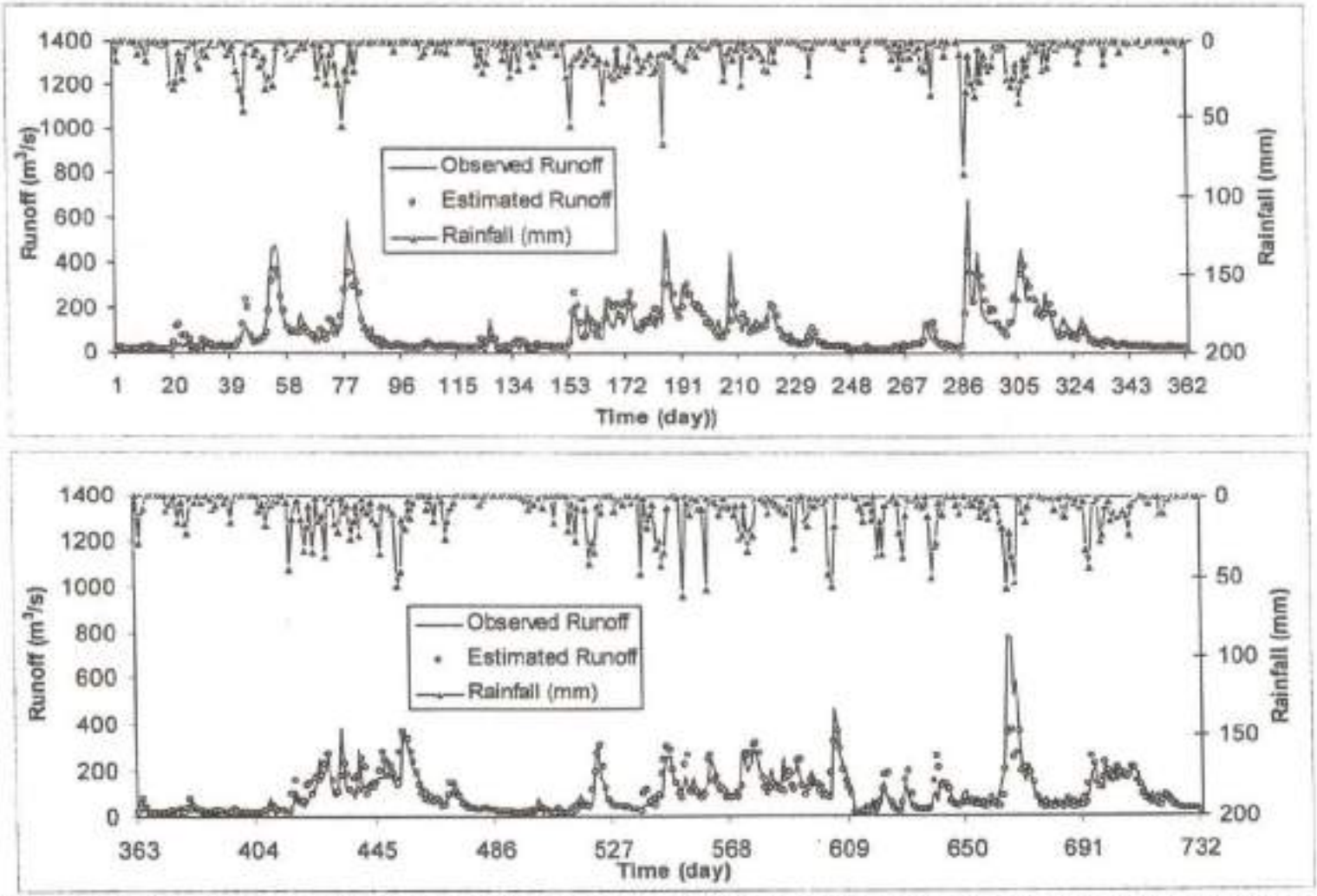

Figure 7.8: Observed and estimated runoff by dynamic RBFANN model during the period of calibration (1979-1984) for (4-16-1) network with ALR as 20 and ALRG as 0.5 for Ramganga watershed

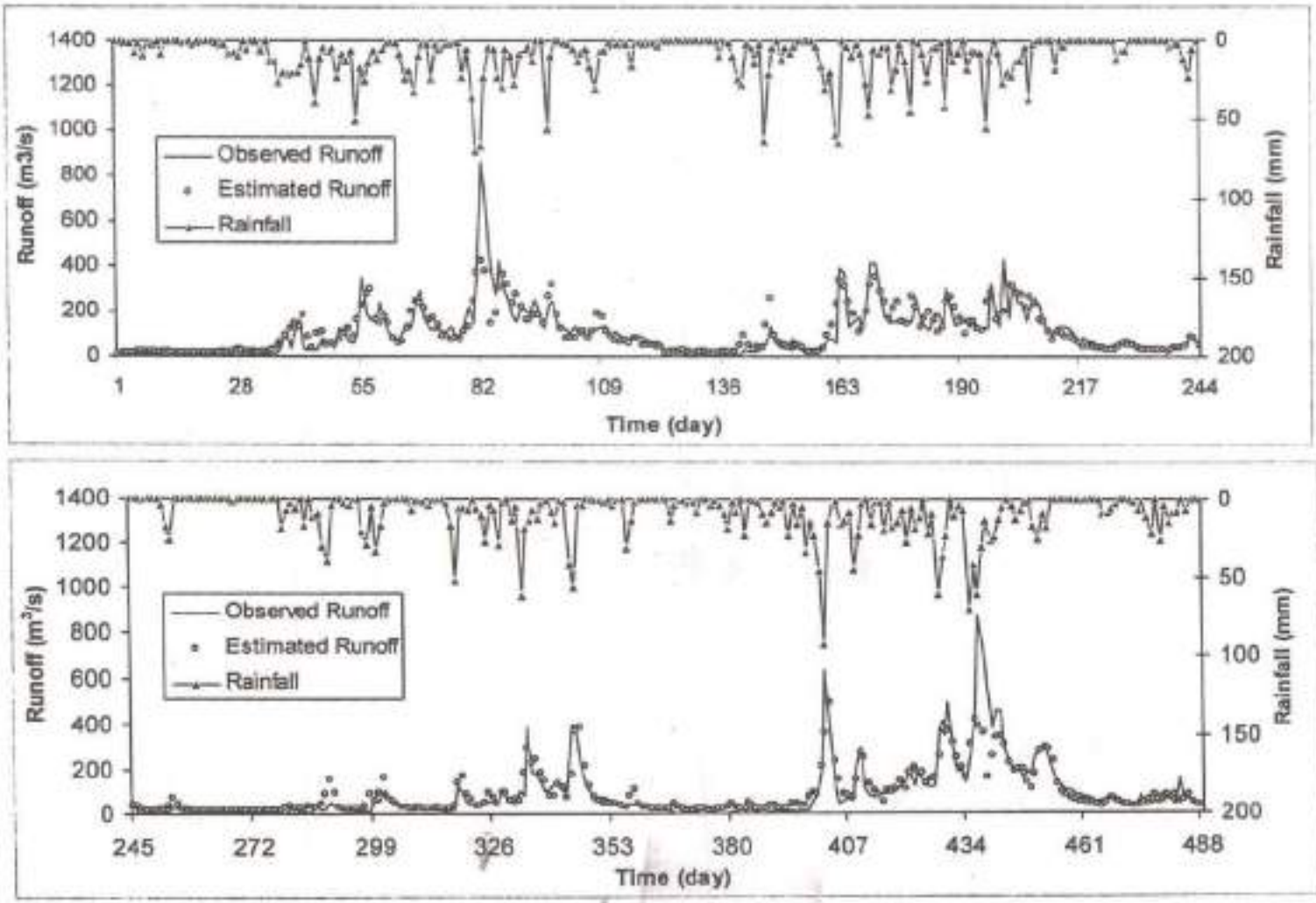

Figure 7.9: Observed and estimated runoff by dynamic RBFANN model during the period of cross-validation (1985-1988) for (4-16-1) network with ALR as 20 and ALRG as 0.5 for Ramganga watershed

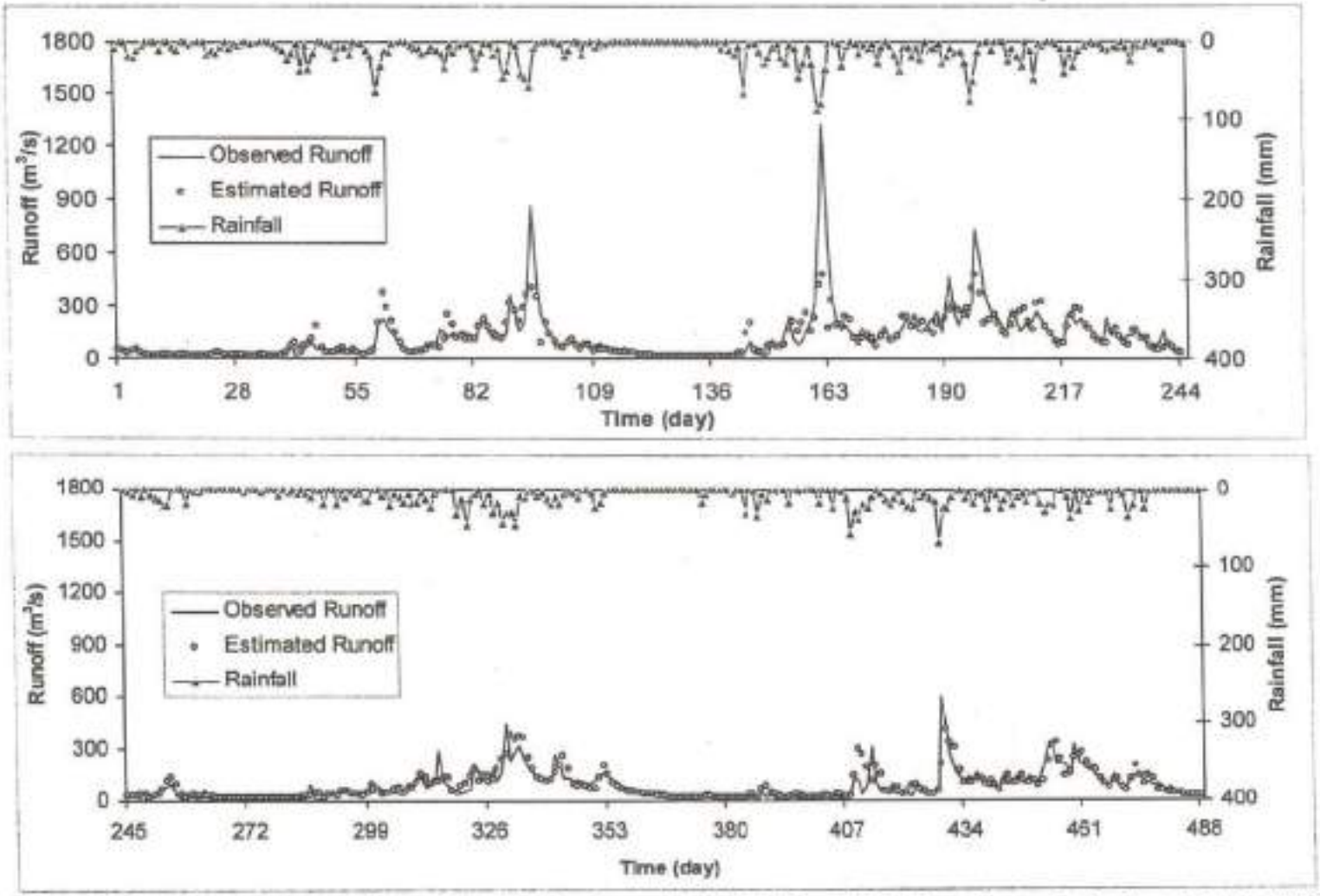

Figure 7.10: Observed and estimated runoff by dynamic RBFANN model during the period of verification (1989-1992) for (4-16-1) network with ALR as 20 and ALRG as 0.5 for Ramganga watershed

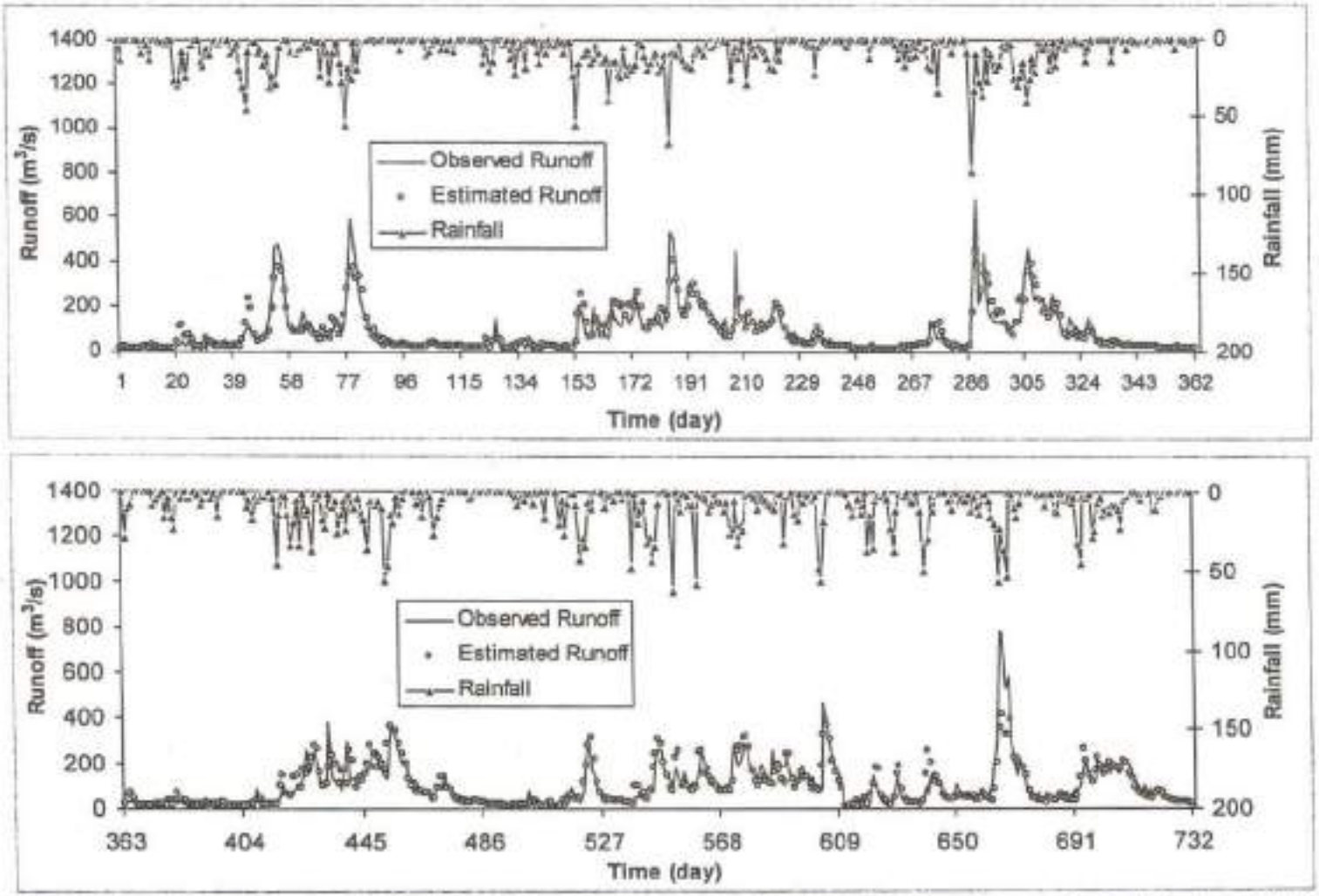

Figure 7.11: Observed and estimated runoff by dynamic RBFANN model during the period of calibration (1979-1984) for (4-32-1) network with ALR as 20 and ALRG as 0.5 for Ramganga watershed

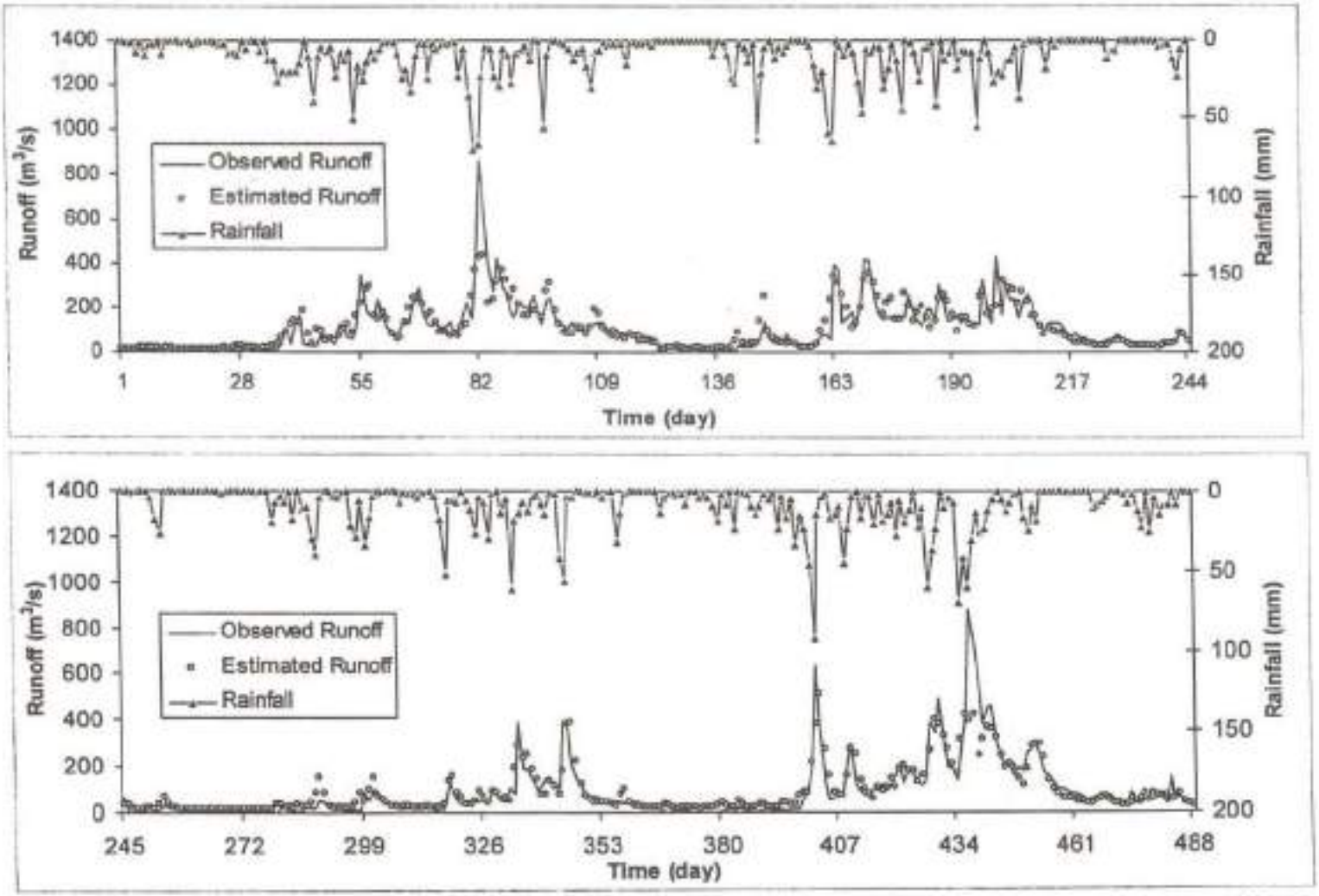

Figure 7.12: Observed and estimated runoff by dynamic RBFANN model during the period of cross-validation (1985-1988) for (4-32-1) network with ALR as 20 and ALRG as 0.5 for Ramganga watershed

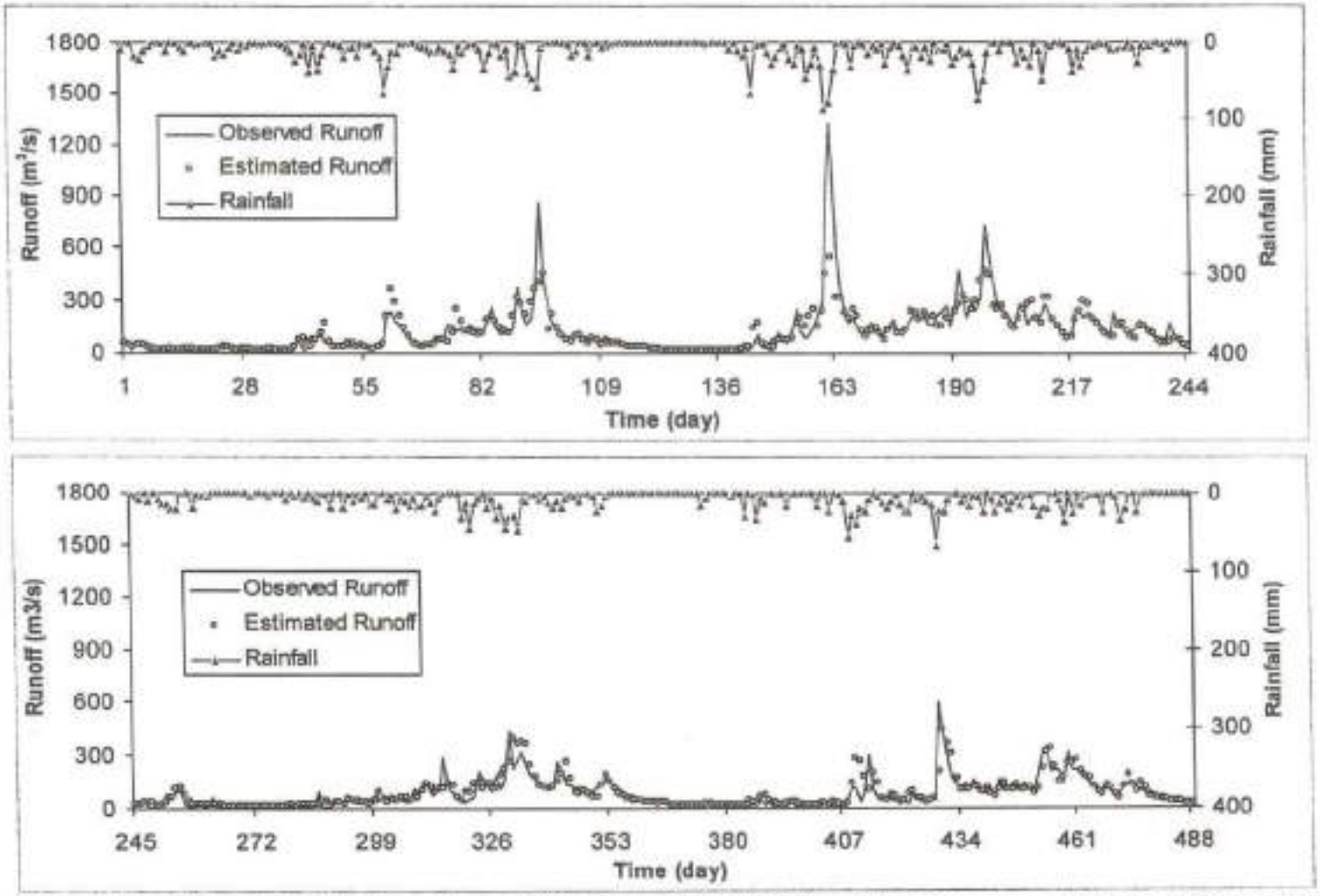

Figure 7.13: Observed and estimated runoff by dynamic RBFANN model during the period of verification (1989-1992) for (4-32-1) network with ALR as 20 and ALRG as 0.5 for Ramganga watershed

7.9.2.2 Naula Watershed

The model performance for different ALR values and three different networks for fixed ALRG (= 0.5) and iterations (= 1000) was evaluated and the results are presented in Table 7.7. The model performance improves rapidly when ALR increases from 0.5 to 20 in calibration, cross-validation, and verification for network (4-4-1). The volumetric error increases as ALR deviates from 20 either higher side or lower side. Thus, ALR = 20 is suitable for network (4-4-1). From Table 7.7, it is seen that the values of CC and CE decrease and RMSE increases as ALR increases beyond 20 in calibration and cross-validation for network (4-16-1). The volumetric errors are quite lower with ALR = 20 than those with ALR different from 20, and therefore, the model performed best at ALR = 20 simulations. For network (4-32-1), efficiencies tend to decrease as ALR deviates from 20 in calibration, cross-validation, and verification. Low value of volumetric error in calibration and cross-validation suggests ALR = 20 for simulation. Highest coefficient of efficiency (CE) is achieved by the network (4-32-1) at ALR = 20 and its values are 86.28%, 84.91%, and 86.81%, in calibration, cross-validation, and verification, respectively. As expected, the model performance is quite poor for ALR values of 0.5 and 5.0, as seen from Table 7.7. Thus, ALR = 20 is adaptable for networks varying from 5-4-1 to 5-32-1 for Naula watershed.

After fixing ALR at 20, learning rate (ALRG) in the output layer was assigned. To this end, different values of ALRG varying from 0.5 to 10 were tried and the results are provided in Table 7.8 for networks 5-4-1, 5-16-1, and 5-32-1. As seen from the table, the model performance is not distinguishable for ALRG ranging from 0.5 to 10 resulting in no significant change in the values of RMSE, CC, and CE. The error in volume however fluctuates with ALRG variation. A lower value of ALRG may be selected (i.e. 0.5) for lower network (i.e. 4-4-1). Notably, selection of a higher value is not preferable if similar model performance can be achieved using the lower value. Therefore, ALRG = 0.5 is suitable for network 5-4-1. Similarly, RMSE, CC, and CE do not change significantly with ALRG varying from 0.5 to 10 for network (4-16-1) (Table 7.8).

The resulting EV however fluctuates with ALRG variation and it considerably increases specially in cross-validation when ALRG is varied from 2 to 10. Therefore, ALRG should lie in the range of 0.5 to 2. It is seen from Table 7.5 that RMSE, CC, and CE values are almost the same for different ALRG values ranging from 0.5 to 10. But at the same time, error in volume gradually increases with increase in ALRG form 0.5 to 10. It follows that ALRG equal to 0.5 is most suitable for network 4-32-1. On the whole, ALRG as 0.5 is the most appropriate value for the range of networks studied.

Fixing ALR = 20 and ALRG = 0.5, the initial selection of the number of iterations is rechecked. To fix the optimum value, the number of iterations in different runs for three networks (5-4-1, 5-16-1, and 5-32-1) were varied from lower (100) to higher (10000) values, and the results are given in Table 7.9. It is seen from the table that CC, and CE values are considerably increases while RMSE decreases up to 1000 number of iterations for network (4-4-1) during calibration, cross-validation, and verification. However, the results are inconclusive as EV fluctuates with increase in number of iterations beyond 100. Therefore, RMSE, CC, and CE suggest 1000 no. of iterations to be suitable for network (4-4-1). The model efficiency due to network (4-16-1) significantly increases up to first 500 iterations, gradually increases up to 1000 iterations, and finally becomes almost stable after 1000 iterations (Table 7.9). The minimum volumetric error occurs around 500 iterations in calibration and cross-validation. In other words, the model performed best around 500 iterations. The performance of network (4-32-1) improves up to 500 iterations, and no further improvement is seen with increasing iterations. EV reduces up to 500 iterations and thereafter it vibrates. Thus, the number of iteration required for optimal results for network 5-4-1 is about 1000, and the number for networks 5-16-1 and 5-32-1 is about 500. It can be inferred that, in general, the number of iterations decreases as the network changes to 5-16-1 or 5-32-1 from 5-4-1.

In all RBFANN structures, ALR = 20. The lower network structure is independent of the ALRG variation from 0.5 to 10. Notably, the higher values of ALRG with higher network resulted in higher volumetric error, and therefore, not suitable for best results. Thus, the value of ALRG is fixed to 0.5 in order to suite all network structures. The maximum number of iterations required for lower networks is 1000, and it reduces to 500 with increase in network structure. The observed and estimated values of

runoff in calibration, cross-validation, and verification for networks (4-4-1), (4-16-1), and (4-32-1) with ALR = 20 and ALRG = 0.5 are shown in Figures 7.14 to 7.22. It is seen that the daily runoff pattern is well simulated by RBFANN model in calibration, cross-validation, and verification as well. The peak flows are underestimated by all networks in calibration, but simulated well in both cross-validation and verification.

Table 7.7: Performance of (4-4-1), (4-16-1), and (4-32-1) dynamic RBFANN models. ALRG = 0.5, No. of iterations = 1000. ALR = 0.5 to 25 for Naula watershed

Period	RMSE			CC			CE			EV		
	4	16	32	4	16	32	4	16	32	4	16	32
						ALR = 0.5						
Calibration	156.57	154.12	153.06	56.27	57.08	57.44	-558.8	-538.4	-529.6	182.3	175.4	172.7
Cross-validation	162.57	159.88	158.82	61.08	61.97	62.28	-1168	-1126.3	-1110.1	236.7	227.8	224.1
Verification	154.18	151.46	150.37	56.21	56.95	57.21	-793.6	-762.3	-750	215.4	206.5	202.7
						ALR = 5						
Calibration	51.28	50.87	50.95	78.56	78.55	78.73	29.32	30.44	30.22	-8.52	-10.85	-10.27
Cross-validation	44.86	44.45	44.58	79.83	79.57	79.78	3.44	5.23	4.66	-13.19	-15.76	-15.31
Verification	44.06	43.89	43.87	81.3	81.17	81.42	27.04	27.58	27.65	-20.7	-22.79	-22.43
						ALR = 10						
Calibration	38.39	30.86	27.29	83.36	86.35	89.07	60.39	74.4	79.24	-1.23	3.92	2.81
Cross-validation	31.08	21.18	20.25	85.19	89.67	90.62	53.66	78.47	80.34	-1.65	8.76	7.47
Verification	31.96	22.34	21.08	86.21	90.38	91.39	61.61	81.24	83.29	-6.74	5.66	4.09
						ALR = 15						
Calibration	30.99	27.74	23.61	87.24	89.11	92.25	74.19	79.31	85.02	-0.94	2.95	2.47
Cross-validation	23.52	19.96	18.58	89.04	90.91	91.99	73.47	80.89	83.44	0.08	7.02	6.27
Verification	24.44	20.95	19.76	90.13	91.6	92.76	77.55	83.49	85.32	-3.43	4.18	5.97
						ALR = 20						
Calibration	29.5	25.77	22.59	87.99	90.77	92.92	76.61	82.16	86.28	-0.31	-0.68	1.61
Cross-validation	21.83	19.37	17.74	89.52	91.79	92.44	77.14	81.99	84.91	1.33	2.61	5.18
Verification	22.92	20.92	18.73	90.67	91.82	93.5	80.25	83.55	86.81	-1.06	-1.29	6.35
						ALR = 25						
Calibration	29.07	26.29	23.01	88.03	90.35	92.66	77.29	81.43	85.77	3.83	3.98	2.52
Cross-validation	20.92	20.05	18.92	89.98	91.3	91.94	78.99	80.72	82.83	7.83	8.11	5.54
Verification	21.83	19.89	19.29	91.04	93.03	93.63	82.09	85.2	86.08	5.65	5.3	5.31

Table 7.8: Performance of (4-4-1), (4-16-1), and (4-32-1) dynamic model. ALR = 20, no. of iterations = 1000, and ALRG = 0.5 to 10 for Naula watershed

Period	RMSE			CC			CE			EV		
	4	16	32	4	16	32	4	16	32	4	16	32
						ALRG = 0.5						
Calibration	29.5	25.77	22.59	87.99	90.77	92.93	76.61	82.16	86.28	-0.31	-0.68	1.61
Cross-validation	21.83	19.37	17.74	89.52	91.79	92.44	77.14	81.99	84.91	1.33	2.61	5.18
Verification	22.92	20.92	18.73	90.67	91.82	93.5	80.25	83.55	86.81	-1.06	-1.29	6.35
						ALRG = 1						
Calibration	29.21	25.37	22.51	88.22	91.11	92.98	77.06	82.69	86.38	-0.56	-1.04	2.02
Cross-validation	21.59	19.35	17.73	89.71	91.95	92.51	77.65	82.04	84.92	0.83	2.11	5.61
Verification	22.52	20.67	18.72	90.47	92.15	93.54	80.94	83.94	86.83	-1.44	-1.63	6.65
						ALRG = 2						
Calibration	29.16	25.17	22.37	88.31	91.3	93.08	77.24	82.97	86.55	-0.63	-1.01	2.4
Cross-validation	21.5	19.48	17.68	89.78	91.95	92.63	77.82	81.79	85	0.68	2.04	6.09
Verification	22.34	20.62	18.65	91.11	92.29	93.63	81.24	84.01	86.93	-1.54	-1.53	6.9
						ALRG = 5						
Calibration	28.95	24.82	22.15	88.43	91.56	93.25	77.47	83.44	86.81	-0.16	0.25	2.72
Cross-validation	21.38	19.58	17.17	89.91	91.95	92.91	78.07	81.6	85.86	1.32	3.27	6.82
Verification	22.16	20.62	18.04	91.24	92.36	93.88	81.54	84.02	87.77	-0.92	0	6.2
						ALRG = 10						
Calibration	28.86	24.25	22.51	88.52	91.98	93.26	77.61	84.19	86.38	0.6	2.2	-1.95
Cross-validation	21.33	19.63	16.62	90.04	91.97	93.2	78.17	81.52	86.74	2.27	5.29	6.89
Verification	22.04	20.61	17.33	91.34	92.4	94.23	81.74	84.03	88.71	0	2.46	6

Table 7.9: Performance of (4-4-1), (4-16-1), and (4-32-1) dynamic RBFANN model. ALR = 20, ALRG = 0.5, and No. of iterations = 100 to 10000 for Naula watershed

Period	RMSE			CC			CE			EV		
	4	16	32	4	16	32	4	16	32	4	16	32
						ITERATION = 100						
Calibration	31.83	29.06	23.89	85.79	88.11	92.14	72.77	77.3	84.66	5.06	1.49	3.38
Cross-validation	23.65	20.97	18.43	88.18	90.14	91.98	73.17	78.91	83.7	9.86	5.06	7.75
Verification	24.64	22.62	19.67	88.99	90.31	92.81	77.19	80.76	85.45	6.36	1.42	8.07
						ITERATION = 500						
Calibration	30.03	26.44	22.7	87.6	90.24	92.87	75.77	81.21	86.15	-0.21	0.08	1.8
Cross-validation	22.32	19.67	17.85	89.12	91.44	92.34	76.09	81.43	84.72	1.63	3.48	5.41
Verification	23.58	21.37	18.86	90.19	91.38	93.4	79.1	82.84	86.62	-0.87	-0.44	6.62
						ITERATION = 1000						
Calibration	29.5	25.77	22.59	87.99	90.77	92.93	76.61	82.16	86.28	-0.31	-0.68	1.61
Cross-validation	21.83	19.37	17.74	89.52	91.79	92.44	77.14	81.99	84.91	1.33	2.61	5.18
Verification	22.92	20.92	18.73	90.67	91.82	93.5	80.25	83.55	86.81	-1.06	-1.29	6.35
						ITERATION = 2000						
Calibration	29.22	25.38	22.48	88.2	91.1	93	77.05	82.68	86.42	-0.65	-1.2	1.55
Cross-validation	21.57	19.34	17.64	89.71	91.94	92.53	77.67	82.06	85.07	0.75	1.94	5.1
Verification	22.51	20.68	18.65	90.97	92.13	93.53	80.96	83.92	86.92	-1.53	-1.82	6.15
						ITERATION = 5000						
Calibration	29.07	25.13	22.26	88.31	91.32	93.14	77.29	83.03	86.68	-0.88	-1.41	1.49
Cross-validation	21.45	19.47	17.49	89.79	91.91	92.67	77.93	81.81	85.32	0.46	1.58	5.01
Verification	22.28	20.64	18.55.	91.12	92.26	93.59	81.34	83.98	87.07	-1.78	-1.97	5.81
						ITERATION = 7500						
Calibration	29	24.98	22.14	88.35	91.42	93.22	77.39	83.23	86.83	-0.87	-1.25	1.44
Cross-validation	21.38	19.46	17.42	89.83	91.9	92.74	78.06	81.83	85.45	0.54	1.7	4.96
Verification	22.2	20.63	18.48	91.17	92.26	93.63	81.48	84	87.17	-1.71	-1.73	5.63
						ITERATION = 10000						
Calibration	28.95	24.82	22.04	88.39	91.52	93.28	77.47	83.44	86.95	-0.85	-1.04	1.41
Cross-validation	21.33	19.43	17.36	89.87	91.89	92.79	78.17	81.89	85.54	0.62	1.89	4.91
Verification	28.45	20.61	18.41	88.39	92.26	93.67	77.47	84	87.25	-0.85	-1.44	5.5

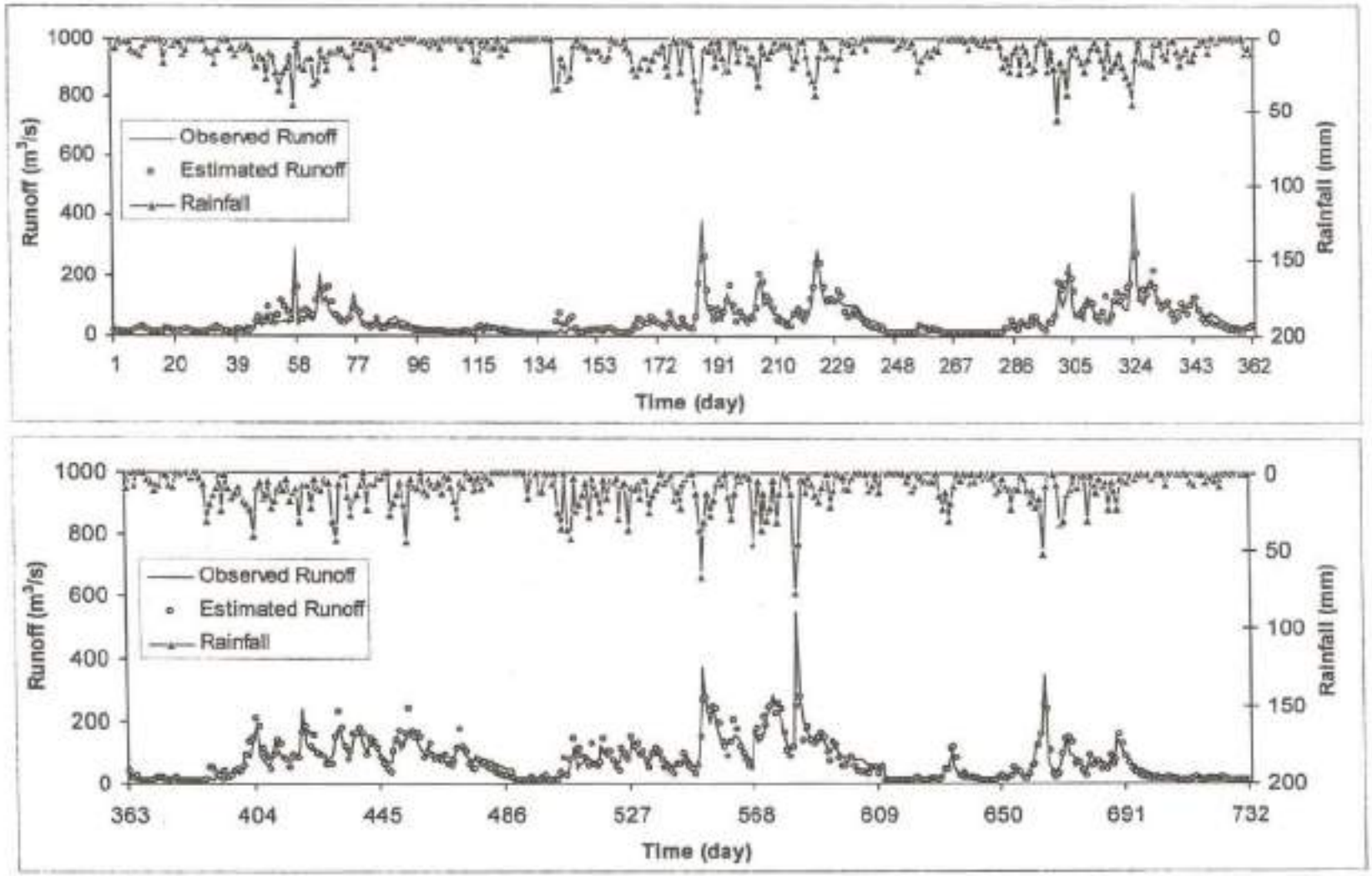

Figure 7.14: Observed and estimated runoff by dynamic RBFANN model during the period of calibration (1979-1984) for (4-4-1) network with ALR as 20 and ALRG as 0.5 for Naula watershed

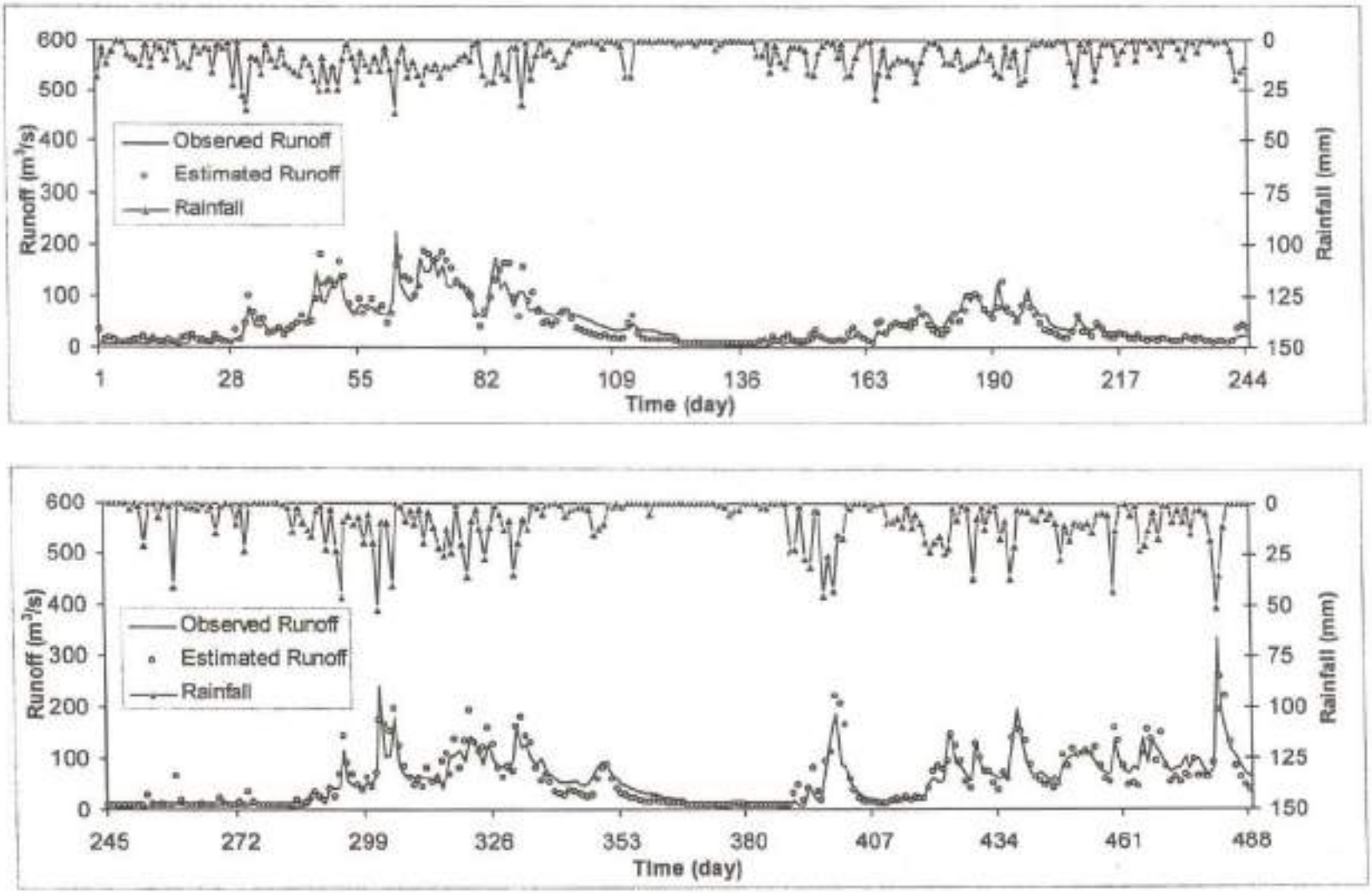

Figure 7.15: Observed and estimated runoff by dynamic RBFANN model during the period of cross-validation (1985-1988) for (4-4-1) network with ALR as 20 and ALRG as 0.5 for Naula watershed

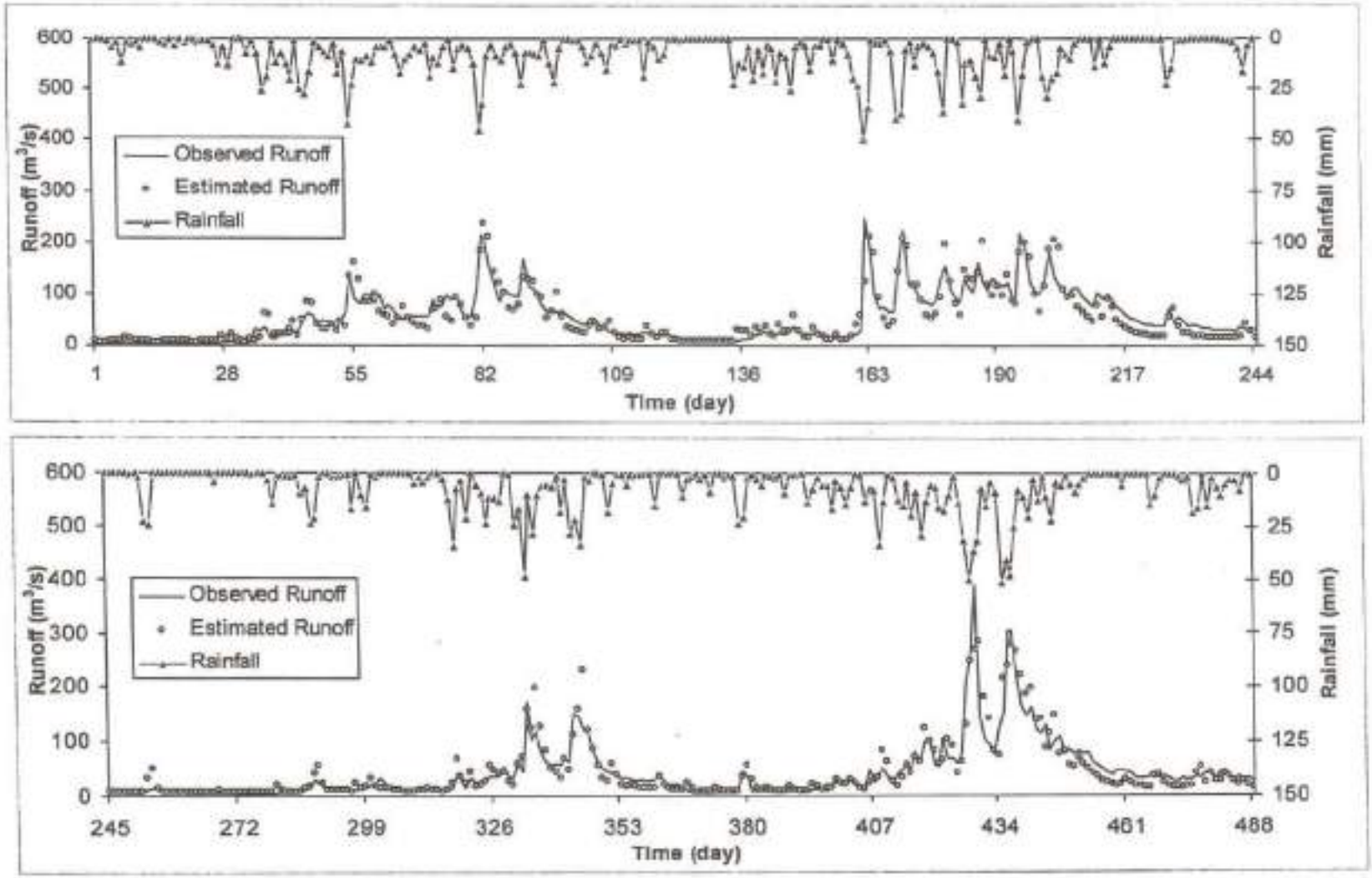

Figure 7.16: Observed and estimated runoff by dynamic RBFANN model during the period of verification (1989-1992) for (4-4-1) network with ALR as 20 and ALRG as 0.5 for Naula watershed

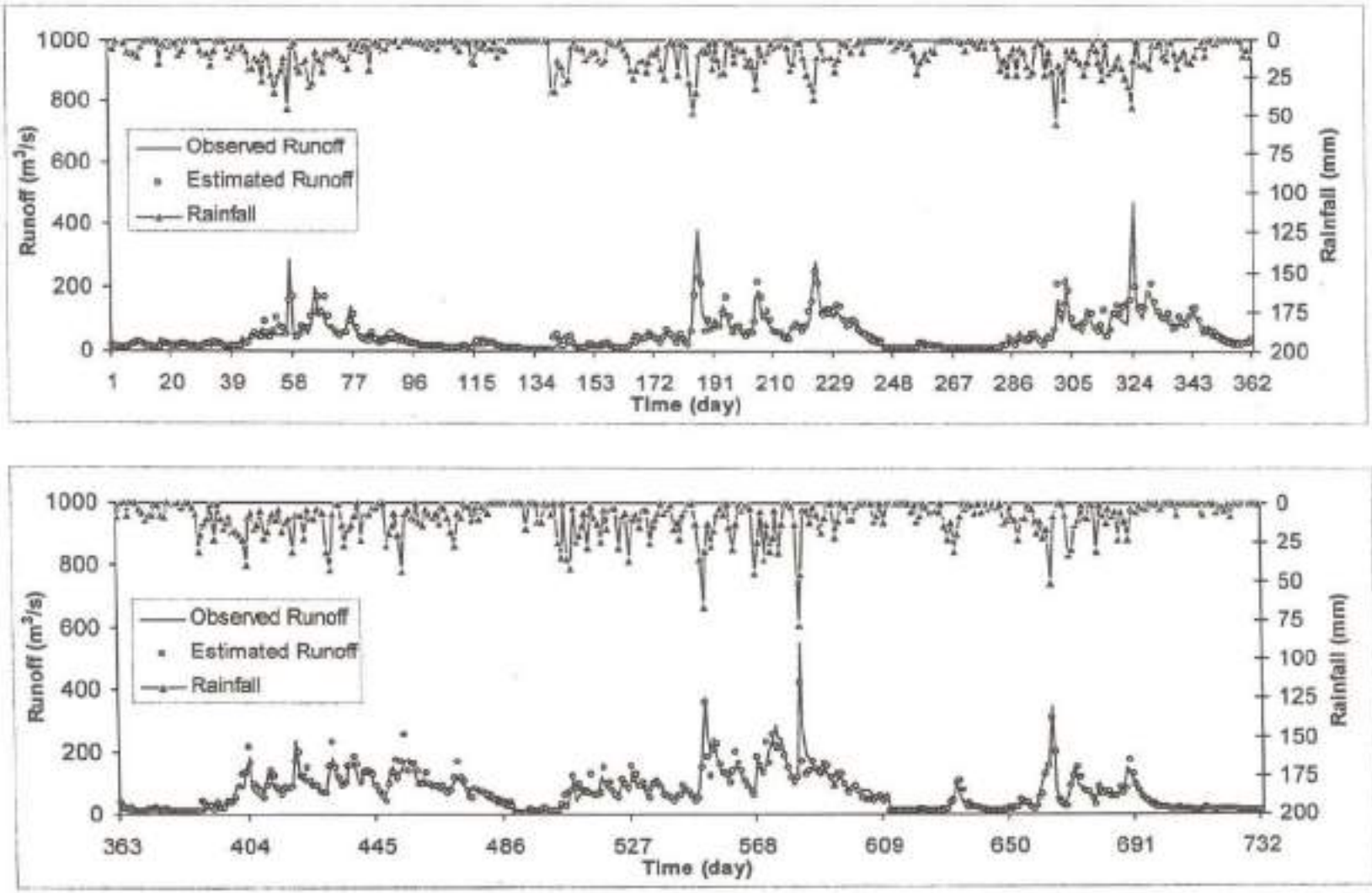

Figure 7.17: Observed and estimated runoff by dynamic RBFANN model during the period of calibration (1979-1984) for (4-16-1) network with ALR as 20 and ALRG as 0.5 for Naula watershed

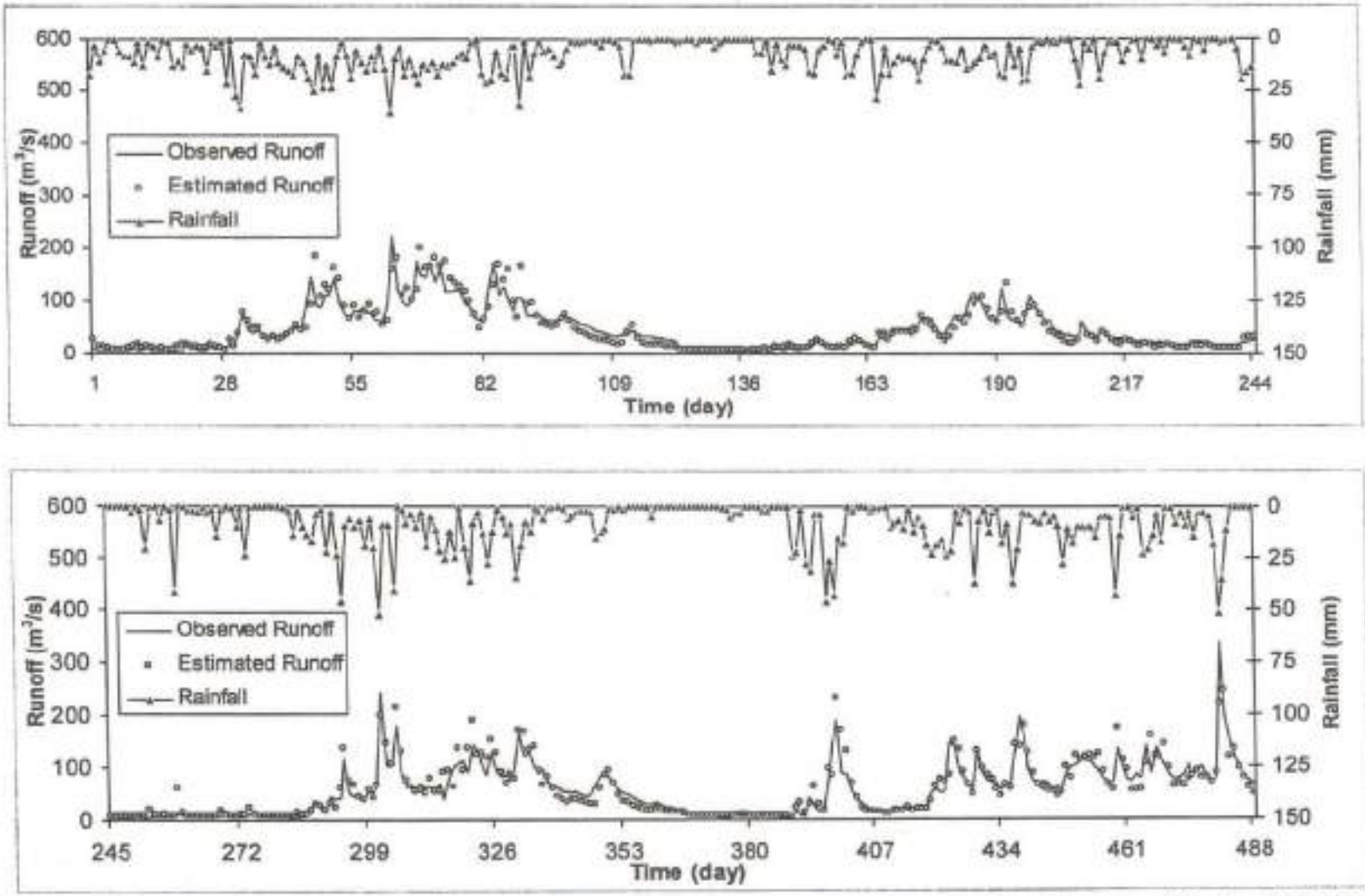

Figure 7.18: Observed and estimated runoff by dynamic RBFANN model during the period of cross-validation (1985-1988) for (4-16-1) network with ALR as 20 and ALRG as 0.5 for Naula watershed

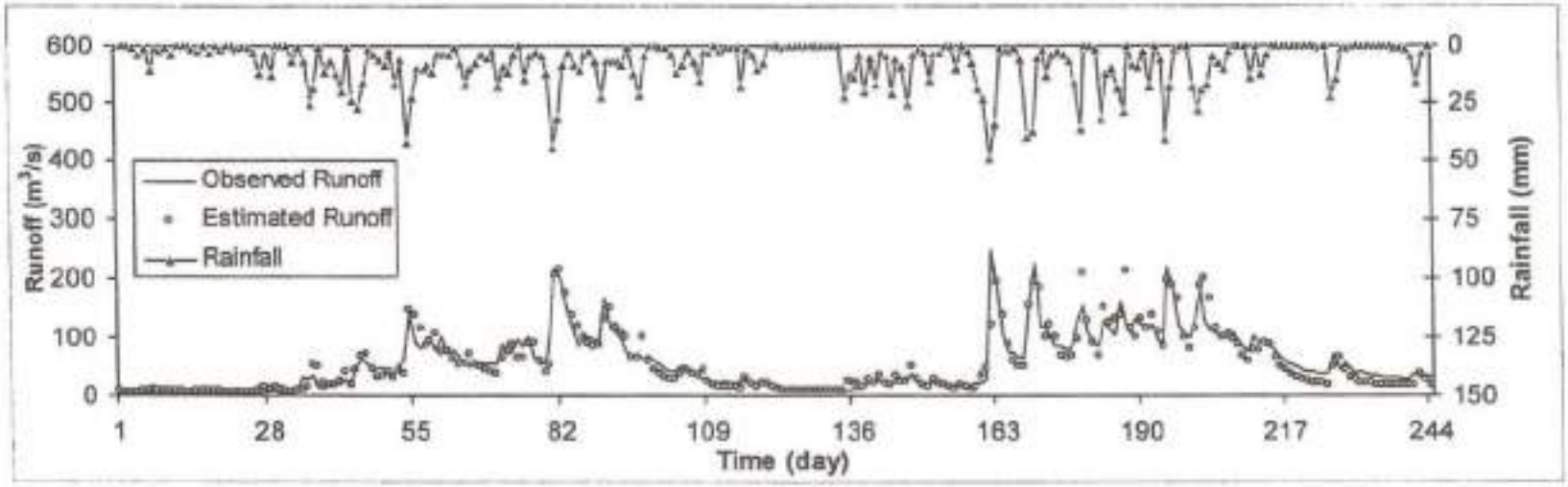

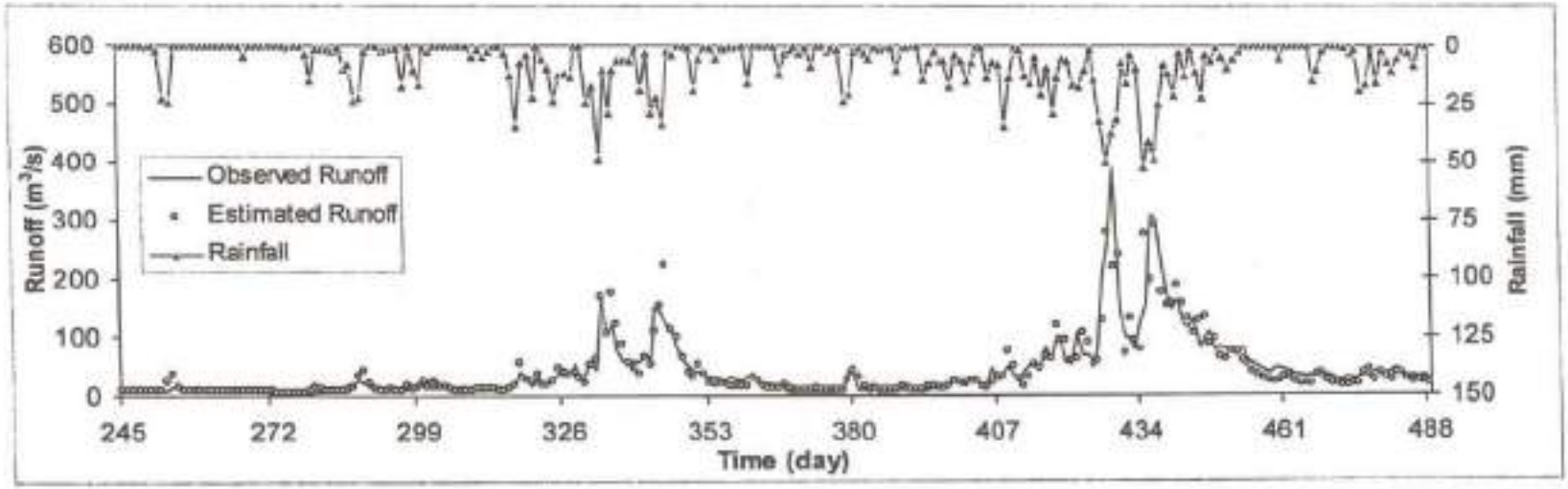

Figure 7.19: Observed and estimated runoff by dynamic RBFANN model during the period of verification (1989-1992) for (4-16-1) network with ALR as 20 and ALRG as 0.5 for Naula watershed

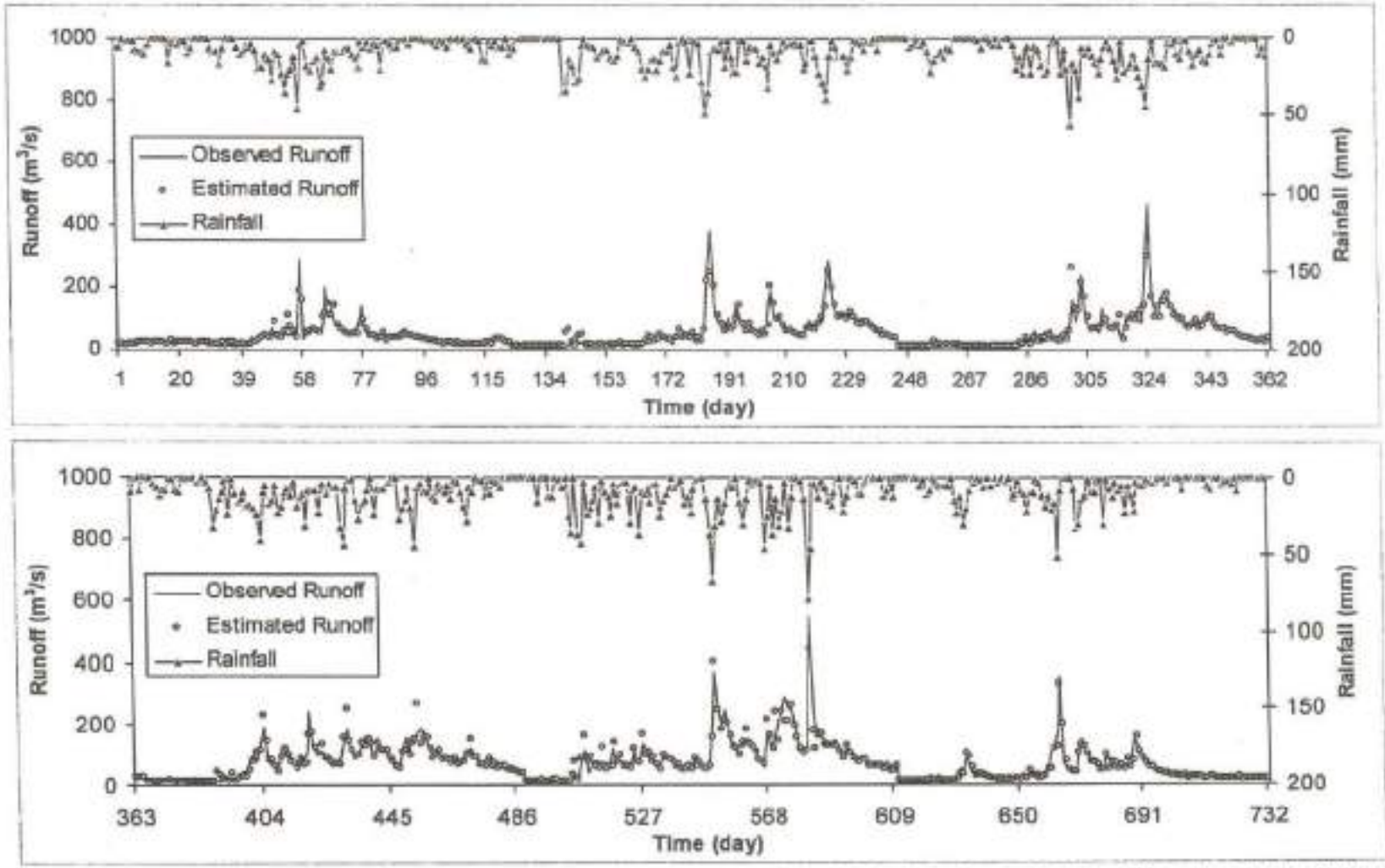

Figure 7.20: Observed and estimated runoff by dynamic RBFANN model during the period of calibration (1979-1984) for (4-32-1) network with ALR as 20 and ALRG as 0.5 for Naula watershed

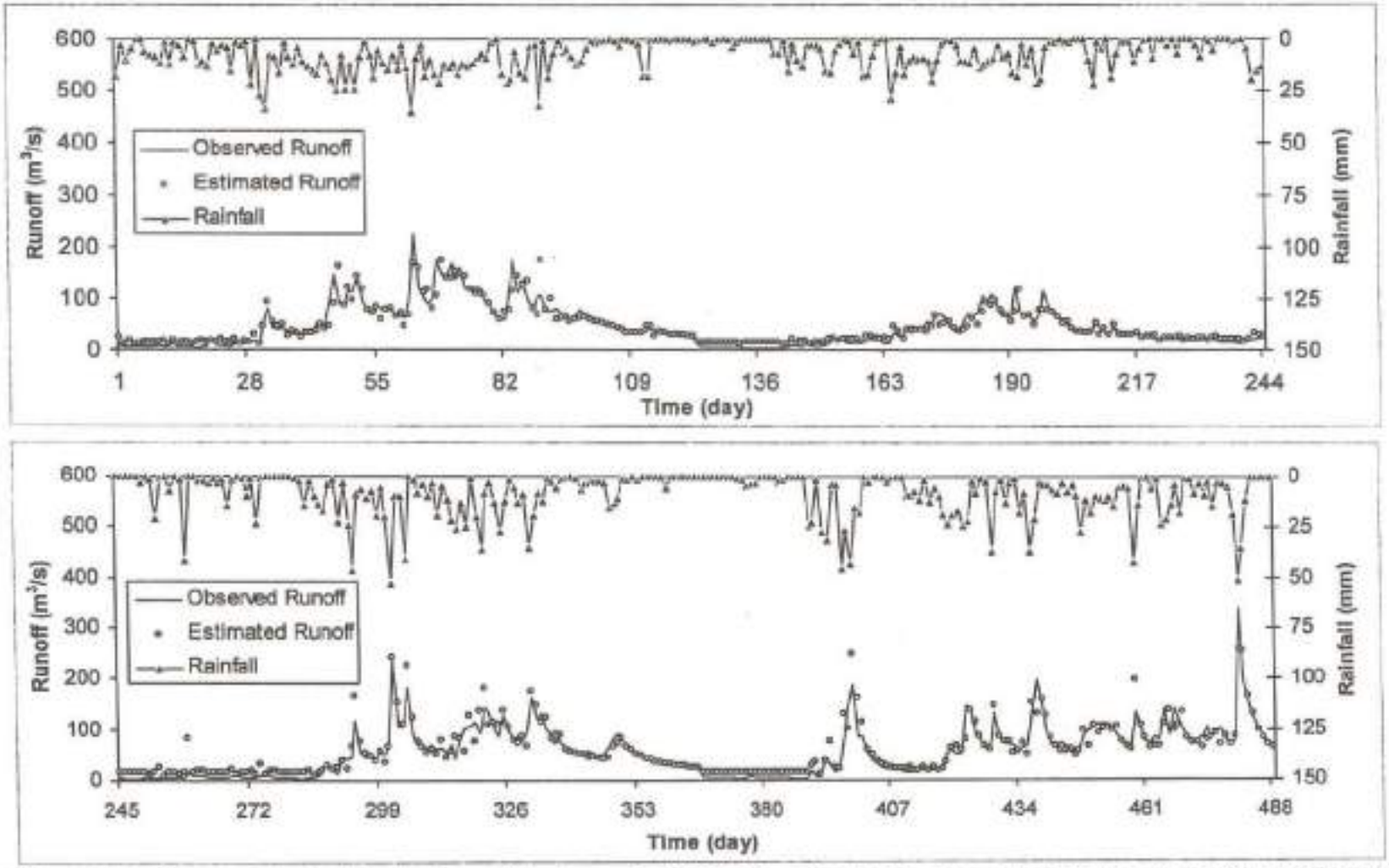

Figure 7.21: Observed and estimated runoff by dynamic RBFANN model during the period of cross-validation (1985-1988) for (4-32-1) network with ALR as 20 and ALRG as 0.5 for Naula watershed

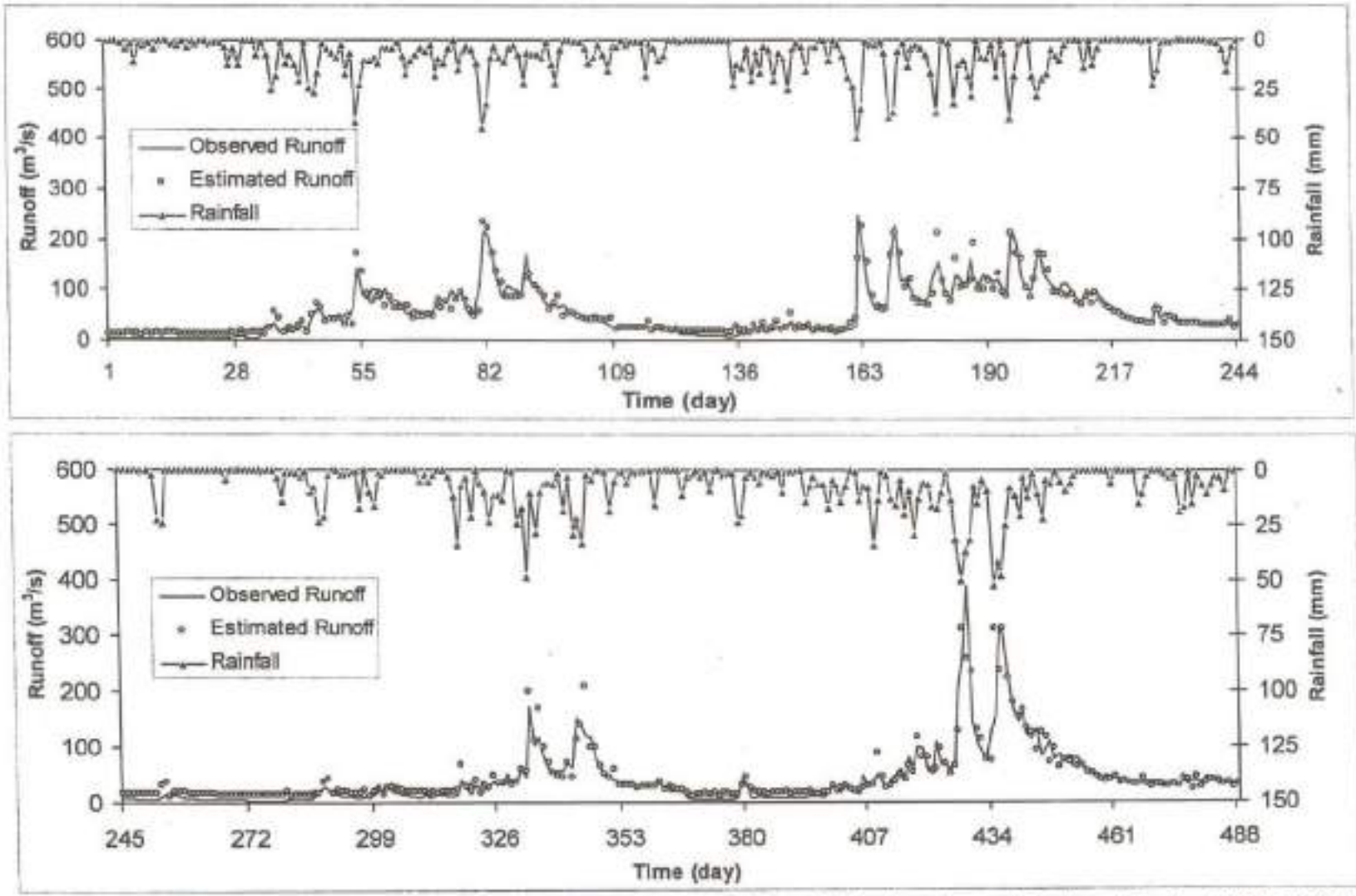

Figure 7.22: Observed and estimated runoff by dynamic RBFANN model during the period of verification (1989-1992) for (4-32-1) network with ALR as 20 and ALRG as 0.5 for Naula watershed

7.9.2.3 Chaukhutia Watershed

The model performance was evaluated for different ALR values and for three different networks with fixed ALRG (= 0.5) and iterations (= 1000) and the results are presented in Table 7.10. It is seen the performance is very poor for ALR values of 0.5 and 5. A drastic improvement in model performance is seen with ALR varying from 5 to 10, and model efficiency increases with increasing ALR. However, EV continuously increases after ALR 15 for network (4-4-1). Considering CE and EV, ALR = 15 is taken to be the most appropriate value.

For network 4-16-1, it is clear from Table 7.7 that RMSE tends to increase and CC, and CE tend to decrease rapidly after ALR = 15 in all three model testing periods. The lowest EV-value also supports that ALR = 15 is the best for network (4-16-1). However, no significant improvement in model efficiency of network 4-32-1 is visible beyond ALR = 15. The low values of EV also support the selection of ALRG as 15. Fixing ALR = 15, ALRG was identified by trials for its value ranging from 0.5 to 10 in networks 5-4-1, 5-16-1, and 5-32-1, and the results given in Table 7.11. RMSE, CC, and CE are seen to improve as ALRG varies from 0.5 to 10, and EV however increases. Thus, it is difficult to suggest a particular value for the selected networks.

In network 4-16-1, RMSE, CC, and CE values are almost constant in the entire range of ALRG selected, but EV increases with ALRG. Thus, ALRG = 0.5 may be best selection for network (4-16-1). It is also supported by network (4-32-1). Moreover, ALRG = 0.5 is suitable for all model networks studied for Chaukhutia watershed. With ALR = 20 and ALRG = 0.5, the optimum number of iterations is fixed by trial and error considering three networks (5-4-1, 5-16-1, and 5-32-1). The number of iteration is varied from 100 to 10000, and the results given in Table 7.12 for all three networks. Similar to the two watersheds discussed above, model performed the best around 5000 iterations for network (4-4-1), around 1000 iterations for (4-16-1), and around 500 iterations for network (4-32-1). This also supports that the lower network required higher number of iterations, and vice versa. Thus, for Chaukhutia watershed, ALR = 15 for all RBFANN structures. The lower network structure is independent of ALRG values ranging (0.5, 10). However, with increase in network structure, ALRG reduces to 0.5 or maximum 1.0. Notably, the higher values of ALRG in a higher network resulted in higher volumetric error. Thus, ALRG of 0.5 is most suitable for all networks. The number of iterations required for lower network

is higher (maximum 5000), and it reduces to minimum 500 with increase in network structure. The observed and estimated values of runoff for the calibration, cross-validation, and verification of networks 5-4-1, 5-16-1, and 5-32-1 with ALR = 10 and ALRG = 0.5 are shown in Figures 7.23 to 7.31.

Table 7.10: Performance of (4-4-1), (4-16-1), and (4-32-1) dynamic RBFANN models. ALRG = 0.5, No. of iterations = 1000. ALR = 0.5 to 25 for Chaukhutia watershed

Period	RMSE			CC			CE			EV		
	4	16	32	4	16	32	4	16	32	4	16	32
						ALR = 0.5						
Calibration	77.52	76.32	75.77	58.7	59.5	59.81	-728.6	-703.1	-691.7	193.7	186.1	182.6
Cross-validation	76.17	75.24	74.76	57.76	58.49	58.85	-503.7	-489.1	-481.5	173.7	169.3	167.1
Verification	75.31	74.38	73.45	56.63	57.08	57.26	-594.3	-577.3	-569.5	188.2	179.1	176.3
						ALR = 5						
Calibration	29.1	28.5	26.36	73.66	72.65	70.45	-16.78	-12.03	4.2	-3.39	-15.89	-9.58
Cross-validation	25.23	24.66	23.86	84.91	84.22	81.4	33.76	36.71	40.75	1.86	-9.71	-3.99
Verification	26.02	25.55	24.51	80.69	80.04	76.42	17.14	20.1	26.44	-5.83	-17.03	-12.36
						ALR = 10						
Calibration	15.31	14.09	13.06	82.29	85.22	87.56	67.68	72.61	76.49	1.53	0.96	0.27
Cross-validation	14.97	13.63	12.49	88.03	90.02	91.98	76.67	80.66	83.76	-0.32	-0.03	-0.48
Verification	14.61	13.03	12.27	86.1	89.1	90.64	73.87	79.23	81.56	1.01	0.39	0.17
						ALR = 15						
Calibration	16.51	13.04	12.78	84.68	87.53	88.15	62.41	76.85	77.48	1.69	0.13	-0.76
Cross-validation	14.16	12.29	12.1	91.65	92.96	92.89	79.13	84.27	84.76	1.06	-1.06	-0.77
Verification	14.28	11.52	11.22	89.78	91.79	92.49	75.04	83.75	84.59	0.12	0.09	-0.39
						ALR = 20						
Calibration	15.22	13.52	12.69	85.76	87.73	88.25	68.07	74.81	77.78	2.18	0.46	-0.61
Cross-validation	13.02	12.38	11.79	91.28	91.79	93.08	82.35	84.06	85.53	4.07	1.71	2.13
Verification	13.01	12.11	11.13	90.64	90.64	92.47	79.29	82.04	84.83	1.15	-0.44	-0.84

Table 7.11: Performance of (4-4-1), (4-16-1), and (4-32-1) dynamic model. ALR = 20, no. of iterations = 1000, and ALRG = 0.5 to 10 for Chaukhutia watershed

Period	RMSE			CC			CE			EV		
	4	16	32	4	16	32	4	16	32	4	16	32
						ALRG = 0.5						
Calibration	16.51	13.04	12.78	84.68	87.53	88.15	62.41	76.85	77.48	1.69	0.13	-1.76
Cross-validation	14.16	12.29	12.1	91.65	92.96	92.89	79.13	84.27	84.76	3.96	-1.06	-3.77
Verification	14.28	11.52	11.22	89.78	91.79	92.49	75.04	83.75	84.59	0.12	0.09	-2.39
						ALRG = 1						
Calibration	15.07	12.86	12.63	86.35	87.9	88.56	68.67	77.18	78	3.42	-1.04	-2.61
Cross-validation	13.2	12.16	12.02	92.39	92.42	93.22	81.87	84.61	84.96	5.4	-2.1	-4.65
Verification	12.76	11.31	11.09	91.43	92.09	92.87	80.08	84.33	84.94	2.45	-1	-3.06
						ALRG = 2						
Calibration	13.94	12.74	12.6	87.2	88.17	88.89	73.2	77.61	78.12	3.57	-1.56	-3.69
Cross-validation	12.24	12.02	12.25	92.75	92.71	93.43	84.42	84.98	84.38	5	-2.72	-6.04
Verification	11.5	11.18	11.21	92.36	92.34	93.11	83.81	84.7	84.62	3.45	-1.53	-4.03
						ALRG = 5						
Calibration	13.36	12.76	13.57	87.28	88.3	88.9	75.4	77.54	74.6	2.73	-2.58	-9.8
Cross-validation	11.6	12.16	14.82	92.86	92.99	92.66	85.99	84.61	77.13	3.33	-4.17	-13.71
Verification	10.88	11.26	13.21	92.6	92.58	92.44	85.52	84.47	78.62	3.37	-2.63	-10.69
						ALRG = 10						
Calibration	13.25	13.31	16.13	87.31	88.2	87.09	75.78	75.57	64.14	2.32	-6.93	-19.38
Cross-validation	11.54	13.39	19.78	92.86	93.09	88.22	86.15	81.35	59.3	2.6	-9.34	-25.91
Verification	10.83	12.17	17.53	92.59	92.68	87.82	85.63	81.86	62.4	2.91	-7.28	-22.03

Table 7.12: Performance of (4-4-1), (4-16-1), and (4-32-1) dynamic RBFANN model. ALR = 20, ALRG = 0.5, and No. of iterations = 100 to 10000 for Chaukhutia watershed

Period	RMSE			CC			CE			EV		
	4	16	32	4	16	32	4	16	32	4	16	32
						ITERATION = 100						
Calibration	19.3	14.57	13.45	81.17	84.16	86.7	48.65	70.74	75.05	4.09	2.44	-0.07
Cross validation	16.24	13.39	13.03	89.62	91.05	91.39	72.54	81.37	82.34	5.75	0.91	-1.47
Verification	17.16	13.56	12.39	86.11	88.48	90.51	63.98	77.48	81.22	1.87	2.4	-0.32
						ITERATION = 500						
Calibration	17.75	13.38	12.94	82.92	86.86	87.81	56.55	75.32	76.91	-1.13	1.21	-1.54
Cross validation	14.98	12.46	12.35	90.73	92.22	92.54	76.64	83.84	84.12	1.31	-0.1	-3.65
Verification	15.59	11.97	11.49	88.06	91.23	92.06	70.26	82.46	83.83	-2.96	1.21	-2.33
						ITERATION = 1000						
Calibration	16.51	13.04	12.78	84.68	87.53	88.15	62.41	76.55	77.48	1.69	0.13	-1.76
Cross validation	14.16	12.29	12.1	91.65	92.26	92.89	79.13	84.27	84.76	3.96	-1.06	-3.77
Verification	14.28	11.52	11.22	89.78	91.79	92.49	75.04	83.75	84.59	0.12	0.09	-2.39
						ITERATION = 2000						
Calibration	15.08	12.83	12.58	86.34	87.95	88.15	68.64	77.31	78.17	3.4	-0.44	-1.63
Cross validation	13.21	12.12	11.86	92.38	92.42	93.2	81.85	84.7	85.37	5.39	-1.65	-3.45
Verification	12.77	11.26	10.96	91.41	92.12	92.88	80.03	84.47	85.3	2.42	-0.53	-1.95
						ITERATION = 5000						
Calibration	13.69	12.61	12.35	87.3	88.38	89.01	74.16	78.07	78.98	3.45	-0.51	-1.62
Cross validation	11.99	11.85	11.6	92.8	92.8	93.46	85.05	85.38	86	4.63	-1.89	-3.27
Verification	11.25	11.02	10.73	92.46	92.48	93.18	84.51	85.13	85.92	3.55	-0.65	-1.66
						ITERATION = 7500						
Calibration	13.42	12.56	12.27	87.33	88.49	89.15	75.17	78.25	79.24	3.07	-0.55	-1.69
Cross validation	11.69	11.77	11.52	92.85	92.91	93.54	85.79	85.85	86.19	3.84	-1.94	-3.36
Verification	10.97	10.96	10.67	92.56	92.58	93.23	85.28	85.3	86.05	3.54	-0.68	-1.72
						ITERATION = 10000						
Calibration	13.33	12.53	12.22	87.3	88.55	89.25	75.49	78.35	79.42	2.79	-0.58	-1.74
Cross validation	11.6	11.72	11.47	92.85	92.68	93.61	86	85.71	86.31	3.35	-1.96	-3.49
Verification	10.9	10.92	10.65	92.56	92.64	93.26	85.46	85.41	86.11	3.4	-0.69	-1.83

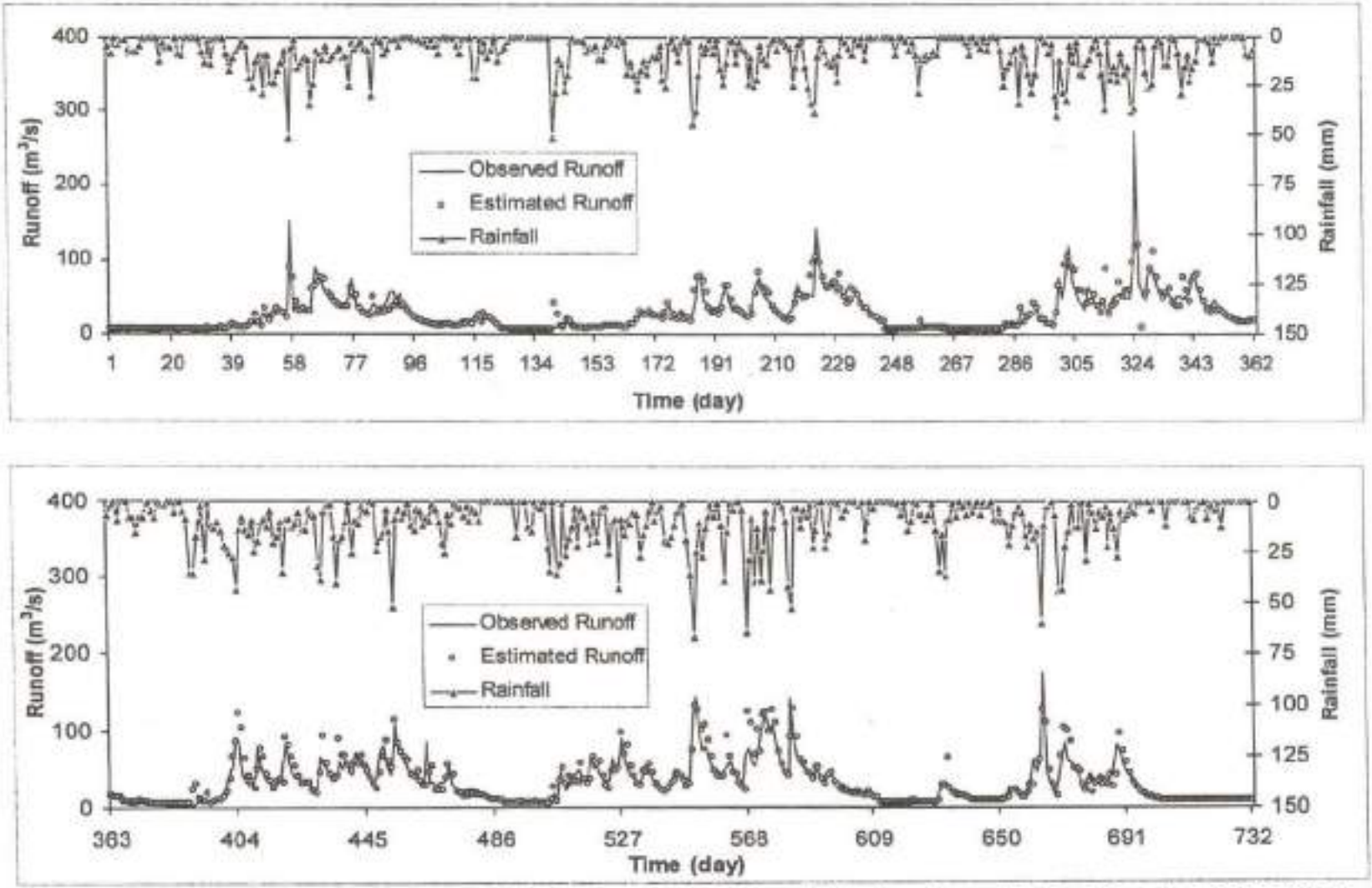

Figure 7.23: Observed and estimated runoff by dynamic RBFANN model during the period of calibration (1979-1984) for (4-4-1) network with ALR as 20 and ALRG as 0.5 for Chaukhutia watershed

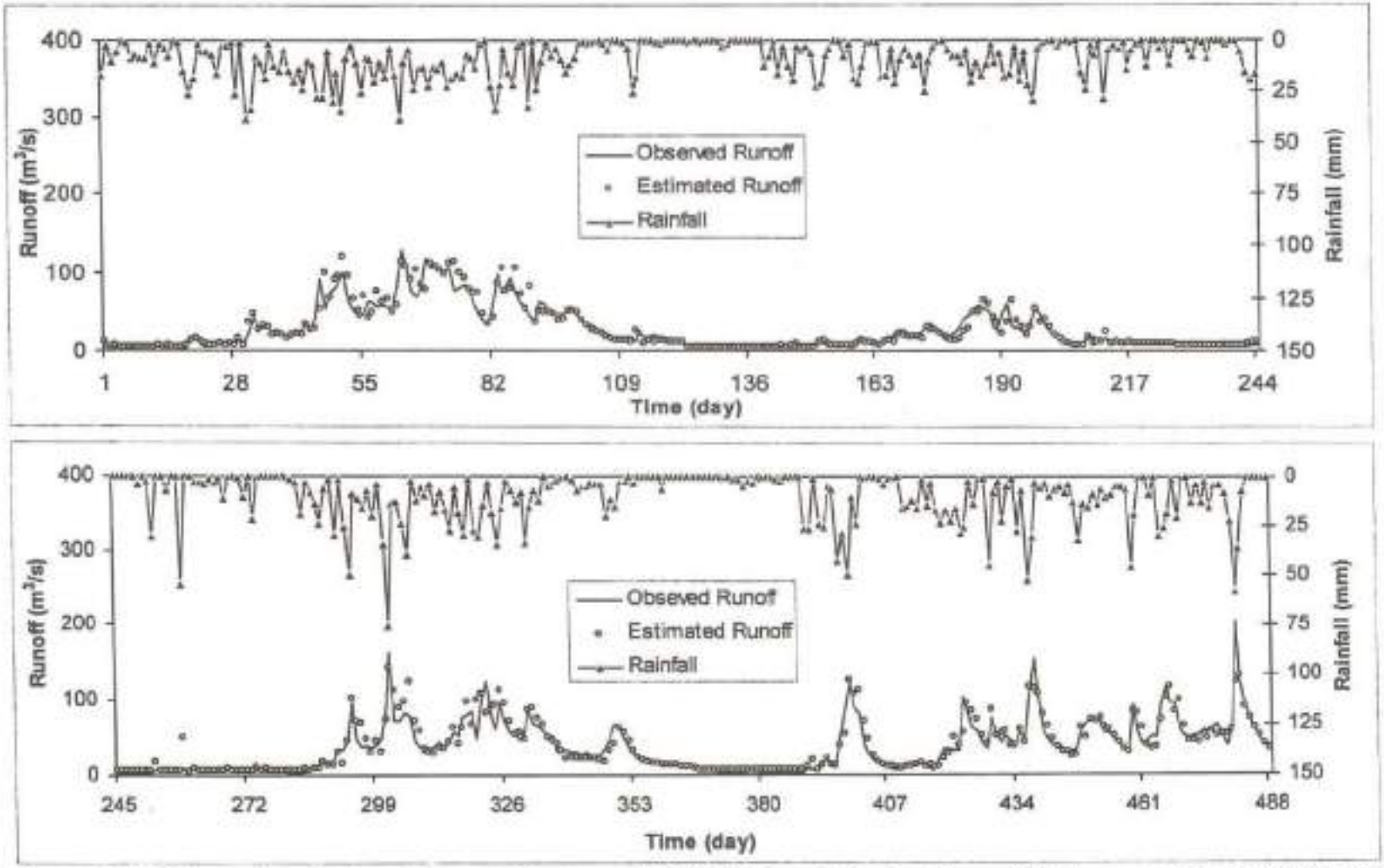

Figure 7.24: Observed and estimated runoff by dynamic RBFANN model during the period of cross-validation (1985-1988) for (4-4-1) network with ALR as 20 and ALRG as 0.5 for Chaukhutia watershed

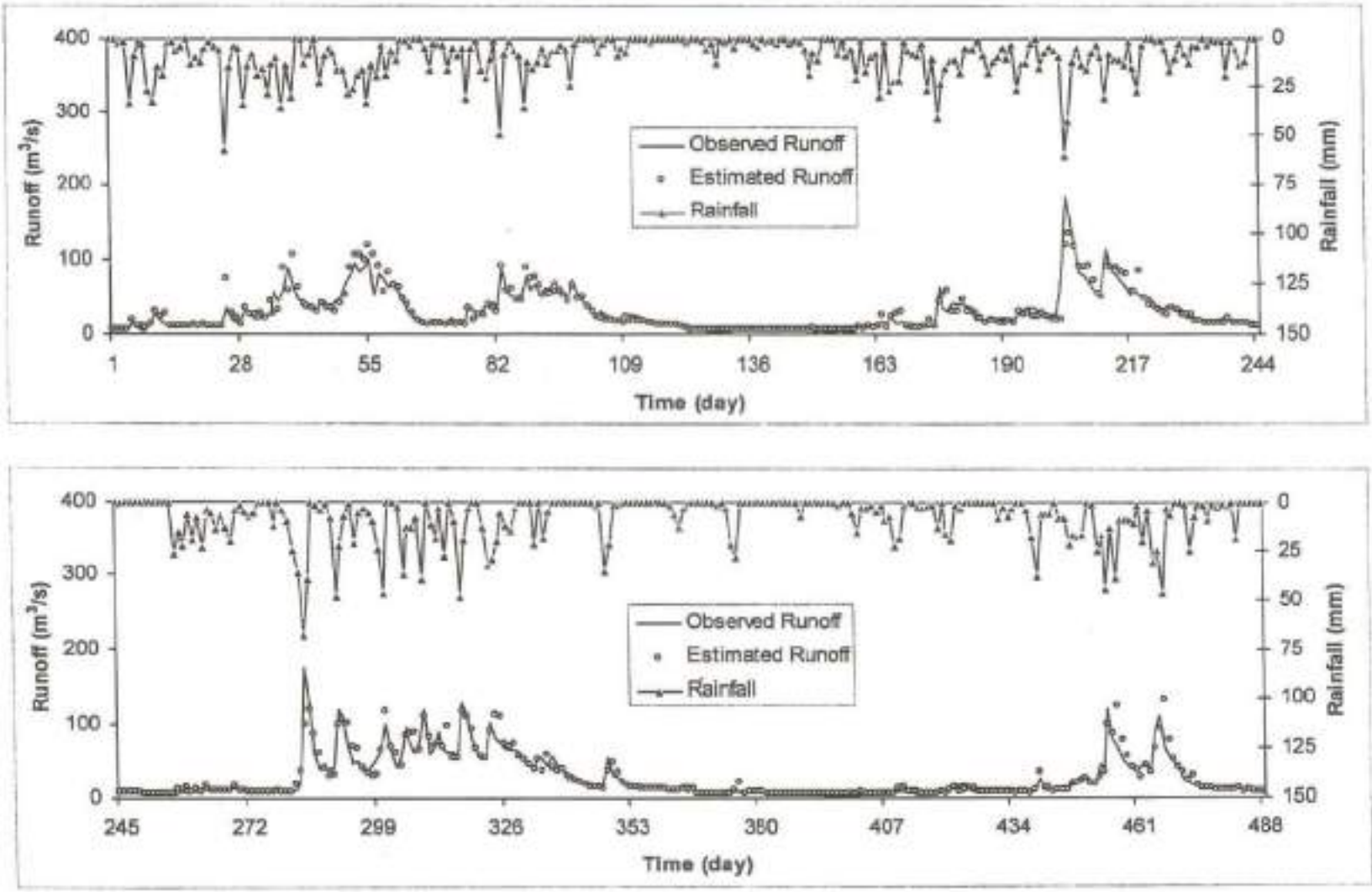

Figure 7.25: Observed and estimated runoff by dynamic RBFANN model during the period of verification (1989-1992) for (4-4-1) network with ALR as 20 and ALRG as 0.5 for Chaukhutia watershed

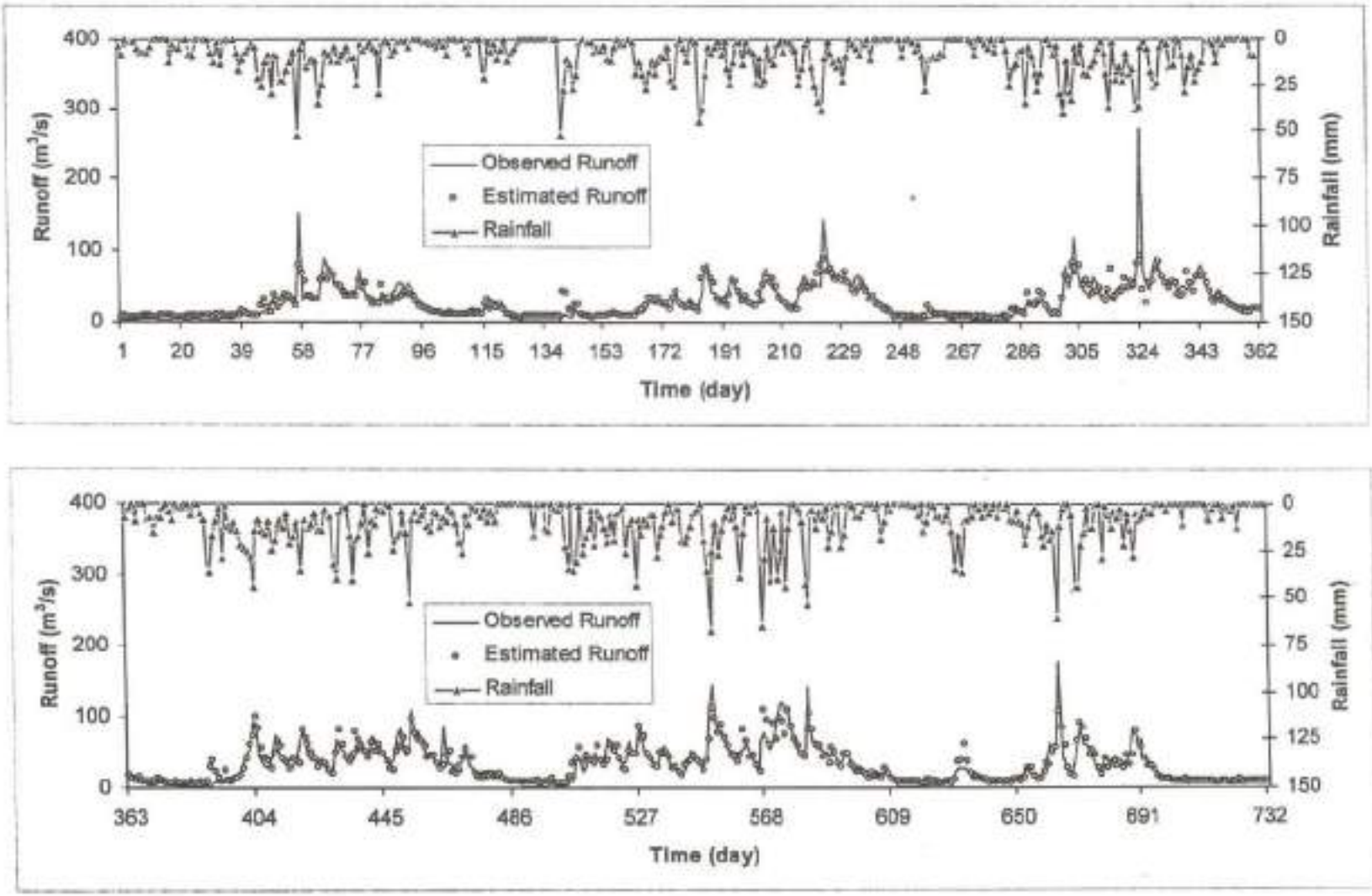

Figure 7.26: Observed and estimated runoff by dynamic RBFANN model during the period of calibration (1979-1984) for (4-16-1) network with ALR as 20 and ALRG as 0.5 for Chaukhutia watershed

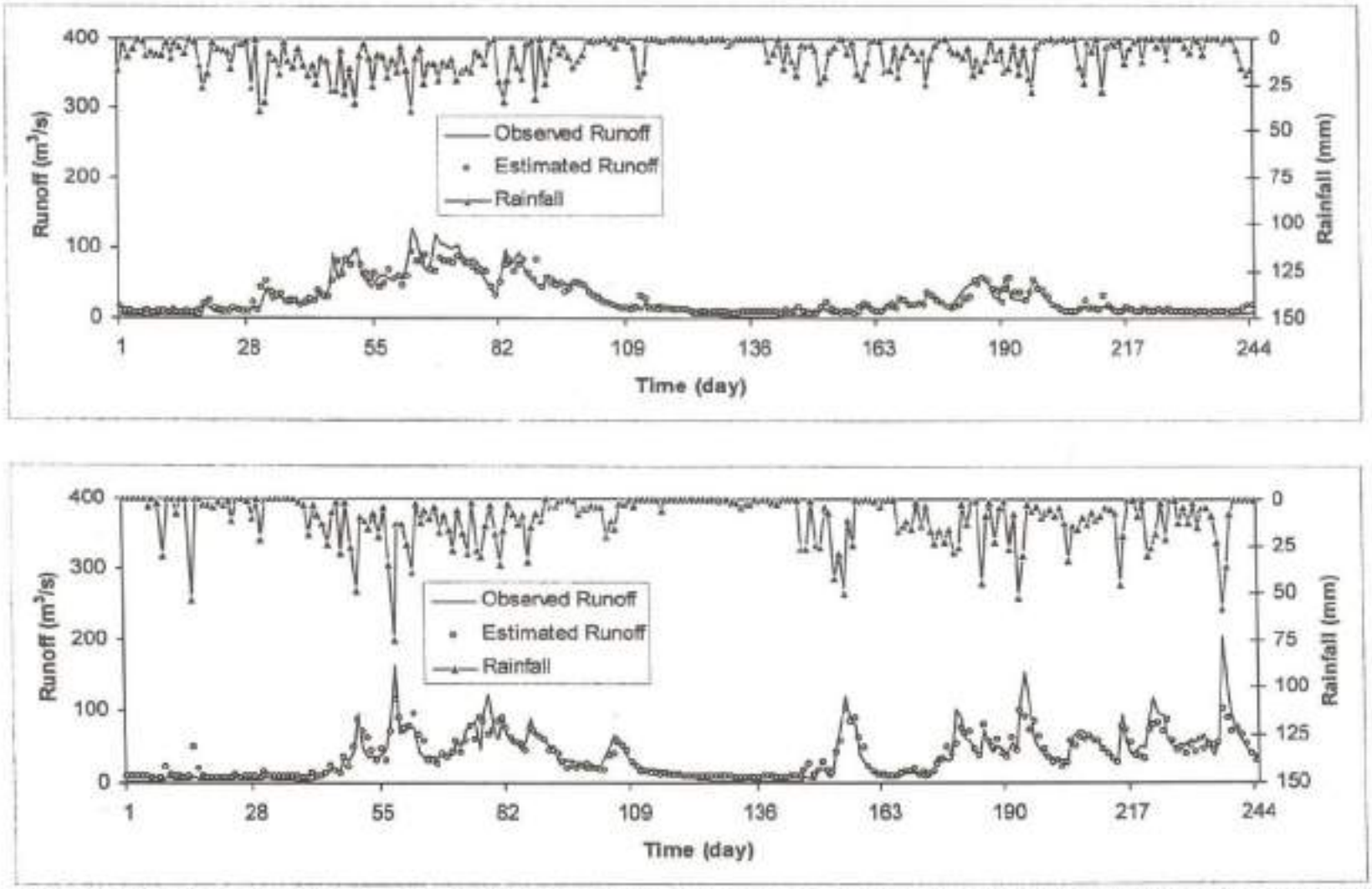

Figure 7.27: Observed and estimated runoff by dynamic RBFANN model during the period of cross-validation (1985-1988) for (4-16-1) network with ALR as 20 and ALRG as 0.5 for Chaukhutia watershed

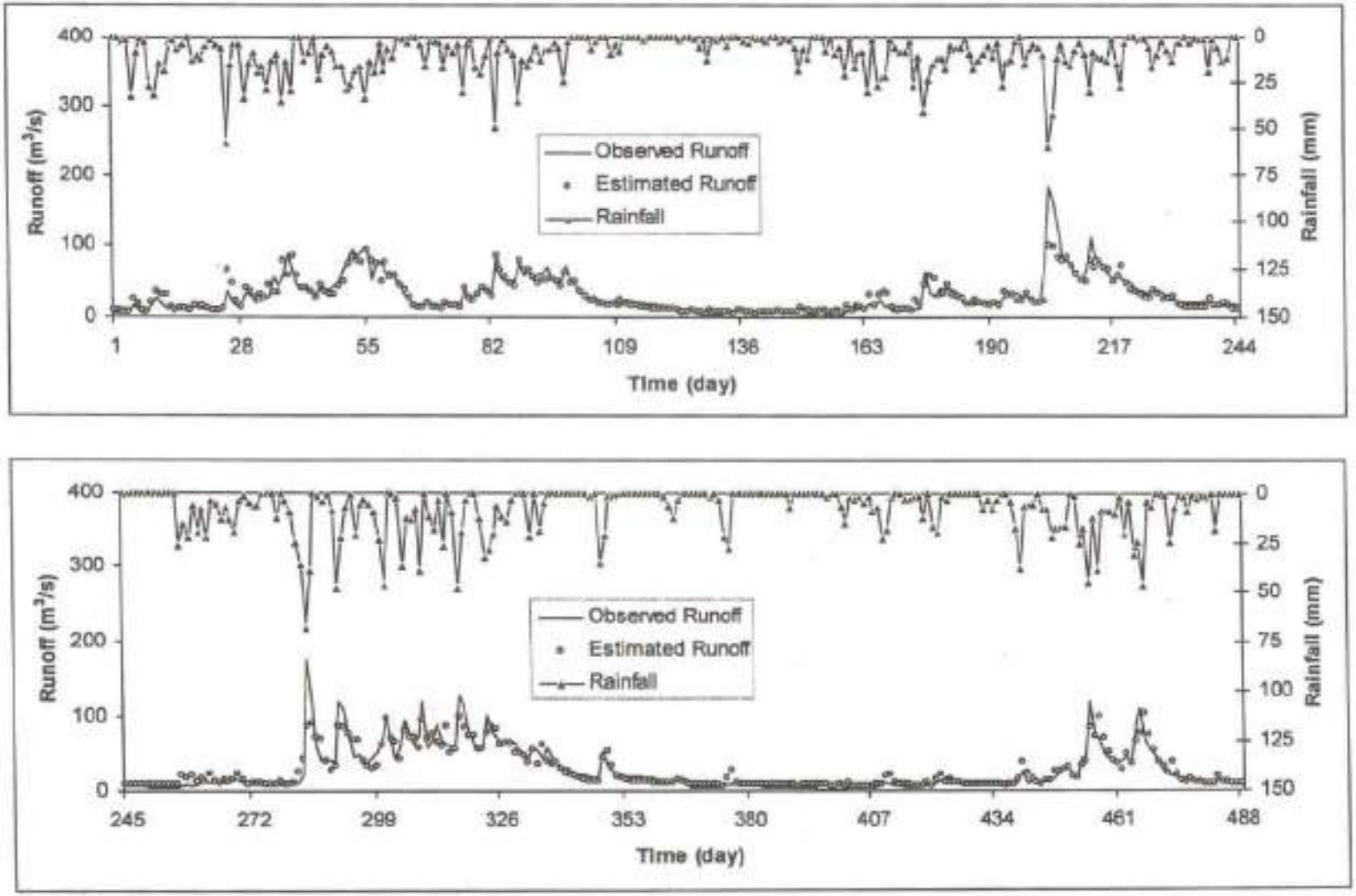

Figure 7.28: Observed and estimated runoff by dynamic RBFANN model during the period of verification (1989-1992) for (4-16-1) network with ALR as 20 and ALRG as 0.5 for Chaukhutia watershed

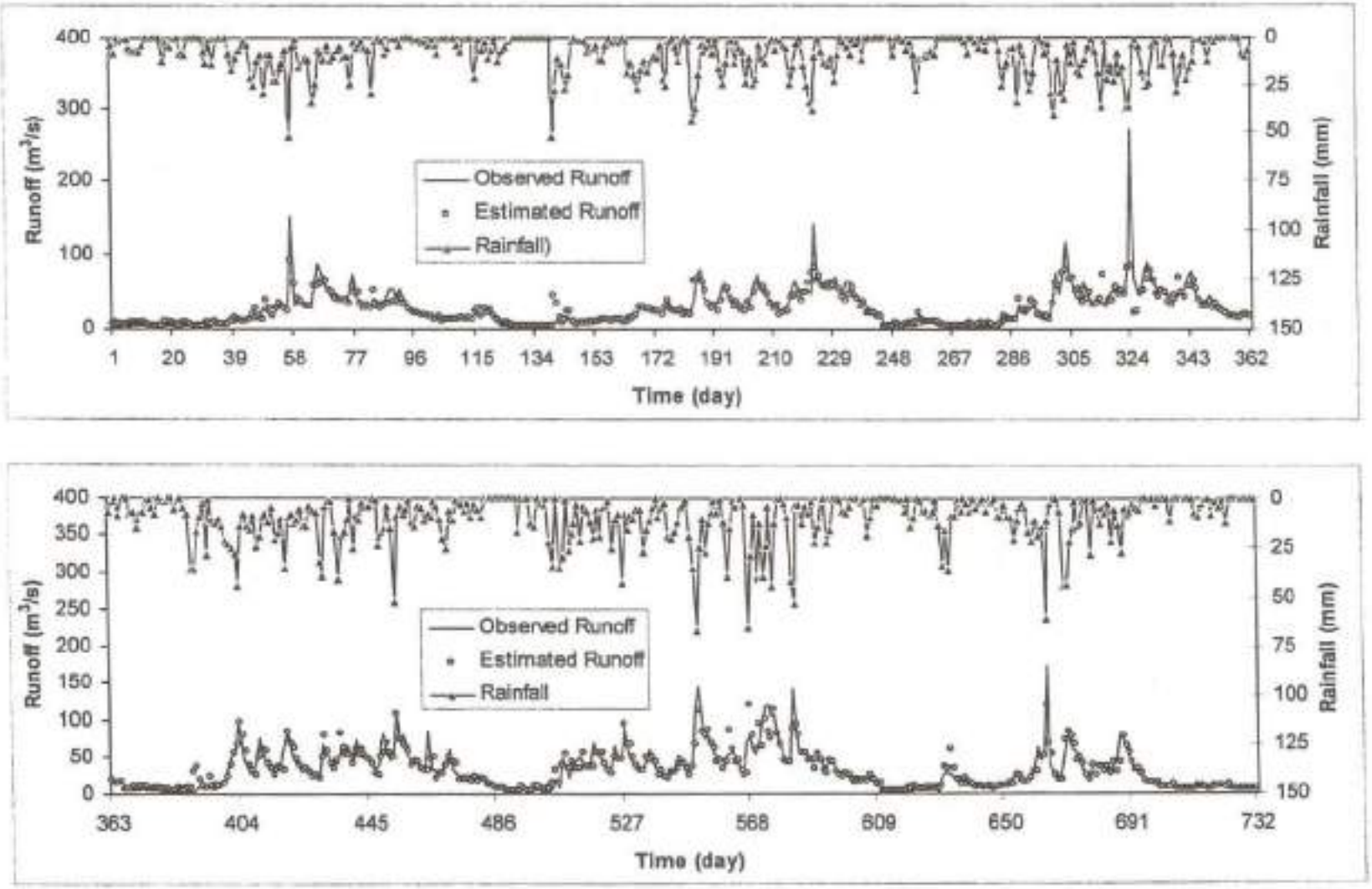

Figure 7.29: Observed and estimated runoff by dynamic RBFANN model during the period of calibration (1979-1984) for (4-32-1) network with ALR as 20 and ALRG as 0.5 for Chaukhutia watershed

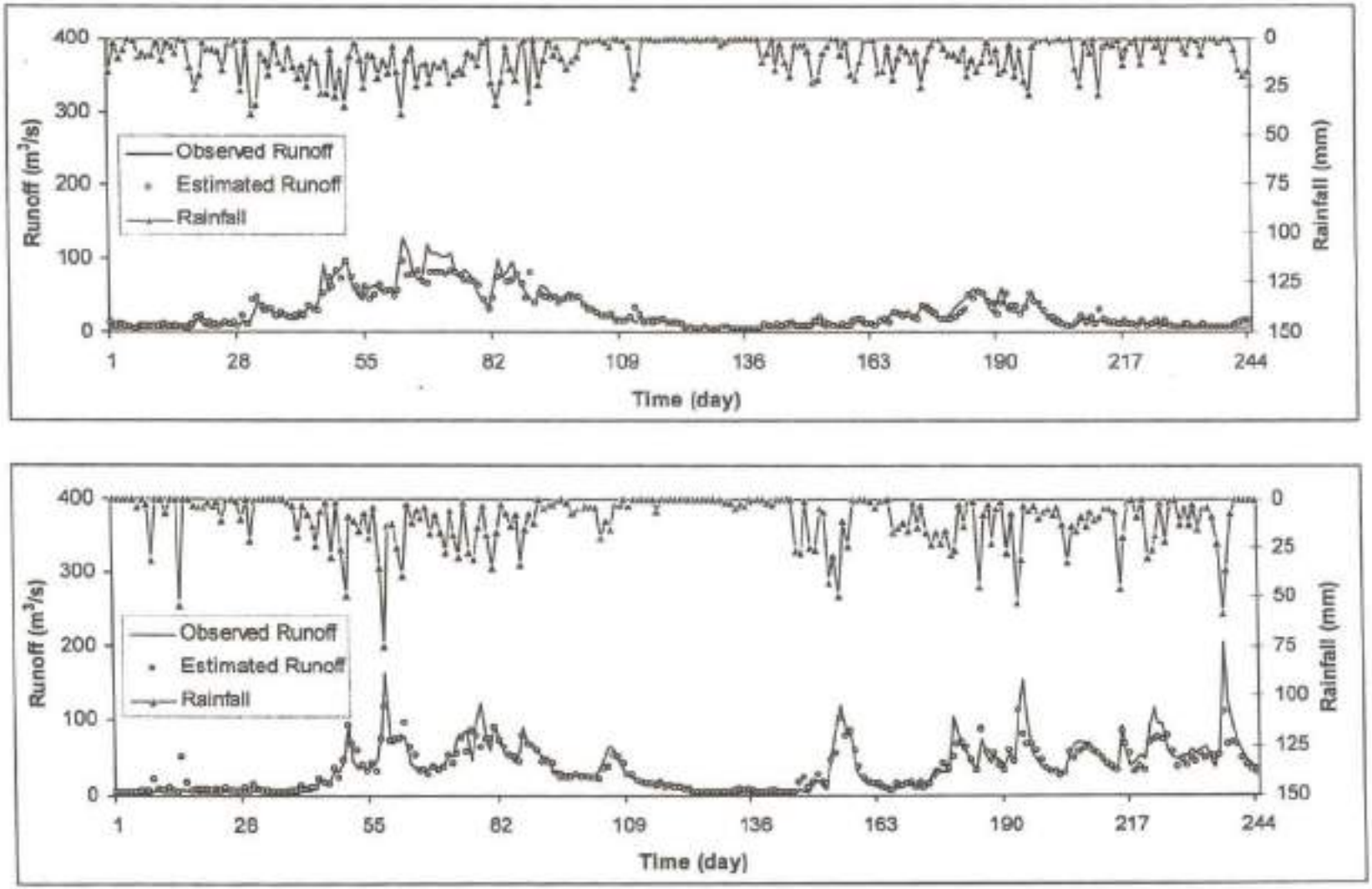

Figure 7.30: Observed and estimated runoff by dynamic RBFANN model during the period of cross-validation (1985-1988) for (4-32-1) network with ALR as 20 and ALRG as 0.5 for Chaukhutia watershed

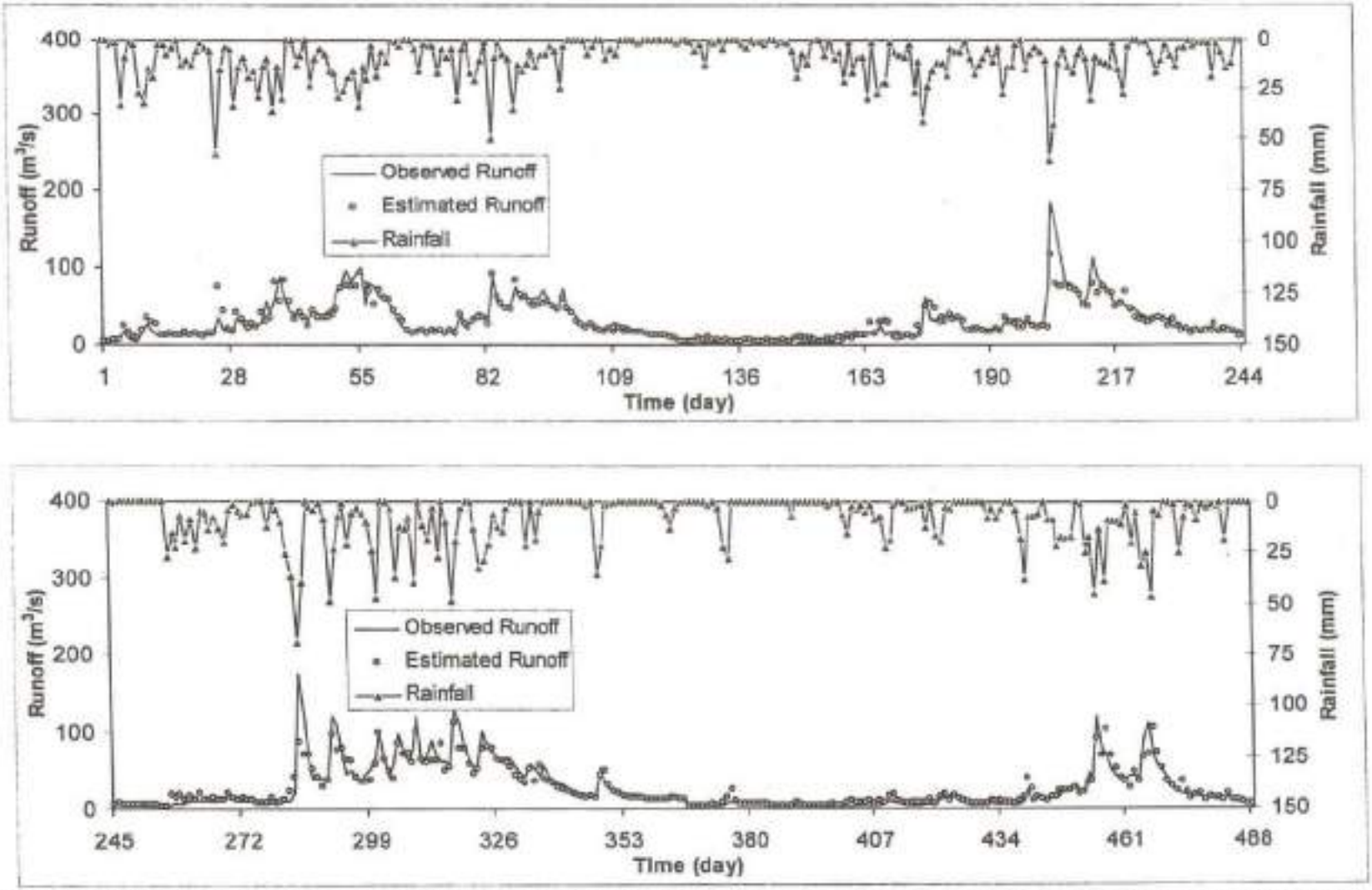

Figure 7.31: Observed and estimated runoff by dynamic RBFANN model during the period of verification (1989-1992) for (4-32-1) network with ALR as 20 and ALRG as 0.5 for Chaukhutia watershed

7.10 CONCLUSIONS

The following conclusions can be derived from this study:

1. Radial Basis Function can be a better solution for rainfall-runoff modeling as physically based models with partial differential equations of mass and energy is difficult to employ due to lack of data. The selection of learning rate as well as the number of iterations required is very important for optimal results. The proposed program has flexibility to change the input and output variables and fix the radial basis nodes.
2. The proposed model performed very well in calibration, cross-validation, and verification for both Chaukhutia and Naula watersheds. However, in case of Ramganga watershed the model performed very well in calibration and cross-validation whereas it performed satisfactorily during verification.
3. The developed RBFANN model in this study simulated the daily runoff quite closely in all watersheds during all periods. The peak flows were however underestimated by the model, and therefore exists a need to modify the proposed model for extreme flows.
4. The proposed model simulates the long-term daily runoff reasonably well in all the considered watersheds, and therefore, its applicability can be generalized for all the sub-watersheds of the Ramganga river basin.

CHAPTER 8

ESTIMATION OF SEDIMENT GRAPH

CHAPTER 8

ESTIMATION OF SEDIMENT GRAPH

The estimation of sediment yield is needed for studies of reservoir sedimentation, river morphology, soil and water conservation planning, and also for estimation of concentration and load of chemicals adsorbed to sediment particles. Sediment yield from a watershed is the output form of an erosion process, and is difficult to estimate as it arises from a complex interaction of various hydro-geological processes, and the knowledge of the actual process and extent of suspended material is far less detailed. Erosion and sediment yield models are broadly classified into three categories viz. empirical models, conceptual models, and process-based models. Merritt et al. (2003) and Aksoy and Kavvas (2005) provided a good review of various models applicable in sediment transport and erosion modeling. The empirical models are based on empirical framework, and therefore, their applicability is limited to the condition for which they are developed (Aksoy and Kavvas, 2005). The feature of this class of models is their high level of spatial and temporal aggregation and their incorporation of a small number of causal variables (Jakeman et al., 1999). The Universal Soil Loss Equation (USLE) (Wischmeier and Smith, 1978) is an empirical model based on exhaustive data from the United States. The conceptual models are based on spatially lumped form of continuity and linear storage-discharge equations of water and sediment yield. Beck (1987) noted that conceptual models play a conciliator role between empirical and physics-based models. Whilst they tend to be aggregated they still reflect the hypotheses about the processes governing system behaviour. This is the main feature that distinguishes conceptual models from empirical models. A watershed is represented by storage systems that include the catchment processes, without including the specific details of process interactions that may require detailed catchment information. Examples of some existing conceptual models include the Unit Sediment Graph (USG) (Rendon-Herrero, 1978) and Instantaneous Unit Sediment Graph (IUSG) (Williams, 1978; Singh et al., 1982; Kumar and Rastogi, 1987; Raghuwanshi et al., 1994; Gracia-Sanchez, 1996; Lee and

Singh, 2005; Singh et al., 2008). If a model is constructed by using mass conservation equation of sediment, it is called a process-based model. Examples of process-based models include Sedimentology Simulation (SEDIMOT) model (Wilson et al., 1984), Agricultural Non-Point Source (AGNPS) model (Young et al., 1987), and Watershed Environmental Hydrology (WEHY) model (Kavvas et al., 2004, 2006). However, due to temporal variations in rainfall inputs and pronounced spatial heterogeneity prevalent in catchment areas, even the process-based models are found to produce unsatisfactory results (Wu et al., 1993; Kothyari et al., 2002).

According to Williams (1978) the unit sediment graph (USG) method of Rendon-Herrero (1978) depends completely on measured data and neglects the effects of watershed cover and conservation practices. Secondly, the method can not be used on ungauged watersheds (Gracia-Sanchez, 1996). On the other hand, to derive direct sediment graphs directly from rainfall of a storm, the regression type relations (between the effective rainfall and mobilized sediment) are in frequent use (Chen and Kuo, 1986; Kumar and Rastogi, 1987; Raghuwanshi et al., 1994; Raghuwanshi et al., 1996; Sharma et al., 1992; and Sharma and Murthy, 1996). The IUSG model based on linear reservoir concept of Nash (1957) has been employed by Kumar and Rastogi (1987), Sharma et al. (1992) and Sharma and Murthy (1996). Raghuwanshi et al. (1994) proposed an IUSG model based on attenuation and translation functions of mobilized sediment. In these models, the mobilized sediment was related with effective rainfall using a regression model. Lee and Singh (1999, 2005) developed the IUSG-based sediment graph models by coupling it with the Kalman filter and Tank model. These models do not explicitly contain any expression or factor in their mathematical formulation to account for major runoff and, in turn, sediment producing watershed characteristics, such as soil type, land use, hydrologic condition, and antecedent moisture. Mishra et al. (2006) developed SCS-CN based sediment yield models which account for various hydrological elements and watershed characteristics such as initial abstraction (I_a) and initial soil moisture (V_0). However, these models are not suitable for time distributed modeling of sediment yield, which is of paramount importance in environmental engineering and water quality modeling.

Recently, Tyagi et al. (2008) developed a time distributed sediment yield model utilizing the SCS-CN based infiltration model for computation of rainfall-

excess rate, and the SCS-CN-inspired proportionality concept for computation of sediment-excess. Finally, for computation of sediment graphs, the sediment-excess is routed to the watershed outlet using a single linear reservoir technique. The developed model can not be used for ungauged catchments, the condition encountered generally for sedimentation studies, and uses single linear reservoir approach for routing the mobilized sediment up to watershed outlet. More recently, Singh et al. (2008) developed new conceptual sediment graph models based on coupling of popular and extensively used methods, viz., Nash model based instantaneous unit sediment graph (IUSG), Soil Conservation Service Curve Number (SCS-CN) method, and Power law. The models can be extremely useful for computing dynamic pollutant loads in water quality modelling if the sediment transports the pollutants that are toxic at high concentrations, requiring determination of peak, rather than average sediment flow rate. Secondly, these models can also be explored for their applicability to ungauged catchments. Increased awareness of environmental quality and desire to control non-point-source pollution has significantly increased the need of sediment yield estimates (Singh, 1989). The sediment graphs are very essential if the sediment transports the pollutants that are toxic at high concentrations, requiring determination of peak, rather than average sediment flow rate.

8.1 OBJECTIVES

Keeping-in-view the foregoing discussions, the main objectives of this chapter are: (i) to formulate a simple conceptual model of sediment yield lying on a strong mathematical foundation and test its workability using data of Chaukhutia watershed of Ramganga catchment, and (ii) to perform sensitivity analysis of model parameters. In a nutshell, the methodology comprises the mobilized sediment estimation by SCS-CN method and Power law, rather than developing a regression relationship between mobilized sediment and effective-rainfall. The mobilized sediment is then routed through Nash (1960) approach. Finally, the direct sediment graphs are computed by convolution of the IUSG with mobilized sediment. It is noteworthy here that the model does not explicitly account for the geometric configuration of a given watershed. The proposed approach is advantageous in the sense that it considers the

rainfall intensity, soil type, land use, hydrologic condition, and antecedent moisture, and thus, it is physically more plausible than the common and less accurate regression type relations.

8.2 PROPOSED MODEL

The proposed model is based on the following assumptions: **(i)** the bed load contributions to the total sediment yield are neglected since they are usually small, and therefore, the suspended sediment yield is considered as the total sediment yield of the watershed; **(ii)** the rainfall, P, grows linearly with time t, i.e. $P = i_0 t$, where i_0 is the uniform rainfall intensity; **(iii)** the inflow is instantaneous and occurs uniformly over the entire watershed producing a unit of mobilized sediment; and (iv) the process is linear and time invariant.

The suspended sediment dynamics for a linear reservoir can be represented by a spatially lumped form of continuity equation and a linear-storage discharge relationship, as follows (Kumar & Rastogi, 1987; Singh et al., 2008; Bhunya et. al., 2009):

First linear reservoir:

$$I_{s1}(t) - Q_{s1}(t) = dS_{s1}(t)/dt \tag{8.1}$$

$$S_{s1}(t) = K_s Q_{s1}(t) \tag{8.2}$$

where, $I_{s1}(t)$ is the sediment inflow rate to the first reservoir $[MT^{-1}]$, and specified in units of (Tons/h), $Q_{s1}(t)$ is the sediment outflow rate $[MT^{-1}]$ in units of (Tons/h), $S_{s1}(t)$ is the sediment storage within the reservoir [M], specified in Tons, and K_s is sediment storage coefficient [T], specified in units of hour.

Defining A_c as the watershed area in km^2, and Y as mobilized sediment per storm in Tons/km^2, then the total amount of mobilized sediment per storm can be given as: $Y_T = [A_c\, Y]$ Tons. However, if it occurs instantaneously and is one unit, then coupling of Eqs. (8.1) & (8.2) results:

$$Q_{s1(t)} = (1/K_s)e^{-t/K_s} \tag{8.3}$$

Eq. (8.3) gives nothing but the rate of sediment output from the first reservoir. This output forms the input to second reservoir and if it goes on up to n_s^{th} reservoir, then the expression for the resultant output from the n_s^{th} reservoir can be given as:

$$Q_s(t) = [(t/K_s)^{n_s-1} e^{-t/K_s}]/K_s\Gamma(n_s) \tag{8.4}$$

where $\Gamma()$ is the Gamma function. Eq. (8.4) represents the IUSG ordinates at time t (h^{-1}). For the condition, at $t = t_{ps}$ or $dQ_s(t)/dt = 0$, yields

$$K_s = t_p/(n_s - 1) \tag{8.5}$$

Coupling of Eqs. (8.4) & (8.5) yields

$$Q_s(t) = (n_s - 1)^{n_s}/[t_p\Gamma(n_s)][(t/t_{ps})e^{-(t/t_{ps})}]^{n_s-1} \tag{8.6}$$

Eq. (8.6) gives the output of the n_s^{th} linear reservoir. where Q_s (t) = Sediment outflow rate from n_s^{th} reservoir or output from the watershed system (Tons/h), t_{ps} = time to peak sediment outflow rate (h).

The SCS-CN method is based on the water balance equation and two fundamental hypotheses, which can be expressed mathematically, respectively, as:

$$P = I_a + F + Q \tag{8.7}$$

$$Q/(P - I_a) = F/S \tag{8.8}$$

$$I_a = \lambda S \tag{8.9}$$

where, P is total precipitation, I_a initial abstraction, F cumulative infiltration, Q direct runoff, S potential maximum retention, and λ initial abstraction coefficient. Coupling of Eqs. (8.7) & (8.8) leads to the popular form of SCS-CN method, expressible as:

$$Q = (P - I_a)^2 / (P - I_a + S) \qquad \text{for } P > I_a \tag{8.10}$$

$$= 0 \qquad \text{otherwise}$$

Following Mishra and Singh (2003), for the condition, $f_c = 0$, the Horton's method (Horton, 1938) can be expressed as:

$$f = f_0 e^{-kt} \tag{8.11}$$

where, f is the infiltration rate ($L\,T^{-1}$) at time t, f_0 is the initial infiltration rate (LT^{-1}) at time t=0, k is the decay constant (T^{-1}), and f_c is the final infiltration rate (LT^{-1}). The cumulative infiltration F can be derived on integrating Eq. (8.11) as:

$$F = f_0 (1 - e^{-kt}) / k \tag{8.12}$$

It can be observed from Eq. (8.12) that as $F \rightarrow f_0/k$, as $t \rightarrow \infty$,. Similarly, for Eq. (8.8) as $Q \rightarrow (P\text{-}I_a)$, $F \rightarrow S$, and time $t \rightarrow \infty$, therefore the similarity between the two yields

$$S = f_0 / k \tag{8.13}$$

On the basis of infiltration tests, Mein and Larson, (1971) have gotten $f_0 = i_0$, where i_0 is the uniform rainfall intensity when t = 0. Substituting this into Eq. (8.13) yields,

$$f_0 = i_0 = kS \tag{8.14}$$

Eq. (8.14) describes the relationship among the three parameters f_0, k, and S. Thus Eq. (8.14) shows that k depends on the magnitude of the rainfall intensity and soil type,

land use, hydrologic condition, and antecedent moisture that affect S and the results are consistent as reported by Mein and Larson (1971). An assumption that rainfall P linearly increases with time t leads to

$$P = i_e t \tag{8.15}$$

which is a valid and reasonable assumption for infiltration rate computation in experimental tests (Mishra and Singh, 2004). Coupling of Eqs. (8.14) & (8.15) gives,

$$P = k S t \tag{8.16}$$

The Power law proposed by Novotny and Olem (1994) can be expressed as:

$$D_R = \alpha C_r^{\beta} \tag{8.17}$$

where D_R = sediment delivery ratio; C_r = runoff coefficient; α and β = the coefficient and exponent of power relationship. It is interesting to note that Eq. (8.17) implicitly considers the two major factors, i.e., D_R and C_r, affecting the erosion and sedimentation process. The sediment delivery ratio, D_R, is dimensionless and is expressed in terms of Sediment yield Y and Potential maximum erosion A as follows:

$$D_R = Y/A \tag{8.18}$$

The coefficient, C is also dimensionless, and expressed in terms of Q and P, as:

$$C_r = Q/P \tag{8.19}$$

Substituting the expressions of D_R and C_r in Eq. (8.17) one gets

$$Y = \alpha A(Q/P)^{\beta} \tag{8.20}$$

Now, for the condition $I_a = 0$, equating Eqs. (8.8) & (8.10) reduces to

$$Q/P = P/(P+S) = F/S \tag{8.21}$$

Substituting the equality $Q/P = P/(P+S)$ (Eq. 8.21) into Eq. (8.20) results

$$Y = \alpha A[P/(P+S)]^{\beta} \tag{8.22}$$

Similarly, the coupling of Eqs. (8.16) & (8.22) yields

$$Y = \alpha A[kt/(1+kt)]^{\beta} \tag{8.23}$$

Thus, Eq. (8.23) gives the expression for mobilized sediment due to an isolated storm event occurring uniformly over the watershed. Hence, total amount of mobilized sediment can be expressed as:

$$Y_T = \alpha A A_c[kt/(1+kt)]^{\beta} \tag{8.24}$$

Finally, coupling of Eqs. (8.6) & (8.24) results

$$Q_s(t) = \left[\alpha A A_c[kt/(1+kt)]^{\beta}(n_s-1)^{n_s}/[t_p\Gamma(n_s)][(t/t_{ps})e^{-(t/t_{ps})}]^{(n_s-1)}\right] \tag{8.25}$$

The expression given by Eq. (8.25) is the proposed model for computations of sediment graphs. The proposed model has four parameters α, β, k, and n_s and A.

8.3 APPLICATION OF THE PROPOSED SEDIMENT GRAPGH MODEL

The workability of the proposed model has been tested on the Chaukhutia watershed of Ramganga catchment. A detailed description of the study watershed has been given in Chapter 2. However, the data specific required for the present study is

being discussed here. Carefully six storms events were selected in such a way that they are falling in the monsoon season during which the chances for erosion and sedimentation are more. The sediment samples were taken at Chaukhutia flow gauging station using a one liter bottle sampler at an interval of 2-4 h, during the rising and falling limbs, at peak, and also during the recession of the events. The base sediment flow of the sediment graph was separated in a manner similar to the separation of the base flow of the runoff hydrograph used by Chow (1964). The basic characteristics of sediment graph data are given in Table 8.1.

Table 8.1: Characteristics of Storm Events

Sl. No.	Date of Event	q_{ps} (Tons/h/Tons)	t_{ps} (h)	β_s	$Q_{s(o)}$ (Tons)	$Q_{ps(o)}$ (Tons/h)
1	July 17, 1983	0.38	2	0.76	2739	1025
2	August 21/22, 1983	0.418	2	0.836	2070	875
3	July 15, 1984	0.397	2	0.794	3145	1250
4	August 18/19, 1984	0.404	2	0.81	2105	850
5	September 1/2, 1984	0.39	2	0.78	1205	475
6	September 17/18, 1984	0.41	2	0.82	963	392

8.3.1 Parameter Estimation

The shape parameter (n_s) was estimated by the relationship given by Bhunya et al. (2009) as:

$$n_s = 5.53\beta_s^{1.75} + 1.04 \qquad \text{for } 0.01<\beta_s<0.35$$

$$n_s = 6.29\beta_s^{1.998} + 1.157 \qquad \text{for } \beta_s \geq 0.35 \qquad (8.26)$$

where, β_s is a non dimensional parameter defined as the product of peak sediment flow rate (q_{ps}) [Tons/h/Tons] and time to peak sediment flow rate (t_{ps}) [h]. β_s is also defined as shape factor (Singh, 2000; Bhunya et al., 2003). The rest of the parameters were estimated using the non-linear Marquardt algorithm (Marquardt, 1963) of the least squares procedure. The estimated parameter values are given in Table 8.2.

Table 8.2: Optimized parameter values for Chaukhutia watershed

Sl. No.	Date of Event	Model parameters				
		n_s	α	β	k	A (Tons/km^2)
1	July 17, 1983	4.79	0.530	0.351	0.029	26.66
2	August 21/22, 1983	5.55	0.727	0.701	0.030	40.78
3	July 15, 1984	5.12	0.735	0.721	0.030	62.69
4	August 18/19, 1984	5.27	0.714	0.663	0.030	38.14
5	September 1/2, 1984	4.99	0.388	0.425	0.030	19.64
6	September 17/18, 1984	5.39	0.587	0.781	0.030	29.34

8.4 PERFORMANCE OF THE PROPOSED MODEL

The performance of the proposed sediment graph model is evaluated on the basis of their (i) closeness of the observed and computed sediment graphs visually; and (ii) goodness of fit (GOF) in terms of model efficiency (ME) and relative error (RE) of the results defined as:

$$ME = 1 - \frac{\sum (Q_{so} - Q_{sc})^2}{\sum (Q_{so} - \overline{Q_{so}})^2}; RE_{(Qs)} = \frac{Q_{s(o)} - Q_{s(c)}}{Q_{s(o)}} \times 100; \quad RE_{(Qps)} = \frac{Q_{ps(o)} - Q_{ps(c)}}{Q_{ps(o)}} \times 100 \tag{8.27}$$

where $Q_{s(o)}$ and $Q_{s(c)}$ = observed and computed total sediment outflow, $Q_{ps(o)}$ and $Q_{ps(c)}$ = observed and computed peak sediment flow rate; $RE_{(Qs)}$ and $RE_{(Qps)}$ are relative errors in total sediment outflow and peak sediment flow rates, respectively.

For visual appraisal, the sediment graphs computed using the proposed model were compared with the observed ones for all the storm events as shown in Figures 8.1 to 8.6. It can be inferred from these figures that the computed sediment graph exhibits fair agreement with the observed graph. Further, Figs. 8.7 & 8.8 show the comparison between computed and observed total sediment outflow and peak sediment outflow rates for all the storm events. The closeness of data points in terms of a best fit line and a higher value of $r^2 \approx 1.000$ indicate a satisfactory model performance for the assigned job.

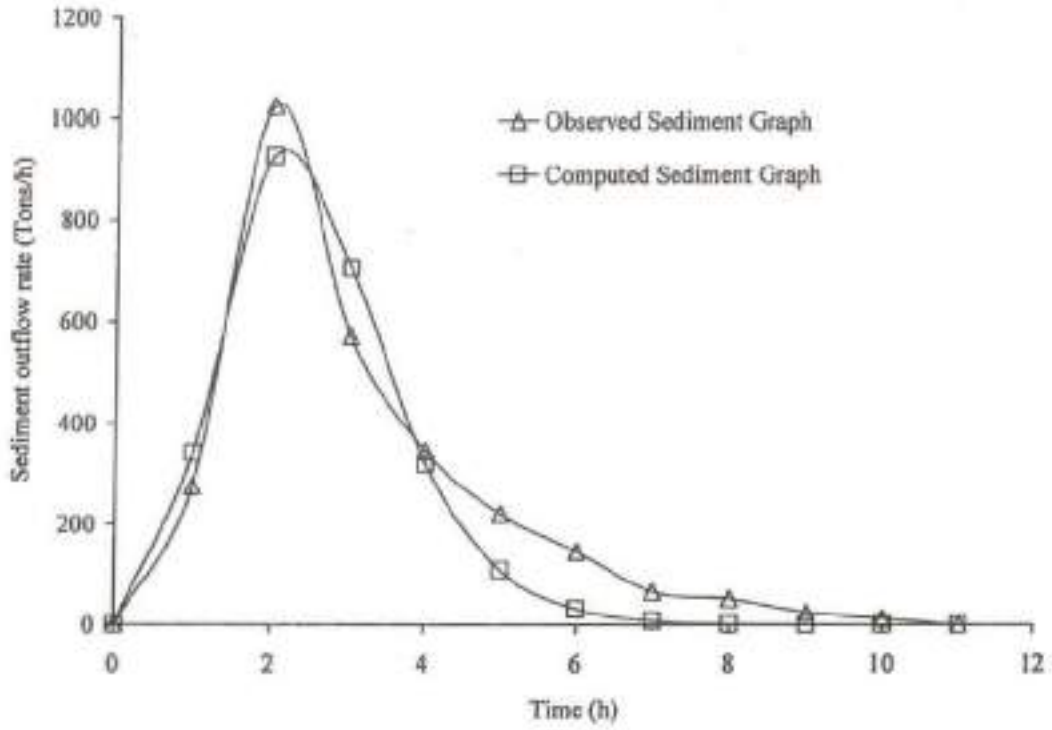

Figure 8.1: Comparison of observed and computed sediment graphs for July 17, 1983

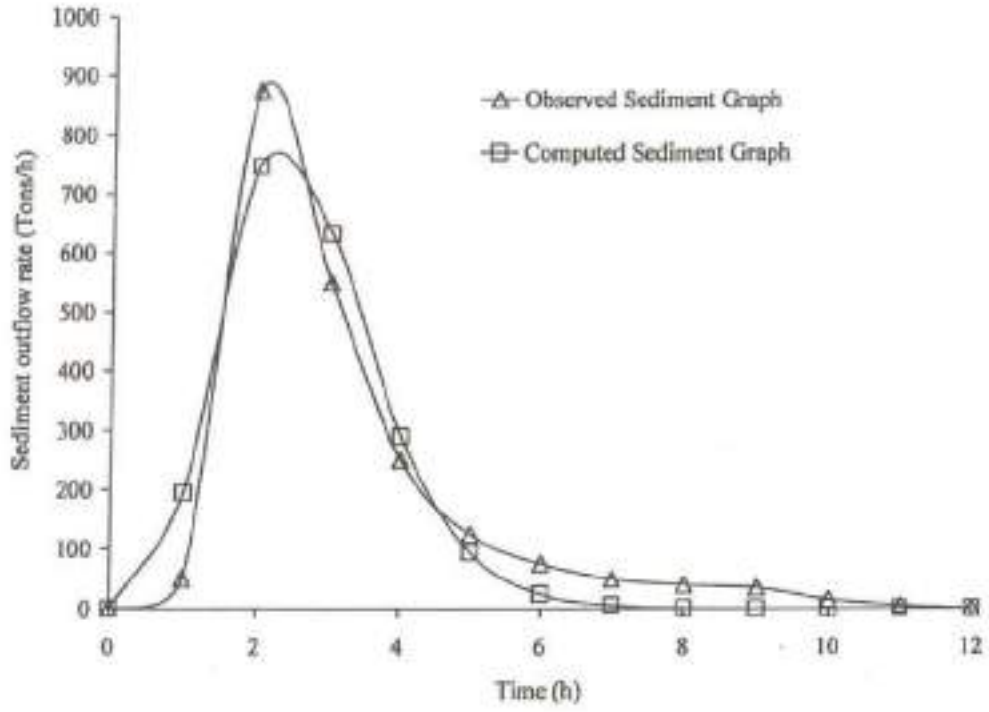

Figure 8.2: Comparison of observed and computed sediment graphs for Aug. 21/22, 1983

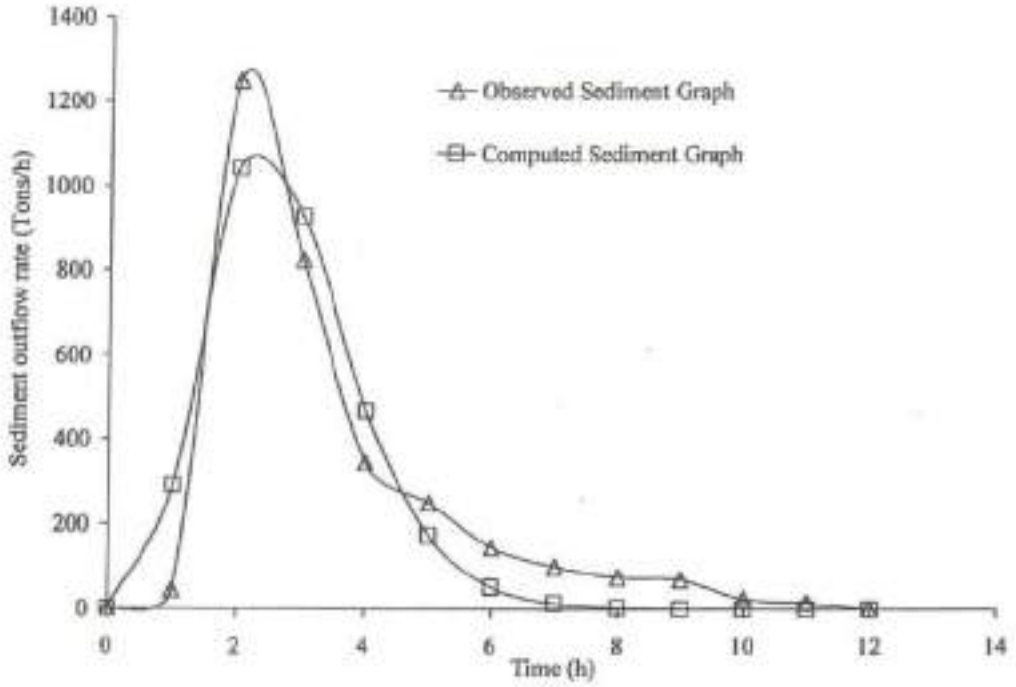

Figure 8.3: Comparison of observed and computed sediment graphs for July 15, 1984

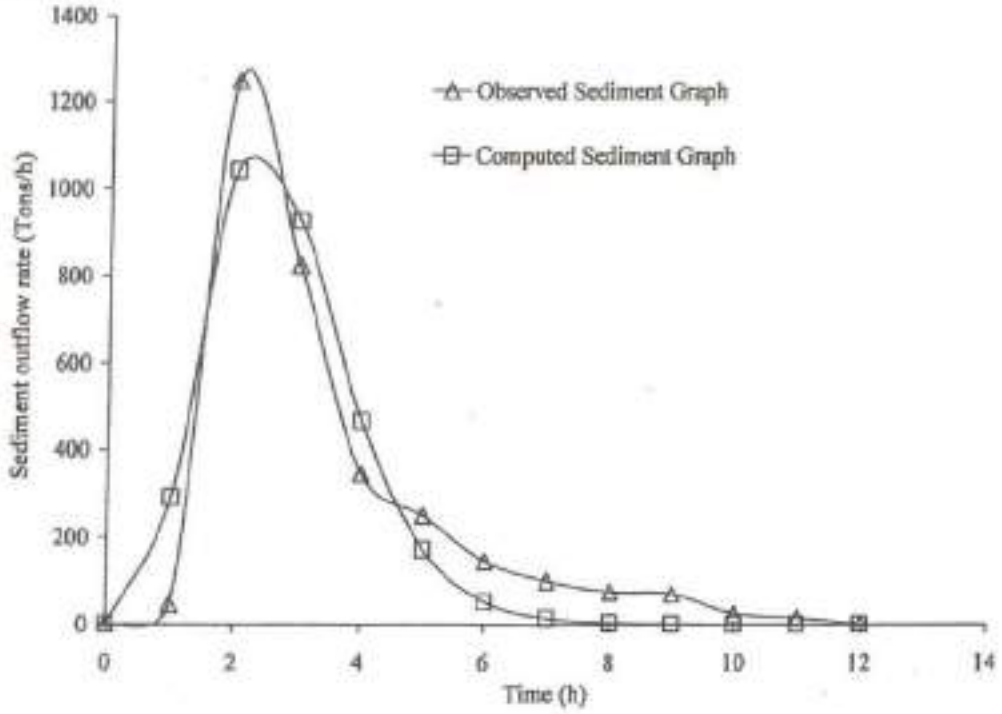

Figure 8.4: Comparison of observed and computed sediment graphs for Aug.18/19, 1984

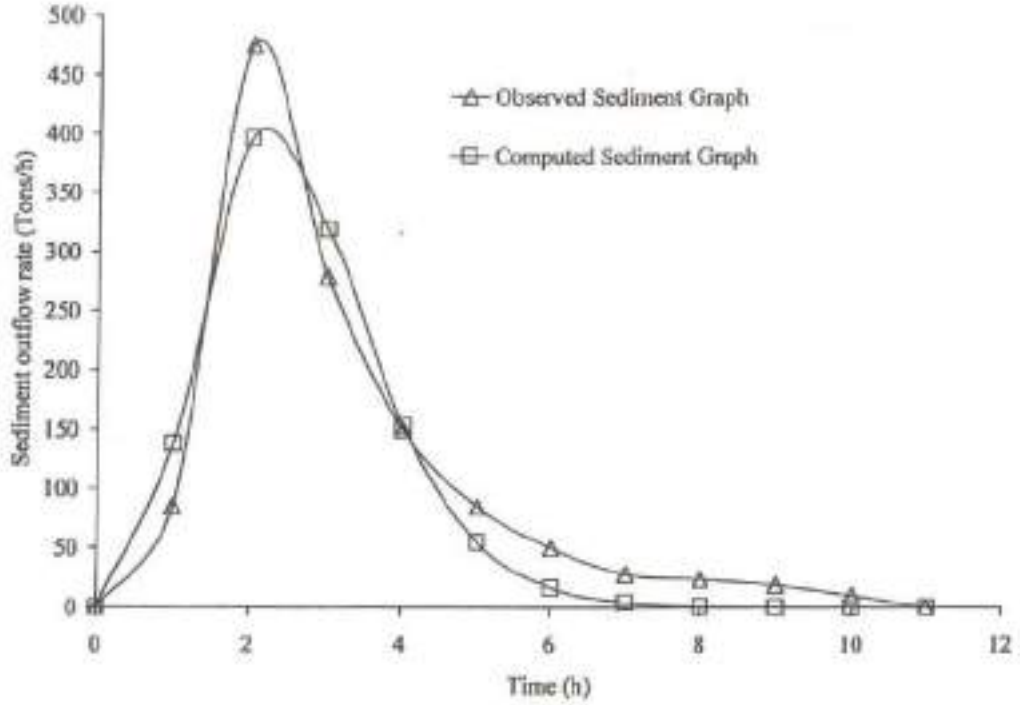

Figure 8.5: Comparison of observed and computed sediment graphs for Sept.1/2, 1984

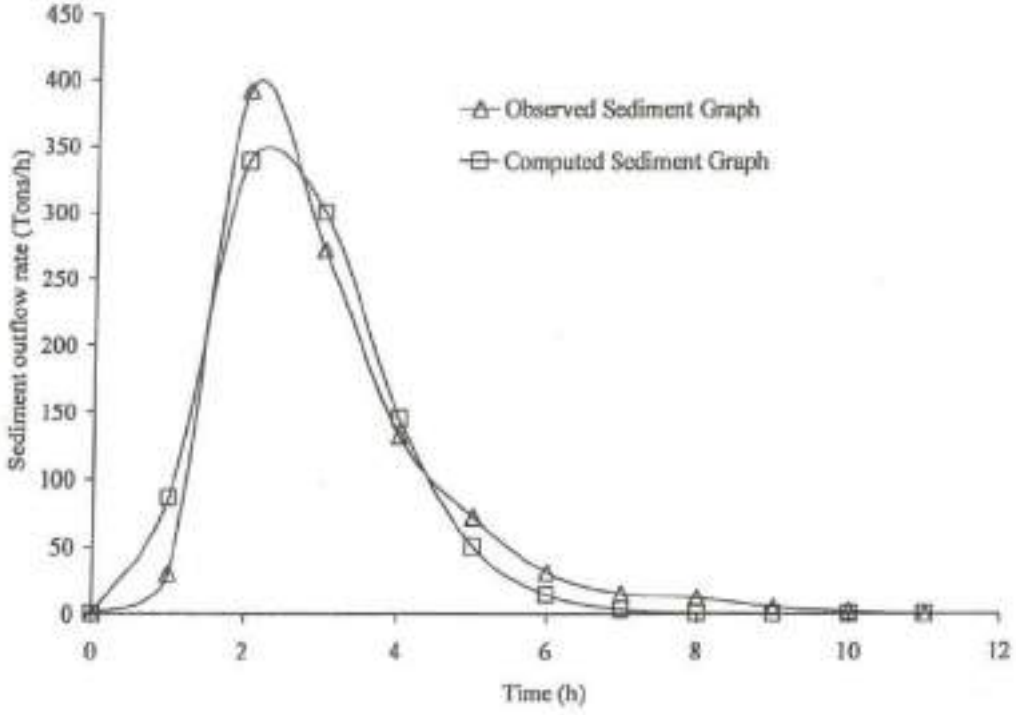

Figure 8.6: Comparison of observed and computed sediment graphs for Sept. 17/18, 1984

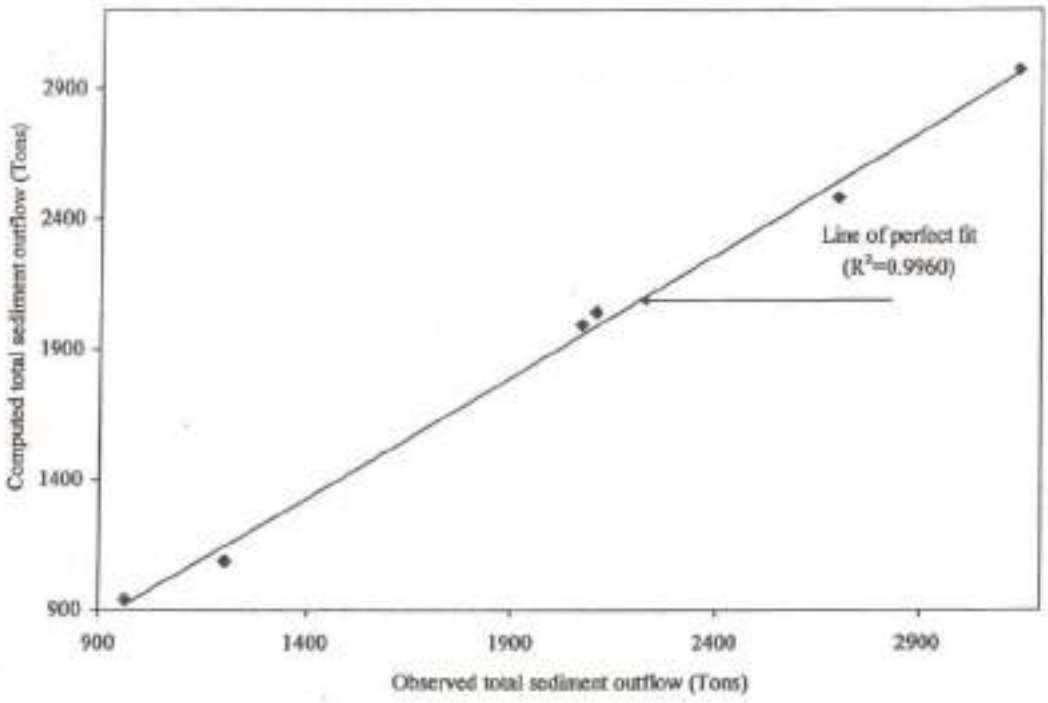

Figure 8.7: Comparison between observed and computed total sediment outflow

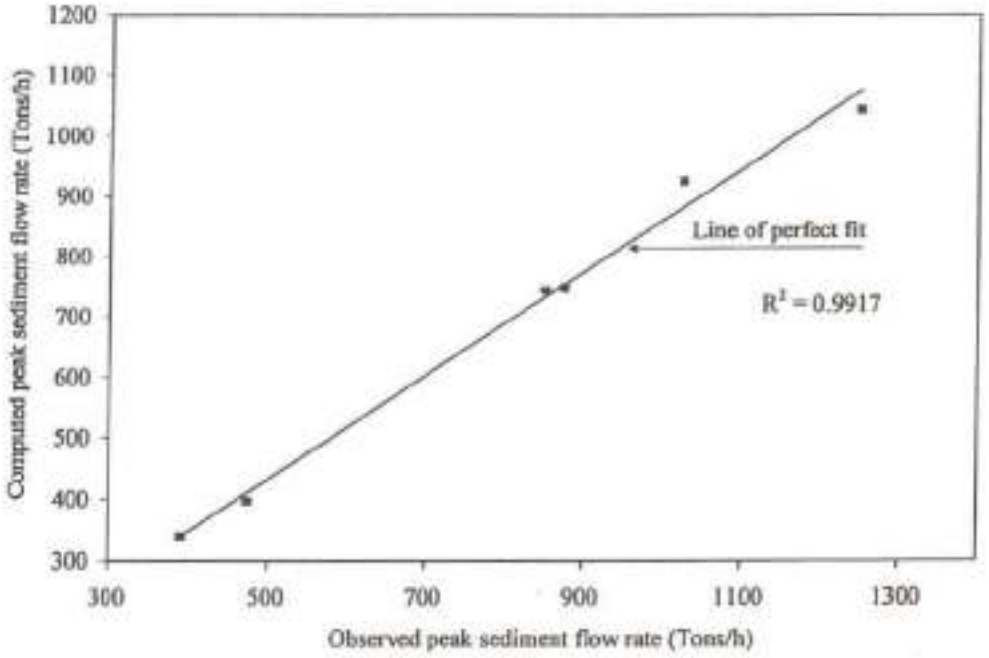

Figure 8.8: Comparison between observed and computed peak sediment flow rates

Further the results of GOF criteria given by Eq. (8.27) for all the events are shown in Table 8.3. The can be observed from Table 8.3 that the relative error in total sediment outflow (RE_{Qs}) varies from 2.49% to 10.04%, whereas the relative error in peak sediment outflow rate (RE_{Qp}) is found to vary from 9.69% to 16.56%. The error percentage can be taken safely because even the more elaborate process-based soil erosion models are found to produce results with still larger errors varying from ± 40% (Vanoni, 1975; Foster, 1982; Hadley et al., 1985; Wu et al., 1993; Wicks and Bathurst, 1996; Kothyari et al., 1996; Jain et al., 2005). Table 3 also shows the GOF in terms of ME for the storm events considered in the application. It is also observed from Table 8.3 that ME varies from 90.52% to 95.41%, indicating a very good performance of the model for sediment graph computations.

Table 8.3: Goodness of fit Statistics

Sl. No.	Date of Event	$RE_{(Qs)}$ (%)	$RE_{(Qps)}$ (%)	ME (Efficiency) (%)
1	July 17, 1983	8.04	9.69	92.91
2	August 21/22, 1983	3.77	14.56	93.48
3	July 15, 1984	5.56	16.56	90.52
4	August 18/19, 1984	3.04	12.47	95.34
5	September 1/2, 1984	10.04	16.42	93.65
6	September 17/18, 1984	2.49	13.52	95.41

8.4.1 Sensitivity Analysis

From the results so far, it is imperative to analyze the sensitivity of different parameters of the proposed model for their effect on overall output. Here, the conventional analysis for sensitivity similar to the work of McCuen and Snyder (1986) and Mishra and Singh (2003) is followed as discussed in the following section. It is evident form Eq. (8.25) that $Q_s(t)$ is a function of α, β, k, n_s, and A i.e. $Q_s(t) = f(\alpha, \beta, k, n_s, A)$. Therefore, the total derivative of Q_s can be given as:

$$dQ_s(t) = \frac{\partial Q_s(t)}{\partial \alpha} d\alpha + \frac{\partial Q_s(t)}{\partial \beta} d\beta + \frac{\partial Q_s(t)}{\partial k} dk + \frac{\partial Q_s(t)}{\partial n_s} dn_s \quad (8.28)$$

where $\frac{\partial Q_s(t)}{\partial \alpha}$, $\frac{\partial Q_s(t)}{\partial \beta}$, $\frac{\partial Q_s(t)}{\partial k}$, and $\frac{\partial Q_s(t)}{\partial n_s}$ are the partial derivatives of $Q_s(t)$ with respect to α, β, k, n_s, respectively. The total derivative, $dQ_s(t)$, corresponding to the increments $d\alpha$, $d\beta$, dk, and dn_s can be physically interpreted as the total variation of $Q_s(t)$ due to the variation of α, β, k, and n_s at any point in the (α, β, k, n_s) domain. The variation of $Q_s(t)$ with respect to the variable under consideration can be derived from Eq. (8.25). A more useful form of Eq. (8.28) can be given as:

$$\frac{dQ_s(t)}{Q_s(t)} = \left(\frac{\partial Q_s(t)}{\partial \alpha}\frac{\alpha}{Q_s(t)}\right)\frac{d\alpha}{\alpha} + \left(\frac{\partial Q_s(t)}{\partial \beta}\frac{\beta}{Q_s(t)}\right)\frac{d\beta}{\beta} + \left(\frac{\partial Q_s(t)}{\partial k}\frac{k}{Q_s(t)}\right)\frac{dk}{k} + \left(\frac{\partial Q_s(t)}{\partial n_s}\frac{n_s}{Q_s(t)}\right)\frac{dn_s}{n_s} \quad (8.29)$$

where, $\left(\frac{\partial Q_s(t)}{\partial \alpha}\frac{\alpha}{Q_s(t)}\right)$, $\left(\frac{\partial Q_s(t)}{\partial \beta}\frac{\beta}{Q_s(t)}\right)$, $\left(\frac{\partial Q_s(t)}{\partial k}\frac{k}{Q_s(t)}\right)$, and $\left(\frac{\partial Q_s(t)}{\partial n_s}\frac{n_s}{Q_s(t)}\right)$ are referred to as the ratio of the error in the sediment flow rate ($dQ_s(t)/Q_s(t)$) to the error in α ($d\alpha/\alpha$), to the error in β ($d\beta/\beta$), to the error in k (dk/k), and to the error in n_s (dn_s/n_s). Now, individual ratio terms corresponding to each parameter can be derived from Eq. (8.25) as follows:

$$\frac{\partial Q_s(t)}{\partial \alpha}\frac{\alpha}{Q_s(t)} = 1 \quad (8.30)$$

A similar error ratio term for parameter 'A' $\left(\frac{\partial Q_s(t)}{\partial A}\frac{A}{Q_s(t)}\right)$ can also be obtained as well.

Similarly, for rest of the parameters, the error ratio terms are derived as:

$$\frac{\partial Q_s(t)}{\partial \beta}\frac{\beta}{Q_s(t)} = \beta \ln\left(\frac{kt}{1+kt}\right) \quad (8.31)$$

$$\frac{\partial Q_s(t)}{\partial k}\frac{k}{Q_s(t)} = \frac{\beta}{t(1+kt)} \tag{8.32}$$

$$\frac{\partial Q_s(t)}{\partial n}\frac{n_s}{Q_s(t)} = \frac{[(n_s-1)(2-n_s)\ln c-(6-3.5ns)]n_s}{(n_s-1)^{2.5}}, \text{ where } c = (t/t_{ps})\exp(-t/t_{ps}),\ n_s>1 \tag{8.33}$$

Eq. (8.33) is based on the expansion of exponential term up to first order only.

8.4.1.1 Sensitivity to α

In order to analyze the model sensitivity to parameter α, the terms pertaining to β, k, and n_s are eliminated from Eq. (8.29) and the resulting expression reduces to

$$\frac{dQ_s(t)}{Q_s(t)} = \left(\frac{\partial Q_s(t)}{\partial \alpha}\frac{\alpha}{Q_s(t)}\right)\frac{d\alpha}{\alpha} \tag{8.34}$$

Coupling of Eqs. (8.34) & (8.30) results

$$\frac{dQ_s(t)}{Q_s(t)} = \frac{d\alpha}{\alpha}, \text{ or } \frac{dQs(t)/Qs(t)}{d\alpha/\alpha} = 1 \tag{8.35}$$

From Eq. (8.35) it can be inferred that the ratio of the error in $Q_s(t)$ to the error in α is 1. This indicate that the any variation (increase or decrease) in α estimate will cause a same amount of variation (increase or decrease) in $Q_s(t)$. Similar pattern can also be observed for parameter A.

8.4.1.2 Sensitivity to β

Similar to the above, the variation of β only is considered after ignoring the impact of α, k, and n, Eq. (8.29) in such case reduces to the following form

$$\frac{dQ_s(t)}{Q_s(t)} = \left(\frac{\partial Q_s(t)}{\partial \beta}\frac{\beta}{Q_s(t)}\right)\frac{d\beta}{\beta} \tag{8.36}$$

or

$$\frac{dQ_s(t)/Qs(t)}{d\beta/\beta} = \left(\frac{\partial Q_s(t)}{\partial \beta}\frac{\beta}{Q_s(t)}\right) \tag{8.37}$$

Equating Eqs. (8.37) and (8.31) one gets

$$\frac{dQ_s(t)/Qs(t)}{d\beta/\beta} = \beta \ln\left(\frac{kt}{1+kt}\right) \tag{8.38}$$

Analogous to the previous analysis, the left hand side of Eq. (8.38) represents the ratio of error in $Q_s(t)$ to the error in β, and the same is shown in Figure 8.9. It is apparent from the figure that any variation (increase) in β for a given t and k causes $Q_s(t)$ to decrease.

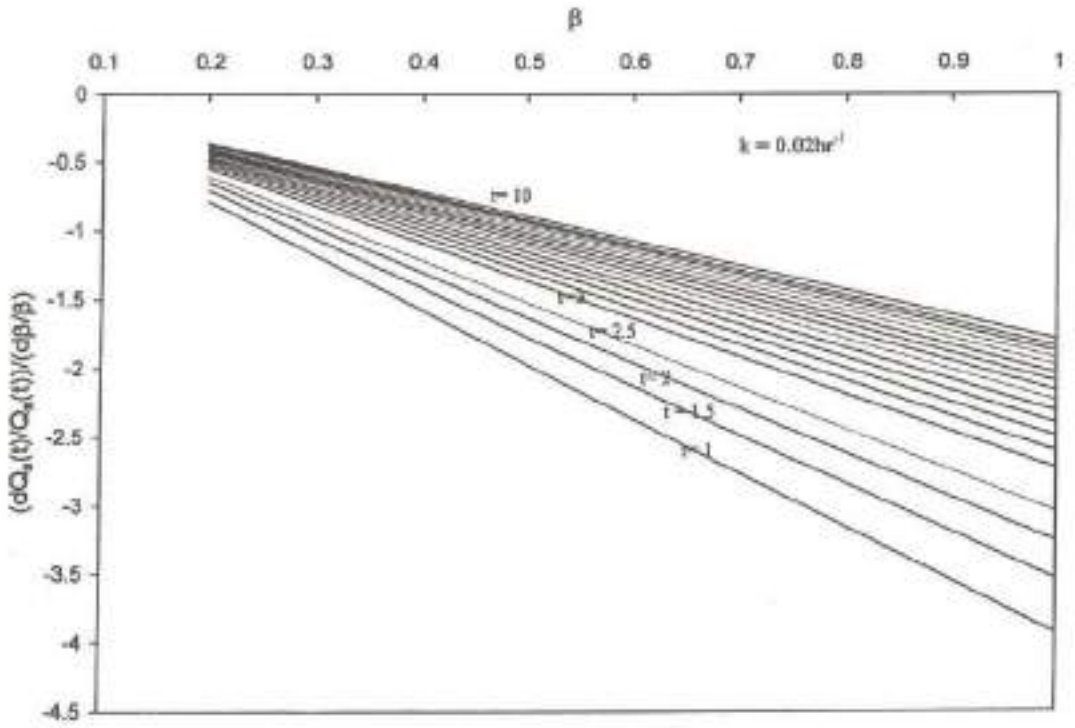

Figure 8.9: Sensitivity of sediment outflow rate to β

8.4.1.3 Sensitivity to k

As above, considering the variation of k only reduces Eq. (8.29) reduces to the following form

$$\frac{dQ_s(t)}{Q_s(t)} = \left(\frac{\partial Q_s(t)}{\partial k}\frac{k}{Q_s(t)}\right)\frac{dk}{k} \tag{8.39}$$

Alternatively, Eq. (8.39) can be expressed as:

$$\frac{dQ_s(t)/Qs(t)}{dk/k} = \left(\frac{\partial Q_s(t)}{\partial k}\frac{k}{Q_s(t)}\right) \tag{8.40}$$

Equating Eqs. (8.40) and (8.32) one gets

$$\frac{dQ_s(t)/Qs(t)}{dk/k} = \frac{\beta}{t(1+kt)} \tag{8.41}$$

As expressed in Eq. (8.41) and shown in Figure 8.10, for any increase in k the ratio of errors tends to decrease, implying the Q_s (t) to increase and vice versa.

8.4.1.4 Sensitivity to n_s

Similar to the preceding analysis, if the variation of only n_s is considered ignoring the impact of α, β, k, Eq. (29) reduces to

$$\frac{dQ_s(t)}{Q_s(t)} = \left(\frac{\partial Q_s(t)}{\partial n_s}\frac{n_s}{Q_s(t)}\right)\frac{dn_s}{n_s} \tag{8.42}$$

Equating Eqs. (8.42) & (8.33) results

$$\frac{dQ_s(t)/Qs(t)}{dn/n_s} = \frac{[(n_s-1)(2-n_s)\ln c-(6-3.5n_s)]n_s}{(n_s-1)^{2.5}}, \text{ where } c = (t/t_{ps})\exp(-t/t_{ps}),\ n_s>1 \quad (8.43)$$

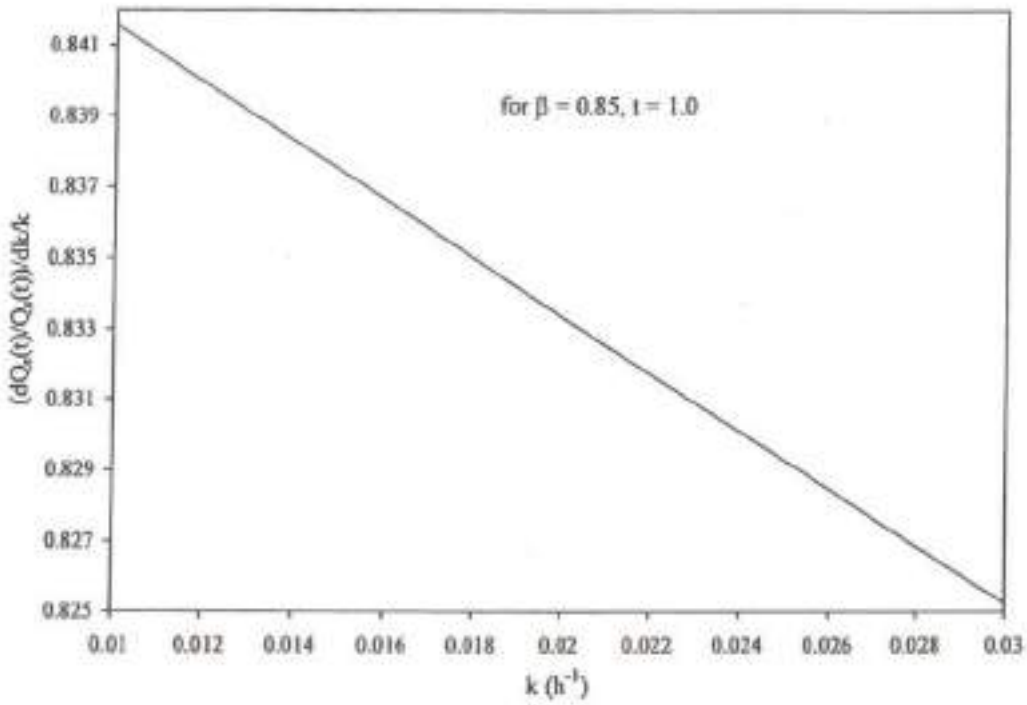

Figure 8.10: Sensitivity of sediment outflow rate to k

Analogous to the previous analysis, the left hand side of Eq. (8.43) represents the ratio of error in $Q_s(t)$ to the error in n_s. It is apparent from Figure 8.11 that any variation (increase) in n_s for a given t/t_p causes the ratio to increase, implying $Q_s(t)$ to increase. Thus the sensitivity analysis shows that any variation (increase or decrease) in parameters 'α' and 'A' will cause a same amount of variation (increase or decrease) in $Q_s(t)$. On the other hand a reverse trend has been observed in the case of parameter β, i.e., for any variation (increase) in β for a given t and k causes $Q_s(t)$ to decrease and vice-versa. A similar trend has also been observed for parameter k, i.e., for any increase in k the ratio of error tends to decrease, implying the Q_s (t) to increase and vice versa. However, in this case rate of change is less as compared to β. The analysis also shows that any variation (increase) in n_s for a given t/t_p causes the ratio to

increase, implying $Q_s(t)$ to increase and vice versa. Overall it can be deduced that parameter β is most sensitive followed by k, α, A, and n_s.

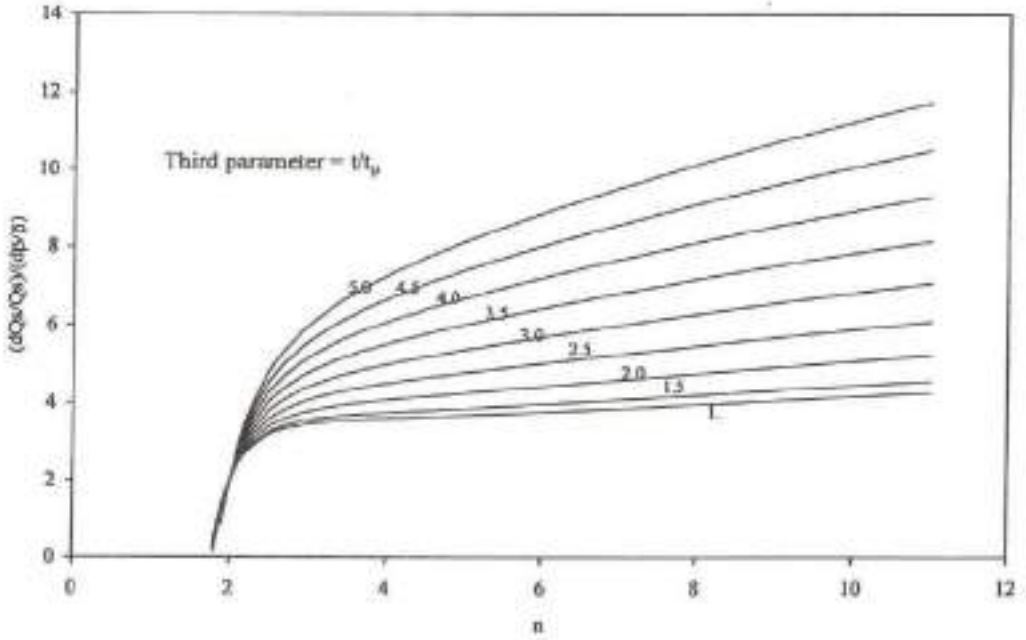

Figure 8.11: Sensitivity of sediment outflow rate to n_s

8.5 CONCLUSIONS

A simple approach incorporating popular and widely used models, i.e., Nash-based IUSG, SCS-CN method, and Power law has been used to develop a simple sediment yield model for computation of sediment graphs. The developed model is mathematically sound and hydrologically improved in the sense that it eliminates the inevitability of a regression based approach used to derive the mobilized sediment and considers rainfall intensity, soil type, land use, hydrologic condition, and antecedent moisture, and thus, physically more plausible than the common and less accurate regression type relations.

A simple relationship has been provided for estimation of number of linear reservoirs (shape parameter, n_s), instead of using graphical and less accurate procedures which are in frequent use. Resulting higher model efficiency (varying from 90.52% to 95.41%) and lower values of relative errors in total sediment outflow

(from 2.49% to 10.04%) and peak sediment flow rate (9.69% to 16.42%) further strengthen the suitability of model for computation of sediment graphs and total sediment outflow. A conventional sensitivity analysis procedure shows that parameter β is most sensitive followed by k, α, A, and n_s. The proposed model has ample scope for estimation of sediment graphs as well as total sediment outflow from ungauged natural watersheds.

CHAPTER 9

IDENTIFICATION OF VULNERABLE AREAS

CHAPTER 9

IDENTIFICATION OF VULNERABLE AREAS

Over the last decade a widely stated objective in land resource management has been the adoption of strategies to ensure the sustainable use of land. The aims of any policy dealing with sustainable use of soils are to maintain soil quality, properties, processes and diversity. At the same time soil erosion continues to degrade the global land resource base with approximately 30 per cent of the present cultivated area having been substantially affected. According to National Commission on Agriculture (Anonymous 1976) 175 million hectares are degraded all over the world. The current rate of annual top soil loss in the world due to water and wind erosion ranging from 20 to 100 tones per ha. This is 16 to 100 times greater than the natural accumulation range, which is estimated at about one centimeter of topsoil formation in 200 years under normal Agricultural practices. Soil erosion rates have increased to such an extent that the material delivery from rivers to the oceans has increased from just 8 billion tons to over 23 billion tons a year, the largest discharge of over 10 billion tones per year coming from Asian rivers alone. If the present trend in the erosion of fertile topsoil of over 23 billion tones per year continues, it will result in the loss of 30 per cent of global soil inventory by 2050.

In recent analysis of annual soil erosion rates in India, it was estimated that about 5334 million tones (1653 tones / ha) of soil is detached annually due to agriculture and associate activities alone. The country's rivers carry about 2052 million tones (626 tones / ha) of this, nearly 1572 million tones are carried away by the rivers into the sea every year and 480 million tones are being deposited in various reservoirs, resulting in the loss of 1 to 2 % of the storage capacity (Anonymous, 1976). Optimal use of soil and land resources to meet the needs of fast growing population is a fundamental issue and promising challenge for the national development.

9.1 SOIL EROSION AND SEDIMENT YIELD

The process of soil erosion involves the processes of detachment, transportation & accumulation of soil from land surface due to either impact of raindrop, splash due to rain impact, shearing force of flowing water, wind, sea waves or moving ice. Erosion due to water is an area of interest to hydrologists and sedimentologists. Various forms of soil erosion due to water are interrill, rill, gully & stream channel erosion. Rain drop plus sheet erosion jointly causes interrill erosion. Concentrated flow causes rill erosion. Gully erosion is an advanced stage of rill on account of head cutting at the gully head. Apart from rainfall and runoff, the rate of soil erosion from the area is also strongly dependent upon its soil, vegetation and topographic characteristics. During the process of erosion and transportation to downstream side, some part of the eroded material may get opportunity to deposit. The net amount of sediment flowing through the watershed is termed as sediment yield.

Deposition of sediment transported by a river into a reservoir reduces the reservoir capacity, thereby adversely affecting the water availability for power generation, irrigation, domestic & industrial use. Sediment deposition on river bed & banks causes widening of flood plains during floods. Control of upland erosion does not always reduce the sediment yield immediately, because of the increased erosivity of channel flow in the downstream. Soil erosion is a serious problem in Lesser Himalayas and foothill ecosystem. Sustainable use of mountains depends upon conservation and potential use of soil and water resources. High population growth has placed a demand on limited natural resources present in the hills. High rainfall coupled with fragile rocks, and high relief conditions in Himalayas are conducive to soil erosion. It is a prime threat to sustained land use for crop production in Himalayan ecosystem. Rapid increase in the developmental activities, mining and deforestation etc. are major factors contributing to soil erosion and thus leading to land degradation.

Empirical models such as Universal soil Loss Equation (USLE) (Wischmeier and Smith, 1965), Revised Universal Soil Loss Equation (RUSLE) (Renard et al., 1991b) and Soil Loss Estimator for Southern Africa (SLEMSA) (Elwell, 1978) as well as physical process based models such as Water Erosion Prediction Project (WEPP) (Nearing et al., 1989), Morgan, Morgan and Finney model (Morgan et al., 1984) and many others are employed for quantitative assessment of soil loss. The soil

loss estimation applying these models indicates the severity of soil erosion under the present land use practices. It aims to identify lands under various kinds of erosion state that serves the basis for planning soil conservation work as well as land use planning. The formulation of proper watershed management programme for sustainable development requires an inventory of the quantitative soil loss erosion and the priority classification of watershed. A watershed with a higher rate of erosion needs to be given higher priority for soil conservation measures to be adopted. Sediment yield from a catchment is one of the main criteria for assessing the vulnerability of a watershed to soil erosion. However, this criterion requires continuous monitoring of sediment samples at the catchment outlet. Such data are hardly available in India and Nepal for small watersheds. Although the sediment yield from large catchment can be obtained from such observations, it is not possible to ascertain the vulnerability to soil erosion of small watersheds within a basin. A soil conservation programme is an expensive and cumbersome process, carried out in steps starting from the most vulnerable (highest sediment producing) region. Therefore, there is a need to assign relative priorities to different regions within a catchment. Development of effective erosion control plans requires the identification of areas vulnerable to soil erosion and quantification of the amounts of soil erosion from various areas. The empirically based USLE and newly revised RUSLE have been used in many countries since the late 1960s for estimation of soil erosion (Wischmeier and Smith, 1978). It is designed to estimate the long-term average annual soil loss for fields with specified cropping and management systems as well as rangeland (Renard et al., 1997). Williams and Berndt (1977) modified the USLE to estimate sediment yield from single storm event. The modified model is referred to as Modified Universal Soil Loss Equation (MUSLE).

9.2 POPULAR EMPIRICAL SEDIMENT YIELD MODELS

A multitude of models are available in hydrologic literature for estimation of soil erosion and sediment yield from watersheds. Most of these models can be grouped in to two broad categories. Models those based on empirical equations generally derived based on analysis of field data are commonly termed as empirical models. Simple methods such as Universal Soil Loss Equation (USLE) (Wischmeier and Smith, 1978), Modified Universal Soil Loss Equation (MUSLE) (Williams, 1975)

or Revised Universal Soil Loss Equation (RUSLE) (Renard et al., 1991), are quite frequently used empirical models for estimation of soil erosion from watersheds (Ferro and Minacapilli 1995; Ferro 1997; Kothyari and Jain, 1997; Ferro et al., 1998; Stefano et al., 1999, Jain and Kothyari, 2000, Kothyari et al., 2002).

The other category of models which use theoretical description of processes involved in the form of mathematical equations are termed as physically based models. These models are intended to represent the essential mechanisms controlling erosion and they incorporate the laws of conservation of mass and energy. Most of them use particular differential equations and generally require more input parameters than empirical models. Numbers of the physical based models are developed in recent past. Examples of physically based models available in literature for estimation of soil erosion are WEPP (Water Erosion Prediction Project, USA) (Nearing et al., 1989), EUROSEM (European Soil Erosion Model), SHESED (Wicks and Bathurst, 1996) and others. The power of physically based models is that they represent a synthesis of the individual components which affect erosion, including the complex interactions between various factors and temporal variability. The result is synergistic, the model as whole represents more than the sum of the individual pieces.

However, the use of physically based models is limited for research use due to their complexity and non-availability of data required to use them. Therefore, empirical models are more commonly in use for field evaluation and modelling for data scarce regions. These are based on inductive logic and generally applicable only to those conditions for which the parameters have been calibrated. Since, this chapter deals with coupling of USLE with GIS for estimation of soil erosion and sediment yield, i.e., to use a empirical model in distributed sense, and hence a brief description of some of the popular empirical models is given here.

USLE: Soil erosion is most frequently assessed by using Universal Soil Loss Equation (USLE) since early 60's. The equation was designed for interrill and rill erosion (Wischmeier and Smith 1978, Renard et al., 1991). Although the equation is described as universal, its database, though extensive, is restricted to slopes normally 0 to 17°, and to soils with a low content of montmorrilonite, it is also deficient in information on erodibility of sandy soils. In addition to the limitation of its database there are theoretical problems with the equation. Soil erosion cannot be adequately described merely by multiplying together six factor values (E = R*K*LS*C*P). There

is considerable interdependence between variables (Morgan, 1995). A flowchart depicting process of using USLE based equations with GIS is shown in Fig. 9.1 as illustration.

MUSLE: It is one of the modified versions of the USLE. In MUSLE (Williams. 1975), the rainfall erosivity factor was replaced by runoff. The runoff factor includes both total storm runoff volume and peak runoff rate. Compared to USLE, this model is applicable to individual storms, and eliminates the need for sediment delivery ratios, because the runoff factor represents energy used in detaching and transporting sediment. The main limitation is that it does not provide information on time distribution of sediment yield during a runoff event.

RUSLE: It is a revised version of USLE, intended to provide more accurate estimates of erosion (Renard et al., 1997). It contains the same factors as USLE, but all equations used to obtain factor values have been revised. It updates the content and incorporates new material that has been available informally or from scattered research reports and professional journals. The major revisions occur in the cover management factor, C, support practice factor, P, and slope length gradient factor, LS, factors. The C is now the product of four sub factors: prior land use; canopy cover, soil surface cover and surface roughness.

MMF Model: is another empirical model for predicting annual soil loss from field-sized area on hill slopes. The model separates the soil erosion process into two phases i.e. the water phases and the sediment phase. In the water phase annual rainfall is used to determine the energy of the rainfall for splash detachment and the volume of runoff, assuming that runoff occur whenever the daily rainfall exceeds a critical value representing moisture storage capacity of the soil-crop complex and that the daily rainfall amounts approximate an exponential frequency distribution. In the sediment phase, splash detachment is modeled using a power relationship with rainfall energy modified to allow for the rainfall interception effect of the crop.

SLEMSA Model: The Soil Loss Estimator for Southern Africa (SLEMSA) was developed largely from data from the Zimbabwe to evaluate the erosion resulting from different farming systems so that appropriate conservation measures could be

recommended. Generally, the model looks like USLE and it has the same limitations as USLE. Empirical Models possess severe limitations. They cannot be universally applied. They are not able to simulate the movement of water and sediment over the land and they cannot be used on scales ranging from individual fields to small catchments.

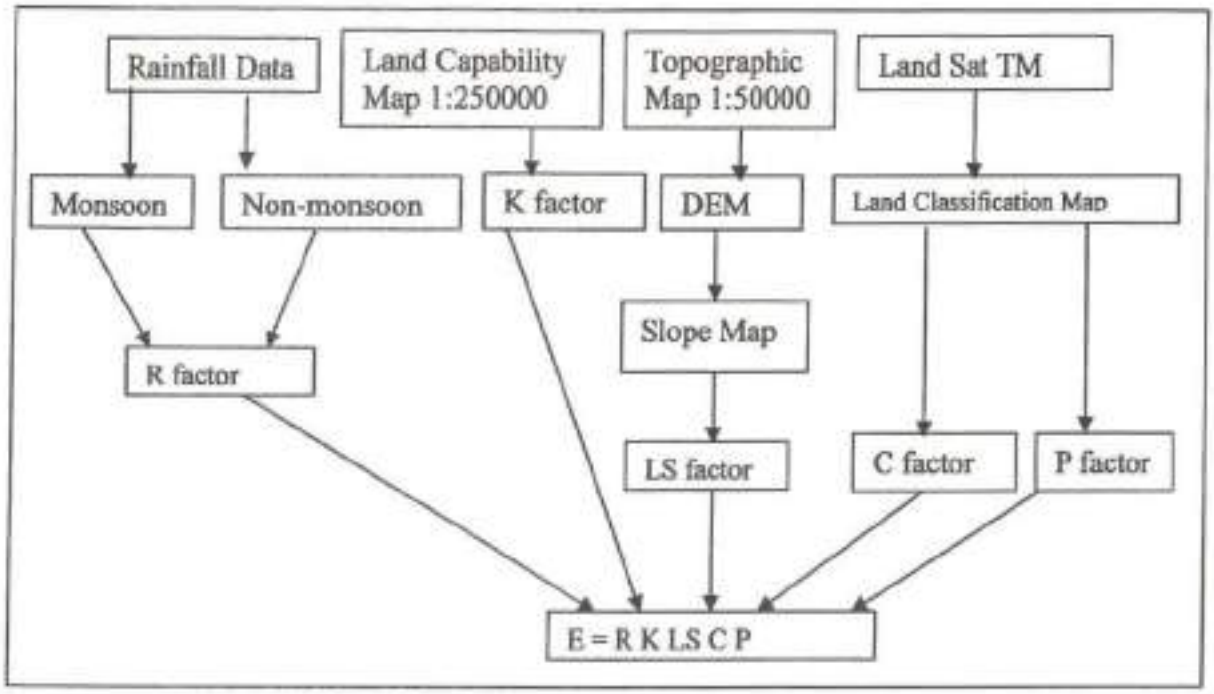

Fig. 9.1: Analysis of flow of USLE model using GIS

9.3 GIS-COUPLED APPLICATIONS OF USLE

A watershed is a land area which drains into a stream system, upstream from its mouth or other designated point of interest. Surface characteristic, soil depth, geological structures, topography and climate of the watershed play an interrelated role in the behavior of water, which flows over or through it. Watersheds are subjected to many types of modifications by human and natural activities. Erosion is a natural geomorphic process occurring continually over the earth's surface. The processes of erosion of soil from earth surface if largely depend on topography, vegetation, soil and climatic variables. These areas found to have pronounced spatial variability in a catchment due to the spatial variation of climatic factors and

catchment heterogeneity. This is one of the reasons given for promoting the use of distributed information of catchment resources using a GIS. By using a GIS the catchment is discretized into sub-areas having approximately homogeneous characteristics and rainfall distribution. The technique of Geographical Information System (GIS) is well suited for quantification of heterogeneity in the topographic and drainage features of a catchment (Shamsi, 1996; Rodda et al., 1999). The remote sensing and GIS techniques have been used for sediment and erosion medaling across the globe (Jain and Kothyari, 2000; Jain et al., 2001; Kothyari et al., 2002; Sarangi & Bhattacharya, 2000; Fistikoglu and Harmancioglu, 2002; Paringitand & Nadaoka, 2003; Chakraborty et al., 2004; Kumar and Sharma, 2005). These models simulate the dynamics of event runoff, soil detachment and transport processes.

Jain and Kothyari (2000) demonstrated the utility of GIS and satellite data in identification of source areas and prediction of storm sediment yield from catchments. The concept of sediment delivery ratio with USLE was used in the study for Karso and Nagwa watersheds in Jharkhand. With the same watersheds and concept of sediment delivery ratio, Kothyari et al. (2002) estimated the temporal variation in sediment yield. Jain et al (2001) coupled USLE and MMF models with GIS for estimation of soil erosion and its spatial distribution for a Himalayan watershed. It was found that GIS platform provides a faster and better method for spatial modeling and gives output maps that can be understood better. Jain and Goel (2002) used these techniques for the assessment of vulnerability of 16 watersheds in the Western India to the soil erosion. The study was reported for catchment of Ukai dam in Gujarat. Fistikoglu & Harmancioglu (2002) integrated a GIS with the USLE model for identification of rainfall based erosion and the transport of non point source pollution loads. They found that GIS permits more effective and accurate applications of the USLE model for small watersheds provided that sufficient spatial data are available.

9.4 OBJECTIVES

The main objectives of this study are:

1. To assess annual rate of soil erosion from the Chaukhutia and Naula watersheds using distributed information for topography, land use, soil etc. derived using GIS.

2. To compute the transport capacity of discretized locations and route the transport limited sediment outflow from each of the discretized cells to the catchment outlet.
3. To compare the simulated sediment yield with the observed sediment yield.
4. To generate maps for sediment outflow from discretized cells.
5. To analyze the rate of soil erosion/deposition maps, and thus identification of areas vulnerable to soil erosion within the watershed.
6. To assess annual rate of soil erosion from catchments using distributed information for topography, land use, soil etc. derived using a GIS.
7. To compute the transport capacity of discretized locations and route the transport limited sediment outflow from each of the discretized cells to the catchment outlet.
8. To compare the simulated sediment yield with the observed sediment yield.
9. To generate maps for sediment outflow from discretized cells.
10. To analyze the rate of soil erosion/deposition maps and then identify areas vulnerable to soil erosion.

In brief, this chapter identifies vulnerable areas from the estimates of soil erosion and sediment yield derived using remotely sensed data and GIS coupled with empirical USLE model.

9.4.1 General Layout

To achieve the aforementioned objectives, the procedural steps are as follows:

1. Calculate Rainfall Erosivity factor, R, from meteorological data
2. Calculate sediment yield from meteorological data
3. Generate Digital Elevation Model (DEM) for the Watershed Study Area
4. Generate Slope, Flow accumulation , Flow direction, and Watershed Network
5. Generate Topographic factor LS Map
6. Generate Land Use Map of study area using digital analysis of satellite data
7. Create Soil Map and its characteristics Database from Satellite data in GIS Environment using ERDAS
8. Generate Cover Management factor C Map
9. Generate Support Practice factor P Map

10. Generate Soil Erodibility factor K Map
11. Generate map for sediment transport capacity
12. Generate maps for transport limited soil accumulation by routing sediment outflow from each of the discretized cells using GIS
13. Generate soil erosion/deposition maps for identification of vulnerable areas.

9.5 MODELLING CONCEPT AND MODEL FORMULATION

Apart from rainfall and runoff, the rate of soil erosion from an area also strongly depends on its soil, vegetation and topographic characteristics. In real situations, these characteristics are found to greatly vary within the various sub-areas of the catchment. Therefore, a catchment can be discretized into various smaller homogeneous units before making the computations for soil loss. The grid based discretization is the most reasonable procedure in both the process-based models and the other simple models (Beven, 1996; Jain and Kothyari, 2000). Therefore, for present study, the grid-based discretization procedure has been adopted. Grid size to be used for discretization should be small enough so that the grid encompasses a hydrologically homogeneous area. As discussed above, the method such as the Universal Soil Loss Equation (USLE) is employed to estimate surface erosion over small size areas, i.e. soil erosion within a grid (or cell).

9.6 Universal Soil Loss Equation (USLE)

The Universal Soil Loss Equation (USLE) is an empirical equation designed for the computation of average soil loss in agricultural fields in USA. However, these days it has globally been accepted as most popular model for erosion prediction and conservation planning technology. The equation predicts losses from sheet and rill erosion under specified conditions. It computes the soil loss for a given site, as product of six potential parameters, whose most likely values at particular location can be expressed numerically (Wischmeier and Smith, 1978; Renard et al., 1991) as:

$$E = R * K * LS * C * P \qquad (9.1)$$

where E is computed soil loss per unit area, expressed in the (tone / ha / yr);

R is rainfall erosivity factor, (MJ*mm / ha*hr);

K is soil erodibility factor, (tone*ha*hr / ha*MJ*mm);

L is slope length factor, (dimensionless);

S is slope steepness factor, (dimensionless);

C is cover and management factor, (dimensionless);

P is support practice factor, (dimensionless);

9.6.1 Rainfall Erosivity Factor, R

Wischmeier and Smith (1958) after evaluation of correlations between soil erosion and a number of rainfall parameters, defined the R factor as the product of rainfall energy and maximum 30-min intensity divided by 100 for numerical convenience, known as the EI_{30} index. On an annual basis, the EI_{30} value is the sum of values over the storms in an individual year. Calculations of rainfall energy require an algorithm relating energy to some measurable paramcter. Up to an intensity of 3 in/hr, rainfall energy increases with storm intensity as a result of the fact that the drop size and fall velocity increase with intensity. Above 3 in/hr, the drop size reaches its maximum size and energy remains constant.

Wischmeier and Smith (1958) proposed that rainfall energy is related to intensity as:

$$E_i = (200 + 87 \log_{10} I_i) P_i \qquad (9.2)$$

where E_i = Kinetic energy of the i^{th} rain increment, J/m^2

I_i = Average intensity of rainfall intensity in the i^{th} increment, cm/hr

P_i = Depth of rainfall in the i^{th} increment, cm

$$R = \sum \text{Erosion index} = \sum_{i=1}^{n} \left(\frac{E_i I_{30}}{100} \right) \quad \text{in} \quad \frac{MJ - mm}{ha - hr} \qquad (9.3)$$

$E = \sum E_i$ = Kinetic energy of rainfall, J/m^2

I_{30} = Maximum intensity of rainfall during a continuous period of 30 minutes, mm/hr

n = Number of rainstorms per year

R = Rainfall Erosivity Factor

Rambabu et al. (1979) developed rainfall intensity-duration-return period relationships for Indian conditions (Fig. 9.2), which can be used with fair accuracy. In these relations (Fig. 9.2), T is the return period (20-25 yr) and t is the duration of rainfall. Furthermore, for Indian conditions, the values of the coefficients a, b, m and n for five zones i.e., North, South, East, West and Centre are given in Table 9.1.

The selection of maximum intensity of rainfall for duration of 30 minutes by Wischmeier and Smith (1978) was based on extensive experimental results. Incidentally, this value has been found to be equally applicable to many parts of India, including Dehradun, by the Central Soil and Water Conservation Research and Training Institute, Dehradun (CSWCRTI). In some tropical and subtropical countries of Asia and Africa, it has been reported that the kinetic energies of individual storms, at intensities 25 mm/hr. are more appropriate for correlating the soil loss. By using this method, only the EI values are required to be considered and not the EI_{30} values.

Table 9.1: Data for intensity-Duration-Return Period Relationships for India

Zone	a	b	m	n
North	5.914	0.500	0.152	1.013
East	6.933	0.501	0.135	0.88
Centre	7.465	0.75	0.171	0.96
West	3.97	0.15	0.165	0.733
South	6.31	0.50	0.152	0.947

9.6.2 Soil Erodibility Factor K

A number of studies of soil erodibility have been made with the USLE. In the USLE, K is assumed to be constant throughout the year. Tables of K values are available from local Soil Conservation Service Offices for most soils in the U.S. In the absence of published data, a widely used relationship for predicting erodibility is a nomograph by Wischmeier et al. (1971), which was developed from the data collected on 55 mid-western agricultural soils. Soil erodibility in the nomograph is predicted as a function of five soil and soil profile parameters as:

1. Percentage silt (MS; 0.002-0.05 mm)
2. Percentage very fine sand (VFS; 0.05-0.1 mm)
3. Percentage sand (SA; 0.1-2 mm)
4. Percentage organic matter (OM)
5. Structure (S_1)
6. Permeability (P_1)

It is important to note that the size ranges given here are not standard for some particle classifications. Codes for structure and permeability are given in USDA soil survey manuals (Soil Conservation Service, 1983) available for most countries in the U.S. and in some foreign countries.

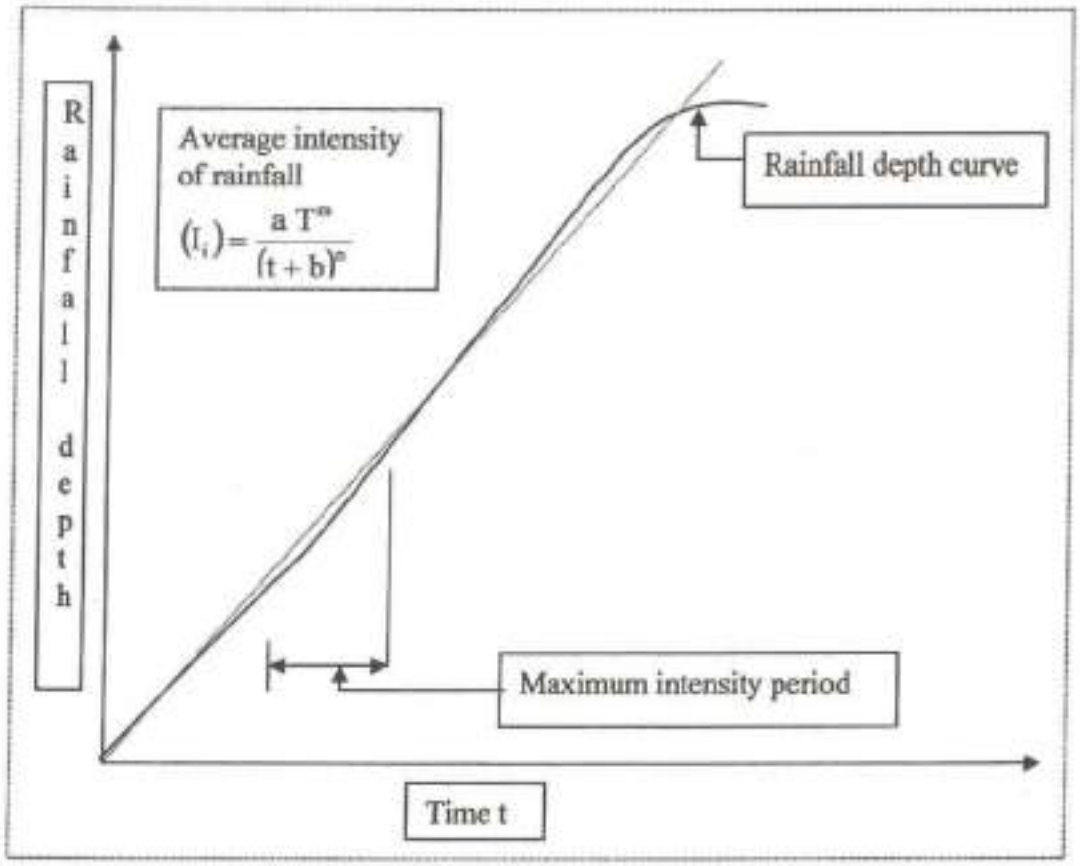

Fig. 9.2: Rainfall Intensity-Duration-Return Period Relationships for Indian Condition

An analytical relationship for the nomograph can be given by the regression equation as Wischmeier et al. (1971):

$$K = \frac{2.1*10^{-4}(12-OM)M^{1.14} + 3.25(S_1 - 2) + 2.5(P_1 - 3)}{100} \quad (9.4)$$

where K is soil erodibility in tons per acre per unit rainfall index (tons-acre-hr/hundreds-acre-ft-tonsf-in), OM is the percentage organic matter, P_1 is the permeability index, S_1 is the structure index, and M is a function of the primary particle size fractions given as:

$$M = (\%\ MS + \%\ VFS)\ (100 - \%\ CL) \quad (9.5)$$

where % CL is percentage clay (<0.002 mm) and other terms are defined as above. The soil erodibility factor K (t*ha*hr / ha*MJ*mm) has been estimated using table values based on the soil textural information given by Haan (1994).

9.6.3 Length and Slope Factors, LS

For computation of LS factor, in a grid-based descretized area as shown in Fig. 9.3, the minimum cell area of about 0.01 km^2 is required to have a representative estimate of LS factor for use in the USLE (Wischmeier and Smith, 1978; Panuska et al., 1991). With this area the maximum permissible length is 141 meters (Panuska et al., 1991) However, cell size smaller than this is to be used for soil loss estimation using GIS. An equation was derived based on unit stream power theory by Moore and Burch (1986a,1986b), Moore and Wilson (1992) for estimating the LS factor in cells smaller than the plots of Wischmeier and Smith (1978). The factor LS in present study is therefore computed for overland grids by using the relationship given by Moore and Wilson (1992) as:

$$LS = \left[\frac{A_s}{22.13}\right]^m \left[\frac{\sin\beta}{0.0896}\right]^n \quad (9.6)$$

where A_s is the specific area (=A/b), defined as the up slope contributing area for overland grid (A) per unit width normal to flow direction (b); β is the slope gradient in degrees; n = 0.4; and m = 1.3. For channel grid areas, the value of A is considered to be equal to the value of the threshold area corresponding to the channel initiation. The use of Eq. (9.6) in the estimation of the LS-factor allows the introduction of the three-dimensional hydrological and topographic effect of converging and diverging terrain on soil erosion (Panuska et al., 1991; Mendicino and Sole, 1997).

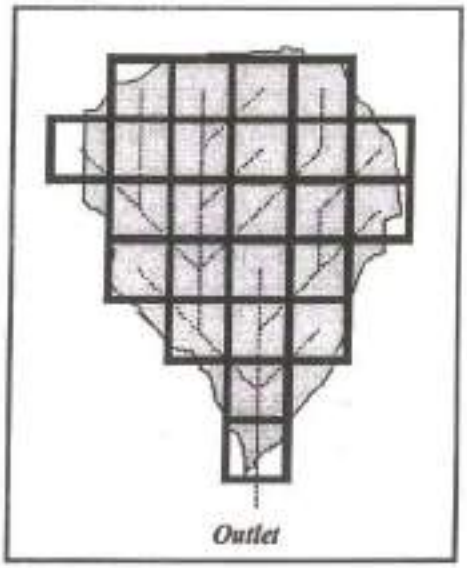

Fig. 9.3: Schematic showing discretized grid cells in a catchment

9.6.4 Cover and Management Factor, C

The cover and management factor is the ratio of soil loss from an area with specified cover and management to that of an identical area in tilled continuous fallow. Vegetative cover dissipates the impact force of raindrops on the soil surface, and protects the soil from splash erosion by modifying the value of volume, drop size, Coefficient of distribution, impact velocity and kinetic velocity of rainfall. The canopy cover is primarily responsible for effectiveness of the vegetative cover. The quality of the cover depends on the foliage characteristics, plant height and the area covered by the vegetation, whereas the leaf area index, height and density of the canopy, foliage characteristics, and the area covered by different species are affected

by the type of vegetation. Splash erosion is caused not only by the direct impact of raindrops on the bare soil surface, but also by the through fall of raindrops from the canopy cover. A dense vegetative cover provides a high protective cover to the ground surface, but a higher height of the canopy, namely from pines, etc. imparts a high terminal velocity to drops of the through fall, which caused heavy soil erosion by splash on the soil surface. The crop cover-management factor C accounts for the effects of cover, crop sequence, and productivity level, length of growing season, tillage practices, residue management, and expected time distribution of erosive events. Based on experimental investigations, values for C factor have been tabulated for many cover conditions (ex. Haan, et al., 1994).

9.6.5 Support Practice Factor, P

The conservation practice factor, P, by definition is the ratio of soil loss from any conservation support practice to that with up and down slope tillage. It is used to evaluate the effects of contour tillage, strip cropping, terracing, subsurface drainage, and dry land farm surface roughening. A bare fallow land surface causes maximum soil erosion especially when it is cultivated up and down the slope or in other words, cultivated across the contours of the land surface. When a sloping land is put under cultivation, it needs to be protected by practices that will attenuate the runoff velocity, so that much less amounts of soil are carried away by the runoff water. P is always ≤ 1.0. In areas with more than one type of practice in use, a weighted value of P as per the area under each practice is considered and *P* is the support practice factor-the ratio of soil loss with a support practice like contouring, strip-cropping, or terracing and down the slope. Based on experimental investigations, values for P factor have been tabulated for many management conditions (ex. Haan, et al., 1994).

9.7 SEDIMENT TRANSPORT AND OUTFLOW

Use of Eq. (9.1) produces the estimate of gross soil erosion in each of the discretized grids of the catchment. Gross amount of soil erosion for each grid area during a year can be generated by multiplying the term KLSCP with the R-factor for the corresponding year. The eroded sediment from each grid follows a defined drainage path – as shown in Fig. 9.4 for a particular cell – to the catchment outlet. The

rate of sediment transport from each of the discretized cell depends upon the transport capacity of the flowing water (Meyer and Wischmier, 1969). The sediment outflow from an area is equal to soil erosion in the cell plus contribution from upstream cells if transport capacity is greater than this sum. However if transport capacity is less then amount of sediment excess of transport capacity get deposited and sediment load equal to transport capacity is discharged to next downstream cell. The concept is shown schematically in Fig. 9.5 (after Meyer and Wischmier, 1969).

9.7.1 Mean Annual Sediment Transport Capacity

The rate of transport of the sediment is governed by the transporting capacity of the flowing water. Most geomorphologic models assume that overland flow is transport limited accumulation and sediment flux Q is mainly predicted by the equation given as:

$$Q = K^*L^*S^n \tag{9.7}$$

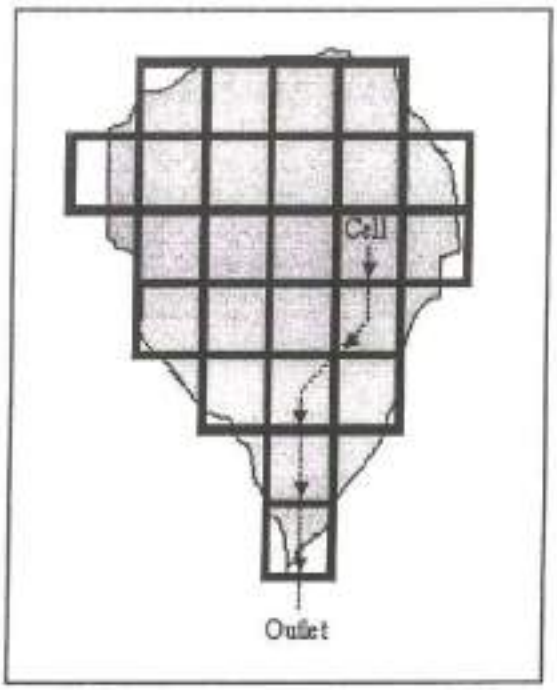

Fig. 9.4: Schematic showing a flow path

where L is the upslope distance (m) and S the local slope gradient (m m^{-1}). For three-dimensional landscapes (Kirkby and Chorley, 1967; Carson and Kirkby, 1972), this equation becomes:

$$Q = K*S*A^m \quad (9.8)$$

where A is the upslope contributing area per unit of contour length. Prosser and Rustomji (2000) made a review on the constants m and n, and found that the median value obtained in experimental studies is 1.4 for both constants. This concept was further studied by Verstraeten et al. (2007) and based on their hypothesis following equation for mean sediment transport capacity was proposed and the same is adopted in this study as:

$$TC = K_{TC}*R*K*A^{(1.44)}*S^{(1.44)} \quad (9.9)$$

where TC is transport capacity ($kg/m^2/yr$). K_{TC} is the transport capacity coefficient and reflects vegetation component within the transport capacity and S the slope gradient.

9.7.2 Transport Limited Accumulation (TLA)

Sediment is routed along the runoff pattern towards the river (Figs. 9.4 & 9.5), taking into account the local transport capacity, TC of each pixel. If the local TC is smaller than the sediment flux, then sediment deposition is modeled. This approach assumes that sediment transport is not necessarily restricted to a transport limited system. If the TC is higher than the sediment flux, then sediment transport supply will be limited. Thus, by introducing the K_{TC}, transport capacity coefficient, a more realistic representation of overland flow along with sediment transport can be simulated. Because much sediment is being routed to these locations from the steeper hill slopes adjoining the thalwegs, it faces high sedimentation rates because the transport potential will also be rather low. The predicted sediment delivery values need to be interpreted as sediment delivery towards the complete length of the river in the catchment. The model produces different maps of erosion, sediment transport and sediment deposition rates, whereby a distinction is made between gross erosion, net

erosion, total sediment deposition and net sediment deposition. Consequently, different total values of erosion and soil loss can be defined.

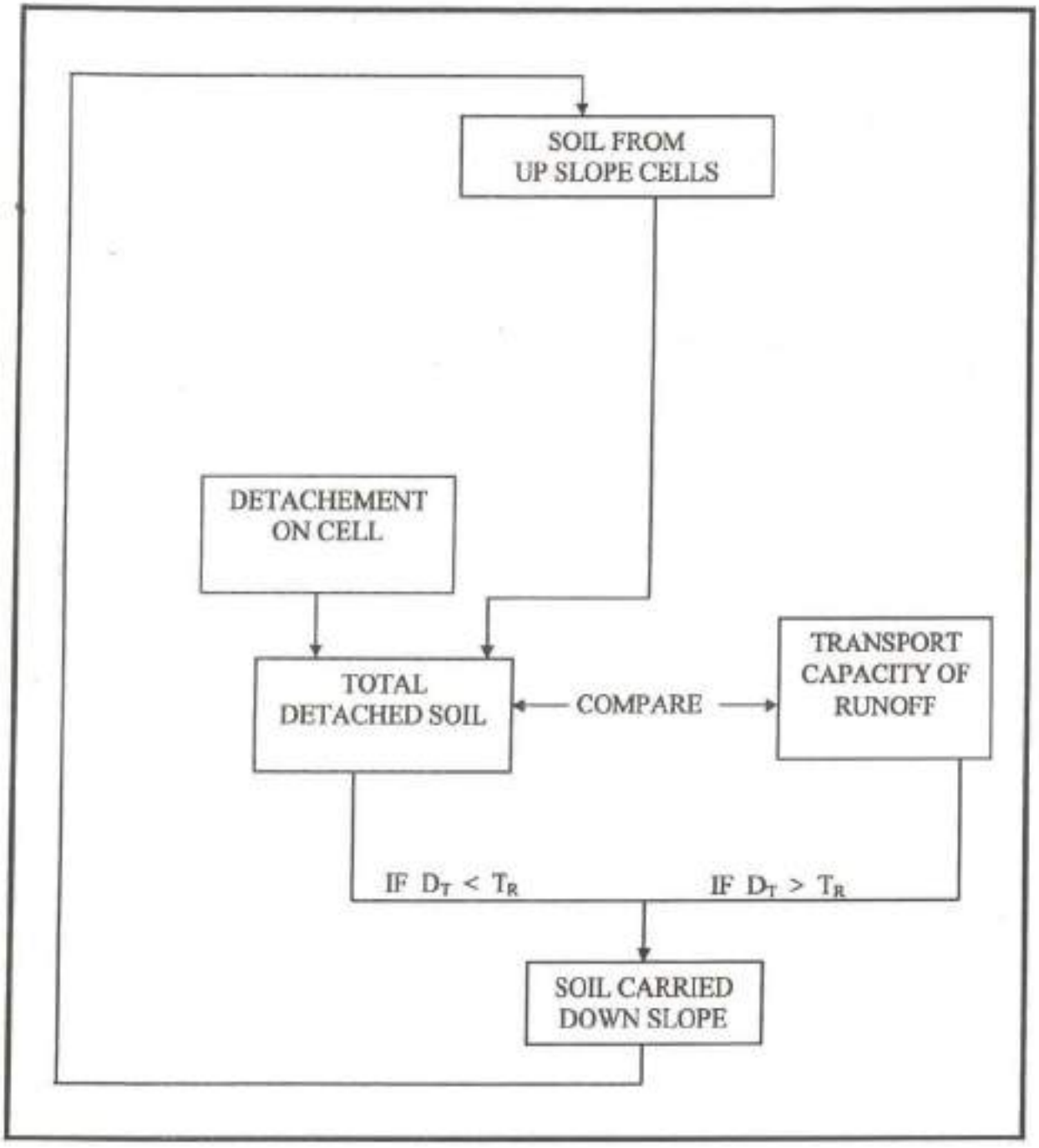

Fig. 9.5: Concepts of Mathematical Modelling of the Process of Soil Erosion by Flow of Water (Meyer and Wischmeier, 1969)

For grid based discretization system transport limited accumulation can be computed as:

$$T_{out} = \min(E + \sum T_{in}, TC) \quad (9.10)$$

$$D = E + \sum T_{in} - T_{out} \quad (9.11)$$

where E = Annual Gross Soil Erosion

TC = Transport Capacity

Tin = Sediment inflow from upstream cells

Tout = Sediment Outflow from the cell

D = Deposition in cell

9.8 STUDY AREA AND DATA AVAILABILITY

In this study, the Chaukhutia and Naula watersheds of Ramganga catchment have been selected to estimate the spatially distributed soil erosion and sediment yield using USLE and GIS. A basic description of the Chaukhutia and Naula watersheds has been given in Chapter 2. However, as per the data specific requirements, a brief description about sediment data is discussed for Chaukhutia watershed only, as the above methodology is first employed to this watershed, and then repeated on Naula watershed.

There is a stream gauging station for measuring runoff and sediment outflow at Chaukhutia Site. The geographic location of this stream gauge station bears latitude of 29°53'10" and longitude of 79°20'40" and this is situated at an altitude of 939.05 m above mean sea level. Daily sediment data from January 1973 to December 1990 was collected from irrigation department, site office Kalagarh. The daily sediment yield data was aggregated to annual series and used in present investigation.

9.9 PREPARATION OF DATABASE FOR CHAUKHUTIA WATERSHED

Computation of soil erosion and sediment yield using the method formulated, and as described above, requires spatial data of Digital Elevation Model (DEM), soil and landuse maps in digital form. In subsequent sections, generation of this database is discussed in a systematic manner.

9.9.1 Digital Elevation Model (DEM) Generation

Digital Elevation Model (DEM) is sampled array of elevations (z) that are spaced at regular intervals in the x & y directions. The various input data are:

- Topographic map
- Data collected by GPS, Total Station
- Stereo Photographs / aerial photographs
- Stereo Satellite images
- Different radar images (LIDAR, IFSARE)

Mainly, there are two ways to generate DEM

- Through raster data by Interpolation
- Through vector data by TIN

9.9.1.1 Generation of DEM and Drainage Network

Add Registered Topographic maps in Polyconic projection system to the Arc Map window in Arc GIS. Create a shape file assigning the same coordinate system as that of registered Toposheet (By importing it). Digitize all the contours of the toposheet. Add "Contour Elevation" as new field to its attribute table and fill up all the contour elevation values against each digitized contour by highlighting them. Repeat above steps for all available toposheets in which study areas lies.

Then Open Arc Toolbox and go to

- 3D Analyst Tools
- Raster Interpolation
- Topo to Raster

Topo to Raster dialog box will be open in which we can add all the digitized Contour layers by changing attribute field to "Contour Elevation" and the tool interpolate contours into DEM of desired pixel size. For the present study a pixel size of 24 m was selected. Following the FLOWCHART shown in Fig 9.6, a DEM of Chaukhutia watershed was generated as shown in Fig. 5.4. Fig. 5.3 shows generated drainage network for the Chaukhutia watershed.

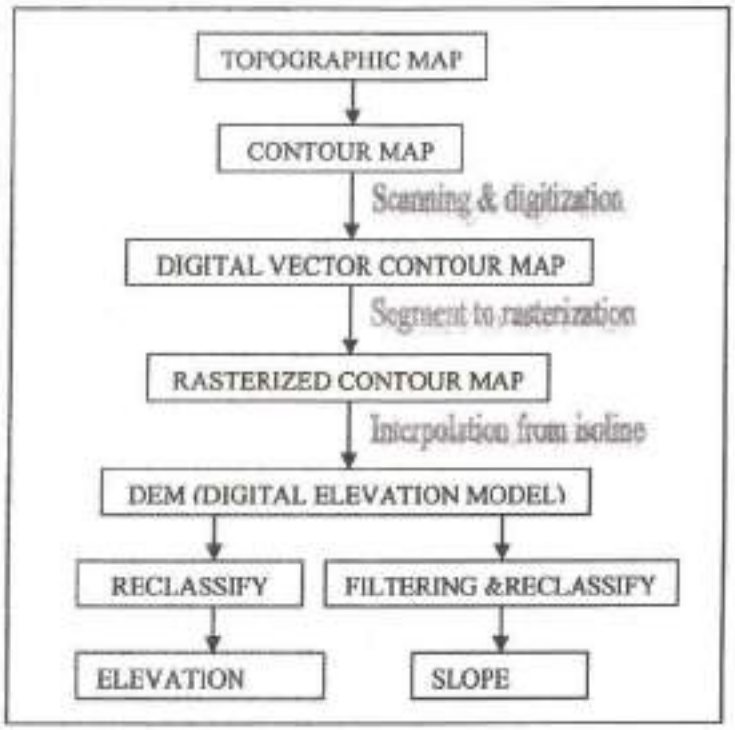

Fig. 9.6: DEM & Slope Generation

9.9.2 Land Use / Land Cover Classification

Satellite data of IRS LISS III sensor was geo-referenced and classified in order to obtain land use/land cover map of the study watershed. In this study unsupervised classification has been carried out to prepare the land use / land cover maps. In unsupervised classification clustering of data is done for given input number of clusters. These clusters are then reclassified into desired number of classes using merging operation. The Chaukhutia sub-catchment has been classified into following seven major land use / land cover classes after merging different clusters. Classified landuse map of the Chaukhutia watershed is shown in Fig. 5.2.

9.9.3 SOIL MAP

The soil map of the present study area was digitized using GIS Software 9.0 version after scanning hardcopy of soil map of the Chaukhutia watershed available from National Bureau of Soil Survey and Land Use Planning, Govt. of India. The

digitized polygon map was then rasterized at 24 m grid cells by using GIS Arc Toolbox. The digitized soil map of the Chaukhutia watershed is shown in Fig. 5.1.

9.10 APPLICATION PROCEDURE, RESULTS & DISCUSSION

As Above, database preparation included generation of spatial data for Digital Elevation Model (DEM), drainage, soil and landuse maps. This sections deals with generation of soil erosion in spatial domain which requires generation of different factor maps in spatial domain. As discussed above, USLE has been used as soil erosion and sediment yield model.

9.10.1 Computation of Rainfall Erosivity Factor, R

The daily rainfall data from year 1973 to 1990 except for year 1974 for Chaukhutia catchment was available. The kinetic energy of daily rainfall was calculated using equation (2). I_{30} was calculated as per concept given by Rambabu et al. (1979) for Indian condition. Then rainfall erosivity factor, R was calculated using Eq. (9.3). The output of R-values for eighteen years i.e. from 1973 to 1990 is presented in Table 9.2.

Table 9.2: Computed rainfall erosivity factor

Year	R [(MJ*mm)/(ha*hr)]	Year	R [(MJ*mm)/(ha*hr)]
1973	4451.11	1982	2211.67
1974	*	1983	2878.17
1975	4047.36	1984	1382.54
1976	3617.62	1985	2071.04
1977	4736.04	1986	4852.98
1978	3431.31	1987	3016.28
1979	1710.64	1988	4843.55
1980	3313.94	1989	3031.21
1981	1716.98	1990	5589.18

* Data not available

9.10.2 Computation of Soil Erodibility Factor, K

The soil map of Chaukhutia catchment dominantly consists of seven categories of soils. The soil erodibility factor, K is dependent on soil profile and the response of the soil to the erosive action of rainfall. The soil erodibility (K) factor identifies the inherent susceptibility of a soil to erode under a standard condition, based on a multivariate nomograph of values for soil structure, permeability, organic matter, and percentage of sand and silt fractions. The soil erodibility factor K (t*ha*hr / ha*MJ*mm) for different type of soil is adopted from Haan et al. (1994). The K factor values are presented in Table 9.3.

Table 9.3: K-Factor for Soil

Type of soil	K (t*ha*hr / ha*MJ*mm)
Thermic fine loamy to loamy skeletal soils	0.020
Thermic loamy skeletal to fine loamy soils	0.023
Thermic to coarse loamy soils	0.032
Thermic sandy skeletal soils	0.042
Thermic coarse to fine loamy soils	0.049
Thermic skeletal to coarse loamy soils	0.057
Thermic coarse to fine loamy soils	0.057

The K factors presented in Table 9.3 were added in the attribute of soil theme's table of Soil Map by opening ERDAS. The output K factor map is presented in Fig. 9.7.

9.10.3 Computation of Topographic Factor, LS

These DEMs were further analyzed to remove pits and flat areas to maintain continuity of flow to the catchment outlets. Using Eq. (9.6), the slope length and gradient factors are linked and, therefore calculated together where flow accumulation is a grid theme of flow accumulation expressed as number of grid cells. The output LS factor map is presented in Fig. 9.8.

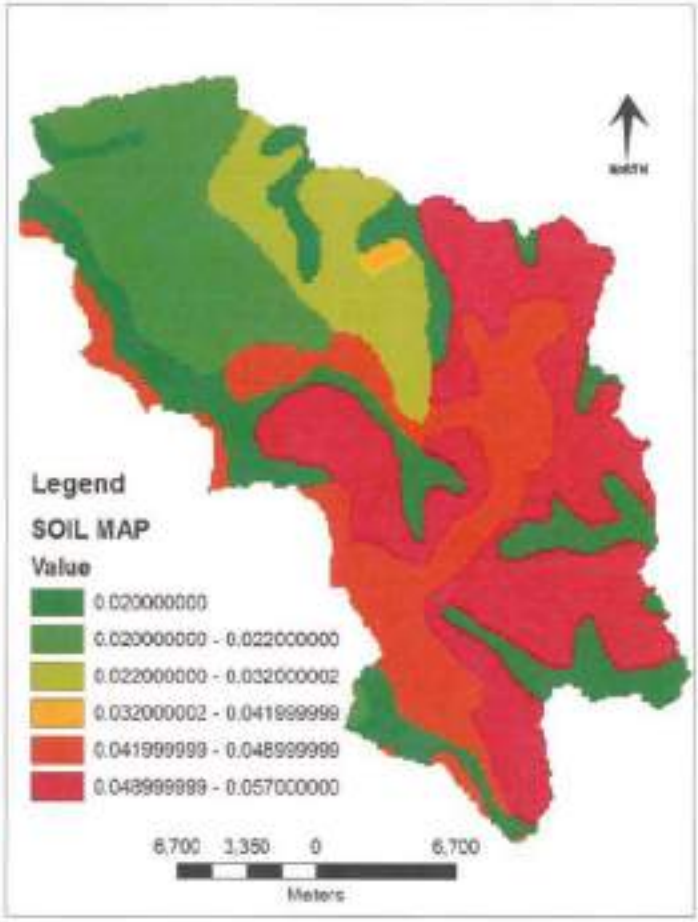

Fig. 9.7: K-Factor Map

9.10.4 Computation of Cover and Management Factor, C

The Chaukhutia catchment has been divided into 7 major coverage's namely cropland, pasture, and forest, road, settlement, rocky and fallow lands. Vegetation cover and cropping systems have a large influence on runoff and erosion rates. Soil erosion can be limited with proper management of vegetation, plant residue and tillage. The crop management factor can be determined with the use of land cover data. A lower C-value represents a cover type that is more effective at defending against soil erosion. The factor C for different type of land cover is taken from Haan et al., (1994) and is presented in Table 9.4. C-factor is added as a field values of given classes of Land use Map by ERDAS 8.5.Version. The map of C factor is presented in Fig. 9.9.

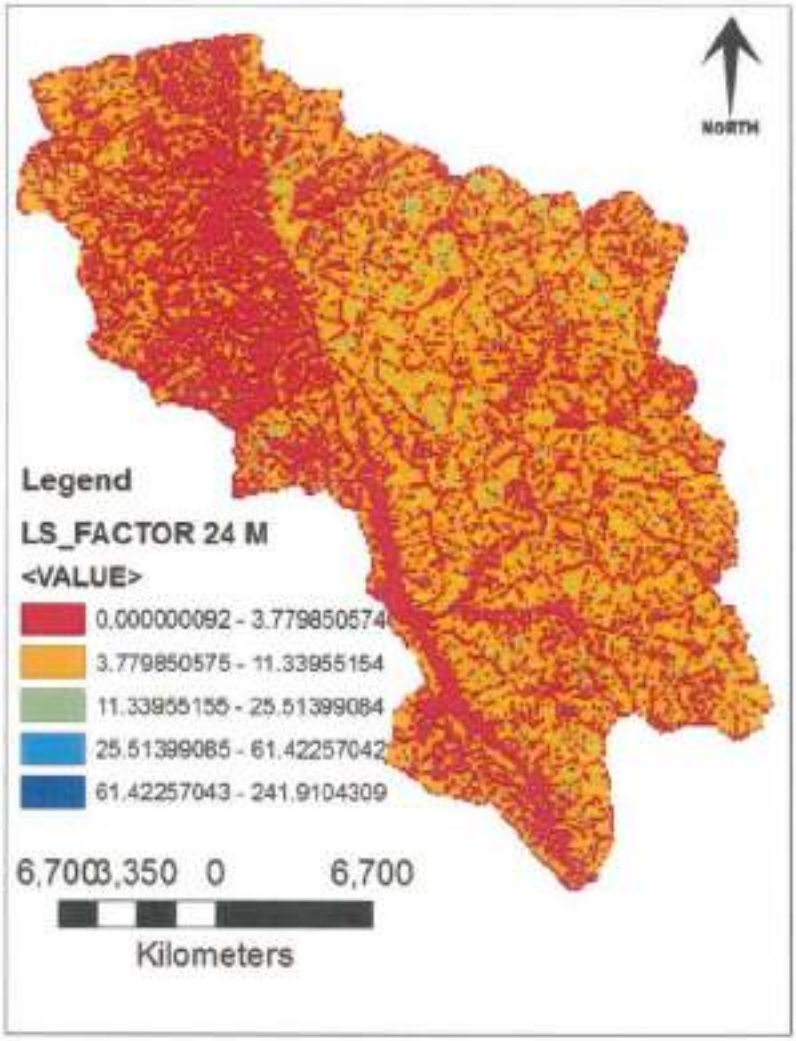

Fig. 9.8: LS-Factor Map

Table 9.4: C factor and P factor related to Land use / Land cover

Land use / Land cover	C factor	P factor
Agriculture	0.34	0.9
Fallow	0.13	1
Undisturbed Forest	0.003	1
Pasture	0.20	1
River	0.13	1
Road	0.13	1
Settlement	0.13	1

9.10.5 Computation of Support Practice Factor, P

The Chaukhutia catchment has been divided into 7 major coverage's namely cropland, pasture, and forest, road, settlement, rocky and fallow lands. The

conservation practices factor takes into account the effects of support and practice management measures which work to reduce the effects of soil erosion. A lower P-value represents a more effective conservation practice. The P factor can be obtained from tables or using the USLE program given information about land use and management. The factor P for different type of land cover is taken from Haan et al. (1994) and is presented in Table 9.4. P factor values are added in the attribute field of land use Map by ERDAS 8.5.Version. The P factor map is presented in Fig. 9.10.

9.11 GENERATION OF THE EROSION POTENTIAL MAPS

The land use, soil, slope steepness and management parameters are the main factors governing soil erosion potential at particular location to the erosive power of rainfall erosivity. The maps for values of USLE parameters, Viz., K, LS, C and P were integrated by GIS Raster Calculator to form a composite map of watershed system. The map of composite parameters KLSCP represents the soil erosion potential of different grid cells as shown in Fig. 9.11. A high value of this term indicates a higher potential of soil erosion in the cell and vice versa.

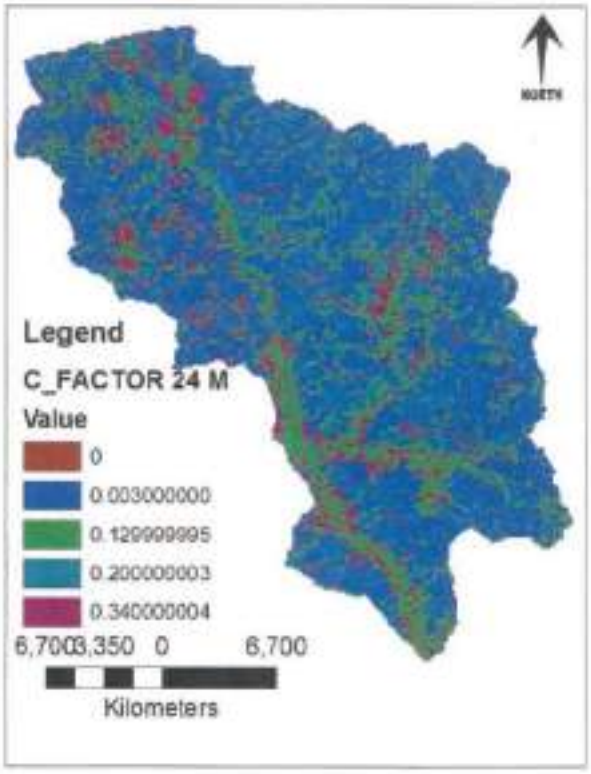

Fig. 9.9: C-Factor 24 m Map

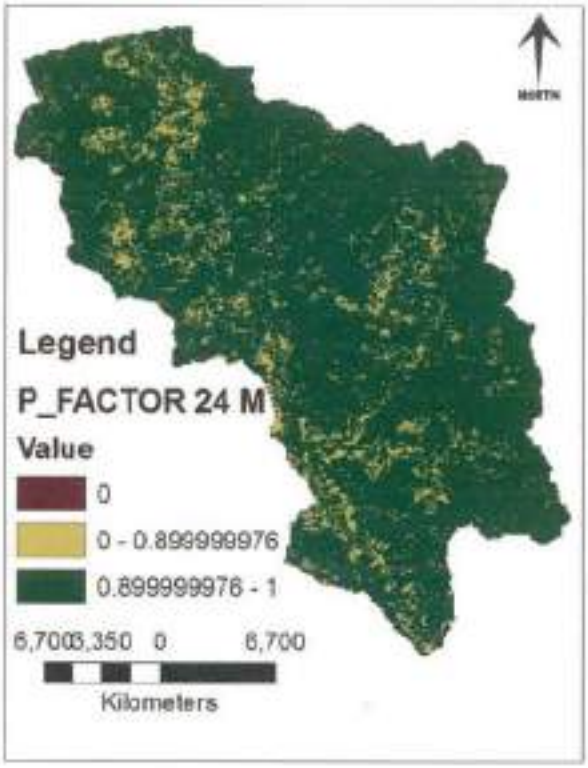

Fig. 9.10: P-Factor 24 m Map

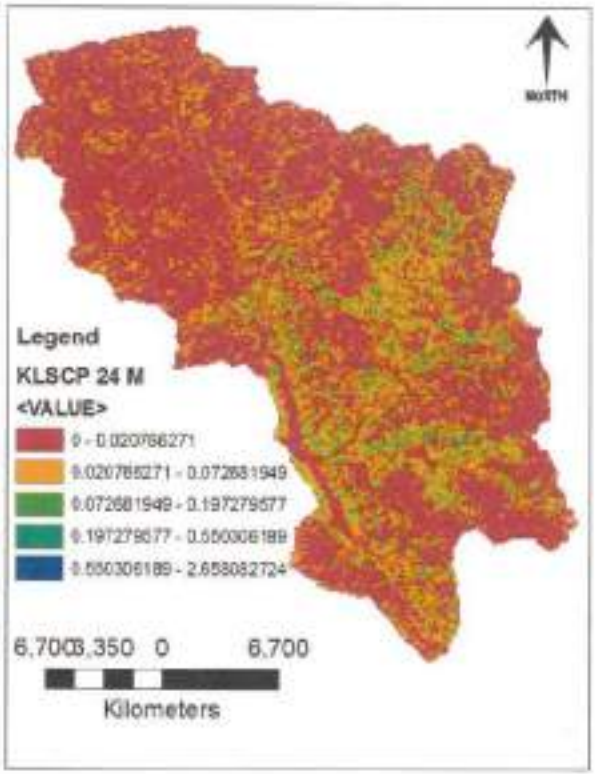

Fig. 9.11: KLSCP Map

9.12 ESTIMATION OF GROSS SOIL EROSION (GSE)

Assessment of gross soil erosion (GSE) of Chaukhutia catchment has been calculated using Arc GIS Raster Calculator. The layers of topographic factor (LS), C factor, Soil Erodibility Factor, K, and Support Practice factor P were overlaid. Then evaluated values of LS, K, C and P maps were multiplied by values of R, rainfall erosivity factor R presented in Table 9.2 from years 1973 to 1990, respectively, to estimate the total soil loss in tones per annum for whole catchment. Multiplication of R factor into KLSCP factor map resulted in maps of gross erosion for different years. Figs. 9.12 to 9.21 present gross soil erosion for some of years. Total computed values of GSE were obtained by summing value of pixels within the catchment to arrive at total gross erosion in the watershed. The value of total GSE for all years is given in Table 9.5.

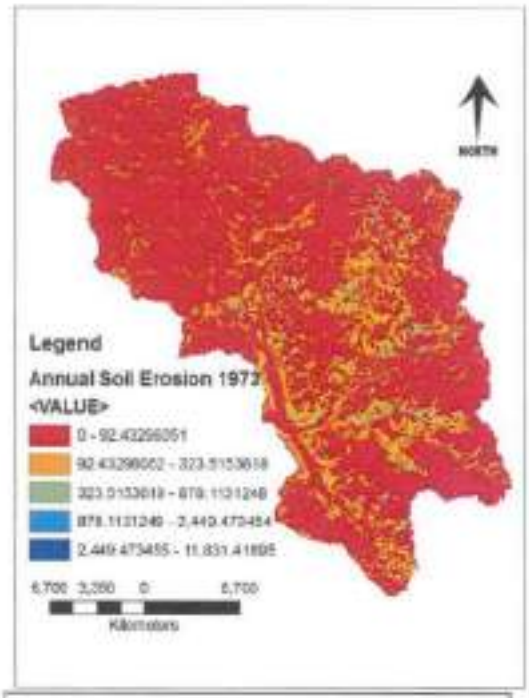

Fig. 9.12: Gross Soil Erosion (GSE) 1973 Map
Computed GSE = 2789489 tones

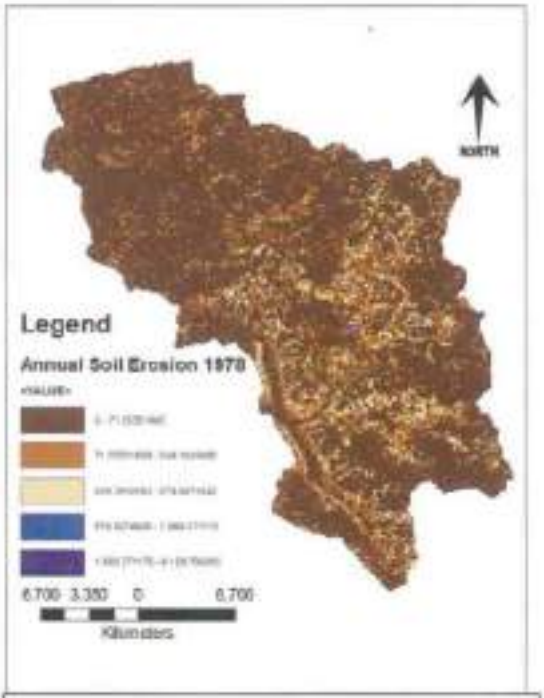

Fig. 9.13: Gross Soil Erosion (GSE) 1978 Map
Comp.GSE= 2154161 tones

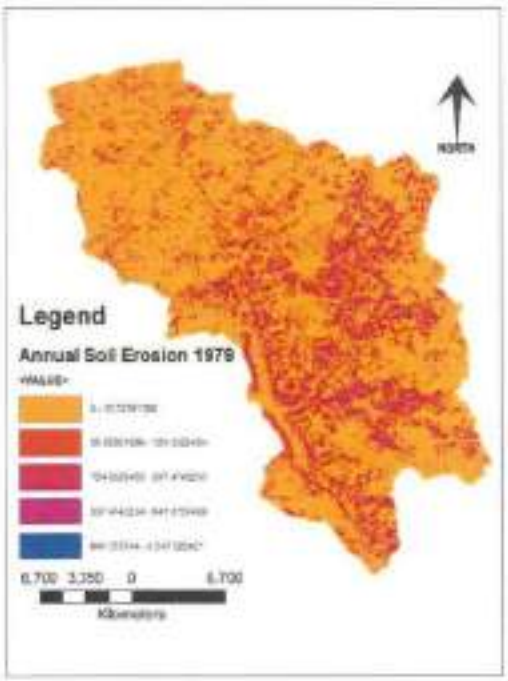

Fig. 9.14: Gross Soil Erosion 1979 Map
Computed GSE= 1058097 tones

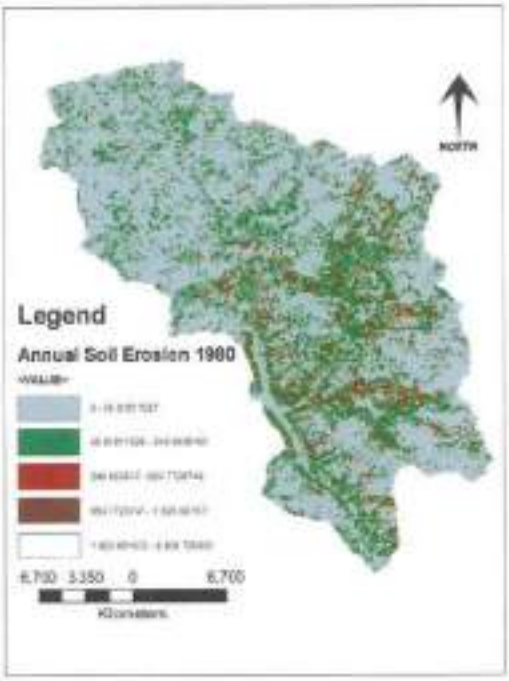

Fig. 9.15: Gross Soil Erosion 1980 Map
Computed GSE = 2144234 tones

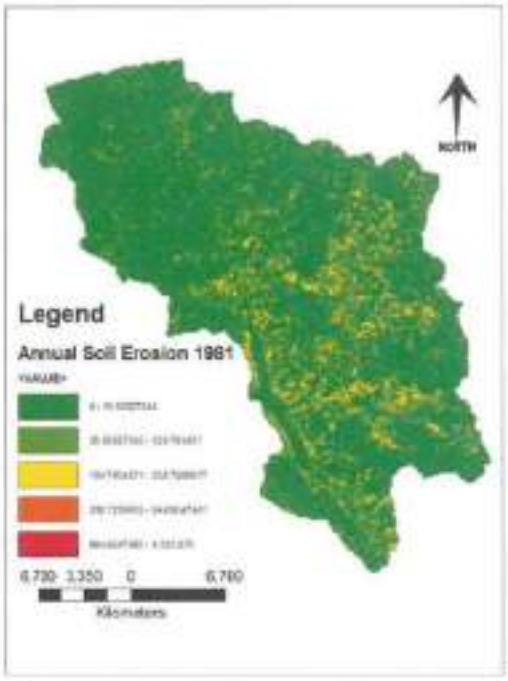

Fig. 9.16 Gross Soil Erosion 1981 Map
Computed GSE= 1058100 tones

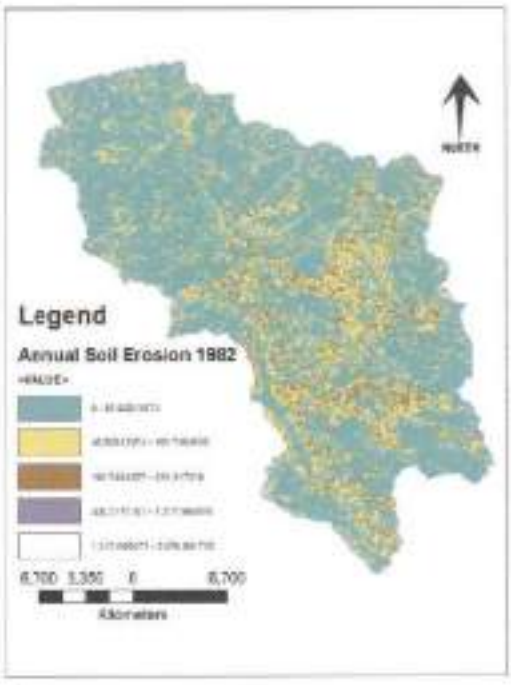

Fig. 9.17 Gross Soil Erosion 1982 Map
Computed GSE= 1368009 tones

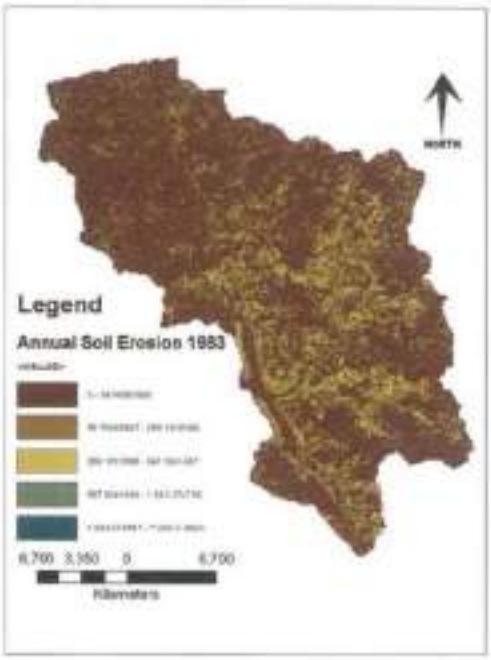

Fig. 9.18. Gross Soil Erosion 1983 Map
Computed GSE= 1780280 tones

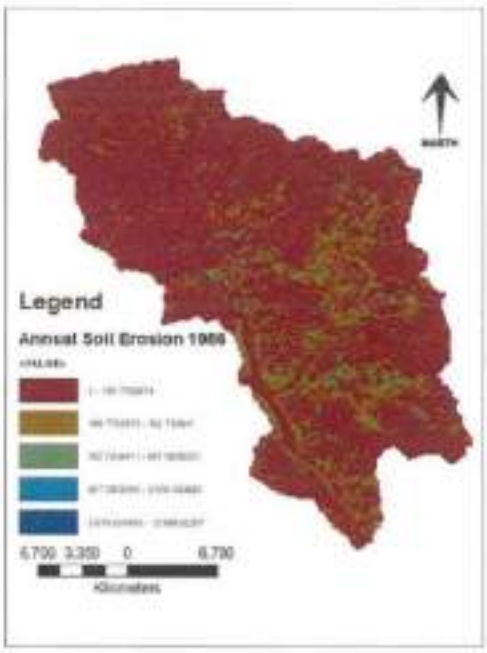

Fig. 9.19. Gross Soil Erosion 1986 Map
Computed GSE= 3146862 tones

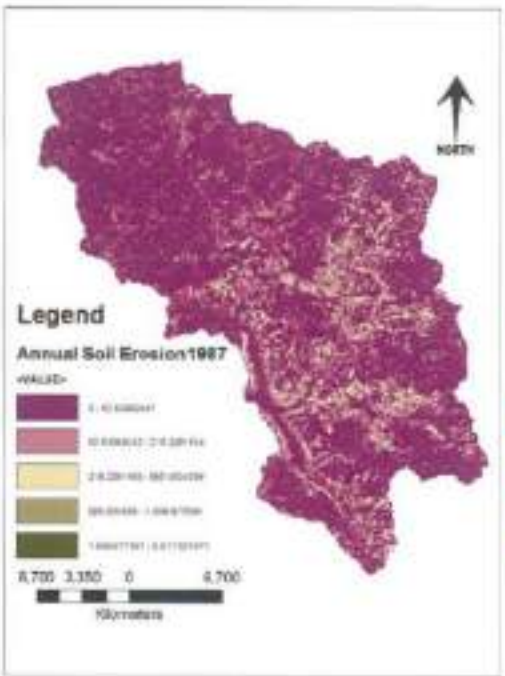

Fig. 9.20. Gross Soil Erosion 1987 Map
Computed GSE= 1894073tones

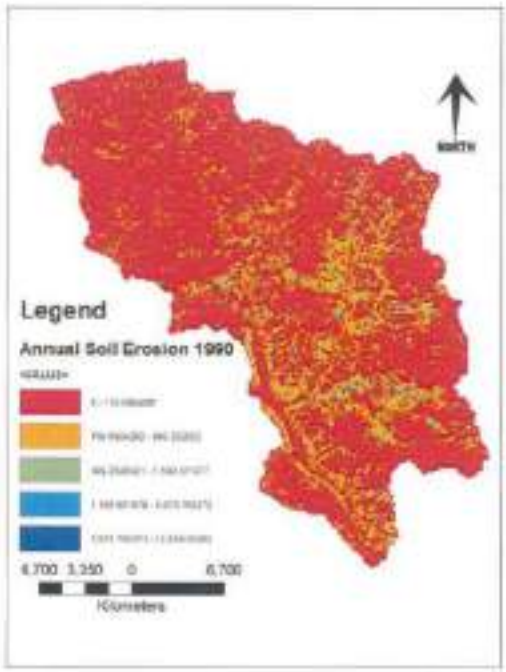

Fig. 9.21. Gross Soil Erosion 1990 Map
Computed GSE= 3504234 tones

Table 9.5: Comparison of Output Results

Year	R [(MJ*mm)/(ha*hr)]	Observed GSY (t)	Computed GSE(t) by USLE	Computed GSY(t) by TLA	% error
1973	4451.11	436847	2789489	565679	-22.77
1974	*	*	*	*	0
1975	4047.36	558067	2541314	787141	-29.10
1976	3617.62	*	2263358	702322	0
1977	4736.04	430557	2268175	621088	-30.67
1978	3431.31	632971	2154161	667341	-5.15
1979	1710.64	753047	1058097	533680	41.10
1980	3313.94	782208	2144234	666902	17.29
1981	1716.98	212706	1058100	297788	-28.57
1982	2211.67	649553	1368009	633600	2.52
1983	2878.17	547775	1780280	586550	-6.61
1984	1382.54	497457	855115	366944	35.57
1985	2071.04	*	1280820	367048	0
1986	4852.98	76048	3146862	97659	-22.12
1987	3016.28	34822	1894073	58660	-40.64
1988	4843.55	175883	3146870	246236	28.50
1989	3031.21	20067	3749799	27094	-25.93
1990	5589.18	41397	3504234	54119	-23.51

*Data Not Available

9.13 COMPUTATION OF SPATIALLY DISTRIBUTED TRANSPORT CAPACITY, TRANSPORT LIMITED ACCUMULATION AND EROSION/DEPOSITION FOR CHAUKHUTIA WATERSHED

As reported earlier, all erosion produced in a grid cell does not find opportunity to get transported to the outlet. Therefore, to convert gross erosion into spatial distribution of sediment yield, annual transport capacity of each grid was computed using Eq. (9.9). The parameter K_{TC} appearing in Eq. (9.9) was taken as unity at the beginning and then calibrated using observed data for 5 years. The calibrated value of K_{TC} equal to 0.005 gave close match between observed and computed sediment yield

and adopted for all other years. Figs. 9.22 & 9.23 shows transport capacity maps for year 1973 and 1990 respectively as illustration.

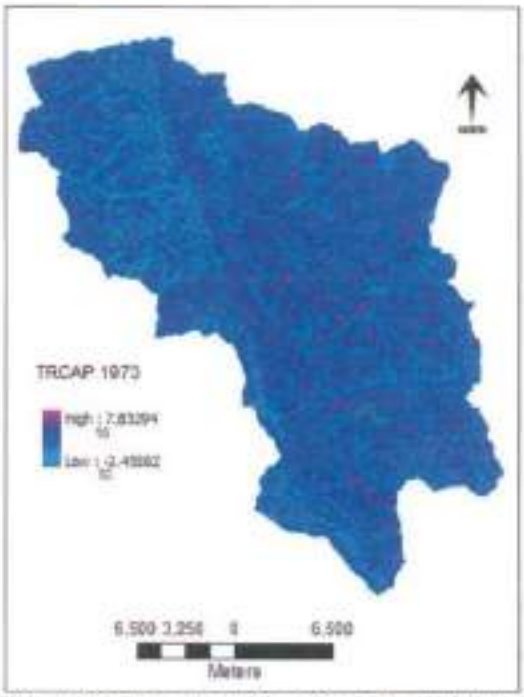

Fig. 9.22: Transport Capacity Map(1973)

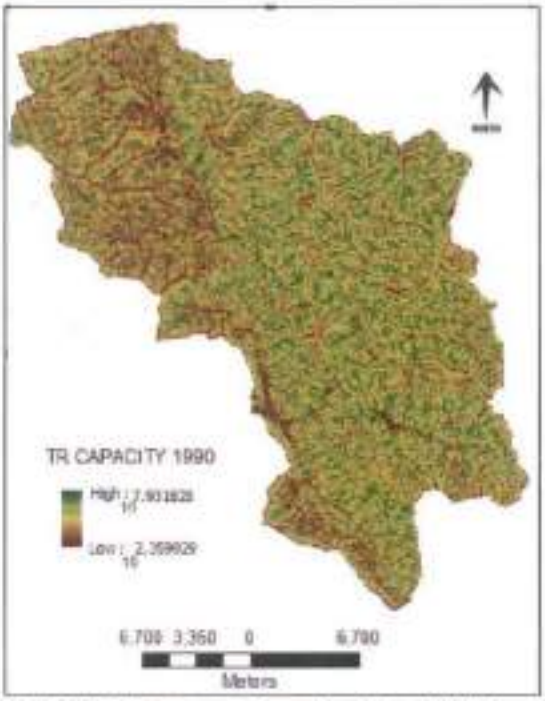

Fig. 9.23: Transport Capacity Map (1990)

Using Eq. (9.8) the gross erosion from each grid was routed downstream to generate map of accumulated sediment yield limited by transport capacity. Such maps give amount of sediment transported from the system at every grid. These maps are useful in knowing value of sediment flowing out of the catchment at any location. Transport limited sediment outflow maps were prepared for all 18 years. Figs. 9.24 & 9.25 depict transport limited sediment outflow or Gross sediment Yield (GSY) maps for year 1973 & 1990, respectively, as an illustration.

The pixel value of the outlet grid of transport limited sediment outflow maps computed above give sediment coming out of the watershed. These values are given in Table 9.5. It can be inferred from Table 9.5, the model over estimates sediment yield for some years and underestimates for some years. Overall the % error between observed and computed value of sediment yield range from - 40% (over estimation) to + 41% (under estimation). Larger errors in a few years are ascribed to uncertainties in the data. Nevertheless the accuracy obtained is considered satisfactory because even the more elaborate process-based soil erosion models are found to produce results

with still larger errors (ASCE, 1975; Foster, 1982; Hadley *et al.*, 1985; Wu *et al.*, 1993; Wicks and Bathurst, 1996).

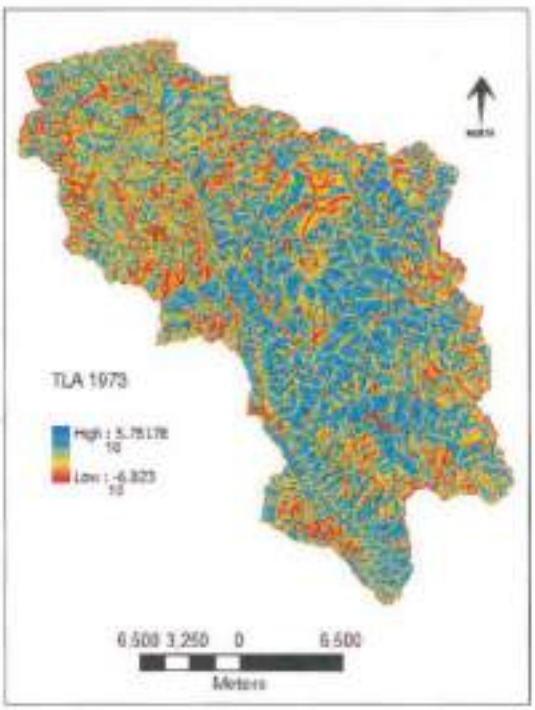

Fig. 9.24: Observed GSY= 436847 tons
Computed GSY= 565679 tones

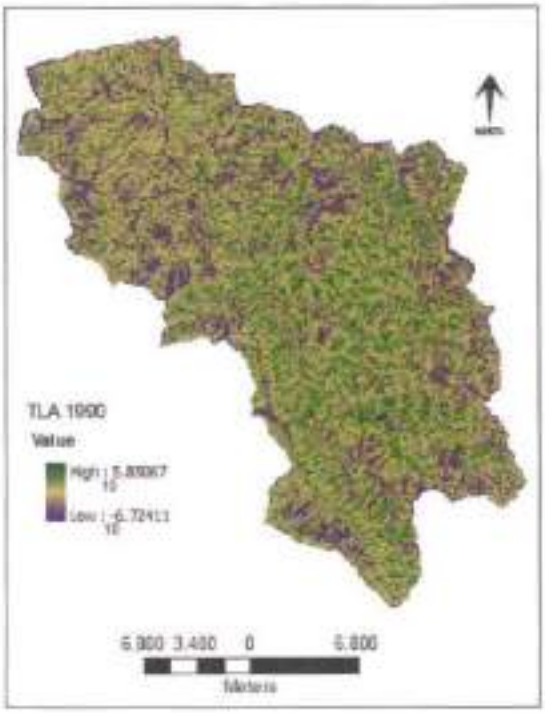

Fig. 9.25: Observed GSY= 41397 tons
Computed GSY= 54119 tones

Using Eq. (9.11) map for deposition of sediment is obtained. Such maps are helpful in identifying areas vulnerable to silt deposition in the catchment. Figs. 9.26 & 9.27 depict sediment deposition maps for year 1973 and 1990 as illustration. As can be seen from these figures, deposition of sediment resulted at grids where transport capacity was low, mostly by the sides of some of the stream reaches. Superimposition of sediment deposition map over gross erosion map resulted in identification of areas vulnerable to soil erosion and deposition. Such maps are extremely important in planning conservation measures. Figs. 9.28 and 9.29 depict erosion/sediment deposition maps for year 1973 and 1990 as illustration.

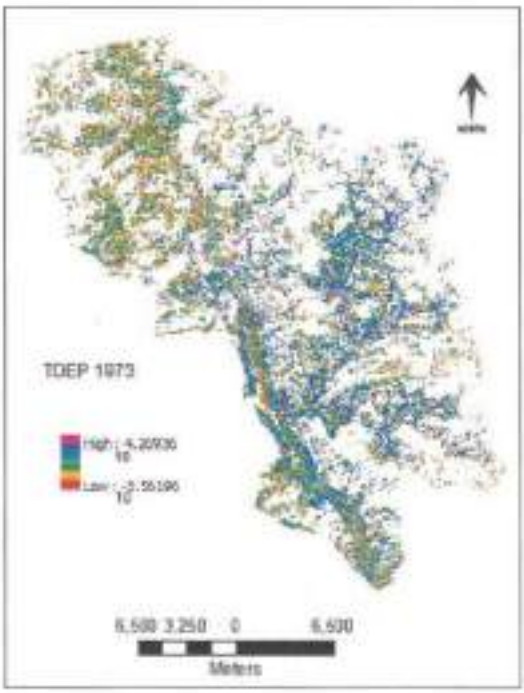

Fig. 9.26: Total deposition 1973 Map

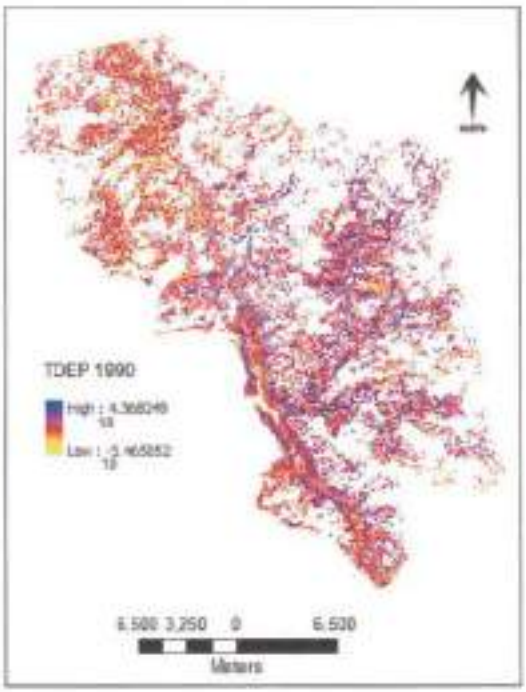

Fig. 9.27: Total deposition 1990 Map

Fig. 9.28: Erosion/deposition 1973 Map

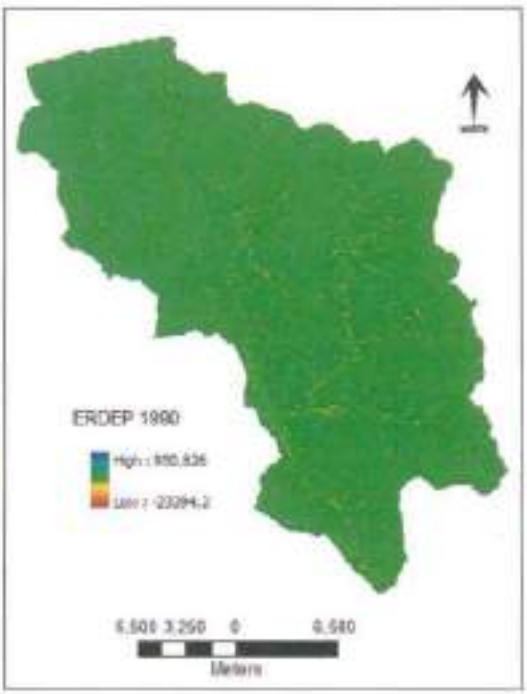

Fig. 9.29: Erosion/deposition1990 Map

9.14 APPLICATION TO NAULA WATERSHED

The basic description of Naula watershed is given in Chapter 2. Following the same procedure, digital elevation model (DEM) and drainage network maps for Naula watershed were prepared as shown in Figs. 9.30 & 9.31, respectively. For identification of vulnerable areas, the above procedure was applied for generation of Gross Soil Erosion (GSE), Transport Capacity (TC) and Transport Limited Accumulation (TLA) maps. The generated maps for GSE, TC and TLA are shown in Figs. 9.32 to 9.34, respectively.

Further, using Eq. (9.11) map for deposition of sediment is also obtained for Naula watershed. Superimposition of sediment deposition map over gross erosion map resulted in identification of areas vulnerable to soil erosion and deposition. Such maps are extremely important in planning conservation measures. Figs. 9.35 depict erosion/sediment deposition maps for year 1987 for Naula watershed as illustration. As can be seen from this figure, majority of the areas in Naula watershed, which include sub-watershed Chaukhutia also, exhibits erosion rates under permissible limits of 10 t/ha/yr. However few areas also exhibits rate of erosion more than permissible limits shown in tones of red in Fig. 9.35 are termed vulnerable and may need to be treated with suitable soil conservation measures.

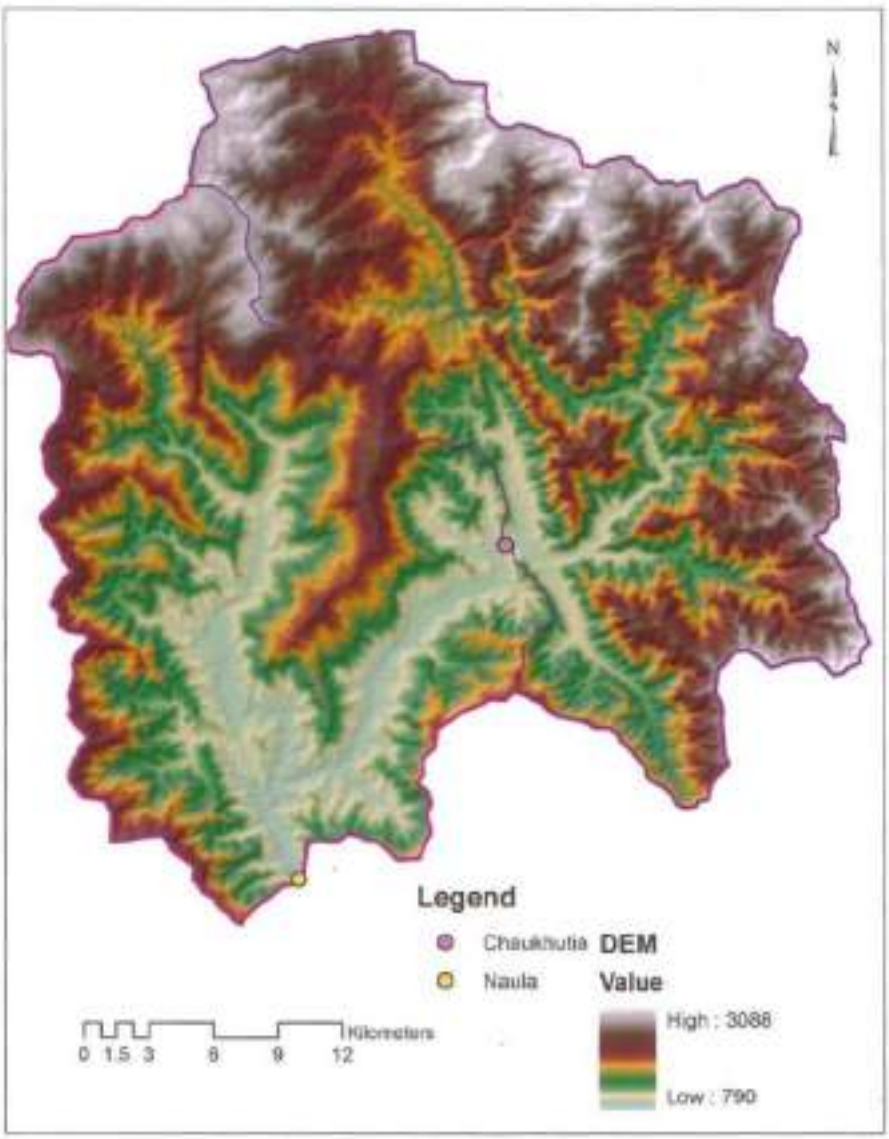

Fig 9.30: Digital Elevation Model of Naula Watershed

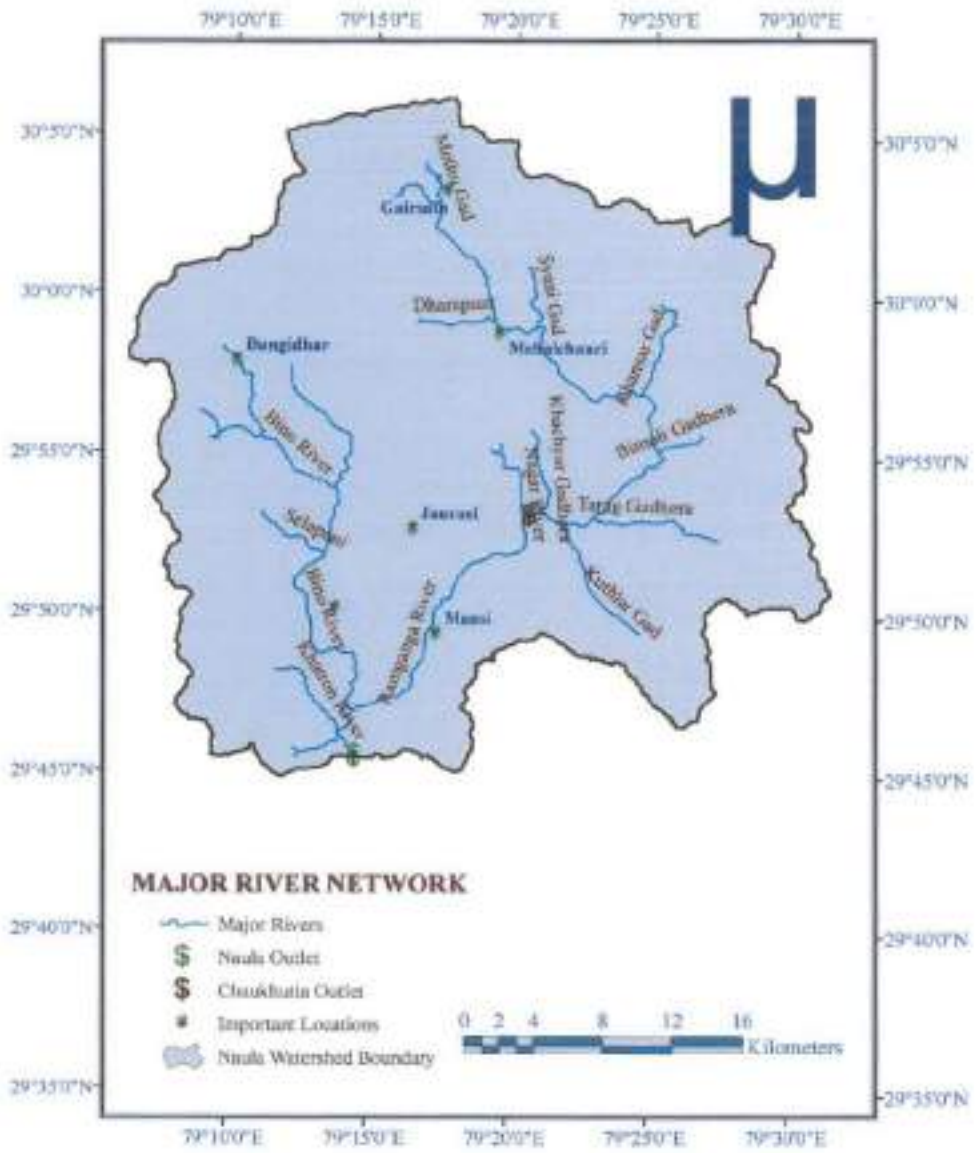

Fig. 9.31: Drainage Network map of the Naula Watershed

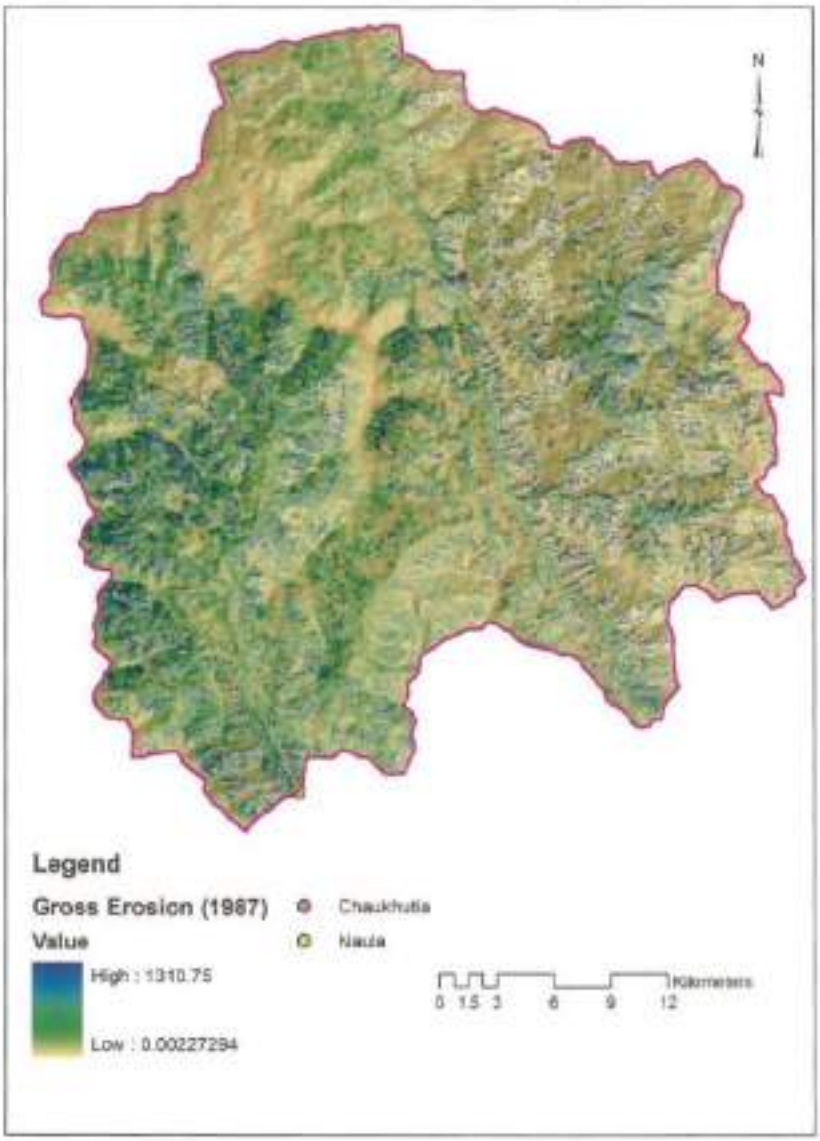

Fig. 9.32. Gross Soil Erosion (GSE) map for Naula watershed for 1987

Fig. 9.33: Transport Capacity map for 1987 for Naula Watershed

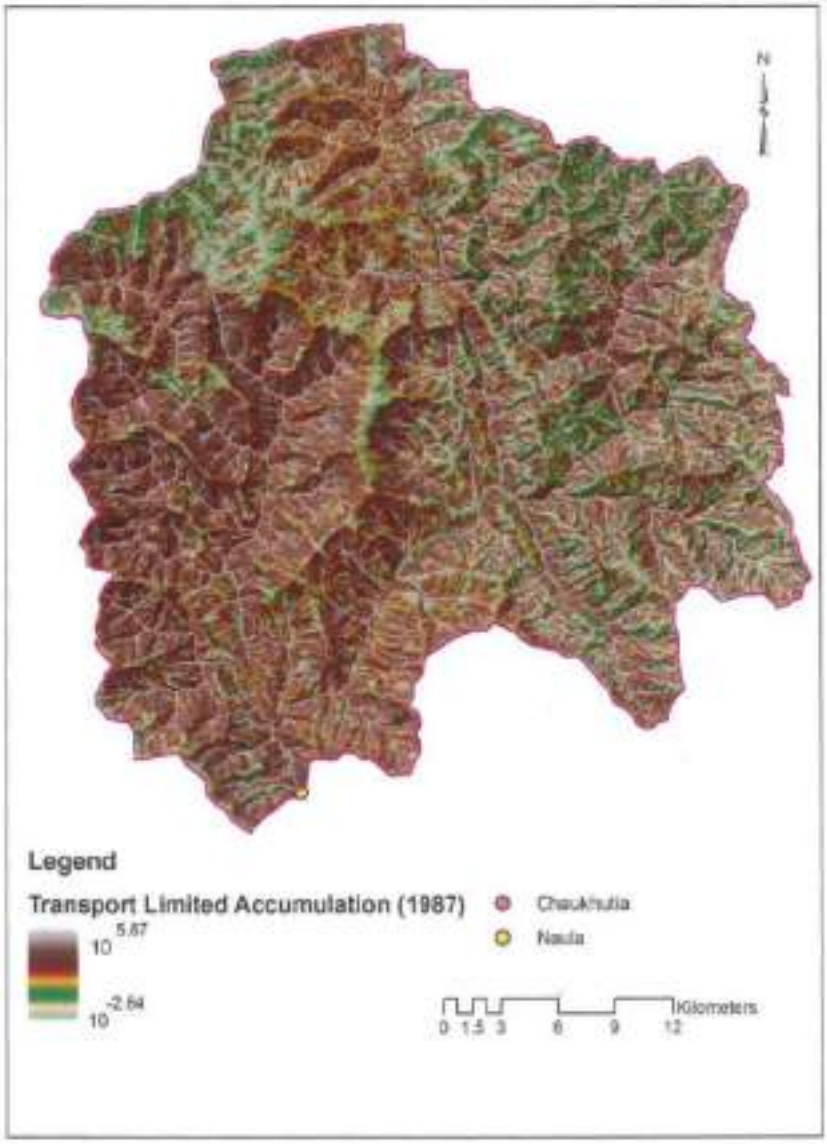

Fig. 9.34. Transport Limited Accumulation map for Naula watershed for 1987

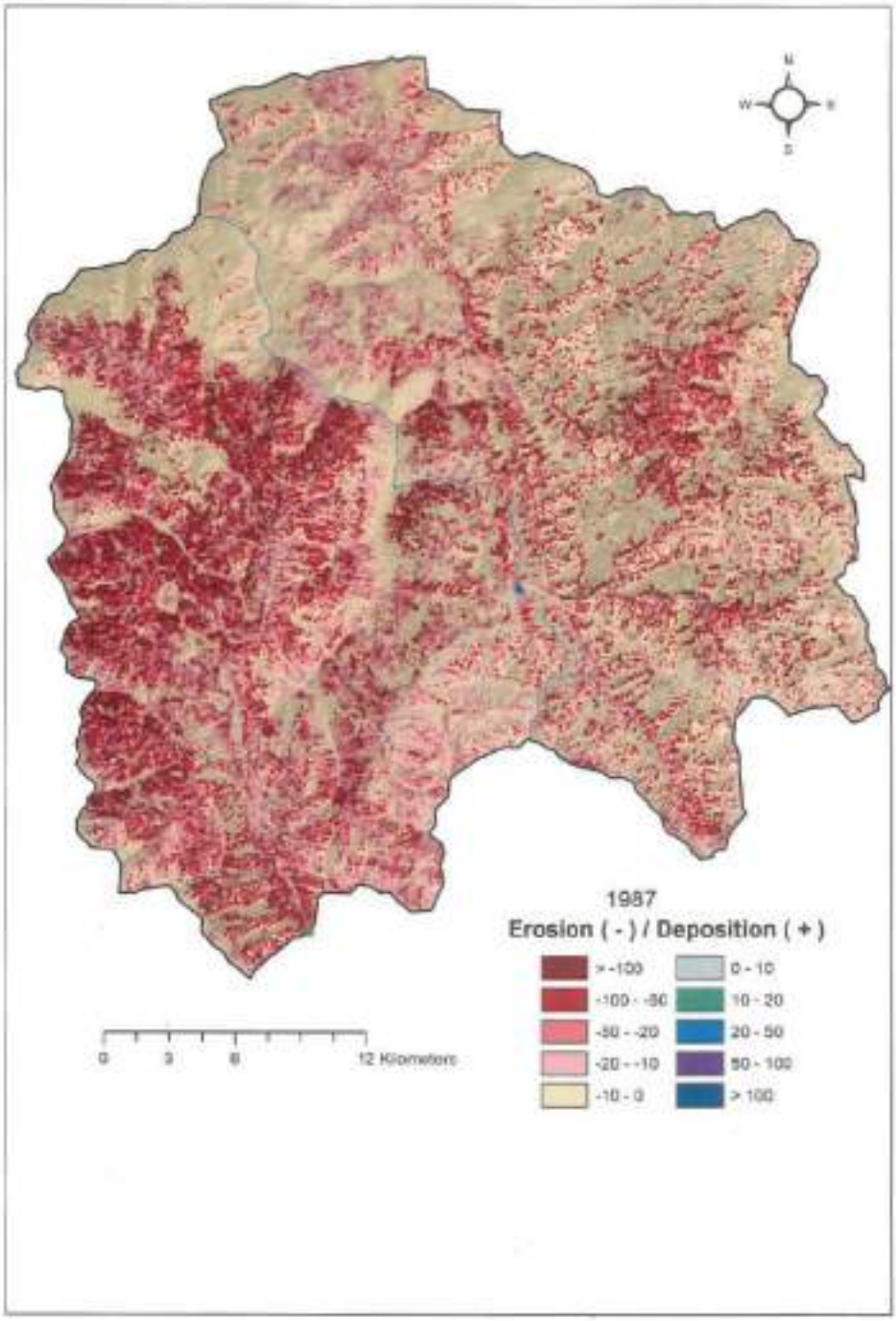

Fig. 9.35. Erosion/depositional map for Naula watershed for 1987

9.15 GUIDELINE FOR SOFTWARE DEVELOPMENT FOR WATERSHED PRIORATIZATION

Fig. 9.36 shows the Flow Chart for watershed prioritization based on vulnerability to soil erosion utilizing remotely sensed data and GIS coupled USLE model. The Flow Chart is self explanatory and can be utilized for developing computer software for watershed prioritization, for use by field engineers, watershed managers and water researchers.

9.16 CONCLUSIONS

Scientific management of soil and water is very important to arrest erosion and enhancing the agricultural production. Soil erosion is the major cause of the loss of fertility, diminishing crop production and land degradation. The deterioration of soil in study area can be controlled effectively by adopting the watershed treatment measures if spatial distribution of soil erosion is known. Erosion is a natural geomorphic process occurring continually over the earth's surface. The processes of erosion of soil from earth surface largely depend on topography, vegetation, soil and climatic variables. These areas are found to have pronounced spatial variability in a catchment due to spatial variation of climatic factors and catchment heterogeneity. This is one of the reasons given for promoting the use of distributed information of catchment resources using a GIS. By using GIS the catchment is discretized into sub-areas having approximately homogeneous characteristics and rainfall distribution. The remote sensing and GIS techniques have been used in this study for generation of spatial information, catchment discretization, data processing and analysis.

Various thematic layers representing different factors of USLE were generated and overlaid to compute spatially distributed gross soil erosion maps for watershed using recorded rainfall for 18 years. A concept of transport limited accumulation was formulated and used in ArcGIS for generating maps for transport capacity and using transport capacity maps, gross soil erosion was routed to the catchment outlet using hydrological drainage paths resulting in generation of transport capacity limited sediment outflow maps. Such maps yield the amount of sediment flowing from a particular grid in spatial domain. The pixel value of the outlet grid of transport limited sediment outflow maps thus computed give sediment coming out of the watershed.

Comparison of observed and computed value of sediment yield revealed that the % error between observed and computed value of sediment yield range from -40% (over estimation) to +41% (under estimation). Larger errors in a few years are ascribed to uncertainties in the data. Nevertheless, the accuracy obtained is considered satisfactory, for the more elaborate process-based soil erosion models also produce results with still larger errors (ASCE, 1975; Foster, 1982; Hadley et al., 1985; Wu et al., 1993; Wicks and Bathurst, 1996). The same procedure was applied to Naula watershed and the maps for gross soil erosion, transport capacity and transport limited accumulation were generated for 1987.

Further, using the above methodology, maps for deposition of sediment were derived. Such maps are helpful in identifying areas vulnerable to silt deposition in the catchment. Analysis of maps reveals that deposition of sediment resulted at grids where transport capacity was low, mostly by the sides of some of the stream reaches. Superimposition of sediment deposition map over gross erosion map resulted in identification of areas vulnerable to soil erosion and deposition. Such maps are extremely useful in planning conservation measures. The method has a potential to assess the impact of different land use covers and soil conservation measures on resulting sediment outflow from the catchment. Therefore, it can be a useful tool in integrated environmental watershed management.

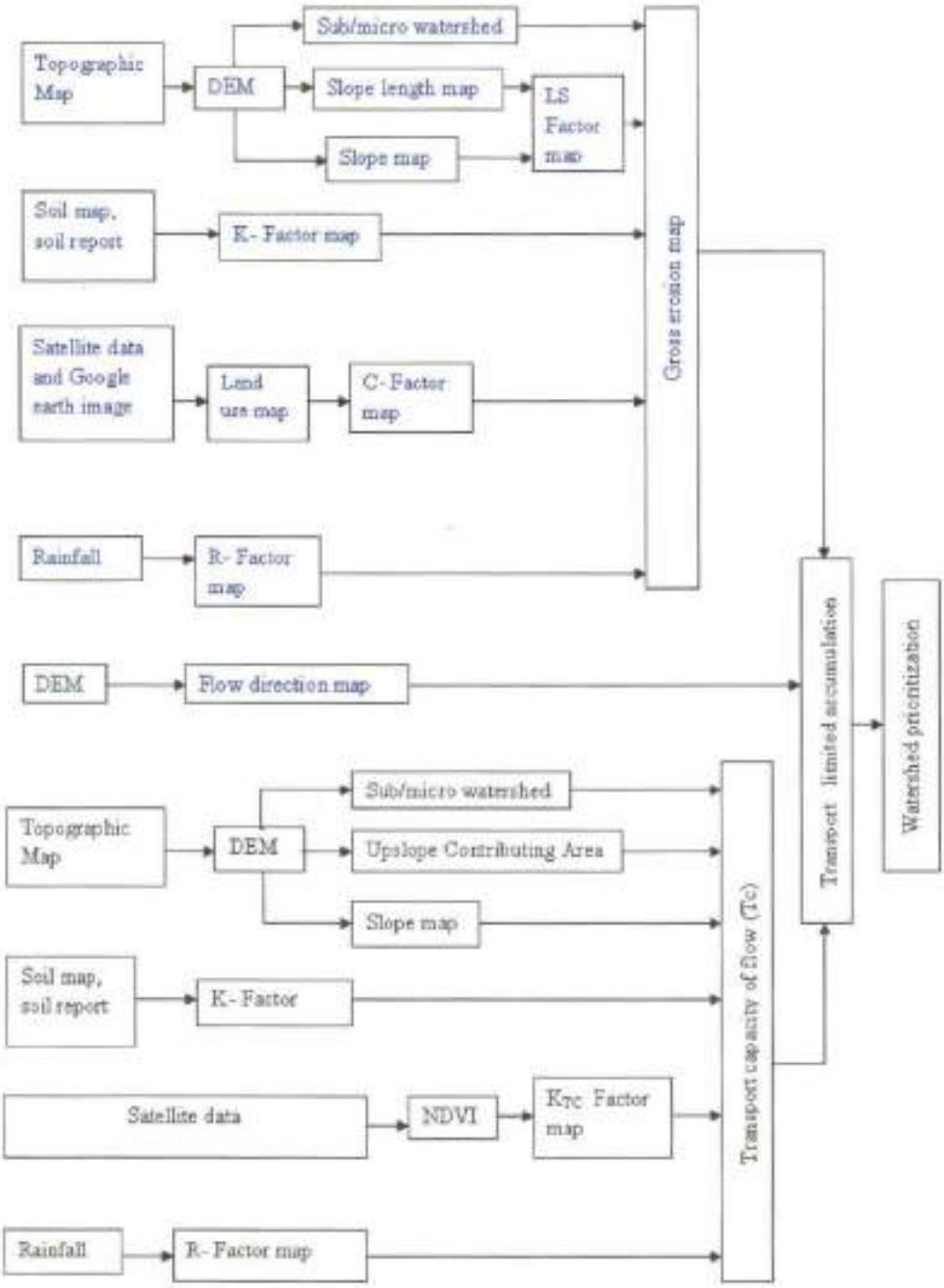

Fig. 9.36: Flow Chart of methodology for watershed prioritization based on GIS coupled USLE model

CHAPTER 10

SUMMARY AND CONCLUSIONS

CHAPTER 10

SUMMARY AND CONCLUSIONS

Identification of vulnerable areas and proper understanding of the complex phenomenon of rainfall-runoff-sediment yield within a drainage basin facilitate improvements in planning and management of soil conservation and water resources and systems. Such identification basically involves quantification of erosion and sediment deposition and its spatial distribution within the watershed. Moreover, in spatially distributed domain, these processes can be effectively addressed with the help of remote sensing (RS) and geographic information system (GIS) techniques.

Notably, only a limited number of studies have been reported in literature applicable to steep Himalayan catchments. These studies indicate that the rate of soil erosion from these catchments is increasing at an alarming rate due to heavy deforestation, urbanization and other developmental activities, and the lack of proper conservation measures. Therefore, a systematic study for quantification of rainfall-generated runoff, soil erosion, sediment yield, areas vulnerable to soil erosion from such catchments was carried out in this project work using different newly developed methodologies/procedures. Under the R&D objective, i.e. Basic Research part, of the project, various hydrological approaches/techniques/models were also tested/investigated for their applicability to Himalayan watersheds. This chapter first summarizes the research outcomes, and finally the identification of vulnerable areas, which forms to be the part of Applied Research. Mainly, the Ramganga, a Himalayan/hilly watershed (area = 3134 km^2), and sub-catchments namely Chaukhutia, Naula, and Gagas are considered for various studies carried out under this project.

10.1 A REVISIT TO UNIT HYDROGRAPH CONCEPT

The concept of unit hydrograph forms to be the key to the development of the field of surface water hydrology despite the fact that it carries fundamental limitations in terms of its guiding principles of linearity, uniformity, and superposition. Since most developing countries face the problem of data scarcity, the synthetic unit hydrographs (SUH) have to be of paramount importance in pragmatic applications. For example, these UHs are frequently used for estimation of flood hydrographs from ungauged catchments. The applicability of UH

concept is tested in terms of their derivation from the catchment characteristics derived with the help of GIS coupled with probability density function (pdf). In this study, the potential of the density functions of Two-parameter Inverse Gamma distribution (2PIGD), Two-parameter Weibull (2PWD) distribution, and Two-parameter Nash geomorphological model (2PNGM) is explored for SUH derivation for Gagas watershed employing Geomorphological Instantaneous Unit Hydrograph (GIUH) approach. The geomorphological parameters of the catchments were extracted from easily available and most updated SRTM data in ILWIS 3.3 GIS environment. Based on the goodnesss-of-fit (GOF) criteria in terms of STDER, RMSE and NSE, 2PIGD was found to perform significantly better than 2PWD and 2PNGM models. The average values of STDER were 6.21, 12.79, and 10.88, respectively, for 2PIGD, 2PWD and 2PNGM models. The average RMSE values were 3.14, 7.13, and 5.96, respectively, for 2PIGD, 2PWD and 2PNGM models. Similarly, NSE values were 92.3%, 68%, and 76.9%, respectively, for 2PIGD, 2PWD and 2PNGM models, an indicator of generally satisfactory application of UH concept. Using the same GIUH concept, the best performing 2PIGD model was also applied to the data of Ramgamga catchment for SUHs derivation for different dynamic velocities, resulting into simple regression models for peak discharge (q_p) and time to peak discharge (t_p) useful for direct field applications.

10.2 A REVISIT TO SCS–CN MODEL

Information regarding flow rates at any point of interest along a stream is necessary in the analysis and design of many types of water resources projects. Although many streams have been gauged to provide continuous records of stream flow, planners and engineers are sometimes faced with little or no available stream flow information and must rely on synthesis and simulation as tools to generate artificial flow sequences for use in rationalizing decisions regarding structure size, the effect of land use, flood control measures, water supplies, and the effect of natural or induced watershed or climatic change. The Soil Conservation Service-Curve Number (SCS-CN) methodology forms to be an important founding stone of surface water hydrology, primarily used to estimate the losses to derive the direct surface runoff from the total amount of rainfall, for use in UH application to convert runoff volumes to runoff rates. Its fields of application, other than rainfall-runoff generation, have varied a lot since its inception.

The long-term hydrologic simulation plays an important role in water resources planning and watershed management, specifically for analysis of water availability,

computation of daily, fortnightly, and monthly flows for reservoir operation and drought analysis. In this study, the applicability of SCS–CN concept has been tested in terms of its utility in long term hydrologic simulation and, in turn, a long-term rainfall-runoff model was proposed and tested on the data of Ramganga catchment using split sampling. The proposed model has four parameters, CN, CN_d, K and K_b. The first two parameters are the curve number for surface flow and drainage flow, respectively; K is the catchment storage coefficient (day); and K_b is the ground water storage coefficient (day).

To check the versatility of the proposed model, the model was further applied to different watersheds located in different hydro-meteorological regions. These are the catchments of Hemavati, Manot, Hridaynagar, Mohegaon, Kalu and Ghodahado. The following conclusions were derived from this study:

- The model generally performed well in both calibration and validation on the data of Ramganga catchment. The resulting efficiencies for all the years varied in the range of 81.82 to 73.62%, showing a satisfactory fit and, in turn, satisfactory model performance.
- The comparison of model efficiencies resulting from model application to other catchments reveals that Hemavati yields maximum efficiency of 83.27% in calibration, and 84.82% in validation. The other catchments like Manot, Kalu and Ghodahado exhibit 60.75, 63.895 and 59.35% efficiencies, respectively, in calibration, and 54.06, 82.014 and 32.31% in validation. The efficiencies of all catchments, except Hemavati and Ramganga, are higher in calibration than in validation, but reverse holds for the others.
- It is seen that the catchment of Hemavati and Kalu can be classified as high runoff producing catchments with runoff coefficient values of 0.83 and 0.91, respectively. Hridaynagar, Mohegaon catchments with low runoff coefficients of 0.25 and 0.27, respectively, behave as dry catchments.
- The model simulated the yearly runoff values with relative error in the range -29.66 to 18.20% for Ramganga catchment. For other catchments it falls within the range of -21.97 to 8.10%. These values indicate good to satisfactory model performance. The negative (-) values of relative error indicate that the model overestimates the runoff values.
- The satisfactory model performance on the high runoff producing watersheds is further appreciable in view of the limited number of model parameters (only four) and its simplicity.

10.3 APPLICATION OF TOPMODEL

The distributed, topographically based hydrological TOPMODEL model was applied to simulate continuously the runoff hydrograph of Chaukhutia watershed of Ramganga catchment. It is a variable contributing area conceptual model in which topography controls the soil water storage and runoff generation. In this model, the total flow is calculated as the sum of two terms: surface runoff and flow in the saturated zone. The TOPMODEL is attractive because of its structural simplicity and consideration of only a few parameters.

Calibration and validation of the TOPMODEL was carried out on the data of Chaukhutia watershed. Raster DEM input for the model is generated through ArcGIS after digitization contour map from Survey of India toposheets. Available data was split into two groups: the first set (1975 – 78) was used for calibration of the model and the other set (1979 – 81) was used to validate model. The model efficiency was 0.58 in calibration, and 0.649 in validation, indicating satisfactory to less than satisfactory model performance. The simulations however provided an insight into the response of the catchment at different periods of the season. TOPMODEL performed only reasonably well as a continuous hydrograph simulator in the Chaukhutia watershed. The model simulated well the base flow, but under-estimated most of the peaks. The use of parameter sets yielding the highest modelling efficiency of 0.57 yields results which are less than encouraging. This may be due to topography of watershed area which has a moderate to steep sloping surface covered with deep forest whereas TOPMODEL is suitable for moderate topography only. In addition, the deep forest contributes less to saturation-excess runoff, an important assumption for direct runoff generation in TOPMODEL formulation.

10.4 APPLICATION OF SWAT MODEL

Among the myriad rainfall-runoff models available in literature, the Soil and Water Assessment Tool (SWAT) has gained immense popularity in the recent past, because it is a distributed watershed model developed by Agricultural Research Service of United States Department of Agriculture to predict the impact of land management practices on water, sediment and agricultural chemical yields in complex watersheds. It is a comprehensive model which requires a significant amount of data and parameters for simulation of runoff and loadings mainly from rural catchments. This study aimed at to test the applicability of SWAT model to simulate runoff response from sub-Himalayan Chaukhutia watershed.

For model run, Digital Elevation Model (DEM), land use map of the study area using satellite data, and digital soil map were prepared, and data base compatible with the latest SWAT-2005 model prepared for runoff simulation. The model was calibrated and validated with different datasets, and finally a sensitivity analysis of model parameters was carried out. The following conclusions were drawn from this study:

- The entire Chaukhutia watershed lies between the elevation 934.845 m and 3099.29 m indicating a mountainous watershed. Its total geographical area is of the order of 57229 ha. Notably, the SWAT model has been suggested to be applicable to only moderately sloping watersheds.
- The Chaukhutia watershed can be broadly categorized as a forest (evergreen) watershed with 33871 ha (of the order of 59%). It is based on the channel initiation threshold (CIT) value of 2500 hectare. It is worth emphasizing that the SWAT model has not been tested for its applicability to such watersheds in the past.
- In general, 133 hydrologic response units (HRU) and 17 sub-basins were considered to be reasonably sufficient to describe the hydrologic response of the watershed.
- In daily flow simulation for the years 1975 to 1980, the values of percent bias (PBIAS) ranged from -9.99 to 6.66 indicated that in some years the runoff was over-estimated (negative PBIAS values) and in others it was under-estimated (positive PBIAS values), but not significantly as the Nash and Sutcliffe efficiency (NSE) ranged from 0.70 to 0.85 indicating a reasonable to very good model fit. It follows that the SWAT model is applicable to even forested sub-Himalayan watersheds.
- The SWAT model parameter "Available water capacity of soil (SOL_AWC)" was found to be the most sensitive parameter for accurate runoff simulation. It implies that this is the most crucial parameter to be assessed from field measurements.

10.5 APPLICATION OF ANN MODEL

The Artificial Neural Network (ANN) models have been applied to several diverse hydrological problems and the results in each case have been found very encouraging. ANNs are capable to handle nonlinearity of the complex systems to be modelled with flexible mathematical structure along with the activation function. Hence in this study, a radial basis function artificial neural network (RBFANN) was developed to model rainfall generated runoff for Ramganga basin and its two sub-watersheds namely Chaukhutia and Naula.

In this study, a computer program was developed using k-means clustering algorithm for the RBF neural network to carry out rainfall-runoff modelling of the Upper Ramganga river basin. The program code was written in FORTRAN environment. The best input combination was decided by cross-correlation matrix method and it consists of rainfall and discharge values. In the present study, dynamic types of approach have been applied for calculation of spread value in radial basis function neural network. The performance of the model is improved by proper selection of suitable learning rates and optimized number of iterations to train the network. The results, i.e. the computed outflows, are compared with the observed flows. The following conclusions were drawn from this study:

- Radial Basis Function can be a better solution for rainfall-runoff modelling as physically based models with partial differential equations of mass and energy is difficult to employ due to lack of data. The selection of learning rate as well as the number of iterations required is very important for optimal results. The proposed program has flexibility to change the input and output variables and fix the radial basis nodes.
- The proposed model performed very well in calibration, cross-validation, and verification for both Chaukhutia and Naula watersheds. However, in case of Ramganga watershed the model performed very well in calibration and cross-validation whereas it performed satisfactorily during verification.
- The developed RBFANN model in this study simulated the daily runoff quite closely in all watersheds during all periods. The peak flows were however underestimated by the model, and therefore, there exists a need to modify the proposed model for extreme flows. It was however due to far exceeding numbers of low flow values than the number of peak values, leading to biasing of optimization to low flow values.
- The proposed model simulates the long-term daily runoff reasonably well in all the considered watersheds, and therefore, its applicability can be generalized for all the sub-watersheds of the Ramganga river basin.

10.6 ESTIMATION OF SEDIMENT GRAPH

Sediment graphs are useful in quick estimation of peak rates of sediment yield that are likely to be experienced at the outlet of the watershed due to a rain storm. In this study, a simple approach incorporating popular and widely used models, Viz., Nash-based

Instantaneous Unit Sediment Graph (IUSG), SCS-CN method, and power law has been used to develop a simple sediment yield model for computation of sediment graphs. The developed model is mathematically sound and hydrologically improved in the sense that it eliminates the inevitability of a regression-based approach that is used to derive the mobilized sediment and considers rainfall intensity, soil type, land use, hydrologic condition, and antecedent moisture, and thus, physically more plausible than the common and less accurate regression type relations.

A simple relationship has been provided for estimation of number of linear reservoirs (shape parameter, n_s), instead of using graphical and less accurate procedures which are in frequent use. Resulting higher model efficiency (varying from 90.52% to 95.41%) and lower values of relative errors in total sediment outflow (from 2.49% to 10.04%) and peak sediment flow rate (9.69% to 16.42%) further strengthen the suitability of the model for computation of sediment graph and total sediment outflow. A conventional sensitivity analysis procedure shows that parameter β is most sensitive followed by k, α, A, and n_s. The proposed model has ample scope for estimation of sediment graphs as well as total sediment outflow from ungauged natural watersheds.

10.7 IDENTIFICATION OF VULNERABLE AREAS

The process of erosion of soil from earth surface largely depends on topography, vegetation, soil, and climatic variables. These factors exhibit pronounced spatial variability in a catchment due to spatial variation of climatic factors and catchment heterogeneity. This is one of the reasons given for promoting the use of distributed information of catchment resources using a GIS. By using a GIS the catchment is discretized into sub-areas having approximately homogeneous characteristics and rainfall distribution. The remote sensing and GIS techniques have been used in this study for generation of spatial information, catchment discretization, data processing and making computations, as follows:

- Various thematic layers representing different factor of USLE were generated and overlaid to compute spatially distributed gross soil erosion maps for watershed using recorded rainfall for 18 years.

- Concept of transport limited accumulation (TLA) was formulated and used in ArcGIS for generating maps for transport capacity (TC). Employing transport capacity maps, gross soil erosion (GSE) was routed to the catchment outlet using hydrological drainage paths resulting in generation of transport capacity limited (TCL) sediment outflow maps. Such maps give amount of sediment flowing from a particular grid in spatial domain.
- Comparison of observed and computed value of sediment yield revealed that the % error between observed and computed value of sediment yield range from -40% (over-estimation) to +41% (under-estimation). Larger errors in a few years are ascribed to uncertainties in the data.
- Maps for deposition of sediment were obtained. Such maps are helpful in identifying areas vulnerable to silt deposition in the catchment. Analysis of maps reveals that deposition of sediment resulted at grids where transport capacity was low, mostly by the sides of some of the stream reaches.
- Superimposition of sediment deposition map over gross erosion map resulted in identification of areas vulnerable to soil erosion and deposition. Such maps are extremely important in planning conservation measures.
- The proposed methodology has the potential to assess impact of different land use scenarios and soil conservation measures on resulting sediment outflow scenario from the catchment. Hence, it is a useful tool for integrated environmental watershed management (IEWM) system.

REFERENCES

REFERENCES

Introduction

1. Geetha, K., Mishra, S.K., Eldho, T.I., Rastogi, A.K. and Pandey, R.P. (2007). Modifications to SCS-CN Method for Long-Term Hydrologic Simulation. DOI: 10.1061/(ASCE) 0733-9437(2007)133:5(475)
2. Rodriguez-Iturbe, I. and Valde's, J.B. (1979). The geomorphologic structure of the hydrologic response. Water Resourcrs Research, 15(6): 1409– 1420.

Study Area

1. Kumar, A. and Kumar, D. (2008). Predicting direct runoff from hilly watershed using geomorphology and stream-order-law ratos: case study. Journal of Hydrologic Enginnering, 13(7): 570-576.
2. Mishra, S.K. and Singh, V.P. (2003b). SCS-CN method Part II: Analytical Treatment, Acta Geophys. Pol. 51(1): 107–123.
3. NBSSLUP (2004). Soils of Uttar Pradesh for optimizing land use: Executive summary. NBSS Publication 68, National Bureau of Soil Survey and Land Use Planning, ICAR, Nagpur 400010.
4. Neitsch, S.L., Arnold, J.G. Kiniry, J.R. and King, K.W. (2005). Soil and Water Assessment Tool theoretical documentation, Version 2005.
5. Sharma, R.P. and Sinha, A, K., (1972). Geology of Ranikhet Area, Kumaon Himalaya. Lucknow University, 137-150.

A revisit to Unit Hydrograph Concept

1. Abramowitz, M. and Stegun, D.I. (1964). Handbook of Mathematical Function. Dover, New York.
2. Aron, G. and White, E.L. (1982). Fitting a gamma distribution over a synthetic unit hydrograph. Water Resources Bulletin, 18(1): 95–98.

3. Bharda, A., Panigrahi, N., Singh, R., Raghuwanshi, N.S., Mal, B.C. and Tripathi, M.P. (2008). Development of geomorphological instantaneous unit hydrograph model for scantly gauged watersheds. Environmental Modelling & Software, 23: 1013-1025.
4. Bhaskar, N.R., Parida, B.P. and Nayak, A.K. (1997). Flood estimation for ungauged catchments using the GIUH. Journal of Water Resource Planning and Management, ASCE, 123(4): 228–238.
5. Bhunya, P.K., Berndtsson, R., Ojha, C.S.P. and Mishra, S.K. (2007). Suitability of gamma, chi-square, weibull and beta distributions as synthetic unit hydrographs. Journal of Hydrology, 334: 28–38.
6. Bhunya, P.K., Singh, P.K. and Mishra, S.K. (2009). Fréchet and chi-square parametric expressions combined with horton ratios to derive a synthetic unit hydrograph. Hydrological sceience, 54 (2): 274-286.
7. Bhunya, P.K., Mishra, S.K. and Berndtsson, R. (2003). Simplified two-parameter gamma distribution for derivation of synthetic unit hydrograph. Journal of Hydrologic Engineering, ASCE, 8(4): 226-230.
8. Bhunya, P.K., Mishra, S.K., Ojha, C.S.P. and Berndtsson, R. (2004). Parameter estimation of beta-distribution for unit hydrograph derivation. Journal of Hydrologic Engineering, ASCE, 9(4): 325–332.
9. Clark, C.O. (1945). Storage and the unit hydrograph. Transactions of American Society of Civil Engineers, 110: 1419–1446.
10. Croley, T.E. (1980). Gamma synthetic hydrographs. Journal of Hydrology, 47: 41–52.
11. Edson, C.G. (1951). Parameters for relating unit hydrograph to watershed characteristics. Transactions of American Geophysical Union, 32(4): 591–596.
12. Gray, D.M. (1961). Synthetic hydrographs for small drainage areas. Proceedings of American Society of Civil Engineers, 87(4): 33–54.
13. Gupta, V.K., Waymire, E. and Wang, C. T. (1980). A representation of an instantaneous unit hydrograph from geomorphology. Water Resources Research, 16(5): 863–870.
14. Haktanir, T., Sezen, N. (1990). Suitability of two-parameter Gamma distribution and three-parameter beta distribution assynthetic hydrographs in Anatolia. Hydrological Sciences Journal, 35 (2): 167–184.

15. Hall, M.J., Zaki, A.F. and Shahin, M.M.A. (2001). Regional analysis using the geomorphoclimatic instantaneous unit hydrograph. Hydrology and Earth System Sciences, 5(1): 93-102.

16. Hann, C.T., Barfield, B.J. and Hayes, J.C. (1984). Design Hydrology and Sedimentology for Small Catchments. Academic Press, New York, USA.

17. Hengl, T., Maathuis, B.H.P. and Wang, L. (2006). Chapter 3: Terrain parameterization in ILWIS. In: New Terrain Parameterization Text Book, (editors), European Commission Joint Research Centre: 29-48.

18. Horton, R.E. (1932). Drainage basin characteristics. Transactions of American Geophysical Union, 13: 350–361.

19. Horton, R.E. (1945). Erosional development of streams and their drainage basins: Hydrophysical approach to quantitative morphology. Geological Society of America Bulletin, 56: 275–370.

20. Itenfisu, D., Elliot, R.L., Allen, R.G. and Walter, I.A. (2003). Comparison of reference evapotranspiration calculations as part of the ASCE standardization effort. Journal of Irrigation and Drainage Engineering, ASCE, 129(6): 440-448.

21. Jain, V. and Sinha, R. (2003). Derivation of unit hydrograph from GIUH analysis for the Himalayan river. Water Resources Management, 17: 355–375.

22. Karvonen, T., Koivusalo, H., Jauhiainen, M., Palko, J. and Weppling, K. (1999). A hydrological model for predicting runoff from different land-use areas. Journal of Hydrology, 217: 253–265.

23. Koutsoyiannis, D. and Xanthopoulos, T. (1989). On the parametric approach of unit hydrograph identification. Water Resources Management, 3: 107– 128.

24. Kumar, A. and Kumar, D. (2008). Predicting direct runoff from hilly watershed using geomorphology and stream-order-law ratos: case study. Journal of Hydrologic Enginnering, 13(7): 570-576.

25. Kumar, R., Chatterjee, C., Lohani, A.K., Kumar, S. and Singh, R.D., (2002). Sensitivity analysis of the GIUH based Clark model for a catchment. Water Resources Management, 16: 263–278.

26. Kumar, R., Chatterjee, C., Singh, R.D., Lohani, A.K. and Kumar, S. (2007). Runoff estimation for an ungauged catchment using geomorphological instantaneous unit hydrograph (GIUH) model. Hydrological Processes, 21: 1829-1840.

27. Lee, K.T. (1998). Generating design hydrographs by DEM assisted geomorphic runoff simulation: a case study. Journal of American Water Resources Association, 34(2): 375-384.

28. Maathuis, B. and Sijmons K. (2005). DEM from Active Sensors – Shuttle Radar Topographic Mission (SRTM), International Institute for Geo-Information Science and Earth Observation.

29. Madsen, H., Wilson, G. and Ammentorp, H.C. (2002). Comparison of different automated strategies for calibration of rainfall- runoff models. Journal of Hydrology, 261(1– 4): 48–59.

30. McCarthy, G.T. (1938). The unit hydrograph and flood routing. Unpublished manuscript presented at a conference of the North Atlantic Division, 24 June 1938, US Army Corps of Engineers.

31. Miller, V.C. (1953). A quantitative geomorphic study of drainage basin characteristics in the Clinch Mountain area, Virginia and Tennessee. Columbia University, Department of Geology, Technical Report, No.3: 271-300.

32. Moore, I.R., Grayson, R.B. and Ladson, A.R. (1992). Digital terrain modelling: A review of Hydrological, Geomorphological and Biological applications. Terrain analysis and distributed modelling in hydrology. (editors), Beven, K. and Moore, I. R., John Wiley and Sons, 7-34.

33. Moradkhani, H., Hsu, K.L., Gupta, H.V. and Sorroshian, S. (2004). Improved streamflow forecasting using self-organizing radial basis function artificial neural networks. Journal ofhydrology, 295: 246-262.

34. Nandrajah, S. (2007). Probability models for unit hydrograph derivation. Journal of Hydrology, 344: 185–189.

35. Nash, J.E. (1957). The form of instantaneous unit hydrograph. International Association of Sciences and Hydrological Publications, 45(3): 114–121.

36. Nash, J.E. and Sutcliffe, J.V. (1970). River flow forecasting through conceptual models. In: A discussion of principles. Journal of Hydrology, 10(3): 282–290.

37. Rodriguez-Iturbe, I. and Valde's, J.B. (1979). The geomorphologic structure of the hydrologic response. Water Resourcrs Research, 15(6): 1409– 1420.

38. Rosso, R. (1984). Nash model relation to Horton order ratios. Water Resources Research, 20(7): 914– 920.

39. Schumn, S.A. (1956). Evolution of drainage systems and slopes in Badlands at Perth Amboy. New Jersey.

40. Sherman, L.K. (1932). Stream flow from rainfall by the unit-graph method. Engineering News-Record, 108(14): 501–505.

41. Singh, S.K. (2000). Transmuting synthetic hydrographs into Gamma distribution. Journal of Hydrologic Engineering, ASCE, 5(4): 380–385.

42. Singh, V.P. (1987). On Application of the Weibull Distribution in Hydrology. Water Resources Management, 1: 33-43

43. Snyder, F.F. (1938). Synthetic unit hydrographs. Transactions of American Geophysical Union, 19: 447–454.

44. Strahler, A.N. (1957). Quantitative Analysis of Watershed Geomorphology. Transaction of American Geophysicsical Union, 38(6): 913–920.

45. Strahler, A.N. (1968). Quantitative geomorphology. In: Fairbridge, R.H. (editor), The Encyclopedia of Geomorphology: Encyclopedia of Earth Sciences Series, III. Dowden, Hutchinson, & Ross, Inc, Stroudsburg, PA, 898–912.

46. Tarboton, D.G., Bras, R.L. and Rodriguez-Iturbe, I. (1991). On the extraction of channel network fron digital elevation data. Hydrological processes, 5: 81-100.

47. United States Army Corps of Engineers, (1994). Flood Hydraulics Package User's Manual for HEC-1, 1990, CPD-1A Version 4.0. US Army Corps of Engineers, Washington DC, USA.

48. Weibull, W. (1939). The phenomenon of ruptures in solids. Ingenior Vetenskaps Akademiens Handlingar, 153: 17.

A Revisit to SCS-CN Methodology

1. Abbott, M.B., Bathurst, J.C., Cunge, J.A., O'Connell, P.E. and Rasmussen, J. (1986a). An introduction to the European Hydrologic System (SHE). 1. History and philosophy of a physically-based, distributed modeling system. Journal of Hydrology, 87: 45–59.

2. Abbott, M.B., Bathurst, J.C., Cunge, J.A., O'Connell, P.E. and Rasmussen, J. (1986b). An introduction to the European Hydrologic System (SHE). 2. Structure of physically-based, distributed modeling system. Journal of Hydrology, 87: 61–77.
3. Andrews, R.G. (1954). The use of relative infiltration indices for computating runoff (unpublished). 'Soil Conservation Service' Fort Worth, Texas, 6P.
4. Bales, J. and Betson. R.P. (1981). The curve number as a hydrologic index. In: Rainfall Runoff Relationship, (editor), Singh, V.P., Littleton, Colo.: Water Resources Publication. 371-386.
5. Boughton, W.C. (1993). A hydrograph-based model for estimating the water yield of ungauged catchments. Hydrology and Water Resources Symposium, Institution of Engineers Australia, Newcastle, 317-324.
6. Burton, J.S. (Compiler) (1993). Proceedings of the federal Interagency Workshop on hydrologic modeling demands for the 90's. USGS Water Resources Investigations report, 93-4018, Federal center, Denver, Colorado.
7. Chapman, T.G. (1991). Comment on 'Evaluation of automated techniques for base flow and recession analyses' by Nathan, R.J. and McMahon, T.A. Water Resources Research, 27: 1783-1784.
8. Chapman, T.G. (1999). A comparison of algorithms for stream flow recession and baseflow separation. Hydrological Processes, 13: 701-714.
9. Chapman, T.G. and Maxwell, A.I. (1996). Baseflow separation- comparison of numerical methods with tracer experiments. Hydrological and Water Resources Symposium, Institution of Engineers Australia, Hobart, 539-545.
10. Chiew, F.H.S., Stewardson, M.J. and McMahon, T.A. (1993). Comparison of six rainfall runoff modelling approaches. Journal of Hydrology, 147: 1–36.
11. Dooge, J.C.I. (1957). The rational method for estimating flood peaks. Engineering, 184: 311-313.
12. Dooge, J.C.I. (1973). Linear Theory of hydrologic systems. Technical Bulletin No.1468, United State Department Of Agriculture, Agriculture Research Service, Washington D.C.
13. Eckhardt, K. (2005). How to construct recursive digital filters for baseflow separation.Hydrological Processes, 19(2): 507-515.

14. Franchini, M. and Pacciani, M. (1991). Comparative analysis of seven conceptual rainfall–runoff models. Journal of Hydrology, 122: 161–219.

15. Furey, P.R. and Gupta, V.K. (2001). A physically based filter for separating baseflow from streamflow time series. Water Resources Research,37(11): 2709-2722.

16. Gan, T.Y., Dlamini, E.M. and. Biftu, G.F. (1997). Effects of model complexity and structure, data quality, and objective functions on hydrologic modeling. Journal of Hydrology, 192(1): 81-103.

17. Geetha, K., Mishra, S.K., Eldho, T.I., Rastogi, A.K. and Pandey, R.P. (2007). Modifications to SCS-CN Method for Long-Term Hydrologic Simulation. DOI: 10.1061/(ASCE) 0733-9437(2007)133:5(475)

18. Grayson, R., Argent, R., Nathan, R., McMahon, T. and Mein, R. (1996). Hydrological recipes: Estimation techniques in Australian hydrology. CRC Catchment Hydrology, Melbourne, 125.

19. Hann, C.T. (1975). Evaluation of a model for simulating monthly water yields from small watersheds. Southern Cooperative Series Bulletin, 201, Agricultural Experimentation of Kentucky, Mossissipi, North Carolina, South Carolina, Tennessee, and Virginia, July.

20. Hawkins, R.H. (1978). Runoff Curve Numbers with varying site moisture. Journal of Irrigation and Drainage Engineering, 104(4): 389-398.

21. Hawkins, R.H., Hjelmfelt, A.T.Jr. and Zevenbergen, A.W. (1985). Runoff probability, storm depth, and curve numbers. Journal of Irrigation and Drainage Engineering, A.S.C.E., 111(4): 330-339.

22. HEC, (2000). Hydrologic Modeling System HEC-HMS. Users Manual, Version2, Hydrologic Engineering Centre, United States Army Corps of Engineers, Davis, CA.

23. Hjelmfelt, A.T.Jr. (1991). Investigation of curve number procedure. Journal Hydraulics Engineering, 117(6): 725–737.

24. Holtan, H.N. and Lopez, N.C. (1971). USDHAL-70 Model of Watershed Hydrology. Technical Bulletin, 1435, United States Department of Agriculture.

25. Huber, W.C., Heaney, J.P., Bedient, B.P. and Bender, J.P. (1976). Environmental Resources Management studies in Kissimmee River Basin. Report, Env-05-76-3, Department of Environmental Engineering and science, University of Florida: Gainesvilla, Florida.

26. Jakeman, A.J. and Hornberger, G.M. (1993). How much complexity is warranted in a rainfall-runoff model? Water Resources Research, 29(8): 2637-2649.

27. James, L.D. (1972). Hydrologic modeling parameter estimation and watershed characteristics. Journal of Hydrology, 17: 283–307.

28. Johnston, P.R. and Pilgrim, D.H. (1976). Parameter optimization for watershed models. Water Resources Research, 12(3): 477–486.

29. Knisel, W.G. (1980). CREAMS, a Field Scale Model for Chemicals, Runoff, and Erosion of Agricultural Management Systems. Conservation Report 26, USDA Agricultural Reserch Service: Washington, DC.

30. Kottegoda, N.T., Natale, L. and Raiteri, E. (2000). Stastistical modeling of daily streamflow using rainfall input and curve number technique. Journal of Hydrology, 234: 170–186.

31. Linsley, R.K., Kohler, M.A., Paulhus, J.L.H. and Wallace, J.S. (1958). Hydrology for engineers. McGraw Hill, New York.

32. Lyne, V.D. and Hollick, M. (1979). Stochastic time-variable rainfall runoff modelling. Hydrology and Water Resources Symposium, Institution of Engineers Australia, Perth, 89-92.

33. Mau, D.P. and Winter, T.C. (1997). Estimating groundwater recharge from stream flow hydrographs for a small mountain watershed in a temperate humid climate, New Hampshire,USA. Ground Water, 35(2): 291-304.

34. Mein, R.G. and Brown, B.M. (1978). Sensitivity of optimized parameters in watershed models. Water Resources Research, 14(2): 299–303.

35. Mishra, S.K. (1998). A Thesis on operation of multipurpose reservoir. Department of hydrology, University of Roorkee, Roorkee 247667 (India).

36. Mishra, S.K., Goel, N.K., Seth, S.M. and Srivastava, D.K. (1998). An SCS-CN based long term daily flow simulation model for a hilly catchment. International Symposium of Hydrology of Ungauged Streams in Hilly Regions for Small Hydropower Development, AHEC, University of Roorkee, 59–81.

37. Mishra, S.K. and Singh, V.P. (1999). Another look at SCS-CN method. Journal of Hydrologic Engineering, ASCE, 4(3): 257–264.

38. Mishra, S.K. and Singh, V.P. (2002a). SCS-CN method: Part I: Derivation of SCS-CN based models, Acta Geophys. Pol. 50(3): 457–477.

39. Mishra, S.K. and Singh, V.P. (2002b). SCS-CN based hydrologic simulation package. In Mathematical Models in Small Watershed Hydrology, (editors, Singh, V.P. and Frevert, D.K.), 391–464. Water Resources Publication, Littleton, CO.

40. Mishra, S.K. and Singh, V.P. (2003). Soil Conservation Service Curve Number (SCS-CN) Methodology. Kluwer Academic: Dordrecht.

41. Mishra, S.K. and Singh, V.P. (2004). Long-term hydrological simulation based on the Soil Conservation Service curve number. Journal of Hydrological Processes, 18(7): 1291–1313.

42. Mishra, S.K., Jain, M.K., Pandey, R.P. and Singh, V.P. (2003a). Evaluation of AMC dependent SCS-CN models using large data of small watersheds. Water and Energy International, 60(3): 13–23.

43. Mishra, S.K., Singh, V.P., Sansalone, J.J. and Aravamuthan, V. (2003b). A modified SCS-CN method: Characterization and Testing. Water Resources Management, 17: 37–68.

44. Mishra, S.K., Jain, M.K. and Singh, V.P. (2004). Evaluation of the SCS-CN based model incorporating antecedent moisture. Water Resources Management, 18: 567–589.

45. Mockus, V. (1964). Letter to Orrin Ferris, March 5, 6P, In: Rallison, R.E., Origin and evolution of the SCS runoff equation, Proc., American Society Civil Engineers, Symposium. Watershed management, Boise, Idaho, July, 1980.

46. Moore, I.D., Colthrap, G.B. and Sloan, P.G. (1983). Predicting runoff from small Appalachian watersheds. Transactions of the Kentucky Academy of Science, 44(3,4): 135–145.

47. Nash, J.E. and Sutcliffe, J.V. (1970). River flow forecasting through conceptual models. Part I. A discussion of principles. Journal of Hydrology, 10: 282–290.

48. Nathan, R.J. and McMahon, T.A. (1990). Evaluation of automated techniques for base flow and recession analyses. Water Resources Research, 26:1465–1473.

49. Neal, C., Skeffington, R., Neal, M., Wyatt, R., Wickham, H., Hill, L. and Hewitt, N. (2004).Rainfall and runoff water quality of the Pang and Lambourn, tributaries of the river Thames, south eastern England. Hydrology of the Earth System and Science, 8: 601-613.

50. Pandit, A. and Gopaikrishnan, G. (1996). Estimation of annual storm runoff coefficients by continuous simulation. Journal of Irrigation and drainage Engineering, 122(4): 211-220.

51. Ponce, V.M. (1989). Engineering Hydrology, Prentice–Hall, Inc., Englewood Cliffs, New Jersey.640PP.

52. Ponce, V.M. and Hawkins, R.H. (1996). Runoff Curve number: Has it reached maturity? Journal of Hydrologic Engineering, 1: 11-19.

53. Poter, J.W. and McMahon, T.A. (1976). The Monash model user manual for daily program HYDROLOG. Department of Civil Engineering, Monash University vic. Research, Report. 2/76, 41.

54. SCS (1956, 1964, 1969, 1971, 1972, 1985, 1993). Hydrology. National Engineering Handbook, Supplement A, Section 4, Chapter 10, Soil Conservation Service, USDA, Washington, D.C.

55. Singh, V.P. (1989). Hydrologic Systems–Watershed Modeling, Vol. II. Prentice Hall: Englewood Cliffs, NJ.

56. Singh, V.P. (1992). Elementary Hydrology. Prentice Hall, Englewood Cliffs, NJ.

57. Singh, V.P. (1995). Computer models of watershed hydrology. Water Resources Publication, Littleton, Colorado.

58. Singh, P. and Singh, V.P. (2001). Snow and Glacier Hydrology. Kluwer Academic Publishers, P.O. Box 322, Dordrecht, The Netherlands.

59. Singh, R.D., Mishra, S.K. and Chowdhary, H. (2001). Regional flow duration models for 1200 ungauged Himalayan watersheds for planning microhydro projects. Journal of Hydrologic Engineering, Technical Note, American Society of Civil Engineers, 6(4): 310–316.

60. Smakhtin, V.Y. (2001). Low flow hydrology: a review. Journal of Hydrology, 240: 147-186.

61. Soil Conservation Service (SCS, 2004). (http://www.wcc.nrcs. usda.gov/ hydro / hydro-techref-neh-630.html).

62. Soni, B. and Mishra, G.C. (1985). Soil water accounting using SCS hydrologic soil classification. Case study, National Institute of Hydrology, Roorkee, India.

63. Williams, J.R. and LaSeur, W.V. (1976). Water Yield model using SCS curve numbers. Journal of Hydraulics Division, ASCE, Vol.102 No. HY9, Proceedings, Paper 12377, 1241-1253.

64. Woodward, D.E. and Cronshey, R. (1992). Investigation of curve number procedure - discussion. Journal of Hydraulic Engineering. 118(6): 951.

65. Woodward, D.E. and Gburek, W.J. (1992). Progress report ARS/SCS curve number work group. Proceedings, ASCE, Water Forum'92, ASCE, New York, 378-382.

66. Wurbs, R.A. (1998). Dissemination of Generalized water resources models in United States. Water International, 23: 190-198.
67. Yao, H., Hashino, M. and Yoshida, H. (1996). Modelling energy and water cycle in a forested head basin. Journal of Hydrology, 174: 221–234.
68. Young Andrew R. (2006). Stream flow simulation within UK ungauged catchments using a daily rainfall-runoff model. Journal of Hydrology, 320: 155–172.
69. Yuan. Y., Mitchell, J.K., Hirschi, M.C. and Cooke, R.A.C. (2001). Modified SCS Curve Number Method for predicting sub surface drainage flow. Transaction of the ASAE, 44(6): 1673- 1682.

Application of TOPMODEL

1. Abbott, M.B., Bathurst, J.C. and Cunge, J.A. (1986). An introduction to the European Hydrological system: System Hydrologique European (SHE). Journal of Hydrology, 87: 45 - 59.
2. Beven, K.J. (1986a). Hillslope Runoff Processes and Flood Frequency Characteristics. In: Abhrahams, A.D., (editor), Hillslope Processes, 187-202, Allen and Unwin, Boston.
3. Beven, K.J. (1993). Prophecy reality and uncertainty in distributed hydrological modeling. Advances in Water Resources, 16: 41-51.
4. Beven, K.J. (1997). TOPMODEL A critique: Hydrological process, Vol. II, 1069–1085.
5. Beven, K.J. and Kirkby, M.J. (1979). A physical based variable contributing area model of catchment hydrology. Hydrologic Sciences Bulletin, 24: 43-69.
6. Beven, K.J. and Wood, E.F. (1983). Catchment geomorphology and dynamics of runoff contributing areas. Journal of Hydrology, 65: 139-158.
7. Beven, K.J. and Binley, A. (1992). The future of distributed models: model calibration and uncertainty prediction. Hydrological Processes, 279–298.
8. Beven, K.J., Lamb, R., Quinn, P., Romanowicz, R. and Freer, J. (1995). TOPMODEL. In Computer Models of Watershed Hydrology, Singh VP (editor).Water Resources Publications: Highlands Ranch, CO, USA; 627–668.
9. Beven, K. TOPMODEL Appendix A: Model Fact Sheets, http://www.cs.laucs.ac.uk/hft/ TOPMODEL.html.

10. Beven, K. TOPMODEL User notes, Window version 97.01, Centre for Research on Environmental Systems and Statistics Lancaster University Lancester.
11. Bhaskar Nageshwar, R., Laura, K., Brummett and Mark, N. (2005). French rainfall-runoff response of a mountainous catchment, Tygarts Creek, using TOPMODEL. Journal of the American Water Resources Association, 41(1):107–121.
12. Blaney, H.F. and Criddle, W.D. (1962). Determining Consumptive use and irrigation water requirements. Technical bulletin, 1275.Washington D.C. U.S. Department of Agriculture.
13. Clark, C.O. (1945). Flood storage accounting. Transactions of American Society of civil Engineers, 110: 1419-46.
14. Campling, P., Gobin, A., Beven, K. and Feyen, J. (2002). Rainfall-Runoff modeling of a humid tropical catchment, the TOPMODEL approach: Hydrological process, 16: 231-253.
15. Costa-Carbal, M. and Burger, S.J. (1994). Digital elevation model networks (DEMON): A model of flow over hill slopes for computation of contributing and dispersal areas. Water Resources Research, 30 (6): 1681-1692.
16. Dooge, J.C.I. (1959). A general theory of unit hydrograph. Journal of Geophysics Resources, 64(2): 241–256.
17. Durand, P., Robson, A. and Neal, C. (1992). Modelling the hydrology of submediterranean mountain catchment (Mont Loneze, Frever) using TOPMODEL: initial results. Journal of Hydrology, 139: 1-14.
18. ERDAS IMAGINE 8.5, (2001). ERDAS.inc, Leica Geo system Geospatial Imaging, Hexagone Group, Sweden.
19. ESRI (2000). Using Arc Map, ESRI, Red lands, California.
20. Fairfield, J. and Leymarie, P. (1991). Drainage networks from grid digital elevation models. Water Resources Research, 27(5): 709-717.
21. Freeman, T.G. (1991). Calculating catchment area with divergent flow based on a regular grid. Computational Geosciences 17: 413-422.
22. Guntner, A., Uhlenbrook, S., Seibert, J. and Leibundgert, C.H. (1999). Multicritical validation of TOPMODEL in a mountainous catchments. Hydrological Processes, 13:1603-1620.

23. Hornberger, G.M., Beven, K.J. and Cosby, B.J. (1985). Shenadcah watershed study: calibration of a topography based, variable contributing area hydrological model to a small forested catchment. Water Resources Research, 21: 1841-1850.

24. Jain, M.K. (1996). GIS based Rainfall-Runoff modeling for Hemavathy catchment, CS (AR) – 22/96-97, N.I.H. Roorkee.

25. Jenson, S.K. and Dominique, J.O. (1988). Extracting topographic structure from digital elevation data for geographic information system analysis. Photogrammetric Engineering & Remote Sensing, 54(11): 1593-1600.

26. Kirkby, M.J. and Weyman, D.R. (1974). Measurements of contributing areas in very small drainage basins. Seminar Series B, No.3, Department of Geography, University of Bristol, Bristol, United Kingdom.

27. Lamb, R., Beven, K.J. and Mayrabe, S. (1998). A generalized topographic soil hydrological index. In: Landform monitoring, Modelling and analysis, Lane, S.N., Richards, K.S. and Chandler, J.H., (editors), Wiley: Chichester, UK, 263-278.

28. Mendicino, G. and Sole, A. (1997). The information content theory for the estimation of topographic index distribution used in TOPMODEL. Hydrological process, 2: 1099-1114.

29. Molicova, H., Grimaldi, M., Bonnel, M. and Hubert, P. (1997). Using TOPMODEL towards identifying and modeling the hydrological patterns within a humid tropical catchment. Hydrological process, 2: 1169 – 1196.

30. Nachabe Mahmood H. (2005). Equivalence between TOPMODEL and the NRCS Curve Number method in predicting variable runoff source areas. Journal of American Water Resources Association, (JAWRA), 42(1): 225–235.

31. Nageshwar, R.B., Brummet, L.K. and French, M.N. (2005). Runoff modeling of a mountainous catchment using TOPMODEL: A case study. Journal of American water resources association, (JAWRA), 107-121.

32. Nash, J.E. (1957). The form of instantaneous unit hydrograph. International Association of Scientific Hydrology Publication, 45(3): 114-121

33. Nash, J.E. and Sutcliffe, J.V. (1970). River flow forecasting through conceptual models I. A discussion of principles. Journal of Hydrology, 10: 282–290.

34. NBSSLUP (2004). Soils of Uttar Pradesh for optimizing land use: Executive summary. NBSS Publication 68, National Bureau of Soil Survey and Land Use Planning, ICAR, Nagpur 400010.

35. Pinol, J., Beven, K. and Freer, J. (1997). Modelling the hydrological response of Mediterranean catchments, PRADES, CATALONIA. Hydrological Processes, 2(9): 1287-1306.

36. Ponce, V.M. (1989). Engineering Hydrology, Prentice–Haii, Inc., Englewood Cliffs, New Jersey.640PP.

37. Quinn, P.F., Beven, K.J., Chevallier, P. and Planchok, O. (1991). The prediction of hill slope flow paths for distributed hydrological modeling using digital terrain models. Hydrological Processes, 5: 59-79.

38. Quinn, P.F., Beven, K.J. and Lamb, R. (1995). The ln (a/tanβ) index; how to calculate it and how to use it within the TOPMODEL framework. Hydrological Processes, 9: 161-182.

39. Robson, A.J., White Lead P.G. and Johuson, R.C. (1993). An application of a physically based semi distributed model to the Balqutidder catchments. Journal of Hydrology, 145: 357-370.

40. Saulnir, A.M., Beven, K.J. and Obled, C. (1997). Digital elevation analysis for distributed hydrological modeling: Reducing scal dependence in effective hydraulic conductivity values. Water Resources Research, 33: 2097-2101.

41. SCS (1956). Hydrology. National Engineering Handbook, Supplement A, Section 4, Chapter 10, Soil Conservation Service, USDA, Washington D.C.

42. Shufen, S., and Huiping, D. (2004). A study of rainfall-runoff response in a catchment using TOPMODEL. Advances in atmospheric sciences, 21(1): 87-95.

43. Tarboton, D.G., TauDEM version 3.1, May 2005, http:/www Engineering.use.edu/dtarb.

44. Tarboton, D.G. (1997). A new method for the determination of flow directions and upslope area in grid digital elevation models. Water Resources research, 33(2): 309-317.

45. Todini, E. (1988b). Rainfall runoff modeling: Past, present and future. Journal of Hydrology, 100: 341–352.

46. Venkatesh, B. and Jain, M.K. (2000). Simulation of daily flows using topography based rainfall-runoff model. Journal of Institution of engineers (India), 81:127-132.

47. Wang, J., Theodore, A.E. and James, M.H. (2006). Power function decay of hydraulic conductivity for a TOPMODEL based infiltration routine. Hydrological processes, 20: 3825 –3834

Application of SWAT Model

1. Arnold, J.G. and Fohrer, N. (2005). SWAT 2000: Current capability and research opportunities in applied watershed modeling. Published in Hydrologic Processes, 19: 563-572.
2. Arnold, J.G. Soil and Water Assessment Tool: Model Fact Sheet, 337-341.
3. Arnold, J.G. and Williams, J.R. (1987). Validation of SWRRB-simulator for water resources in rural basins. Journal of Water Resources Planning and Management, ASCE, 113(2): 243-256.
4. Arnold, J.G., Williams, J.R. and Maidment, D.R. (1995). Continuous-time water and sediment –routing model for large basins. Journal of Hydraulic Engineering, 121(2):171-183.
5. Arnold, J.G., Williams, J.R., Nicks, A.D. and Sammons, N.B. (1990). SWRRB: A basin scale simulation model for soil and water resources management. Taxes A&M University Press, College Station, TX.
6. Benaman, J., Christine, A., Shoemake and Dauglas, A.H. (2005). Calibration and validation of soil and water assessment tool on an agriculture watershed United State New York. Published in Journal of Hydrologic Engineering, ASCE, 363-374.
7. Busche, H., Heipe, C. and Diekkruger, B. (2005). Modeling the effects of land use and climate change on Hydrology and soil erosion in a sub humid African catchment. Published in 3rd International SWAT Conference Proceeding, July 11-15, 2005, Zurich, held at Eawag, Switzerland, 433-443.
8. Cho, S.M. and Lee, M.W. (2001). Sensitivity considerations when modeling hydrologic processes with digital elevation model. Journal of the American Water Resources Association, 37(4): 931-934.
9. Chow V.T., Maidment, D.R. and Mays, L.W. (1988). Applied Hydrology. Publisher: McGraw- Hill Book Company.

10. Donigian, A.S., Imhoff, J.C. and Bicknell, B.R. (1983). Predicting water quality resulting from Agricultural non point source pollution via simulation - HSPE. Agricultural management and water quality, Iowa State University Press Ames Iowa, 200-249.

11. Eckhardt, K. and Arnold, J.G. (2001). Automatic calibration of a distributed catchment model. Journal of Hydrology, 251: 103-109.

12. Gassman, P.W., Jha, M., Secchi, S. and Arnold J. (2003). Initial calibration and validation of the SWAT model for the Upper Mississippi river basin. Diffuse pollution Conference Dublin, 2003, 35- 40.

13. Gholami, S.A. and Gosain, A.K. (2005). Distributed watershed modeling mountainous catchment: A case study in the Amameh catchment in Iran. Published in 3rd International SWAT Conference Proceedings July 11-15,2005, Zurich, held at Eawag, Switzerland, 408-414.

14. Gosain, A.K., Rao, S., Ray, D.B., Bhandari, A., Calder, I., Amezaga, J. and Garratt, J. (2006). Hydrological modeling in the micro watersheds of Madhaya Pradesh and Himachal Pradesh –Internal Report XII-Feb, 2006.

15. Gosain, A.K., Rao, S., Srinivasan, R., Reddy, N. and Gopal (2005). Return flow Assessment for irrigation command in the Palleru river basin using SWAT model. Published in Hydrological Processes, 19(3, 28): 673-682.

16. Gupta, H.V., Sorooshian, S. and Yapo, P.O. (1999). Status of automatic calibration for hydrologic models: Comparision with multilevel expert calibration. Journal of Hydrologic Engineering, 4(2): 135-143.

17. Harmel, R.D., Cooper, R.J., Slade, R.M., Haney, R.L. and Arnold, J. G. (2006). Cumulative uncertainty in measured streamflow and water quality data for small watersheds. Transactions of ASABE, 49(3): 689-701.

18. Haan, C.T., Barifield, B.J. and Hayes, J.C. (1994). Design Hydrology and Sedimentology for Small Catchments.

19. Hao Fanghua, Cheng Hongguange, Yang Stengtian, Qi Ye and Ren Xeihe river. (2005). Published in 3rd International SWAT Conference Proceeding, July 11-15, 2005, Zurich, held at Eawag, Switzerland, 423-433.

20. Jirayoot, K. and Trung, L. D. (2005). Application of SWAT model to the Decision Support Framework of the Mekong River Commission. Published in 3rd International SWAT Conference Proceeding, July 11-15, 2005, Zurich, held at Eawag, Switzerland, 320-329.

21. Kannan, N., White, S.M., Worrall, F. and Whelan, M.J. (2007). Sensitivity analysis and identification of the best evaportranspiration and runoff options for hydrological modeling in SWAT -2000. Published in Journal of Hydrology, 332: 456–466.

22. Kim, C., Kim, H., Jang, C., Shin, S. and Kim, N. (2003). SWAT application to the Yongdam and Bocheong watersheds in the Korea for daily stream flow estimation. Published in 2nd International SWAT Conference Proceeding, July 01-04, 2003, Bari, Itali, 283-292.

23. Knisel, W.G. (1980). CREAMS, a Field Scale Model for Chemicals, Runoff, and Erosion of Agricultural Management Systems. Conservation Report 26, USDA Agricultural Reserch Service: Washington, DC.

24. Krysanova, V., Hatterman, F., Post, J., Habeack, A. and Wechsung, F. (2005). Application of SWIM model with Elbe basin : Experiment and new developments. Published in 3rd International SWAT Conference Proceeding, July 11-15, 2005, Zurich, held at Eawag, Switzerland, 19-29.

25. Lenhart, T., Kckhardt, K., Fohrer, N. and Frede, H.G. (2002). Comparison of two different approaches of sensititivity analysis. Physics and Chemistry of Earth, 27: 645–654.

26. Leonard, R.A., Knisel, W.G. and Still, D.A. (1987). GLEAMS:Groundwater loading effects of agricultural management systems. Transactions of ASAE, 30(5): 1403-1418.

27. Liew Van, M.W., Veith, T.L., Bosch, D.D. and Arnold, J.G. (2007). Suitability of SWAT for the conservation effects assessment project: A comparison on USDA-ARS experimental watersheds.Journal of Hydrologic Engineering, 12(2): 173-189.

28. Luzio, M.D., Mitchell, G. and Sammons, N. (2005). AVSWAT- X Tutorial for Workshop on Watershed Modeling using SWAT 2003. March 5, 2005.

29. Luzio Mauro, D., Srinivasan, R. and Arnold, J.G. (2002). Integration of Watershed Tools and SWAT Model into Basins. Journal of the American Water Resources Association, 38(4): 1127-1141.

30. Mausbach, M.J. and Dedrick, A.R. (2004). The length we go: measuring environmental benefits of conservation practices. Journal of Soil and Water Conservation, 5915: 96A–103A.

31. Mishra, A., Froebrich, J. and Kar, S. (2003). Potential and applicability of SWAT model in check dam management in small watershed. Published in 2nd International SWAT Conference Proceeding, July 01-04, 2003, Bari, Itali, 283-292.

32. Motovilov, Y.G., Gottschalk, L., Engeland, K. and Rodhe, A. (1999). Validation of distributed hydrological model against spatial observation. Agicultural and Forest Meteorology, 98: 257-277.

33. Muleta, K., Misgana., Nicklow, J.W. and Bekele, G. (2007). Sensitivity of distributed watershed simulation model to spatial scale. Published in Journal Of Hydrologic Engineering, ASCE / March /April, 2007, 163-172.

34. Muthuwatta, L.P. (2004). Long term rainfall – runoff lake level modeling of the lake Naivasha basin, Kenya. Information Institute for Geo- information and Earth Observation Enschede, The Netherlands.

35. Neitsch, S.L., Arnold, J.G. Kiniry, J.R. and King, K.W. (2002). Soil and Water Assessment Tool theoretical documentation, Version 2000.

36. Neitsch, S.L., Arnold, J.G. Kiniry, J.R. and King, K.W. (2005). Soil and Water Assessment Tool theoretical documentation, Version 2005.

37. Nash, J.E. and Sutcliffe, J.V. (1970). River flow forecasting through conceptual models. Part 1- A discussion of principles. Journal of Hydrology, 10 (3): 282-290.

38. National Bureau of Soil Survey and Land Use Planning, ICAR, Negpur – 400010. Soils of Uttar Pradesh for optimizing land use: Executive summary. Publication number 68.

39. Patra, K.C. (2008). Hydrology and Water Resources Engineering. Published by Narosa Publishing House, New Delhi.

40. Sevat, E. and Dezetter, A. (1991). Selection of calibration of objective functions in the context of rainfall – runoff modeling in a Sudanese savannah area. Hydrologic Sciences Journal, 36: 307-330.

41. Tideman, E.M. (1999). Watershed Management – Guidelines for Indian Condition.

42. Tripathi, M.P., Panda, R.K. and Raghuvansi, N.S. (2005). Development of effective management plan for critical sub watershed using SWAT model. Published in Hydrological Processes, 28th Feb.2005, 19(3): 809-826.

43. Watson, B.M., Ghafouri, M. and Selvalingam, S. (2003). Applications of SWAT to model the water balance of the Woady Yalok River Catchments, Australia. Published in 2nd International SWAT Conference Proceeding, July 01-04, 2003, Bari, Itali, 94-110.

44. Williams, J.R, Nicks, A.D. and Arnold, J.G. (1985). Simulator for water resources in rural basins. Journal of Hydraulic Engineering, 111(6): 970-986.

45. Williams, J.R., Jones, C.A. and Dyke, P.T. (1984). A modeling approach to determining the relationship between erosion and soil productivity. Transactions of ASAE, 27(1): 129-144.

46. White, S.M., Kannan, N., Grizzetti, B. and Hollis, J. (2005). Catchments scale modeling of pesticides losses with imperfect data. Published in 3rd International SWAT Conference Proceeding, July 11-15, 2005, Zurich, held at Eawag, Switzerland, 30-39.

Application of ANN Model

1. Abrahart, R.J. and See, L. (2000). Comparing neural network and autoregressive moving average techniques for the provision of continuous river flow forecasts in two contrasting catchments.Hydrologic Processes, 14: 2157–2172.

2. Agarwal, A., Singh, R.D., Mishra, S.K. and Bhunya, P.K. (2005). ANN-based sediment yield models for Vamsadhara river basin (India). Water SA, 31(1): 95-100.

3. Agarwal, P.K., Senthil Kumar, A.R., Sudheer, K.P. and Jain, S.K. (2004). Rainfall-Runoff Modeling using Artificial Neural Networks: Comparison of Network Types. Journal of Hydrological Processes, 19: 1277-1291.

4. Agarwal, A. (2002). Artificial neural networks and their application for simulation and prediction of runoff and sediment yield. Unpublished PhD thesis work.

5. Anctil, F., Perrin, C. and Andreassian, V. (2004). Impact of the length of observed records on the performance of ANN and of conceptual parsimonious rainfall-runoff forecasting models. Environ.Modell.Software, 19: 357-368.

6. ASCE Task Committee on Application of Artificial Neural Networks in Hydrology. (2000). Artificial neural networks in hydrology-I: preliminary concepts. Journal of Hydrologic Engineering, ASCE, 5(2): 115–123.

7. Bhattacharya, B. and Solomatine, D.P. (2000). Application of artificial neural network in stage discharge relationship. Proceedings of 4th International Conference on Hydroinformatics, Iowa, USA.

8. Broomhead, D.S. and Lowe, D. (1988). Multivariable functional interpolation and adaptive networks. Complex Systems, 2: 321-355.

9. Bustami, R., Nabil, B., Charles, B. and Suhaila, S. (2007). Artificial Neural Network for precipitation and water level predictions of bedup river IAENG. International Journal of Computer Science, 34(2).

10. Chenard, J. And Caissie, D. (2008). Stream temperature modelling using artificial neural networks: application on Catamaran Brook, New Brunswick, Canada. Hydrological processes, 22: 3361-3373.

11. Chiang, Y.M., Chang, L.C. and Chang, F.J. (2004). Comparison of static feed forward and dynamic-feedback neural networks for rainfall–runoff modeling. Journal of Hydrology, 290: 297–311.

12. Coulibaly, P., Anctil, F. and Bobe´e, B. (1998). Real time neural network based forecasting system for hydropower reservoirs. In: Miresco, E.T. (editor), Proceedings of the First International Conference on New Information Technologies for Decision Making in Civil Engineering, University of Quebec, Montreal, Canada, 1001–1011.

13. Coppola, Emery, A., Rana, A. J., Poulton, M.M., Szidarovszky, F. and Uhl, V.W. (2005). A neural network model for predicting aquifer water level elevations. Ground Water, 43(2): 231 -241.

14. Cryer, J.D. (1986). Time Series Analysis. Boston: PWS-KENT Publishing Company.

15. Dawson, C.W., Harpham, C., Wilby, R.L. and Chen, Y. (2002). Evaluation of artificial neural network techniques for flow forecasting in the River Yangtze, China Hydrology and Earth System Sciences, 6(4): 619-626.

16. Dawson, C.W. and Wilby, R.L. (2001). Hydrological modelling using artificial neural networks, Progress In Physical Geography, 25:80–108.

17. de Vos N.J. and Rientjes, T.H.M. (2005). Constraints of artificial neural networks for rainfall-runoff modeling: Trade-offs in hydrological state representation and model evaluation. Hydrology and Earth System Sciences, 9: 111–126.

18. Deco, G. and Obradovic, D. (1996). An information theory based learning paradigm for linear feature extraction, Neurocomputing, 12: 203-221.

19. Fernando, D.A.K. and Jayawardena, A.W. (1998). Runoff forecasting using RBF networks with OLS algorithm. The Journal of Hydrologic Engineering, ASCE, 3(3): 203-209.

20. French, M.N., Krajeswski, W.F. and Cuykendall, R.R. (1992). Rainfall forecasting in space and time using a neural network. Journal of Hydrology, 137: 1-31.

21. Gaume, E. and Gosset, R. (2003). Over-parameterisation: A major obstacle to the use of artificial neural networks in hydrology. Hydrology and Earth System Sciences, 7(5): 693–706.

22. Graham, E., Clive, W.J.G. and Timmermann, A. (2006). Handbook of Economic Forecasting. Published by Elsevier.

23. Haykin, S. (1999). Neural networks: a comprehensive foundation. New Jersey: Prentice Hall.

24. Hsu, K.L., Gupta, H.V. and Sorooshian, S. (1995). Artificial neural network modeling of the rainfall–runoff process. Water Resources Research, 31: 2517-2530.

25. Jain, A. and Srinivasulu, S. (2004). Development of effective and efficient rainfall-runoff models using integration of deterministic, real-coded genetic algorithms and artificial neural network techniques. Water Resources Research, 40(4).

26. Jain, S.K., Das, D. and Srivastava, D.K. (1999). Application of ANN for reservoir inflow prediction and operation. Journal of Water Resources Planning and Mgnagement, ASCE, 125 (5): 263–271.

27. Jain, S.K., Nayak, P.C. and Sudheer, K.P. (2008). Models for estimating evapotranspiration using artificial neural networks and their physical interpretation. Hydrologic Processes, 22: 2225–2234.

28. Jalili, M., Kharaajoo, and Bubak, M. (2004). Proposing a new learning algorithm to improve fault tolerance of neural networks. ICCS 2004, LNCS 3037, 717-721.

29. Kachroo, R.K. and Natale, L. (1992). Non-linear modelling of the rainfall-runoff relation. Journal of Hydrology, 135: 341–369.

30. Kadri, Y. and Ahmet, K. (2005). Performances of stochastic approaches in generating low streamflow data for drought analysis. Journal of spatial hydrology spring, 5: 20-31.

31. Krishna, B., Satyaji Rao, Y.R. and Vijaya, T. (2008). Modelling groundwater levels in an urban coastal aquifer using artificial neural networks. Hydrological processes, 22: 1180-1188.

32. Komda, T. and Makarand, C. (2000). Hydrological forecasting using neural networks. Journal of Hydrologic Engineering, 5: 180-189.

33. Kuligowski, R.J. and Barros, A.P. (1998). Experiments in short-term precipitation forecasting using artificial neural networks. Monthly Weather Review, 126: 470–482.

34. Lin, G.F. and Chen, L.H. (2004). A non-linear rainfall–runoff model using radial basis function network. Journal of Hydrology, 289: 1–8.

35. MacQueen, J. (1967). Some methods for classification and analysis of multivariate observations, Proceedings of the 5th Berkeley Symposium on Mathematical Statistics and Probability, 1: 281–297.

36. Maier, H.R. and Dandy, G.C. (2000). Neural networks for the prediction and forecasting of water resources variables: a review of modeling issues and applications. Environmental Modeling & Software, 15: 101–124.

37. Makridakis, Spyros, Winkler, and Robert, L. (1983). Averages of forecasts: Some empirical results. Management Science, 29: 987-996.

38. Marina, C., Paolo, A. and Alfredo, S. (1999). River flood forecasting with a neural network model. Water Resources Research, 35: 1191-1197.

39. Mason, J.C., Price, R.K. and Temme, A. (1996). A neural network model of rainfall-runoff using radial basis functions. Journal of Hydraulic Research, 34(4): 537-548.

40. Miksovsky, J. and Raidl, A. (2005). Testing for nonlinearity in European climatic time series by the method of surrogate data.Theoretical and Applied Climatology.

41. Minns, A.W. and Hall, M.J. (1996). Artificial neural networks as rainfall runoff models. Hydrologic Sciences, 41(3): 399-417.

42. Miyoung, S. and Cheehang, P. (2000). A radial basis function approach to pattern recognition and its application. ETRI Journal, 22(2).

43. Moradkhani, H., Hsu, K.L., Gupta, H.V. and Sorroshian, S. (2004). Improved streamflow forecasting using self-organizing radial basis function artificial neural networks. Journal ofhydrology, 295: 246-262.

44. Napiorkowski, Jarosław, J. and Adam, P. (2005). Artificial neural networks as an alternative to the volterra series in rainfall-runoff modelling. Acta Geophysica Polonica, 53(4): 459-472.

45. Nash, J.E. and Sutcliffe, J.V. (1970). River flow forecasting through conceptual models. In: A discussion of principles. Journal of Hydrology, 10(3): 282–290.

46. Nayak, P.C., Rao, Y.R.S. and Sudheer, K.P. (2006). Groundwater level forecasting in a shallow aquifer using artificial neural network approach. Water Resources Management, 20: 77-90.

47. Peralta, J., German, G. and Araceli, S. (2007). Design of artificial neural networks based on genetic algorithms to forecast time series. Innovations in Hybrid Intelligent Systems, ASCE 44: 231-238.

48. Piotrowski, A., Napi´orkowski, J.J. and Rowi´nski, P.M. (2006a). Flash-flood forecasting by means of neural networks and nearest neighbour approach – a comparative study. Nonlinear Processes Geophysics, 13: 443–448.

49. Poggio,T. and Girosi, F. (1990). Networks for approximation and learning. Proceedings of IEEE, 78:1481-1497.

50. Rajurkar, M.P., Kothyari, U.C. and Chaube, U.C. (2004). Modeling of the daily rainfall-runoff relationship with artificial neural network. Journal of Hydrology, 285: 96-113.

51. Ralph, W., Libin, S. and Jinxi, X. (2008). A new string-to-dependency machine translation algorithm with a target dependency language model. In Proceedings of the 46th Annual Meeting of the Association for Computational Linguistics (ACL).

52. Raman, H. and Sunilkumar, N. (1995). Multivariate modelling of water resources time series using artificial neural networks. Hydrological Sciences Journal, 40(1): 145-163.

53. Senthil Kumar, A.R., Sudheer, K.P., Jain, S.K. and Agarwal, P.K. (2005). Rainfall-runoff modelling using artificial neural networks: comparison of network types. Hydrologic Processes, 19: 1277-1291.

54. Shamseldin, A.Y. (1997). Application of a neural network technique to rainfall–runoff modeling. Journal of Hydrology, 199: 272–294.

55. Slawomir, G. (2005). Induced Weights Artificial Neural Network. ICANN 2005, LNCS 3697: 295-300.

56. Sudheer, K.P., Srinivasan, K., Neelakantan, T.R. and Srinivas, V.V. (2008). A nonlinear at a driven model for synthetic generation of annual stream flows. Hydrologic Processes 22: 1831–1845.

57. Tokar, A.S. and Johnson, P.A. (1999). Rainfall–runoff modeling using artificial neural networks. Journal of Hydrological Engineering, ASCE, 4(3): 232-239.

58. Tokar, A.S. and Markus, M. (2000). Precipitation – Runoff Modeling using Artificial Neural Networks and Conceptual Models. Journal of Hydrologic Engineering, ASCE, 5(2): 156-161.

59. Venkatesan, P. and Anitha, S. (2006). Application of a radial basis function neural network for diagnosis of diabetes mellitus. Current science, 91(9): 1195-1199.

60. Vieira, A. (2005). A multi-objective evolutionary algorithm using neural networks to approximate fitness evaluations. International Journal of Computer System and Signals, 6:18-36.

61. Wagener, T. (2003). Evaluation of catchment models. Hydrologic Processes, 17: 3375-3378.

62. Wei, S., Zhenghong, G. and Yingtao, Z. (2008). Application of RBF neural network ensemble to aerodynamic optimization. 46th AIAA Aerospace Sciences Meeting and Exhibit, Nevada.

63. Yang, C.C., Prasher, S.O., Lacroix, R., Sreekanth, S., Patni, N.K. and Masse, L. (1997). Artificial neural network model for subsurface-drained farmland. Journal of Irrigation and Drainage Engineering,123: 285–292.

64. Yu, P.S., Liui, C.L. and Lee, T.Y. (1994). Application of transfer function model to a storage runoff process. Stochastic and Statistical Methods in Hydrology and Environmental Engineering, 3: 87-97.

65. Zakermoshfegh, M., Ghodsian, M. and Montazer Gh, A. (2004). River flow forecasting using artificial neural networks. Hydraulics of Dams and River Structures, 7: 425-430.

66. Zhang, M., Fulcher, J. and Scofield, R.A. (1997). Rainfall estimation using artificial neural network group. Neurocomputing, 16: 97–115.

67. Zhigang, J. and Yajing, L. (2009). The application of RBF neural network on construction cost forecasting. Second international workshop on knowledge discovery and data mining

Estimation of Sediment Graph

1. Aksoy, H. and Kavvas, M.L. (2005). A review of hillslope and watershed scale erosion and sediment transport models. Catena 64: 247–271.
2. Beck, M.B. (1987). Water quality modelling: a review of uncertainty. Water Resources Research, 23(8): 1393–1442.
3. Bhunya, P.K., Mishra, S.K. and Berndtsson, R. (2003). Simplified two-parameter gamma distribution for derivation of synthetic unit hydrograph. Journal of Hydrologic Engineering, ASCE, 8(4): 226-230.
4. Bhunya, P.K., Singh, P.K. and Mishra, S.K. (2009). Fréchet and chi-square parametric expressions combined with horton ratios to derive a synthetic unit hydrograph. Hydrological sceience, 54 (2): 274-286.
5. Chen, V.J. and Kuo, C.Y. (1986). A study of synthetic sediment graphs for ungauged watersheds. Journal of Hydrology, 84: 35–54.
6. Chow, V.T. (1964). Handbook of applied hydrology. McGraw-Hill, New York, N.Y.

7. Foster, G.R. (1982). Modeling the erosion processes. Hydrological modelling of small watersheds, Haan, C.T., Johnson, H. and Brakensiek, D.L. (editors), ASAE Monograph No. 5. American Society of Agricultural Engineers St. Joseph Mich. 297–380.
8. Gracia-Sanchez, J. (1996). Generation of Synthetic Sediment Graphs. Hydrologic Processes, 10: 1181-1191.
9. Hadley, R.F., Lal, R., Onstad, C.A., Walling, D.E. and Yair, A. (1985). Recent developments in erosion and sediment yield studies. IHP-II Project A.1.3.1 United Nations Educational Scientific and Cultural Organization Paris.
10. Horton, R.I. (1938). The role of infiltration in the hydrologic cycle. Transactions of American Geophysical Union, 14: 446-460.
11. Jain, M.K., Kothyari, U.C. and Ranga Raju, K.G. (2005). GIS based distributed model for soil erosion and rate of sediment outflow from catchments. Journal of Hydraulic Engineering, ASCE, 131(9): 755-769.
12. Jakeman, A.J., Green, T.R., Beavis, S.G., Zhang, L., Dietrich, C.R. and Crapper, P.F. (1999). Modelling upland and in-stream erosion, sediment and phosphorus transport in a large catchment. Hydrologic Processes, 13(5): 745–752.
13. Kavvas, M.L., Yoon, J.Y., Chen, Z.Q., Liang, L., Dogrul, C., Ohara, N., Aksoy, H., Anderson, M.L., Reuters, J. and Hackley, S. (2006). Watershed environmental hydrology model: environmental module and its application to a California watershed. ASCE Journal of Hydrologic Engineering, 11 (3): 261-272.
14. Kavvas, M.L., Chen, Z.Q., Dogrul, C., Yoon, J.Y., Ohara, N., Liang, L., Aksoy, H., Anderson, M.L., Yoshitani, J., Fukami, K. and Matsuura, T. (2004). Watershed environmental hydrology (WEHY) model based on upscaled conservation equations: hydrologic module. Journal of Hydrologic Engineering, ASCE, 9(6): 450–464.
15. Kothyari, U.C., Jain, M.K. and Ranga Raju, K.G. (2002). Estimation of temporal variation of sediment yield using GIS. Hydrological Sciences, 47(5): 169–176.
16. Kothyari, U.C., Tiwari, A.K. and Singh, R. (1996). Temporal variation of sediment yield. Journal of Hydrologic Engineering, ASCE, 1(4): 169–176.
17. Kumar, S. and Rastogi, R.A. (1987). Conceptual catchment model for estimation of suspended sediment flow. Journal of Hydrology, 95: 155-163.

18. Lee, Y.H. and Singh, V.P. (1999). Prediction of sediment yield by coupling Kalman filter with instantaneous unit sediment graph. Hydrologic Processes, 13: 2861-2875.

19. Lee, Y.H. and Singh, V.P. (2005). Tank model for sediment yield. Water Resources Management, 19: 349-362.

20. Marquardt, D.W. (1963). An algorithm for least-square estimation of non-linear parameters. Journal of the Society for Industrial and Applied Mathematics, 11(2): 431-441.

21. McCuen, R.H. and Snyder, W.M. (1986). Hydrologic modeling: Statistical methods and applications. Prentice-Hall, Englewood Cliffs, New Jersy, 07632.

22. Mein, G.R. and Larson, C.L. (1971). Modeling the infiltration component of the rainfall-runoff process, WRRC Bulletin 43. Water Resources Research Center, University of Minnesota, Minneapolis, Minnesota.

23. Merritt, W.S., Letcher, R.A. and Jakeman, A.J. (2003). A review of erosion and sediment transport models. Environ Model Software, 18: 761–799.

24. Mishra, S.K. and Singh, V.P. (2003). Soil Conservation Service Curve Number (SCS-CN) Methodology. Kluwer Academic Publishers, P.O. Box 17, 3300 AA, Dordrecht, The Netherlands.

25. Mishra, S.K. and Singh, V.P. (2004). Validity and extension of the SCS-CN method for computing infiltration and rainfall-excess rates. Hydrologic Processes, 18(17): 3323-3345.

26. Mishra, S.K., Tyagi, J.V., Singh, V.P. and Singh, R. (2006). SCS-CN-based modeling of sediment yield. Journal of Hydrology, 324: 301-322.

27. Nash, J.E. (1957). The form of the instantaneous unit hydrograph. Hydrological Sciences Bulletin, 3: 114–121.

28. Nash, J.E. (1960). A unit hydrograph study with particular reference to British catchments. Proceedings of the Institution of Civil Engineers, London 17: 249–282.

29. Novotny, V. and Olem, H. (1994). Water Quality: prevention, identification and management of diffuse pollution. John Wiley & Sons, New York.

30. Raghuwanshi, N.S., Rastogi, R.A. and Kumar, S. (1996). Application of linear system models for estimation of washload. Proceedings International Conference on Hydrology & Water Resources, Singh, V.P. and Kumar, B. (editors), 3: 113-123, New Delhi, India.

31. Raghuwanshi, N.S., Rastogi, R.A. and Kumar, S. (1994). Instantaneous-unit sediment graph. The Journal of Hydrologic Engineering, ASCE, 120(4): 495-503.

32. Rendon-Herrero, O. (1978). Unit sediment graph. Water Resources Research, 14(5): 889-901.

33. Sharma, K.D. and Murthy, J.S.R. (1996). A conceptual sediment transport model for arid regions. Journal of Arid Environments, 33: 281-290.

34. Sharma, K.D., Dhir, R.P. and Murthy, J.S.R. (1992). Modelling suspended sediment flow in arid upland basins. Hydrologic Sciences, 37(5): 481-490.

35. Singh, P.K., Bhunya, P.K., Mishra, S.K. and Chaube, U.C. (2008). A sediment graph model based on SCS-CN method. Journal of Hydrology, 349: 244-255.

36. Singh, S.K. (2000). Transmuting synthetic hydrographs into gamma distribution. Journal of Hydrologic Engineering, ASCE, 5(4): 380-385.

37. Singh, V.P. (1989). Hydrologic Systems: Vol. 2: Watershed Modeling, Prentice Hall, Englewood Cliffs, N. J.

38. Singh, V.P., Baniukiwicz, A. and Chen, V.J. (1982). An instantaneous unit sediment graph study for small upland watersheds. Water Resources Publications, Littieton, Colorado.

39. Tyagi, J.V., Mishra, S.K., Singh, R. and Singh, V.P. (2008). SCS-CN based time distributed sediment yield model. Journal of Hydrology, 352: 388–403.

40. Vanoni, V.A. (editor) (1975). Sedimentation Engineering. ASCE, New York.

41. Wicks, J.M. and Bathurst, J.C. (1996). SHESED: A physically based, distributed erosion and sediment yield component for the SHE hydrological modeling system. Journal of Hydrology 175: 213–238.

42. Williams, J.R. (1978). A sediment graph model based on an instantaneous unit sediment graph. Water Resources Research, 14(4): 659–664.

43. Wilson, B.N., Barfield, B.J., Moore, I.D. and Warner, R.C. (1984). A hydrology and sedimentology watershed model. II: Sedimentology component. Transactions of ASAE 17: 1378-1384.

44. Wischmeier, W.H. and Smith, D.D. (1978). Predicting rainfall-erosion losses-A guide to conservation planning. Agricultural Handbook No. 537, Science and Education Administration, U.S. Department of agriculture, Washington D.C

45. Wu, T.H., Hall, J.A. and Bonta, J.V. (1993). Evaluation of runoff and erosion models. Journal of Irrigation and Drainage Engineering, ASCE, 119(4): 364-382.

46. Young, R.A., Onstad, C.A., Bosch, D.D. and Anderson, W.P. (1987).AGNPS: an agricultural non-point source pollution model: a large water analysis model. US Department of Agriculture, Cons. Res. Report, No. 35: 77.

Identification of Vulnerable Areas

1. Anonymous, (1976). Report of the National Commission on Agriculture, Part 5, Chapters, 17 and 18, Ministry of Agriculture & Irrigation, New Delhi.
2. Beven, K.J. (1996). A discussion of distributed hydrological modeling. In: Abbott, M.B. and Refsgaard, J.C. (editors), Distributed hydrological modeling. Kluwer, Dordrecht, The Netherlands, 278–255.
3. Carson, M.A. and Kirkby, M.J. (1972). Hillslope form and process. Cambridge University Press, Cambridge, 475.
4. Chakraborty, D., Dutta, D. and Chandrasekharan, H. (2004). Satellite remote sensing application in assessing soil erosion of a watershed. Journal of Soil and Water Conservation, India, 3(1,2): 21-28.
5. Elwell, H.A. (1978). Soil Loss Estimation: Compiled Works of the rhodesian multi-disciplinary team on soil loss estimation. Institute of Agricultural Engineering, Salisbury (Harare), Zimbabwe.
6. ERDAS (Earth Resources Data Analysis System) (1998). ERDAS Imagine 8.5. ERDAS Inc., Atlanta, Georgia, USA.
7. Ferro, V., Porto, P. and Tusa, G. (1998). Testing a distributed approach for modelling sediment delivery. Hydrologic Sciences Journal, 43(2): 425-442.
8. Ferro, V. (1997). Further remarks on a distributed approach to sediment delivery. Hydrological Sciences, 42(5): 633-647.
9. Ferro and Minacapilli, M. (1995). Sediment delivery processes at basin scale. Hydrological Sciences, 40(5): 703-717.
10. Fistikoglu, O. and Harmancioglu, N. (2002). Integration of GIS with USLE in assessment of soil erosion, Kluwer Academic Publishers, Netherlands, 447-467.

11. Haan, C.T., Barfield, B.J. and Hayes, J.C. (1994). Design Hydrology and Sedimentology for Small Catchments. Academic Press, New York.

12. Hadley, R.F., Lal, R., Onstad, C.A., Walling, D.E. and Yair, A. (1985). Recent developments in Erosion and Sediment Yield studies. UNESCO (IHP) Publication, Paris, France.

13. Jain, M.K. and Kothyari, U.C. (2000). Estimation of soil erosion and sediment yield using GIS, Hydrological Sciences Journal, 45(5):771-786.

14. Jain, S.K., Kumar, S., and Varghese, J. (2001). Estimation of soil erosion for a himalayan watershed using GIS technique. Kluwer Academic Publishers, Printed in Netherlands, 41-54.

15. Jain, S.K. and Goel, M.K. (2002). Assessing the vulnerability to soil erosion of the Ukai Dam catchments using remote sensing and GIS, Hydrological Sciences Journal, February 2002, 47(1): 31-40.

16. Kirkby, M.J. and Chorley, R.J. (1967). Throughflow, overland flow, and erosion. Bulletin, International Association of Eci. Hydrology. 12: 5-21.

17. Kumar, S. and Sharma, S. (2005). Soil erosion risk assessment based on MMF model using remote sensing and GIS, Journal of Hydrology, March-June 2005, 28 (1-2): 47-58.

18. Kothyari, U.C., Jain, M.K. and Ranga Raju, K.G. (2002). Estimation of temporal variation of sediment yield using GIS, Hydrological Sciences, April 2002, 47(5): 693-705.

19. Kothyari, U.C. and Jain, S.K. (1997). Sediment yield estimation using GIS. Hydrological Sciences Journal, 42(6): 833-843.

20. Mendicino, G. and Sole, A. (1997). The information content theory for the estimation of topographic index distribution used in TOPMODEL. Hydrological process, 2: 1099-1114.

21. Meyer, L.D. and Wischmeier, W.H. (1969). Mathematical simulation of the processes of soil erosion by water. Transactions of American Society of Agricultural Engineers, 12: 754-759.

22. Moore, I. and Burch, G. (1986a). Physical basis of the length-slope factor in the universal soil loss equation. Soil Science Society of America Journal, 50: 1294-1298.

23. Moore, I. and Burch, G. (1986b). Modeling erosion and deposition: topographic effects. Transactions of ASAE, 29(6): 1624-1630, 1640.

24. Morgan, R.P.C. (1995). Soil erosion and conservation, 2nd edition. Longman, Essex.

25. Morgan et al., (1984). A predictive model for the assessment of soil erosion risk. Journal of Agricultural Engineering Research, 30: 245-253.

26. Moore, I. and Wilson, J.P. (1992). Length slope factor for the Revised Universal Soil Loss Equation: simplified method of solution. Journal of Soil and Water Conservation, 47(5): 423-428.

27. Nearing, M.A., Foster, G.R., Lane, L.J. and Finkner, S.C. (1989). A process based soil erosion model for USDA water erosion prediction project technology. Transactions of American Society of Agricultural Engineers, 32(5): 1587-1593.

28. Panuska, J.C., Moore, I.D. and Kramer, L.A. (1991). Terrain analysis: integration into the agricultural nonpoint source (AGNPS) pollution model. Journal of soil and water conservation 46(1): 59–64.

29. Paringitand, E.C. and Nadaoka, K. (2003). Sediment yield modeling for small agricultural catchments: land-cover parameterization based on remote sensing data analysis. Hydrological Processes, 17: 1845-1866.

30. Prosser, I.P. and Rustomji, P. (2000). Sediment transport capacity relations for overland flow. Progress In Physical Geography, 24(1):179-193.

31. Rambabu, Tejwani, K.K., Agrawal, M.C. and Bhusan, L.S. (1979). Rainfall intensity duration-return period equations and nomograph of India, Bulletin No. 3, CSWCRTI, Dehradun.

32. Renard, K.G., Foster, G.R., Weesies, G.A., McCool, D.K. and Yoder, D.C. (1997). Predicting soil erosion by water: a guide to conservation planning with the revised universal soil loss equation (RUSLE). US Government Printing Office, Washington DC, 384.

33. Renard, K.G., Foster, G.R., Weesies, G.A., McCool, D.K. and Yoder, D.C. (1991a). Predicting soil erosion by water- a guide to conservation planning with the Revised Universal Soil Loss Equation (RUSLE), Report ARS-703, US Dept Agriculture, ARS, Washington D.C., USA.

34. Renard, K.G., Foster, G.R., Weesies, G.A., McCool, D.K. and Yoder, D.C. (1991b). RUSLE, Revised Universal Soil Loss Equation. Journal of Soil and Water Conservation, 46 (1), 30-33.

35. Rodda, H.E., Demuth, S. and Shankar, U. (1999). The application of a GIS-based decision support system to predict nitrate leaching to groundwater in southern Germany. Hydrologic Sciences Journal, 44(2): 221-236.

36. Sarangi, A. and Bhattacharya, A.K. (2000). Use of Geomorphologic parameters for sediment yield prediction from watershed, IARI, New Delhi-110012. 99-106.
37. Shamsi, U.M. (1996). Storm-Water Management Implementation through Modeling and GIS. Journal of Water Resources Planning and Management, 22(2): 114-127.
38. Stefano, C.Di., Ferro, V. and Porto, P. (1999). Modelling sediment delivery processes by a stream tube approach. Journal of Hydrological Sciences, 44(5): 725–742.
39. Verstraeten, G., Prosser, I.P. and Fogarty, P. (2007). Predicting the spatial patterns of hill slope sediment delivery to river channels in the Murrumbidgee catchment, Australia. Journal of Hydrology, doi:10.1016/j.jhydrol.2006.10.025.
40. Wicks, J.M. and Bathurst J.C. (1996). SHESED: a physically based, distributed erosion and sediment yield component for the SHE hydrological modelling system. Journal of Hydrology, 175: 213-238.
41. Williams, J.R. (1975). Sediment routing for agricultural watersheds. Water Resources, Bulletin, 11: 965-974.
42. Williams, J.R. and Berndt, H.D. (1977). Sediment yield prediction based on watershed hydrology. Transactions of American Society of Agricultural Engineers, 20: 1100-04.
43. Wischmeier, W.H. and Smith, D.D. (1978). Predicting rainfall erosion losses. Agricultural Handbook no. 537, US Dept of Agriculture, Science and Education Administration.
44. Wischmeier, W.H. and Smith, D.D. (1965). Predicting rainfall-erosion losses from cropland east of Rocky Mountains. U.S.D.A. Agricultural Handbook No. 282, Washington D.C.
45. Wischmeier, W.H. and Smith, D.D. (1958). Rainfall energy and its relationship to soil loss. Transactions AGU, 39 (3): 285-291.
46. Wischmeier, W.H., Johnson, C.B. and Cross, B.V. (1971). A soil erodibility nomograph for farmland and construction sites. Journal of soil and water conservation, 26: 189-192.
47. Wu, T.H., Hall, J.A. and Bonta, J.V. (1993). Evaluation of runoff and erosion models. Journal of Irrigation and Drainage Engineering, ASCE, 119(4): 364-382.

Appendix-III

1. Aksoy, H. and Kavvas, M.L. (2005). A review of hillslope and watershed scale erosion and sediment transport models. Catena 64: 247–271.

2. Andrews, R.G. (1954). The use of relative infiltration indices in computing runoff (unpublished), Soil Conservation Service, Fort Worth, Texas, 6.
3. Arnold, J.G., Williams, J.R., Griggs, R.H. and Sammons, N.B. (1990). SWRRB – A basin scale simulation model for soil and water resources management, A&M Press, Texas.
4. Aron, G., Miller, A.C.Jr. and Lakatos, D.F. (1977). Infiltration formula based on SCS curve number. Journal of Irrigation and Drainage Engineering Division, ASCE, 103(4): 419–427.
5. Bhunya, P.K., Jain, S.K., Singh, P.K. and Mishra, S.K. (2009). A simple conceptual model of sediment yield, accepted manuscript, WARM967R1.
6. Bonta, J.V. (1997). Determination of watershed curve number using derived distributions. J. Irrigat. Drain. Eng., ASCE, 123(1), 234–238.
7. Boszany, M. 1989 Generalization of SCS curve number method. Journal of Irrigation and Drainage Engineering, ASCE, 115(1): 139–144.
8. Boughton, W.C. (1989). A review of the USDA SCS curve number method. Australian Journal of Soil Research, 27(3): 511–523.
9. Cazier, D.J. and Hawkins, R.H. (1984). Regional application of the curve number method. Water Today and Tomorrow, Proceedings ASCE, Irrigation and Drainage Division Special Conference. ASCE, New York, NY, 710.
10. Chen, C. (1982). An evaluation of the mathematics and physical significance of the Soil Conservation Service Curve Number procedure for estimating runoff volume. Proceedings International Symposium on Rainfall-Runoff Relationship, Singh, V.P. (editor), Water Resources Publications, Littleton, CO, 387–418.
11. Chow, V.T., Maidment, D.R. and Mays, L.W. (1988). Applied Hydrology. McGraw Hill, New York.
12. Garen, D. and Moore, D.S. (2005). Curve number hydrology in water quality modeling: use, abuse, and future directions. Journal of American Water Resources Association, 41(2): 377–388.
13. Gaur, M.L. (1999). Modeling of surface runoff from natural watersheds with varied roughness. Unpublished Ph.D. thesis, Department of Hydrology, Indian Institute of Technology, Roorkee, India, 1–270.
14. Gaur, M.L. and Mathur, B.S. (2003). Modeling event based temporal variability of flow resistance coefficient. Journal of Hydrologic Engineering, ASCE, 8(5): 266–276.

15. Gaur, M.L. and Mathur, B.S. (2009). Predicting varied kinematic roughness parameter during storm durations under ungauged catchment situations. In Water, Environment, Energy and Society – Volume I – Hydrologic and Hydraulic Modeling, (editors, Jain, S.K., Singh, V.P., Kumar, V., Kumar, R., Singh, R.D and Sharma, K.D.), 264–274. Allied Publishers Pvt Ltd, ISBN 81-8424-398-7.

16. Geetha, K., Mishra, S.K., Eldho, T.I., Rastogi, A.K. and Pandey, R.P. (2008). SCS-CN based continuous model for hydrologic simulation. Water Resources Management, 22: 165–190.

17. Geetha, K., Mishra, S.K., Eldho, T.I., Rastogi, A.K. and Pandey, R.P. (2007). Modifications to SCS-CN method for long-term hydrologic simulation. Geetha, K., Mishra, S.K., Eldho, T.I., Rastogi, A.K. and Pandey, R.P. (2008)., 133(5): 475–486.

18. Golding, B.L. (1979). Discussion of runoff curve numbers with varying soil moisture. Geetha, K., Mishra, S.K., Eldho, T.I., Rastogi, A.K. and Pandey, R.P. (2008). Division, ASCE, 105(IR4): 441–442.

19. Grove, M., Harbor, J. and Engel, B. (1998). Composite vs. distributed curve numbers: Effects on estimates of storm runoff depths. Journal of American Water Resources Association, 34(5): 1015–1033.

20. Haith, D.A. and Shoemaker, L.L. (1987) Generalized watershed loading functions for stream flow nutrients. Water Resources Research, 23: 471–478.

21. Hawkins, R.H. (1975). The importance of accurate curve numbers in the estimation of storm runoff. Water Resources Bulletin, 11(5): 887–891.

22. Hawkins, R.H. (1978). Runoff curve numbers with varying site moisture. Journal of Irrigation Drainage Division, ASCE, 104(IR4): 389–398.

23. Hawkins, R.H. (1979). Runoff curve numbers with varying site moisture. Journal of Irrigation Drainage Division, ASCE, 105(IR4): 375–389.

24. Hawkins, R.H. (1984). A comparison of predicted and observed runoff curve numbers. Proceedings, ASCE, Irrigation and Drainage Division Special Conference. ASCE, New York, NY, 702–709.

25. Hawkins, R.H. (1993). Asymptotic determination of runoff curve numbers from data. Journal of Irrigation and Drainage Engineering, 119(2): 334–345.

26. Hawkins, R.H., Hjelmfelt, A.T.Jr. and Zevenbergen, A.W. (1985). Runoff probability, storm depth and curve numbers Journal of Irrigation and Drainage Engineering, 111(4), 330–340.

27. Hawkins, R.H., Woodward, D.E. and Jiang, R. (2001). Investigation of the runoff curve number abstraction ratio. Paper presented at USDA-NRCS Hydraulic Engineering Workshop, Tucson, Arizona.

28. Hjelmfelt, A.T.Jr. (1980). Empirical investigation of curve number technique. Journal Hydraulics Division, ASCE, 106(9): 1471–1477.

29. Hjelmfelt, A.T.Jr. (1991). Investigation of curve number procedure. Journal Hydraulics Engineering, 117(6): 725–737.

30. Hjelmfelt, A.T.Jr., Kramer, L.A. and Burwell, R.E. (1982). Curve numbers as random variable. Proceedings International Symposium on Rainfall-Runoff Modeling (editor, Singh, V.P.), 365–373. Water Resources Publications, Littleton, CO.

31. Horton, R.I. (1938). The interpretation and application of runoff plot experiments with reference to soil erosion problems. Proceedings, Soil Science Society America, 3: 340–349.

32. Huang, M., Gallichand, J., Wang, Z. and Goulet, M. (2006). A modification to the Soil Conservation Service curve number method for steep slopes in the Loess Plateau of China. Hydrologic Processes, 20: 579–589.

33. Jain, M.K., Mishra, S.K., Babu, S. and Singh, V.P. (2006a). Enhanced runoff curve number model incorporating storm duration and a nonlinear I_a-S relation. Journal of Hydrologic Engineering, 11(3): 131–135.

34. Jain, M.K., Mishra, S.K., Babu, S. and Venugopal, K. (2006b). On the Ia–S relation of the SCS-CN method. Nord. Hydrol. 37(3): 261–275.

35. Knisel, W.G. (1980). CREAMS: a field-scale model for chemical, runoff and erosion from agricultural management systems. Conservation Research Report No. 26, South East Area, US Department of Agriculture, Washington, DC.

36. McCuen, R.H. (1982). A Guide to Hydrologic Analysis Using SCS Methods. Prentice Hall, Englewood Cliffs, NJ.

37. McCuen, R.H. (1989). Hydrologic Analysis and Design. Prentice Hall, Englewood Cliffs, NJ.

38. McCuen, R.H. (2002). Approach to confidence interval estimation for curve numbers. Journal of Hydrologic Engineering, 7(1): 43–48.

39. Merritt, W.S., Letcher, R.A. and Jakeman, A.J. (2003). A review of erosion and sediment transport models. Environmental Modelling Software, 18: 761–799.

40. Michel, C., Andreassian, V. and Perrin, C. (2005). Soil Conservation Service Curve Number Method: How to mend a wrong Soil Moisture Accounting procedure. Water Resources Research, 41, W02011, doi: 10.1029/2004WR003191.

41. Miller, N. and Cronshey, R. (1989). Runoff curve numbers, the next step, Proceedings, International Conference on Channel Flow and Catchment Runoff. University of Virginia, Charlottesville, VA.

42. Mishra, S.K. and Singh, V.P. (1999). Another look at SCS-CN method. Journal of Hydrologic Engineering, ASCE, 4(3): 257–264.

43. Mishra, S.K. and Singh, V.P. (2002a). SCS-CN method: Part I: Derivation of SCS-CN based models, Acta Geophys. Pol. 50(3): 457–477.

44. Mishra, S.K. and Singh, V.P. (2002b). SCS-CN based hydrologic simulation package. In Mathematical Models in Small Watershed Hydrology, (editors, Singh, V.P. and Frevert, D.K.), 391–464. Water Resources Publication, Littleton, CO.

45. Mishra, S.K. and Singh, V.P. (2003a). Soil Conservation Service Curve Number (SCS-CN) Methodology. Kluwer Academic Publishers, P.O. Box 17, 3300 AA Dordrecht, The Netherlands.

46. Mishra, S.K. and Singh, V.P. (2003b). SCS-CN method Part II: Analytical Treatment, Acta Geophys. Pol. 51(1): 107–123.

47. Mishra, S.K. and Singh, V.P. (2004a). Long-term hydrologic simulation based on the Soil Conservation Service curve number. Hydrologic Processes, Mishra, S.K. and Singh, V.P., 1291–1313.

48. Mishra, S.K. and Singh, V.P. (2004b). Validity and extension of the SCS-CN method for computing infiltration and rainfall-excess rates. Hydrologic Processes, 18, 3323–3345.

49. Mishra, S.K. and Singh, V.P. (2006). A re-look at NEH-4 curve number data and antecedent moisture condition criteria, Hydrologic Processes, 20, 2755–2768.

50. Mishra, S.K., Jain, M.K. and Singh, V.P. (2004a). Evaluation of the SCS-CN based model incorporating antecedent moisture. Water Resources Management, 18: 567–589.

51. Mishra, S.K., Jain, M.K., Pandey, R.P. and Singh, V.P. (2003a). Evaluation of AMC dependent SCS-CN models using large data of small watersheds. Water and Energy International, 60(3): 13–23.

52. Mishra, S.K., Sansalone, J.J. and Singh, V.P. (2004b). Partitioning analog for metal elements in urban rainfall-runoff overland flow using the soil conservation service curve number concept. Journal of Environmental Engineering, ASCE, 130(2): 145–154.

53. Mishra, S.K., Sansalone, J.J., Glenn III, D.W. and Singh, V.P. (2004c). PCN based metal partitioning in urban snow melt, rainfall/runoff, and river flow systems. Journal of American Water Resources Association, Paper No. 01043, 1315–1337.

54. Mishra, S.K., Singh, V.P., Sansalone, J.J. and Aravamuthan, V. (2003b). A modified SCS-CN method: Characterization and Testing. Water Resources Management, 17: 37–68.

55. Mishra, S.K., Tyagi, J.V., Singh, V.P. and Singh, R. (2006a). SCS-CN-based modeling of sediment yield. Journal of Hydrology, 324: 301–322.

56. Mishra, S.K., Jain, M.K., Babu, P.S., Venugopal, K. and Kaliappan, S. (2008). Comparison of AMC-dependent CN-conversion Formulae. Water Resource Management, 22: 1409–1420.

57. Mishra, S.K., Sahu, R.K., Eldho, T.I. and Jain, M.K. (2006b). An improved I_a-S relation incorporating antecedent moisture in SCS-CN methodology. Water Resources Management, 20: 643–660.

58. Mockus, V. (1949). Estimation of total (peak rates of) surface runoff for individual storms. Exhibit A of Appendix B, Interim Survey Report Grand (Neosho) River Watershed, USDA, Dec. 1.

59. Moore, R.J. and Clarke, R.T. (1981). A distribution function approach to rainfall–runoff modeling. Water Resources Research, 17(5): 1367–1382.

60. Moore, R.J. (1983). The Probability-Distributed Approach to Spatial Conceptual Rainfall–Runoff Modeling. Report to Flood Protection Commission, Ministry of Agriculture, Fisheries and Food, Institute of Hydrology, Wallingford.

61. Moore, R.J. (1985). The probability-distributed principle and runoff production at point and basin scales. Journal of Hydrological Sciences, 30(2): 273–297.

62. Morel-Seytoux, H.J. and Verdin, J.P. (1983). Correspondence between the SCS CN and infiltration parameters. In Advances in Irrigation and Drainage: Surviving External Pressures (editors, Borelli, J. Hasfurther, V. R. & Burman, R. D.), 308–319. Proceedings, ASCE Special Conference, Jackson, WY, July.

63. Nash, J.E. (1957). The form of the instantaneous unit hydrograph. Hydrological Sciences Bulletin, 3: 114–121.

64. Neitsch, S.L., Arnold, J.G., Kiniry, J.R., Williams, J.R. and King, K.W. (2002). Soil and Water Assessment Tool (SWAT): Theoretical documentation, Version 2000, Texas Water Resources Institute, College Station, Texas, TWRI Report TR-191.

65. Novotny, V. and Olem, H. (1994). Water Quality: Prevention, Identification, and Management of Diffuse Pollution. John Wiley & Sons, New York, NY.

66. Ogrosky, H.O. (1956). Service objectives in the field of hydrology, Unpublished, Soil Conservation Service, Lincoln, Nebraska, 5 pp.

67. Pandit, A. and Gopalakrishnan, G. (1996) Estimation of annual storm runoff coefficients by continuous simulation. Journal of Irrigation and Drainage Engineering, ASCE, 122(40): 211–220.

68. Perrone, J. and Madramootoo, C.A. (1998). Improved curve number selection for runoff prediction. Canadian Journal of Civil Engineering, 25(4): 728–734.

69. Plummer, A. and Woodward, D.E. (2002). The origin and derivation of Ia/S in the runoff curve number system. Available at the NRCS website: http://www.wcc.nrcs.usda.gov/water/quality/common/techpaper/don1.pdf

70. Ponce, V.M. (1989) Engineering Hydrology: Principles and Practice. Prentice-Hall, Englewood Cliffs, NJ.

71. Ponce, V.M. and Hawkins, R.H. (1996). Runoff Curve Number: Has it reached maturity? Journal of Hydrologic Engineering, 1(1): 11–19.

72. Rallison, R.E. (1980). Origin and evaluation of the SCS runoff equation. Proceedings, Symposium, Watershed Management, ASCE, Idaho, July, 1980, 912–924.

73. Rallison, R.E. and Miller, N. (1982). Past, present, and future. Proceedings, International Symposium, Rainfall-Runoff Relationship (editor, Singh, V.P.). Water Resources Publicatios, P.O. Box 2841, Littleton, CO.

74. Ramasastry, K.S. and Seth, S.M. (1985). Rainfall-runoff relationships. Rep. RN-20, National Institute of Hydrology, Roorkee, India.

75. Sahu, R.K., Mishra, S.K., Eldho, T.I. and Jain, M.K. (2007). An advanced soil moisture accounting procedure for SCS curve number method. Hydrologic Processes, 21(21): 2872–2881.

76. Schneider, L.E. and McCuen, R.H. (2005). Statistical guidelines for curve number generation. Journal of Irrigation and Drainage Engineering, ASCE, 131(3): 282–290.

77. SCS 1972. Hydrology. National Engineering Handbook, Supplement A, Section 4, Chapter 10, Soil Conservation Service, USDA, Washington, DC.

78. SCS 1985. National Engineering Handbook. Supplement A, Section 4, Chapter 10, Soil Conservation Service, USDA, Washington, DC.

79. Sharpley, A.N and Williams, J.R. (1990). EPIC – Erosion/Productivity Impact Calculator: 1. Model Documentation. US Department of Agriculture Technical Bulletin No. 1768. US Government Printing Office, Washington, DC.

80. Sherman, L.K. (1949). The unit hydrograph method. In Physics of the Earth (editor, Meinzer, O.E.), 514–525. Dover Publications, Inc., New York, NY.

81. Simanton, J.R., Hawkins, R.H., Mohseni-Saravi, M. and Renard, K.G. (1996). Runoff curve number variation with drainage area, Walnut Gulch, Arizona, Soil and Water Division, Transactions of ASAE, 39(4): 1391–1394.

82. Singh, P.K., Bhunya, P.K., Mishra, S.K. and Chaube, U.C. (2008). A sediment graph model based on SCS-CN method. Journal of Hydrology, 349: 244–255.

83. Singh, V.P. (1992). Elementary Hydrology. Prentice Hall, Englewood Cliffs, NJ.

84. Singh, V.P. (1995). Chapter 1: Watershed modeling. In Computer Models of Watershed Hydrology (editor, Singh, V.P.), 1–22. Water Resources Publications, Littleton, CO.

85. Singh, V.P. and Frevert, D.K. (2002). Mathematical Models of Small Watershed Hydrology and Applications. Water Resources Publications, Highlands Ranch, CO.

86. Singh, V.P. and Woolhiser, D.A. (2002). Mathematical modeling of watershed hydrology. 150th anniversary paper, Journal of Hydrologic Engineering, ASCE, 7(4): 271–292.

87. Sobhani, G. (1975). A review of selected small watershed design methods for possible adoption to Iranian conditions. M.S. thesis, Utah State University, Logan, Utah.

88. Springer, E.P., McGurk, B.J., Hawkins, R.H. and Goltharp, G.B. (1980). Curve numbers from watershed data. Proceedings, Irrigation and Drainage Symposium on Watershed Management, ASCE, New York, NY, 938–950.

89. Steenhuis, T.S., Winchell, M., Rossing, J., Zollweg, J.A. and Walter, M.F. (1995). SCS runoff equation revisited for variable-source runoff areas. Journal of Irrigation and Drainage Engineering, 121(3): 234–238.

90. Svoboda, A. (1991). Changes in flood regime by use of the modified curve number method, Journal of Hydrological Sciences, 36(5): 461–470.

91. Tyagi, J.V., Mishra, S.K., Singh, R. and Singh, V.P. (2008). SCS-CN based time distributed sediment yield model. Journal of Hydrology, 352: 388–403.

92. Valdes, J.B., Diaz-Grandos, M. and Brass, R.L. (1990). A derived PDF for the initial soil moisture in a catchment. Journal of Hydrological, 113: 163–176.

93. Van-Mullem, J.A. (1989). Runoff and peak discharges using Green-Ampt model. Journal of Hydraulics Engineering, ASCE, 117(3): 354–370.

94. Walter, M.T. and Stephen, B.S. (2005). Discussion: curve number hydrology in water quality modeling: uses, abuses, and future directions, by David, C., Garen, Daniel, S. and Moore, Journal of American Water Resources Association, (JAWRA), 41(6): 1491–1492.

95. Williams, J.R. and LaSeur, W.V. (1976) Water yield model using SCS curve numbers. Journal of Hydraulics Division, ASCE, Proc. Paper 12377, 102(HY9): 1241–1253.

96. Woodward, D.E., Hawkins, R.H., Hjelmfelt, A.T.Jr., Van Mullem, J.A. and Quan, D.Q. (2002). Curve number method: origins, applications and limitations. In Second Federal Interagency Hydrologic Modeling Conference, Las Vegas, NV, 1–10. Available at: http://www.wcc.nrcs.usda.gov/water/quality/common/

97. Young, R.A., Onstad, C.A., Bosch, D.D. and Anderson, W.P. (1989). AGNPS: a nonpoint-source pollution model for evaluating agricultural watersheds. Journal of Soil and Water Conservation, 168–173 (March–April).

98. Yu, B. (1998). Theoretical justification of SCS method for runoff estimation. Journal of Irrigation and Drainage Engineering, 124(6): 306–310.

99. Yuan, Y., Mitchell, J.K., Hirschi, M.C. and Cooke, R.A.C. (2001). Modified SCS curve number method for predicting sub-surface drainage flow. Transactions of ASAE, 44(6): 1673–1682.

100. Zhi-Hua, S., Li-Ding, C., Nu-Fang, F., De-Fu, Q. and Chong-Fa, C. (2009). Research on the SCS-CN initial abstraction ratio using rainfall-runoff event analysis in the Three Gorges Area, China. Catena, 77: 1–7.

BIBLIOGRAPHY

BIBLIOGRAPHY

1. Agarwal, A. and Singh, R.D. (2004). Runoff modelling through back propagation artificial neural network with variable rainfall-runoff data. Water resources management, 18(3): 285-300.
2. Alan J., Nonnan, E.P. and Allan R. (1994). Biogeochemistry of small catchments: A tool for Environmental Research. John Wiley & Sons Ltd., ©SCOPE.
3. Ampofo, E.A., Muni, R.K. and Bonsu, M. (2003). Estimation of Soil losses within plots as affected by different agricultural land management. Soil and water Management Division, Soil Research Institute, CSIR, Kumasi, Ghana, 957-967.
4. Arnold, J.G., Bernhadit, P.M. and G. (1993). A comprehensive surface-groundwater flow model. Journal of Hydrology, 142: 47-69.
5. Arnold, J.G., William, J.R., Sriniwasan, R. and King, K.W. (1996). SWAT-Soil and Water Assessment Tool USDA-ARS: Temple, TX.
6. Arnold, J.G., Neitesh, S.L., Kiniry, J.R., Sriniwasan, R. and Williams, J.R. (2002). Soil and Water Assessment Tool, User's Manual, Version 2000.
7. Arnold, J.G., Jaikrishan, R., Srinivasan, R. and Santhi, C. (2005). Advances in the application of the Swat model for water resources management. Published in Hydrological Processes, 19(3, 28): 749-762.
8. Bednarz, S.T., Dybala T., Muttiah, R.S., Rosenthal, W. and Dugas, W.A. Technical Appendices (Water Yield Feasibility Studies).
9. Beven, K.J. (2002). Rainfall–runoff modeling: The Primer. John Wiley and Sons Limited, England, 360.
10. Boyce, R.C. (1975). Sediment routing with sediment delivery ratios. In: Present and Prospective Technology for Predicting Sediment Yields and Sources, 61-65. US Department of Agriculture Publications, ARS-S-40.
11. Campbell, D.J., Guha, A. and Sackfield, C. (2003). SWAT2000- (First Report October 27, 2003).
12. Central Unit for Soil Conservation (Hydrology and Sedimentation), (1972). Handbook of Hydrology. Soil Conservation Division, Ministry of Agriculture, Government of India.

13. Clark, C.O. (1945). Storage and unit hydrograph. Transactions of ASCE, 110: 1419-1446.

14. Cunderlik, J.M. (2003). Hydrologic model selection for the CFCAS project: Assessment of water resources risk and vulnerability to changing climatic condition. Project Report, October 2003.

15. Dickey, E.C., Mitchell, J.K. and Scarborough, J.N. (1979). The application of hydrologic models to small watersheds having mild topography. Water Resources Bulletin, 156: 1753-1769.

16. Dingman, S.L. (1994). Physical hydrology. Prentice-Hall, Inc., Englewood Cliffs, NJ.

17. ESRI (Environmental Systems Research Institute) (1994). Cell based modeling with GRID. Environmental Systems Research Institute Inc., Redlands, California, USA.

18. Fernandez, C. (2001). Predicting Erosion and Sediment Yield using GIS: Application to the Lawyers Creek Watershed M. S. thesis; Washington State University.100 p.

19. Flugel, W.A., Marker, M., Moretti, S., Rodolfi, G. and Sidrochuk, A. (2003). Integrating geographical information systems, remote sensing, ground truthing and modeling approaches for regional erosion classification of semi-arid catchments in South Africa, Hydrologic Processes, 17: 920-942.

20. Gassman, W.P., Reyes, M.R., Green, C.F. and Aronold, J.G. (2005). SWAT Peer Reviewed literature: A Review. Published in 3rd International SWAT conference Proceeding, July 11-15, 2005, Zurich, held at Eawag, Switzerland, 01-18.

21. Gosian, A.K., Rao, S. and Ray, D.B. (2006). Climate change impact assessment on hydrology of Indian river basins. Current Science, 90(3):346-353.

22. Gosian, A.K., Rao, S. and Ray, D.B. (2005). Vulnerability assessment of climate change impact on Indian Water Resources using SWAT model. Published in 3rd International SWAT Conference Proceeding, July 11-15, 2005, Zurich, held at Eawag, Switzerland, 231-240.

23. Green, C.G., Luzio, M.D., Arnold, J.G. and Tomer, M.D. (2005). SWAT model development for a large agricultural watershed in Iowa. Published in 3rd International SWAT Conference Proceeding, July 11-15,2005,Zurich, held at Eawag, Switzerland, 414-422.

24. Jayasekare, A.S., Dayawansa, N.D.K., Silva, R.P.D. and Muthuwatta, L.P. Development of Agriculture engineering, Faculty of Agriculture, University of Paradenia (Sri Lanka) :

Spatially distributed hydrological modeling of upper umaoya catchment using Soil and Water assessment Tool (SWAT).

25. Jha, M., Gassmam, P.W., Secchi, S., Arnold, J.G., Kurkalova, L.A., Fenl, H.L. and Kling, C.C. (2005). An assessment of alternative conservation practices and land use strategies on the hydrology and water quality of the Upper Mississippi river basin. Published in 3rd International SWAT Conference Proceeding, July 11-15, 2005, Zurich, held at Eawag, Switzerland, 444-453.

26. Koskova, R., Buchtele, J. and Volos, B. (2005). Evaluation of SAC-SMA and HSPF rainfall-runoff simulations in upper parts of Vltava basin. Geophysical Research Abstracts, 7.

27. Lal, R. (1994). Soil Erosion Research Methods. Second Edition, Soil and Water Conservation Society, Columbus.

28. Leaf, C.F. and Brink, G.E. (1973). Hydrologic simulation model of Colorado subalpine forest. USDA Forest Service research paper RM-107, U.S. Department of Agriculture, Washington, D.C.

29. Liew M.W.V., Veith, T.L., Bosch, D.D. and Arnold J.G. (2002). Suitability of SWAT for the conservation effects assessment project: Comparison on USDA Agricultural Research Service Watershed. Published in Journal Of Hydrologic Engineering, ASCE /March/April, 2002. 173-189.

30. Lu, H., Moran, C.J. and Prossor, I.P. (2006). Modeling sediment delivery ratio over the Murray Darling Basin. Environmental Modeling & Software, 21(2005): 1297-1308.

31. Markus, M. and Baker, D. (1994). The Fraser River: Streamflow forecasting and simulation computer package. Technical Report, Northern Colorado Water Conservancy district, Loveland, Colorado.

32. Maidment, D.R. (1994). Digital delineation of watersheds and stream networks in the Allegheny basin. Prepared for Hydrologic Engineering Centre, Davis, California, USA.

33. Maner, S.B. (1958). Factors affecting sediment delivery ratio in the red hill physiographic area. Transactions, AGU 39(4): 669-675.

34. McCool et al., (1989). Revised slope length factor for the Universal Soil Loss Equation. Transactions of American Society of Agricultural Engineers, 32: 1571-1576.

35. Meamarian, H., Esmaeilzadeh, H. and Tajbakhsh, S.M. (2005). Sediment yield potential estimation of Kashmir Urban Watershed using MPSIAC model in the GIS framework, college of Agriculture University of Birjand, Tehran,Iran, 1-3.

36. Mendas, A., Errih, M., Benhanifia, K., Maidi, M. and Rahmani, M.A. Hydrologic model and GIS to estimate hydrologic balance at watershed scale – Application to the watershed of Macta (Western Algerian).

37. Mishra, S.K., Geetha, K., Rastogi, A.K. and Pandey, R.P. (2005). Long-term hydrologic simulation using storage and source area concepts. Journal of Hydrological Processes, 19(14): 2845–2861.

38. Mishra, S.K. (2000). A modified SCS-CN based hydrologic model. Technical Report (BR) 2/1999-2000, National Institute of Hydrology, Roorkee, UP, India, 51.

39. Mishra, S.K. (1998). A Thesis on operation of multipurpose reservoir. Department of hydrology, University of Roorkee, Roorkee 247667 (India).

40. Mishra, S.K. and Dwivedi, A.K. (1998). Determination of curve numbers for a watershed, 9th National Symposium On Hydrology, Indian National Committee on Hydrology (INCOH), Amritsar, India, November 26-27.

41. Mishra, S.K., Jain, M.K., Pandey, R.P. and Singh, V.P. (2005b). Catchment area-based evaluation of the AMC-dependent SCS-CN-based rainfall–runoff models. Journal of Hydrological Processes, 19(14): 2701–2718.

42. Molnar, D.K. and Julien, P.Y. (1998). Estimation of upland erosion using GIS, Computers & Geo Sciences. 24: 183-192.

43. Mosher, T. (2004). SWAT Model: a Review. Term Paper Presentation Geog 590-602 Land Use Modeling April 29, 2004.

44. O'Connell, P.E. and Clarke, R.T. (1981). Adaptive hydrological forecasting - A review. Hydrological Sciences-Builetin-des Sciences Hydrologiques, 26: 2-6.

45. Reungsang, P., Kanwar, R.S., Jha, M., Gassman, P.W. Ahmad, K. and Saleh, A. (2005). Calibration and Validation of SWAT for the Upper Maquoketa river watershed. Working paper, 05-396, June 2005.

46. Richard, K. (1993). Sediment delivery and the drainage network. In: Channel Network hydrology, (Edited By Bevan, K. and Kirkby, M.J.). Willy, Chichester, West Sussex, UK, 222-254.

47. Rodriguez-Iturbe, I., Gonzalez-Sanabria, M. and Bras, R.L. (1982). The geomorphoclimatic theory of the instantaneous unit hydrograph. Water Resources Research, 18(4): 877–886.

48. Roehl, J.W. (1962). Sediment source areas, delivery ratios and influencing morphology factors. In: Symposium of Bari (1-8 October 1962), 202-213. IAHS Publ. no. 59.

49. SCS (Soil Conservation Service) (1975). Urban hydrology for small watersheds. Technical release no. 55, Soil Conservation Service , United States Dept. of Agric., Washington DC, USA.

50. Sharma, R.P. and Sinha, A, K., (1972). Geology of Ranikhet Area, Kumaon Himalaya. Lucknow University, 137-150.

51. Singh, V.P. (1988). Hydrologic Systems. Volume I Rainfall Runoff Modeling. Publisher, Prentice Hall, Englewood Cliffs, New Jersey.

52. Simulation and prediction of runoff and sediment yield. Unpublished PhD thesis work.

53. Spangler, M.G. and Handy, R.L. Iowa State University: Soil Engineering. Fourth edition.

54. Srinivasan, R. Jacobs, J.H., Day. D. and Karim, A. (2005). 3rd International SWAT Conference Proceeding, July 11-15, Zurich, held at Eawag, Switzerland.

55. Srinivasan, R. Jacobs, J.H. and Jenson, R. (2003). 2nd International SWAT Conference Preceding, July 01-04, 2003, Bari, Itali.

56. Takle, S., Eugene, Jha, M., Gassman, P.W., Anderson, J. and Secchi, S. (2005). Climate change impacts on the hydrology and water quality of the Upper Mississippi River basin. Published in 3rd International SWAT Conference Proceeding, July 11-15, 2005, Zurich, held at Eawag, Switzerland, 559-608.

57. Tripathi, M.P. (2005). Hydrological modeling using SWAT for effective managements of a small agricultural Watershed. Published in 3rd International SWAT Conference Proceeding, July 11-15,2005, Zurich, held at Eawag, Switzerland, 279-290.

58. USACOE (1998). HEC-1 flood hydrograph package user's manual, Technical Report. CPD-1A, U. S. Army Corps of Engineers, Hydrologic Engineering Centre, 609, Second Street, Davis, CA 95616–4687.

59. Van Oost, K., Govers, G. and Desmet, P.J.J. (2000). Evaluating the effects of changes in landscape structure on soil erosion by water and tillage. Landscape Ecology, 15 (6): 579-591.

60. Van Rompaey et al (2005). Modeling sediment yields in Italian Catchments. Geomorphology 65: 157-169.

61. Van Rompaey, A., Verstraeten, G., Van Oost, K., Govers, G. and Poesen, J. (2001). Modeling mean annual sediment yield using a distributed approach. Earth Surface Processes and Landforms, 26 (11): 1221-1236.

62. Verstraeten, G., Van Oost, K., Van Rompaey, A., Poesen, J. and Govers, G. (2002). Evaluating an integrated approach to catchment management to reduce soil loss and sediment pollution through modeling. Soil Use and Management, 18: 386-394.

63. Walling, D.E. (1983). The sediment delivery problem. Journal of Hydrology, Data 65, 209-237.

64. Walling, D.E. (1988). Erosion and sediment yield research- some recent perspectives. Journal of Hydrology, 100: 113-141.

65. White, K. and Chaubey, I. (2005). Sensitivity analysis, calibration and validation for a multi site and multi variable SWAT model. Journal of the American Water Resources Association, Oct. 2005, 1077-1083.

66. Williams, J.R. (1975) and Berndt, H.D. (1972). Sediment yield computed with universal equation. Journal of Hydraulic Division, ASCE, 98(12): 2087-2098.

67. Wischmeier, W.H. (1959). A rainfall erosion index for a universal soil loss equation. In: Proceedings Soil Science Society of America, 23: 246-249.

LIST OF PUBLICATIONS

LIST OF PUBLICATIONS

1. Geetha, K., S.K. Mishra, T.I.Eldho*, A.K. Rastogi, R.P. Pandey (2008),'SCS-CN-based continuous simulation model for hydrologic forecasting,' J. Water Resources Management, Vol. 22, No. 2, Feb., pp. 165-190.
2. Singh, P.K., P.K. Bhunya, S.K. Mishra, U.C. Chaube (2008),'A sediment graph model based on SCS-CN method,' J. Hydrology, Vol. 349, pp. 244-255.
3. Bhunya, P.K., P.K. Singh, S.K. Mishra, and N. Panigrahy (2008),'A variable storage coefficient model for rainfall-runoff computation,' Hydrological Sciences Journal, Vol. 53, No. 2, pp. 338-352.
4. Bhunya*, P.K., P.K. Singh, and S.K. Mishra (2009),'Fréchet and Chi-square distributions combined with Horton order ratios to derive a synthetic unit hydrograph (SUH),' Hydrological Sciences–Journal–des Sciences Hydrologiques, 54(2), pp. 274-286.
5. Jain, M.K., S.K. Mishra, R.B. Shah (2009),'Identification of Sediment Source and Sink Areas in a Himalayan Watershed using GIS and Remote Sensing,' J. Land Degradation & Development, 20: 1-17, DOI: 10.1002/ldr.952.
6. Bhunya, P.K., S.K. Jain, P.K. Singh, and S.K. Mishra (2009),' A simple conceptual model of sediment yield,' J. Water Resources Management, DOI 10.1007/s11269-009-9520-4, WARM967R1.
7. Singh, P. K., M. L. Gaur, S. K. Mishra and S. S. Rawat (2010),'An updated hydrological review on recent advancements in Soil Conservation Service-Curve Number technique,' Journal of Water and Climate Change, IWA Publishing, 01.2, pp. 118-134.
8. Singh, P.K., S.K. Mishra, ML Gaur, SS Rawat (2009),'GIUH-based probability models for SUH derivation from ungauged catchments using SRTM data and ILWIS,' Sci-fronts, An Annual J. of Multiple Sciences, Vol. III(3), Dec., pp. 57-68.
9. Rawat, SS, PK Singh, S.K. Mishra, (2009),'Estimation of direct runoff hydrograph using two parameters inverse gamma distribution function employing Horton ratios,' Sci-fronts, An Annual J. of Multiple Sciences, Vol. III(3), Dec., pp. 69-81.

10. Singh*, P.K., U.C Chaube, S.K. Mishra, M.L. Gaur, S.S. Rawat (2010),"GIUH based probability models for flood prediction from ungauged basins using remote sensing and GIS," Dept. of Civil and Env. Engg., Utah State University, USA, Sept. 28-30. (Accepted)
11. Singh, P.K., Mishra, S.K., Jain, M.K., Bhunya, P.K. (2008),'A Review on Synthetic Unit Hydrograph Methods,' EGU General Assembly 2008, Assembly of the European Geophysical Union, EGU, Vienna, Austria, April 13-15.

APPENDICES

Appendix-I

SHORT-TERM TRAINING

On

IDENTIFICATION OF VULNERABLE AREAS IN HIMALAYAN WATERSHEDS

(November 22-23, 2010)

I.1 INTRODUCTION

Our country experiences soil erosion of the order of 5334 million tones (1653 tones / ha) every year due to agriculture and other associated human activities. Of this, about 2052 million tones (626 tones / ha) are carried by rivers, nearly 1572 million tones taken into the sea, and 480 million tones deposited in various multipurpose reservoirs, resulting in the loss of 1 to 2 % of the storage capacity. Thus, it adversely affects the availability of water for power generation, irrigation, domestic & industrial use. Since the process of soil erosion from the earth surface largely depends on topography, vegetation, soil, and climatic variables, it is a serious problem in lower Himalayas and foothill ecosystems. To circumvent, watershed management programs are taken up and these require an inventory of the quantitative soil loss erosion and the priority classification of watershed. Sediment yield from a catchment is the main criteria for assessing the vulnerability of a watershed to soil erosion. Since the measurement of sediment yield in a watershed at a fine grid scale is a cumbersome task, the geographic information systems (GIS) and remote sensing techniques are widely used for the assessment of sediment yield through rainfall-runoff-sediment yield models. In this study, Universal Soil Loss Equation (USLE) coupled with GIS is employed for soil loss estimation and, in turn, for identification of vulnerable areas in the Chaukhutia sub-watershed of Ramganga catchment.

I.2 ORGANIZATION OF WORKSHOP

A two days workshop on "**Identification of vulnerable areas in Himalayan watersheds**" has been conducted by the Department of Water Resources Development and Management, during November 22-23, 2010 at Engineers' Academy, Kalagarh.

I.2.1 Course Curriculum and Mode of Training

The course curriculum was decided in consultation with the sponsor and is given in Appendix-IA. It was covered in the form of class-room lectures, practical sessions, laboratory works, field visits, and panel discussion, as shown in the Time Table (Appendix-IA).

I.2.2 Resource Persons

The following persons were involved in the completion of the project.

Dr. Surendra Kumar Mishra — Principal Investigator
Associate Professor
Dept. of Water Resources Development and Management
IIT Roorkee, Roorkee-247667 (UK)

Dr. Manoj Kumar Jain — Co-Principal Investigator
Assistant Professor
Dept. of Hydrology
IIT Roorkee, Roorkee-247667 (UK)

I.2.3 Course Participants

Twenty seven participants from the level of Superintending Engineer, Executive Engineers, Assistant Engineers and Junior Engineers from Uttarakhand Irrigation Department and two participants from Forest Research Institute have participated in the course. A list of the participants is enclosed as in Appendix-IB. Photographs show the class room training of the participants.

I.2.4 Boarding & Lodging of Participants

The participants were accommodated in the Guest House of Uttarakhand Irrigation Departmmt at Kalagarh, which provides excellent boarding and lodging facilities.

I.2.5 Course Evaluation

The participants were asked to rate and comment on different aspects of training such as subject coverage, study tour, course organization, boarding & lodging facility etc. Most of these aspects were rated as either excellent or very good, as seen in Appendix-IC.

I.2.6 Course Material

A brief description of the project work including results of the study has been prepared in the form of a pamphlet and it was supplied to the participants of the workshop. The details of the pamphlet are given in Appendix-II.

Appendix-IA

Training Workshop

R&D Project on

Identification of Vulnerable Areas in Himalayan Watersheds

(November 22-23, 2010)

Sponsor: INCOH, MoWR, New Delhi **Venue: Engineers' Academy, Kalagarh, Pauri Garhwal**

TIME TABLE

Date	0930-1100	1100-1115	1115-1245	1245-1415	1415-1545	1545-1600	1600-1730
22.11.2010	Registration & Inauguration	Tea break	L-1 (SKM)	Lunch Break	L-2 (MKJ)	Tea break	L-3 (SKM)
23.11.2010	L-4 (SKM)		L-5 (MKJ)		Practical Session (SKM/MKJ)		Panel Discussion & Valedictory

L. No.	Topic
L-1	Project Objectives & Rainfall –Runoff Modelling
L-2	GIS and Remote Sensing & Sediment Yield Assessment
L-3	SCS-CN Methodology
L-4	Assessment of Runoff and Sediment Yield using SCS-CN Concept
L-5	Application of SWAT Model- Ramganga Case Study

SKM: Dr. SK Mishra, PI: 9411100753; MKJ: Dr. M.K. Jain, Co-PI: 9410371758

Appendix-IB

LIST OF PARTICIPANTS

S. N.	Name & Address of Participant	S. N.	Name & Address of Participant
1	Dev Karan, A.E.Civil Engineers' Academy, Kalagarh, Pauri Garhwal	11	Rishi Pal Sigh, J.E. Camp Management Division-Kalagarh Bijnor
2	S.K.Garg, S.E Ramganga Dam Circle, Kalagarh, Pauri Garhwal	12	Manohar Datt Joshi, J.E Camp Management Division-Kalagarh Bijnor
3	Yogendra Kumar, Executive Engineer Central Stores Division, Kalagarh, Pauri Garhwal	13	Dr SES Rawat Scientist –F Climate Change & Forest Infulences Div. FRI, Dehradun
4	Ashok Kumar Mishra, J.E. Engineers' Academy, Kalagarh, Pauri Garhwal	14	Tarun Johri,Deputy Conservator of Forests Climate Change & Forest Infulences Div. FRI, Dehradun
5	Gagan Deep Singh, J.E. Engineers' Academy, Kalagarh, Pauri Garhwal	15	Ramesh Chand, J.E. Engineers' Academy, Kalagarh, Pauri Garhwal
6	Phool Singh,A.E Ramganga Dam Circle, Kalagarh, Pauri Garhwal	16	Rajendra Prasad, A.E Engineers' Academy, Kalagarh, Pauri Garhwal
7	Suresh Chandra Sharma, Executive Engineer Ramganga Dam Circle, Kalagarh, Pauri Garhwal	17	Satya Prakash Naroriya, A.E Engineers' Academy, Kalagarh, Pauri Garhwal
8	Arjun Singh, J.E. Engineers' Academy, Kalagarh, Pauri Garhwal	18	Gaj Raj Singh, J.E. Engineers' Academy, Kalagarh, Pauri Garhwal
9	Jai Prakash Sharma,A.E Camp Management Division-Kalagarh Bijnor	19	Bhanu Pratap Singh, J.E Ramganga Dam Circle, Kalagarh, Pauri Garhwal
10	Surendra kumar, J.E. Engineers' Academy, Kalagarh, Pauri Garhwal	20	Anwar Bahdur Khan, J.E Ramganga Dam Circle, Kalagarh, Pauri Garhwal
21	Anil Kumar, J.E Ramganga Dam Circle, Kalagarh, Pauri Garhwal	25	Raj Kumar Verma, J.E Engineers' Academy, Kalagarh, Pauri Garhwal
22	Piyush Chandra Gaur, Executive Engineer Camp Management Division-Kalagarh Bijnor	26	Rajneesh Kumar, A.E Engineers' Academy, Kalagarh, Pauri Garhwal
23	Jabar Singh, J.E Ramganga Dam Circle, Kalagarh, Pauri Garhwal	27	Pramod Kumar, A.E Engineers' Academy, Kalagarh, Pauri Garhwal
24	Veer Singh, J.E Ramganga Dam Circle, Kalagarh, Pauri Garhwal		

Appendix-IC

COURSE EVALUATION BY PARTICIPANTS (% NO. OF PARTICIPANTS)

Sl. No.	Head	Rating			
		Excellent	Very good	Good	Fair
1	Subject coverage				
	(a) Course content	11.11	88.89	0	0
	(b) Lectures	22.22	77.78	0	0
	(c) Teaching method	55.56	44.44	0	0
	(d) Knowledge gained	11.11	55.56	33.33	0
2	Boarding & lodging				
	(a) Rooms	77.78	22.22	0	0
	(b) Fooding	55.56	44.44	0	0
	(c) General	55.56	22.22	22.22	0
3	Educational tour				0
	(a) Informationwise	66.67	33.33	0.00	0
	(b) Recreationwise	33.33	22.22	33.33	11.11
4	Organisers				
	(a) Institution	88.89	11.11	0	0
	(b) Cooperation	77.78	22.22	0	0
	(c) Helpfulness	77.78	22.22	0	0
5	Programme analysis				
	(a) Utility	33.33	55.56	11.11	0
	(b) Learning opportunity	44.44	55.56	0	0
	(c) Practical value	22.22	66.67	11.11	0
	(d) Understanding	11.11	77.78	11.11	0
	(e) Confidence development	22.22	77.78	0	0


IDENTIFICATION OF VULNERABLE AREAS IN
HIMALAYAN WATERSHEDS
11/22/2010


11/22/2010


11/22/2010


11/22/2010

Appendix-II

IITR Project No. MOW-281-WRC

R&D Project

IDENTIFICATION OF VULNERABLE AREAS IN HIMALAYAN WATERSHEDS

Sponsored by
Indian National Committee for Hydrology (INCOH)
National Institute of Hydrology, Roorkee
(Ministry of Water Resources, Government of India)

Department of Water Resources Development and Management
Indian Institute of Technology Roorkee
Roorkee (Uttaranchal) 247 667, India

INTRODUCTION

Our country experiences soil erosion of the order of 5334 million tones (1653 tones / ha) every year due to agriculture and other associated human activities. Of this, about 2052 million tones (626 tones / ha) are carried by rivers, nearly 1572 million tones taken into the sea, and 480 million tones deposited in various multipurpose reservoirs, resulting in the loss of 1 to 2 % of the storage capacity. Thus, it adversely affects the availability of water for power generation, irrigation, domestic & industrial use. Since the process of soil erosion from the earth surface largely depends on topography, vegetation, soil, and climatic variables, it is a serious problem in lower Himalayas and foothill ecosystems. To circumvent, watershed management programs are taken up and these require an inventory of the quantitative soil loss erosion and the priority classification of watershed. Sediment yield from a catchment is the main criteria for assessing the vulnerability of a watershed to soil erosion. Since the measurement of sediment yield in a watershed at a fine grid scale is a cumbersome task, the geographic information systems (GIS) and remote sensing techniques are widely used for the assessment of sediment yield through rainfall-runoff-sediment yield models. In this study, Universal Soil Loss Equation (USLE) coupled with GIS is employed for soil loss estimation and, in turn, for identification of vulnerable areas in the Chaukhutia sub-watershed of Ramganga catchment.

METHODOLOGY

The methodology includes determination of soil erosion by USLE and then its transportation to the outlet using transport limited capacity. Use of USLE equation (E = RKLSCP, where E = computed soil loss per unit area in tons/ha/ yr), R = rainfall erosivity factor in MJ-mm/ha-hr, K= soil erodibility factor in tones-ha-hr/ha-MJ mm, L= slope length factor, S= slope steepness factor, C= cover and management factor, P= support practice factor) produces the estimates of gross soil erosion in each of the discretized grids of the catchment (Fig. 1). The eroded sediment from each grid (Fig. 1) follows a defined drainage path (as in Fig. 2 for a particular cell) to the catchment outlet. The rate of sediment transport from each of the discretized cell depends on the sediment transport capacity (T_C) of the flowing water. The sediment outflow from an area is equal to soil erosion in the cell plus contribution from upstream cells if transport capacity exceeds the sum. However, if T_C is less than this amount, the sediment excess of transport capacity gets deposited and sediment load equal to T_C is discharged to next downstream cell, as shown schematically in Fig.3. For the most part, the approach encompasses two computational steps: determination of mean annual sediment transport capacity and transport limited accumulation.

- **Mean annual sediment transport capacity (T_C):** The rate of sediment transport is governed by T_C (= $K_{TC} R K A^{(1/6)} S^{(1/6)}$, where T_C is transport capacity (kg/m^2/yr), K_{TC} is the transport capacity coefficient depends on land use and reflects vegetation component within the transport capacity, A is the upslope contributing area per unit of contour length, and S is the slope gradient).
- **Transport Limited Accumulation (TLA):** The sediment is routed along the runoff pattern towards the river as shown in Figs. 1 & 2, taking into account the local T_C of each pixel. If the local T_C is smaller than the sediment flux, sediment deposition is modeled. This approach assumes that sediment transport is not necessarily restricted to a transport limited system. If T_C is higher than the sediment flux, sediment transport supply will be limited. Thus, by introducing K_{TC}, the overland sediment transport is simulated more realistically. The predicted sediment delivery is interpreted as the sediment delivery for the complete length of the river in the catchment.

General procedure of the proposed methodology can be described as follows:

i. Calculate rainfall erosivity factor R using meteorological data.
ii. Generate Digital Elevation Model (DEM), slope, flow accumulation, flow direction, and drainage network maps for the study area.
iii. Generate topographic factor LS Map
iv. Generate land use map of the study area using digital analysis of satellite data.
v. Generate soil map and its characteristic database from satellite data in GIS environment using ERDAS.
vi. Generate soil erodibility factor K, topographic factor LS, cover management factor C, and support practice factor P maps.
vii. Generate sediment transport capacity map.

viii. Generate maps for transport limited soil accumulation by routing sediment outflow from each discretized cell using GIS.

ix. Finally, generate soil erosion/deposition maps for identification of vulnerable areas.

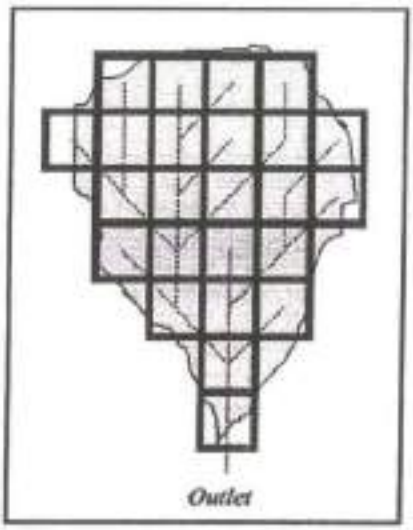

Fig. 1: Schematic showing discretized grid cells in a catchment

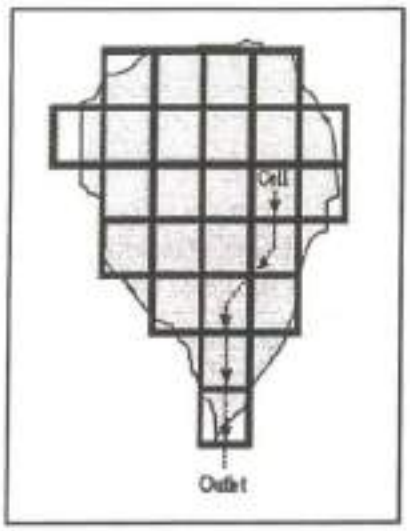

Fig. 2: Schematic showing a flow path

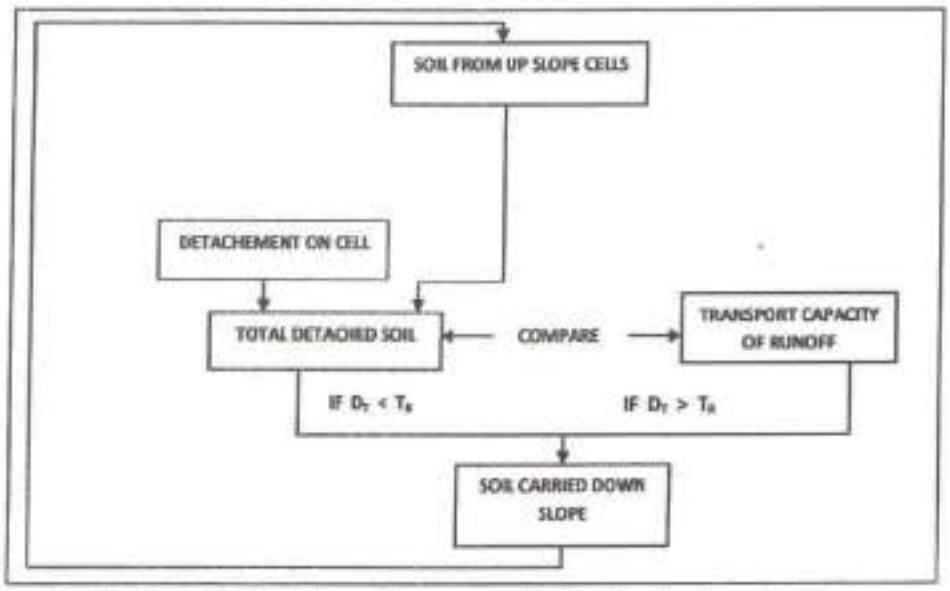

Fig. 3: Concepts of mathematical modelling of the process of soil erosion by flow of water

STUDY WATERSHED

The Chaukhutia watershed is the uppermost part of Ramganga catchment. Ramganga catchment is located in the foothills of Himalayas in the Uttarakhand state of India. The river Ramganga originates at Diwali Khel of Chamoli district. It is a major tributary of river Ganga and emerges out of the hills at Kalagarh (District Almora). The outlet of Chaukhutia watershed is located in Chaukhutia block headquarter under Ranikhet sub-division of Almora district. It is forest dominated, and geographically, it is bounded between

latitudes of 29° 46' 35" N to 30° 06' 11" N and longitudes of 79° 11' 23" E to 79° 31' 21" E. The drainage area above the gauging station at Chaukhutia, which is more or less rectangular shaped, covers an area of 452.25 km^2. The elevation of the watershed varies from 929 m to 3114 m above mean sea level. The climate of this watershed varies from sub-tropical in the lower region to sub-temperate and temperate in upper region with a mean annual temperature of 24.5°C and a mean minimum temperature of 17.3°C. The significant portion of total precipitation in the form of rainfall in the watershed occurs mainly during the four months of the monsoon, i.e. from June to September with a mean annual total precipitation of 1357.8 mm. In the watershed, the main soil type is clayey loam falling under hydrologic soil groups B & C and the landuse is forest dominated. Figs. 4 & 5 show the DEM and drainage network maps of the Chaukhutia watershed.

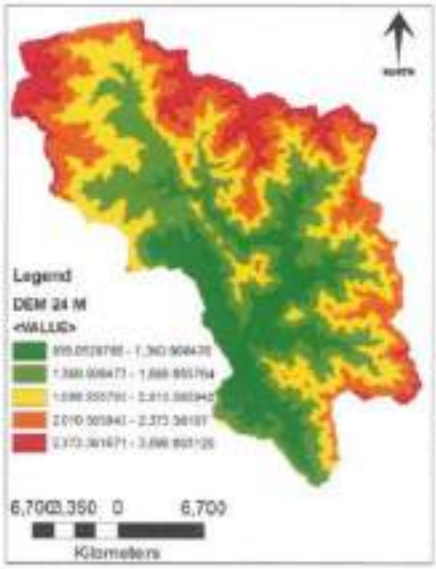

Fig. 4: DEM of Chaukhutia watershed

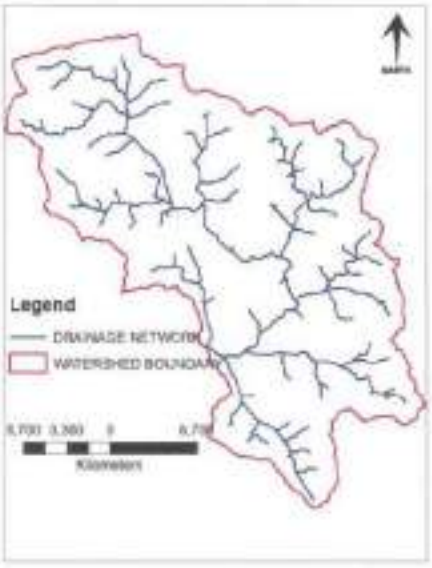

Fig. 5: Drainage network of Chaukhutia watershed

LAND USE AND SOIL MAPS

Satellite data of IRS LISS III sensor were geo-referenced and then, landuse/land cover map were prepared using ERDAS imagine and ArcGIS 9.1 software employing unsupervised classification. In this classification, data are clustered for given input numbers. These clusters are then reclassified into desired number of classes using merging operation. The Chaukhutia sub-catchment has been classified into seven major land use / land cover classes after merging different clusters as shown in Fig. 6. The soil map of the study area was digitized (Figure 7) using GIS Software 9.0 version from the scanned copy of the soil map available from National Bureau of Soil Survey and Land Use Planning (NBSSLUP), Govt. of India. The digitized polygon map was then rasterized at 24 m grid cells using GIS Arc Toolbox.

Estimation of soil erosion

Maps depicting gross amount of soil erosion from different discretized cells of the Chaukhutia catchment were computed by multiplication of the erosion potential map produced by integration of KLSCP maps with corresponding annual values of rainfall erosivity factor R. Fig. 8 depicts the gross soil erosion for the year 1975 as illustration. Such maps indicate the gross amount of soil erosion from each cell in a year.

Computation of Transport Limited Sediment Accumulation and Outflow

The gross erosion from each grid was routed downstream to generate map of the accumulated sediment yield limited by transport capacity and depicted in Fig. 9. Such maps provide the amount of sediment transported from the system at every grid and are useful for determination of sediment flowing out of the catchment at any location. The pixel value of the sediment outflow map denotes the amount of sediment

leaving the current cell to the next downstream cell. The pixel value of the cell at the catchment outlet denotes the sediment coming out of the watershed.

Fig. 6: Classified landuse map of Chaukhatia watershed

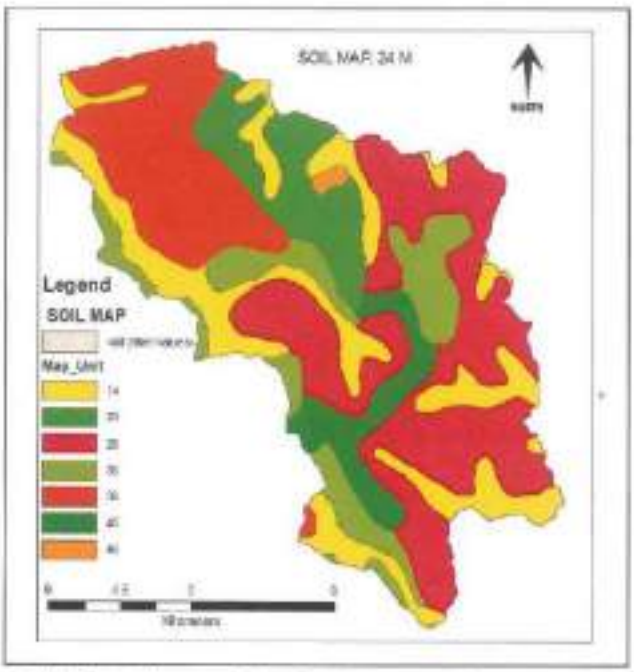

Fig.7: Soil map of Chaukhutia watershed

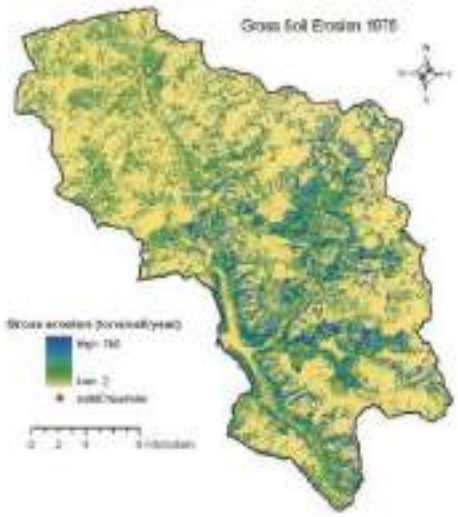

Fig. 8: Gross soil erosion map for the year 1975

Fig. 9: Transport limited sediment outflow for year 1975

Vulnerable Areas

Net erosion maps for different years were calculated by subtracting the deposition rates for each grid cell from the gross erosion rates for each grid cell. Negative values on the net erosion map are the areas where sediment deposition occurs (i.e. true sediment deposition), whereas positive values correspond to grid cells with net sediment erosion. High values of erosion/deposition in Fig. 10 represents the areas vulnerable to sediment erosion/deposition, respectively. As seen, deposition of sediment resulted at the grids where transport capacity was low, mostly by the sides of some of the stream reaches in valleys and flatter land areas found in the cultivated valley lands in the catchment. Such maps are extremely important in planning conservation measures, for the areas producing more sediment receive priority for their implementation.

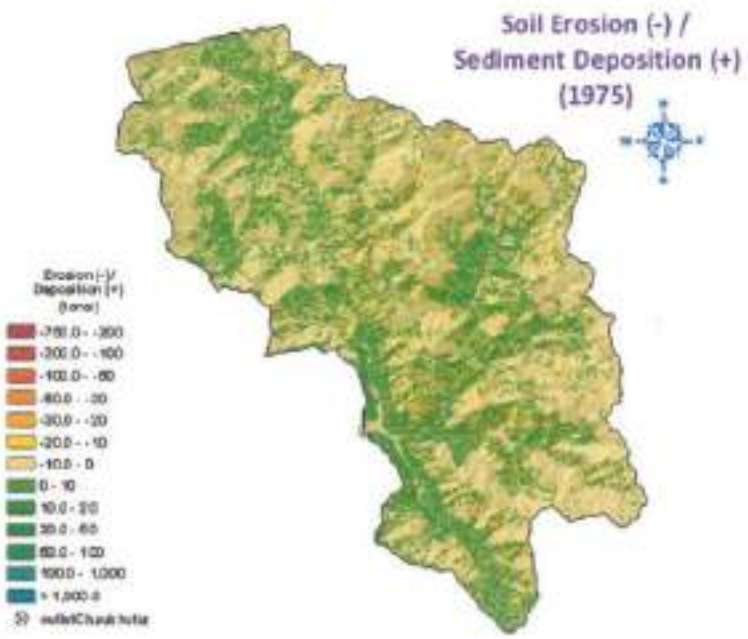

Fig. 10: Vulnerable areas in Chaukhutia watershed regarding soil erosion/sediment deposition for year 1975.

"Save Land and Water, both are Precious"

Project Team

Dr. Surendra Kumar Mishra Associate Professor Dept. of Water Resources Development and Management IIT Roorkee, Roorkee-247667 (UK)	Principal Investigator
Dr. Manoj Kumar Jain Assistant Professor Dept. of Hydrology IIT Roorkee, Roorkee-247667 (UK)	Co-Principal Investigator
Dr. Pushpendra Kumar Singh Dept. of Water Resources Development and Management IIT Roorkee, Roorkee-247667 (UK)	Research Associate
Mr. Sanjay Kumar Gupta Dept. of Hydrology IIT Roorkee, Roorkee-247667 (UK)	Senior Research Assistant
Mr. Soban Singh Rawat Dept. of Water Resources Development and Management IIT Roorkee, Roorkee-247667 (UK)	Research Scholar
Ms. Vibha Agarwal Dept. of Water Resources Development and Management IIT Roorkee, Roorkee-247667 (UK)	Project Staff

SCS-CN METHODOLOGY: AN UPDATED REVIEW

A number of hydrologic models are available for the estimation of direct runoff from storm rainfall. Most models are however limited because of their intensive input data and calibration requirements. The Soil Conservation Service-Curve Number (SCS-CN) technique has been applied successfully throughout the entire spectrum of hydrology and water resources, even though originally it was not intended to deal with and solve certain issues such as erosion and sedimentation and environmental engineering. This chapter includes an updated review of this popular technique with its critical performance analysis under various hydrological applications. The study highlights its provenance and its conceptual and empirical foundations followed by relative significance of the parameter CN and various estimation methods and issues related to the I_a and S relationship. Finally, notable recent advancements available in the literature are discussed for their structural strengths and applicability in real world problems.

III.1 INTRODUCTION

Mathematical modelling of watershed responses is employed to address a wide spectrum of environmental and water resources problems (Singh & Woolhiser 2002). Central to addressing these issues is rainfall-runoff modelling, which is particularly used in water resources management, flood and drought mitigation and water resources assessment (Mishra & Singh 2003a). The Soil Conservation Service-Curve Number (SCS-CN) rainfall-runoff technique is a well-recognized method, widely used to estimate runoff from total event rainfall, and thus water recharge, stream flow, infiltration and soil moisture content. Its popularity is rooted in convenience, simplicity, authoritative origin and responsiveness to four readily grasped catchment properties viz., soil type, land use/treatment, surface condition and antecedent moisture condition. The method is simple to use and requires basic descriptive inputs that are converted to numeric values for estimation of watershed direct runoff volume (Bonta 1997). A curve number (CN) that is descriptive of runoff potential of watershed is required in this method, which is widely preferred by hydrologists, engineers and watershed managers as an independent simple watershed model, as well as the runoff estimating

component in many complex watershed models such as AGNPS (Young *et al.* 1989), and SWAT (Neitsch *et al.* 2002). Accordingly it has witnessed myriad applications all over the world. Because of its simplicity, it has been applied throughout the entire spectrum of hydrology and water resources, even for problems the SCS-CN was not originally intended to solve. According to Garen & Moore (2005) '...the reason for the wide application of curve number method includes its simplicity, ease of use, widespread acceptance, and the significant infrastructure and institutional momentum for this procedure within NRCS. To the date, there has been no alternative that possesses so many advantages, which is why it has been and continues to be commonly used, whether or not it is, in a strict scientific sense, appropriate...'. The method, though appealing to many practising hydrologists by its overwhelming simplicity, contains some unknowns and inconsistencies (Chen 1982). Due to its origin and evolution as agency methodology, it is effectively isolated from the rigors of peer review, other than the information contained in NEH-4, which was not intended to be exhaustive. No complete account of the method's foundation is available to date, despite some noteworthy attempts made by Rallison (1980), Chen (1982), Miller & Cronshey (1989), Ponce & Hawkins (1996), Yu (1998), Mishra & Singh (1999), Mishra & Singh (2002a,b), Mishra & Singh (2003a,b), Mishra & Singh (2004a,b), Michel *et al.* (2005) and Mishra & Singh (2006). Realizing these vital facts and expressions of the researchers, the authors considered it an apt effort to attempt a state-of-art review of such a popular hydrological technique.

Looking into more than five decades of its provenance and application in various fields (even for those it was not originally intended to solve) it is a pressing need at the moment to examine the mathematical and physical significance of the method and its various parameters. The ultimate aim remains to highlight its strengths and weaknesses together with a thorough review of its application in various fields followed by suggesting certain future courses of action of research in curve number method so that the method can still enjoy an esteemed place among the hydrologists and practising engineers community.

The major objectives of this review paper are as follows:

- To explore the provenance and original intentions of the SCS-CN method;
- To diagnose conceptual and empirical base and highlight the strengths and weaknesses;
- To diagnose relative significance of the parameter CN and its estimation methods;

- To explore notable recent applications in the realms of hydrology and water resources;
- To summarize a review for a future course of action of research.

III.1.1 Provenance and original intentions

The origin of the SCS-CN technique can be traced back to the establishment of the Soil Conservation Service (SCS) (previously the Soil Erosion Service (SES)) to obtain hydrologic data and to establish a simpler procedure for estimating runoff rates changed with setting up demonstration conservation projects and overseeing the design and construction of soil and water conservation measures for retarding water flow to prevent erosion – a classic hydrological problem of the time. In 1954, the United States Department of Agriculture (USDA) (presently known as the Natural Resources Conservation Service (NRCS)) developed a unique procedure known as the SCS-CN method for estimating direct runoff from storm rainfall. It is well documented and found a place in the National Engineering Handbook Section 4: Hydrology (SCS 1985). The ultimate method is the result of more than 20 years of studies of rainfall-runoff relationships carried out during the late 1930s and early 1940s for certain small, rural watersheds supplemented by the works of several investigators including Mockus (1949), Sherman (1949), Andrews (1954) and Ogrosky (1956). In these efforts, thousands of infiltrometer tests on field plots were conducted to develop a rational method for estimating runoff under various cover conditions.

Following a historical attempt by Sherman (1949) to plot direct runoff versus storm rainfall, Mockus (1949) came up with a finding that the estimation of direct runoff for ungauged watersheds depends on soils, land use, antecedent rainfall, duration of storm, associated rainfall amount, average annual temperature and date of storm. Mockus (1949) also communed these factors into an empirical index value b and proposed the following relationship between storm rainfall depth P and direct runoff Q (Mishra & Singh 1999):

$$Q = P(1 - 10^{-bP}) \tag{III.1}$$

Mockus (1949) further realized that Eq. (III.1) gave better results for shorter duration storms in comparison to longer ones; and also the end results were found to be better on watersheds having mixed-cover rather than single-cover watersheds. Andrews (1954) independently

grouped the infiltrometer data collected from Texas, Oklahoma, Arkansas and Louisiana, where he developed a graphical rainfall-runoff procedure taking into account the soil texture, type and amount of cover and conservation practices, combined into what is referred to as soil-cover complex or soil-vegetation-land use (SVL) complex (Miller & Cronshey 1989). According to Rallison & Miller (1982) the empirical P-Q rainfall-runoff relationship from Mockus and the SVL complex concept from Andrews were the true building blocks of the existing SCS-CN method documented in NEH-4 (SCS 1985).

III.1.2 Theoretical, conceptual and empirical architecture

The SCS-CN method is based on the water balance equation along with two fundamental hypotheses. The *first hypothesis* equates the ratio of actual amount of direct surface runoff (Q) to the total rainfall (P) (or maximum potential surface runoff) to the ratio of actual infiltration (F) to the amount of the potential maximum retention (S). The *second hypothesis* relates the initial abstraction (I_a) to S, also described as potential post initial abstraction retention (McCuen2002).

(a) Water balance equation

$$P = I_a + F + Q \tag{III.2}$$

(b) Proportional equality (first hypothesis)

$$\frac{Q}{P - I_a} = \frac{F}{S} \tag{III.3}$$

(c) I_a-S relationship (second hypothesis)

$$I_a = \lambda S \tag{III.4}$$

The values of P, Q and S are in-depth dimensions, while the initial abstraction coefficient (λ) is dimensionless. In a typical case, a certain amount of rainfall is initially abstracted as interception, infiltration and surface storage before runoff begins. A sum of these three at initiation of surface runoff is usually termed 'initial abstraction'.

The first hypothesis (Eq. (III.3)) is primarily a proportionality concept (Figure III.1) and incorporates three major envelopes of interpretation (Mishra & Singh 2003a): (i) it reconciles the popular concept of partial area contributing with the curve number (Hawkins 1979); (ii) it undermines the source area concept (Steenhuis *et al.* 1995), allowing runoff generation only from saturated or wetted fractions of the watersheds; and (iii) it ignores the statistical theory (Moore & Clarke 1981; Moore 1983; Moore 1985), based on the runoff production from only the saturated (independent or interacting) storage element.

The second hypothesis (Eq. (III.4)) is a linear relationship between initial abstraction I_a and potential maximum retention S. Coupling Eqs. (III.2) and (III.3), the expression for Q can be written as:

$$Q = \frac{(P - I_a)^2}{P - I_a + S} \tag{III.5}$$

Equation (III.5) is the general form of the popular SCS-CN method and is valid for $P \geq I_a$; $Q = 0$ otherwise. For $\lambda = 0.2$, the coupling of Eqs. (III.4) and (III.5) results in:

$$Q = \frac{(P - 0.2S)^2}{P + 0.8S} \tag{III.6}$$

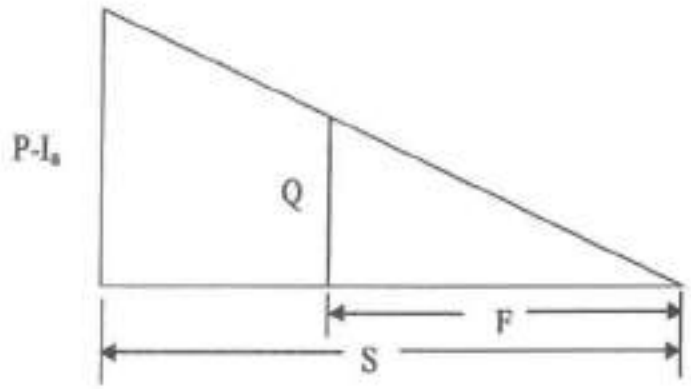

Figure III.1: Proportionality concept of the existing SCS-CN method (after Mishra and Singh, 2003a)

Equation (III.6) is well recognized as a popular form of the existing SCS-CN method. Thus, the existing SCS-CN method with $\lambda = 0.2$ is a one-parameter model for computing surface runoff from daily storm rainfall, having versatile importance, utility and vast untapped potential. The parameter S of the SCS-CN method depends on soil type, land use, hydrologic condition and antecedent moisture condition (AMC). Similarly, the initial abstraction coefficient λ is frequently recognized as a regional parameter depending on geologic and climatic factors (Ramasastry & Seth 1985; Boszany 1989).

The existing SCS-CN method assumes λ to be equal to 0.2 for practical applications, which has frequently been questioned for its validity and applicability (Hawkins *et al.* 2001), invoking many researchers to carry out a critical examination of the I_a–S relationship for pragmatic applications. A detailed diagnosis on the studies carried out by various researchers on the I_a–S relationship has been given in the forthcoming section. This altogether establishes the spatial variability and sensitivity of λ to the technique.

Since the parameter S can vary in the range of $0 \leq S \leq \infty$, it is mapped onto a dimensionless curve number CN, varying in a more appealing range $0 \leq CN \leq 100$, as:

$$S = \frac{1000}{CN} - 10 \qquad \text{(III.7)}$$

where S is in inches. The difference between S and CN is that the former is a dimensional quantity (L) whereas the latter is non-dimensional. The highest possible numerical value of CN (i.e. 100) symbolizes a condition of zero potential maximum retention ($S = 0$), which in a real physical situation represents an impermeable watershed. On the contrary the lowest possible numerical value of CN indicates a situation of highest potential maximum retention ($S = \infty$), reflecting a physical situation of an infinitely abstracting watershed (because of the assumption that $I_a = \lambda.S$, which remains an unlikely situation in real field conditions. Many researchers attempted the practical design values validated by experience lying in a realistic range (40, 98) (Van-Mullem 1989). The CN has no intrinsic meaning; it is only a convenient transformation of S to establish a 0–100 scale (Hawkins 1978).

Here, it is interesting to quote Michel *et al.* (2005): '...it is the empirical framework within which the method was developed did not incite hydrologists to check its consistency...'. However, recently, the method has undergone various stages of peer review and has been diagnosed to achieve enhanced performance without disfiguring its simplicity. In this direction some notable works have been carried out by Chen (1982), Rallison & Miller (1982), Ponce & Hawkins (1996), Yu (1998), Mishra & Singh (1999; 2002a,b; 2003a,b; 2004a,b), Mishra *et al.* (2003a,b) and Michel *et al.* (2005). Mishra & Singh (2002a; 2003a,b) revisited the empirical rainfall-runoff models proposed by Mockus (1949) and Horton (1938) and they derived the existing SCS-CN method using these models. In an advanced form, Mishra & Singh (2002a; 2003b) derived the existing SCS-CN method using second-order storage hypothesis, which leads its categorization as a conceptual model. Furthermore, the proportionality concept (Eq. (III.3)) of the SCS-CN method represents the $C = S_r$ concept (Mishra & Singh 2003a; Mishra *et al.* 2006a,b) that is truly based on the volumetric concept of soil physics and categorically emphasizes the conceptual basis of the SCS-CN technique. Further, it is only under a conceptual modelling framework that we are able to discern why the retention and runoff ratios ought to be equal now popularly transformed into the Proportionality concept (Mishra & Singh 2003a; Mishra *et al.* 2006a,b). As a concluding thought, following Ponce & Hawkins (1996) and Mishra & Singh (2003a) the authors are in a position to succinctly conclude that the SCS-CN technique is a conceptual model of

hydrologic abstraction of storm rainfall, supported by empirical data dedicated to estimate direct runoff volume from storm rainfall depth based on a single numeric parameter CN.

III.1.3 I_a-S examination

The I_a-S concept has also been a topic of research by many for pragmatic applications. According to Plummer & Woodward (2002) I_a was not a part of the SCS-CN model in its initial formulation but, as the developmental stages continued, it was included as a fixed ratio of I_a to S (Eq. (III.4)). The relationship was justified on the basis of measurements for watersheds of fewer than 10 acres, despite a considerable scatter in the resulting I_a–S plot (SCS 1985). Because of this large variability, the $I_a = 0.2S$ relationship has been the focus of discussion and modification since its very inception. For example, Aron *et al.* (1977) suggested $\lambda \leq 0.1$ and Golding (1979) provided λ values for urban watersheds depending on CN as $\lambda = 0.075$ for $CN \leq 70$, $\lambda = 0.1$ for $70 < CN \leq 80$, and $\lambda = 0.15$ for $80 < CN \leq 90$. Hjelmfelt (1991) pointed out that many storm and landscape factors interact to define the initial abstraction. Many other studies carried out in the United States and other countries (SCS 1972; Springer *et al.* 1980; Cazier & Hawkins 1984; Ramasastry & Seth 1985; Boszany 1989) report λ to vary in the range of (0, 0.3). However, as the initial abstraction component accounts for the short-term losses such as interception, surface storage and infiltration before runoff begins, λ can take any non-negative value (Mishra & Singh 1999). Ponce & Hawkins (1996) suggest that the fixing of the initial abstraction ratio at 0.2 may not be the most appropriate number, and that it should be interpreted as a regional parameter.

Mishra & Singh (2004b) developed a criterion for validity of the SCS-CN method with λ variation using the following relationships:

$$\lambda = \frac{CIa^*}{\left(1 - Ia^*\right)\left(1 - Ia^* - C\right)} \tag{III.8a}$$

and

$$S \leq \frac{(P - Q)}{\lambda} \tag{III.8b}$$

where $I_a^* = Ia/P$ varies as $0 \leq Ia^* \leq 1$, and for $Ia^* > 1$, $C = Q/P = 0$.

Equation (III.8b) was developed by coupling Eqs. (III.8a) and (III.3) for $\lambda \geq 0$ and $Ia^* + C \leq 1$. Graphically, Eqs. (III.8a) and (III.8b) are shown in Figure III.2. It can be inferred from the figure that λ can take any non-negative value (0, ∞); for a given value of Ia^*, λ

increases with C and reaches ∞ as (C + Ia*) approaches 1; for a given value of C, λ increases with Ia*; as Ia* → 0, λ → 0.

Thus the use of Eq. (III.4) with λ = 0.2 (the case for the existing SCS-CN method) will yield Ia much larger than zero. For this reason, the existing SCS-CN method performs poorly on very low runoff-producing (or low C-value) lands, such as sandy soils and forest lands. Figure III.2 also shows that the existing SCS-CN method has widest applicability on those watersheds exhibiting C values in the approximate range of (0.4–0.6) and the initial abstraction amount of the order of 10% of the total rainfall. On the basis of Figure III.2, they defined the applicability bounds for the SCS-CN method as: λ ≤ 0.3; Ia* ≤ 0.35 and C ≥ 0.23. A study by Hawkins *et al.* (2001) suggested that a value of λ = 0.05 gives a better fit to data and would be more appropriate for use in runoff calculations.

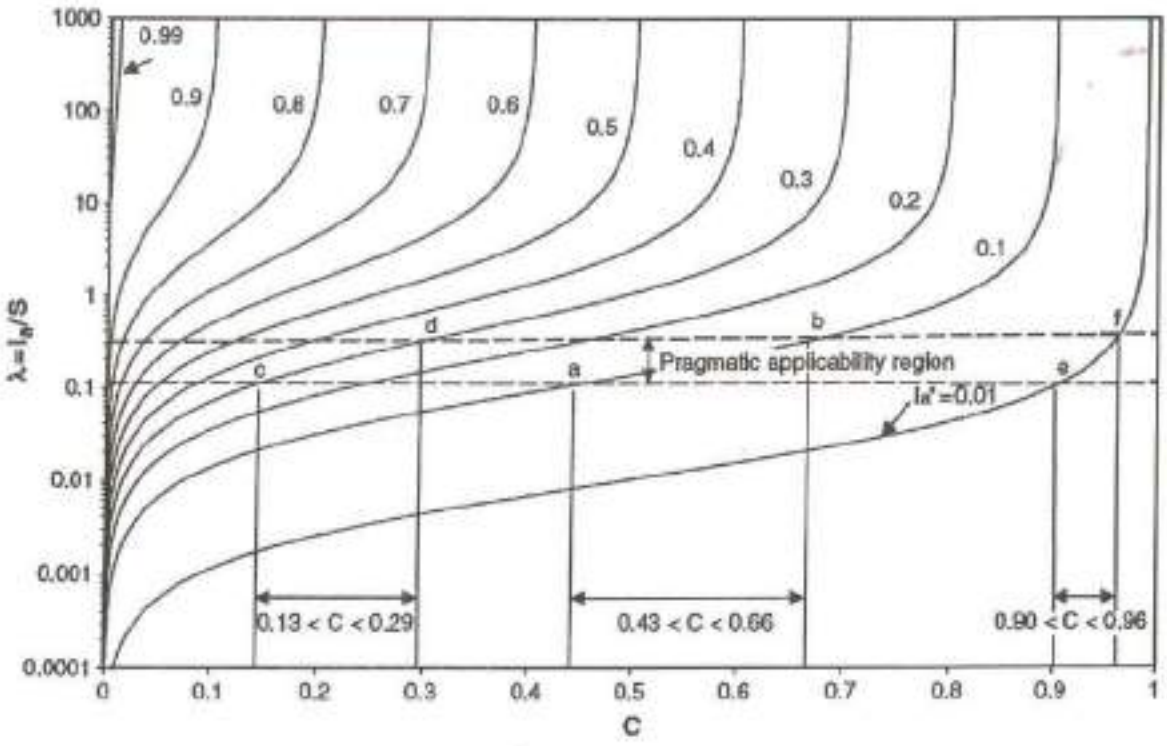

Figure III.2: Variation of initial abstraction coefficient λ with runoff factor C and non-dimensional initial abstraction I_a^* (Mishra and Singh, 2004).

According to Plummer & Woodward (2002) each relationship of I_a to S requires a unique set of CNs; a change in the I_a-S relation would require a change in the runoff equation.

The I_a-S relationship proposed by Woodward *et al.* (2002) requires further refinement for several reasons (Jain *et al.* 2006a). Bonta (1997) showed that the number of methods increased if CN was determined from measured P-Q data and λ was allowed to vary from 0.2. Thus, a proper λ value in Eq. (III.4) is crucial for accurate runoff estimation, and it can vary from 0 to ∞ (Mishra & Singh 1999; Mishra & Singh 2003a). Mishra & Singh (1999; 2003a) suggest λ to be implicitly related to both S and P, and it is also described as a regional and climatic parameter. Since P is an implicit function of climatic/meteorological characteristics, a more general non-linear I_a-S relation including P was proposed by Jain *et al.* (2006b) expressed as:

$$I_a = \lambda S\left(\frac{P}{(P+S)}\right)^{\alpha} \qquad \text{(III.9)}$$

where α is a constant. Since Eq. (III.9) reduces to Eq. (III.4) for $\lambda = 0.2$ and $\alpha = 0$, the former is a generalized form of the latter. The model resulting from the coupling of Eq. (III.5) and Eq. (III.9) and its variants for $\lambda = 0.3$ and $\alpha = 1.5$ were found to perform much better than the existing SCS-CN method (Eq. III.6) for $\lambda = 0.2$.

In this direction, Mishra *et al.* (2006b) developed a modified non-linear I_a-S relationship, owing to the fact that I_a largely depends on initial soil moisture M, as:

$$I_a = \frac{\lambda S^2}{(S+M)} \qquad \text{(III.10)}$$

The generalized nature of the above equation can be seen as, for M = 0 or a completely dry condition, $I_a = \lambda S$, which is the same as Eq. (III.4). Thus, Eq. (III.3) is a specialized form of Eq. (III.10). Readers should refer to the cited works for their detailed implication. The model resulting from the coupling of Eq. (III.5) and Eq. (III.10) and its variants were found to perform much better than the existing SCS-CN method (Eq. III.6) for $\lambda = 0.2$. More recently, Zhi-Hua Shi *et al.* (2009) examined the I_a-S relationship using six years of rainfall and runoff event data from the Three Gorges area of China. The results indicated that the I_a/S values, using event rainfall-runoff data, varied from 0.010 to 0.154, with a median of 0.048. The average initial abstraction ratio of the watershed was equal to 0.053. The standard SCS-CN method underestimates large runoff events and yielded a slope of the regression line of 0.559 and an intercept of 0.301. The modified I_a/S value was about 0.05, which better predicted runoff depths with a coefficient of determination (COD) of 0.804 and a linear regression slope of 0.834.

Thus, it can be concluded from the above discussions of I_a-S examination that there is still ample scope for better refinements for better results and structural improvements in the existing I_a-S relationship and hence the improvements will produce an enhanced performance of the SCS-CN technique.

III.1.4 Critical scrutiny of SCS-CN technique with major strengths and weaknesses

Though the technique is versatile in its conceptual as well as application domain, the ultimate success is often governed by the precision with which the values of CN and I_a are assigned, which indeed are most sensitive but typically assumed constant over space and time. Previous researches have well established that even for the same location these values are highly changeable during a year owing to factors like changes in land use, crop cover, crop growth, land treatment etc. One more critical analysis of this popular technique could be towards its dependency on the process of infiltration. The SCS-CN infiltration rate only produces a monotonic decreasing infiltration curve for constant rainfall intensity. Morel-Seytoux & Verdin (1983) have verified and reported that infiltration rates implied in the SCS-CN procedure fluctuate with rainfall intensity, which often disagrees with real field situations. When the SCS method is expressed as an infiltration equation, the infiltration rate becomes dependent on both total storm rainfall and rainfall intensity. Contrarily, when the technique is expressed as a spatially varied saturation overland flow model, the technique implies that some part of the catchment has infinite storage capacity. With this it is evident that there exists the lack of physical reality in the formulation of the SCS method, which seems to be an inherent limitation to any further development.

The method, though alluring to many practising hydrologists by its overwhelming simplicity, contains some unknowns and inconsistencies (Chen 1982). Recently the method has been critically reviewed and diagnosed by various researchers for its structural inconsistencies (Michel *et al.* 2005) and uses and limitations (Ponce & Hawkins 1996; Garen & Moore 2005). The major strengths and weaknesses of the SCS-CN technique can be summarized as follows:

Major strengths

- It is a simple, predictable, stable and lumped conceptual model.
- It relies on only one parameter CN and is well suited for ungauged situations.

- It is the single available technique for wider applications in the majority of computer-based advanced hydrologic simulation models (Singh 1995).
- Its responsiveness to four readily grasped catchment properties: soil type, land use/treatment, surface condition and antecedent moisture condition.
- It requires only a few basic descriptive inputs that are convertible to numeric values for estimation of direct surface runoff.
- The method does best in agricultural sites (for which it was originally intended) but has equally extendable utility on urban or forest sites.
- The technique has tremendous capabilities for its adoption towards environmental and water quality modelling.
- It is well compatible with recent GIS and remote sensing tools in hydrological applications.

Major weaknesses

- Lack of clear guidance on how to clearly accommodate varied antecedent moisture conditions.
- Choice of fixing the initial abstraction coefficient $\lambda = 0.2$ leads to preempted regionalization based on geologic and climatic conditions.
- The method has no explicit provisions for spatial scale effects on the CN, which remains highly sensible and truly governs the runoff.
- The discrete relationship between CN and AMC classes permits a sudden jump in CN, resulting in an equivalent quantum jump in computed runoff.
- It does not have any expression of time and ignores the impact of rainfall intensity and its temporal distribution.
- It lacks the expression for antecedent moisture, which plays a crucial and significant role in governing runoff generation process.

III.1.5 CN estimation methods

The soil moisture concentration on a catchment just before a rainfall event occurs is of great importance in hydrology. According to Hawkins (1975): '...that the errors in CN may have much more consequences on runoff estimation than errors of similar magnitude in storm rainfall P...' This establishes enough about the importance of accurate CN estimation. Major watershed characteristics such as soil type, land use/treatment classes, hydrologic soil group,

hydrologic condition and, most importantly, antecedent moisture condition play a significant role in accurate CN estimation. In the words of Hawkins *et al.* (1985) '...the antecedent moisture condition (AMC) is one of the most influential watershed characteristics in determining curve number (CN).' This reflects the fact that AMC is relatively less important in extremely wet or dry conditions, but at the same time very important in catchments with highly variable soil moisture. The AMC is extremely dependent on catchment conditions and plays a dominating role while applying the SCS-CN technique in a variety of situations. It remains highly dependent on prevailing soils, land cover, land treatment and runoff generating processes. Often the applicability of the technique is questioned, owing to the variability in one of these factors. Perrone & Madramootoo (1998) have revealed that three AMCs used in the SCS-CN technique are inapplicable for catchments lying in humid regions as the technique was developed in semi-arid and arid locations in the USA, where the majority of runoff is generated as excess infiltration.

The SCS defines AMC as an index of the watershed wetness (Hjelmfelt 1991). NEH uses the antecedent 5-day rainfall as antecedent precipitation index (API) for three AMCs as AMC I through AMC III. These three conditions of the watershed correspond respectively to 90%, 10% and 50% cumulative probability of exceedance of runoff depth for a given rainfall (Hjelmfelt *et al.* 1982). These antecedent conditions are usually defined in a heuristic manner by means of empirical coefficients like CN used in the SCS-CN approach. Even though CNs are related to soil and land use characteristics, the basic question remains: what is the most likely state of the soil concentration moisture just before a storm reaches a catchment? (Valdes *et al.* 1990.) Despite widespread use of the SCS-CN technique, the accurate estimation of the parameter CN, depending on antecedent conditions (soil concentration moisture just before a storm), is a topic of continued discussions among hydrologists and the water resources community e.g. Hawkins 1978; Hawkins 1979; Hjelmfelt 1980; Springer *et al.* 1980; Chen 1982; Hawkins 1984; Hjelmfelt 1991; Hawkins 1993; Steenhuis *et al.* 1995; Ponce & Hawkins 1996; Simanton *et al.* 1996; Bonta 1997; Mishra & Singh 1999; McCuen 2002; Mishra & Singh 2002a; Garen & Moore 2005; Sahu *et al.* 2007; Walter & Stephen 2005; Mishra & Singh 2006.

Originally CNs were developed using daily rainfall-runoff records corresponding to the maximum annual flows from gauged watersheds, for which information on their soils, cover and hydrologic condition was available (SCS 1972). The rainfall (P)-runoff (Q) data were plotted on arithmetic paper having a grid of plotted curve number (Figure III.3). The CN value corresponding to the curve that separated half of the plotted data from the other half

was taken as the median curve number for the watershed. Thus the developed curve numbers represented the averages or median site values for soil groups, cover and hydrologic condition and corresponds to AMC II (CN_{II}). The upper enveloping curve was taken to correspond to AMC III (CN_{III}) and the lower curve to AMC I (CN_I). The average condition was taken to mean average response, which was later extended to imply average soil moisture condition (Miller & Cronshey 1989). For any change in AMC condition (say from AMC_I to AMC_{III}) on a given catchment, a sudden jump in CN value (i.e. from CN I to CN III) invariably occurs. And this variability is discontinuous in nature, which ultimately results in a sudden jump in computed runoff. Thus, indirectly, it gives a reflection of the discrete nature of the CN-AMC relationship.

Depending on 5-day antecedent rainfall, CN_{II} is convertible to CN_I and CN_{III} using the relationships given by Sobhani (1975), Hawkins *et al.* (1985) and Neitsch *et al.* (2002) and directly from the NEH-4 tables (SCS 1972; McCuen 1982; McCuen 1989; Ponce 1989; Singh 1992; Mishra & Singh 2003a).

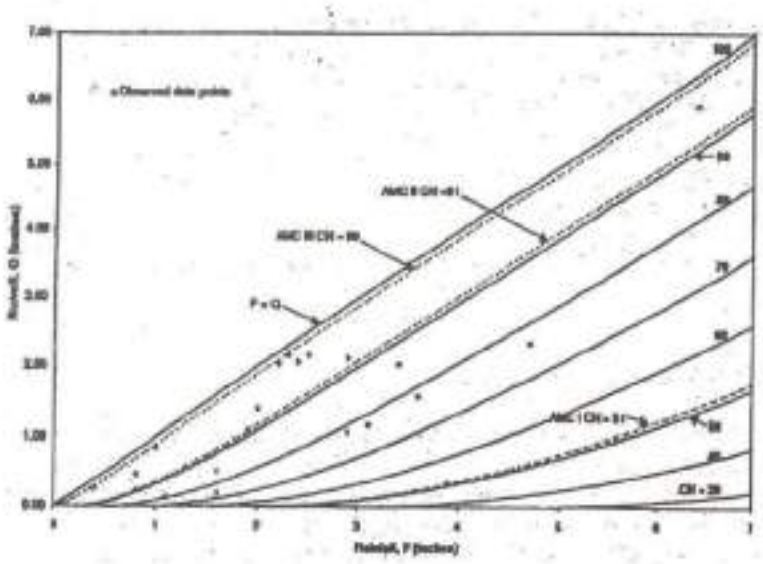

Figure III.3: Determination of CN for AMC I through AMC III using SCS-CN method (after Mishra and Singh, 2003a)

To get the average CN values (CN_{II}) from the rainfall (P)-runoff (Q) data of a gauged watershed, Hawkins (1993) suggested S (or CN) computation using the expression given below:

$$S = 5\left[P + 2Q - \sqrt{Q(4Q + 5P)}\right] \qquad \text{(III.11)}$$

Another group of researchers believed in adopting an alternative approach termed the rank-order approach to estimate CN from rainfall (P)-runoff (Q) data (Hjelmfelt 1980). Here P-Q data were sorted and rearranged on rank-order basis to have equal return periods. Bonta (1997) evaluated the potential of such derived distributions to derive curve numbers from measured P-Q data, treating them as separate distributions. The derived-distribution method also identifies watershed as 'standard', 'violent' and 'complacent', similar to Hawkins (1993). Such a derived-distribution method has ample potential even when data availability is limited. Schneider & McCuen (2005) developed a new log-normal frequency method to estimate curve numbers from measured P-Q data. The developed method was found to be more accurate than the rank-order method. Mishra & Singh (2006) investigated the variation of CN with AMC and developed a new power relationship between the CN and the 5-day antecedent rainfall. The resulting CN-AMC relationship is well applicable for both gauged and ungauged watersheds and eliminates the problem of sudden jump from one AMC level to another.

A few researchers belong to another school of thought that in CN estimation slope should also be considered as a factor, e.g. Sharpley & Williams (1990) and Huang *et al.* (2006). Sharpley & Williams (1990) incorporated slope factor in CN estimation assuming that CN_2 obtained from the NEH Handbook (SCS 1972) corresponds to a slope of 5%. The slope adjusted CN_2 named $CN_{2\alpha}$ were represented as:

$$CN_{II\alpha} = \frac{1}{3}(CN_{III} - CN_{II})\left(1 - 2e^{-13.86\alpha}\right) + CN_{II} \qquad \text{(III.12)}$$

where α is the soil slope in m/m. Huang *et al.* (2006) tested the above equation and found that the equation has limited applications and, as an improvement, they developed another set of equations for climatic and steep slope conditions observed in Loess Plateau of China, expressed as:

$$CN_{II\alpha} = CN_{II}\left[\frac{322.79 + 15.63\alpha}{(\alpha + 323.52)}\right] \qquad \text{(III.13)}$$

However, the credibility of the above equation needs to be validated for other regions having similar climatic and slope conditions. They also tested the slope-adjustment CN method, used in EPIC, in both its original and optimized forms, and found that in both cases the runoff prediction was improved for steep slopes.

Recently, Mishra *et al.* (2008) compared AMC-dependent CN conversion formulae (Table III.1) developed by Sobhani (1975), Hawkins *et al.* (1985), Chow *et al.* (1988) and Neitsch *et al.* (2002) and a new formula proposed by them using the NEH-4 CN values as the target values. Using relative error (RE) and root mean square error (RMSE) as the statistical performance evaluation criteria, it was found that the Sobhani (1975), Hawkins *et al.* (1985), Chow *et al.* (1988) and Neitsch *et al.* (2002), and the proposed formulae, yield RE values in the respective percent range of (3.25, −17.16) and (11.26, −5.19); (1.68, −19.68) and (15.59, −1.95); (4.59, −15.01) and (16.94, −0.92); (4848.83, −2.04) and (27.11, −1.68); and (1.51,−19.96) and (16.10,−1.55) respectively for CN_I and CN_{III} conversion. The results show that the Neitsch formulae yield abnormally high RE-values, especially for low (1, 40) CN, showing the poorest performance in fitting NEH-4 values. On the other hand, the Hawkins formulae exhibit the narrowest range of RE-variation and, therefore, are closest to NEH-4 data. Thus it can be interpreted that the Sobhani formula performs the best in CN_I-conversion, and the Hawkins formula in CN_{III}.

Table III.1: Popular AMC dependent CN conversion formulae (Mishra et al., 2008)

Method	AMC I	AMC III
Sobhani (1975)	$CN_I = \frac{CN_{II}}{2.334 - 0.01334CN_{II}}$	$CN_{III} = \frac{CN_{II}}{0.4036 + 0.005964CN_{II}}$
Hawkins et al. (1985)	$CN_I = \frac{CN_{II}}{2.281 - 0.01281CN_{II}}$	$CN_{III} = \frac{CN_{II}}{0.427 + 0.00573CN_{II}}$
Chow et al. (1988)	$CN_I = \frac{4.2CN_{II}}{10 - 0.058CN_{II}}$	$CN_{III} = \frac{23CN_{II}}{10 + 0.13CN_{II}}$
Neitsch et al. (2002)	$CN_I = CN_{II} - \frac{20(100 - CN_{II})}{\{100 - CN_{II} + \exp[2.533 - 0.0636(100 - CN_{II})]\}}$	$CN_{III} = CN_{II}\exp\{0.0067(100 - CN_{II})\}$
Mishra et al. (2008)	$CN_I = CN_{II} - \frac{20(100 - CN_{II})}{2.274 - 0.012754CN_{II}}$	$CN_{III} = \frac{CN_{II}}{0.430 + 0.0057CN_{II}}$

Table III.2 also shows the RMSE values for different AMC-dependent CN conversion formulae taking SCS (1972; 1985) CN values as target values. A high value of RE indicates greater deviation of the computed values from the observed ones, and vice versa, whereas RE equal to zero shows a perfect fit. They further evaluated the performance of the above

conversion formulae (Table III.1) using the *filed data* taken from USDA-ARS Water Database, which is a collection of rainfall and stream flow data from small agricultural watersheds of the United States, and found that the proposed formulae perform the best, and those due to Neitsch the poorest in field application. Hawkins' formulae ranked second, while Sobhani & Chow ranked third and fourth. On the whole, the overall performance of the proposed and Neitsch formulae was found to be the best and poorest on field data, respectively.

Table III.2: RMSE values for different AMC-dependent CN conversion formulae taking SCS (1972, 1985) CN values as target values (Mishra et al., 2008)

Method	RMSE	
	CN_I	CN_{III}
Sobhani (1975)	0.8293	1.2703
Hawkins et al. (1985)	0.9247	0.7652
Chow et al. (1988)	0.8937	0.8106
Neitsch et al. (2002)	6.8255	1.6038
Mishra et al. (2008)	0.9445	0.7681

III.1.6. Applications with recent advancements

Since its inception the SCS-CN method has witnessed myriad and a variety of applications to real fields for reasons such as its simplicity, stability and accountability for most runoff producing watershed characteristics (soil type, land use treatment, surface condition and antecedent moisture condition). Recently Singh & Frevert (2002) edited a book titled '*Mathematical Models of Small Watershed Hydrology and Applications*', in which at least 6 of the 22 chapters have mathematical models of watershed hydrology based on SCS-CN approach. This reflects the robustness and eternal popularity of the SCS-CN technique. Walter & Stephen (2005) add that efforts to merge the curve number model with distributed and variable source area concepts will provide the initial steps of incorporating better hydrological science into existing water quality models by improving water quality models that are already being used widely. A considerable amount of literature on the method has been published and the method has gone through various stages and phases of critical reviews (Rallison 1980; Chen 1982; Ponce & Hawkins 1996; Mishra & Singh 2003a; Garen & Moore 2005; Michel *et al.* 2005; Walter & Stephen 2005; Mishra & Singh 2006). Rallison (1980) provided detailed information about the origin and evaluation of the technique and highlighted major concerns to its application to the hydrology and water resources problems

it was designed to solve and suggested future research areas. Chen (1982) evaluated the mathematical and physical significance of the technique for estimating the runoff volume.

Though primarily intended for event-based rainfall-runoff modelling on ungauged watersheds, the SCS-CN method has been applied successfully in the wider realm of hydrology and watershed management and environmental engineering with notable contributions from Williams & LaSeur (1976), Hawkins (1978), Mishra & Singh (1999), Mishra & Singh (2002a), Mishra & Singh (2004a,b) and Mishra *et al.* (2004b,c). Svoboda (1991) used the curve number concept to calculate soil water content for deriving rainfall contribution to direct runoff and groundwater. The method has also been successfully applied to sediment yield modelling (Mishra *et al.* 2006a; Singh *et al.* 2008; Tyagi *et al.* 2008; Bhunya *et al.* 2009) and determination of sub-surface flow (Yuan *et al.* 2001). The vast applicability described above reflects the important status of the SCS-CN method in the prevailing hierarchy of hydrologic models.

The concept and status of the SCS-CN-based method have become so popular and versatile that, beside direct replications, many prominent researchers have well integrated the core concept of the technique into their new hydrological models. It is interesting to mention Walter & Stephen (2005): 'It is worth specifically noting that criticisms of the curve number method, like that of Garen & Moore (2005), should not be interpreted as reflecting negatively on its creator(s). Rather, these types of comments are an incentive to engage the same creative effort that these early 'modelers' invoked to find appropriate approaches to current problems based on current science', which fortifies ongoing developmental efforts towards SCS-CN technique. Hence, in this paper an attempt has been made to present an abstracted review of some of the notable developments based on the SCS-CN technique and to highlight their strengths and weaknesses.

III.1.7 The SCS-CN method in hydrologic simulations

This section briefly discusses some of the notable works carried out for long- as well as short-term hydrologic simulation applications.

For the first time, Williams & LaSeur (1976) introduced the concept of Soil Moisture Accounting (SMA) procedure to develop a Water Yield Model (WYM) based on the SCS-CN technique. The developed model has various advantages such as eliminating sudden jumps in the CN-values while changing from one AMC to the other and it can be applied to a nearby ungauged watershed by adjusting the curve number for the ungauged watershed in proportion to the ratio of the AMC II curve number to the average estimated curve number

for the gauged watershed. On the other hand, the model has some perceived limitations and disadvantages as it utilizes an arbitrary assigned value of 50.8 cm for absolute potential maximum retention S_b with faulty assumption of decay of soil moisture based on lake evaporation. Also the model describes the variation of direct runoff Q with P analogous to F and, thus, contrasts the existing SCS-CN technique. Hawkins (1978) outlined serious flaws associated with the CN and AMC relationships such as: (i) the discrete relationship between CNs and AMC class, leading to a sudden jump in CN and a corresponding quantum jump in calculated runoff; (ii) the lack of assumptions in the development of the NEH-4 table and, thus, no physical reasoning or reconciliation with reality. To circumvent these flaws, he proposed a daily flow simulation model, which accounts for the site moisture on a continuous basis. However, the model also has disadvantages of concern such as: (i) the model assumes that the SCS-CN method is based on the $(I_a + S)$ scheme, whereas I_a is separate from S (Mishra & Singh 2003a); and (ii) the model still uses the conventional empirical S-CN mapping relationship for computing CN for the various time steps. Pandit & Gopalakrishnan (1996) developed a continuous simulation model using the existing SCS-CN method for computing annual pollutant loads based on annual storm runoff coefficient (ASRC) and degree of perviousness/imperviousness of watershed.

In a new attempt, Yu (1998) developed relationships between rainfall and runoff similar to the SCS-CN method based on two simple but reasonable assumptions that the spatial variation of infiltration capacity has an exponential distribution while the lumped variation of rainfall follows an exponential distribution. Grove *et al.* (1998) studied the feasibility of the distributed CN approach compared to the composite approach for estimation of runoff depths using the SCS-CN method. The distributed approach may have an advantage for analysis of urbanizing watersheds with the proliferation of remote sensing and geographic information systems. Mishra & Singh (1999) discussed the origin and heritage of the existing SCS-CN technique in a sound analytical environment. They derived analytically the existing SCS-CN method from the empirical method of Mockus (1949) and proposed a general form of the modified SCS-CN method.

The application of the existing SCS-CN method (model 1; Eq. (III.6)) and the modified SCS-CN method (model 2; $Q = P^2/(S + 0.5P)$) to 3-Bar D watershed is shown in Figure III.4. It can be observed from Figure III.4 that the modified SCS-CN method (model 3) fits most of the observed data points, whereas the existing SCS-CN method (model 2)

deviates greatly from the observed data points; the latter model attempts to fit only a few high rainfall-runoff data.

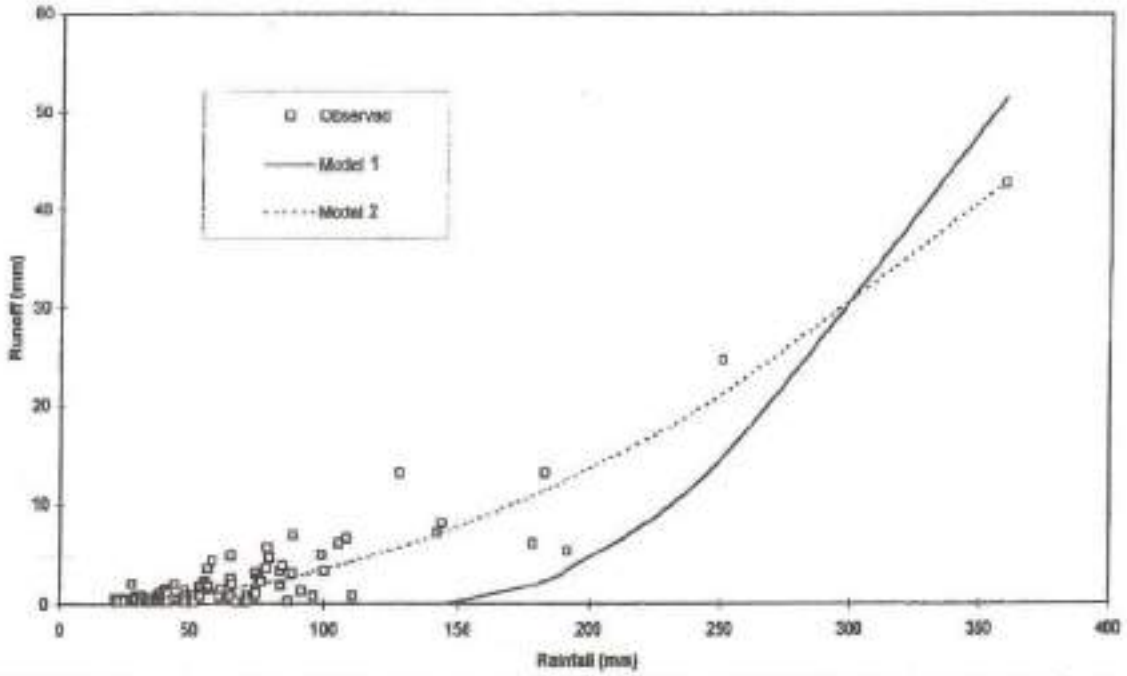

Figure III.4: Fitting of the existing SCS-CN method (model 1 for λ=0.2) and the modified SCS-CN method (model 2 for λ=0.5) (model 2) to 3-Bar D Watershed Data

Mishra *et al.* (2003b) addressed many intrinsic issues related to the SCS-CN method such as estimation of CNs from the recorded rainfall and runoff data and CNs variability associated with antecedent moisture and variability due to temporal and spatial variation of rainfall. They suggested a modified SCS-CN method based on the $C = S_r$ concept accounting for the static portion of infiltration and antecedent moisture and provided a simple spreadsheet estimation of the potential maximum retention from P and Q data, and 5-day antecedent precipitation (P_5). Mishra & Singh (2004a) developed a four parameter 'Versatile SCS-CN Model' to remove the inconsistencies and complexities associated with the existing models of long-term hydrologic simulation. The developed model obviates the sudden jumps in CN values and exclusively considers the soil moisture budgeting on a continuous basis, evapotranspiration and watershed routing procedures. Unlike the original SCS-CN method (as described in the preceding paragraphs), the modified SCS-CN method accounts for the static portion of the infiltration as well as the antecedent moisture. It incorporates a volumetric analysis which shows that the ratio of the potential maximum retention (S) to the precipitation amount versus runoff factor relation is equivalent to the average suction pressure–moisture content

relation for a unit rainfall amount and a given soil porosity. These characteristics make the model versatile. However, the versatile model contains a higher number of parameters and does not distinguish between the intrinsic parameter and the initial condition of watershed.

Mishra & Singh (2004b) established the criterion for the applicability of the SCS-CN method and extended the SCS-CN concept to derive a time-distributed runoff model and infiltration model. Mishra *et al.* (2004a) discussed the inherent sources of variability as spatial and temporal variation of rainfall and variation of CNs with the antecedent moisture. To circumvent the variability due to antecedent moisture they developed a modified form of Mishra & Singh (MS) (2002b) model using the $C = S_r$ concept by incorporating the antecedent moisture or initial soil moisture (V_0) into the basic proportionality concept.

In an attempt to restructure the mathematical and conceptual foundations of the SCS-CN technique, Michel *et al.* (2005) highlighted the major inconsistencies associated with the age-old but most popular SCS-CN technique and proposed a renewed SCS-CN procedure. Some of the inconsistencies noticed by them are: (i) it ignores the initial soil moisture, i.e. the moisture storage at the beginning of the storm event in its formulation; (ii) it is applicable only for the end of the storm event, i.e. it is silent within the storm event; and (iii) the relationship between the initial abstraction I_a and the potential maximum retention S is not justifiable, although presenting uniqueness in terms of parameter i.e. one-parameter model characteristics. They introduced a renewed SCS-CN procedure based on the SMA procedure, while keeping the acknowledged efficiency of the original technique. The SMA procedure was re-addressed by Sahu et al. (2007) that resulted in a simple expression for V_0 to avoid a sudden jump in runoff computations. Recently, Geetha *et al.* (2007; 2008) developed new lumped conceptual models based on SCS-CN for long-term hydrologic simulations.

III.1.8 The SCS-CN method in sedimentation and environmental engineering

A number of popular computer-based runoff and erosion simulation models such as AGNPS (Young *et al.* 1989), CREAMS (Knisel 1980), SWRRB (Arnold *et al.* 1990), SWAT (Neitsch *et al.* 2002), EPIC (Sharpley & Williams 1990) and GWLF (Haith & Shoemaker 1987) use the SCS-CN method as a component model for runoff estimation. A detailed description of many of the above-mentioned models can be found in Merritt *et al.* (2003) and Aksoy & Kavvas (2005). In the recent past, one interesting review paper by Garen & Moore (2005) titled '*Curve Number Hydrology in Water Quality Modeling: Uses, Abuses, and Future Directions*', followed by fine discussions by Walter & Stephen (2005),was widely

appreciated and centred by the hydrologic community particularly the water quality modellers. Hence, it can be stated that the SCS-CN method is still a central tool available to the scientific community with its broad and user-friendly acceptance to address real world problems.

Mishra *et al.* (2004b) employed the basic proportionality concept (Eq. III.3) of the SCS-CN method for partitioning 12 metal elements, Zn, Cd, Pb, Ni, Mn, Fe, Cr, Mg, Al, Ca, Cu and Na, between dissolved and particulate-bound form. For this they postulated two parameters, namely the potential maximum desorption (Ψ) and partitioning curve number (PCN), as analogous to the SCS-CN parameters S and CN, respectively. In an another attempt, again Mishra *et al.* (2004c) suggested a new partitioning curve number (PCN) approach for partitioning heavy metals into dissolved and particulate-bound forms in urban snow melt, rainfall/runoff and river flow environments on the basis of an analogy between SCS-CN method-based infiltration and metal sorption processes as discussed above.

In another endeavour to develop an SCS-CN-based sediment yield model, Mishra *et al.* (2006a) coupled the popular SCS-CN method with the Universal Soil Loss Equation (USLE) for modelling rain-storm generated sediment yield from a watershed. The generalized expression for the models can be expressed as:

$$Y = \left[\frac{(1-\lambda_1)[P-\lambda S+V_0]}{P+(1-\lambda)S+V_0}+\lambda_1\right]A \qquad \text{(III.14)}$$

where Y = sediment yield, A = the potential maximum erosion, P = total rainfall, S = potential maximum retention, V_0 = initial soil moisture, λ = initial abstraction coefficient and λ_1 is the initial flush coefficient. This reflects that the SCS-CN technique is equally applicable in sediment yield modelling. Despite having a hydrologically sound procedure and a firm mathematical base, the models are not applicable for modelling time-distributed suspended sediment yield or sediment graph applications (Singh *et al.* 2008; Bhunya *et al.* 2009). More recently, Singh *et al.* (2008) came up with new conceptual sediment graph models based on the coupling of popular and extensively used methods, viz., Nash model (Nash 1957) -based instantaneous unit sediment graph (IUSG), SCS-CN method and power law (Novotny & Olem 1994). The generalized form of the model can be expressed as:

$$Qs = \frac{\left[\alpha A A_w\left[(kt-\lambda+\theta)/(1-kt-\lambda+\theta)\right]^{\beta} n_s^{(n_s-1)}\left[(t/t_{ps})\exp(-t/t_{ps})\right]^{(n_s-1)}\right]}{t_{ps}\Gamma(n_s)} \qquad \text{(III.15)}$$

where α and β = coefficient and exponent of power law; k = infiltration decay coefficient; λ, $\theta = V_0/s$ and n_s is the number of reservoirs and constitutes the set of model parameters. The

models consider major runoff-producing characteristics, and watershed characteristics such as soil type, land use, hydrologic condition, antecedent moisture and rainfall intensity. It is physically more plausible than the common regression relations-based models. Such models can be exceptionally useful for computing dynamic pollutant loads in water quality modelling if the sediment transports the pollutants that are toxic at high concentrations, requiring determination of peak, rather than average, sediment flow rate.

Tyagi *et al.* (2008) developed a time-distributed sediment yield model (sediment graph model) utilizing the SCS-CN-based infiltration model for computation of rainfall-excess rate, and the SCS-CN-inspired proportionality concept for computation of sediment-excess. Finally, for computation of sediment graphs, the sediment-excess is routed to the watershed outlet using a single linear reservoir technique. The expression for the model can be expressed as:

$$Y_t = \frac{A}{P_{\Delta t}}\left[1-\frac{S^2}{(P+S-\lambda S)^2}\right](i-f_c) \qquad \text{(III.16)}$$

where A is the actual potential maximum erosion of the watershed, dependent on the soil properties and storage capacity (S); and $P_{\Delta t}$ is the rainfall amount during time interval Δt; i is the rainfall intensity and f_c is the final infiltration rate.

III.1.9 Application of the SCS-CN technique for ungauged catchments

The problem of estimation of flood rates from small ungauged basins still remained one of the biggest issues for researchers. A plethora of research findings has clearly established that even the simplest SCS-CN technique is quite capable of providing the volume and peak discharge rates in accordance with prevailing rainfall events. The technique could be effectively extended for its application under ungauged situations. Moreover, before the method can be applied to an ungauged catchment, its parameters need to be calibrated from certain nearby gauged catchments having similar land use and physical characteristics as ungauged catchment e.g. slope, hydrologic soil conditions etc.

While attempting such extended application of the SCS-CN technique to ungauged situations , the popular Unit Hydrograph (UH) concept is often adopted to yield calibrated parameters (may be termed correlated coefficient), which will then be applied to the SCS-CN method to estimate even the flood hydrographs from ungauged catchments. One such exertion was attempted by Gaur (1999), where the applicability of SCS Synthetic UH was

successfully demonstrated to predict surface-runoff responses from a few natural catchments initially assuming them as ungauged. The observed depths of daily rainfall and runoff were utilized to derive truer CN values, which were used to compute peak runoff rate (Q_p) and time to Q_p. Integrating these computed values with SCS dimensionless unit hydrograph shape function, the representative SCS-Synthetic UH of relevant unit duration (near to time of concentration of catchment) were derived, which in turn were utilized to compute direct runoff hydrographs under real input rainfall pulses. The computed surface runoff responses were quite satisfactory. Gaur & Mathur (2009) confirmed another indirect utility of such synthetic SCS unit pulse hydrographs for generating overland roughness predictive equations for facilitating application of the kinematic wave modelling approach on ungauged situations applying optimization under kinematic wave flow conditions (Gaur & Mathur 2003). It clearly justified another indirect potential of the SCS-CN technique for hydrological evaluation of ungauged catchments. Boughton (1989) examined the SCS-CN technique for estimating runoff from small ungauged rural catchments. He collated the results of some Australian studies where curve numbers were calibrated against actual runoff data. A major weakness realized was the sensitivity of estimated runoff to errors in the selection of the curve number as the changes of about 15–20% in the curve number doubles or halves the total estimated runoff.

III.2 REMARKS

The SCS-CN method has gained applicability among all sorts of hydrological modelling approaches attempted across the globe by an enormous number of researchers, field engineers and academicians in the domain of earth system sciences. The method is simple to use and requires basic descriptive inputs that are converted to numeric values for estimation of watershed direct runoff volume (Bonta 1997). Within the tremendous literature available on applications of the SCS-CN technique in hydrological sciences, a relevant updated review dealing with its origin, historical background, nature, advantages and limitations, CN estimation methods, CN vs. AMC description, I_a-S relationship and recent notable advanced applications for areas other than originally intended have been presented and discussed for their merits and demerits. The application on ungauged basins remains one of the important future prospects of the techniques. On the basis of some structural advancements and vast applications, it is found that the technique would always enjoy its simplicity, applicability and wider acceptability among the hierarchy of available hydrologic models for the benefits

of society as a whole. The presented review of this vital hydrological tool may serve the purpose of better understanding and practical applications of the SCS method at the levels of basic academics as well as practising hydrologists in order to facilitate better and fruitful advanced applications of the technique in their fields. At the end, the contents provided in this review paper may serve as a guiding principle to synchronize our futuristic research efforts harmonizing with the emerging swiftness of developmental laws of nature in the context of hydrological progress.